Novel Isocyanide Chemistry for the Synthesis of Defined (Macro-)Molecules

Zur Erlangung des akademischen Grades eines

DOKTORS DER NATURWISSENSCHAFTEN

(Dr. rer. nat.)

von der KIT-Fakultät für Chemie und Biowissenschaften
des Karlsruher Instituts für Technologie (KIT)

genehmigte

DISSERTATION

von

M. Sc. Kevin Andreas Waibel

aus Karlsruhe

Dekan: Prof. Dr. Manfred Wilhelm
1. Referent: Prof. Dr. Michael A. R. Meier
2. Referent: Prof. Dr. Joachim Podlech
Tag der mündlichen Prüfung: 14.04.2021

„Die Welt machte mich zu einem Chemiker,
nun mache ich sie zu meinem Labor.”

Frei nach Friedrich Dürrenmatts „Besuch der alten Dame”

Declaration of authorship

Die vorliegende Arbeit wurde von März 2018 bis März 2021 unter Anleitung von Prof. Dr. Michael A. R. Meier am Karlsruher Institut für Technologie (KIT) angefertigt.

Hiermit versichere ich, dass ich die Arbeit selbständig angefertigt, nur die angegebenen Quellen und Hilfsmittel benutzt und mich keiner unzulässigen Hilfe Dritter bedient habe. Insbesondere habe ich wörtlich oder sinngemäß aus anderen Werken übernommene Inhalte als solche kenntlich gemacht. Die Satzung des Karlsruher Instituts für Technologie (KIT) zur Sicherung wissenschaftlicher Praxis habe ich beachtet. Des Weiteren erkläre ich, dass ich mich derzeit in keinem laufenden Promotionsverfahren befinde und auch keine vorausgegangenen Promotionsversuche unternommen habe. Die elektronische Version der Arbeit stimmt mit der schriftlichen Version überein und die Primärdaten sind gemäß Abs. A (6) der Regeln zur Sicherung guter wissenschaftlicher Praxis des KIT beim Institut abgegeben und archiviert.

Karlsruhe, 26.05.2021 _____

Kevin Waibel

I Danksagung

Die wohl fundamentalste Lehre der Wissenschaft ist, dass Fortschritt niemals Einzelnen zugeschrieben werden kann, sondern dass er aus Zusammenarbeit und regem Austausch resultiert. Meiner Promotion will ich also ein großes Dankeschön an all jene voranstellen, die es mir ermöglicht haben, diesen Weg zu beschreiten und/oder mich dabei begleitet haben.

Zunächst möchte ich dir, Michael Meier, danken, dass du mich damals (schon für die Masterarbeit) in deinen Arbeitskreis aufgenommen und mir das nötige Vertrauen entgegengebracht hast, diesen langen Weg erfolgreich zu meistern. Deine offene, persönliche und studentennahe Art haben meine Zeit in deinem AK bereichert und mich niemals daran zweifeln lassen, dass die Promotion unter deiner Betreuung die richtige Entscheidung war. Du warst immer zu einem Gespräch bereit, wenn es um Probleme und Herausforderungen ging, und hast immer versucht, meine Ideen und Motivation in die richtigen Bahnen zu lenken, auch in den Zeiten, in denen ich vor lauter Molekülen keine Atome mehr sehen konnte. Vielen Dank dafür!

An zweiter Stelle möchte ich dem Arbeitskreis von ganzem Herzen danken. Ihr alle habt diese drei Jahre zu einer unvergesslichen Zeit gemacht, egal ob wir gemeinsam im Praktikum saßen und uns die wildesten Fragen für mögliche Kolloquien ausgedacht haben oder bei den Studenten- und Arbeitskreisfeiern die Nacht zum Tag gemacht haben. Ich hoffe ich konnte euch allen etwas zurückgeben und sei es nur durch meine literarischen Beiträge zur Weihnachtsfeier. Euer Lachen klang zumindest immer ehrlich!

Namentlich möchte ich den fleißigen Korrektoren meiner Arbeit danken: Teşekkürler Eren. Grazie Federico e Luca. Danke Julian, Philipp und Roman. Dafni, I surely did not forget you! Thank you for your invaluable input and for proofreading my thesis, and last but not least for our nonsensical chit-chat on *Teams* and face-to-face. I will miss your humor.

Danke, Roman, für die unzähligen Stunden wissenschaftlichen Geplauders und unserer erfolgreichen Kooperation. Danke, Philipp, für die Stunden gemeinsamer Arbeit in 408, das während der Promotion für uns beide wohl zu einem zweiten zu Hause geworden ist. Danke auch für deine wilden Playlists und die unzähligen Lieder, die ich wohl nie wieder hören kann!

Ein besonderes Dankeschön auch nochmal an euch, Eren, Julian, Luca, Maximiliane und Philipp. Wir haben alle fast gleichzeitig angefangen, und nun stehen wir am Ende unserer gemeinsamen Zeit im AK Meier. Ich werde diese Zeit und entspannte Arbeitsatmosphäre vermissen. Genauso möchte ich den Alumni des AK Meier danken, die mich damals herzlich in den Arbeitskreis aufgenommen und ihre Expertise mit mir geteilt haben. Weiterhin auch dir vielen Dank, Eduard Spuling, du hast mit deiner unmittelbaren Labornachbarschaft die Laboratmosphäre in 408 immer bereichert, genauso wie die unzähligen Freitagmorgenfrühstücke im MZE.

Genauso möchte ich Rebecca Seim danken, die mit ihrer Expertise immer eine tatkräftige Unterstützung ist und ohne die so Einiges im Arbeitskreis nicht funktionieren würde. Die Zusammenarbeit mit dir war immer bereichernd!

Vielen Dank an Camilla, Dasha, Ninon und Triantafillia, die ihre Bachelor- oder Vertieferarbeit unter meiner Betreuung angefertigt haben, sowie an Helene und Moritz, die mich als HiWis bei der Laborarbeit unterstützt haben.

Ich danke unseren Sekretärinnen, Ann-Kathrin und Pinar, die immer eine willkommene Stütze für die unzähligen bürokratischen Hürden sind, die einem während der Promotion begegnen.

Nicht zuletzt gilt mein Dank auch den Angestellten des IOC, die immer für Nachschub an Glasware und Chemikalien gesorgt und meine unzähligen Massenproben vermessen haben.

Weiterhin möchte ich denjenigen danken, die den Grundstein für meinen Lebensweg gelegt haben: meinen Eltern und Verwandten. Ich danke euch, Mama und Papa, Carmen und Andreas, dass ihr mich immer gefördert und motiviert habt, nicht nur eine, sondern unzählige Fragen zu stellen. Vom Tag meiner Geburt an habt ihr mir mitgegeben, dass ich niemals aufhören sollte, neues Wissen in mich aufzusaugen wie ein Schwamm. Ihr hattet nie Zweifel an mir und habt mich in meiner Entwicklung immer bestärkt und ermuntert, diesen Weg einzuschlagen. Zu Beginn des Studiums schien die Doktorwürde wie ein fernes, unerreichbares Ziel, und jetzt fehlen nur noch wenige Schritte. Danke, dass ihr immer für mich da seid!

Ich möchte auch euch, Frank und Joachim, danken, so wie meiner restlichen Familie.

Ganz besonders hervorheben möchte ich noch euch, Harald und Pia, die ihr mich, genau wie meine Eltern, schon mein Leben lang unterstützt, finanziell wie auch mit der

Weisheit von Großeltern. Die unzähligen Gespräche, Ausflüge, Telefonate und gemeinsamen Essen werde ich niemals vergessen. Als unwissendes Kind habe ich euch immer den Nobelpreis versprochen, jetzt als Erwachsener sehe ich das natürlich realistischer. Ich danke euch auch dafür, dass ihr jede meiner wissenschaftlichen Arbeiten gelesen habt, auch wenn die wohl in eines der wenigen Fachgebiete fallen, in denen ihr euch nicht so gut auskennt. Vielen lieben Dank!

Ich möchte auch meiner Schwester Leonie und meinem „Schwager" Marius danken, ihr seid schon immer eine Bereicherung in meinen Leben.

Natürlich gebührt auch Judith und Winfried ein großer Dank, den Eltern meiner Freundin, die mich seit ich sie kennengelernt habe wie ein weiteres Mitglied ihrer Familie behandeln. Die Anerkennung, die ihr mir entgegengebracht habt, ist unersetzlich.

Auch meinem Freundeskreis gebührt ein großes Dankeschön. Ihr alle habt mit eurem Humor, unseren unzähligen Vogelbräu- und Spieleabenden, Erster-Mai-Maiwanderungen, Volleyballspielen, Reisen, Grillfeiern und Dungeons & Dragons Sessions dazu beigetragen, dass ich heute hier stehe.

Zu guter Letzt möchte ich dir, Samira, danken. Wenn die griechische Legende stimmt und die Menschen in zwei Teile zerbrochen wurden, um ihre Stärke zu schmälern, so bin ich überzeugt, dass du meine zweite Hälfte bist. Du bereicherst mein Leben in einem so unvorstellbaren Maße, dass es sich kaum in Worte fassen lässt. Du weißt, was ich meine. Danke für alles, was du für mich tust und getan hast.

II Kurzzusammenfassung

Die Substanzklasse der Isocyanide wurde bereits im späten 19. Jahrhundert entdeckt, allerdings wurde damals eine breitere Anwendung von ihrem meist penetranten Geruch und den wenigen bekannten Darstellungsmöglichkeiten limitiert. Im folgenden Jahrhundert wurden neuartige Methoden zur Synthese dieser Verbindungen etabliert, die jedoch meist auf der Verwendung von gefährlichen bzw. toxischen Chemikalien wie Phosphoryltrichlorid oder Phosgen und seinen Derivaten basierten. Trotzdem wurde ihr Potential von der Wissenschaft schnell erkannt und genutzt. Dies führte zum neuartigen Forschungsgebiet der isocyanidbasierten Chemie, in der die isocyanidbasierten Multikomponentenreaktionen eine der wichtigsten Untergruppen darstellt. Mögliche Anwendungsbereiche umfassen die kombinatorische und medizinische Chemie sowie die Synthese von definierten als auch dispersen Makromolekülen, wodurch die vielseitige Reaktivität von Isocyaniden bereits angedeutet wird. Dennoch ist ihr Potential bei weitem nicht ausgeschöpft und neuartige Anwendungen und Synthesen werden immer noch regelmäßig publiziert. Moderne Ansätze konzentrieren sich darauf, den ökologischen sowie ökonomischen Einfluss ihrer gefährlichen und teuren Herstellung zu verbessern, da dieser eine breitere industrielle Anwendung bisher verhindert hat. In dieser Arbeit wurden die Synthese von Isocyaniden untersucht und ihre Verwendung in organischer wie auch makromolekularer Chemie erweitert.

Im ersten Teil der Arbeit wird die Synthese von Isocyaniden im Sinne der Nachhaltigkeit kritisch bewertet und nachgehend bezüglich ihrer Umweltfreundlichkeit verbessert. Hierfür werden mehrere nachhaltige Lösungsmittel und weniger gefährliche Reagenzien eingesetzt. Weiterhin wird eine Bibliothek an verschiedenen Isocyanidverbindungen hergestellt, um die Effizienz des überarbeiteten Syntheseprotokolls zu aufzuzeigen.

Zweitens wird eine neuartige *One-pot*-Reaktion von Isocyaniden mit Sulfoxiden untersucht und deren Reaktionsparameter verbessert. Mehrere verschiedene Experimente werden durchgeführt, um ein tieferes Verständnis der Reaktion zu ermöglichen, nach deren Auswertung ein möglicher Mechanismus vorgeschlagen wird. Das Reaktionsprotokoll wird benutzt, um eine Bibliothek an Verbindungen sowie neuartige Monomere für die Polymerchemie herzustellen.

Im letzten Teil werden definierte, amphiphile, sternförmige Makromoleküle mittels des *Arm-first*-Ansatzes hergestellt. Die dafür benötigten Armmoleküle werden über einen linearen iterativen Reaktionszyklus synthetisiert, mit uniformem Octa(ethylenglykol) modifiziert und unter Einsatz der kupfer-katalysierten Azid-Alkin-Cycloaddition an eine Kerneinheit gebunden. Danach werden die erhaltenen Sternmoleküle in qualitativen Einkapselungsexperimenten eingesetzt, um mögliche Anwendungen als Phasen-Transfer-Katalysator oder als *Drug-Delivery*-System zu evaluieren.

III Abstract

The substance class of isocyanides was already discovered in the late 19th century. However, its broader application suffered due to their noxious smell and the limited procedures for their preparation. In the following century, several methods to synthesize these interesting compounds were published, yet they were mostly based on the application of hazardous chemicals, like phosphoryl trichloride or phosgene and its derivatives. Still, scientific research recognized and exploited the tremendous potential of isocyanides. This led to the establishment of isocyanide-based chemistry, featuring isocyanide-based multi-component reactions (IMCRs) as one of the most important areas. Applications were found in combinatorial and medicinal chemistry, as well as in the synthesis of defined and disperse macromolecules, which already hints at their highly versatile reactivity. Still, their potential is far from exhausted as novel applications and syntheses are regularly being developed. Modern approaches focus on changing the ecologic and economic impact of their hazardous and costly preparation, which has so far prevented their application in industrial use. The present work investigates the synthesis of isocyanides and extends their use in organic and macromolecular chemistry.

In the first part of the thesis, the synthesis of isocyanides is critically evaluated in terms of sustainability and thereafter improved to be environmentally more benign. Therefore, a set of sustainable solvents as well as less hazardous reagents are employed. Furthermore, a library of different isocyanides is synthesized to demonstrate the efficiency of the reworked protocol.

Secondly, a novel one-pot reaction featuring isocyanides and sulfoxides is investigated and its reaction parameters are improved. A mechanism is proposed and supported based on a variety of control experiments to gain further understanding of this novel reaction. The procedure is applied for the synthesis of a library of compounds and novel monomers for polymer chemistry.

Finally, defined, amphiphilic star-shaped macromolecules were synthesized *via* an arm-first approach. The respective arm molecules were obtained from a linear iterative growth strategy, modified with uniform octa(ethylene glycol) and coupled to a core moiety *via* copper-catalyzed azide-alkyne cycloaddition. The star molecules were then employed in qualitative encapsulation experiments to investigate potential applications in phase-transfer catalysis and drug-delivery.

IV Table of contents

Table of contents

1 Introduction

Mankind has been using (bio)polymers because of their natural abundance and special properties, mainly derived from their high molecular weight, for a long time.[1–7] However, starting from the 19th century, industrialization and scientific progress not only made processing of those resources much easier, but also enabled the synthesis of new manmade macromolecules. In the early 20th century, polymer chemistry was shaped by Hermann Staudinger as a new research area,[8–10] for which he was later awarded the Nobel Prize. Since then, different polymers (thermosets, thermoplastics, and elastomers) have been synthesized and found their way into our daily lives.[11]

As synthesis and corresponding processing of polymers significantly advanced over time, so did the control over the polymerization process itself, e.g. Ziegler-Natta-catalysts allowed for the production of linear high- and low-density polyethylene as well as stereo-controlled polypropylene.[12,13] Hence, dispersity of polymers has decreased over time, structures have become more precise and sophisticated, which has even lead to complex molecules like dendrimers and star-shaped polymers. However, where nature has been able to synthesize perfectly defined macromolecules in all different kinds of architectures for billions of years, e.g. observed in deoxyribonucleic acid (DNA) or proteins, synthetical alternatives fail to reach such perfection.[14,15] Even the most advanced techniques like ‘living’ polymerizations do not get close to the precision required for a perfectly defined macromolecule.[16–19]

Recently, however, the research area of synthetic *sequence-defined macromolecules*, which is inspired by nature’s precision engineering in chemistry, has seen rising interest and therefore increasing numbers of publications.[20,21] This field has its roots in Merrifield’s groundbreaking work on solid phase peptide synthesis in 1963, which allowed for the first man-made defined oligo-/polypeptides.[22] Contrary to standard polymers, which always come with a length and monomer distribution, their sequence-defined counterparts are perfectly determined in terms of monomer sequence as well as size uniformity, hence exhibiting no dispersity at all ($Đ = 1$).[21,23] In the past years, the synthesis and application possibilities of those defined macromolecules has advanced.[23–28] For the latter, molecular data storage and cryptography are often mentioned as potentials for future developments.[25,29–32]

Research on behavior and properties of these sequence-defined macromolecules has also gained a lot of interest. Commonly referred to as *structure-property-relationship*,

it focuses on new insights into the understanding and comparison of disperse and uniforms systems.[23,33] Furthermore, investigations aim to build structures, which allow for a defined three dimensional architecture based on their molecular sequence just like proteins.

Modern synthetic strategies mostly rely on linear and bidirectional approaches, as well as on so-called iterative exponential growth (IEG) methods.[34] In-solution approaches are often weighted against solid-supported protocols (**Chapter 2.4.1**). Hence, mostly linearly and bidirectionally synthesized oligomers are obtained in their corresponding processes. Also the synthesis of defined macrocycles is reported in the literature,[28,35] while more sophisticated architectures like star-shaped molecules have been avoided due to high costs in time and effort.

However, star-shaped macromolecules promise diverse applications,[36] one of the most important ones being drug delivery by encapsulation and subsequent targeted release of guest molecules.[37,38] In the present work, established synthetic methods toward uniform macromolecules are combined with the general idea of molecular architectures that allow encapsulation. Next, the focus is shifted on establishing new structure property-relations of the highly defined star-shaped structures.

2 Theoretical background

2.1 On the term *macromolecule*

The word *macromolecule* consists of two sub terms being macro- (large, in a large scale)[39] and molecule (a group of atoms that forms the smallest unit that a substance can be divided into without a change in its chemical nature).[40] Both meanings do not leave much room for interpretation, yet their combination does. Finding a consistent definition for *macromolecule* is not as easy as it seems. A quick look up in the *Duden – deutsche Rechtschreibung* states: “a molecule, which is built up by a thousand or more atoms”.[41] However, consulting the *Römpp – encyclopedia* further aspects to the definitions are added: First, it sets the lower boundary of molecular weight to roughly 10000 g/mol and states that molecular weight can reach into millions. Still, more importantly it enlarges the definition of *macromolecules* by adding a size-property relationship: the properties of a *macromolecule* do not change by addition or subtraction of a few atoms or atom groups. This statement makes the transition from *low molecular* to *high molecular* a property rather than a size requirement. Last, it is stated that a *polymer* nearly always comes with a distribution in size/mass instead of being a perfectly defined molecule.[42] Yet, exceptions like specialized *biomacromolecules* (for example enzymes or nucleic acids) are known,[43] and recent research has focused on synthetic defined *macromolecules*,[17,19,20,44] which make up the very foundation of this thesis. The term *macromolecule* itself goes back to Nobel laureate Hermann Staudinger, who shaped the field in the 1920s. Yet, in the first relevant publication on *polymer chemistry* he calls them *high molecular weight compounds*.[8,45] However, *macromolecules* are as old as life in the universe, as they make up important parts of every organism even the tiniest of them.[46,47] Therefore, any scientific discussion about *macromolecules* is inevitably bound to their natural origin.

2.2 Natural macromolecules

Natural macromolecules are versatile and come in a wide variety of sizes, structures and purposes. Common examples are polynucleotides,[48] proteins,[49] polysaccharides,[7] lignin,[3] but also polyhydrocarbons like in natural rubber.[50] If divided into only two particular categories, natural macromolecules either belong to the class of polymers with defined structure and molecular weight (sequence-defined, *i.e.* RNA, DNA, proteins) and polymers with a distribution in size (non-sequence-defined,

i.e. polysaccharides, lignin and polyhydrocarbons). A small selection of biomacromolecules and their properties are evaluated in the following sections (**Chapters 2.2.1** and **2.2.2**).

2.2.1 Ribonucleic acid and deoxyribonucleic acid

The most renowned biomacromolecules are ribonucleic acid (RNA) and deoxyribonucleic acid (DNA), as they represent the most important building blocks of a living organism.[14] These macromolecular compounds not only enable the complex mechanisms of evolution, but also resemble nature's analogue of today's silicon-based data storage (**Chapter 2.4.2**). However, it is rather quaternary instead of binary as it uses four base pairs. The DNA structure, which was first decrypted by F. H. C. Crick and J. D. Watson in 1953, consists of two separate molecular strains twisting into a double helix.[43] This ground-breaking discovery unveiled the characteristic pairing of pyrimidines (thymine and cytosine) and purines (adenine and guanine), resulting in a helical secondary and tertiary structure of the two strains (**Figure 1**).

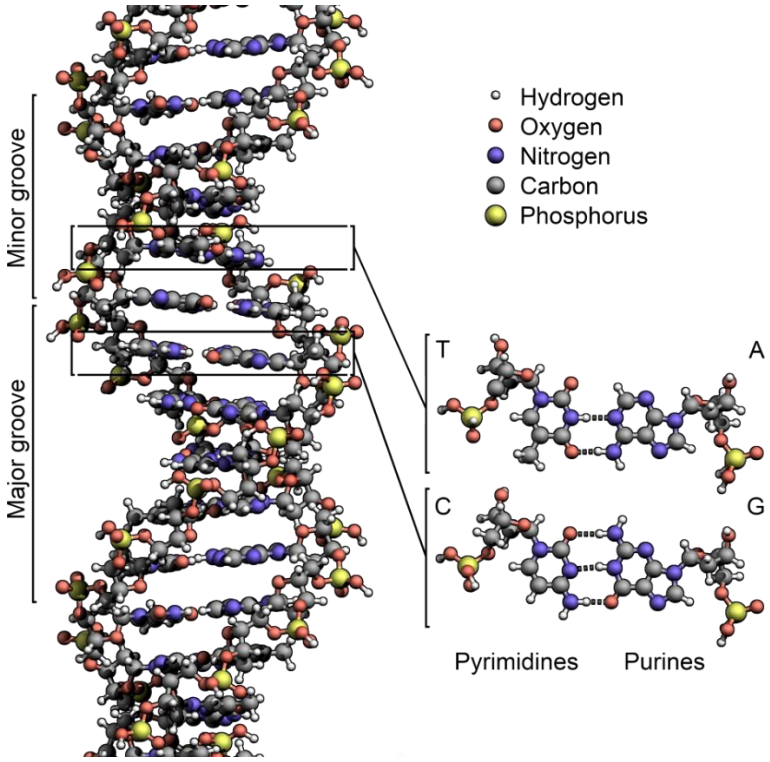

Figure 1: Left side: Double-helical structure of DNA. Right side: Characteristic base pairing of adenine and thymine as well as guanine and cytosine with respective hydrogen-bonding.[51] Reprinted with permission (Creative Commons).

Overall, the above mentioned nucleobases are essentially side chains of a sequence-defined phosphate-deoxyribose polymer.[14] Based on the variation of the nucleobase sequence, information is stored in the DNA strains. RNA, however, consists of only

one strain and is obtained by untwisting the double helix of DNA and replicating one strain. In contrast to DNA, the nucleobase uracil is used instead thymine and ribose is employed instead of deoxyribose. RNA is the actual molecule being read by enzymes to synthesize proteins based on their information, which is encrypted in their sequence of nucleobase sidechains. Therefore, specialized enzymes, which can read, decrypt and replicate RNA, are necessary. These also belong to the group of sequence-defined macromolecules called proteins.

2.2.2 Proteins and their structure-property-relationship

Proteins are, like DNA, macromolecular structures, but consist of amino acids rather than nucleobases. However, they also represent an essential requirement for life and are involved in nearly every biological process. Their presence is responsible for the respective function, metabolism and structure of each living cell.[49] For human beings, those proteinogenic building blocks consist of twenty-two amino acids, which are subdivided into twenty canonical and two non-canonical representatives.[52] The analysis of the respective monomeric units is not sufficient to understand the final structure of a protein, as the analysis of their intra- and intermolecular interaction is also necessary (**Figure 2**)

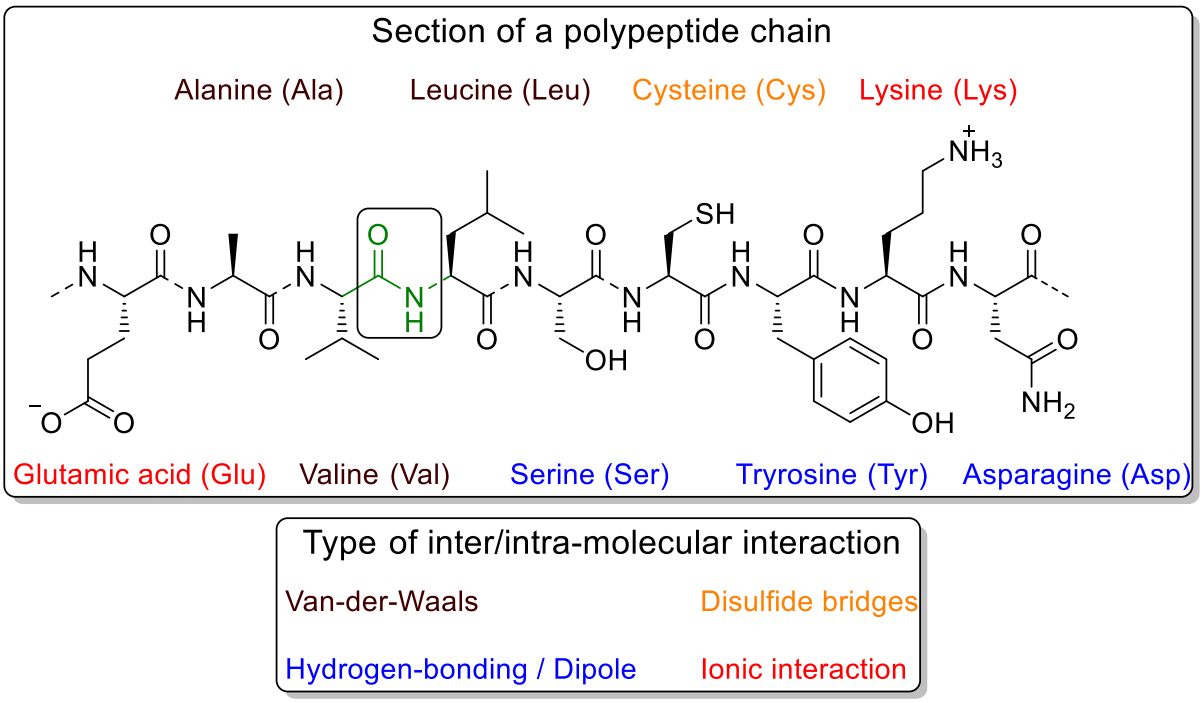

Figure 2: Section of a sequence-defined polypeptide chain: the basic framework of a protein. The respective *peptide bond* is highlighted in green. The broken lines show the connection of the different amino acids, whereas the color coding of the amino acid names shows their predominant inter/intra-molecular interaction. Note, that also the *peptide bond* itself is capable of hydrogen-bonding.

The order of amino acids within a protein is called *primary structure*.[53] Subsequently, the defined order and intramolecular interactions of amino acids in their *primary structure* shape the polypeptide into *β-sheets* or *α-helices*, called *secondary structure*.[49,53] When the chain reaches a certain size, two or more *secondary structures* are able to form into a *tertiary structure*. Finally, different polypeptide-chain-monomers agglomerate to oligomers, which form a *quaternary structure* describing the protein as its whole (**Figure 3**).[53] Countless proteins are currently known and each possesses its own defined order in which the monomers are sorted. In today's chemical terms, this property is called *sequence-defined*, as mass and order of the polypeptide are not random but are biosynthesized with exact precision in a function-orientated way. These molecularly defined chains are folded into a certain structure, which is inherent for fulfilling their natural purpose (e.g. enzymatic catalysis).[54] Altering the secondary structure by increasing the temperature, adding strong acids/bases or reacting the side chain moieties renders the protein useless. This process, which is called denaturation,[55] is a proof that the complex interactions of the polypeptide chains lead to a structure-property-relationship.[49] Therefore, deeper analysis of protein structuring is necessary to understand this sophisticated interaction, which leads to highly functionalized protein structures (DNA replication, enzyme synthesis, transport proteins, enzymatic catalysis).

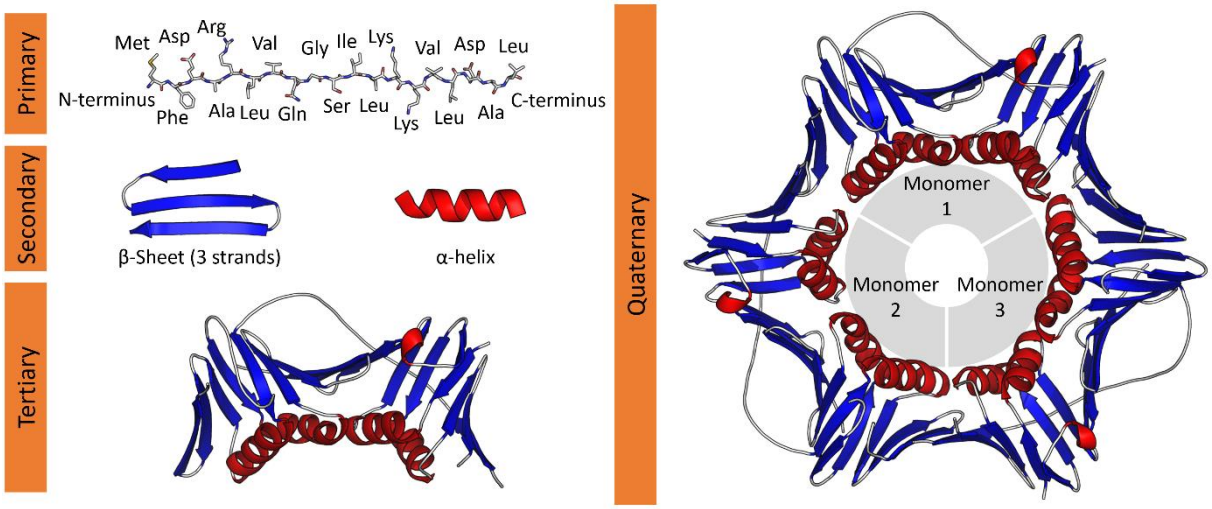

Figure 3: Left side: Primary, secondary, tertiary structure of proteins. Right side: Quaternary structure.[56] Reprinted with permission (Creative Commons).

Over the course of time, nature has developed and optimized its biosynthesis methods for defined structures like DNA and proteins that enabled the complex mechanisms of cellular life.[57] Yet, the focus to copy or imitate such highly ordered structures in the

field of polymer chemistry is a rather recent development in scientific research.[44] However, publications and advances on this topic have drastically increased over the last years, which highlights the interest in understanding and eventually exploiting structure-property relationships for further development and applications.[17,19,20,44] Therefore, a whole new topic of synthetic macromolecules evolved, namely, sequence control and finally sequence definition. These two concepts are explained more thoroughly in the **Chapters 2.4** and **2.5**.

2.3 Precision engineering tools in chemistry

In **Chapter 2.2**, natural macromolecules were discussed and roughly divided into two main classes: sequence-defined macromolecules like DNA or proteins and non-sequence-defined macromolecules like cellulose, lignin, and natural rubber. Processing of natural abundant polymers by mankind was followed by the development of new materials, which began in the 19th century and has since then shaped a whole era in human progress and still does. Our dependence as well as our benefits offered by those materials are the reason why the current era is often referred to as the *plastic age*. Science, however, did not stop at this point, and shaped a new field of research starting in the middle of the 20th century: the synthesis of precise macromolecular structures, which is strongly based on nature's architecture and step-wise synthesis found in the molecules of life.[22] Thus, sequence-control and sequence-definition came into focus of polymer science in the last few decades.[17–19,21,44,58] It is noteworthy that both terms are not used consistently in literature. Hence, it is necessary to define them, as they both are inevitably bound to this topic.

The term *sequence-controlled* is the generic term for a group of highly specialized macromolecules. Furthermore, it describes polymers with well-arranged blocks of different monomers, differing in their chain length. Therefore, every AB block-copolymer can be seen as a *sequence-controlled* polymer and as its name states, the property of the polymer is its degree of control in sequence and length, although both are never perfectly defined.[21,59] Thus, the dispersity $Đ$ of a *sequence-controlled* polymer is $Đ \geq 1$. In contrast, a *sequence-defined* macromolecule must have a dispersity of one ($Đ = 1$) and the order and position of each and every monomer unit must be strictly determined, thus it is a perfectly defined molecule. Concluding, *sequence-defined* macromolecules are a subgroup within this class of *sequence-controlled* polymers, in which the degree of control/definition is at its maximum. Besides the certain chain length and sequence the term *sequence-defined* can be

extended and is often applied to each subunit/monomer of the macromolecule, meaning also precise tailoring of tacticity and chirality of the monomer units (**Figure 4**).[21,58] The latter has not been achieved yet.

Sequence-defined macromolecules can, as discussed in the last paragraph, also be named as *sequence-controlled* polymers, but they always have to have a dispersity of $Đ = 1$. When a sequence-defined macromolecule is built up from a variety of different monomers, the position of each monomer within the chain is known, as well as the exact molecular weight (**Figure 4**).[20,21] It is noted that the term *sequence-defined polymer* is intrinsically misleading, as a sequence-defined polymer is uniform, a polymer however comes always with a distribution in size. Thus, those two terms contradict each other and are therefore omitted as compositum in this thesis. Instead, the more neutral word *macromolecule* is used, as it covers both the uniform and non-uniform species.

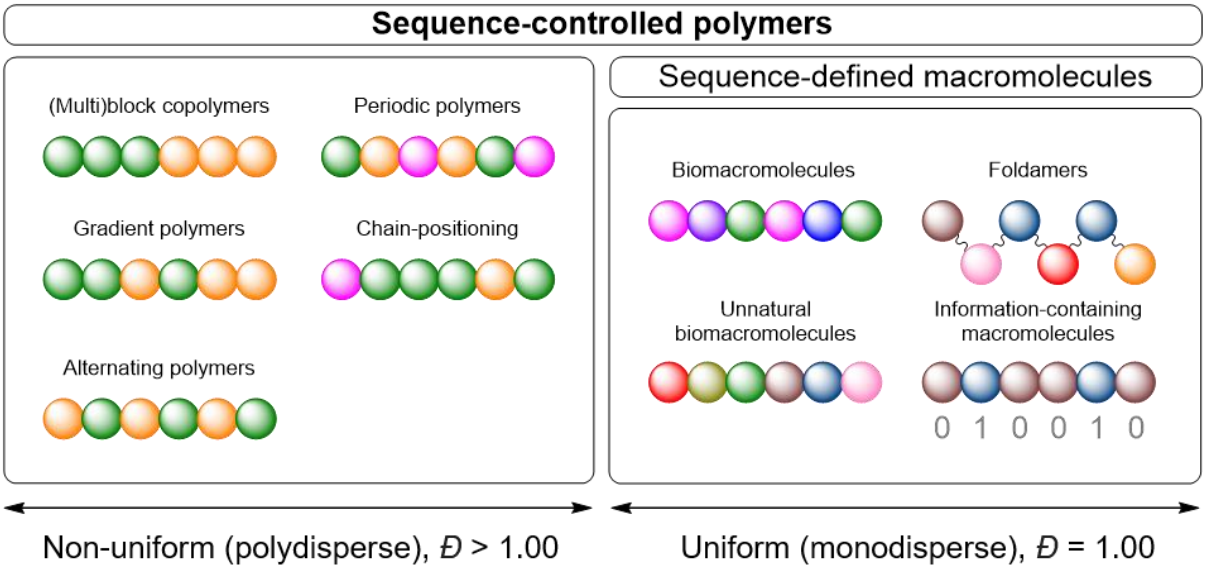

Figure 4: Representation of the polymer class of sequence-controlled polymers ($Đ > 1$, yet some degree in its sequence) and its subgroup sequence-defined macromolecules ($Đ = 1$, absolute control of sequence). Each colored dot represents one monomer unit. Adapted from [21].

Another way to differentiate between those two classes apart from the dispersity $Đ$ is their path of synthesis. *Sequence-controlled* polymers are nearly always synthesized in a *sophisticated* polymerization reaction often using unique catalysts or specialized AB-monomers for higher degree of control. Associated publications feature the synthesis of *sequence-controlled* polymers *via* polyaddition, polycondensation, as well as the whole spectrum of ‘living’ polymerizations, like reversible addition-fragmentation

chain transfer (RAFT) polymerization, nitroxide-mediated polymerization (NMP), ring-opening metathesis polymerization (ROMP) and atom transfer radical polymerization (ATRP).[18,19,60]

On the other hand, *sequence-defined* macromolecules cannot be synthesized in this way, as even the most controllable polymerization reactions, like 'living' polymerizations yield polymers with a *Đ* higher than unity. Thus, sequence-defined macromolecules can only be obtained by iterative and/or stepwise syntheses, which are combined with purification steps in-between, making them far more time-consuming and resource-costly than just *sequence-controlled* polymers.[21,23,26,61] An in-detail definition and general strategies of synthesis approaches as well as recent progress and their application are explained in detail in **Chapter 2.4**.

However, nature's precision in designing macromolecules remains unchallenged and will most likely never be matched by humankind. Two common examples for its well-defined and application-oriented expertise are DNA/RNA – *the* natural data storage system, which was already discussed in **Chapter 2.2.1**, and hemoglobin – an iron-containing metalloprotein, which transports oxygen and carbon-dioxide and is found in red blood cells of vertebrates. Both underline the basic thought behind sequence-definition: The so-called structure-property relationship. Perfectly defined structure enables a certain function (data encoding in DNA, oxygen transport in the hemoglobin) which could not be achieved to such an extent by a polydisperse polymer.[14,62]

2.3.1 Ideal synthesis

Still, even though nature has developed and perfected its synthetic routes to sequence-defined macromolecules over the course of time, mistakes are prone to happen, leading to different outcomes depending on what errors were made. A worst-case scenario is a single monomer (*i.e.* amino acid) mistake that renders the function obsolete, for example sickle cell disease, which not only reduces the efficiency of oxygen transport in affected erythrocytes but also increases the probability of blood clotting.[63] Furthermore, spontaneous mutations can arise, which can be beneficial, unproblematic or malicious. In some cases, small deviations from the aimed macromolecule are desired like in the replication of the RNA of a virus which is quite often replicated with minor deviations but is used as basic survival strategies of their class (e.g. flu-virus, human immunodeficiency virus (HIV), *etc.*).[46] On the other hand, the shift of the original brown eye color of a Homo Sapiens in a wider variety, which

also features blue and green can be considered a unproblematic mutation.[64,65] Finally, an exemplary malicious mutation alters the cell-growth and disables apoptosis, which can ultimately lead to cancer.[66] This small summary leads to the statement that “no synthesis is without error”. Thus, evolution has found its way to either exterminate or at least reduce those mutations. Not a single organism, but evolution can of course benefit from them. Transferring the above-mentioned to sequence-definition in chemistry, suitable approaches should fulfill the same criteria of an *ideal synthesis* – a hypothetic term or rather a principal, which is well known in *Green/Sustainable Chemistry*.[67,68] Thus, a high control over the synthesis and the possibility to eliminate errors by purification should be ensured. Both properties are elementary for a approach leading to sequence-definition.[21]

Possible features of such a synthesis are displayed in **Figure 5** and divided into two main groups: preparatively and sustainably ideal. Note, that the division is not fixed as for some both categories would suffice.

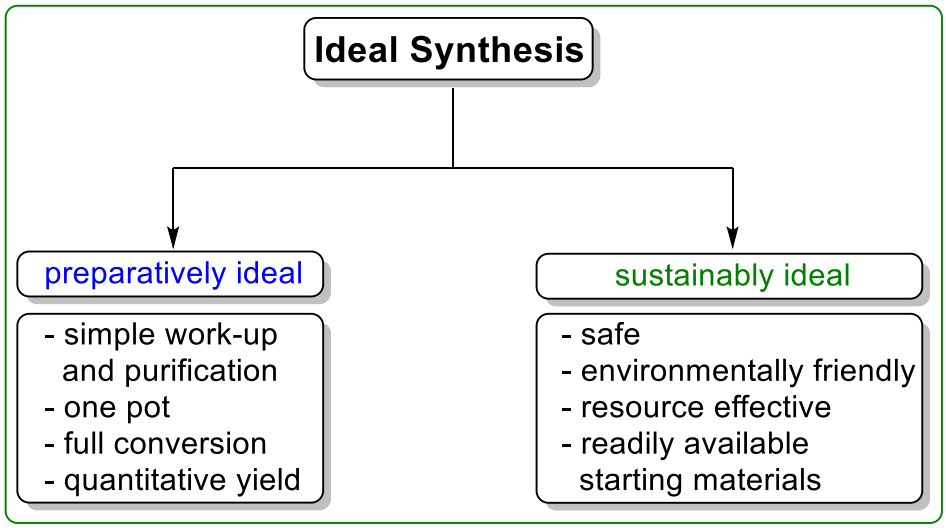

Figure 5: Possible features of an *ideal synthesis* split into two subcategories for increased clarity. Adapted from [67,68].

Ideal synthesis can be described as a chemical utopia, as it can never be achieved. Concurrently, it enables the drive to reach those noble goals. However, sustainability cannot be considered as a static ideal. Much more, it is dynamic and responds and adapts as progress is made and is a relative measure – maybe the tower of babel can serve as allegory: no matter how many stories are built, the sky is never to be reached. Yet, it is of great importance to apply those ideals to each synthesis carried out. Precision engineering of macromolecules, like in sequence-definition, benefits greatly and is only possible by holding onto those values.

It has already been established that sequence-defined macromolecules are synthesized utilizing stepwise procedures that either involve orthogonal protecting groups or at least orthogonal reactions (**Chapter 2.5**). Therefore, their synthesis always consists of multiple steps, which underlines the importance of high conversion and high yields: a yield of 90% is commonly considered excellent in laboratory scale chemistry (this does not count for industrial processes, in which yield equals profit/loss), however iterating this synthesis just five times in a row totals in an overall yield of only 59%. Respectively, a consistent 95% or 99% of yield total in 77% and 95% after five consecutive steps, respectively, which underlines the outmost importance of high conversion and high yields in sequence-defined chemistry. Furthermore, readily available starting materials and resource effectiveness lower the price and also the ecological footprint of the reaction – a goal which is always to be considered. Applying safe and environmentally friendly chemicals and benign reaction conditions are getting increased attention in recent publications and in general, as science bares the responsibility to develop a more sustainable future.[69–73] However, replacing toxic chemicals is not always possible yet should always be considered. Cost-benefit-ratio sometimes demands the application of less favorable chemicals and processes, but advantages and disadvantages are to be carefully weighed against each other to find optimal conditions in a given frame. Likewise, simple reaction set-ups as well as easy work-up and purification are a necessity in sequence-definition. Especially multi-component reactions (MCRs) have gained value as a robust and reliable working horse for monodisperse macromolecules, but are also applied in polyaddition-polymerizations and in combinatorial chemistry as they often combine simplistic set-ups with straight-forward purification.[26,35,74–76] A short overview about their history and applications besides sequence-definition is given in **Chapter 2.3.3**. Furthermore, the Passerini-3-component reaction (P-3CR), which was applied for the oligomer synthesis in this thesis, is discussed in detail (**Chapter 2.3.4**). Next to multi-component chemistry, other synthetic procedures have proven their reliability and simplicity. Noteworthy is the azide-alkyne-Huisgen cycloaddition (CuAAC), which quickly rose to attention after its initial discovery by German chemist Rolf Huisgen in the late 20th century.[77] Since then, hundreds of reviews and publications have featured this cycloaddition and have defined and shaped a whole field of science: the so-called ‘click’-chemistry.[78–80] This reaction was also applied in the featured synthesis of uniform star-block-co-macromolecules and is discussed in **Chapter 2.3.6**.

2.3.2 Isocyanides

As the attention in the next chapter is focused on isocyanide-based multi-component reactions (IMCR), key compounds throughout this thesis, a previous introduction to this versatile substance class is important. Isocyanides, which is their given name by IUPAC, are sometimes also called isonitriles (outdated), were initially discovered by Lieke in 1859, who reacted allyl iodide with silver cyanide to form allyl cyanide.[81] However, the silver ion masked the cyanide, only allowing an nucleophilic attack of the nitrogen, which rather resulted in allyl isocyanide or an inseparable mixture of both. Additionally, he found one of the most characteristic properties of isocyanides, especially the volatile ones, their rather noxious odor:

"*Es besitzt einen penetranten, höchst unangenehmen Geruch; das Öffnen eines Gefäßes mit Cyanallyl reicht hin, die Luft eines Zimmers mehrere Tage lang zu verpesten, weshalb alle Arbeiten mit demselben im Freien vorgenommen werden müssen*."[81]

"It possesses a pungent, highly unpleasant odor; opening a vial containing allyl cyanide is sufficient to contaminate the air in a room for several days, hence working with this substance is only possible outdoors."

Note that the pungent odor of the mentioned *allyl cyanide* mainly originated from the isocyanide impurity within and not the actual cyanide.

Indeed, even Ivar Ugi, who discovered the Ugi-4-component reaction (U-4CR), another IMCR, in 1962 and developed a simpler reaction route to isocyanides, stated that the further exploitation of isocyanide chemistry was delayed by their terrible smell.[82–84] There are however exceptions,[85] and non-volatile isocyanides are intrinsically easier to handle without extreme precautions. In **Scheme 5**, common isocyanide syntheses are displayed in their chronological order. [81,86–90]

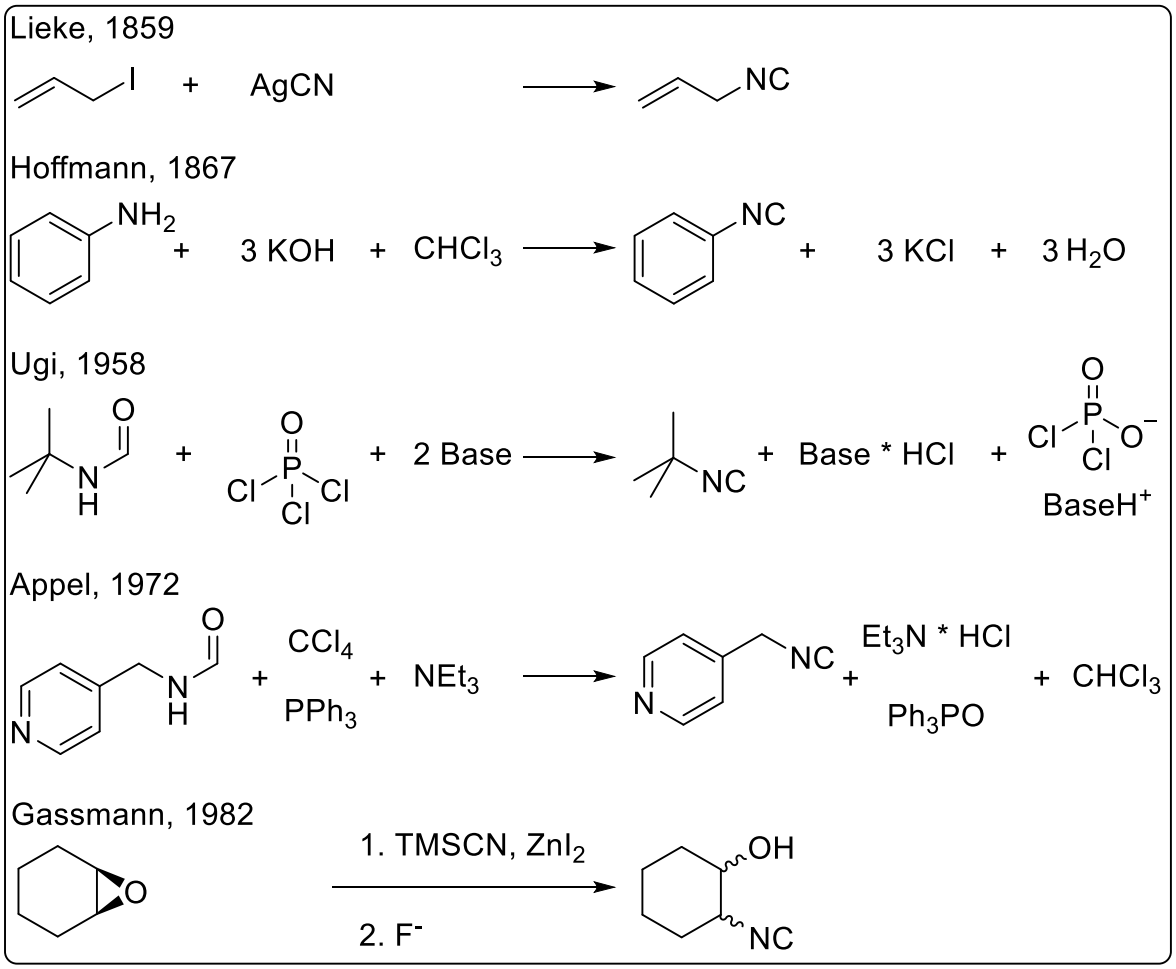

Scheme 1: Common isocyanide syntheses in chronological order.[81,86–90] Today, mostly the Ugi-approach is applied, with phosphoryl trichloride as dehydrating agent.[26,91–95]

Hoffmann discovered the first applicable synthesis, which featured the direct reaction of amines with dichlorocarbene, prepared by an *in situ* reaction of chloroform with potassium hydroxide. Yet, the number of isocyanides, prepared *via* this or any fashion, reported in the literature until 1950 was low:

“For a whole century only twelve not yet easily available isocyanides had been prepared, and since the then known isocyanides smelled very unpleasantly, their chemistry was only moderately investigated.”[84]

Their first synthetic application was the Passerini-3-component reaction (P-3CR), which was published in 1921 by Mario Passerini (**Chapter 2.3.4**).[74] Then, in 1950, xantocillin was isolated from *Penicillium notatum* and has remained one of few natural products bearing isocyanide groups,[96–98] the latter being the reason, why isocyanide smell is hardly categorizable: a natural connection is often necessary (e.g. rotten fish for amines), which is missing for isocyanides. Nonetheless, Ivar Ugi provided a simpler reaction path toward isocyanides by dehydrating *N*-formamides, which, together with

the contemporary discovery of the Ugi-4-component reaction (U-4CR) resulted in an increasing interest in these compounds.[82,83,87] Today, phosphoryl trichloride ($POCl_3$) is reported most frequently in scientific publications to synthesize isocyanides by dehydrating the respective *N*-formamides. [26,91–95] However, the isocyanide synthesis opposes the principal goals of sustainability. As a reagent is necessary to dehydrate the *N*-formamide as well as two equivalents of base are needed in the Ugi-approach, the atom economy is rather poor (**Scheme 1**). Furthermore, toxic reagents and solvents ($POCl_3$, dichloromethane and triethyl amine) are applied in the synthesis, rendering the reaction non-sustainable. The generally accepted mechanism of the isocyanide dehydration is shown in **Scheme 2** and proceeds *via* a nucleophilic attack of the formamide-oxygen at the electro-/oxyphilic center of the dehydrating agent (**a**). Next, the base deprotonates the amide forming an imidate adduct (**b**), which is then protonated by the ammonium salt (**c**). Subsequently, the intermediate undergoes an α-elimination in which the formamide proton and the phosphor species are eliminated (**d**). The $POCl_3$ is an example for a typical dehydration agents but as also *p*-toluenesulfonyl chloride (*p*-TsCl), (di-, tri-)phosgene or the *Burgess reagent* are used to dehydrate *N*-formamides in a similar mechanism.[68,99–101]

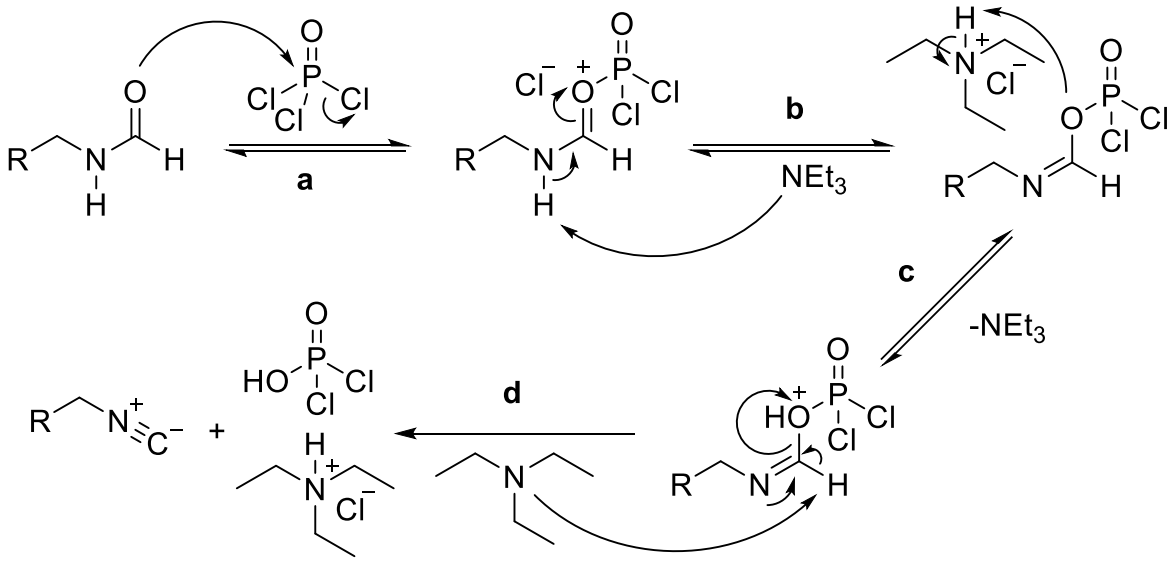

Scheme 2: Proposed mechanism of the isocyanide dehydration.[87,102] Next to $POCl_3$ also *p*-TsCl, (di-, tri-)phosgene or the *Burgess reagent* can be employed as dehydrating agent.[68,99–101]

In early 2020, an environmentally more benign approach was reported by the author of this thesis (**Scheme 3**), which uses *p*-TsCl, a waste product in the commercial saccharin production, as dehydrating agent.[103]

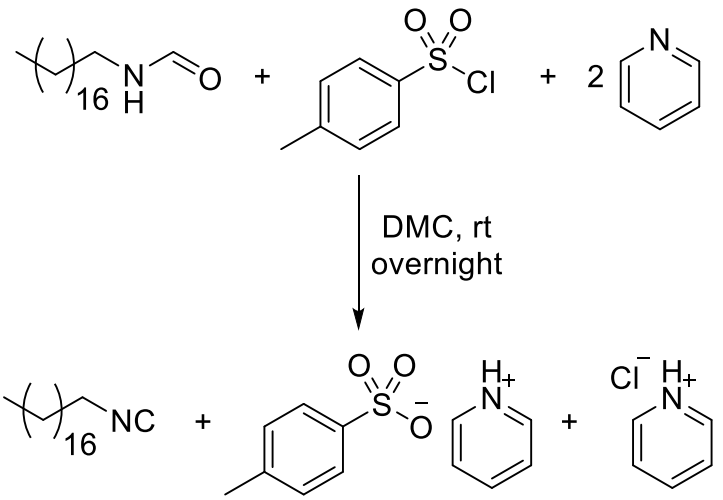

Scheme 3: More sustainable approach to aliphatic isocyanides utilizing *p*-TsCl, which is a waste product in the commercial saccharin production, thus readily available and also non-toxic.[103]

Recently, Dömling *et. al.* published a time- and resource-effective procedure toward an exceptional variety of different isocyanide compounds.[104] This method increased the overall sustainability of the Ugi-approach, since some criteria of combinatorial chemistry (e.g. feasible and fast reaction, easy and fast purification) meet also the expectations of Green Chemistry.

Before continuing with the main application of isocyanides, the IMCRs, their general properties are explained, as they are unique to this substance class and resemble the driving force of IMCRs.

Lieke was most likely unaware of the structural nature of the allyl isocyanide, which he accidently synthesized, as it was Gautier, who evaluated the isomeric relationship between organic cyanides and isocyanides in 1867.[84] Later, the electronic and orbital properties of isocyanides were evaluated in detail and have shown to be isoelectronic to carbon monoxide, thus explaining why also isocyanides are suitable ligands in metal-organic complex chemistry.[84] Chemically, the isocyanide carbon is capable of reacting as a nucleophile as well as an electrophile. Contrary, cyanides are attacked by electrophiles at the nitrogen atom, and by nucleophiles at the carbon center.[68]

Furthermore, isocyanides feature α-acidity, which can be further increased by electron-withdrawing groups. They are prone to hydrolysis in acidic (aqueous) environments, which reconverts them to their respective *N*-formamides or amines. Applying Lewis

acid catalysis, they are converted to poly(iminomethylene)s. In basic media, however, isocyanides are quite stable.[68]

Yet, their unique reaction with both electrophiles and nucleophiles (α-addition) can be considered their most important feature. It promotes isocyanides to a highly versatile tool in organic synthesis allowing for metal-catalyzed insertions,[105–108] the Van Leusen reactions,[109] interactions with a wide variety of different functional groups as well as their application in multi-component reactions (MCR polymerizations included).[68,74,76,82,110–115] The latter are discussed in the following chapter. First, however, a short outlook on novel isocyanide-based syntheses is given as these are also within the scope of this thesis.

Recently, isocyanides were employed toward the synthesis of thiocarbamates,[116–119] which generally require phosgene, a hazardous and highly toxic substance (**Scheme 4**). Thiocarbamates are often biologically active and serve for a variety of applications. For example, they are employed as antivirals, antifertility agents as well as pesticides and herbicides (Thiobencarb, Orbencarb, and Molinate).[116] In 2016 Maes *et al.* published a procedure employing isocyanides, thiosulfonates and non-hazardous sodium iodide as catalyst to access thiocarbamates. The sulfinate side product can, in principle, even be reconverted to a thiosulfonate by sulfenylation or from disulfides by selective oxidation.[116] In 2018, Sun and coworkers introduced another pathway toward thiocarbamates starting from differently substituted *tert*-butyl sulfoxide, which was thermolyzed in toluene to give a sulfenic acid as highly reactive intermediate. Subsequent reaction with one equivalent of isocyanide and water yielded thiocarbamates in moderate to high yields.[117] In the same year, a photochemical approach was published. Herein, thiols were reacted with isocyanides and water as co-solvent and oxygen source.[118] Rather recently, Wei Wei and coworkers showed that also sulfinates can be reacted with isocyanides to form thiocarbamates, when energy supply is sufficient and catalytic amounts of iodine and water are present.[119] Most of these synthesis are described as more sustainable by their authors, yet one crucial factor remains neglected: the synthesis of isocyanides, as already described above, employs phosphoryl trichloride or even more hazardous chemicals like phosgene as well as di- and triphosgene. Hence, the synthesis leaves room for improvement regarding overall sustainability, a topic, which is targeted in the **Chapters 4.1** and **4.2** together with the alternative isocyanide synthesis discussed previously.[103]

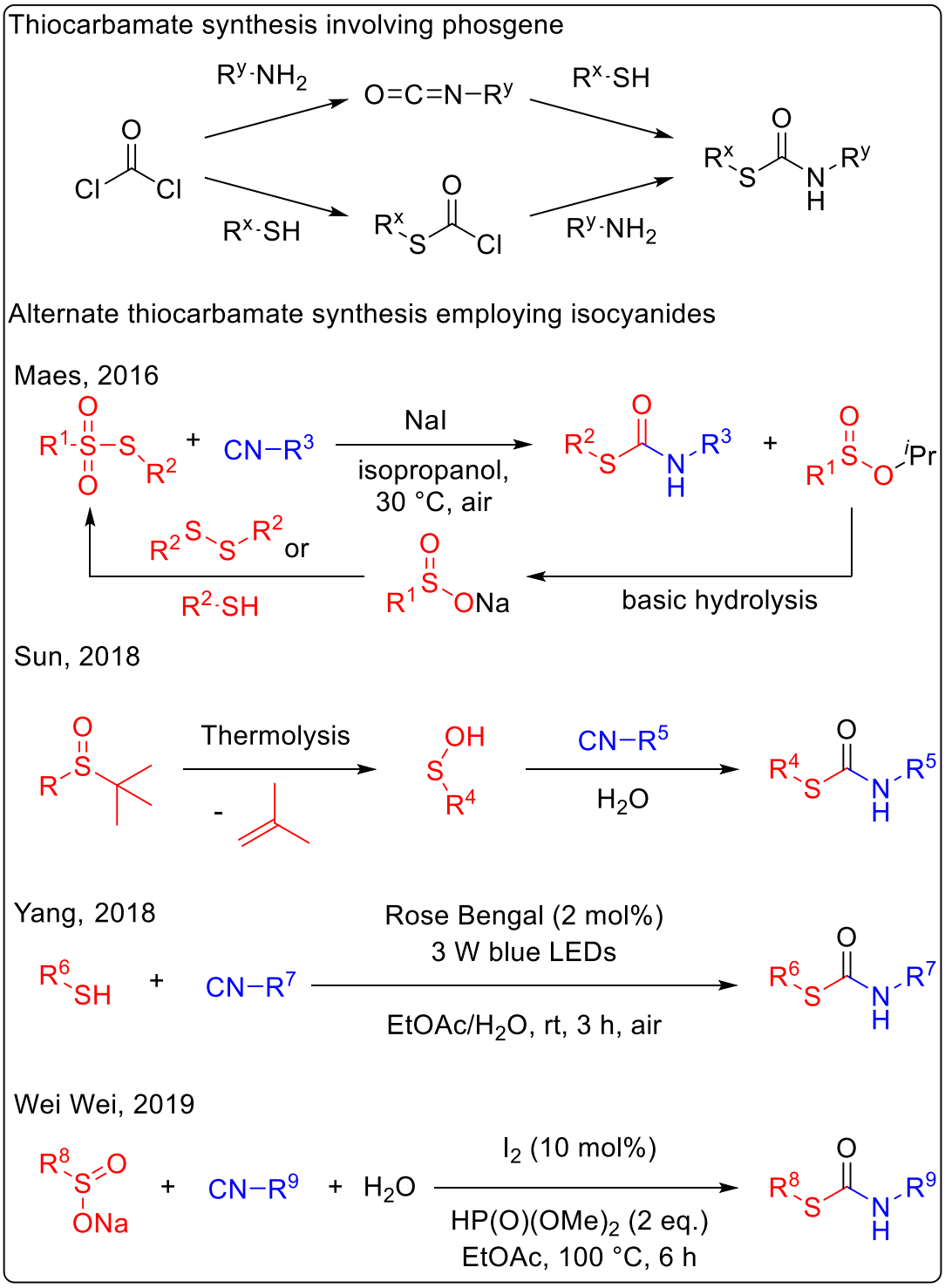

Scheme 4: Top: Industrial synthesis of thiocarbamates involving phosgene and toxic intermediates. Bottom: Four alternative routes toward thiocarbamates, which utilize isocyanides instead.[116–119]

However, reconsidering the main use of isocyanides: isocyanide-based multi component reactions, these and also non-isocyanide-based ones are now evaluated regarding their history, synthetic details and applications in the following chapter.

2.3.3 Multi-component-reactions

The discovery of MCRs began in 1850, when Adolph Strecker published the Strecker amino acid synthesis,[120] making them contemporary to the first vulcanization (start of the synthetic polymer age, Goodyear, 1840) and the discovery of isocyanides (Lieke, 1859). Yet, it took sixty years to connect isocyanides and MCRs (Passerini, 1921),[74] and another ninety years to broadly apply MCRs in polymer chemistry (Meier, 2011).[121,122] By definition, a multi-component reaction involves at least three different reactants, which either react simultaneously or in a cascade of reactions (some mechanisms will be discussed in this chapter)[68,123] and as a result, most of the atoms of the starting materials are incorporated in the product. Thus, a high atom economy of up to 100% is characteristic for MCRs. Often, the mechanism involves a condensation giving a small molecule as a side-product such as water in the U-4CR. Apart from excellent atom economy, MCRs often differ from common syntheses by several features related to the previously discussed *ideal synthesis*: high conversions, high yields, readily available starting materials and low synthetic effort. The latter is underlined by their robustness as typically no dry solvents are necessary, impurities do not significantly alter the outcome, or inert gas is seldomly applied). Moreover, they often feature simple one-pot protocols. Hence, rather complex structures can be achieved by relatively few operating steps, omitting the time-consuming isolation of intermediates, which is one of their greatest benefits compared to multistep synthesis. Especially in combinatorial chemistry toward drug syntheses and discovery, MCRs are an invaluable tool (**Scheme 5**).[68,110,124,125] As an example, the commercial two step synthesis of lidocaine is weighted against its one-pot synthesis *via* a U-3CR. Also, the U-4CR has been employed in the synthesis of indinavir (Crixivan®), which was used to treat the HIV and the resulting acquired immune deficiency syndrome (AIDS).

a) Two-step synthesis of **Lidocaine**

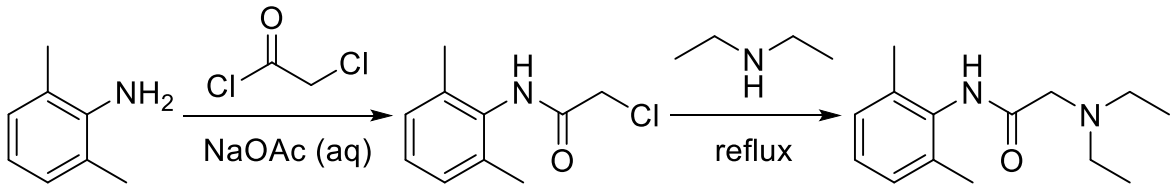

b) One-pot reaction of **Lidocaine** utilizing an Ugi-3CR

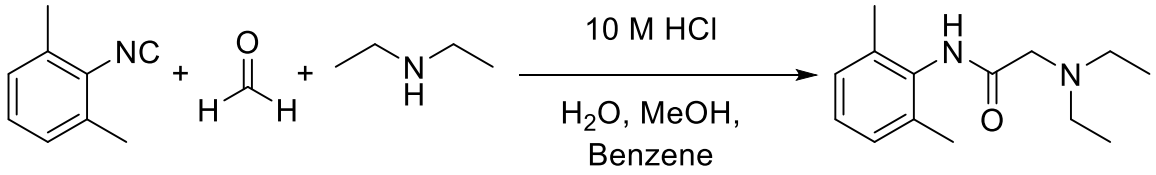

c) Synthesis of **Crixivan®** **(MD 639)** involving an Ugi-4CR

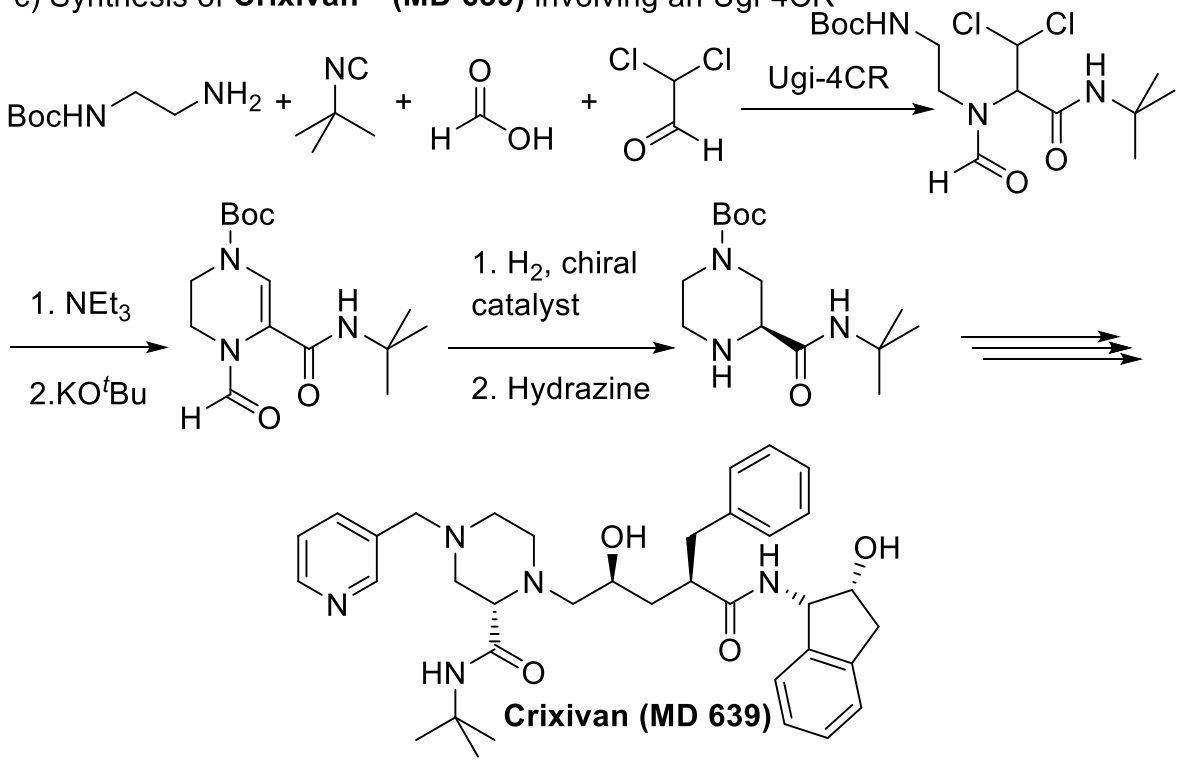

Scheme 5: a) Comparison between the two-step and one-pot synthesis of the local anesthetic lidocaine. b) Schematic synthesis of indinavir (Crixivan®, produced by Merck), which was used to treat HIV/AIDS in which a key intermediate is synthesized by an U-4CR.[124,125]

However, as they use multiple reactants, which are often transformed in a cascade of reaction steps, more insight in their mechanistical advance is necessary to understand their preparative benefits. Generally, chemical reactions follow the basic rules of a dynamic equilibrium, which was first described by Henry Louis Le Chatelier at the end of the 19th century and is either known as *Le Chatelier's principle* or *The Equilibrium Law*. The dynamic nature of chemical reactions is of great importance to characterize

MCRs and allows to categorize them into three distinct types (**Scheme 6**). Reaction type I solely consists of reversible reactions, significantly decreasing its value for preparative chemistry: theoretical yields between 0 and 100% are possible, yet a mixture of reactants, intermediates as well as product is far more likely. Additionally, incomplete conversion fosters side-reactions, which further increases the difficulty of product isolation.

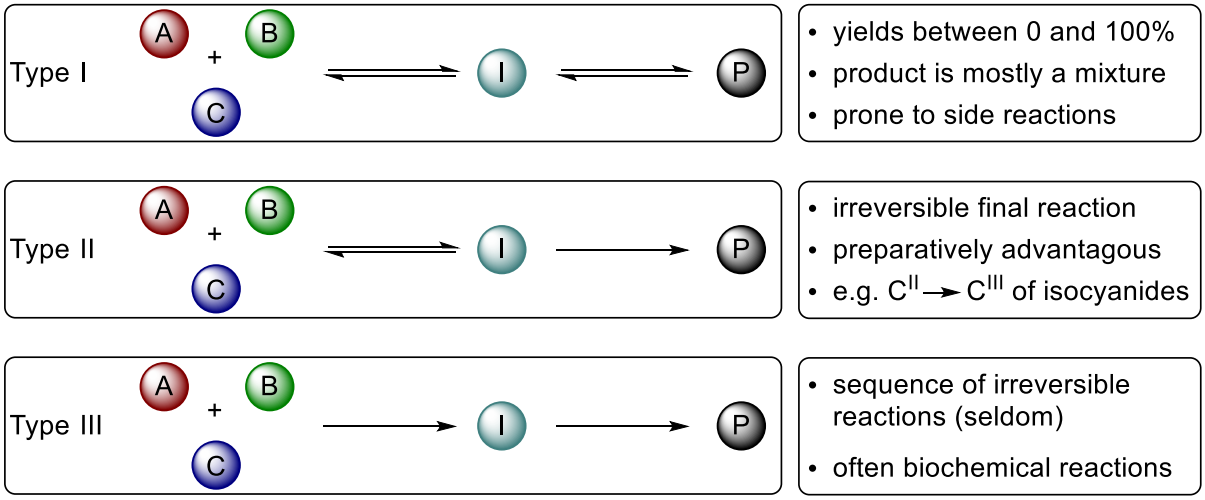

Scheme 6: The three basic types of MCRs and their features. Adapted from [68].

Type II also involves reversible elementary reaction steps, which proceed *via* intermediates, yet the final reaction step is irreversible. Therefore, the equilibrium is generally shifted to the product. A common example is the strongly exothermic oxidation of the isocyanide C^{II} to a C^{III} in the P-3CR and U-4CR. In general, every step that leads to the formation of a thermodynamically highly stable compound is suitable, therefore ring-closure or aromatization can serve as such steps. Most MCRs, which are of preparative value, belong to this type. Type III solely consist of irreversible steps yet occurs seldomly in preparative chemistry but is often seen in biochemical reactions, for example reactant transformation *via* enzymatic catalysis. It is noted that this is a schematic overview meant for simplification. Often an exact assignment is not possible.

The first reported MCR, the Strecker synthesis, involves an aldehyde or ketone, which is reacted with ammonia and hydrocyanic acid in a 3-component condensation reaction, thus, justifying its MCR character. Subsequent hydrolyzation yields the respective racemic amino acid (**Scheme 7**). In the first step, an iminium ion is formed *via* the reaction of an aldehyde and ammonia. Subsequently, the cyanide starts a nucleophilic attack on the intermediate to form an α-aminonitrile, the irreversible step

of this MCR. The final product is a racemic mixture of the amino acid, which is obtained by hydrolyzing the corresponding aminonitrile.[120]

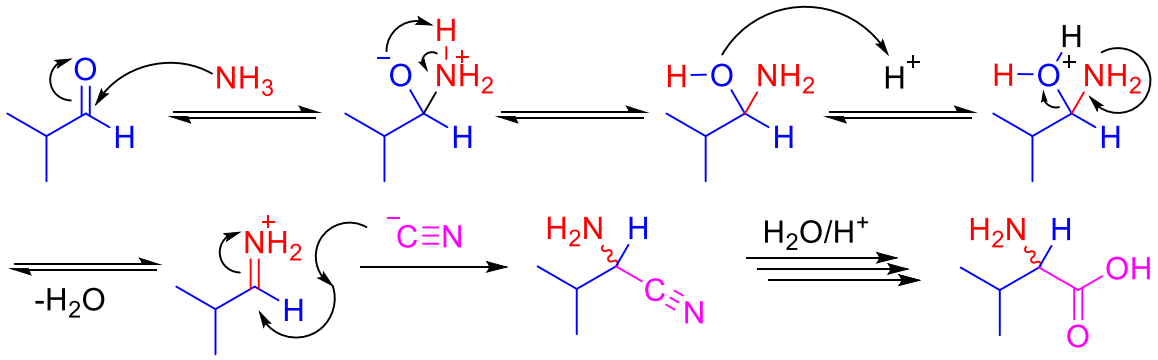

Scheme 7: Strecker synthesis utilizing isopropyl aldehyde (blue). The reaction proceeds *via* imine formation with ammonia (red) and subsequent nucleophilic attack of the cyanide (pink). The final product is a racemic mixture of the amino acid valine, which is obtained by hydrolyzing the corresponding aminonitrile.[120]

Asymmetric variations of the Strecker synthesis are nowadays known. They either involve asymmetric catalysts or asymmetric auxiliaries and thus allow both laboratory and industrial synthesis of pure L-amino acids or their non-natural enantiomeric analogs.[126–130]

An example of a MCR involving an ring-closure as final irreversible step and the possibility of a subsequent aromatization is the Hantzsch 1,4-dihydropyridine synthesis, which was reported in 1881 by Arthur Rudolf Hantzsch,[131] making it the second reported MCR after the Strecker amino acid synthesis.

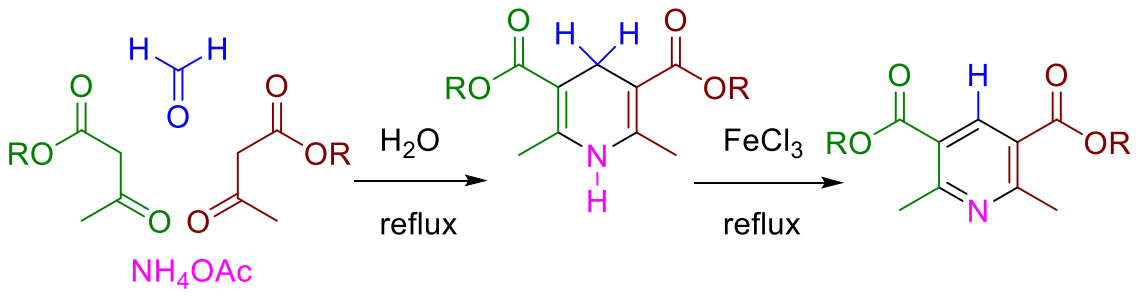

Scheme 8: Hantzsch 1,4-dihydropyridine synthesis. The initial condensation reaction of two β-keto esters (green and brown), ammonium acetate (pink) and an aldehyde (blue) yields a dihydropyridine, which subsequently can be oxidized to yield the respective pyridine derivative often under decarboxylating conditions.[131]

The reaction involved formaldehyde, two equivalents of a β-keto ester and a nitrogen donor, e.g. ammonia or an ammonium salt (**Scheme 8**). In this case, ammonium acetate and formaldehyde react with one equivalent of β-keto ester each to form an

enamine and an unsaturated carbonyl compound, respectively. Both intermediate compounds condense yielding the 1,4-dihydropyridine, which can be oxidized to form the pyridine derivative (Hantzsch pyridine synthesis).[131] Recent studies have shown that the reaction can be carried out in a one-pot synthesis in water with direct aromatization by either ferric chloride, manganese dioxide or even potassium permanganate, further underlining its multi-component character.[132] Besides the countless pyridine derivatives that can be synthesized by applying this strategy, also dihydropyridines find their application – for example Nifepidine (**Scheme 9**), which is used to treat angina, high blood pressure, Raynaud's phenomenon, suppression of preterm labor and acute myocardial infarction, again underlining the value of MCRs in drug synthesis.[133]

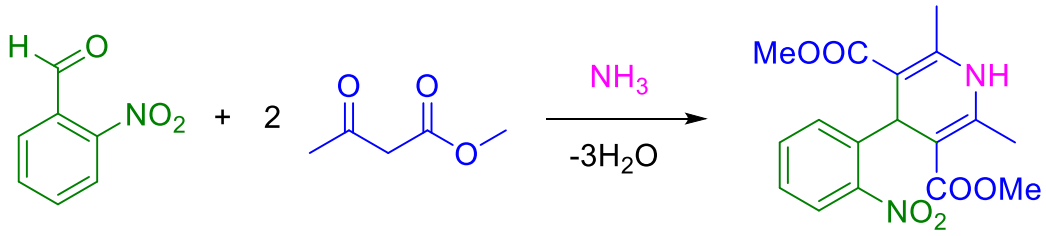

Scheme 9: Synthesis of Nifepidine involving 2-nitrobenzaldehyde, methyl acetoacetate and ammonia, which are reacted in a Hantzsch dihydropyridine synthesis, omitting the final aromatization step toward the pyridine species.[134]

Other strategies even involve solid-phase approaches toward the combinatorial synthesis of those heterocycles.[135] As 1,4-dihydropyridines are known for their use as calcium antagonists, further trials in medicinal use were conducted,[136,137] while they were recently also investigated for chemotherapeutic activities.[138]

In 1891, Pietro Biginelli enlarged the repertoire of β-keto ester-involving MCRs. The so-called Biginelli reaction utilizes a β-keto ester, which is reacted with an aryl aldehyde and a urea forming 3,4-dihydropyrimid-2(1*H*)-ones. Here, no increase in thermodynamic stability by aromatization can take place, yet the ring closure acts as the irreversible step (**Scheme 10**).[139,140]

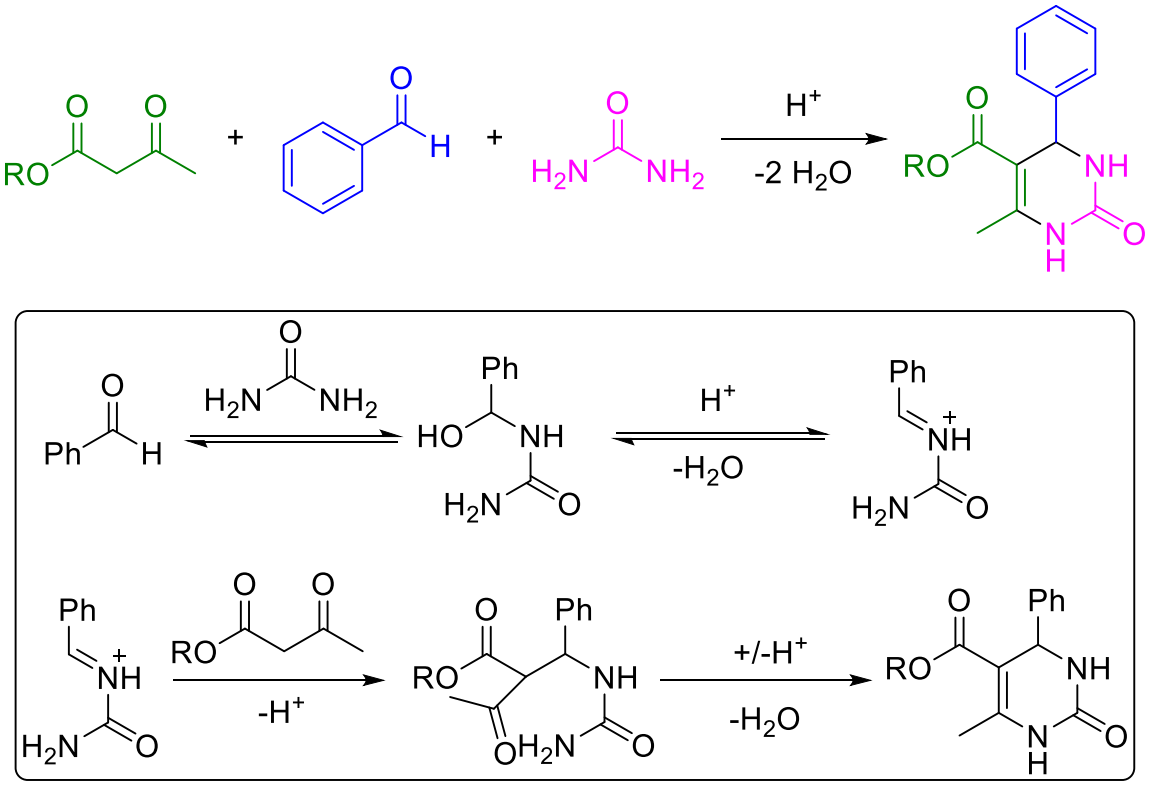

Scheme 10: Top: Example of the Biginelli reaction: the reaction of an aryl aldehyde (blue), urea (pink) and a β-keto ester (green) yields a 3,4-dihydropyrimidin-2(1*H*)-one and two equivalents of water as condensation products.[139,140] Bottom: Accepted mechanism proposed by Kappe in 1997.[141]

In a first reaction step, the aryl aldehyde adds to the urea forming an α-hydroxyalkyl urea. After acidic activation and cleavage of one equivalent of water the intermediate reacts with the β-keto ester. A final ring-closing condensation yields the desired product.[141] Like the dihydropyridines, also dihydropyrimidones are used as drug derivatives in the pharmaceutical industry, for example as calcium channel blockers.[142] The Biginelli reaction can also be carried out applying simple solid phase protocols, which highlights its use in combinatorial synthesis toward the discovery of drugs.[143–146] Also, this reaction is still is widely applied in terms of polymerization and combinatorial chemistry (**Scheme 11**).[147,148] More recently, a synthesis utilizing sequential Biginelli and Passerini reactions was published and was later extended toward molecular data storage – a “hot” topic in combinatorial and also macromolecular chemistry.[149,150]

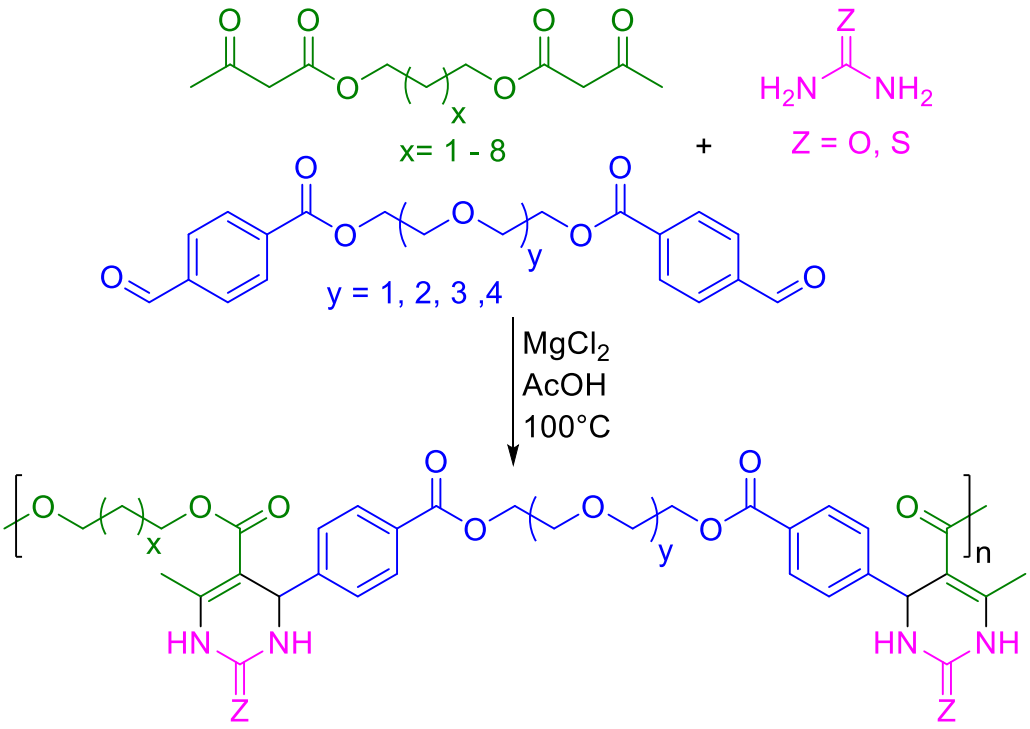

Scheme 11: Biginelli polycondensation toward Biginelli polymers. The versatility of the polyethylene glycol, acetoacetate ester backbones as well as the urea component allow for rapid synthesis of a theoretical number of 64 different polymers (**8** × **4** × **2**) – one of the main features of combinatorial chemistry.[148]

It was already established that carbonyl compounds play an important role in MCRs, due to their electronic properties. They are known for their strong electrophilicity as electron density of the carbonyl carbon is quite low because of the electron-withdrawing oxygen. Furthermore, their adjacent methylene group can be deprotonated allowing for versatile reaction pathways – a property called α-acidity and both aldehydes and ketones undergo the so-called keto-enol tautomerism, which leads to interesting properties regarding the hard and soft acids and bases (HSAB) concept and enables reactions with different electrophiles and nucleophiles.

A prominent MCR exploiting ketone and aldehyde reactivity is the Mannich reaction – a concise traverse from acetoacetate to aldehyde chemistry, which eventually leads to the key to this thesis: the two isocyanide-based multi component reactions – the Passerini and Ugi reaction, in which carboxylic acids, aldehydes, ketones, amines and isocyanides are utilized.

In the Mannich reaction, formaldehyde reacts with a primary or secondary amine to form an iminium intermediate. Subsequently, this iminium species (electrophile) reacts with a α-CH acidic compound such as an aldehyde or ketone, which serves as nucleophile. Also nitriles and acetylenes can be applied in this step. After addition of

both species, a β-amino enone derivative is formed (**Scheme 12**). Molecules synthesized by the Mannich reaction after often called Mannich bases as they contain a tertiary amine.

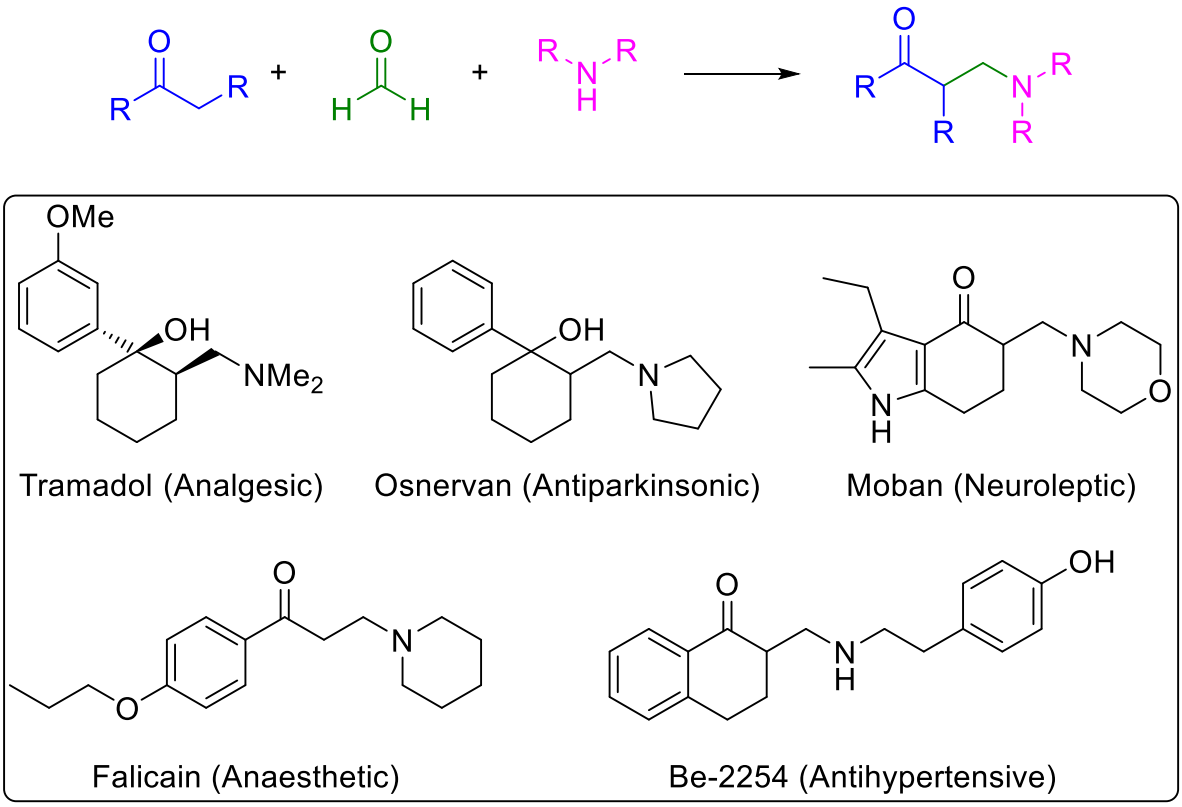

Scheme 12: Top: The Mannich reaction, a three-component reaction toward molecules that are commonly referred to as Mannich bases.[151] As reactants an α-CH acidic component (blue), formaldehyde (green) and a secondary amine (pink) are employed. Bottom: Examples of Mannich bases and their derivatives used in medicine.[152]

As for the previously discussed MCRs, applications of the Mannich reaction also lay in drug synthesis and combinatorial chemistry, and asymmetric approaches have gained popularity.[152–154]

Finally, in 1921 a new class of MCRs emerged: the so-called isocyanide based MCRs (IMCRs). IMCRs combine the reaction of carbonyl compounds with the outstanding reactivity of isocyanides (**Chapter 2.3.2**), and are known for their fast reaction rate, high yield, and high atom economy. The two most prominent representatives are the Passerini-3-component reaction (P-3CR – 1921),[74] which entails an acid component, an aldehyde/ketone and an isocyanide – and the Ugi-4-component reaction (U-4CR – 1959),[102] which involves an acid component, an aldehyde/ketone, a primary amine and an isocyanide. Both reactions have been used in combinatorial chemistry,[84,110] polymer chemistry[37,76,92,111,115,155,156] and also in the synthesis of

uniform macromolecules.[26,31,35,112,157–160] As the P-3CR is also applied for the synthesis of star-shaped macromolecules herein, it is discussed more thoroughly in **Chapter 2.3.4**, whereas the U-4CR is explained in the next paragraph.

Although the two reactions are related and largely share the same scope of reactants, there are distinct differences: an additional amine component in the case of the U-4CR and their mechanism (**Scheme 13**).

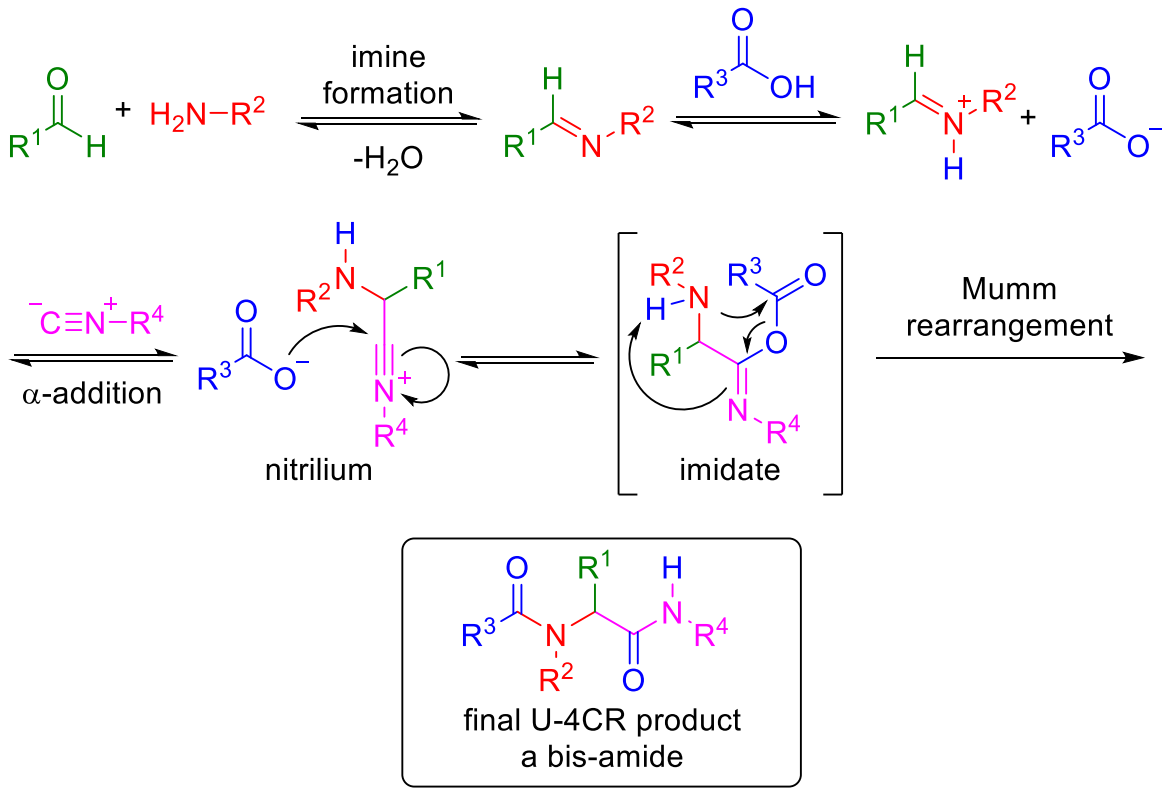

Scheme 13: Generally accepted mechanism of the Ugi-4-component reaction. The pathway proceeds *via* initial imine formation (aldehyde green and amine red), which is then activated by a carboxylic acid (blue), followed by α-addition of an isocyanide (pink). After reacting with the carboxylate, an imidate is formed and a final [1,4]-Mumm rearrangement yields a bis-amide as product.

The U-4CR starts with the formation of an imine by a condensation reaction between a carbonyl compound (either ketone or aldehyde) and an amine. Generally, precondensation of this component is beneficial in terms of obtained yield as it suppresses the P-3CR that can occur as a side reaction,[68] whereas the opposite is not possible due to the missing amine component. Subsequently, the imine is activated by protonation, which allows further advance of the proposed mechanistic pathway: the isocyanide component reacts in an α-addition, subsequently forming a nitrilium species, which is then transformed by the carboxylate to an secondary amine-bearing acyl imidate as intermediate.[161] This structure is unstable and consequently

rearranges into the thermodynamically more stable final product, a bis-amide, *via* [1,4]-Mumm rearrangement, a reaction already described in 1910.[162] As the final rearrangement is irreversible, the reaction is to be classified as type II MCR (**Scheme 6**, p. 20). Further differences between the P-3CR and the U-4CR are in the choice of solvent, as the latter tends to proceed more efficiently in polar protic solvents, like methanol.[68]

Recently, Rocha *et al.* published a report on the Ugi reaction mechanism, in which charge-tagged reactants were employed to clarify reactive intermediates *via* electrospray ionization fragmentation mass spectrometry (ESI-MS(/MS)) analysis. Next to the imine formation, the nitrilium species (**Scheme 14**) was also found, thus further solidifying the evidence for the proposed mechanism (**Scheme 13**).[163]

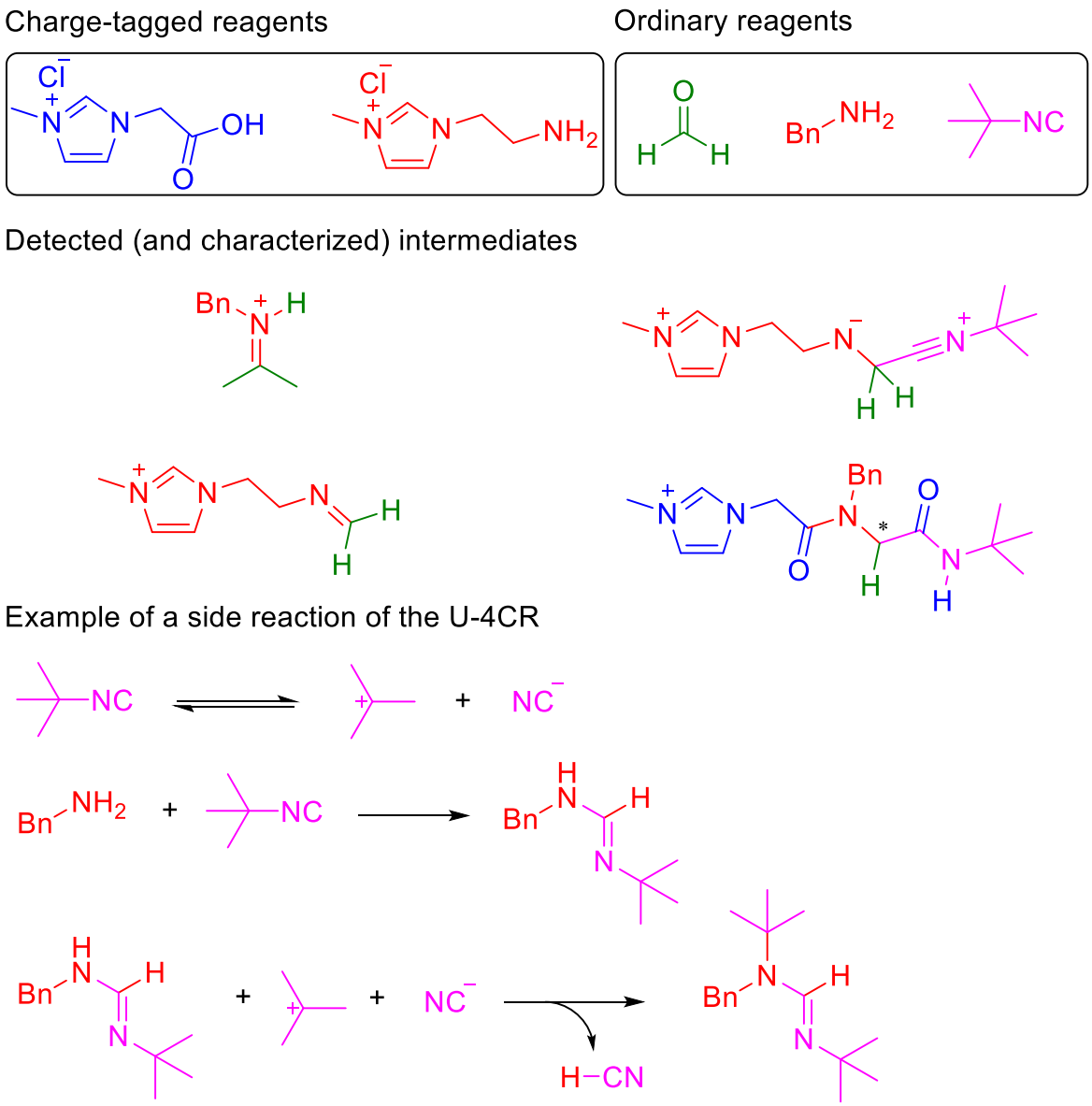

Scheme 14: Top: U-4CR mechanism evaluation by applying charge-tagged reagents. Middle: Detected and characterized intermediates, which support the suggested mechanism in **Scheme 13**. Bottom: Side reaction, which was found by ESI-MS(/MS) evaluation.[163]

Additionally, a side reaction was found, whereby the amine component reacts with the isocyanide and the organic side group of another isocyanide, which has formally split into its alkyl part and a cyanide ion. The latter is transformed into one equivalent of hydrogen cyanide.

Besides the classic U-4CR (**Scheme 15 a**) yielding diversely substituted bis-amides, research has found a significant number of variants that employ a broad spectrum of subsidiary acid components (**Scheme 15**).

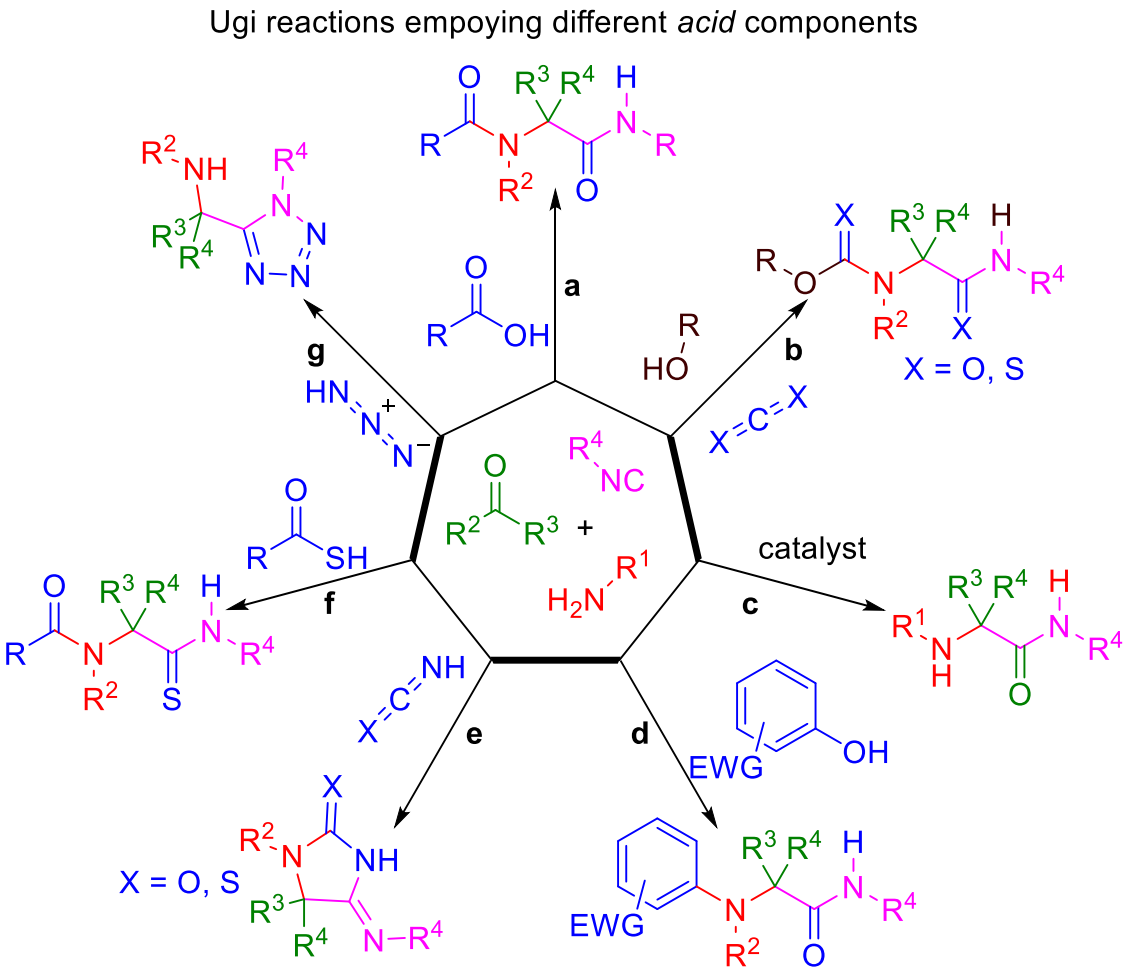

Scheme 15: Different Ugi reactions using isocyanide (pink), carbonyl compound (aldehyde or ketone, green) and primary amine, which employ a broad spectrum of an acid component. **a**: classic U-4CR. **b**: U-5CR, which utilizes carbon dioxide or carbonyl sulfide and an alcohol. **c**: U-3CR utilizing phenylphosphinic acid as catalyst **d**: Ugi-Smiles reaction of phenols, which are substituted with electron withdrawing groups (EWG). **e**: Ugi reaction employing iso(thio)cyanic acids. **f**: U-4CR with thiocarboxylic acids. **g**: Tetrazole synthesis *via* Ugi reaction of hydrazoic acid. Adapted from [164].

Synthesis of substituted carbamates is possible *via* the U-5CR, in which the acidic component is replaced by an *in situ* formed carbonate species, which is generated by reacting carbon dioxide with an alcohol under pressure (**Scheme 15 b**).[165] Furthermore, carbonyl sulfide and carbon disulfide have been shown in this variation yielding α-carbamate thioamides or α-thionocarbamate thioamides. Another approach, which has recently exploited to synthesize polymers, employs phenylphosphinic acid as a catalyst, subsequently leading to α-amino-amides (**Scheme 15 c**).[166] In the Ugi-Smiles variant, phenols substituted with electron withdrawing groups (EWG) are employed as the acid component, as EWGs increase the acidity of the phenol (**Scheme 15 d**).[167] It is noteworthy that the mechanism does not proceed with a final Mumm-rearrangement, but rather a Smiles-rearrangement, lending this reaction its

characteristic name. Also, pyridine and quinoline derivatives are employed in the Ugi-Smiles reaction.[168] Subsequent exchange of the carboxylic acid with an iso(thio)cyanic acid derivative yields so-called hydantoin analogues (**Scheme 15 e**).[82] Thiocarboxylic acids lead to thioamides (**Scheme 15 f**) and if hydrazoic acid is employed as carboxylic acid substitute, 1,5-substituted tetrazoles are obtained (**Scheme 15 g**).[165]

Concluding, the diverse variations of the Ugi reaction render it a powerful synthetic tool in combinatorial chemistry as well as pharmaceutical chemistry, which was already mentioned earlier (**Scheme 5**), while their utilization in polymer chemistry is briefly discussed in the following paragraph.[92,115,121,166]

U-4CR polymers yield interesting and diverse structures due to the high variability of the components, which are employed in their synthesis (**Scheme 16**). As four components are used in total, two difunctional and two monofunctional ones are typically employed to form linear polymers *via* step-growth mechanism. Hence, the control of the backbone structure is altered by changing the di-components, whereas the variation of the mono-component allows for introduction of different sidechain structures.[92] The general motif, the bis-amide, is of great significance as it is generally seen in protein structures and therefore the obtained polymers (polypeptoids) are, to a certain degree, capable of biomimicry.[169] Furthermore, diversification and availability of the components allow high output of polymers with different properties and key features, especially as also isocyanides, which have been a limiting factor of IMCRs, are readily obtained.[103,104] A wide variety of dicarboxylic acids and diamines are commercially available making backbone variation for these polymerizations rather simple and cost effective. Same goes for the sidechain iteration, as mono-carboxylic acids, amines and aldehydes come in very diverse structural motifs. Limiting factor is often only the isocyanide component that is rather costly (monoisocyanides) or has to be synthesized individually (diisocyanides).

Besides these polycondensations, there are reports about the U-4CR as synthetic tool for the synthesis of ROMP monomers,[170] monomers for acyclic diene metathesis (ADMET),[121,171] diversely substituted polyacrylamides,[172] as well as its use in post-polymerization modifications.[156]

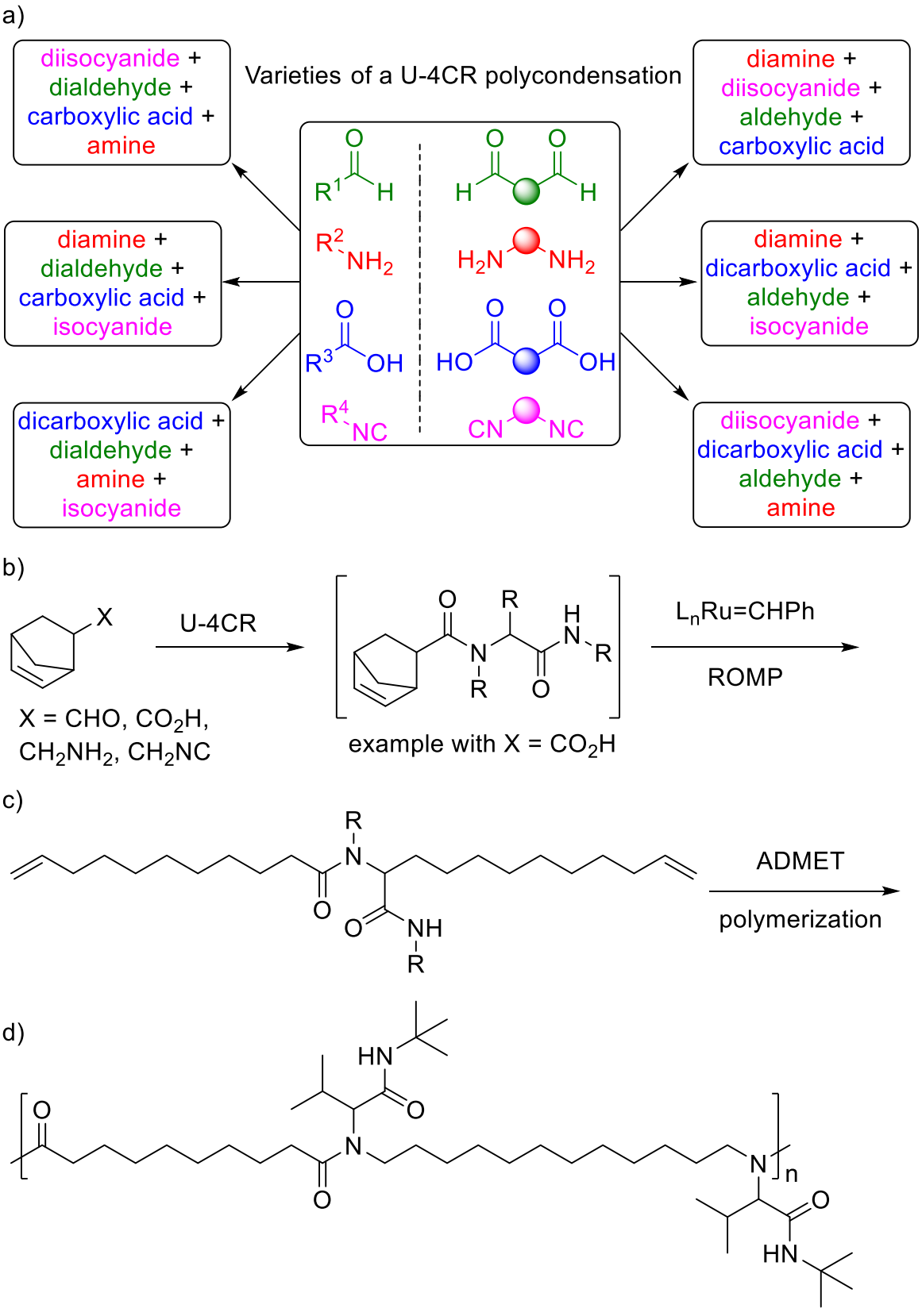

Scheme 16: a) Possible combinations for a Ugi-4-component reaction toward polymers utilizing variable acid components (blue), primary amines (red), aldehydes (green) and isocyanides (pink). Adapted from [92]. b) Functionalization of norbornene derivatives *via* U-4CR and subsequent ROMP. Adapted from [170]. c) ADMET monomer obtained from castor oil basted reactants. Adapted from [171]. d) Example of a polymer obtained *via* U-4CR polycondensation. Adapted from [92].

2.3.4 The Passerini reaction

As already mentioned in the previous chapter, the Passerini-3-component reaction was first described in 1921,[74] therefore being the solid foundation of isocyanide-based multicomponent chemistry.

The most typical variant of the reaction employs a carboxylic acid, an aldehyde, and an isocyanide, which are converted into an α-acyloxy amide (**Scheme 17**). As every atom of the reactants finds itself in the product, the Passerini reaction can be considered as an addition reaction giving it an outstanding atom economy of 100%. In contrast, the U-4CR is condensation reaction, as one equivalent of water is removed in the process of the imine formation. However, both reactions share an irreversible rearrangement as last step and therefore also the P-3CR reaction is to be considered a MCR type II (**Scheme 6**).[68]

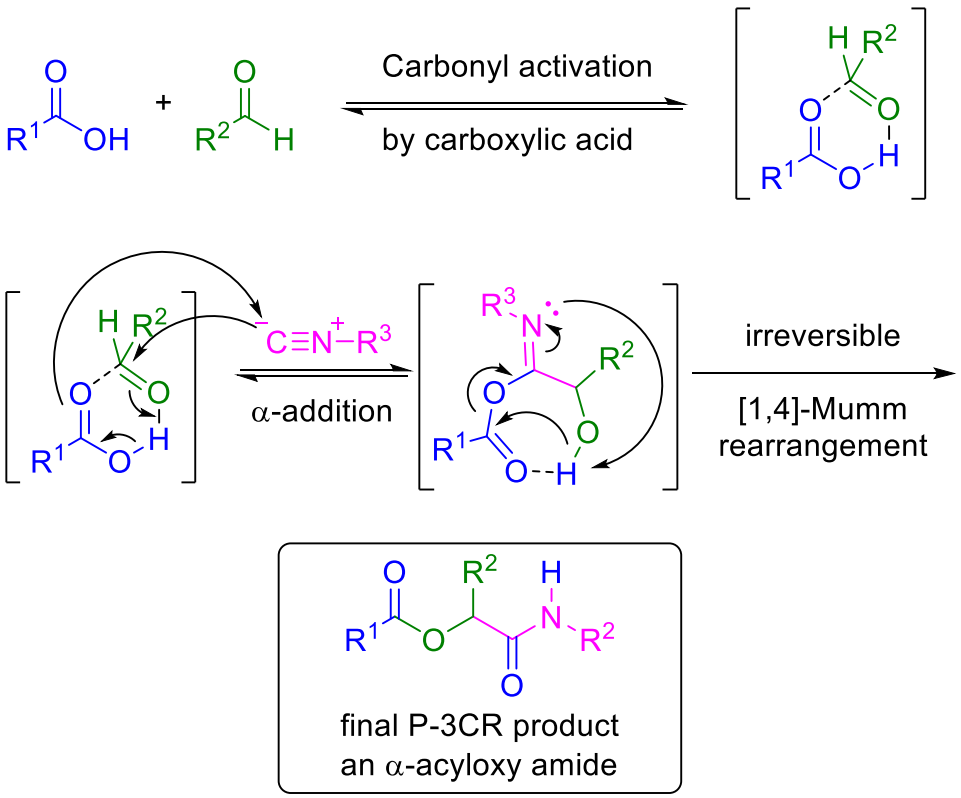

Scheme 17: Proposed mechanism of the Passerini reaction: The carboxylic acid (blue) activates the carbonyl compound (green) by forming a hydrogen bonded adduct. Then, the isocyanide (pink) attacks *via* α-addition – a concerted reaction step. After final and irreversible [1,4]-Mumm rearrangement of the seven-membered transition state, an α-acyloxy amide is obtained.[74,165,173]

One of the proposed mechanisms starts *via* an activation of the carbonyl compound by the acidic component, leading to a hydrogen-bonded adduct. Next, the isocyanide component adds to this loosely bound adduct *via* α-addition. A final and irreversible

[1,4]-Mumm rearrangement yields the Passerini product, an α-acyloxy amide. Nonetheless, the mechanism of the P-3CR is still not fully understood. In 1965, Eholzer published a variety of the Passerini reaction, in which the water-free carboxylic acid component was replaced with a mineral acid.[174] Instead of the proposed hydrolysis of the isocyanide compound toward its *N*-formamide or even amine, which occurs normally if such compounds are subjected to acidic aqueous conditions, they isolated the α-hydroxyamide. Concludingly, they proposed an acceleration of the reaction, which is in accordance with the findings of Sarma and Pirrung, who also reported acceleration of multicomponent reactions in aqueous media.[175] In 2011, an alternative mechanism was postulated by Maeda *et al.*, which involves a second carboxylic acid as a fourth, but catalytic component (**Scheme 18**).[176] Herein, a second acid molecule is involved in the rearrangement of the α-addition adduct, as the calculated energy of the transition state is significantly lower than without the additional fourth component. Subsequently, the product is formed *via* a cyclic transition state. Those findings were supported by density functional theory (DFT) calculations carried out in 2015.[177]

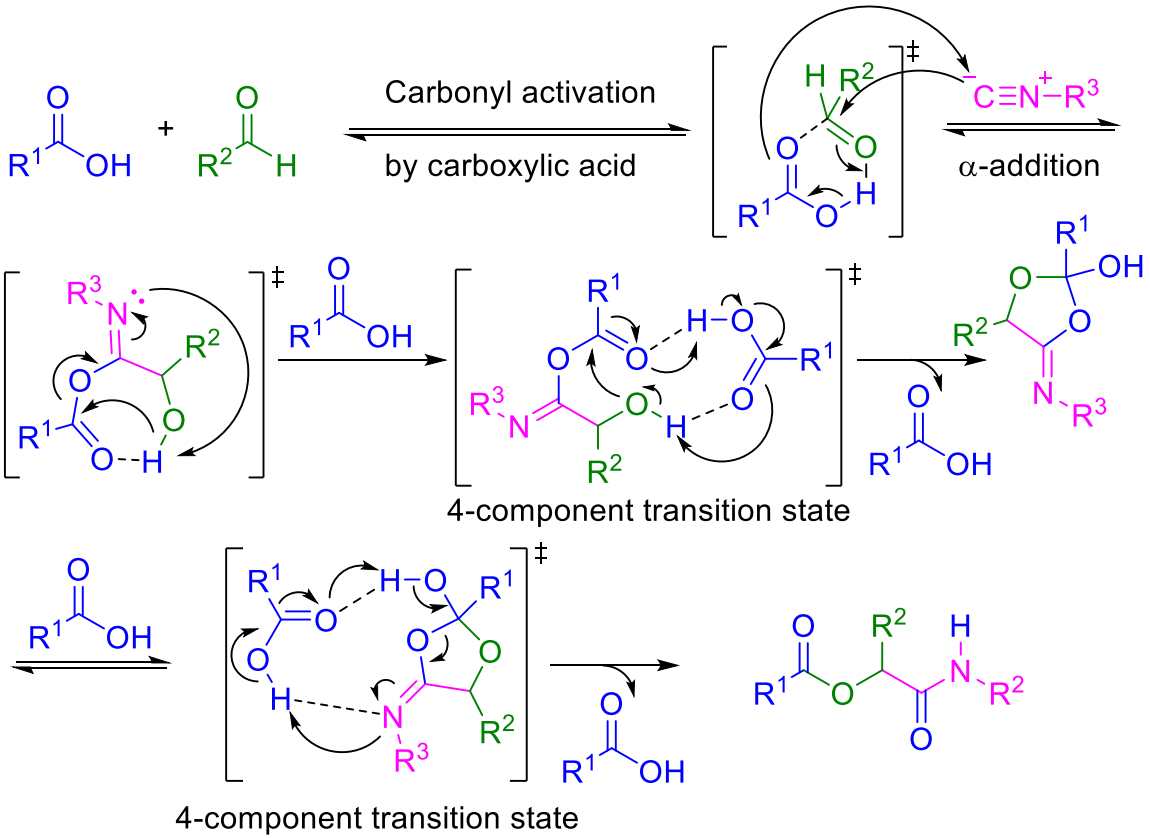

Scheme 18: Proposed mechanism of the P-3CR involving two 4-component transition states. This mechanism was based on quantum mechanical calculations in the gas phase.[176] The mechanism was backed up by DFT calculations.[177]

Similarly to the Ugi-4-component reaction, which was previously discussed, the P-3CR is a powerful tool in preparative chemistry. Its modular and robust character led to a wide scope of achievable motifs with structural diversity in only one single step. Next to its classical variation (**Scheme 19 a**), the applied acid and carbonyl components can be replaced with a variety of other substance classes, which increases its scope even further (**Scheme 19 b-g**).

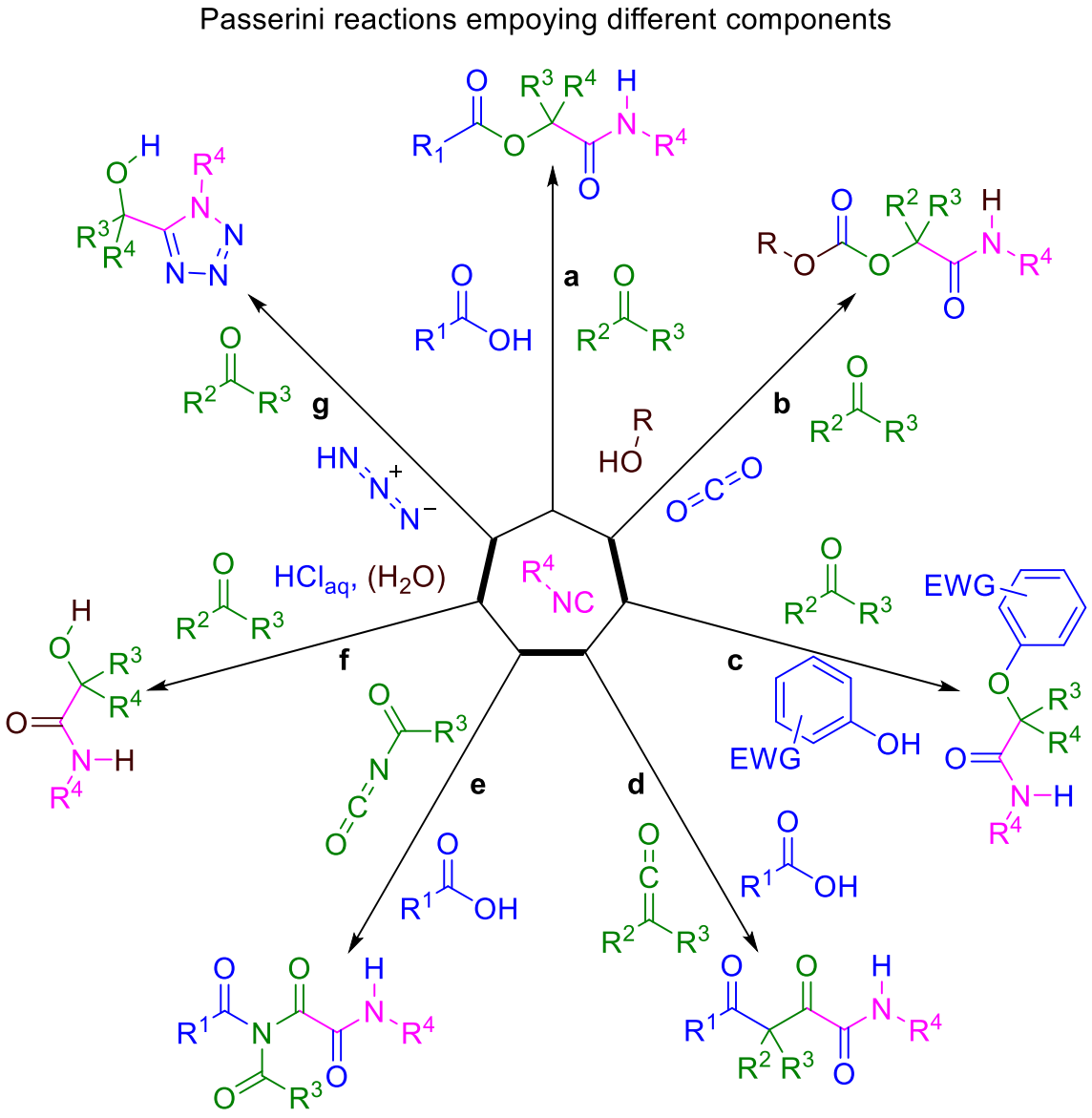

Scheme 19: Different Passerini reactions employing a broad spectrum of acid (blue) and carbonyl (green) compounds. **a**: classic P-3CR. **b**: P-4CR, which utilizes carbon dioxide and an alcohol, which *in situ* form carbonic acid. **c**: Passerini-Smiles reaction of phenols, which are substituted with electron withdrawing groups (EWG). **d**: Passerini reaction employing ketenes. **e**. Passerini reaction employing acylisocyanates as carbonyl compound leading to *N,N*-diacyloxoamides. **f**: P-3CR with catalytic/stochiometric amounts of mineral acids – here water is the third component, respectively. **G**: tetrazole synthesis *via* Passerini reaction of hydrazoic acid. Adapted from [164].

If an alcohol in the presence of carbon dioxide is employed, carbonic acid is generated *in situ*. A subsequent P-3CR leads to carbonic ester amides, yet this reaction is often accompanied by hydrolysis, leading to α-hydroxyamides (**Scheme 19 b**).[178] Similar to the corresponding Ugi variant, reaction of EWG-substituted phenols leads to the Smiles-variation of the Passerini reaction (**Scheme 19 c**).[179] A recent publication also found 1,1,1,3,3,3-hexafluoro-propan-2-ol (HFIP) capable of replacing the acid component. Herein, the characteristic Smiles rearrangement is avoided and the stable imidate is directly hydrolyzed to obtain α-hydroxyamines.[180] As alternative carbonyl compounds, ketenes as well as acylisocyanates can be employed, leading to α,γ-diketoamides or *N,N*-diacyloxoamides (**Scheme 19 d/e**).[68] If mineral acids like HCl replace the carboxylic acid, α-hydroxyamides can be obtained (**Scheme 19 f**)[174] and hydrazoic acids leads to substituted tetrazoles, respectively (**Scheme 19 g**).[181] This procedure was later revised and improved to avoid the toxic hydrazoic acid, as it was found that also trimethylsilyl azide reacts in Passerini reactions.[182] Another variation employs alcohols as surrogates for carbonyl compounds, which were oxidized *in situ* by 2-iodoxybenzoic acid (IBX).[183] This alternative avoids storage of aldehydes, which are easily oxidized on air and allows for a quick and easy conversion with subsequent consumption of those sensitive compounds.

Cyclization reactions have also been reported, either directly *via* the Passerini reaction or as a quick and simple post-reaction modification (**Scheme 20**).[184,185]

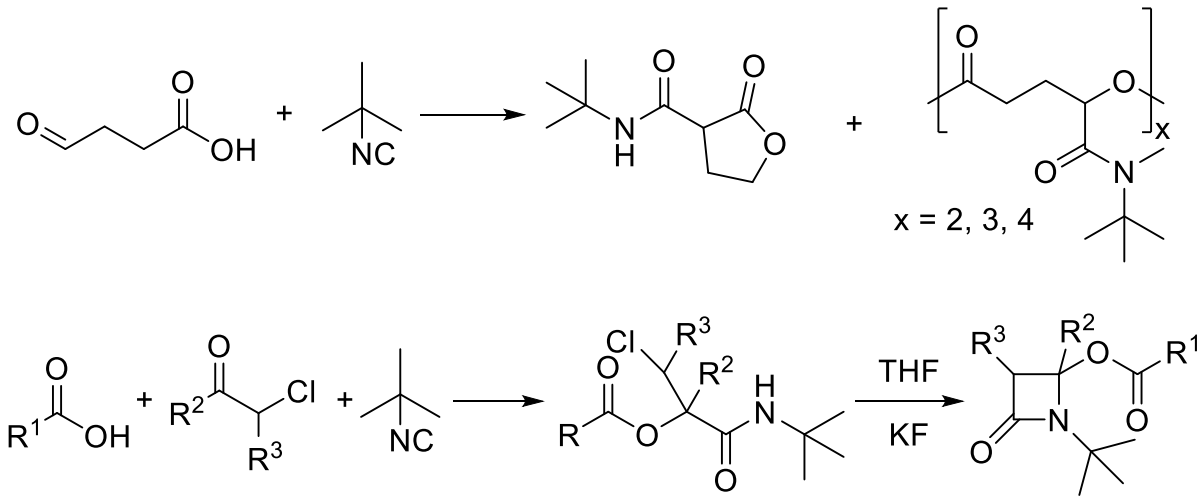

Scheme 20: Top: Passerini cyclization with an AB monomer, yielding linear oligomers as side products. Bottom: Passerini reaction with α-chloro aldehydes/ketones and subsequent cyclization with potassium fluoride toward azetidinones.[184,185]

The first approach employs an AB type compound toward direct cyclization. However, oligomers are also obtained and favoring the cyclization over linear oligomerization has

to be carefully evaluated *via* the reaction conditions.[184] Likewise, the P-3CR is also utilized in polymerizations, as shortly discussed at the end of this chapter. Post-reaction cyclization can be achieved by employing α-chloro carbonyls in the P-3CR. This is performed by refluxing the compound in tetrahydrofuran (THF) in the presence of an excess of potassium fluoride.[185] The resulting azetidinone structure is found in penicillin and is therefore the core motif for a wide variety of antibiotics.

Stereo controlled P-3CRs have also gained interest in the scientific community, however their enantioselectivity does not match that of other asymmetric syntheses, like for example the Sharpless epoxidation. Such enantioselective reactions employ either stereo specific (chiral) reactants or asymmetric catalysts (**Scheme 21**).[186–189]

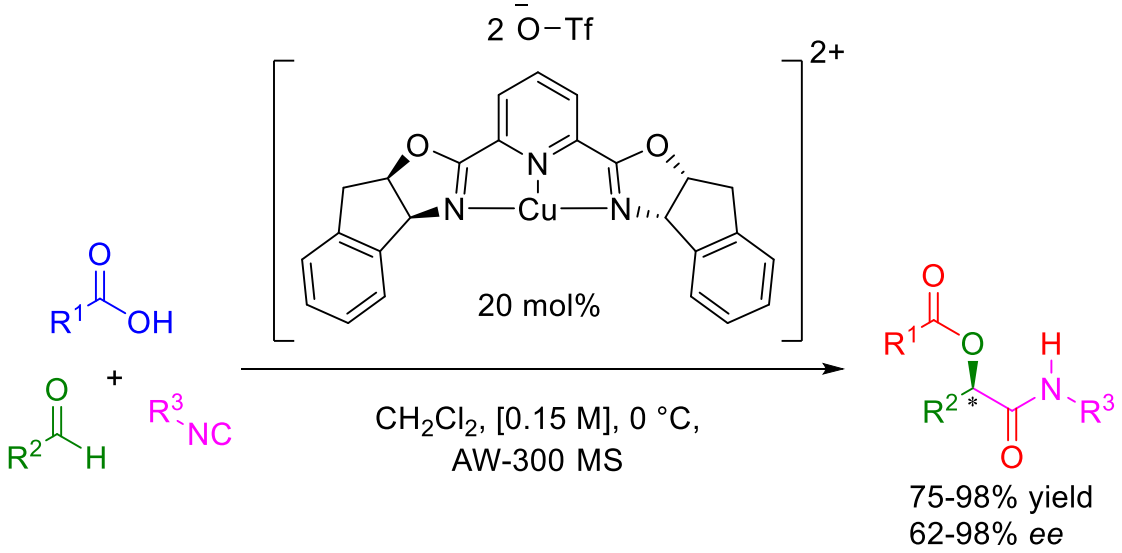

Scheme 21: Asymmetric P-3CR with a tridentate indan (pybox) Cu(II) Lewis acid complex.[188]

The modular character of the P-3CR also supports its application in medicinal chemistry. Fast screening of vast amounts of reactants to synthesize libraries, toward specific motifs has yielded several products, which have found application as drugs. A common example is biculatamide (Casodex®), which is synthesized by employing water, a ketone as well as an isocyano compound and titanium(IV)chloride as catalyst. It is a nonsteroidal selective antiandrogen for the treatment of prostate cancer.[190] The P-3CR was also utilized to synthesize an HIV-1 protease enzyme inhibitor.[191,192] A combinatorial approach published in 2007 by Dömling *et al.* reported the compilation of three libraries of 88 compounds each. Dicarboxylic acids where applied in Passerini or Ugi reactions and the final products where screened for compounds, which mimic the hormone erythropoietin.[193] Further understanding and deeper insights are given in reviews about medicinal and combinatorial chemistry.[194]

In 2011, the P-3CR was first introduced as synthetic tool in polymer chemistry.[121] Two distinct approaches where reported. The first combines IMCR and acyclic diene metathesis (ADMET): a monomer featuring terminal double-bonds is synthesized *via* P-3CR employing an aldehyde and carboxylic acid, which can be obtained *via* pyrolysis of ricinoleic acid. Subsequent ADMET of those monomers, which bear terminal alkenes on each side, afforded polymers with a number average molar mass (M_n) ranging from 11.5 kDa to 21.7 kDa and dispersity $Đ$ between 1.35 and 1.45. Furthermore, direct polymerization of dialdehydes and dicarboxylic acids was conducted by employing different isocyanides. In the following years, further publications of several working groups featured the P-3CR as reliable tool for macromolecular chemistry:[111] P-3CR derived acrylate monomers were radically polymerized,[76] an AB-monomer approach was evaluated,[195] graft-copolymerization approaches were conducted[114] and photo-cleavable polymers were synthesized by employment of 2-nitrobenzaldehyde.[196] Hence, the P-3CR has been employed as versatile synthetic instrument in macromolecular chemistry and new findings are constantly being published.

A recent approach by Barner-Kowollik *et al.* published in 2019 featured the visible-light-induced Passerini multicomponent polymerization of *in situ* photogenerated thioaldehydes (**Scheme 22**).[197] The obtained poly(thioesteramide)s were then subjected to either thiirane insertion, which allowed a shift toward lower retention time due to an increase in hydrodynamic radius, as the linear backbone of the polymer was *internally* enlarged, or aminolysis *via* employment of butylamine yielding diamides and dithiols.

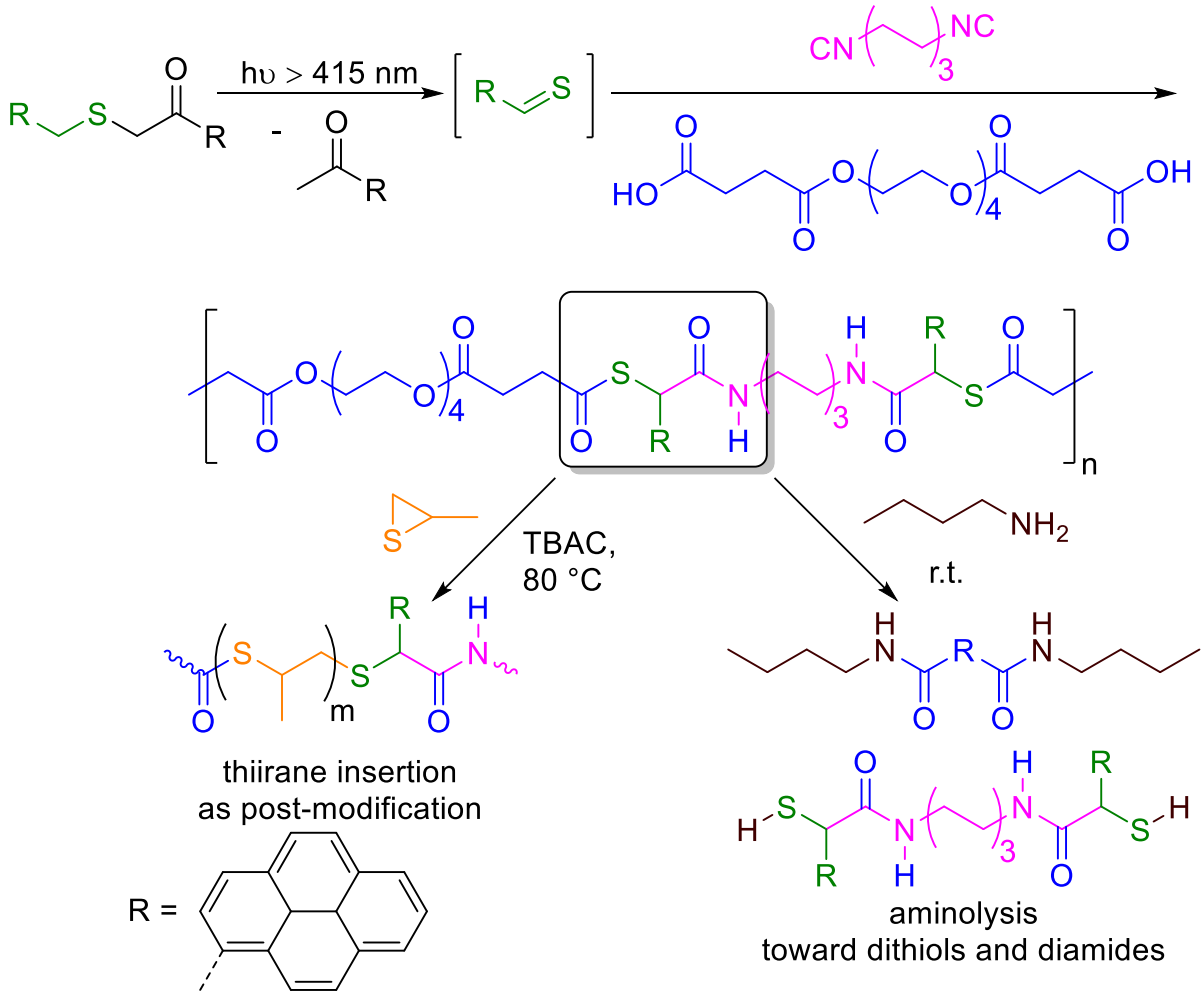

Scheme 22: Top: Passerini polymerization utilizing *in situ* photogenerated thioaldehydes. Bottom left: Thiirane insertion (internal backbone growth). Bottom right: Aminolysis. Adapted from [197].

Another interesting report from of Tunca *et al.* is about the modification of electron deficient polyesters trough combination of the azide-alkyne Huisgen cycloaddition as well as the P-3CR reaction (**Scheme 23**).[198] The authors report a post polymerization modification of an alkyne containing polyester by reacting it with a mixture of benzyl azide and 3-azidopropionic acid toward 1,2,3-triazoles. Subsequently, a P-3CR is employed to introduce two sidechain moieties. Azides, or rather their protonated variation, hydrazoic acid, can be employed as carboxylic acid substitute in either the P-3CR or U-4CR reaction. Their main area of application is, however, the azide-alkyne Huisgen cycloaddition, which was also employed in this thesis. Hence, in the next two chapters, a short overview about the substance class and the Huisgen cycloaddition is given.

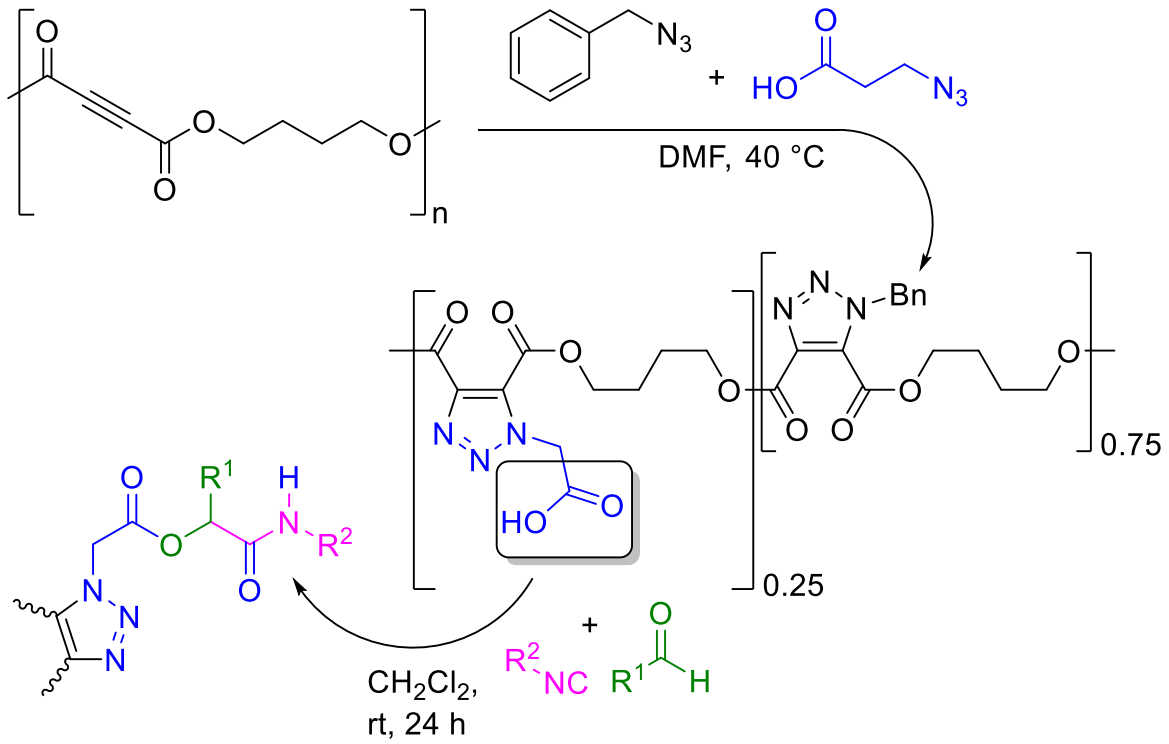

Scheme 23: Tandem post modification of an electron deficient polyester *via* initial azide-alkyne cycloaddition and subsequent P-3CR.[198]

2.3.5 Azides

An azide is the conjugated base of the so-called hydrazoic acid HN_3 (**Figure 6**). It is isoelectronic to carbon dioxide (CO_2), the cyanate ion (NCO^-), nitrous oxide (N_2O) and the nitronium ion (NO_2^+). Next to inorganic azides, also organic ones are known, and find application in a wide variety of syntheses, mainly the synthesis of primary amines or the Huisgen cylcoaddition (**Chapter 2.3.6**).

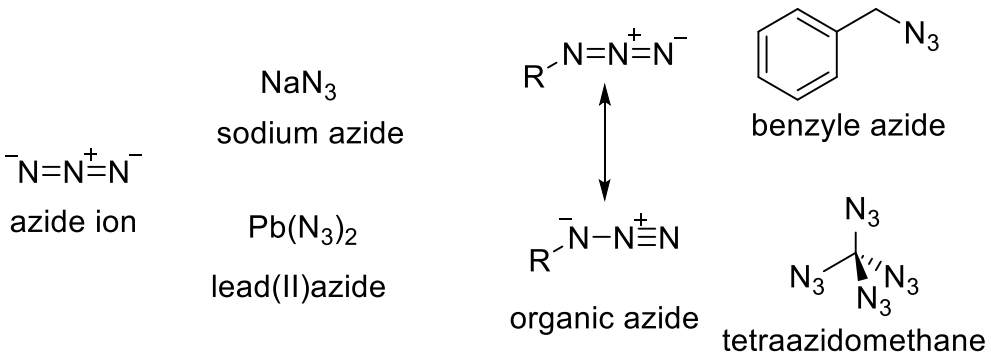

Figure 6: Left side: most important resonance structure of the azide ion and two inorganic salts of the hydrazoic acid. Right side: Resonance structure of organic azides as well as benzyl azide and tetraazidomethane as prominent examples.

Inorganic azides are severely toxic, especially the soluble ones, and nearly all of them are explosive.[199] Sodium azide, which is often used in organic synthesis, is absorbed

through skin and, if treated with water, it releases the highly volatile and toxic hydrazoic acid. Its main area of application, aside from organic chemistry, is as nitrogen source for airbag inflation.[200] Other inorganic azides like lead(II)azide are used as potent initiating explosives. The biochemical mode of action of an azide is the irreversible blocking of the active center in cytochrome c oxidase, which is normally reserved for oxygen. Hence, ATP production in the cell is stopped, consequently leading to cell death, in the same way as cyanide or carbon monoxide do.[199]

Organic azides are often toxic and smaller ones tend to be explosive.[199] Yet, in 2006 tetraazidomethane was isolated, a highly thermally instable compound with a nitrogen mass content of 93.3%. Other organic azides, however, are far easier to handle and allow for a wide variety of subsequent reactions. They can be obtained by several different procedures, of which a few are presented in **Scheme 24**.

Activated electron poor aromatic systems can undergo a nucleophilic aromatic substitution with sodium azide, likewise standard nucleophilic substitution applying sodium azide is known to work with a wide variety of substrates, even with weak leaving groups, as an azide is an excellent nucleophile. As solvent, DMSO and DMF are often applied either at room temperature or up to 100 °C.[201–204] Aryl halides are reacted with organolithium compounds, like *n*-butyllihtium and afterwards converted into the corresponding azides *via* employment of trimethylsilylazide. Other routes feature the application of azide transfer reagents like trifluoromethanesulfonyl, tosyl or imidazole-1-sulfonyl azide, which directly afford the azide from amine substituted substrates. In summary, the simple and efficient synthesis of azide-bearing compounds enables a diverse range of substrates, which subsequently can be employed as reactants in the Huisgen cycloadditon.

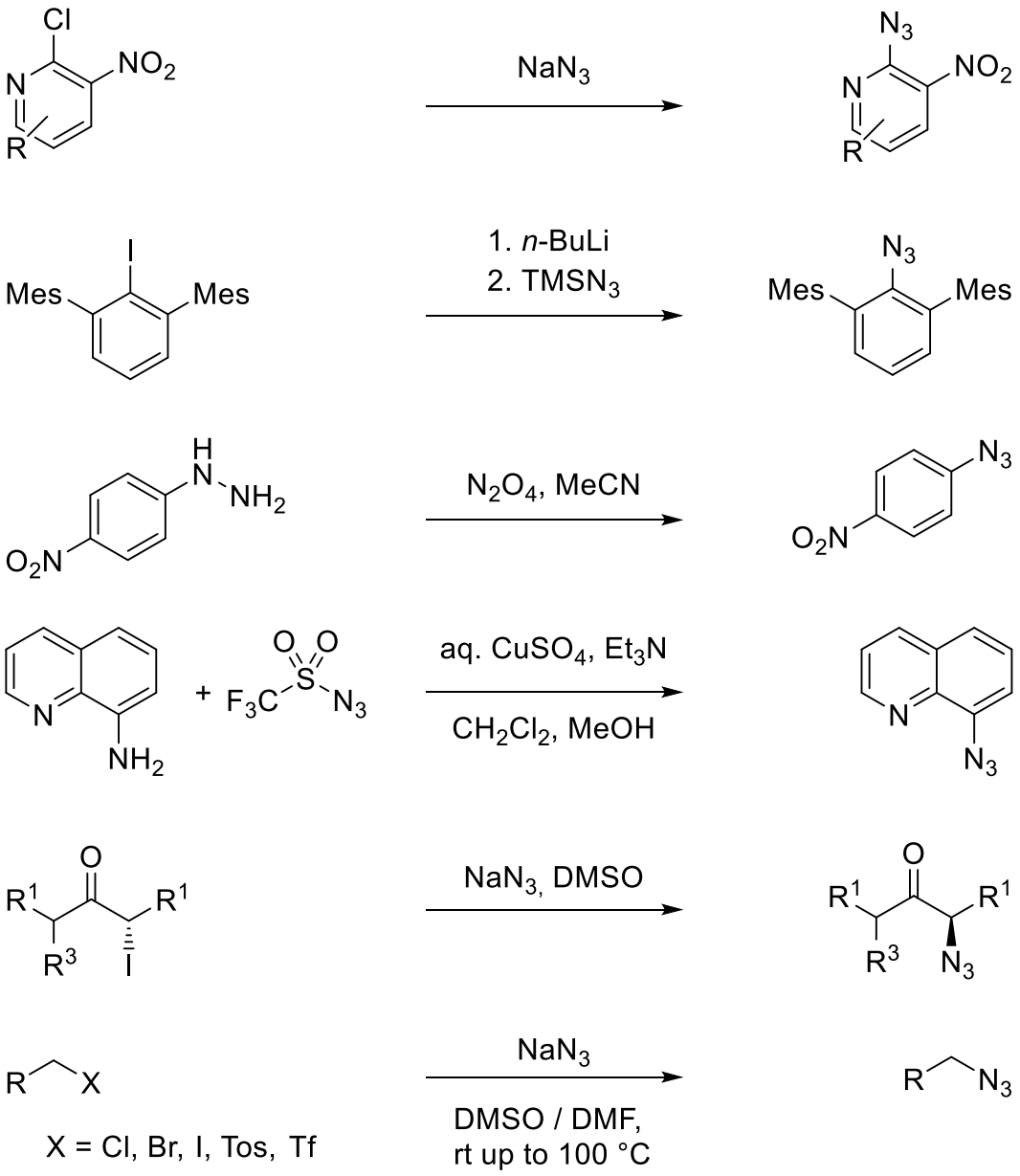

Scheme 24: A short overview of syntheses that allow the introduction of an azide group.[199]

2.3.6 The azide-alkyne Huisgen cycloaddition

In the azide-alkyne Huisgen cycloaddition, an alkyne is reacted with an azide yielding a 1,2,3-triazole (**Scheme 25**, bottom). In terms of reaction type, it is defined as a 1,3-dipolar cycloaddition. It was named by Rolf Huisgen, who studied reaction kinetics and conditions of this family of cycloadditions in the middle of the 20th century.[205] However, the reaction of a terminal alkyne with an azide is slow, often needs temperatures around 100 °C and yields both regio-isomers of the heterocycle in equal amounts – several disadvantages, which render the basic reaction rather inefficient for an application in combinatorial chemistry or high-throughput screening (HTS) toward large molecule libraries.

Upon targeting the missing regioselectivity of the Huisgen cycloaddition, a highly efficient and selective variation was found independently by Sharpless *et al.*[206] and Meldal *et al.* in 2002:[207] the copper-catalyzed azide-alkyne cycloaddition, mostly abbreviated to CuAAC. It is either carried out by *in situ* reduction of copper(II)salts, which is mostly achieved by reacting copper(II)sulfate with sodium ascorbate (NaAsc) in a THF/water mixture,[206] or alternatively by using copper(I)salts and amine bases as ligand (pyridine/diisopropylethylamine amine (DIPEA)) in a wide variety of organic solvents (chloroform or toluene are often utilized (**Scheme 25**)).[78,207] For the latter, often heating is applied, yet is no necessity for a successful reaction, but increases solubility of the copper complexes in organic solvents.

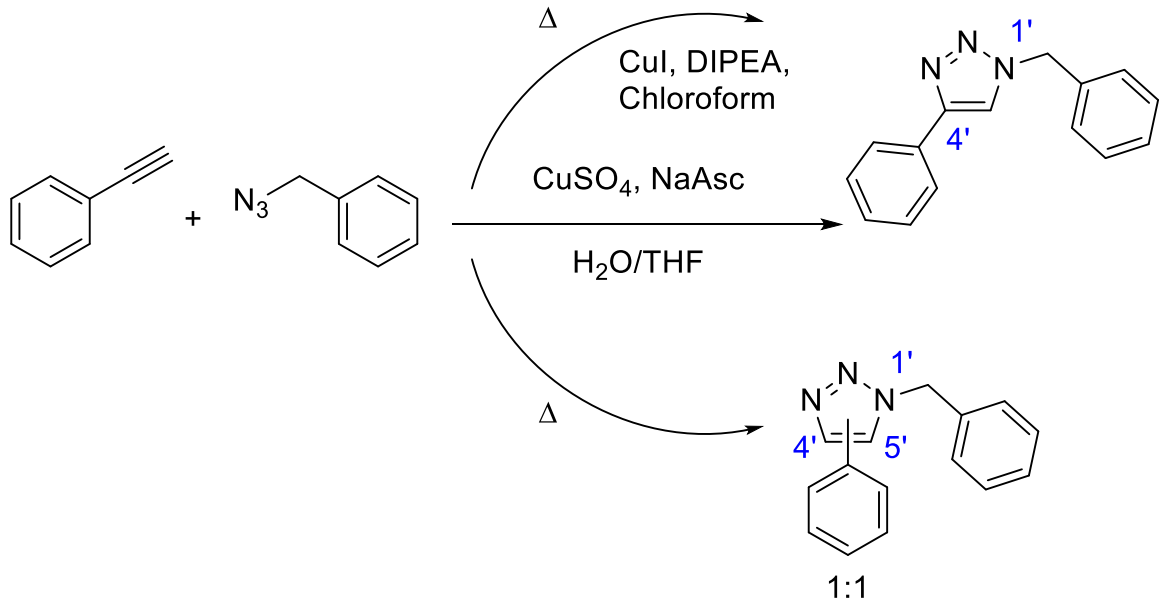

Scheme 25: Top: CuAAC employing copper(I)salts and an organic ligand, here DIPEA toward the 1,4-substituted product. Middle: CuAAC carried out with *in situ* reduction of copper(II)salts, here copper(II)sulfate and the sodium salt of ascorbic acid (NaAsc). Bottom: Non-selective thermally driven azide-alkyne cycloaddition.

These variations yield solely the 1,4-substituted product yet work only with terminal alkynes. Nonetheless, this not only brought the Huisgen cycloaddition into focus, but also shaped a whole new field of chemical reactions: ‘Click’ chemistry.

Like the definition of MCRs, the definition of ‘click’ chemistry is bound to certain parameters, or rather requirements that all have to apply to the reaction.

‘Click’ reactions offer high yields, are insensitive to solvent parameters as well as oxygen and water residues, while still featuring a high modularity and absolute regio- and stereospecificity. Generally, the reaction is driven by a considerable

thermodynamic force (>20 kcal/mol). Ideally, ‘click’ reactions proceed under simple reaction conditions and employ readily available starting materials and maintain high atom economy. Often, they use benign solvents and rely on simple work-up procedures (crystallization/distillation) rather than chromatography. Next to the [3+2] cycloadditions, like the CuAAC,[78,79,206,207] also [4+1] cycloadditions between isocyanides and tetrazines,[208] Diels-Alder- and inverse electron demand Diels-Alder reactions,[209,210] as well as thiol-ene/thiol-yne chemistry[211–213] are considered to be ‘click’-chemistry.

Consequently, research on the CuAAC evaluated potential mechanisms, strongly focusing on the interaction between the copper(I) and alkyne component. Already Sharpless *et al.* proposed a mechanism for the catalytic cycle of the Cu(I) ligation (**Scheme 26**) when they first published their findings on the CuAAC in 2002.[206]

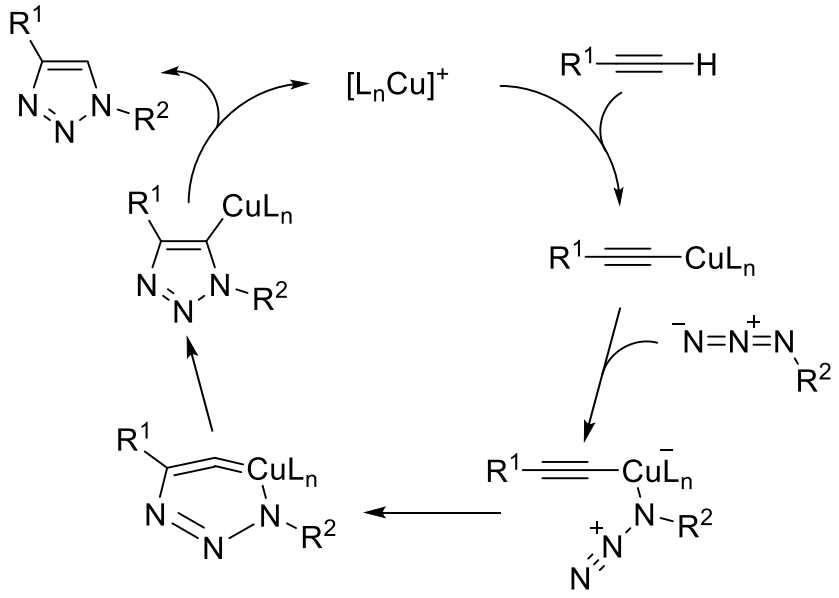

Scheme 26: Proposed catalytic cycle of the CuAAC leading to the 1,4-substituted triazole.[206]

The reaction starts with the alkyne forming a ligand-stabilized copper-acetylide. Afterwards, the azide coordinates with its alkylated/arylated nitrogen onto a free orbital of the copper species allowing for direct influence of the regioselectivity in the following ring closure. After eliminating the copper species, solely the 1,4-subsituted 1,2,3-triazole is yielded as product.

The proposed mechanism features only one copper atom, which takes part in the catalytic cycle, yet in the following years kinetic and isotope studies proposed and favored a mechanism involving a dicopper species.[214–217] In 2015, de Angelis *et al.*

employed charge-tagged reagents in the azide-alkyne cycloaddition and subsequently used electrospray ionization mass spectrometry (ESI-MS) to assess possible intermediates solidifying their proposal (**Scheme 27**).[215]

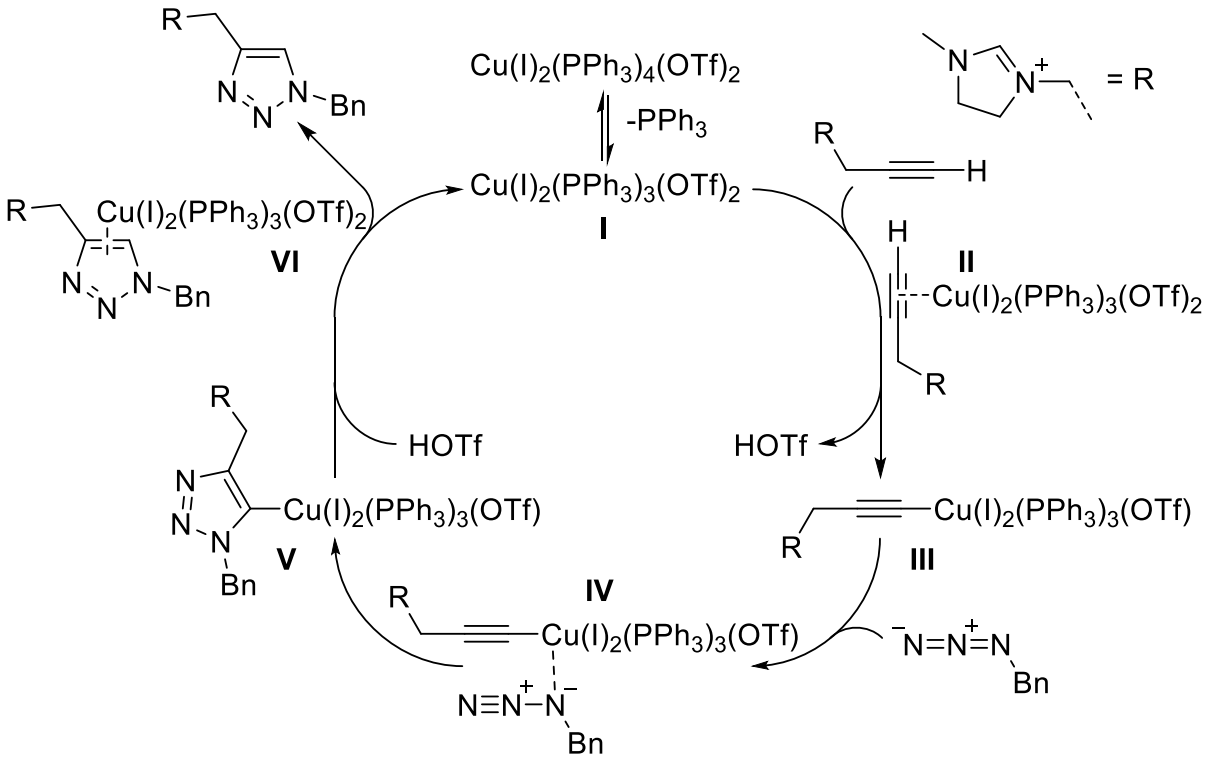

Scheme 27: Proposed mechanisms of the azide-alkyne cycloaddition, which was backed up by employing a charge-tagged alkyne and reacting it with benzyl azide *via* Cu(I) catalysis. The results confirmed a dicopper species, which first forms a copper acetylide complex with the alkyne and subsequently coordinates the azide component. The reaction proceeds with absolute stereo control.[215]

Instead of a single copper species, the active complex is assumed to consist of a dicopper species, which coordinates to the alkyne over π-orbital interactions (**Scheme 27 II**). After eliminating a ligand, a copper(I)acetylide is formed (**Scheme 27 III**). Subsequently, the azide loosely coordinates to the dicopper species, allowing for a shift in partial charge distribution in the azide enabling subsequent reaction (**Scheme 27 IV** and **V**). After triazole formation, the copper species is replaced *via* a proton transfer yielding the final product as well regenerating the active catalytic species (**Scheme 27 VI** and **I**). Due to its robust and versatile character, the CuAAC is employed in many research fields. As substituted triazole compounds often exhibit biological activity, the reaction is applied in medicinal and combinatorial chemistry to screen and evaluate new drugs, bio-mimics, nucleotides and peptides, often in combination of techniques involving solid support (**Scheme 28**).[218–220]

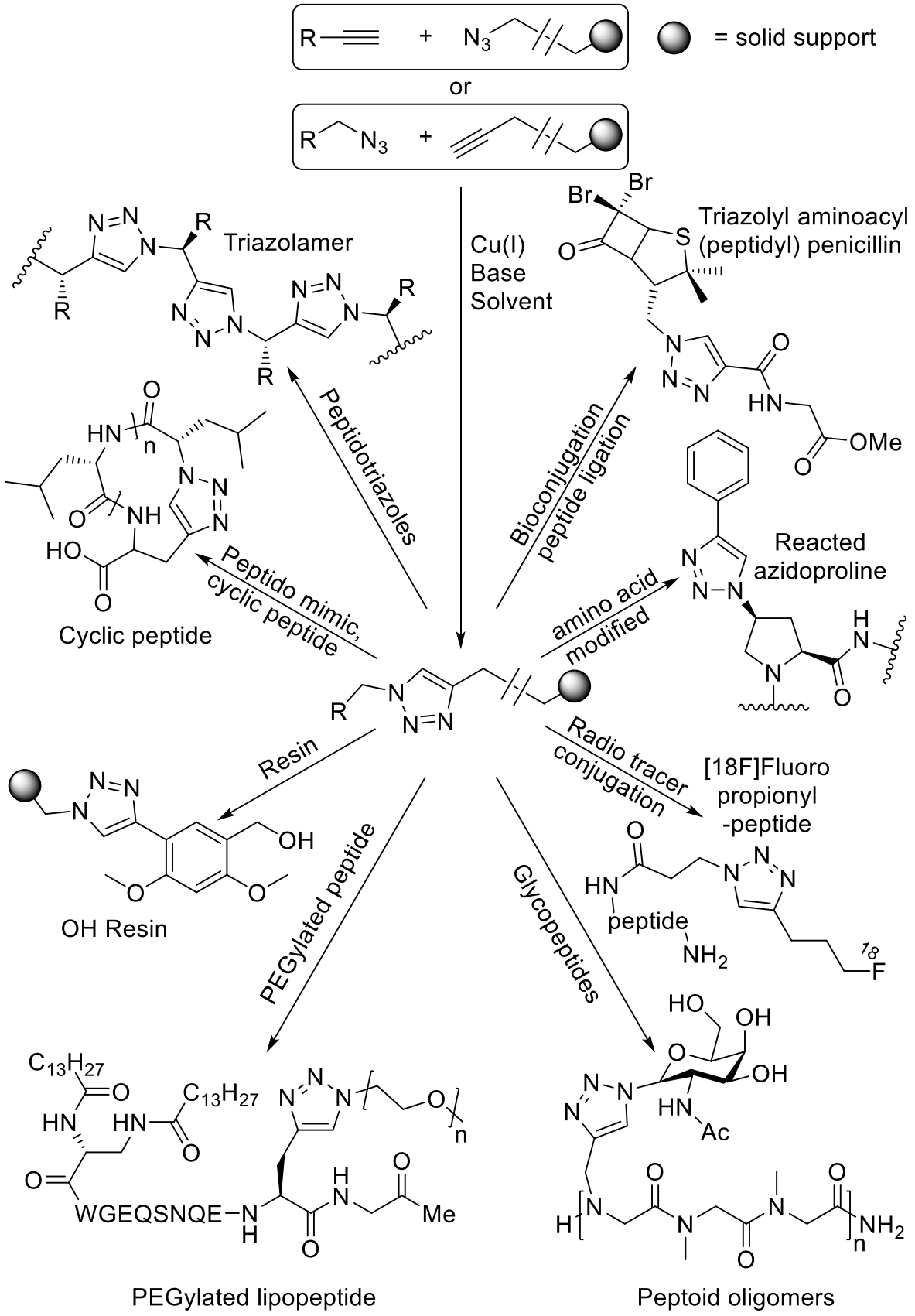

Scheme 28: Selection of solid-supported syntheses involving the CuAAC toward modified peptides and peptoides. Adapted from [220].

Furthermore, the CuAAC has been applied in polymer chemistry and also in the synthesis of complex dendrimers.[80,221–223] In 2015, Jamison and coworkers demonstrated the first application of the CuAAC in the synthesis of sequence-defined, unimolecular macromolecules *via* a multistep flow synthesis and iterative exponential growth (FLOW-IEG) (**Scheme 29**).[24]

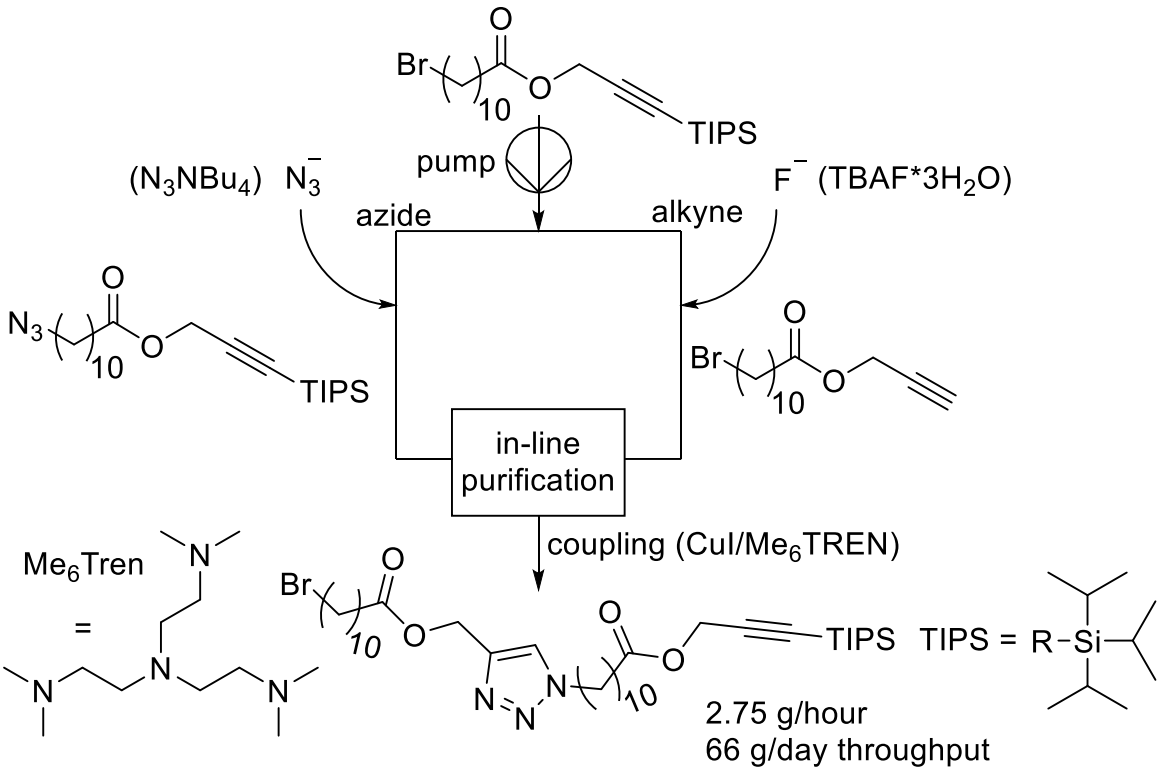

Scheme 29: Application of the CuAAC in a multistep flow synthesis employing the iterative exponential growth strategy toward uniform macromolecules. Adapted from [24].

The synthesis started from 11-bromoundecanoic acid, which was converted to a triisopropylsilyl protected propargyl ester. Subsequent splitting of the batch allowed for selective deprotection of the silyl group and selective conversion of the bromide into an azide moiety. After in-line purification, the two compounds were reunited and coupled *via* CuAAC employing copper(I)iodine as catalyst and Me_6Tren as basic ligand. The automated flow synthesis system provided a highly pure product output of 2.75 g/hour with a 66 g throughput per day. This was one of the first connecting syntheses with an automated process, which was not based on solid-support protocols.

After having established and elaborated some of the chemical tools that allow the synthesis of such highly defined compounds, their history as well as present strategies of their synthesis are described in the following chapter.

2.4 Sequence-definition and application of sequence-defined macromolecules

Parts of this chapter and following subchapters have been adapted with permission from previous passages written by the author.[224]

The origins of sequence-definition lay, as already discussed earlier, in nature, in which associated molecules fulfill certain tasks only because of their precisely defined structure. Alteration of the latter, be it through physical or chemical influences, inevitably renders their function obsolete. Recently, synthesis of such highly defined macromolecular species came into focus of polymer science and, in the 21th century, this topic has seen increasing output as well as media attention.[225] Driving force of this development is data storage based on organic molecules and not on silicon, as the latter cannot fulfil rising demands in *cold data storage* (data which has to be saved, yet is not required to be retrievable in seconds) due to the immense consumption of silicon as well as energy.[164] First synthetic approaches toward unimolecular and/or sequence-defined molecules date back to 1963, the year in which Merrifield published a first approach to man-made oligopeptides, which were synthesized in a step-wise procedure applying a strategy today known as solid phase peptide synthesis (SPPS) (**Scheme 30**).[22]

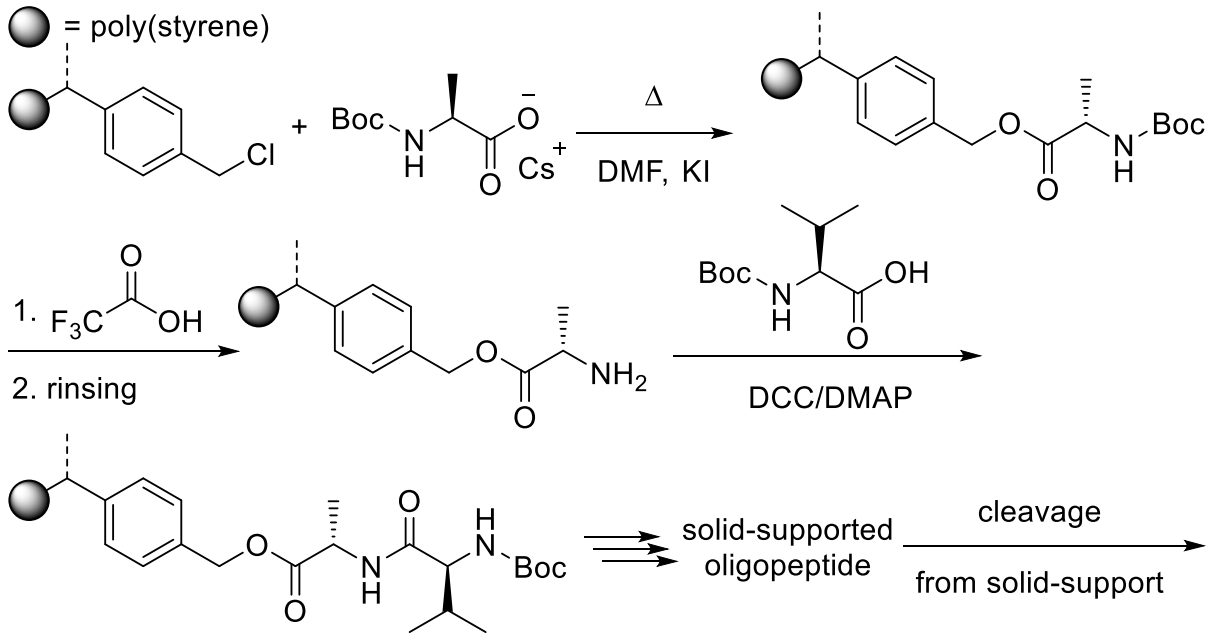

Scheme 30: Simplified solid-support protocol toward oligopeptides. A *tert*-butyloxycarbonyl (Boc)-protected amino acid is reacted with a poly(styrene) based solid-support. Afterwards, the Boc-protection group is cleaved with trifluoro acetic acid (TFA) and the obtained amine is subsequently coupled with another Boc-protected amino acid, which is activated by *N,N'*-dicyclohexylcarbodiimide (DCC) and dimethyl aminopyridine (DMAP). The step-wise procedure is continued and in the end, the obtained polymer bound oligopeptide is selectively cleaved from its solid support.[22]

In the given example, a *tert*-butyloxycarbonyl (Boc)-protected amino acid is reacted with a poly(styrene) based solid-support. Afterwards, the Boc-protecting group is cleaved with trifluoro acetic acid (TFA) and the obtained amine is subsequently coupled with another Boc-protected amino acid, which is activated by *N,N'*-dicyclohexylcarbodiimide (DCC) and dimethyl aminopyridine (DMAP). The step-wise procedure is continued and finally, the obtained oligopeptide is selectively cleaved from its solid support.

Unknowingly, Merrifield set the cornerstone of sequence-defined macromolecules: stepwise procedures with absolute control over the synthesis, and protection group chemistry or alternatively the application of orthogonal reactions. At that time, sequence-definition was solely used for biochemistry, and not applied in polymer sciences. However, the latter had also seen groundbreaking innovations and in the second half of the 20th century, as theoretical knowledge increased and synthesis as well as the corresponding industrial processes of polymers were significantly improved, and finally resulted in higher control over the polymerization process itself.[12,13,16] Yet, sequence-definition cannot even be achieved by the application of highly advanced polymerization techniques.[16,18,19,226] Most of them allow for a high control correlating with a narrow dispersity, but do not reach 100% control as it is necessary for sequence-definition. Hence, the synthesis of unimolecular molecules involves the application of specialized stepwise strategies, which are described in the following chapter.

2.4.1 Basic strategies for synthesis

Absolute control over the reaction and possible side-reactions remains crucial to achieve sequence-definition. Therefore, common protocols employ protecting groups paired with high-conversion and -selectivity reactions or orthogonal reactions as strategy, which are both always carried out in a stepwise procedure coupled with in-between purification. Hence, most syntheses of uniform macromolecules feature a highly specialized iterative cycle of alternating reaction procedures (one, which increases the degree of oligomerization and one deprotecting/connecting reaction) allowing the build-up of precise molecular architectures, either in a linear or bidirectional way. Alternatively, an iterative exponential growth (IEG) strategy can be employed, which is also known as the divergent/convergent approach (**Scheme 31**).[34]

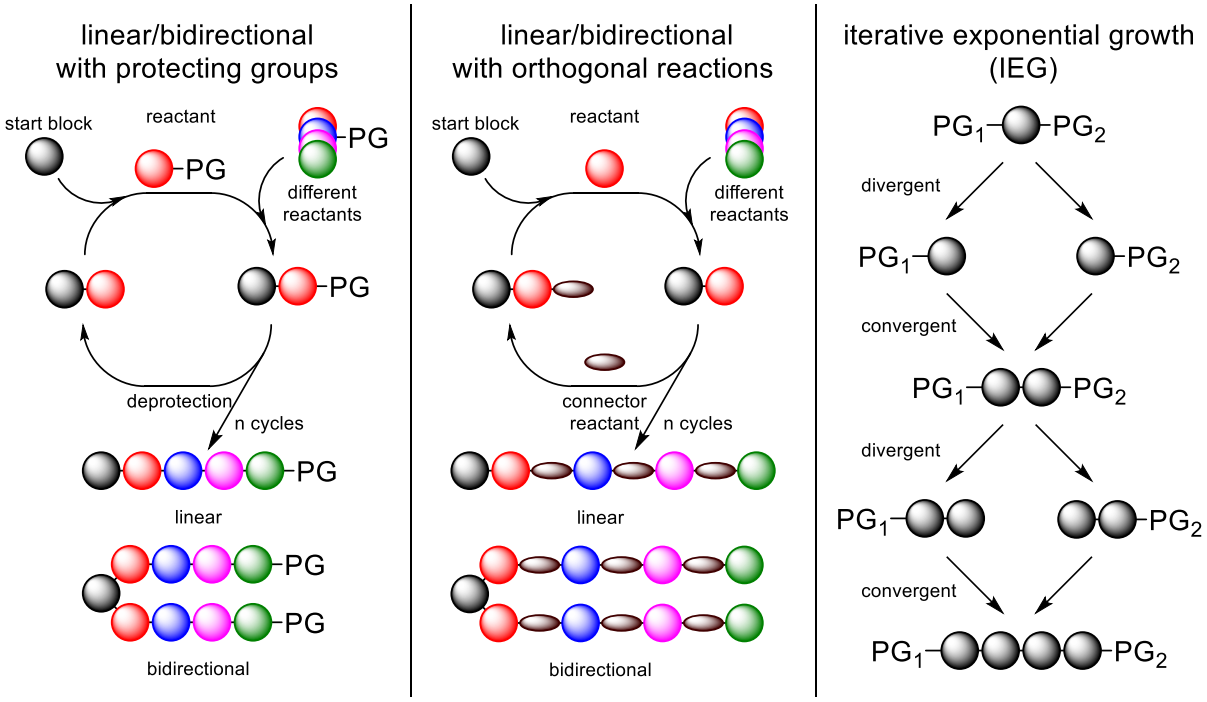

Scheme 31: Overview of the three main strategies toward uniform/sequence-defined macromolecules. Left: Linear/bidirectional approach, which utilizes **protecting groups** (PGs): after initial reaction of a start block with a building block, the isolated product is deprotected allowing for subsequent reactions. After finalizing, a linear or a symmetric bidirectional oligomer is obtained. Middle: Linear/bidirectional approach, which utilizes **orthogonal reactions**: after initial reaction of a start block with a building block, the isolated product is reacted with a connector molecule allowing for subsequent reactions. After finalizing, a linear or a symmetric bidirectional oligomer is obtained. Right: The iterative exponential growth starts from an orthogonally deprotected start block, which is **divergently deprotected** on each side and then **coupled convergently**. As the name states, this approach features an exponential growth in oligomer size (1-2-4-8-16-etc.). Adapted from [34].

In the linear approach utilizing protecting groups, a start block is reacted with a protected building block. After isolation, the protecting group is cleaved allowing for further reactions. The same approach can also be carried out utilizing orthogonal reactions instead of protecting groups. Instead of a deprotection step to restore the reactive functionality for further reactions, the necessary functional group is introduced. Both approaches can also be carried out bidirectionally. As a third option, the iterative exponential growth approach is well established. Here, the start block is functionalized with two orthogonal protecting groups. Subsequently, orthogonal deprotection on either side and subsequent convergent coupling of the separate and differently deprotected batches allows for exponential growth of the molecule.

All three approaches have been exploited toward the synthesis of highly defined structures and can often be individually fine-tuned, if necessary, as each class of uniform macromolecules has their own challenges, which have to be addressed in their

synthesis. Often, solid-supported approaches are compared to in-solution, an issue, which is discussed in a later paragraph of this chapter.[160]

The above-mentioned strategies are specifically bound to the targeted applications of the synthesized sequence-defined macromolecules. In fact, there are two distinct areas of application until now, which are discussed in the following paragraphs: first, the synthesis of sequence-defined macromolecules as tool to evaluate differences and similarities between polymers and their uniform macromolecule counterparts (often termed structure-property-relationship), which are obtained *via* the linear, bidirectional or IEG approach and second, the synthesis of molecules used for data storage or sequencing, which requires applying the linear approach.[23,24,27,35,112,160,227] As of 2009, advances in molecular data storage and sequential reading were predominantly reported with decreasing intervals by the groups of Lutz,[17,21,29,59,228–233] Meier[26,30,31,33,150,157,158,234] and Du Prez.[32,61,160,235]

One of the first scientific works featuring uniform macromolecules in terms of synthetic polymer-related species was published in 1999 by Burns and coworkers.[236] They focused on the synthesis of poly(ethylene glycol)s (PEGs) as such structures are regularly employed for ion binding, but also find application in bio chemistry as PEGs show nonspecific binding of proteins to membrane surfaces.[236] They used protecting groups (tetrahydropyrane (THP) and benzyl (Bn)) paired with good leaving groups (tosylate (OTos), or halides) to synthesize a doubly protected undeca(ethylene glycol). In 2004, Hill reported the first uniform PEG synthesis, while specifically mentioning that they were synthesized employing the IEG approach.[237] Again, mainly THP and Bn were utilized as orthogonal protecting groups and likewise they applied tosylation as tool of activation for the Williamson ether synthesis toward oligo(ether)s. They reported high yields, while maintaining high purities, which were verified by elemental analysis and mass spectrometry. Nonetheless, their length record of a 24mer was already beaten in 2006, when the synthesis of a 44mer PEG was reported.[238]

In 2009, Davis and coworkers reported the synthesis of uniform oligo(ethylene glycol)s, and verified their uniformity employing size exclusion chromatography (SEC) analysis (**Scheme 32**).[239]

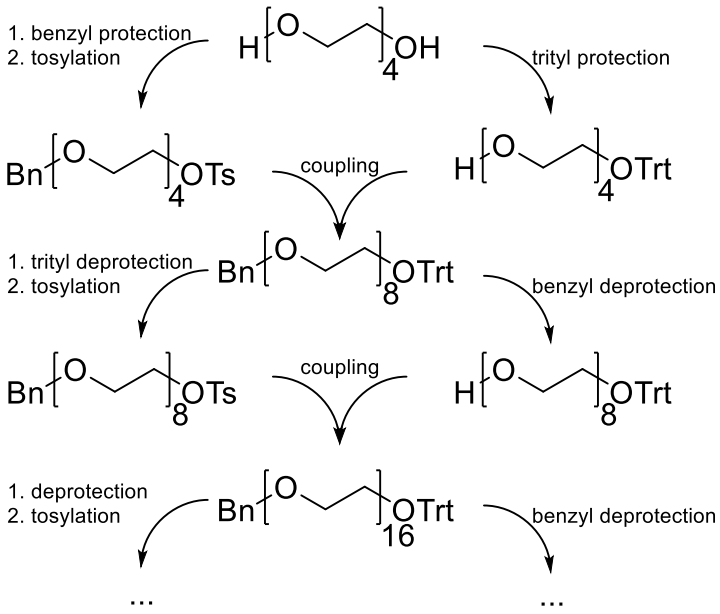

Scheme 32: Scheme of the synthesis toward uniform oligo(ethylene glycol)s, which was applied by Davis and coworkers in 2009. They employed the IEG approach, which features exponential growth of oligomer length.[239]

Recently, a comparative study was published that carefully examined different reported strategies of synthesis toward uniform oligo(ethylene glycol)s.[240] It was demonstrated that SEC is the only reliable analysis method to verify uniformity, albeit it also has its limits, if comparing, for example, a 15mer with a 16mer due to their small difference in hydrodynamic radius.

SEC analysis of uniform macromolecules was not prominent before 2008, when Hawker and his coworkers started the “hype” toward the synthesis of uniform macromolecules (**Scheme 33**).[23] They reported a stepwise procedure based on the iterative divergent/convergent approach toward uniform oligo-(ε-caprolactone) and managed to synthesize oligomers up to a 64mer. They applied orthogonal protecting groups and combined those with the common protocol of the Steglich esterification. The synthesis started with ***ε***-caprolactone, which is opened and monofunctionalized on both ends employing a *tert*-butylsilylether and a benzyl ester as protecting groups, respectively. The coupling was achieved by Steglich esterification, which applies DCC and DMAP. Subsequently, orthogonal deprotection and repetitive coupling allowed for a synthesis of a 64mer. Even at high molecular weight, they reached yields between 80 and 95% and prepared dimer to 64-mer in a multigram scale, which allowed complete characterization with a range of techniques.

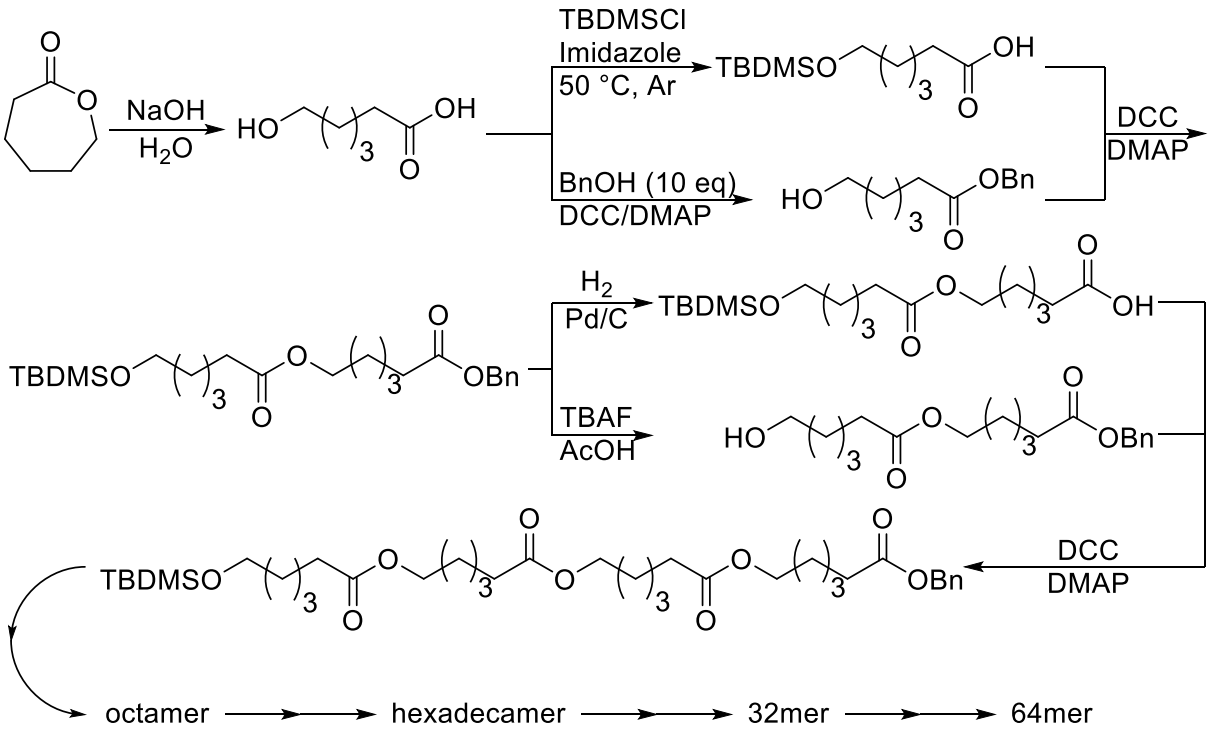

Scheme 33: IEG approach toward uniform oligo-(ε-caprolactone) by Hawker.[23]

As already mentioned in **Chapter 2.3.6**, in 2015 Jamison and coworkers embedded the IEG-approach into an automated synthesis, which was specialized to the CuAAC as coupling reaction.[24] In contrast to Hawkers work, they also prepared additional building blocks, which allowed the synthesis of symmetric AB- and AABB-co-hexadecamers (8 blocks of each species) (**Scheme 34**). They also introduced a further aspect in controlling the oligomeric architecture: a branched building-block. However, the SEC analysis showed a shoulder at higher retention times (smaller size), after they reacted the branched oligomer with an AB-dimer, which is herein suggested to mean that the branched species was probably not fully converted.

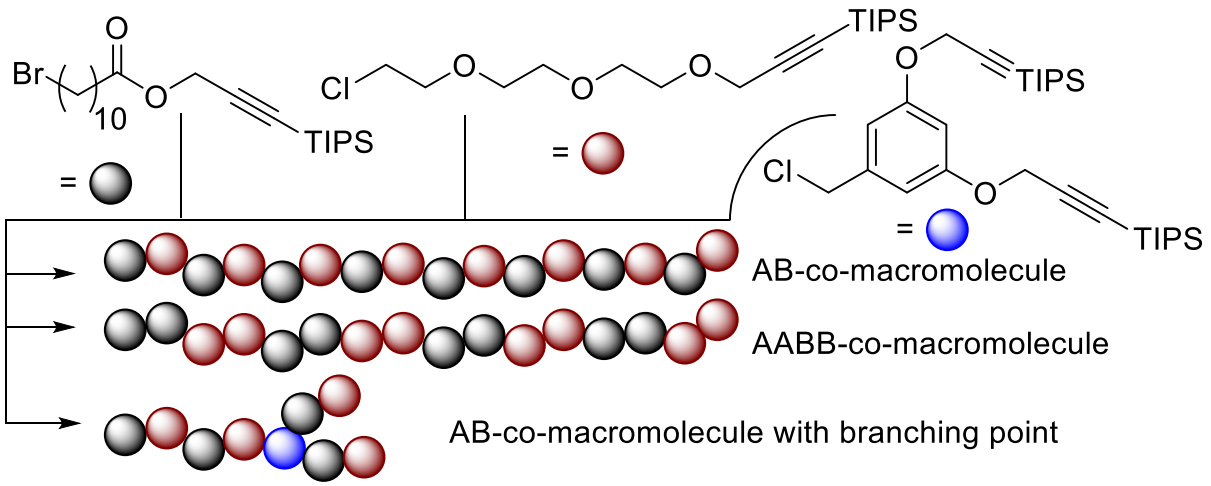

Scheme 34: Jamison and coworkers employed three different building blocks, which allowed them to synthesize different co-macromolecules, and a third one, containing a branching point.[24]

In the following years, however, the focus of synthesizing uniform macromolecules shifted toward a new-found application, when Lutz *et al.* proposed that man-made sequence-defined macromolecules could be used for molecular data storage. His first publications features the whole topic of sequence-controlled polymers as the “holy grail in polymer science”,[18] yet in the next years refinement and advances highlighted that it is sequence-defined macromolecules that allow application in this futuristic approach of data handling. So far, sequence-controlled polymers have found application in biocatalysis, molecular transport, signal transduction, cell signaling and molecular motors.[59] For these, the absolute accuracy of monomer positioning within the polymer was not necessary, yet for data storage it his. Hence, Lutz proposed that such molecules have to be synthesized in a stepwise procedure, which allows absolute control over the reaction, and therefore provides the necessary accuracy for monomer positioning in the chain.[21]

In 2013, Li and coworkers presented one of the first bidirectional approaches toward uniform oligomers utilizing the P-3CR, which allowed synthesis of symmetric macromolecules with precisely defined side-chains (**Scheme 35**).[112]

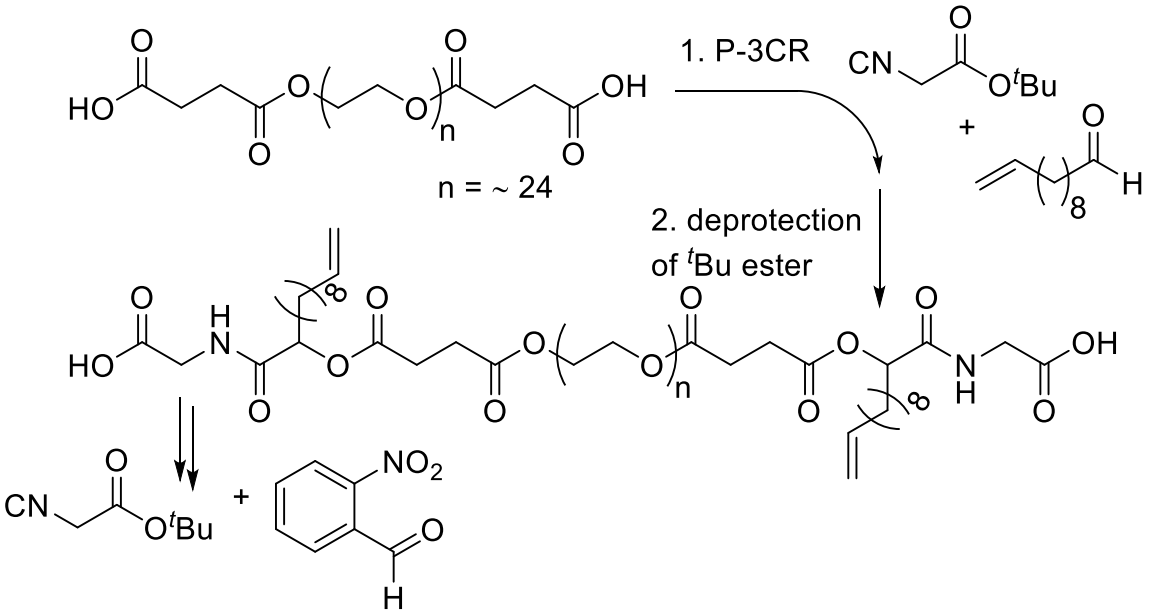

Scheme 35: Schematic representation of the synthetic approach toward highly controlled oligomers utilizing the P-3CR employed by Li and co-workers. Adapted from[112].

They started from a diacid based on commercial PEG, which was functionalized in an iterative cycle using the P-3CR and a deprotection reaction. Herein, varying the employed aldehyde allowed introduction of a sequence. Yet, as the PEG-core still featured dispersity so did the derived macromonomers. Hence, those molecules were only to an extent sequence defined.

In the following year, Meier *et al.* reported the first iterative cycle yielding uniform macromolecules utilizing the P-3CR *via* a linear approach as this allows the synthesis of defined unsymmetric molecules.[157] Instead of relying on protecting groups, orthogonal reactions were applied: a P-3CR employing octadecanoic acid, undecanal and an varying isocyanide was combined with a subsequent thiol-ene reaction utilizing mercaptopropionic acid as linker molecule. This allowed introduction of a new carboxylic acid moiety, which closes the reaction cycle. They synthesized a sequence-defined tetramer weighing 1.6 kDa, which contained four different side chains (cyclohexyl, *tert*-butyl, *n*-pentyl and *n*-butyl). The final molecule was prepared in seven steps with an overall yield of 26%, yet also all intermediates were fully characterized by NMR spectroscopy, mass spectrometry and SEC, to validate the successful synthesis and most importantly the purity of the obtained compounds. Building on the initial success, a similar approach was published in 2015, albeit using the U-4CR as tool of synthesis as it allowed dual side chain control: in the P-3CR only the isocyanide component was varied, whereas in the U-4CR approach both the isocyanide and the

amine were varied. As linking reaction, thiol-ene addition with mercaptopropionic acid was once again employed. The obtained structures were analyzed to certify their uniformity. However, 15% overall yield of the obtained pentamer proved to be quite low and hence restricting in terms of long-chained sequence-defined macromolecules.

In 2016, a novel approach toward sequence-defined macromolecules was published, which addressed the improvable overall yields of previous reports (**Scheme 36**).[26] It was based on the synthesis of an AB-monomer, in which the second functionality (the carboxylic acid) was protected *via* benzylation. Employing the AB-monomer allowed variation of aldehydes and subsequent hydrogenation of the benzyl functionality enabled iteration of the synthesis cycle. Both, P-3CR and hydrogenation proved to give high yields, even as molecular weights of the oligomers increased. Consequently, a sequence-defined decamer featuring 10 different side chains was prepared with an overall yield of 44% after 19 steps. Furthermore, the iterative cycle was carried out in a multi-gram scale as 2.40 g of the final decamer were isolated, equaling about 0.67 mmol. SEC and ESI-MS were employed to prove uniformity. Later, also ^{1}H pulsed field gradient (PFG) NMR spectroscopy studies of the decamer were conducted to evaluate its uniformity.[241]

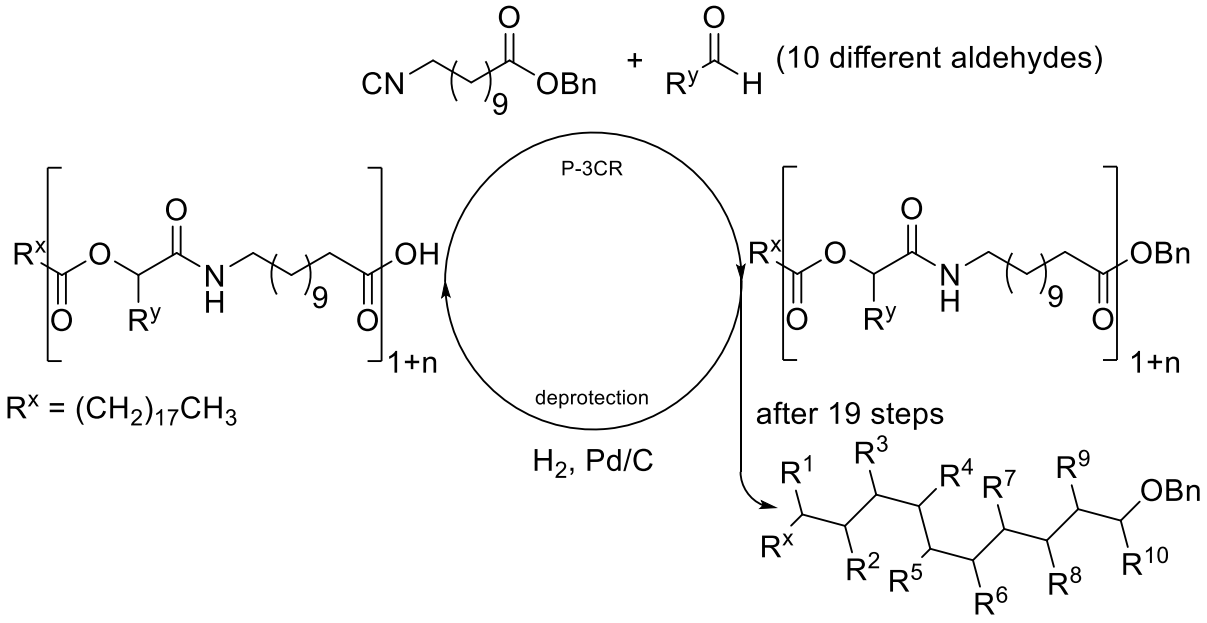

Scheme 36: Iterative cycle toward sequence-defined macromolecules *via* P-3CR and subsequent hydrogenation by Meier *et al*.[26]

This iterative cycle was later applied bidirectionally to evaluate the limits of ring-closing metathesis[35] and it was also improved to allow for dual sequence-control by synthesizing a set of 9 different AB-monomers.[31] There, the backbone as well as the

side-chains were both varied allowing for a denser information content within the molecule.

In 2017, the group of Li reported dual sequence control by exploiting a newfound selectivity of the P-3CR.[159] Two building blocks (AB and AC) were synthesized, which allowed a selective P-3CR by consecutive single additions. Employing those building blocks allowed for rapid alternation of different side chains, as no linking or deprotection reaction is necessary.

Nonetheless, all these approaches share the time-consuming process of purification, which is normally carried out by applying column chromatography. Often the choice is between a more time consuming in-solution approach like the above-mentioned processes, or rather a more resource and time efficient solid-supported or a non-column chromatography-based synthesis, which both will be covered in the next paragraphs before finalizing this chapter by evaluating the main field of applications: data storage and cryptography.

Lutz and coworkers regularly publish about the synthesis of sequence-defined macromolecules with the main goal of applying them as molecular data storage.[25,229–231,242] Therefore, they mostly rely on solid-support synthesis as this allows for a much faster synthesis than in-solution approaches. Furthermore, Lutz *et al.* suggest that high purity is not a necessity for a successful read-out of the sequences by MS, hence SEC data is typically not shown.

In 2019, Meier and Du Prez published studies about a direct comparison of a solid-supported and an in-solution approach, both of which combined the P-3CR with 1,2,4-triazoline-3,5-dione (TAD) chemistry (**Figure 7**).[160] For the solid phase cycle, solely washing was applied whereas in the solution-based approach, column chromatography was employed for purification. In both approaches, the degree of polymerization was nine. Overall yield, purity and scale were superior in the in-solution approach, whereas reaction time and overall required time were lower for the solid-supported approach by orders of magnitude. Contrary to three weeks of synthesis for the solution phase, the solid-phase approach was carried out in merely two days. This comparative study confirmed the predominant assumptions regarding these two synthesis techniques. Hence, choosing one or the other is not only about the time consumed, but rather a more complex balance between the targeted purity, scale of reaction, overall yield and required time in the laboratory. Obviously, the latter three

can be seen as overall resource consumption, as they can be easily translated into actual expenses in terms of an economical value: chemicals have to be acquired, and the work forces have to be paid, which both have to be taken into account when planning to synthesize such sophisticated structures.

	Solid phase	Solution phase
Yield (%)	5	18
Purity (%)	84	>99
Scale (mg)	50	200
Degree of polymerization	9	9
Purification method	Washing	Column chromatography
Reaction time	<5 min,[a] 30-120 min[b]	5 min,[a] 8-48 h[b]
Overall required time	2 days	3 weeks

Figure 7: Direct comparison of solid phase and solution phase approach. [a] reaction time for TAD Diels-Alder reaction. [b] reaction time for P-3CR including purification. Adapted from [160].

In 2016, Anderson and coworkers published a solution-based synthesis of sequence-defined hydroxyproline-based oligo(carbamate)s, which exploited fluorous solid-phase extraction (FSPE) as method for purification.[243] Therefore, as starting material a fluorinated hydroxyproline was employed, which allowed rinsing of the non-fluorous impurities that were generated over the course of synthesis. The reaction mixture was subjected to fluorous silica and impurities were rinsed by applying a mixture of methanol/water. Afterwards the fluorous products were eluted by employing pure acetone. Consecutive high yields and purities were achieved and finally a 91% pure sequence-defined hexamer was obtained with the impurity being unreacted pentamer, thus effectively combining the benefits of both the solid-supported (*i.e.* purification) and solution-based (e.g. high yields) syntheses. Applying fluoro-tagged starting materials was later taken up by Meier *et al.* to synthesize molecular passwords, which, however, were not sequence-defined macromolecules, but rather small sized molecules obtained *via* a single U-4CR.[30]

In 2019, Gao and coworkers reported the scalable synthesis of positively charged sequence-defined functional polymers in a bidirectional fashion (**Scheme 37**).[27] Uniform and also sequence-defined macromolecules were synthesized.

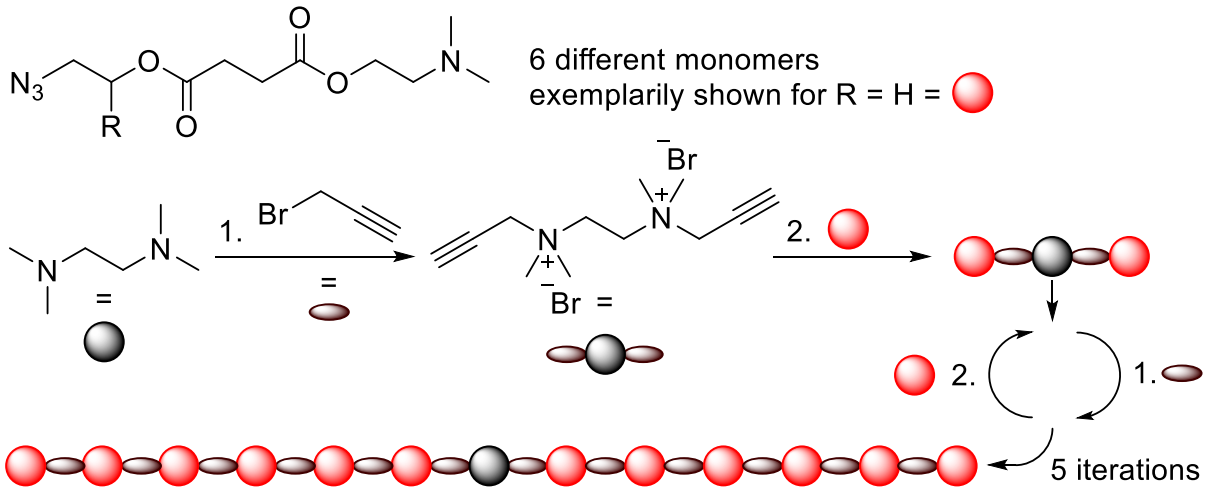

Scheme 37: Bidirectional synthesis of uniform oligomers baring quaternary ammonium groups in the backbone. The latter was exploited to purify the product *via* precipitation and subsequent centrifugation. By employing 6 different monomers, also sequence-defined macromolecules were synthesized.[27]

Solution-based approaches discussed so far heavily rely on column chromatography as means of purification. Gao however, established a solution phase protocol that featured simple precipitation and centrifugation as method of purification. Hence, the time consumed by purification was comparable to solid support-based approaches. Furthermore, they maintained high yields (overall yield: 68% over 12 steps, 96.8% average yield per step) and excellent purity. NMR spectroscopy, SEC and matrix-assisted laser desorption ionization-time of flight (MALDI-ToF) experiments were conducted to characterize the compounds and confirmed the uniformity. They were also able read-out the sequence *via* fragmentation spectrometry. Hence, these molecules were deemed useful for application in information transmitting and reading. Furthermore, it was suggested that due to the water-solubility of the positively charged molecules bio applications such as condensing DNA or drug delivery are possible.

More recently, an approach toward sequence-defined polyurethanes (PU) was published that were then used to build up 3D-networks *via* subsequent thiol-ene reactions.[244] Similarly to the work of Gao, they did not employ column chromatography for purification, but rather developed an iterative cycle in which solely washing was applied as a time- and resource-saving alternative. As sidechains, either methyl or allyl groups were introduced. Finally, three PU-oligomers with distinct sequences were

synthesized and characterized by HPLC, NMR spectroscopy, mass spectrometry, before ultimately being converted to networks.

Approaches that apply column chromatography have also seen advances in the last years. In 2019, Junkers reported quasi-uniform-sized poly(methacrylate) (PMA) ($Đ$ = 1.005 – 1.040), which was obtained *via* flash column chromatography of its disperse equivalent ($Đ$ = 1.130).[245] As such, the limitations of chromatographic polymer separation are evaluated and discussed, stating that separation of polymeric and oligomeric species becomes increasingly difficult with increasing size (degree of oligomerization). This was attributed to minimal differences in affinity between the oligomeric species. However, in 2020 Kim *et al.* reported a synthesis of sequence-defined macromolecules, cyclic and co-oligomers, *via* the IEG approach, which overcame this issue (**Scheme 38**).[28]

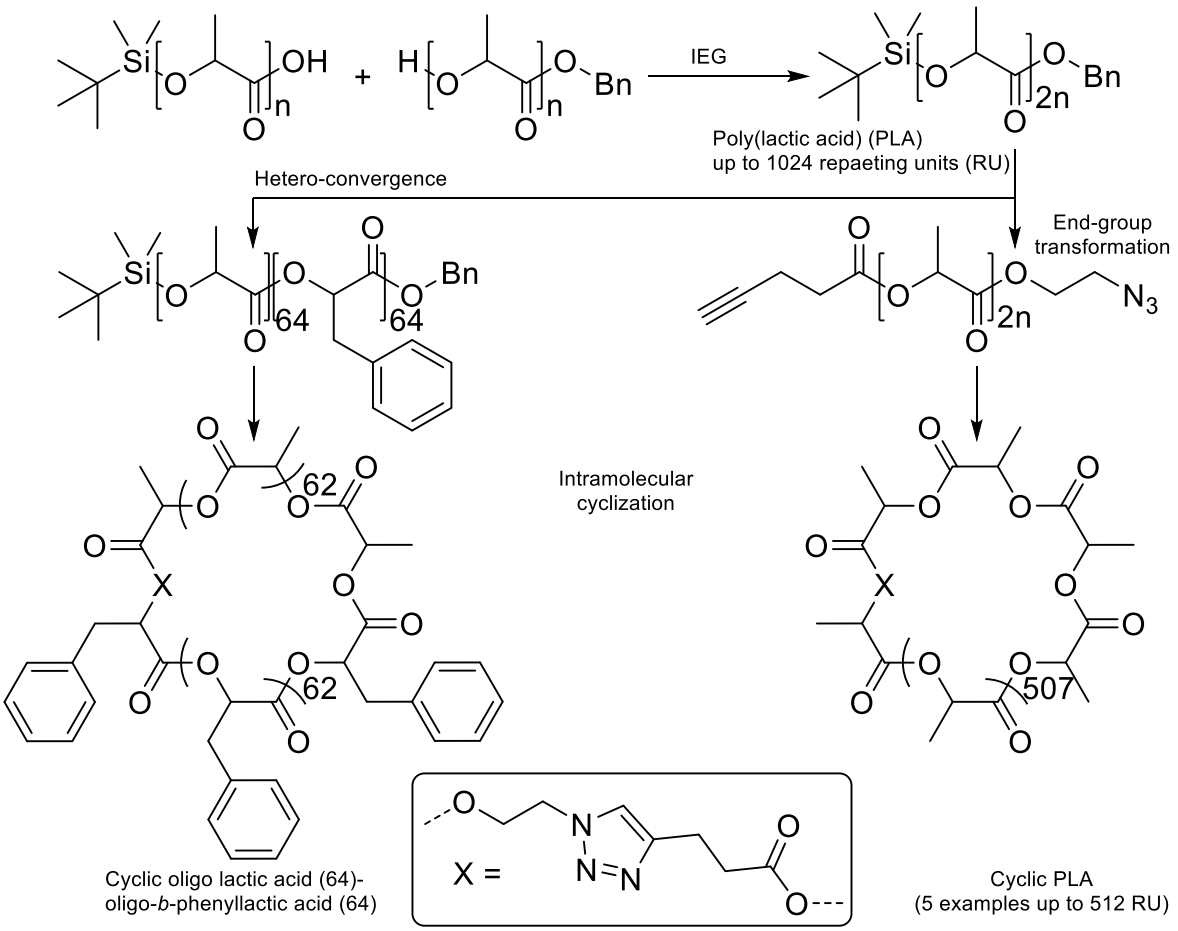

Scheme 38: Synthesis of uniform macromolecules *via* IEG. Subsequent end-group transformation allowed for intramolecular cyclization. For the larger species, preparative SEC was used for purification.

While early stages with low molecular weight were separated with standard column chromatography, larger oligomeric species were purified *via* a preparative SEC

system. As their synthesis protocol featured exponential growth, the hydrodynamic radius of the respective molecules drastically increased from step to step in late stages of their synthesis, allowing for easy separation in an automated system. Hence, a 64-64-co-oligomer and a homo-512mer were prepared and converted to their cyclic equivalents by internal cyclization. The oligomers were synthesized *via* Steglich esterification, whereas for the final ring-closing CuAAC was employed.

Furthermore, Kim and coworkers used this IEG approach to synthesize information containing sequence-defined copolyesters and hence, also sought to employ molecules as potential media for data storage.[246]

2.4.2 Sequence-defined macromolecules in data storage

As previously mentioned, molecular data storage is inspired by DNA, which is the only natural data storage system discovered so far. The complex interplay between DNA and proteins allows nature not only for the synthesis of such sophisticated structures, but also the read-out and replication. Contrary to the binary system used by computers, nature relies on the four nucleobases adenine, cytosine, guanine, and thymine. Hence, a sequence-defined tetramer, which used these nucleobases as sidechains, would contain 8 bits. This is a result of to the logarithmic character of the system and is explained in the following three equations.[31]

$$\left(n_{permutations}\right) = \left(n_{variations\ per\ repeating\ number}\right)^{degree\ of\ oligomerization} \qquad \text{(eq. 1)}$$

$$bit = \frac{\log\left(n_{permutations}\right)}{\log(2)} \qquad \text{(eq. 2)}$$

$$8\ bits = 1\ byte \qquad \text{(eq. 3)}$$

Already in 2013, Lutz *et al.* mentioned that DNA data storage surpasses the commercial silicon based one and that also man-made data-containing macromolecules allow for a much higher information density.[59] Hence, a variety of strategies aiming to develop synthetic macromolecules as media for data storage were developed. Key element of these syntheses is the iterative build-up of a linear oligomeric chain, which contains information on a molecular level just like DNA. Crucially, a second criterion is the read-out of the sequence-defined macromolecules often conducted *via* ESI-MS/MS. The synthesis of information-containing molecules, which find their origin in the binary system, is depicted in **Scheme 39**.[229]

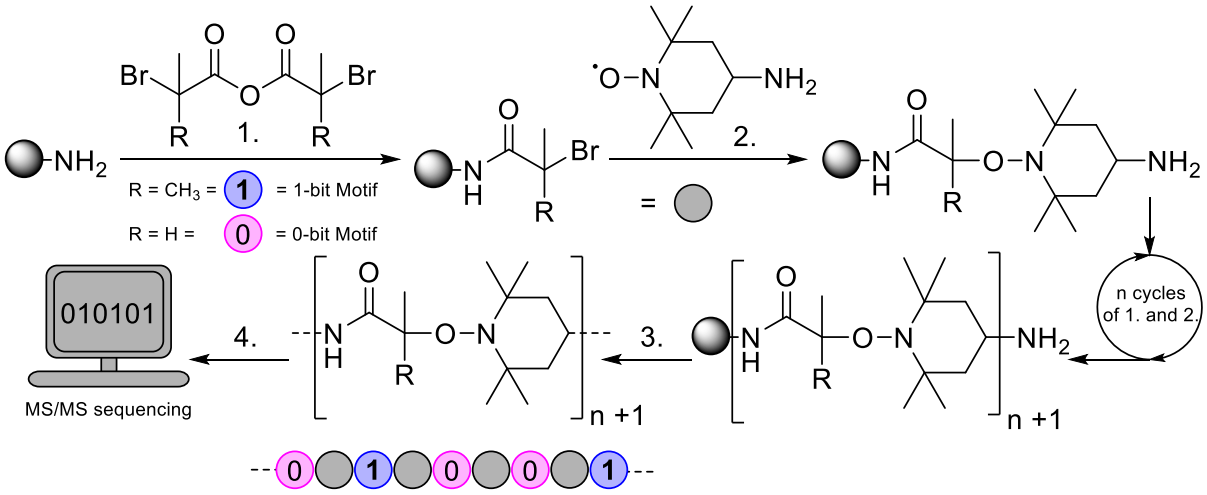

Scheme 39: Iterative solid-supported synthesis of an information-containing macromolecule. Sidechains, which resemble the 1-bit/0-bit motif used in binary data storage, are used. Subsequent, cleavage of the sequence-defined oligomer allows for sequential read-out *via* MS/MS. Adapted from [229].

The authors developed a synthesis applying an information-containing anhydride (its sidechain is either hydrogen or a methyl group) as well as amino-functionalized 2,2,6,6-tetramethylpiperidinyloxyl (TEMPO) to establish an iterative procedure toward monodisperse macromolecules. The starting material was a solid support, from which the oligomer was built and later cleaved for subsequent analysis *via* ESI-MS/MS. They state that theoretically any sequence could be written in these macromolecules and managed to synthesize a 12mer, which corresponds to 2^{12} = 12 bits or rather 1.5 kB of information. Nonetheless, the read-out was only possible for small chains. Hence, poly(alkoxyamine phosphodiester)s were used instead of the poly(alkoxyamine amide)s as they proved to be more reliable and offered greater potential.[25,231,232,247] Lutz and coworkers also improved the read-out by designed inter-byte fragmentation to be able to read longer sequences.[29] Data storage density, however, does not only increase by prolonging the oligomers, although length is the most influential factor (confirmed by eq. 1). Additionally, increasing the variants of molecules used to build up the oligomers greatly increases data density. As already mentioned, in DNA, four different information containing molecules can be found (max. storage density of 2 bits/monomer), however in non-natural sequence-defined oligomers even higher numbers can be achieved. In 2015, a system that relied on binary dyads was implemented. They were based on four different building blocks greatly simplifying the data extraction and therefore allowed for an increase in storage density.[231] In the following years, Lutz and coworkers improved these building blocks and finally utilized a coding library, which was based on either 4 or 8 phosphoramidites, equaling a

storage density of 2 or 3 bits/monomer.[247] They were able two encode pictures with sizes ranging from 80 to 144 pixels into macromolecules and were still able to decode the information *via* electrospray pseudo-MS^3 sequencing. It was stated that "a macromolecular storage capacity of 144 bits per chain was achieved […], which is the highest capacity ever attained for a synthetic informational [macromolecule]."[247] However, Lutz also states: "A few examples […] have been reported, with theoretical storage densities ranging from 2 to 24 bits/monomer."[61,150,231,247,248] These publications all feature an expanded alphabet of molecules, which introduce information into the macromolecule. Hence, the theoretical length to store the same amount of data as in a system relying on 4 or 8 building blocks is far lower, giving excess to other applications such as cryptography or[31] molecular pin codes.[32]

In 2014, when Meier *et al.* implemented multi-component reactions as a valuable tool toward uniform sequence-defined macromolecules.[157] However, the first approaches which utilized either the P-3CR or U-4CR coupled with subsequent thiol-ene addition showed moderate to good yields and thus were not optimal for the synthesis of larger oligomers (only a tetramer/pentamer were obtained).[157,158] In 2016, these drawbacks were addressed (**Chapter 2.3.4**) when an alternative system relying on P-3CR and subsequent hydrogenation was employed toward the synthesis of sequence-defined macromolecules.[26] In this work, a decamer bearing ten different sidechains (they were introduced by varying the aldehyde component in the P-3CR) was synthesized, which corresponds to 10^{10} = 10,000,000,000 permutations = 33.22 bits. In 2020, the same strategy was further improved by synthesizing 9 different backbone molecules, the number of aldehydes utilized was increased to 11 and a tetramer was synthesized.[31] By only varying the backbones or sidechains either 9^4 = 6561 permutations = 12.68 bits or 11^4 = 14.641 permutations = 13.84 bits would be possible. However, by combining the two strategies, the data density significantly increased to $(9 \times 11)^4$ = 96,069,601 permutations = 26.52 bits for a tetramer and peaking at $(9 \times 11)^9 = 9.14*10^{19}$ = 59.7 bits for a theoretical nonamer. A novel publication even features the read-out of mixtures of uniform sequence-defined macromolecules, which further increases the data-storage capacity.[249]

However, all these publications focus on writing data into molecules and improving automated read-out of the synthesized sequences. Yet, if compared to their natural counterparts – DNA and proteins – they leave one key component behind. Not only does nature encrypt information into its macromolecules, but also the sequence of the

natural building blocks, e.g. amino acids, influences the 3D-structure of the molecules (**Chapter 2.2.2**). Hence, the molecular sequence of amino acids in proteins is far more than just an information-containing sequence as it alters shape and subsequently also the function of the whole protein. As this is strongly bound the (self)-assembly of molecules, this key feature resembles sequence-definition not only within a chain but rather in the third dimension as interaction between molecules and within.

2.5 Sequence-definition in the third dimension

As discussed in **Chapter 2.2**, DNA and proteins are the key molecules of life on earth. Herein, sequence-definition enables structure as well as function. Thus, the inevitable question arises, if also man-made macromolecules allow for these features. In 2020, Lutz published two philosophical essays toward synthetic life based on sequence-defined macromolecules.[250,251] At the moment, this may seem futuristic, but nevertheless his thoughts, which are based on our current knowledge about DNA, deliver the key elements necessary for such a sophisticated project (**Figure 8**).

Property	Molecular reason
Information storage	Controlled nucleotide sequence
Hybridization	Supramolecular base-pairing
[(Self-)assembly]	Conformation, supercoiling
Self-replication	Template enzymatic polymerization
Transcription	Enzymatic polymerization
Random mutations	Depurination, deamination, dimerization[a]
Repair	Mostly enzymatic
Epigenetics·	Methylation, hydromethylation[a]

Figure 8: Important features that make DNA a life-bearing macromolecule. [a] The listed terms are examples of more complex mechanisms. Adapted from [251].

All of those features are important yet discussing them in detail would reach too far. Hence only three will be evaluated further: Information storage, hybridization and (self-)assembly. Information storage has already been covered in **Chapter 2.4.2**, whereas the two other categories remain unanswered regarding man-made macromolecules.

For this thesis and its short outlook, hybridization and (self-)assembly will be combined into the generic term *structure* or rather *3D-sequence-definition*. Also, proteins are evaluated as they offer more structural diversity than the predominant double-helix of DNA. It has already been established that peptides arrange into secondary, tertiary

and quaternary structures (**Chapter 2.2.2**). They do so, because of complex inter- and intramolecular interactions based on certain functional groups (carboxylic acid, amine, hydroxy, thiol *etc.*) that allow for van-der-Waals-, hydrogen bridge-, dipole- and ionic bonding.[15] Ultimately, the sequence of amino acids will dictate how those chains will coil or fold and structure themselves in the three dimensions. However, what is easy to understand in theory, is hard to prove or rather to validate. Encrypting proteinic structures has remained one of the most difficult tasks in science and even computer based calculations have their limitations due to the necessity of massive computing power, yet progress is constantly made.[252] The same is for molecules like lipids or cyclodextrins, which are also known to form interesting supramolecular structures.[253] However, a wealth of knowledge has been accumulated based on the self-assembly of block copolymers.[254] These serve as role models to molecular interaction, which is derived from their macromolecular structure, but also the properties of their subunits. Sequence-controlled polymers in particular have added a lot to the current understanding in this area of research.[44] However, the molecular interactions of such polymers are often random or rather just dictated by their general structure. Proteins on the other hand, are complex three-dimensional structures and whose interactions (inter- and intramolecular) are based on the strategically positioned groups. Hence, their assembly is far more sophisticated than in other polymers. This is why besides simple block copolymers, also dendrimers and star-shaped polymers are listed as keys toward understanding supramolecular structuring of organic matter, as their architecture is globular.[36,255,256] Especially the latter have not been explored in a sequence-defined approach and hence offer new insights in their structure-property relationship. Hence, the theoretical background of this thesis is concluded with a short overview about synthetic approaches toward, and applications of, dendrimers and star-shaped macromolecules (**Chapters 2.5.1** and **2.5.2**).

2.5.1 Dendrimers

Dendritic structures came into focus in the last quarter of the 20th century. The first procedures followed the divergent approach and were conducted by Vögtle *et al.* in 1978,[257] and in the following years several patents and reports on dendrimers were published.[258–262] In 1990, Hawker introduced a convergent synthesis (**Scheme 40**, **Scheme 41**).[263] In the divergent synthesis starts with a multifunctional core **A** (at least three reactive functionalities), which is extended outward by iteratively reacting it with

a specialized building block. This allows for exponential branching and subsequently yields the dendrimers G1, G2 and G3.

The convergent synthesis features the build-up of so-called dendrons. Herein, the start molecule will find itself on the surface of the sphere in the final molecule and hence the reactions proceed inward. In a final step, these dendrons are coupled to a multifunctional core utilizing their focal point **E** to obtain the dendrimer.

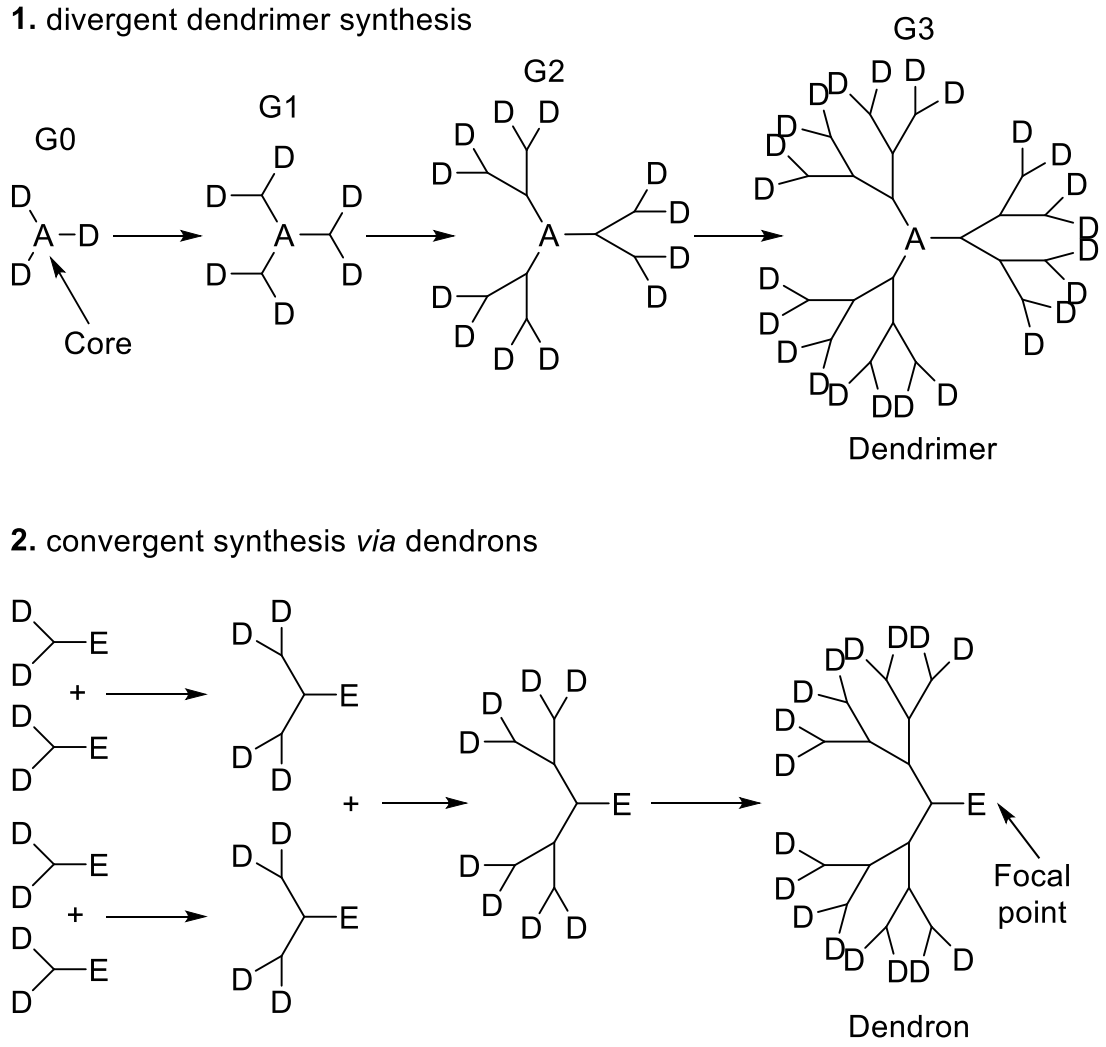

Scheme 40: 1. Divergent synthesis of dendrimers. **A** resembles the initiating core molecule, D are reactive sites. 2. Convergent synthesis of dendrons. **E** is called focal point.[264] The respective dendrimer is obtained in a final coupling step, which attaches the dendrons to a multifunctional core moiety (**Scheme 41**).

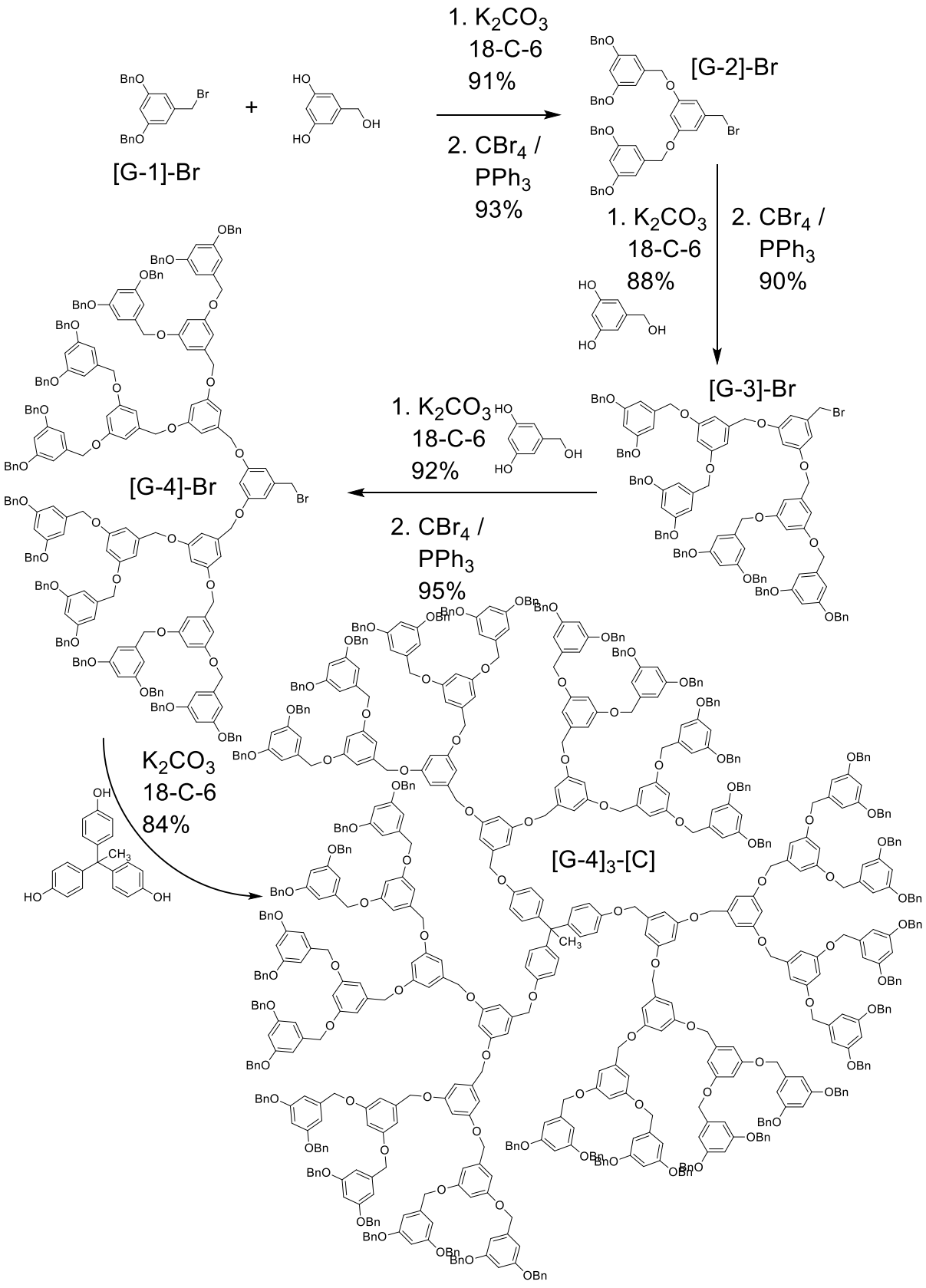

Scheme 41: First convergent synthesis of dendrons [G-1-3] and a dendrimer $[G\text{-}4]_3$-[C] published by Hawker *et. al.* in 1990.[263] Even larger dendrimers than the pictured $[G\text{-}4]_3$-[C] were reported, however were not displayed due to reasons of clarity.

The convergent synthesis started with a di-benzylether-substituted benzyl bromide [G-1]-Br, which was reacted with 2,4-dihydroxybenzyl alcohol utilizing potassium carbonate and 18-crown-six ether (18-C-6) in a simple Williamson ether synthesis. Afterwards the unreacted hydroxy function was converted to a bromide by applying tetrabromo methane and triphenyl phosphane in an Apple reaction. This yielded the dendron [G-2]-Br, from which the synthesis was continued toward [G-3]- and [G-4]-Br by iterating the aforementioned protocols. Finally, the dendron [G-4]-Br is coupled with 1,1,1-tri(hydroxyphenyl)ethane to yield the dendrimer $[G\text{-}4]_3$-[C], a monodisperse structure with the molecular formula $C_{671}H_{576}O_{93}$. It was analyzed by NMR spectroscopy as well as SEC and exhibited a $Đ$ = 1.02. Next to this dendrimer, also the successful synthesis of the even larger species, $[G\text{-}5]_3$-, $[G\text{-}6]_3$- and $[G\text{-}6]_3$-[C] were reported within this publication. The latter exhibits a molecular mass of over 40000 g/mol and has remained one of the largest monodisperse structures ever made.

Since then, publications in this field have increased tremendously and feature but are not limited to the synthesis of metallodendrimers,[265–270] dendrimers *via* 'click' chemistry[222,271,272] and multi-component reactions.[273–279]

Dendrimers are known for their symmetric and spherical structure and should by definition be monodisperse and hence highly defined compounds. Developed in the late 20th century, they were already a well-studied topic, when the topic sequence-control and sequence-definition in macromolecules was only emerging. The properties of dendrimers are mostly a result of the functional groups on their molecular surface, however, also internal functionality has been implemented,[280–282] often toward biochemical applications like encapsulation of guest molecules with subsequent isolation of the active site and biomimicking.[283,284] Often drugs are hydrophobic compounds with low water-solubility, and hence absorption into the bloodstream is restricted. This often limits their potential and can even be responsible for negative side effects, which are a result of the necessary overdose of the drug to achieve its wanted effect. However, functionalizing the molecular surface of these highly defined structures has also enabled water-solubility. This phenomenon is surprising as generally only few polymeric structures exhibit water-solubility (e.g. PEGs). However, dendrimers that are functionalized with hydrophilic moieties on their outmost sphere have shown unimolecular micellar behavior with the ability to carry hydrophobic payloads in aqueous solutions and hence allow for application toward drug delivery systems.[285,286] Thus, these water soluble dendrimers are prime candidates for applied

host-guest chemistry as they are capable of encapsulating drugs or solubilizing drug compounds.[287–292] Additionally, the size of dendrimers can be precisely tailored as they are uniform per definition, which fosters their application in biomedicine. Often drugs are functionalized with PEG to increase their size, which prolongs their length of stay in hosts before they are eliminated. However, if their hydrodynamic radius is increased too much, unbeneficial side-effects can occur supporting the need of uniform, structures for biomedical applications. Furthermore, introduction of binding motifs in such well-defined structures can help to control the area of effect, e.g. by specialized surface functionalization of dendrimers. Hence, latest research on dendrimers often focusses on tailoring and manipulating those structures to employ them as drug delivery systems[293,294] and even target specific carriers.[295–297] Various publications and reviews allow for deeper insights.[256,264,298–305]

2.5.2 Star-shaped macromolecules

Star-shaped macromolecules represent the simplest class of branched polymers and generally consist of a core unit baring three or more linear chains. Hence, it is the branching point in the chains, where star-shaped macromolecules and dendrimers differ from each other. Likewise to the latter, they represent a unique sub-class of macromolecules and come with a variety of different properties allowing for a broad area of applications, which are based on their special shape. These are discussed later in this paragraph.

The first report on star-shaped macromolecules dates back to 1948, when Schaefgen and Flory published a synthesis toward star-shaped polyamides/polyesters. They employed amino acids or hydroxy acids together with a small amount of a multifunctional core molecule, which was either a “polyamine” or “polycarboxylic acid”.[306] Furthermore, six years after Szwarc published his results on polymerization,[16] his ground breaking discovery was employed to synthesize star-shaped macromolecules by Morton *et al*. in 1962.[307] Since then, all kinds of synthesis strategies have been developed to obtain star-shaped macromolecules and active research on their unique properties is being conducted toward specialized applications such as gene- and drug delivery, as nano reactors or in phase-transfer catalysis.[36,308–310] Generally, there are two well-established procedures to synthesize star-shape macromolecules, which are termed arm-first (convergent approach) or core-first (divergent approach) (**Scheme 42**).[36]

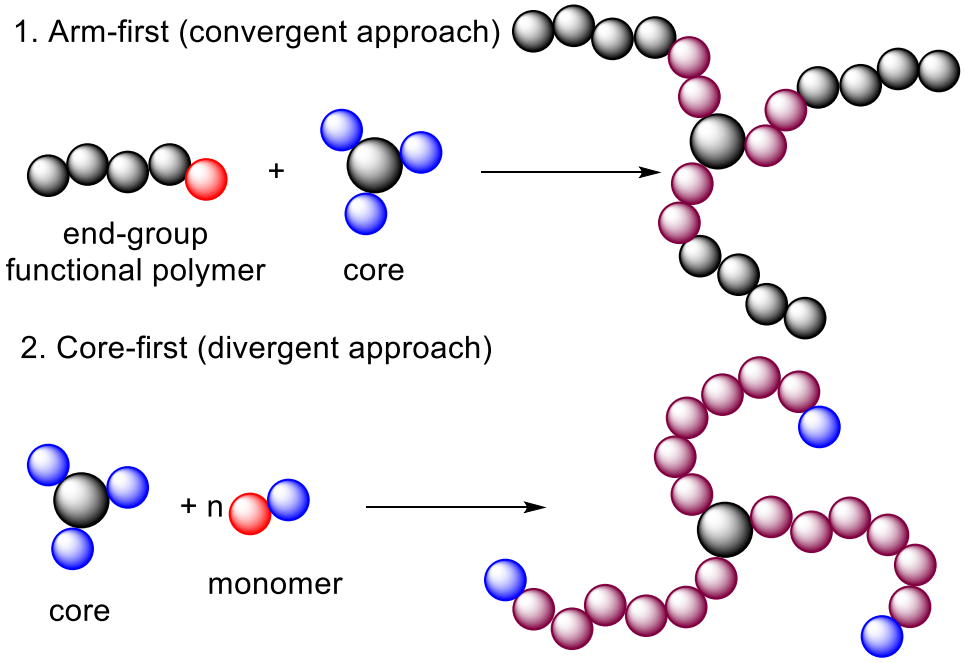

Scheme 42: 1. Arm-first approach toward star-shaped macromolecules; pre-synthesized arm (end-group functional polymer) and core are connected in a final coupling. 2. Core-first approach. The core molecule acts as multi-functional initiator from which the arms are polymerized. Blue and red represent functionalities, which become violet when reacted with each other.[36]

The arm-first approach is considered the more elaborate route of synthesis, as it consists of two parts: first, the synthesis of the arms, and second coupling of arm and core. In contrast, the core-first approach starts from a core, which acts as the polymerization initiator, and hence the procedure consists of only one step. However, synthesis of a suitable core,[306,311] monomer[312] and possible post-polymerization functionalization also must be taken into account.[37] Hence, choosing between one or the other is often more complex than just evaluating the total amount of steps, which are necessary for the synthesis to be completed. This recurs in **Chapter 4.3** of the results and discussion, in which both strategies were employed and compared to each other.

Next to the variable synthesis routes, several different architectures of star polymers are also known from the literature (**Figure 9**). Star-shaped macromolecules that bear arms consisting of the same polymer backbone and all at roughly the same length are generally termed as *homo star polymers* akin to their linear counterparts.[36,312] Consequently, also *star-block copolymers* are known, which can be either synthesized by a single 'living' polymerization with differing monomers being sequentially added or rather a combination of techniques or even post-polymerization functionalization.[36,37,313] However, the term *functionalized stars* refers to star polymers

with either functional groups along the chain (in-chain) or at the end (end-functionalized stars). These often serve as role models to evaluate fundamental properties like chain dynamics as well as absorption and association.[314]

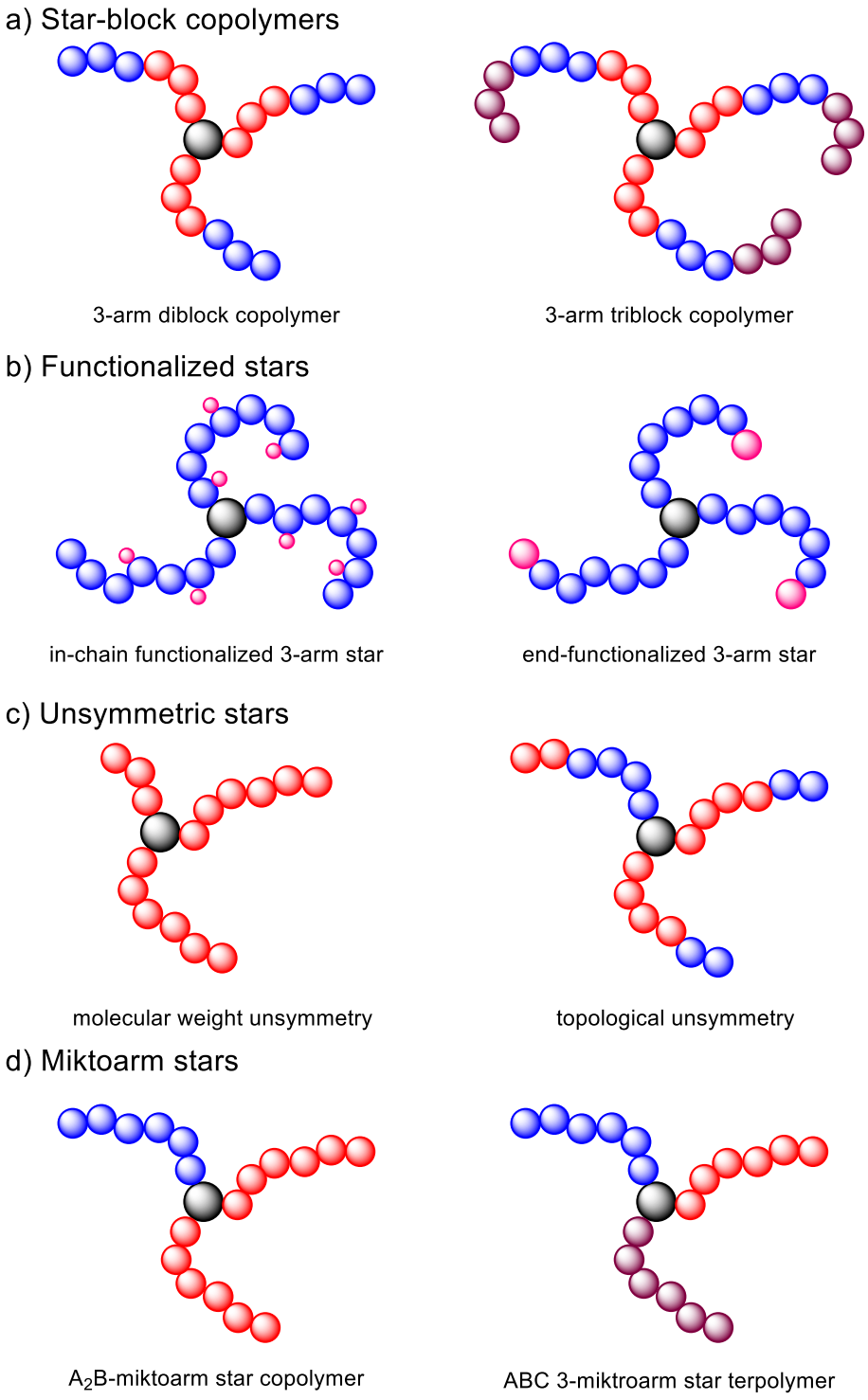

Figure 9: Examples of different star polymer architectures. Adapted from [36]. Red, blue and violet represent different topologies, whereas pink is a reactive functionality.

As also symmetry plays a key role in molecular/polymer interaction, the synthesis of unsymmetric stars has emerged in literature involving molecular weight-, functional

group- or topological unsymmetry in the arms.[36] Finally, so-called miktoarm stars were developed to give further insights to the complex interactions deriving from polymeric architectures. Miktis is derived from the Greek word μικτός and translates to mixed. Hence, miktoarm stars bear chemically different arms and can occur in a variety of designs.[36,315,316]

Syntheses of star-shaped macromolecules feature the application of 'living' anionic-, or cationic,[317,318] reversible deactivation radical polymerization (RDRP),[319–321] group transfer polymerization,[322] ROMP,[323] as well as 'click' and[324–326] multi-component chemistry,[37,38,224,312] or even a combination of techniques.[327] Hence, backbones and architecture of star polymers are as diverse as their synthesis and therefore allow for high tunability toward their targeted application. Next, the synthesis of star polymers *via* MCRs is depicted in **Scheme 43**, as a significant part of the thesis is dedicated to this approach.[37]

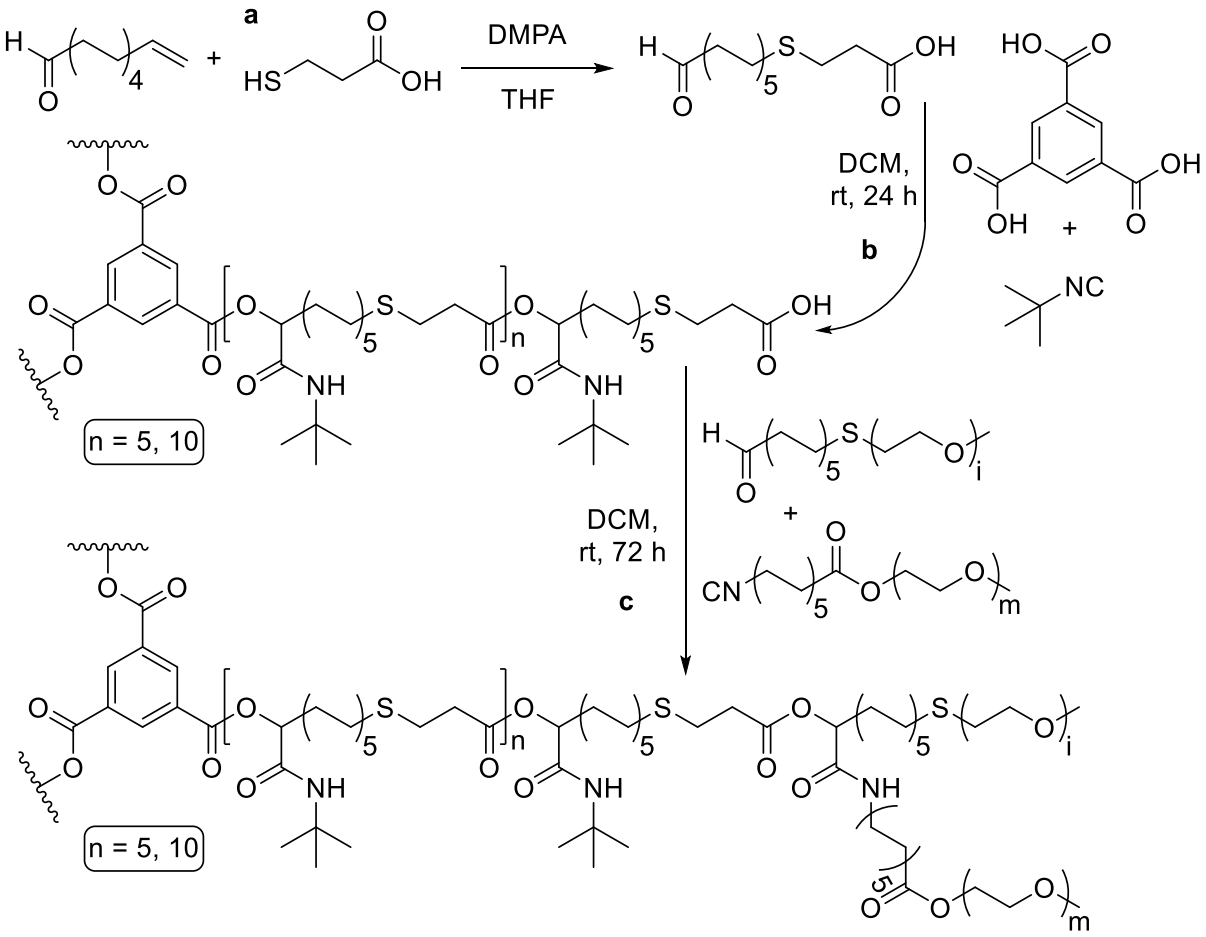

Scheme 43: a: Synthesis of an AB-monomer *via* thiol-ene reaction. **b**: Synthesis of a star homo polymer *via* P-3CR polymerization. **c**: Post-polymerization modification with PEG-bearing aldehyde and isocyanide toward amphiphilic star-shaped block copolymers.[37]

In this study, the authors described the synthesis of an AB-monomer bearing an aldehyde as well as a carboxylic acid as functionalities. Employing the monomer together with an isocyanide and a multifunctional core molecule (in this case a benzene-1,3,5-carboxylic acid) allowed for synthesis of a homo star polymer *via* a P-3CR polymerization.[312] Subsequent post-polymerization modification with a PEG-bearing aldehyde and isocyanide yielded star-block copolymers in good yields and with moderate dispersity (*Đ* = 1.23 and 1.40). These star-block copolymers showed amphiphilic character due to their hydrophilic PEG shell and the hydrophobic core and hence were employed for phase-transfer experiments using the organic dyes Orange II and Para red.[37] It was demonstrated that the polymers were able to encapsulate the Orange II dye molecules and transport them into the organic phase (DCM), in which they are normally insoluble. In a following publication, even star polymers with four arms were synthesized and oxidation of the sulfide moieties in the backbone to their respective sulfones was introduced as a second post-polymerization modification. Encapsulation and targeted release of Azithromycin, which is a semisynthetic macrolide antibiotic, was evaluated.[38] With these experiments, it was demonstrated that the antibiotic was successfully encapsulated and that a selective release is possible *via* the alteration of the pH-value. It was also shown that the polymers are not cytotoxic and hence allow for an *in vitro* application.

Drug delivery is not the only, however one of the main targeted applications of star polymers.[316,328–330] They are also employed as thermoplastics[331] and catalysts,[332] in biomedicine,[333,334] and other applications such as nano structured thin films, nano reactors or even in industry.[36,310]

It is therefore evident that despite the increased synthetic effort required for the synthesis of star polymers their structural uniqueness endows them with properties otherwise unattainable. Since their initial discovery in the middle of the 20th century, progress has been made at a steady pace. However, despite significant advances in the field, the structure-property relationships of star polymers are rarely described. Therefore, the synthesis and characterization of uniform star shaped macromolecules can serve as pioneering field of research to achieve novel insights to the inter- and intramolecular interactions of these highly defined three-dimensional structures and establish said structure-property relations, which result from their targeted uniformity.

3 Aims

The main objective of this thesis is a synthetic evaluation and a preparative investigation of novel approaches and applications of isocyanide chemistry. The thesis is divided into three main topics:

1. The evaluation and improvement of isocyanide synthesis regarding its sustainability (employed solvents, base and dehydrating agent) as well as the synthesis of a large isocyanide library and the application of sustainable isocyanides in polymer chemistry.

2. The evaluation of a novel one-pot synthesis of thiocarbamates, which was discovered while employing the newly established protocols detailed in the first part in the synthesis of a novel building block for part three of the thesis. The reaction was investigated to gain mechanistical insights and was employed to synthesize a library of thiocarbamate compounds.

3. (a) The synthesis of novel uniform star-shaped macromolecules *via* the core-first approach. As such, an established procedure was adapted and employed, which did not prove to be effective.

   (b) The synthesis of uniform star-shaped macromolecules *via* the arm-first approach. P-3CR and hydrogenation were combined with the azide-alkyne cycloaddition. Challenges and limits were evaluated and finally the target molecules were employed in qualitative phase-transfer experiments.

Aims

4 Results and discussion

In the following chapters, the results of this thesis are presented and thoroughly discussed. Macromolecules are, as previously mentioned, built up from subunits, called monomer (or larger building blocks), and hence the presented sequence starts from the improvement of this building block synthesis before the protocols toward sequence-defined macromolecules are established and evaluated.

4.1 Improvement of isocyanide synthesis/application of isocyanides

Parts of this chapter contain results that have already been published:

K. A. Waibel, R. Nickisch, N. Möhl, R. Seim, M. A. R. Meier, *Green Chem.* **2020**, *22*, 933–941.

(The author conducted the planing and evaluation of the experiments, and most of the writing. R. Nickisch contributed to the writing and co-supervised N. Seul, a "Vertieferstudent", who was also involved in the synthesis of the compounds. C. Rieker conducted first experiments (Bachelor thesis under the author's co-supervision),[335] *N. Möhl carried out the GC screening (Bachelor thesis under the author's co-supervision),*[336] *whereas R. Seim applied the improved conditions to synthesize an isocyanide library under the author's supervision.)*

In **Chapter 2.3.1** of the theoretical background, a brief introduction to the principles of Green Chemistry is given. It has already been established that a hypothetical *fully* sustainable synthesis is hardly possible. However, scientific research in the last years has revealed the tremendous changes our society has to face regarding the climate crisis and environmental pollution. Hence, also chemistry has established the noble goal of reducing emissions and replacing hazardous chemicals, which, at the moment, are quite often involved in the industrial synthesis of commercially available chemicals. Furthermore, laboratory syntheses rely even more on such chemicals, as basic research sees them as necessity for progress in certain areas.

Abstract

In this chapter, the general synthesis of the benzyl 11-isocyanoundecanoate building block for P-3CR based sequence-definition, which was developed by Meier *et al.* in 2016,[26] is revised in terms of sustainability. Especially the *N*-formamide dehydration to the isocyanide is thoroughly evaluated and improved. Therefore, three common synthesis protocols for isocyanide dehydrations (dehydrating agent: $POCl_3$, *p*-TsCl and

PPh_3/I_2) are investigated and optimized regarding their sustainability. E-factors as well as the general sustainability of the applied reagents are considered and discussed. After establishing the superiority of *p*-TsCl for dehydration of aliphatic *N*-formamides to isocyanides, the reagent was used in eleven examples, with special focus on the benzyl 11-isocyanoundecanoate.

State of the art

Benzyl 11-isocyanoundecanoate **4** is a highly specialized building block, which was designed to be employed in an iterative stepwise synthesis toward sequence-defined macromolecules *via* the P-3CR. The molecule bears an isocyano moiety, which allows its application in IMCRs. Additionally, it contains a benzyl-protected carboxylic acid and hence can be subjected to a further P-3CR after deprotecting the benzyl ester under mild conditions (H_2 and Pd/C).[26] However, until now the building block was obtained *via* a three-step synthesis involving multiple chemicals that are classified as toxic, corrosive and hazardous (**Scheme 44**).

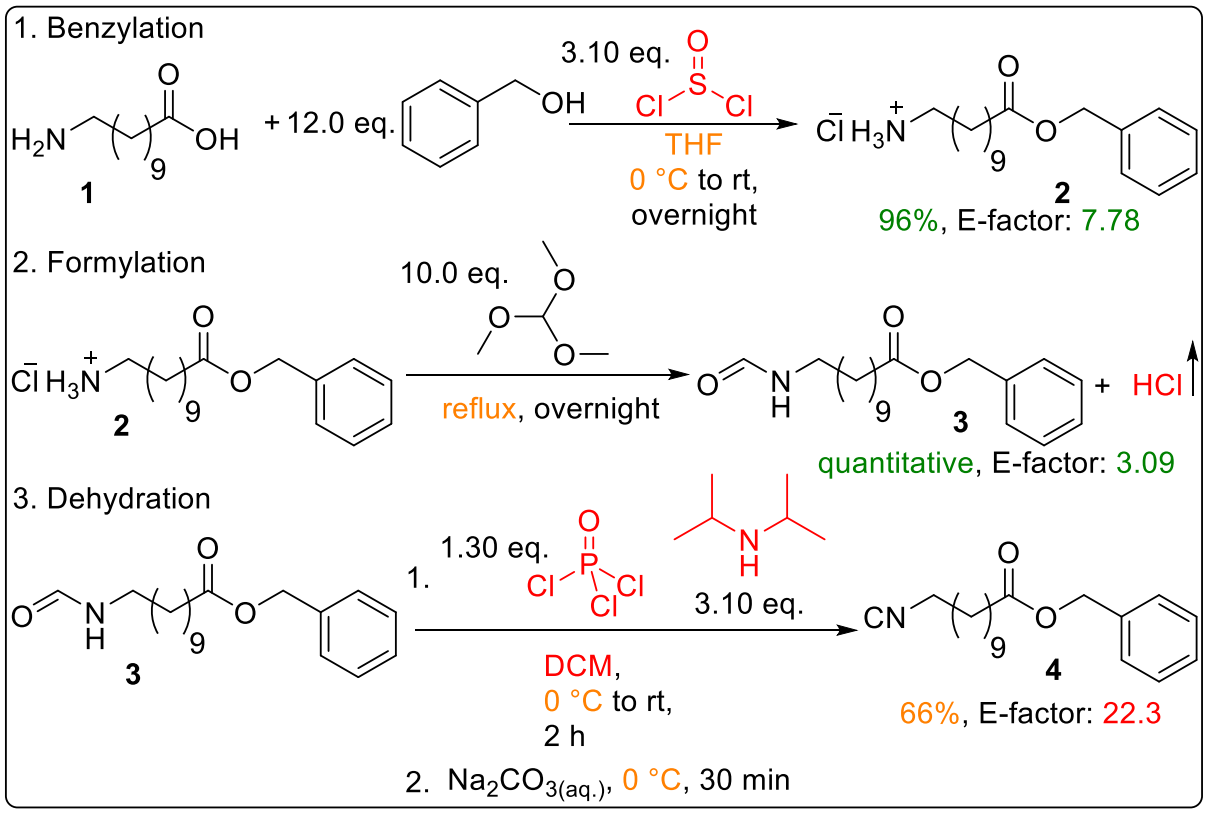

Scheme 44: Reported three-step synthesis of benzyl 11-isocyanoundecanoate **4** *via* subsequent benzylation, formylation and dehydration of 11-aminoundecanoic acid **1**. Hazardous chemicals as well as non-ideal reaction conditions or yield are colored regarding their sustainability from low (red) to high (green).[26] For the herein calculated E-factors, all chemicals and solvents are included except for solvents needed for precipitation/extraction or column chromatography.

Furthermore, IMCRs, like the previously mentioned U-4CR or P-3CR, are often considered as sustainable/green reactions because of the availability of the (mostly) benign reactants (especially carboxylic acids, aldehydes/ketones) that are often employed. Additionally, atom economy, as well as yield, are typically high. Purification is often easy because of the virtually absent side reactions (for example in the P-3CR) and the high difference of polarity between the employed reactants and the targeted product, allowing for a simple chromatographic purification. However, these calculations often neglect the isocyanide component, which is often bought from chemical suppliers and used without questioning further its route of synthesis. Generally, isocyanides are synthesized by either employing di/triphosgene or phosphoryl trichloride together with an amine base (for example triethylamine (TEA), or diisopropyl amine (DIA)) in dichloromethane (DCM). However, this reaction not only requires active cooling due to the high reactivity of the dehydrating agent, but also all the employed chemicals are highly toxic and hence diminish the sustainable character of IMCRs.

Hence, in this thesis, the sustainability of isocyanide synthesis was sought to be improved to omit the highly toxic reagents. Special attention lay on the benzyl 11-isocyanoundecanoate **4**, as this compound was the solid base in the synthesis of star-shaped macromolecules (**Chapter 4.3**).

Results and discussion

First, the benzylation and formylation steps of 11-aminoundecanoic acid were improved. In the established protocol, the compound is first benzylated and then formylated, as *N*-formamides are not stable in acidic conditions: they decompose into the respective amine and carbon monoxide. Furthermore, trimethyl orthoformate is not the standard chemical for formylation, yet it was found that the hydrochloride **2** obtained in the benzylation was not reactive enough to attack ethyl formate, which is normally employed in formylation of amines.

Therefore, the first two steps of the synthesis were inverted to omit the thionyl chloride in the benzylation step. 11-Aminoundecanoic acid **1** was directly formylated by employing an ethyl formate/DMF mixture (volumetric, 2:1) (**Scheme 45**).

1. Formylation

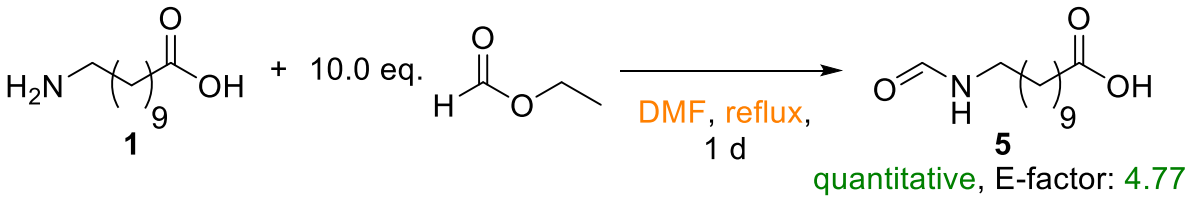

Scheme 45: Direct formylation of **1** employing ethyl formate in DMF.

As **1** is present as zwitterionic salt (11-ammoniumundecanoate), the nucleophilic character of the amine, which is necessary to attack the ethyl formate, is suppressed. Also, the solubility of the compound in the employed mixture is poor, even at elevated temperature (boiling point of the mixture was between 60 and 70 °C). However, it was found that the theoretically unfavorable reaction of ammonium attacking the formic ester still took place, yet only slowly. Qualitative screening *via* atmospheric solids analysis probe mass spectrometry (ASAP-MS) revealed a rather interesting side reaction, which matched the visual observation of an increase in reaction speed in the last quarter of the reaction time, *i.e.* the initially white suspension turns clear, which indicates full conversion. The mass spectrum showed a peak of higher *m/z* besides the reactant and the targeted product, namely the ethyl ester of the 11-formamidoundecanoic acid **5**. It is to assume acidic catalysis by the free carboxylic acid leads to a certain amount of transesterification or even esterification with the equivalents of ethanol, which are released in the actual formylation reaction. Nevertheless, esterification of the reactants leads to an increase in solubility and, as the *N*-formylation is not reversible in this chemical environment, the reaction proceeds to full conversion. Work-up of the reaction mixture was done *via* rotary evaporation to first collect the remaining excess of ethyl formate and then, at higher temperatures the DMF, which both can be reused in subsequent formylations. Nearly all DMF was removed at 80 °C under reduced pressure, as the ^{1}H NMR spectrum of the obtained compound showed no characteristic signals of the solvent (**Figure 10**). Also, not even traces of the ethyl 11-formamido undecanoate side product were detected by the ASAP-MS. Supposedly, the ester is reconverted to the carboxylic acid when ethanol is evaporated under reduced pressure. The purity of **5** was confirmed by several analytical methods (**Chapter 6.3.3.1**). In terms of sustainability, the novel synthesis does not surpass the established one utilizing trimethyl orthoformate and may even fall short, as longer reaction times and the employment of DMF was necessary. Furthermore, synthesis of **3** is quantitative and purification (besides evaporation of the

solvent) was not necessary. As expectations for the alternate procedure were high and thus, having found another quantitative synthesis, the environmental factors of the DMF were neglected. However, the hydrochloride **2** proved to be unstable over longer periods of storing as it was hygroscopic, subsequently leading to decomposition of the benzyl ester, whereas **5** was stored for months under air at room temperature in a glass flask without any degradation. Hence, the alternative procedure allows for the synthesis of larger quantities (up to 150 mmol was shown to be viable) as **5** does not require direct conversion and, synthetically, both approaches are equally elaborate.

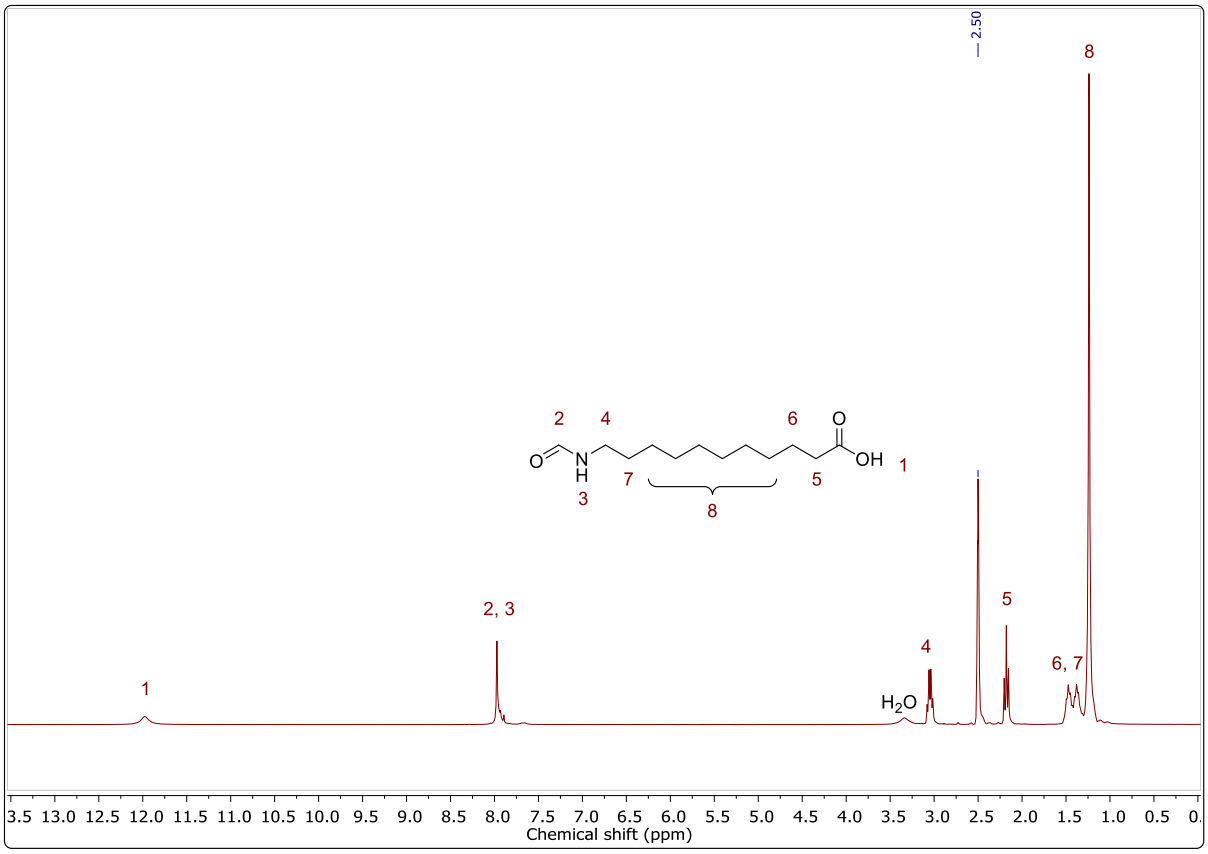

Figure 10: ^{1}H NMR spectrum of **5** in deuterated DMSO (DMSO-d_6). Ethyl ester peaks at around 4 ppm and characteristic signals of DMF at around 2.90 ppm are absent confirming the purity of the obtained compound. Reprinted with permission from [103,224].

Subsequently, **5** was converted to the benzyl ester by employing benzyl bromide (BnBr) and diisopropylethylamine (DIPEA) in dichloromethane (**Scheme 46**).

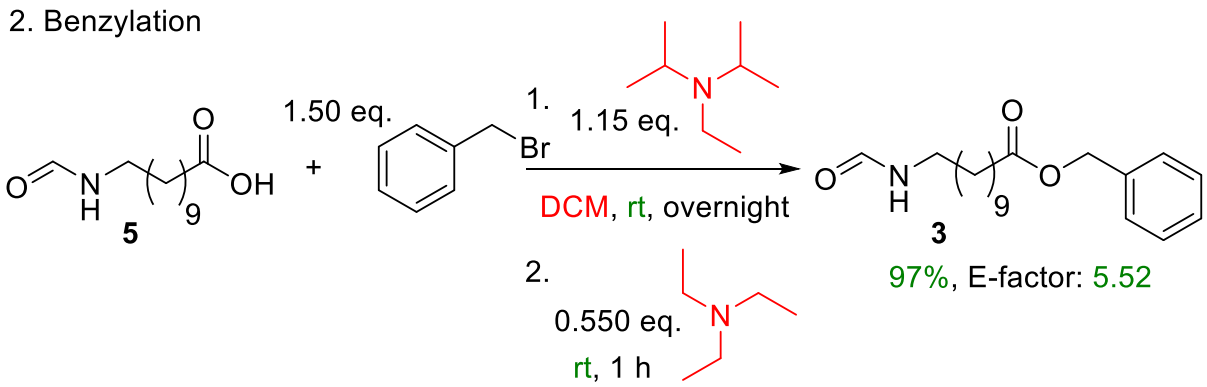

Scheme 46: Synthesis of **3** *via* benzylation of **5**. As reagents benzyl bromide, DIPEA and TEA were employed.

N-formamide **5** was suspended in a solution of DIPEA in dichloromethane and benzyl bromide was added. Poor solubility of **5** required a long reaction time, yet after stirring overnight, the solution turned clear and ASAP-MS measurements did not detect any remaining starting material, nor did thin-layer chromatography (TLC). As the original benzylation only required precipitation of the reaction mixture into ice-cold diethyl ether, the challenge was to find a comparably simple work-up procedure. Benzyl-bromide, however, cannot be easily evaporated under reduced pressure nor extracted into the aqueous phase, the second being the standard work-up procedure for such reactions. Hence, after full conversion, 0.550 eq. of triethylamine were added to the reaction mixture and stirring was continued for another hour. Contrary to DIPEA, TEA can still take part in a Menschutkin reaction and thus is converted by the remaining benzyl bromide to yield benzyl triethyl ammonium bromide (BTEAC). The latter is quite soluble in water as well as the DIPEA hydrobromide, which was formed during the esterification reaction. Subsequently, aqueous work-up was employed and yielded **3** in sufficient purity and high yield (95%) for further reactions (**Chapter 6.3.3.1** and **Figure 13**). Only minor impurities are visible at 3.40 ppm, around the benzylic protons (5.10 ppm) and at about 6.25 and 9.50 ppm. The second can be attributed to remaining BTEAC or benzyl bromide.

In terms of sustainability, thionyl chloride and THF as well as diethyl ether for purification were omitted. Also, no cooling of the reaction and for the precipitation was required. However, as simple esterification *via* acid catalysis (benzyl alcohol and sulfuric acid) was not possible due to the acid sensitivity of the *N*-formamide, an alternative procedure was needed. Regarding reactants, DIPEA as well as TEA count toward toxic compounds as amine bases are quite toxic and also dichloromethane

should generally be avoided if possible.[71,73,337] As an alternative, a protocol utilizing DMF and potassium carbonate as base could replace DIPEA and dichloromethane, however these conditions were not tested. TEA however, which quenches the remaining benzyl bromide, still has to be employed to omit column chromatography. Regarding the overall sustainability, it is hypothesized that quenching could be left out, as benzyl bromide does not react in the following dehydration to the respective isocyanide, however this was not attempted.

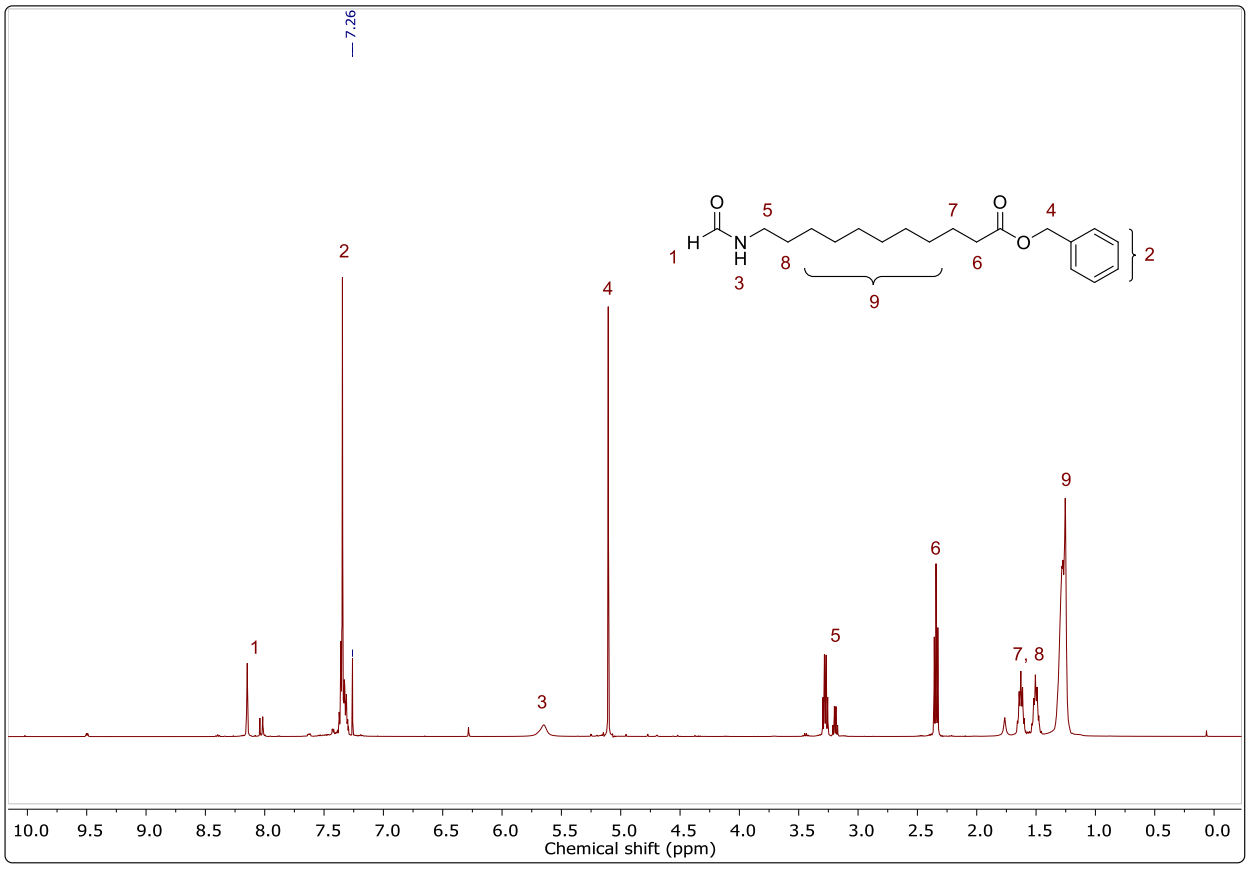

Figure 11: ^{1}H NMR spectrum of **3** in deuterated chloroform ($CDCl_3$). Reprinted with permission from [103,224].

Having established an alternative way toward **4**, the reaction to the isocyanide was evaluated and subsequently altered to better fit the principles of Green Chemistry. To not interrupt continuity, the final reaction conditions are presented in **Scheme 45**, whereas the process of reaction optimization and its related discussion is described afterwards. Initially, **3** was suspended in dimethyl carbonate (DMC) and pyridine. The flask was placed into a water bath to allow for passive cooling as the reaction was carried out in large batches of up to 100 mmol. Afterwards, solid *p*-TsCl is added into the flask *via* solid funnel in one portion. After overnight stirring, TLC confirmed the completion of the reaction and subsequently the mixture was cooled to 0 °C by placing

the flask into an ice bath. Addition of aqueous 20wt% sodium carbonate was carried out *via* dropping funnel. After quenching was completed (ca. 30 minutes; bubbling subsided), the standard protocol of aqueous work-up was done (separation of aqueous and organic phase, 3 times extraction of the organic phase, 3 times washing of the combined organic phases, drying and solvent removal under reduced pressure). It is noted that for some batches, repeated washing steps lead to slow phase separation, therefore it was omitted for some batches and no loss in yield was observed. Subsequent flash column chromatography to remove residual *p*-toluenesulfonic acid (*p*-TsOH) and pyridine yielded the product in a yield of 97% and high purity (**Chapters 6.3.1**, **6.3.3.1** and **Figure 12**).

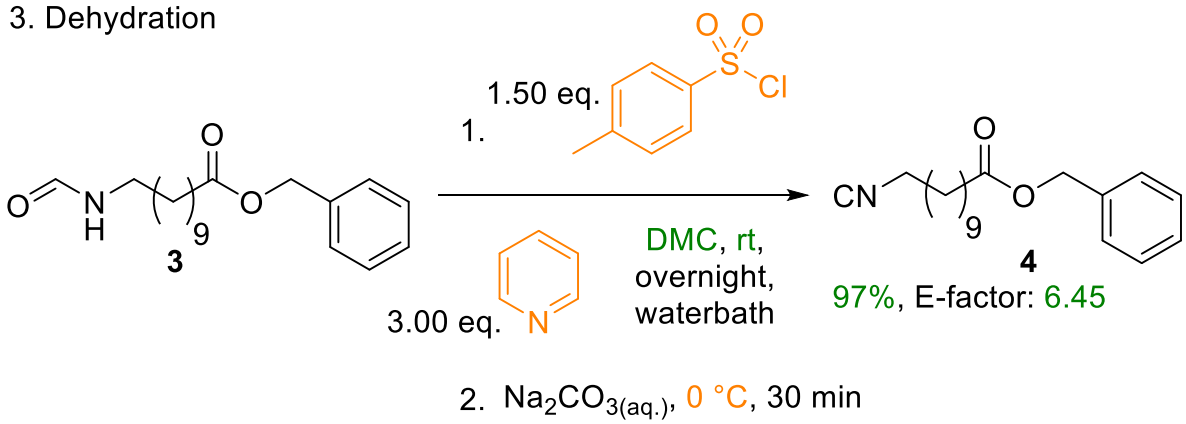

Scheme 47: More sustainable dehydration of **3** to **4** by employing *p*-TsCl and pyridine in dimethyl carbonate (DMC).

The E-factor of the synthesis of **4** was reduced to less than a third of the original value (22.3 to 6.45), while increasing the yield from 66% to 97% and avoiding the hazardous chemicals phosphoryl trichloride, DIA and dichloromethane. Over the three-step synthesis, the overall yield of the new protocols was 94% and the total E-factor was 16.7, the original values were 63.4% and 33.2, respectively. Concluding, the synthesis of the isocyano building block necessary for the work in **Chapter 4.3** was improved in terms of sustainability, efficiency and overall yield, which allowed to produce large amounts in little time (about 100 mmol in four days).

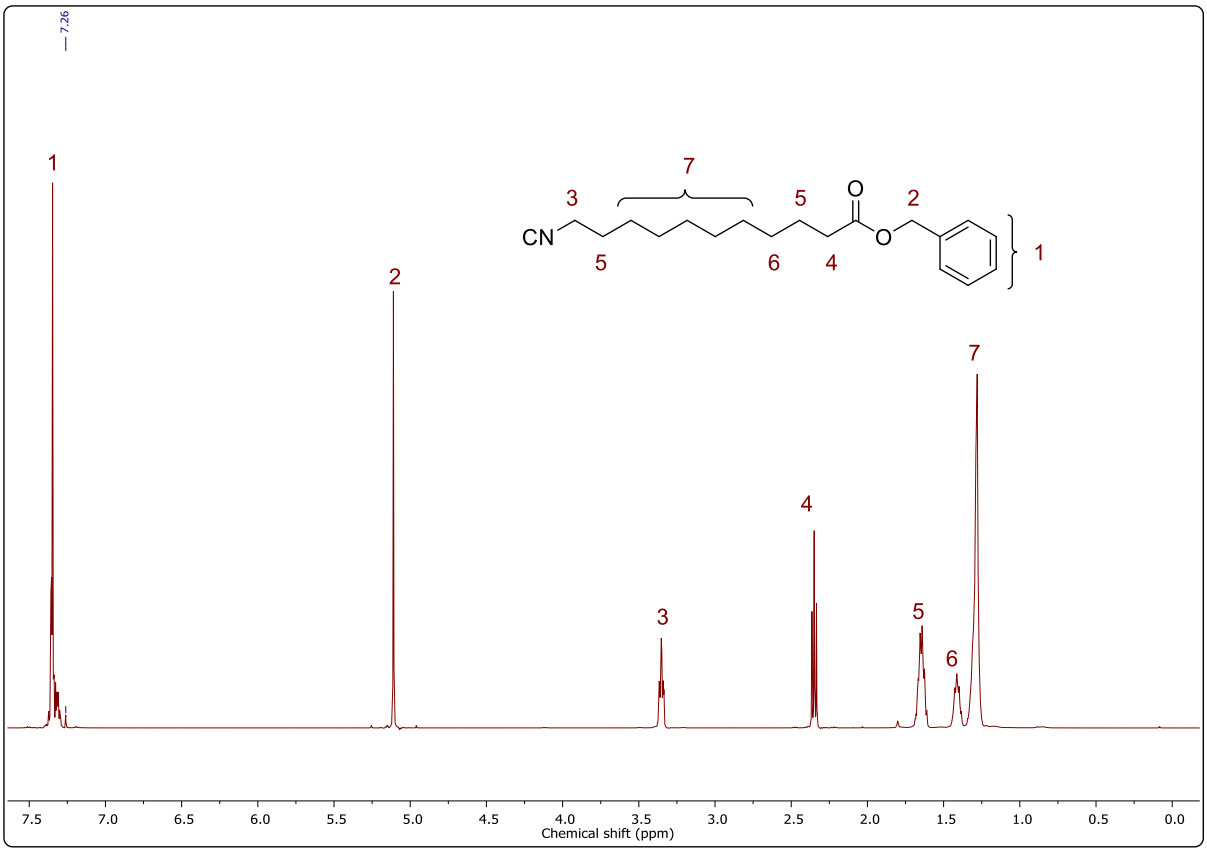

Figure 12: ^{1}H NMR of **4** in deuterated chloroform ($CDCl_3$). The characteristic proton signal of the CH_2 adjacent to the isocyano group is marked with number 3. Reprinted with permission from [103,224].

In the following paragraphs, the detailed optimization of isocyanide dehydration is described. For this, *N*-octadecyl formamide **7** was chosen as model compound for an internal standard based reaction optimization *via* gas chromatography (GC), as high molecular weight decreases volatility and hence the noxious smell of isocyanides. The compound was synthesized from octadecyl amine **6** by employing 10 eq. of ethyl formate and refluxing overnight, which yielded the formamide in quantitative yield and high purity after evaporation of the solvent.

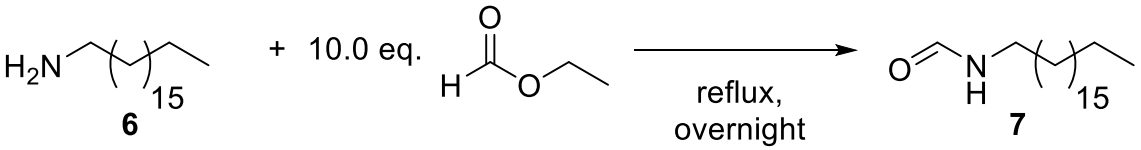

Scheme 48: Synthesis of **7** by refluxing **6** in an excess of ethyl formate.

First, different literature procedures, which are known to convert *N*-formamides into their respective isocyanides, were reviewed and applied (**Scheme 49**). The chosen procedures were selected taking into account the toxicity of their reagents, hence reactions employing neither phosgene derivatives nor the specialized dehydration

agent, *Burgess reagent*, were considered. Isocyanide **8** was isolated after aqueous work-up and flash-column chromatography, yielding 96% and 42% of the desired product, respectively. Note that the exact procedures can be found in **Table 1** and **Table 2**.[103] The E-factor, as already mentioned above, is calculated using Sheldons formula,[338] yet only reagents and solvents utilized for the reaction itself (quenching included) are taken into account. Solvent amounts for extraction as well as silica and solvent for chromatography were not taken into account as this would not have allowed a consistent comparison of the reactions with literature procedures.

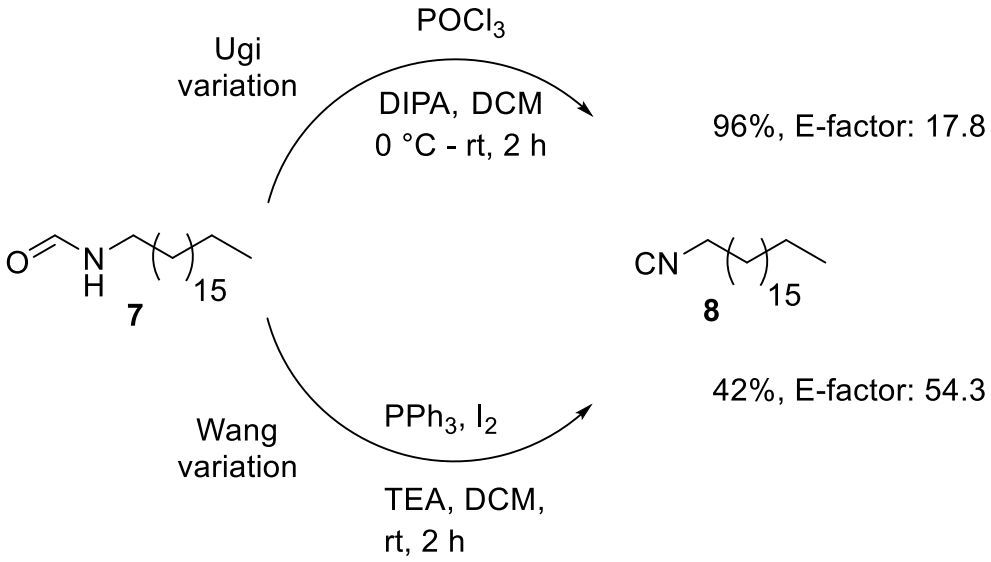

Scheme 49: Synthesis of octadecyl isocyanide by the Ugi and Wang procedure. Both reactions were carried out in DCM as it is employed in most isocyanide syntheses.

After having established the protocols, alterations toward a more sustainable solvent were carried out, as DCM is considered toxic and health hazardous (Global harmonized system (GHS) 07/08, H315/319/336/351/373) like most chlorinated solvents and is suspected of causing cancer. However, alternative solvents have to fulfill certain criteria to be viable substitutes. As highly reactive phosphoryl trichloride and amine bases are used, the selected solvents have to be chemically inert toward those reagents, which exclude alcohols, ketones, water and primary amines. Hence, to find suitable solvents, several sustainability selection guides were considered[69–73] and for a first test, three more sustainable alternatives were chosen: ethyl acetate (EA, GHS 02/07, H225/319/336), 2-methyl tetrahydrofuran (Me-THF, GHS 02/05/07, H225/302/315/318) and dimethyl carbonate (DMC, GHS 02, H 225), which all were found to be inert toward the reaction conditions. Additionally, EA and DMC are both relatively non-toxic, whereas Me-THF exhibits slight toxicity and all of them can be

synthesized utilizing resources from renewable feedstocks. Ethyl acetate is produced *via* acid-catalyzed esterification of acetic acid and ethanol, dimethyl carbonate *via* carbonylation of methanol utilizing carbon monoxide on copper catalysts,[339] whereas Me-THF can be obtained from furfural or pentoses.[340]

The yields and respective E-factors of the Ugi procedure in DCM, and its substitutes are summarized in **Table 1**.

Table 1: Solvent variation for the Ugi dehydration of **7** utilizing $POCl_3$ and DIPA.

Entry	*Solvent*	*Yield (%)*[a]	*E-factor*
1	DCM	96	17.8
2	EA	90	13.9
3	Me-THF	94	12.6
4	DMC	90	15.9

[a] The corresponding solvent, formamide (0.33 M in solvent, 3.00 mmol, 1.00 eq.), $POCl_3$ (1.30 eq.) and base (2.60 eq.) were utilized under ice-bath cooling and the reaction was stirred for two hours at room temperature.

Generally, the Ugi procedure is known to achieve high yields for a variety of substrates. Thus the high yield of **8** in its standard variation in DCM was to be expected.[26,75,87,91–93,341] Yet, also the alternative and more environmentally benign solvents gave consistently high yields, the best being Me-THF with 94% and an E-factor of 12.6, which already hinted to the possibility to improve the procedure regarding sustainability.

However, besides the toxicity of DCM, more challenges lie within the isocyanide synthesis. Generally, the dehydration of a compound, if not done catalytically, is considered none-sustainable, especially regarding its below average atom economy. Phosphoryl trichloride (GHS 05/05/08, H302/330/314/372) is extensively used in the Ugi procedure to dehydrate the employed *N*-formamides, however it is a highly toxic and reactive reagent, which not only requires careful handling but also cooling when being quenched with aqueous sodium carbonate solution, as well as for the initial addition to the reaction solution. Therefore, the reaction has to be cooled twice to 0 °C, which is energy consuming and further contradicting the principles of Green Chemistry. Moreover, the compound has a problematic life cycle as also its industrial production involves highly reactive reagents and requires high amounts of energy as it is commonly synthesized by reacting phosphorus with elemental chlorine and

subsequent oxidation. Hence, the goal was to find a more environmentally benign substitute, while maintaining the high yields and versatility of the Ugi procedure.

As a first alternative, a publication of Wang and coworkers from 2015 was considered.[342] There, aliphatic *N*-formamides are dehydrated utilizing triphenylphosphane (PPh_3), iodine and triethyl amine. The authors stated that their motivation was driven by convenience, as $POCl_3$ is not easily available in China and hence they were in need for a more benign yet still efficient isocyanide synthesis. PPh_3 as well as iodine are both far less reactive and toxic as well as bench stable in contrast to the above mentioned $POCl_3$. Iodine, however, has skin irritating properties and can sublime and hence be inhaled. Nonetheless, the overall toxicity of the new combination is significantly lower.

Therefore, a brief solvent evaluation was carried out (**Table 2**), revealing that at least for isocyanide **8**, the highest yield, and lowest E-factor (93%, 54.3, respectively) were achieved by employing the more sustainable Me-THF, whereas DCM as solvent yielded only 42% and an E-factor of 54.3. However, the reaction yielded triphenylphosphane oxide as a side product, which cannot be removed by aqueous extraction like the water-soluble residues of phosphoryl trichloride, making column chromatography inevitable. On the other hand, the reaction required no initial cooling when the dehydrating agents were added and hence is less energy consuming.

Table 2: Solvent variation for the Wang dehydration of **7** utilizing PPh_3, iodine and TEA.

Entry	*Solvent*	*Yield (%)*[a]	*E-factor*
1	DCM	42	54.3
2	EA	37	49.2
3	Me-THF	93	18.4
4	DMC	33	60.8

[a] The corresponding solvent, formamide (0.33 M in solvent, 3.00 mmol, 1.00 eq.), PPh_3 (1.50 eq.), iodine (1.50 eq.) and base (3.00 eq.) were utilized and the reaction was stirred for two hours at room temperature.

Encouraged by these results, another dehydration agent was investigated, *para*-toluenesulfonyl chloride (*p*-TsCl), which had been the dehydrating agent of choice in a publication about synthesis of small and volatile isocyanides like methyl isocyanide.[99] However, in this specific publication, the reagent was employed at 75 °C under vacuum together with quinoline as a base, as this allowed for continuous distillation of the volatile and potentially explosive isocyanide. Additionally, the authors

mention that especially low molecular weight isocyanides exclude aqueous work-up as they exhibit decent water solubility. However, as those volatile isocyanides did not lie within our targeted scope and the employed conditions were quite different from our expectations, a complete GC-screening was carried out to identify the optimal reaction conditions. This included but was not limited to the solvent and with a final aqueous work-up in mind. Already the properties of *p*-TsCl directed our main efforts toward its application, as it still exhibits strong oxophilicity, yet is far easier to handle than $POCl_3$. The compound is a bench-stable solid being only prone to hydrolysis, which can be prevented by storing it in a sealed container and flushing it with argon or nitrogen after application. In contrast to phosphoryl trichloride, *p*-TsCl is less-toxic, however, it is, like $POCl_3$, corrosive, albeit to a much less extent. The safety data sheets of Merck KGaA were considered for both chemicals: $POCl_3$ exhibits a LD50 oral of 380 mg kg^{-1} in rats in terms of acute toxicity, whereas for *p*-TsCl it is 4680 mg kg^{-1}, respectively.[343,344] Furthermore, $POCl_3$ exhibits a LD50 for inhalation over 4 h of 0.303 mg L^{-1} in rats, whereas for *p*-TsCl such a value is absent (however, it has to be considered that hydrolysis of both $POCl_3$ and *p*-TsCl produces HCl gas, which is also toxic and corrosive). In terms of its reactivity, employment at room temperature without any cooling (small batches, <5 mmol) or passive cooling by just a water bath when applying large amounts (batches up to 100 mmol were tested) was deemed unproblematic. Finally, *p*-TsCl is a waste product of the industrial saccharine synthesis by the Remsen-Fahlberg process,[345,346] which aligns perfectly well with the principles of Green Chemistry as it gives a waste product new value.

To learn about its reactivity in isocyanide synthesis, the reaction conditions of the Ugi procedure were adapted (**Scheme 50**) and employed for the GC screening (tetradecane was used as an internal standard). The results are presented in **Table 3** beginning with the alteration of the amine base.

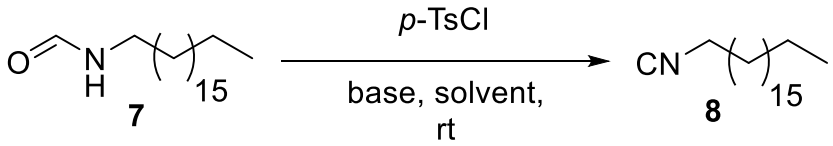

Scheme 50: Starting point for reaction optimization of dehydration of **7** utilizing *p*-TsCl, a solvent and a base.

In **Chapter 2.3.2**, it was already discussed that the general mechanism for the *N*-formamide dehydration proceeds *via* an adduct consisting of the formamide and the

dehydrating agent that undergoes elimination to form the respective isocyanide. As both reaction steps require proton subtraction by a base, at least two equivalents of a base are necessary for full conversion. Whereas the base was seen as a "*lesser evil*" for the two previous reaction optimizations, it was now within the given criteria for improvement. Generally, the GHS rates most amine bases as toxic, with pyridine being an exception as it is only rated health hazardous.[73] Hence, diisopropylamine (DIPA), diisopropylethylamine (DIPEA), pyridine (Py) and triethylamine (TEA) were chosen as they are all commercially available and can at least be produced quite sustainably.[347–352]

Table 3: Optimization of reaction parameters for the dehydration of **7** utilizing *p*-TsCl and a base in given solvents.[103]

Entry	*Solvent*	*Base*	*c (mol L^{-1})*	*t (h)*	*Yield (%)*[a]	*E-factor*
1	DCM[a]	DIPA	0.330	21	35[b]	51.3
2	DCM[a]	DIPEA	0.330	7.80	14[b]	132
3	DCM[a]	TEA	0.330	1.50	25[b]	72.2
4	DCM[a]	Py	0.330	2	66[b]	26.4
5	Me-THF[a]	Py	0.330	2	12[c]	106
6	DMC[a]	Py	0.330	2/18	7/85[c]	217/31.8
7	MeCN[a]	Py	1.00	4/18	70/56[c]	8.2/10.5
8	Cyrene™[a]	Py	1.00	1/2	10/2.4[c]	80.2/324
9	GBL[a]	Py	1.00	1/2	28/22[c]	26.5/34.8
10	DCM	Py	1.00	2	96[c, d]	7.76
11	DMC	Py	1.00	18	89[c, d]	7.41

[a] Yields calculated by GC using a calibration curve of product **8**. [b] The corresponding solvent, 5.00 mmol formamide (1.00 eq.), *p*-TsCl (1.30 eq.) and the base (2.60 eq.) were applied. [c] The corresponding solvent, 5.00 mmol formamide (1.00 eq). *p*-TsCl (1.50 eq.) and the base (3.00 eq.) were applied. [d] Isolated yield after work-up.

In the course of the experiment, pyridine was found to be the most reactive base in combination with the new dehydrating agent as it gave the highest yields in the shortest reaction time. As such, pyridine was used for all forthcoming experiments. In addition to Me-THF and dimethyl carbonate, acetonitrile (MeCN), Cyrene™ and γ-butyrolactone (GBL) were also tested yet all found inferior to dimethyl carbonate in regard of the yield. Most of the evaluated solvents also exhibited a decrease in yield after a certain reaction time, whereas dimethyl carbonate distinguished itself by a slow reaction yet high conversion and yield after overnight stirring (only 7% yield after 2 h,

yet 85% after 18 h). Additionally, the concentration of the reaction was increased threefold, as the low concentration of the Ugi procedure results from the high reactivity and hence highly exothermic reaction of $POCl_3$. The amount of *p*-TsCl was increased from 1.30 to 1.50 eq. to compensate the loss of dehydrating agent due to hydrolysis to *para*-toluenesulfonic acid (*p*-TsOH) by water residue in the solvent or reactants. In doing so, also the ratio of the base was adjusted from 2.60 to 3.00 eq. The evaluation was finalized by carrying out the reaction in DCM and DMC with subsequent aqueous work-up and isolation *via* flash column chromatography and gave **8** in a yield of 96% and 89% with a respective E-factor of 7.76 and 7.41. Although the results from these two reactions are rather similar, toxicity is not counted toward the final E-factor, meaning the procedure utilizing DCM is faster (reaction time 2 h), whereas the procedure employing DMC as solvent can be considered the more sustainable (no toxic solvent, reaction time 18 h). This was further observed in a comparison with the altered Ugi and Wang procedures (**Table 4**).

Table 4: Comparison of the solvent optimized dehydration of **7** with $POCl_3$ and PPh_3/I_2 as well as the optimized reaction condition employing *p*-TsCl.

Entry	*Method*	*Solvent*	*Yield (%)*	*E-factor*
1	Ugi[a]	Me-THF	94	12.6
2	Wang[b]	Me-THF	93	18.4
3	*p*-TsCl[c]	DMC	89	7.41

[a] see**Table 1**, [b] see **Table 2**, [c] see **Table 3**.

Contrary to the Ugi procedure, the *p*-TsCl containing one offers low toxicity and easy handling, which was confirmed *via* a visible comparison between $POCl_3$ and *p*-TsCl as dehydrating agents (**Figure 13**). There, the characteristic HCl vapors, which evolve even after dropwise $POCl_3$ addition at 0 °C, are absent when p-TsCl is added, while higher concentration of reactant is possible (0.333 mol L^{-1} *versus* 1.00 mol L^{-1}) due to the diminished exothermic character of the reaction. However, also the Wang procedure offers reagents of lower toxicity, but it is the work-up in which they differ. Triphenylphosphane oxide is not removable by aqueous extraction, whereas the *in situ* produced *p*-TsOH is. Hence, the Wang procedure requires flash chromatography, whereas the new established procedure allows for omitting time- and resource consuming chromatography if the reaction solution is washed thoroughly (note that this counts mostly for the long chained, respectively highly nonpolar isocyanides, as the small ones – for example 1,5-diisocyanopentane or cyclohexyl/benzyl isocyanide –

exhibit a certain water solubility, which leads to a decrease in yield if extracted too often). This was later confirmed in a P-3CR polymerization utilizing 1,12-diisocyanododecane – only washed and chromatographed (**Figure 14**, **Figure 15** and **Scheme 51**).

Figure 13: Top left: dehydration of *tert*-butyl formamide (11.6 mmol in 35 mL DCM, (0.33 M)), cooling is applied for subsequent addition of $POCl_3$. Bottom left: reaction after dropwise addition of $POCl_3$, internal temperature at 0 °C, still HCl vapors are evolving clouding the flasks. Top right: dehydration of *tert*-butyl formamide (35 mmol in 35 mL DCM, 1.00 M), a water bath is applied for subsequent addition of *p*-TsCl. Bottom right: reaction after addition of *p*-TsCl. No visible hints of an exothermic reaction are observed. In some dehydrations, the temperature increased slightly – sometimes indicated by statistical bubbling of the low temperature boiling DCM. Reprinted with permission from [103].

Furthermore, the optimized reaction procedures, one carried out in DCM (*Procedure A* (*Proc. A*), shorter reaction time, toxic solvent), the other one in DMC (*Procedure B* (*Proc. B*), longer reaction time, non-toxic solvent), were then employed to synthesize a library of different isocyanide compounds (**Table 5**), which did not only show their value but also their limitations. Both the standard procedures, as well as the analytical data of the compounds, are listed within the experimental section (**Chapter 6.3.1**).[103]

Table 5: Synthesized isocyanides *via* formamide dehydration utilizing the optimized reaction conditions with *p*-TsCl in either DCM or DMC. n.L. = no literature available.

Entry	*Substrate*	*Proc. A[a] – yield (%)*	*E-factor A*	*Proc. B[b] – yield (%)*	*E-factor B*	*Lit. Yield (%)*	*Lit. E-factor[c]*
1	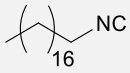	96	7.76	89	7.40	87[91]	36.9
2	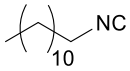	90	11.9	94	9.93	94[91]	48.8
3	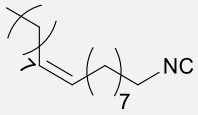	97	7.73	98	6.68	n.L.	–
4	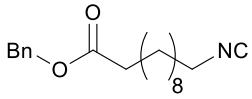	97	7.11	97	6.45	66[26]	22.3
5	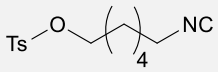	53	15.0	68	11.0	n.L.	–
6	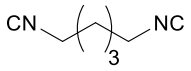	48	49.0	82	25.7	n.L.	–
7	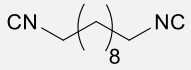	93	15.8	89	15.0	71[353]	33.6
8	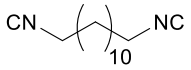	87	14.8	97	12.0	75[92]	33.6
9	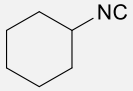	67	28.8	68	24.9	76[94]	62.0
10	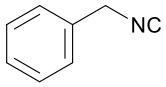	44	41.5	62	25.6	64[75]	22.2
11	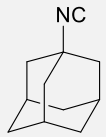	79	16.5	78	14.7	93[95]	28.9
12	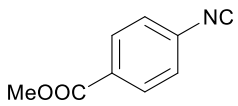	13[d]	108.6	–	–	96[93]	12.9

[a] Formamide (5.00 mmol, 1.00 eq.) in DCM (1 M), 1.50 (3.00)/3.00 (6.00) eq. *p*-TsCl/pyridine at rt for 2 h. [b] Formamide (5.00 mmol, 1.00 eq.) in DMC (1 M), 1.50 (3.00)/3.00 (6.00) eq. *p*-TsCl/pyridine at rt for 2 h. [c] E-factors were calculated using the values in the respective literature. [d] Adjusted equivalents: Formamide (5.00 mmol, 1.00 eq.) in DCM (1 M), 1.70/3.40 eq. *p*-TsCl/pyridine at rt for 2 h.

Furthermore, yields as well as E-factors were compared with literature data, which always rely on $POCl_3$ in DCM. Note that for a concise comparison only literature and *Proc. B* are collated as it is the most sustainable alternative and nearly always exceeds *Proc. A* in yield and E-factor with **Table 5**, entry 1, 7 and 11 being expectations with slightly higher yields for *Proc. A*.

Long-chain alkyl isocyanides (**Table 5**, entry 1-3) were obtained in similar yields to the ones in literature: (89/94/98% in DMC, compared to literature 87/84/n.L.%). However, the E-factor is 80% lower for entry 1 and 2, which is major improvement toward sustainability. In numbers, this implies that 37 kg of waste is produced according to the literature for the synthesis of 1 kg octadecyl isocyanide, whereas *Proc. B* only produces 7.40 kg – a trend that is consistent within the library but more pronounced for entries 1-3 (note that benzyl isocyanide (entry 10) and methyl 4-isocyano benzoate (entry 12) are certainly exceptions, however, they are not aliphatic isocyanides, but rather benzylic or aromatic ones, which is hypothesized to influence the efficiency of the method).

Entry 4, 11-isocyano undecanoate, was already mentioned at the beginning of the chapter. Here, both the yield as well as the E-factor were significantly improved, which was of great importance, as this compound is used for P-3CR-based sequence-definition in **Chapter 4.3**.

For entry 5, a simultaneous tosyl protection and *N*-formamide dehydration was tried, which resulted in moderate yield and E-factor. By activating the hydroxy functionality post-reaction functionalization is enabled.

Also, diisocyanides (**Table 5**, entries 6-9) benefit from the newly established procedure. Herein, yields were improved (*Proc. B*: 89 and 97%, literature 71 and 75%, respectively) and the E-factor was lowered about 55 and 65%, respectively. Also, entries 3, 7 and 8 were of special interest, as the reactants from which the respective *N*-formamides are synthesized (oleyl amine, 1,10-diaminodecane and 1,12-diaminododecane) originate from renewable feedstocks.

The synthesis of three otherwise commercially available isocyanides (**Table 5**, entries 9-11) revealed the limitations of our approach. The lower obtained yields were attributed to water solubility as well as steric hindrance/electronic effects, the latter being confirmed by **Table 5**, entry 12, which is an aromatic isocyanide. Whereas the

E-factor was still better than in literature for adamantyl and cyclohexyl isocyanide (E-factor 14.7/24.9 *versus* 28.9/62.0), it was worse for benzyl isocyanide (25.6 *versus* 22.2). The yields were lower for all three samples (*Proc. A* 68/62/78% *versus* literature 76/64/93%). Further, Kim *et al.* reported high yields for benzyl and cyclohexyl isocyanide utilizing a novel synthesis protocol in 2013, which was based on continuous flow microreactors (99% yield). However, they still relied on $POCl_3$ in DCM, which should be omitted.[341] Also, microreactors were not available and thus the results were compared with the classical procedure.

Finally, the aromatic isocyanide (**Table 5**, entry 12) underlined the limitations of the new procedure, as it was only obtained in 13% yield with a related E-factor of about 109. This was also confirmed in test reactions with other aromatic formamides, yet these are not listed within this thesis as they gave similar or even worse results.

All the yields given in **Table 5** refer to isocyanides being purified *via* flash column chromatography after initial quenching and aqueous work-up. Chromatography produces waste (solvent, and silica). Thus, it was investigated to avoid this last step of purification and to see if simple extraction yielded isocyanide pure enough for further reactions. Therefore, 1,12-diisocyano dodecane was resynthesized and solely purified by washing. The ^{1}H NMR spectra of both compounds are compared in **Figure 14**, which only shows small amounts of an impurity in the region of aromatic protons (possibly remaining *p*-TsOH/pyridine) for the non-chromatographed product.

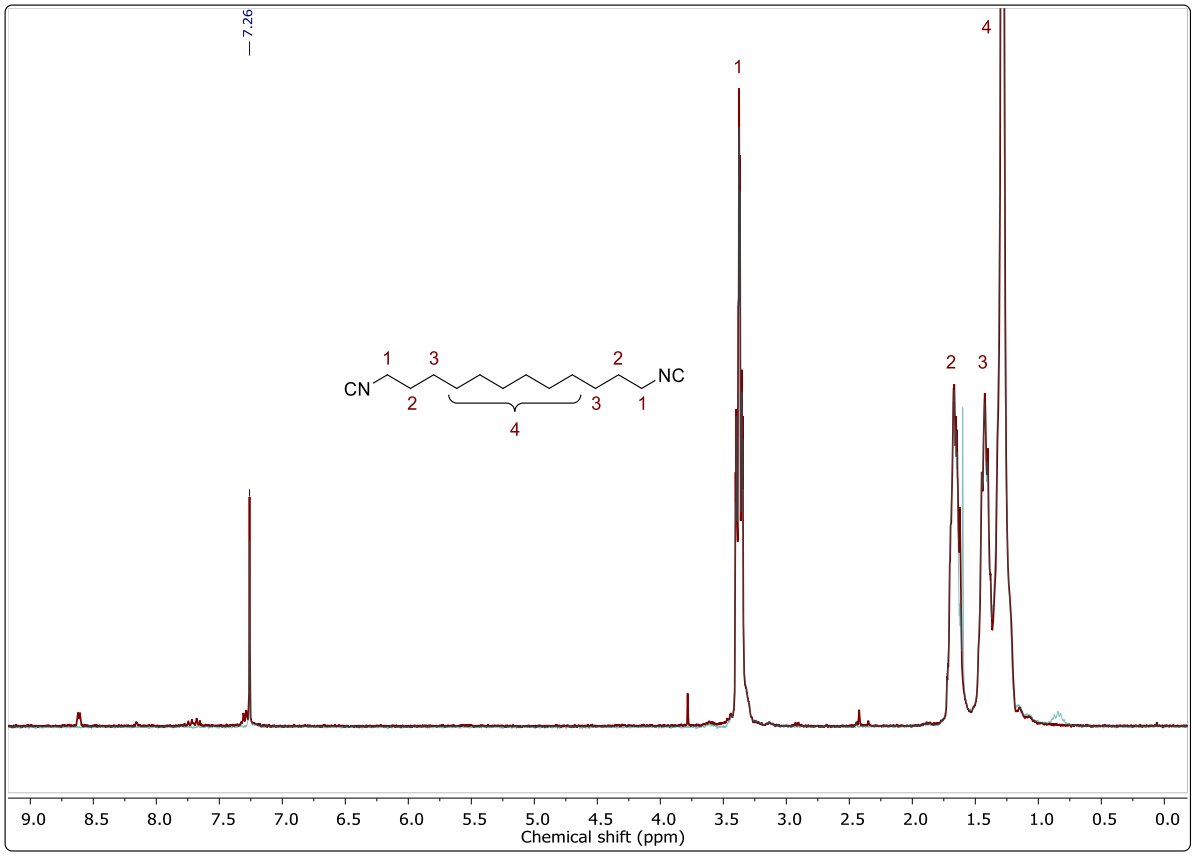

Figure 14: ^{1}H NMR spectrum of 1,12-diisoyano dodecane after extraction and washing (red line), and after purification by flash column chromatography (blue line) in deuterated chloroform ($CDCl_3$). Reprinted with permission from [103].

Based on these results, we deemed the impurities to be negligible and employed both compounds in a P-3CR polymerization, as step-growth polymerizations are quite sensitive to reactant purity due to the necessity of a balanced stoichiometry (**Scheme 51**). Both polymerizations were carried out in bulk utilizing sebacic acid and heptanal (both are available from castor oil)[354] together with either purified or non-purified diisocyanide.

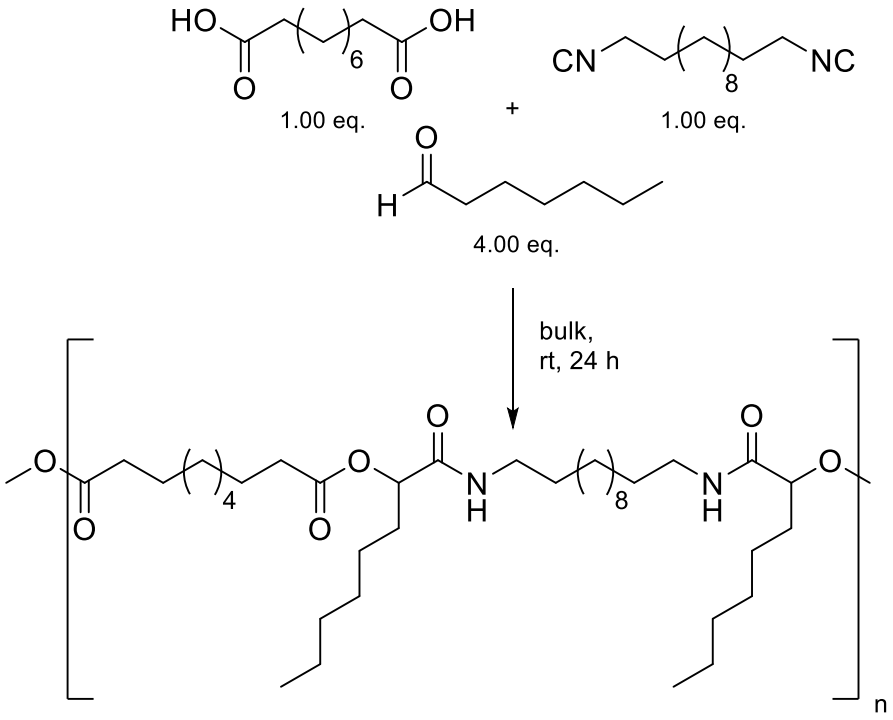

Scheme 51: P-3CPR of sebacic acid, heptanal and 1,12-diisocyano dodecane. The latter being purified either by sole washing or by washing and flash chromatography. Reprinted with permission from [103].

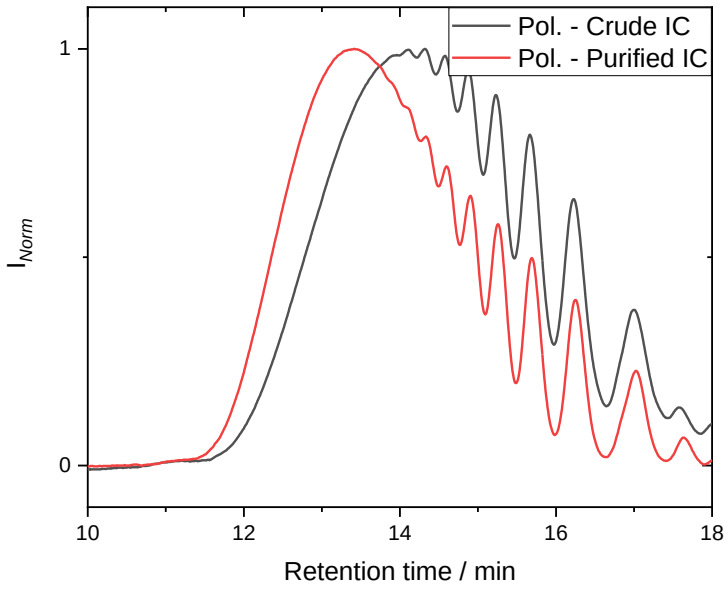

Figure 15: Molecular weight distribution of the two obtained polymers measured in THF. The polymer using the purified isocyanide (red line) has a slightly higher molecular weight than the one that was synthesized with the *crude* isocyanide. Reprinted with permission from [103].

After simple precipitation in cold diethyl ether, the samples were analyzed by SEC and compared (**Figure 15**). The number averaged molecular weight (M_n) of the obtained

polymer utilizing the pure isocyanides was at 10500 g/mol, whereas utilizing the crude isocyanide led to a slightly lower M_n of 8350 g/mol, indicating that washing is enough to yield isocyanide in sufficient purity for further reactions. Visibly, the crude isocyanide polymer distinguished itself by a darker color, yet both were waxy solids.

Concludingly, protocols utilizing $POCl_3$ or PPh_3/I_2 in DCM were applied to synthesize octadecyl isocyanide as model compound and to evaluate yield and most importantly E-factor. Subsequently, these protocols were improved toward sustainability by substituting the toxic DCM by environmentally more benign solvents like ethyl acetate, Me-THF, or DMC. However, as toxicity of $POCl_3$ and low yields of its PPh_3/I_2 counterpart remained a challenge, a third protocol, which aimed to combine efficiency of the first with the lower toxicity of the second was adapted from previous literature. The herein employed *p*-TsCl proved to be the dehydration agent of choice for aliphatic isocyanides, as it exhibits no toxicity, is less corrosive than $POCl_3$, less reactive and considered a bench-stable chemical. Furthermore, it occurs as a side product in the large-scale industrial production of *o*-TsCl, which is a precursor molecule in the saccharin production *via* the Remsen-Fahlberg process. Hence, the procedure gives a waste product new value, which is in line with the principles of Green Chemistry. The protocol was improved by GC optimization *via* an internal standard to maximize yield and hence minimize the E-factor. 1.00 eq *N*-formamide in DMC (1 M) together with 1.50 eq. *p*-TsCl and 3.00 eq. pyridine stirred for 18 h at room temperature were found to give the best results and hence were applied to synthesize a library of aliphatic mono- and diisocyanides. As most of these compounds were literature-known, a concise comparison of yields and E-factors was carried out, which further underlined the benefits of our novel procedure in terms of sustainability and also efficiency. Limits of the procedure lie in the dehydration of *N*-formamides yielding commercially available isocyanides like adamantly, benzyl and cyclohexyl isocyanide, which it only exceeds in terms of E-factor values but not the yields (benzyl isocyanide is an exception). Furthermore, aromatic substrates give rather low yields (about 10%) and hence exhibit higher E-factors than in literature. Finally, it was evaluated if flash column chromatography, which is normally conducted to purify isocyanides after aqueous work-up, is necessary, as this also produces high amounts of waste (solvent/silica). 1,12-Diisocyano dodecane was applied either crude or purified in a polymerization and showed only small differences in the molar mass of the resulting polymers. Hence, flash column chromatography was deemed to be a no absolute necessity depending

on the targeted application of the obtained isocyanides. However, for the comparison with literature, chromatography is applied to allow for a consistent comparison.

4.2 A novel one-pot synthesis of thiocarbamates

Parts of this chapter contain results that were conducted by T. Malliaridou in her Bachelor thesis, which was co-supervised by the author.[355]

The synthetic value of isocyanides in organic synthesis has already been described in the **Chapters 2.3.2** and **2.3.3**. Their versatile character enables countless pathways of reaction and hence allows for application in multi-component chemistry[68,74,76,82,110–115] but also metal-catalyzed insertions[105–108] or Van Leusen reactions.[109] Still, research on isocyanide-based reactions is conducted and novel areas of application have emerged over the last decade, e.g. thiocarbamates.[116–119] Furthermore, with the publications of Meier *et al.* (**Chapter 4.1**) and Dömling *et al.*, the time- and resource-consuming synthesis of isocyanides has been simplified.[103,104] Hence, aliphatic isocyanides can be obtained quite sustainably *via* dehydration utilizing *p*-TsCl and pyridine in DMC/DCM or in a wider scope with $POCl_3$ and TEA in DCM, yet in a rather resource-saving procedure, which allows for diverse research to unveil new areas of application for those compounds.

Abstract

In this chapter, a novel one-pot synthesis toward different thiocarbamates is described, which was discovered due to accidental contamination of an *N*-formamide with dimethyl sulfoxide (DMSO). As a result, dehydration of said *N*-formamide to its respective isocyanide yielded not only product, but also non-negligible quantities of an unknown side product, which proved to be the corresponding thiocarbamate. Thus, investigations of this newly found reaction were conducted. First, the reaction was briefly optimized toward higher selectivity and yield. Second, several experiments toward mechanistical studies were conducted to establish a potential reaction mechanism. Third, the optimized protocol was utilized to synthesize a library consisting of 16 thiocarbamates, which were obtained in moderate to good yields. Several strategies toward thiocarbamate-based polymers were investigated, ultimately leading to four novel norbornene-based monomers, which can be applied in a ring-opening metathesis polymerization.

State of the art

At the end of **Chapter 2.3.2** of the theoretical background, a brief introduction to isocyanide-based synthesis of thiocarbamates was given. Herein, isocyanides are shown to substitute the hazardous and extremely toxic phosgene, which is industrially applied in a two-step synthesis toward thiocarbamates. Therefore, it is either reacted with an amine first and subsequently with a thiol or *vice versa*. Although, phosgene is invaluable, its use strongly contradicts the principles of Green Chemistry and is generally a chemical to avoid. It is mostly synthesized locally and directly converted to its less hazardous derivatives to omit transports of the reagent, which always come with an exceptionally high risk. Hence, laboratory work with phosgene is only possible to a limited extent, which is where phosgene substitutes like diphosgene and triphosgene find their application. However, these are still quite toxic and hence should be omitted as well, if possible. There were only few substitute reactions to target the synthesis of thiocarbamates, yet as off 2016 several working groups published alternative routes based on isocyanides toward those compounds.[116–119] However, as previously discussed, the synthesis of isocyanides is often neglected in terms of overall sustainability, yet it relies on highly toxic reagents like $POCl_3$. Having established a more sustainable synthesis of isocyanides (**Chapter 4.1**), a coincidence led to the discovery of the herein discussed novel pathway to thiocarbamates. This route still relies on *p*-TsCl as a dehydrating agent and yields the respective thiocarbamate after addition of an aliphatic or benzylic sulfoxide before work-up. This not only gives access to novel thiocarbamate compounds, but also completely circumvents the isolation of the isocyanide compound used in literature-known thiocarbamate syntheses. Hence, only one work-up has to be conducted, which increases the overall sustainability of the obtained compounds.

Results and discussion

Discovery of the novel route toward thiocarbamates resulted from the synthesis of a building block for the arm-first approach described in **Chapter 4.3.2**. The reaction leading to the thiocarbamate side product is shown in **Scheme 52**. The aim was the synthesis of a novel building block utilizing **4**, **5** and aldehyde **9** by reacting them *via* P-3CR and subsequent dehydration utilizing the new protocol described in **Chapter 4.1**. However, **5** is quite insoluble in DCM, which is why 5% DMSO (with respect to the DCM volume) was added to the reaction mixture, to assist with the

dissolution. As later described in **Chapter 4.3.2**, this is not necessary as even the minute solubility is enough to ensure full conversion over time, yet its addition in first test reactions proved to be the driving force in the discovery of the new thiocarbamate synthesis as is described in this section. After evaporation of aldehyde **9** and DCM under reduced pressure, compound **10** was subjected to column chromatography to separate it from remaining isocyanide **4**. As **4** is far less polar than **10**, it was eluted with cyclohexane/ethyl acetate 7:1 and then the product was eluted by adjusting the gradient to cyclohexane/ethyl acetate 1:2 + 5% methanol. However, this also led to partial elution of the DMSO, and residual solvent stayed in the obtained product as impurity. To evaluate if the DMSO impurity interferes with the planned dehydration to compound **11,** a small test reaction was conducted, in which not only **11** was detected, but also an unknown species, which later proved to be thiocarbamate **12**. However, the only two species containing sulfur in the reaction were the dehydration agent *p*-TsCl and DMSO. The first was excluded, as such a side reaction would have already taken place in the reaction optimization described in **Chapter 4.1**, which was never observed. Concludingly, DMSO was rather quickly identified as the assumed reactant, yet in the beginning it remained unclear how the side reaction proceeded.

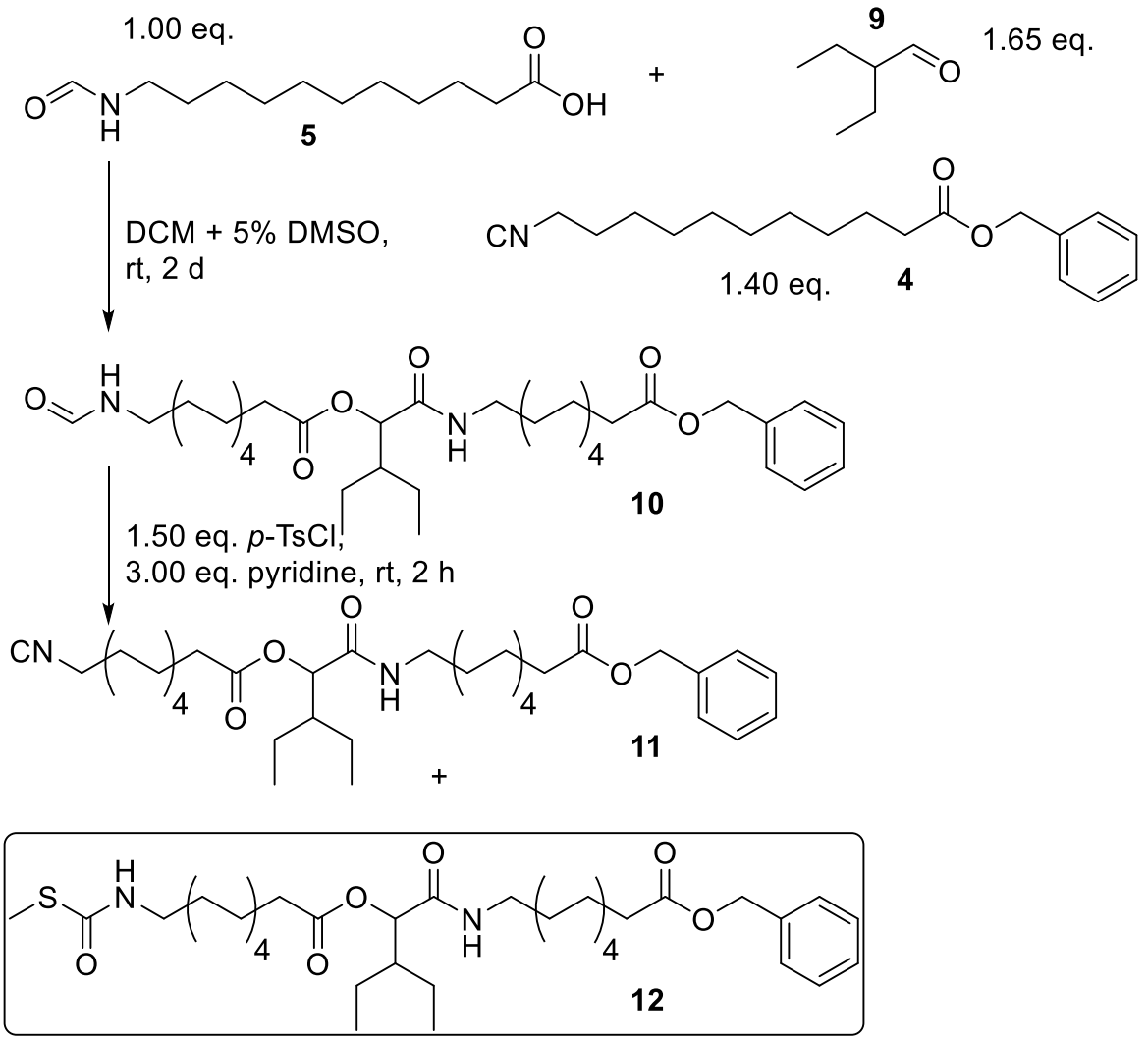

Scheme 52: Two-step synthesis of a longer building block **11** by P-3CR of **4**, **5** and **9** toward *N*-formamide **10**. Subsequent dehydration yielded desired product **11** but also a side product, which proved to be thiocarbamate **12**.

After several test reactions, it became clear that the addition of DMSO at a later stage (typically after the 2 h reaction time of the dehydration) is beneficial for the yield of the thiocarbamate.[355] With this information in hand, an internal standard-based GC reaction optimization conducted by T. Malliaridou under the author's co-supervison.[355] This time, *N*-dodecylformamide was used (instead of *N*-octadecyl formamide, which was used in **Chapter 4.1**) considering the volatility of the theoretical product, *S*-methyloctadecyl thiocarbamate, which would not be suitable for GC analysis. The formamide was therefore obtained quantitively from refluxing dodecyl amine in 10.0 eq. of ethyl formate (**Scheme 53**).

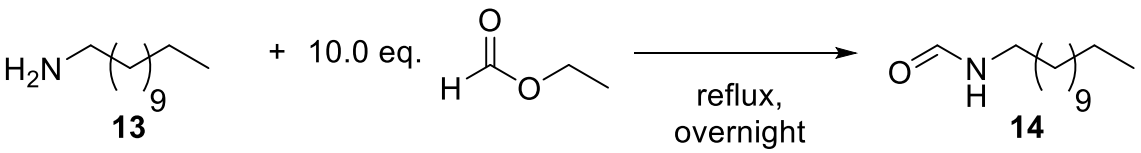

Scheme 53: Synthesis of **14** by refluxing **13** in an excess of ethyl formate.

However, the reaction system was found to be non-ideal for a standard-based GC analysis, as non-reproduceable and inexplainable results were obtained, for instance yields exceeding 100%. It is herein hypothesized that the inhomogeneity of the respective samples caused the deviations in the GC-based yield calculations as the preparation of these samples was sometimes accompanied by precipitation of solids. Therefore, a rough reevaluation of reaction conditions was conducted to obtain more reliable results. This was done by working up the respective reactions by flash column chromatography (**Scheme 54**, **Table 6**).

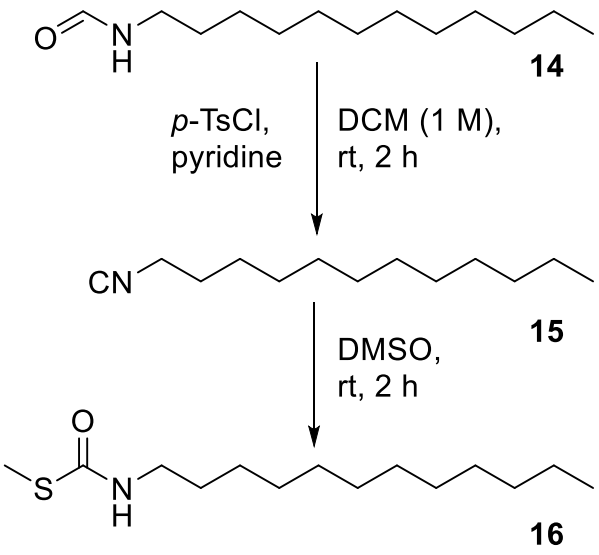

Scheme 54: Dehydration of formamide **14** to isocyanide **15** and subsequent reaction to obtain thiocarbamate **16**. The reaction was conducted in one pot without any purification.

Formamide **14** was dissolved in DCM (1 M) and reacted with pyridine and *p*-TsCl for 2 h, after which DMSO was added to the reaction mixture and stirring was continued for another 2 h. Then, the reaction mixture was directly subjected to column chromatography and the product was eluted with cyclohexane/ethyl acetate 10:1.

Table 6: Optimization of the thiocarbamate one-pot synthesis starting from *N*-formamide 14.

Entry	*Eq. p-TsCl/py*	*Eq. DMSO*	*Yield (%)*
1	1.00/2.00	1.50	0.00[a]
2	1.10/2.20	1.50	10.2[b]
3	1.20/2.40	1.50	45.1[b]
4	1.30/2.60	1.50	68.2[b]
5	1.40/2.80	1.50	74.8[c]
6	1.50/3.00	1.50	76.8[c]
7	1.60/3.20	1.50	76.5[c]
8	1.50/3.00	1.00	81.2[c]
9	1.50/3.00	1.25	76.5[c]
10	1.50/3.00	1.40	70.0[c]
11	1.50/3.00	1.50	76.8[c]
12	1.50/3.00	1.60	74.4[c]
13	1.50/3.00	2.00	47.0[c]

[a] Only isocyanide was obtained. [b] Mixtures of product and isocyanide were obtained and hence the yield was calculated by ^{1}H NMR spectroscopy. Therefore, the CH_2 adjacent to the isocyanide functionality and the NH of the thiocarbamate were integrated and compared. [c] Only product was obtained.

Adjusting the amount of dehydrating agent, which was always utilized in a 1:2 ratio with pyridine, like in the previous isocyanide synthesis, gave a maximum of yield (76.8%) at 1.50 eq. *p*-TsCl regarding the *N*-formamide. Further increase was not reflected in an increased yield of thiocarbamte. Lowering its amount, however, was connected not only with decreasing yield, but also in a change of the main product. Equivalents above 1.40 yielded solely the thiocarbamate **16**, whereas at 1.30 to 1.10 eq., a mixture of thiocarbamate **16** and isocyanide **15** was obtained. However, as in the applied work-up procedure (flash column chromatography), isocyanide and product were not separable and thus the yields were calculated by peak integration of the ^{1}H NMR spectrum of the obtained isocyanide/product mixture. At 1.00 eq., no traces of product were observed anymore, already hinting a participation of *p*-TsCl in the mechanism of the thiocarbamate formation. In contrast to that, altering the DMSO equivalents gave an inconsistent trend, as the maximum (81.2%) was achieved at 1.00 eq. with decreasing yields thereafter. Surprisingly, at 1.50 eq., another increase in yield was observed: 76.8% (**Table 6**, entries 6/11). However, as some of the later employed *N*-formamides and sulfoxides exhibited differences in reactivity, any further

procedure (e.g. for the library synthesis describe later) was conducted utilizing 1.50 eq. *p*-TsCl, 3.00 eq. pyridine and 1.50 eq. of sulfoxide (**Scheme 55**).

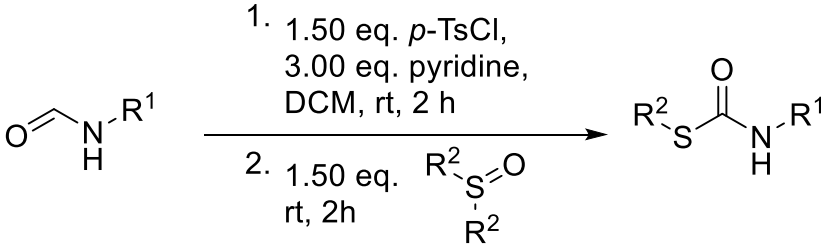

Scheme 55: Optimized conditions of thiocarbamate synthesis starting from *N*-formamides in a one pot procedure.

Next, a library of thiocarbamates was synthesized utilizing four different *N*-formamides and four commercially available sulfoxides, also to investigate if different sulfoxides would lead to the respective now expected products. The reaction was worked up by loading the crude reaction mixture onto a column and flushing with different gradients of cyclohexane/ethyl acetate. As the results of these reactions also helped with the evaluation of a mechanism, its evaluation is targeted in the paragraphs thereafter.

Table 7: Thiocarbamates synthesized *via* one-pot dehydration and sulfoxide addition Optimized conditions from **Scheme 55** were applied for all sixteen compounds. The batch size was 2.50 mmol for the first three entries and 10.0 mmol for entry 4.

Entry	*N-formamide*	*Sulfoxide 1* *yield (%)*	*Sulfoxide 2* *yield (%)*	*Sulfoxide 3* *yield (%)*	*Sulfoxide 4* *yield (%)*
1	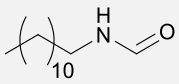	77	85	80	53
2	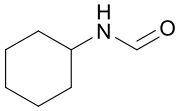	69	70	70	25
3	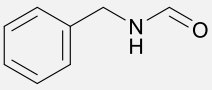	72	59	81	46
4	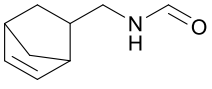	60	73	79	50

Originally, this direct application onto silica without any quenching and aqueous work-up was also tried for some procedures of **Chapter 4.1** (sustainable isocyanide synthesis), yet had to be abandoned because of some unreacted *p*-TsCl, which remained in the crude mixture (indicated on the TLC and visualized by UV light). The remaining *p*-TsCl was often not separable from the product on the column, hence aqueous work-up had to be conducted for the isolation of isocyanides. However, in the thiocarbamate synthesis, no such spot was visible on the TLC after the mixture had reacted with the sulfoxide. As product and side products (*p*-TsOH, pyridine and pyridinium hydrochloride) exhibit a large difference in polarity, direct subjection to column chromatography without any aqueous work-up was possible for most derivatives. However, reactions utilizing benzyl sulfoxide led to impure product after flash chromatography, as it was contaminated with an unknown compound, which was later identified as benzyl sulfide (this was yet invaluable for the mechanistical studies, which are described in a later paragraph, **Scheme 56**).

Regarding the library displayed in **Table 7**, the thiocarbamates were isolated in medium to good yields (exception is *N*-cyclohexyl formamide being reacted with benzyl sulfoxide). The benzylic sulfoxide proved to be the least reactive in the thiocarbamate synthesis, whereas the cyclic tetrahydrothiophene-1-oxide and DMSO gave consistently high yields. Butyl sulfoxide exhibited the highest yield if reacted with dodecyl isocyanide, yet gave only moderate yield with benzyl isocyanide. Interestingly, the thiocarbamates derived from benzyl isocyanide gave higher yields than just the synthesis of intermediate benzyl isocyanide with *Proc. A* from **Chapter 4.1** (44% for benzyl isocyanide isolation *versus* 72/59/81/46% for the resulting thiocarbamates), further implying that some benzyl isocyanide is getting lost in the aqueous work-up. However, employment of the cyclic sulfoxide (**Table 7**, tetrahydrothiophene-1-oxide) was of more interest as further information regarding the mechanism were expected from its products. As the resulting thiocarbamates always contain one of the alkyl chains of the sulfoxides, the cyclic sulfoxide was employed to evaluate the fate of the second alkyl chain. For tetrahydro thiophen-1-oxide, ring-opening was observed with the open end being attacked by chloride as nucleophile, yielding the 4-chlorobutyl thiocarbamate as final product (**Scheme 56**). Note that full analytical characterization of the obtained compounds can be found in **Chapter 6.3.2**. Next to ^{1}H and ^{13}C NMR spectroscopy, also mass and IR analysis were conducted. As an example, the ^{1}H NMR

spectrum of **16** depicted in **Figure 16**, which stands for the respective purity of the isolated thiocarbamates.

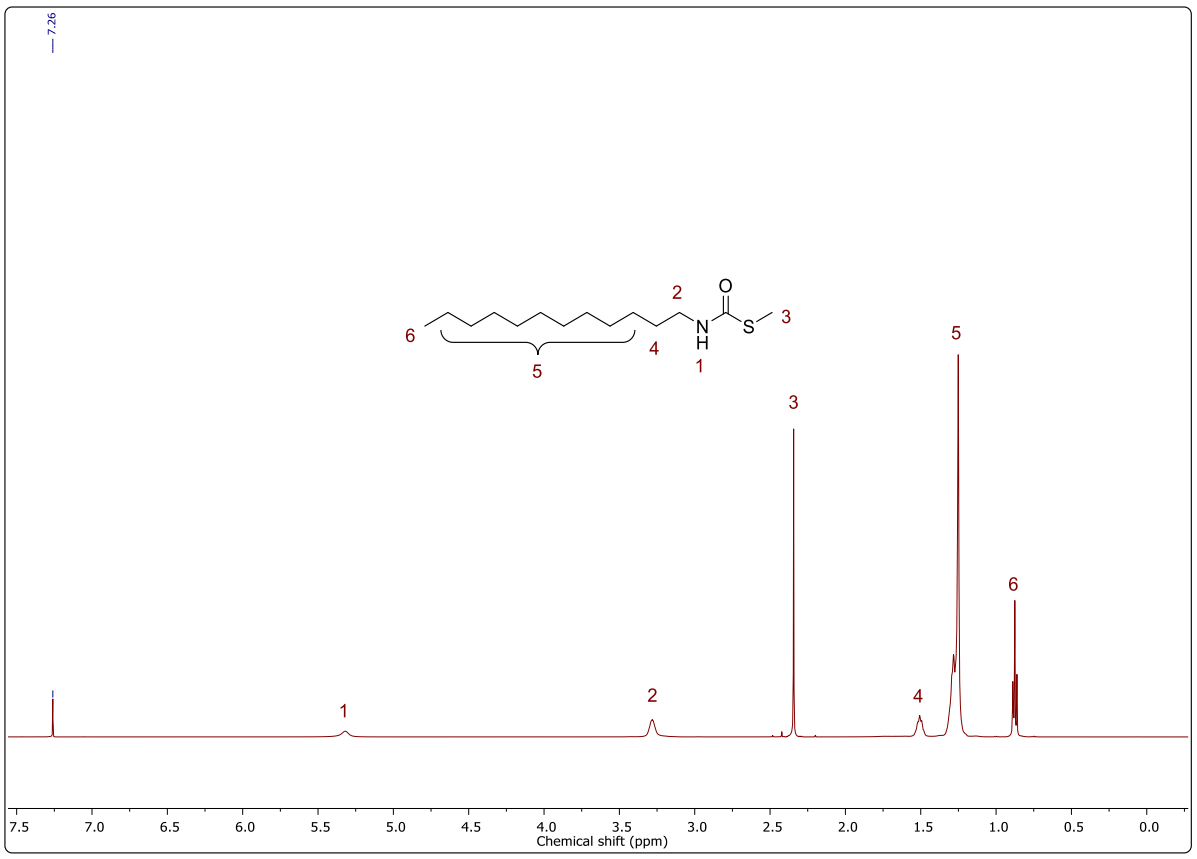

Figure 16: ^{1}H NMR spectrum of **16** in deuterated chloroform ($CDCl_3$). Peak number one belongs to the amide proton, whereas peak number three belongs to the methyl group adjacent to the sulfur atom.

However, the mechanism of the reaction was still not resolved and hence was the main focus of further experiments. As already mentioned, both the reaction with benzyl sulfoxide and tetrahydrothiophene-1-oxide provided invaluable insights toward a mechanism. Also, GC analysis of a reaction utilizing butyl sulfoxide and benzyl sulfoxide was conducted (**Scheme 56**). These experiments further pointed to an alternative redox reaction, which occurred simultaneously. Furthermore, the formation of dimethyl sulfide in the reactions that employed DMSO as reagent, was indicated by the unpleasant characteristic smell of rotten cabbage attributed to the sulfide. However, due to its volatility, it was not possible to isolate nor to measure said compound by GC-MS analysis, whereas the butyl sulfoxide as well as benzyl sulfoxide clearly indicated the formation of their respective sulfides in the chromatogram of the GC-MS. The paired mass spectrometer indicated masses that were assigned to

benzyl/butyl sulfide (note that for this experiment *N*-cyclohexyl formamide and not *N*-dodecyl formamide was employed).

Following literature research revealed a publication from 2011, in which DMSO was used in the oxidation of isocyanides toward isocyanates.[356] There, trifluoroacetic anhydride was utilized as catalyst and the reaction was carried out at -60 °C to 0 °C in DCM. To trap the highly reactive isocyanate, primary amines were employed, and the respective urea compounds were isolated. However, it was also shown that cyclohexyl isocyanate could be isolated by just evaporating the solvents, yielding the desired isocyanate in high yield and purity (albeit some residual DMSO was detected). With this knowledge in hand, the GC chromatograms were carefully reevaluated, yet only traces of cyclohexyl isocyanate were found. However, the chromatogram revealed benzyl chloride as side product for the reaction utilizing benzyl sulfoxide **17**, which confirmed the assumption made from the reaction employing tetrahydrothiopen-1-oxide **18**: the second substituent of the sulfoxide forms the respective chloro-hydrocarbon (**Scheme 56**).

1. Reaction of benzyl sulfoxide and tetrahydrothiophen-1-oxide

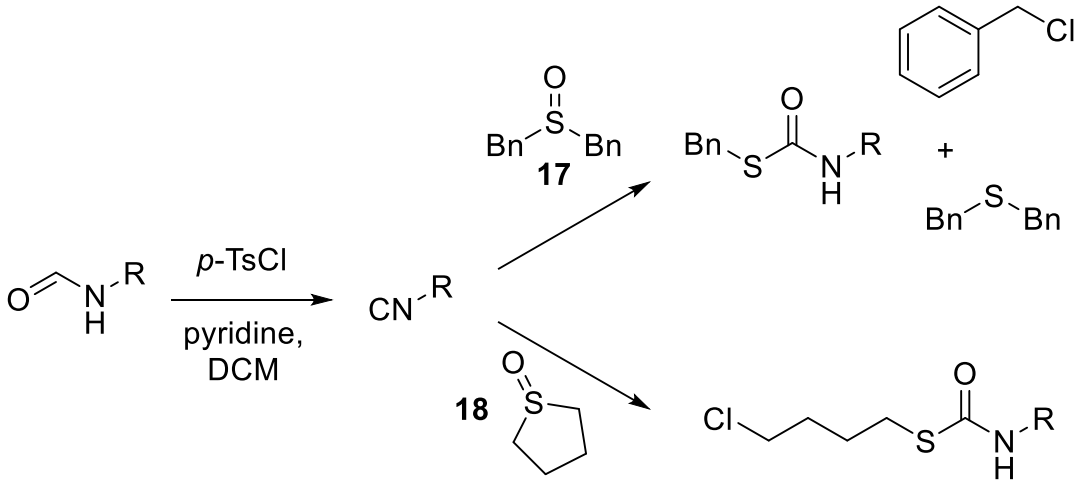

2. Oxidation state of the involved species

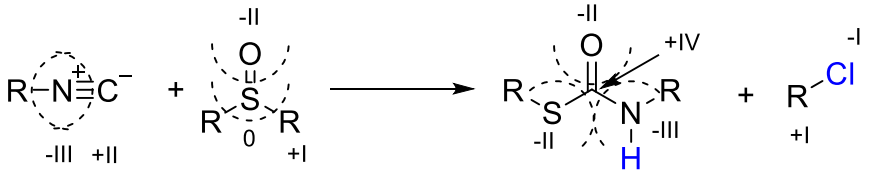

Scheme 56: 1. Employment of benzyl sulfoxide and tetrahydrothiophene-1-oxide for the synthesis of thiocarbamates. For the first, benzyl chloride and benzyl sulfide were confirmed as side products. For the second, a 4-chlorobutyl thiocarbamate was identified as product, indicating a nucleophilic attack of chloride at the open end of the ring-opened sulfoxide. 2. Oxidation states of the assumed reactants indicating an oxidation of the isocyanide carbon from +II to +IV and a reduction of the sulfoxide sulfur from 0 to -II. The assumed byproduct

consisting of a chloride and the second sulfoxide alkyl chain retain their oxidative state of -I/+I, respectively. The necessary proton and chloride (blue) however cannot stem from the main participants of the reaction (isocyanide and sulfoxide).

However, for DMSO and butyl sulfoxide, this was not detectable as methyl chloride as well as butyl chloride are too volatile to be either isolated or be distinguishable from the solvent peak in the GC-MS. Surprisingly, alkyl-phenyl substituted sulfoxides (e.g. methylphenyl sulfoxide), which theoretically have to react with the phenyl substituent as the existence of cationic phenyl moiety can be excluded, did not react at all.

Subsequently, the already identified reagents were examined regarding their oxidation state. In the reaction, the isocyanide carbon is oxidized from +II to +IV, whereas the sulfur of the sulfoxide is reduced from 0 to -II, confirming the assumption that the observed transformation is a redox reaction. Hence, the number of electrons is already balanced for the involved compounds. However, neither the sulfoxide nor the isocyanide can provide the proton and chloride ion, which are necessary for the correct stoichiometry of the reaction. Reconsidering the first part of the reaction, dehydration of a *N*-formamide with *p*-TsCl and pyridine yields an equimolar amount of pyridinium tosylate and pyridinium hydrochloride as byproducts, which represent the missing piece of the puzzle in the reaction equation: the *in situ* produced pyridinium hydrochloride is reconverted to pyridine, while the proton is subtracted by the thiocarbamate nitrogen, and thus the chloride finds itself in the second alkyl chain of the sulfoxide.

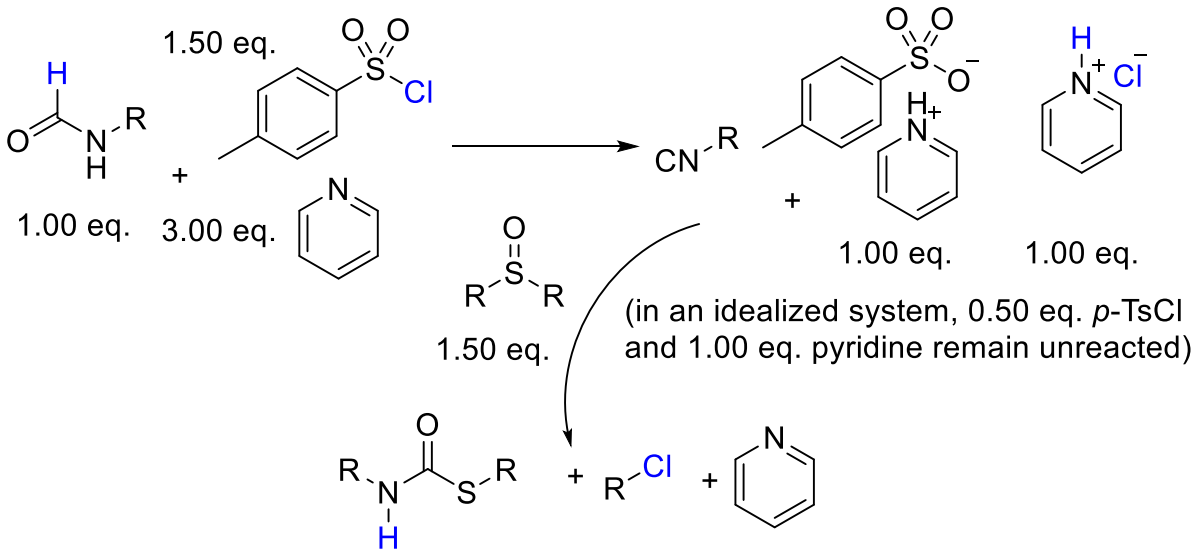

Scheme 57: Idealized dehydration of a formamide yields its respective isocyanide as well as 1.00 eq. of pyridinium tosylate and pyridinium hydrochloride. Theoretically, an excess of

0.50 eq. of *p*-TsCl remains unreacted within the reaction mixture. After sulfoxide addition, the isocyanide is converted to the thiocarbamate formally utilizing one equivalent of HCl. After the reaction, no *p*-TsCl is detectable in the GC or on TLC indicating a certain relevance for conversion.

Having established the complete reaction equation, only the mechanism remained unknown, next to the role of the *p*-TsCl, which seemed to be connected as remaining *p*-TsCl from the isocyanide dehydration was consumed over the course of the thiocarbamate formation. To get further insights, the synthesis of thiocarbamates from isocyanides was targeted. Therefore, commercially available cyclohexyl isocyanide was reacted with DMSO to form *S*-methyl cyclohexyl thiocarbamate. Different conditions were tried and are summarized in **Table 8**. The reactions were analyzed by GC in 15 min intervals. 1.50 eq. DMSO and pyridinium hydrochloride were deemed obligatory to ensure full conversion in stoichiometric terms. As before, the reactions were carried out in dichloromethane.

Table 8: Reaction conditions for the evaluation of the role of *p*-TsCl in the thiocarbamate formation.

Entry	*Eq. DMSO*	*Eq. p-TsOH*	*Eq. p-TsOPyrH*	*Eq. Pyr*HCl*	*Eq. p-TsCl*	*Eq. pyridine*
1	1.50	0.50		1.50		
2	1.50		1.50	1.50		
3	1.50			1.50		
4[a]	1.50		1.50	1.50	0.50	1.00
5[a]	1.50			1.50	0.50	1.00

[a] These entries feature the same conditions as entry 2 and 3 yet also contain the theoretical excess of dehydrating agent and pyridine from the isocyanide dehydration.

Table 8, entry 1 was conducted under acidic conditions utilizing 1.50 eq. of pyridinium hydrochloride and 0.50 eq. of *p*-TsOH, however, after one hour only formamide was detected indicating the decomposition of cyclohexyl isocyanide. For **Table 8**, entries 1 and 2, no reaction was observed, yet the isocyanide remained stable over the course of the screening (2 h). Hence, after 2 h, 0.50 eq. *p*-TsCl and 1.00 eq. pyridine, which resemble the theoretical excess in an isocyanide dehydration, were added. The following GC measurements indicated thiocarbamate formation, which proceeded until the isocyanide was completely consumed. Whereas the reaction was normally completed in 15 min to 1.5 h, these batches had to be stirred overnight to ensure full completion. It was noticed that the pyridinium hydrochloride was hardly soluble in DCM, which is most likely the reason for the prolonged reaction time. However, it remained

unclear why the compound exhibited such bad solubility. In the isocyanide dehydration, precipitation of the highly polar salts (*p*-TsOPyrH and Pyr*HCl) was only witnessed in dimethyl carbonate, never in dichloromethane. Nevertheless, the experiments confirmed that the presence of unreacted *p*-TsCl is necessary for the reaction to proceed as not a trace of thiocarbamate was detected in the blank feed.

Finally, an experiment was conducted to exclude a radical based mechanism. Therefore, the standard procedure was employed, yet 1.50 eq. benzophenone was added after the dehydration, before addition of the sulfoxide. As the reaction proceeded normally, it is highly unlikely that a radical species is involved.

Based on all results, a possible mechanism was proposed and is depicted in **Scheme 58**. The crucial reaction steps are marked with letters, whereas important intermediates carry the abbreviation **I+number**. The assumed reaction mechanism considers the whole chemical environment after the dehydration to the isocyanide and begins with addition of the sulfoxide (here DMSO). Note that due to the dehydration, excess *p*-TsCl (theoretically 0.50 eq.) as well as the dehydration byproducts pyridinium tosylate and pyridinium hydrochloride are present, the latter being important for complete stoichiometry. In reaction step **a**, the remaining *p*-TsCl reacts with DMSO to form **I1** in a Swern-like reaction. This is backed by recent literature, which proposed that *p*-TsCl is indeed capable of replacing oxalyl chloride, which is utilized in the standard protocol of a Swern oxidation.[357] As the sulfoxide is now activated, the isocyanide component acts as nucleophile (step **b**), yielding the hypothetical and rather unstable transition state **TS1**. After rearrangement **c** into intermediate **I2**, the reaction proceeds in three different pathways. However, pathways 1 and 2 featuring steps $\mathbf{d}_a$ + $\mathbf{e}_a$/$\mathbf{d}_b$ + $\mathbf{e}_b$ are basically the same, yet in inverted order and, finally, both lead to the expected thiocarbamate. Step $\mathbf{d}_a$ features the separation of the alkyl chloride (methyl chloride in this case) yielding **I3a**, whereas in $\mathbf{d}_b$ the *p*-TsCl species is recovered and the isocyanide nitrogen subtracts the proton from pyridinium hydrochloride giving **I3b**. After step $\mathbf{e}_a$/$\mathbf{e}_b$, the product **TC1** is obtained, respectively. These pathways are confirmed by the presence of benzyl chloride in the GC measurement for the reaction utilizing benzyl sulfoxide as reagent. Furthermore, even in an idealized reaction, only 0.50 eq. *p*-TsCl remain after the dehydration to the isocyanide, yet the reaction proceeds to full conversion. This suggests the recovery of the activating *p*-TsCl species. However, it remains unclear if actually chloride attacks as a nucleophile or rather the conjugated base of *p*-TsOH (leading to the symmetric

anhydride of *p*-TsOH, which should also allow for activation), as they both are below-average nucleophiles. The designation *catalysis* is omitted as no such proof was obtainable. In the remaining pathway 3, step **d*c*** targets the side reaction leading to the respective sulfide. Herein, the tosyl species is eliminated from **I2** without any further reaction, yielding the sulfide **SU1** (in this case dimethyl sulfide, which evaporates due to its low boiling point) as well as an isocyanate **ICA1**.

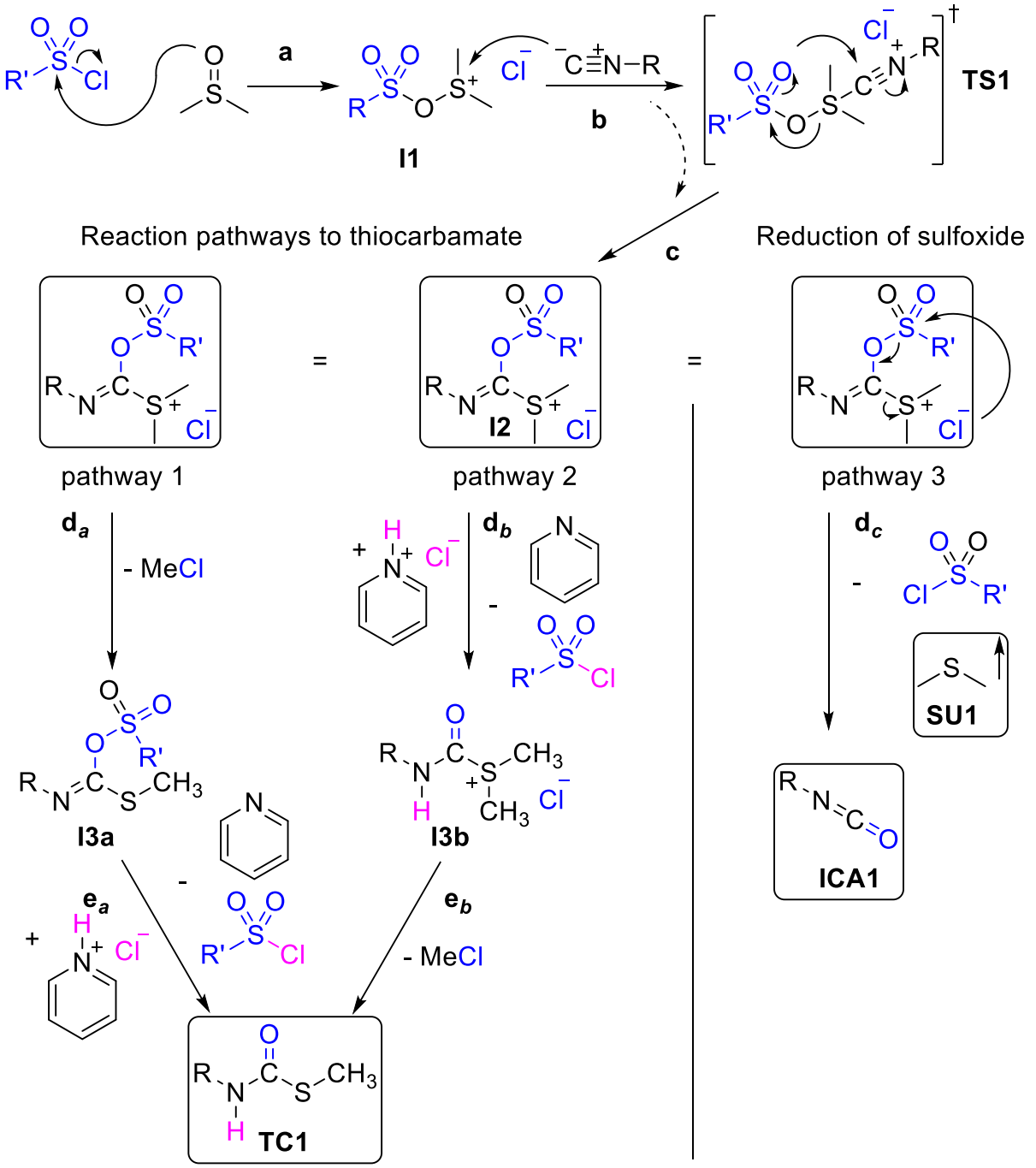

Scheme 58: Proposed mechanism of thiocarbamate formation utilizing DMSO and an isocyanide by *p*-TsCl activation. **a** DMSO and *p*-TsCl react to form a Swern-like intermediate **I1 b** the isocyanide component (nucleophile) attacks **I1** to form the hypothetical transition state **TS1**, **c** which rearranges to **I2**. From here, the reaction continues in three potential pathways:

d_a and **d_b** lead to the expected product, whereas **d_c** targets the sulfoxide reduction to sulfide **SU1** also yielding the isocyanate **ICA1**.

The catalytic oxidation of isocyanides utilizing DMSO[356] and the detection of butyl sulfide/benzyl sulfide as well as the isolation of benzyl sulfide confirm the assumed pathway. However, the respective isocyanate compound was only detected in small amounts by GC and could not be isolated. It is hypothesized that it decomposes under the applied conditions. Originally, it was planned to underline the presumed mechanism *via* theoretical calculations, yet due to time restrictions, only basic values regarding the reaction enthalpy and stability of the postulated intermediates were received. Hence, these are not presented within this thesis.

Furthermore, this novel reaction was attempted to be employed in the synthesis of thiocarbamate-based monomers suitable for subsequent polymerization toward applications in material sciences (**Scheme 59**)

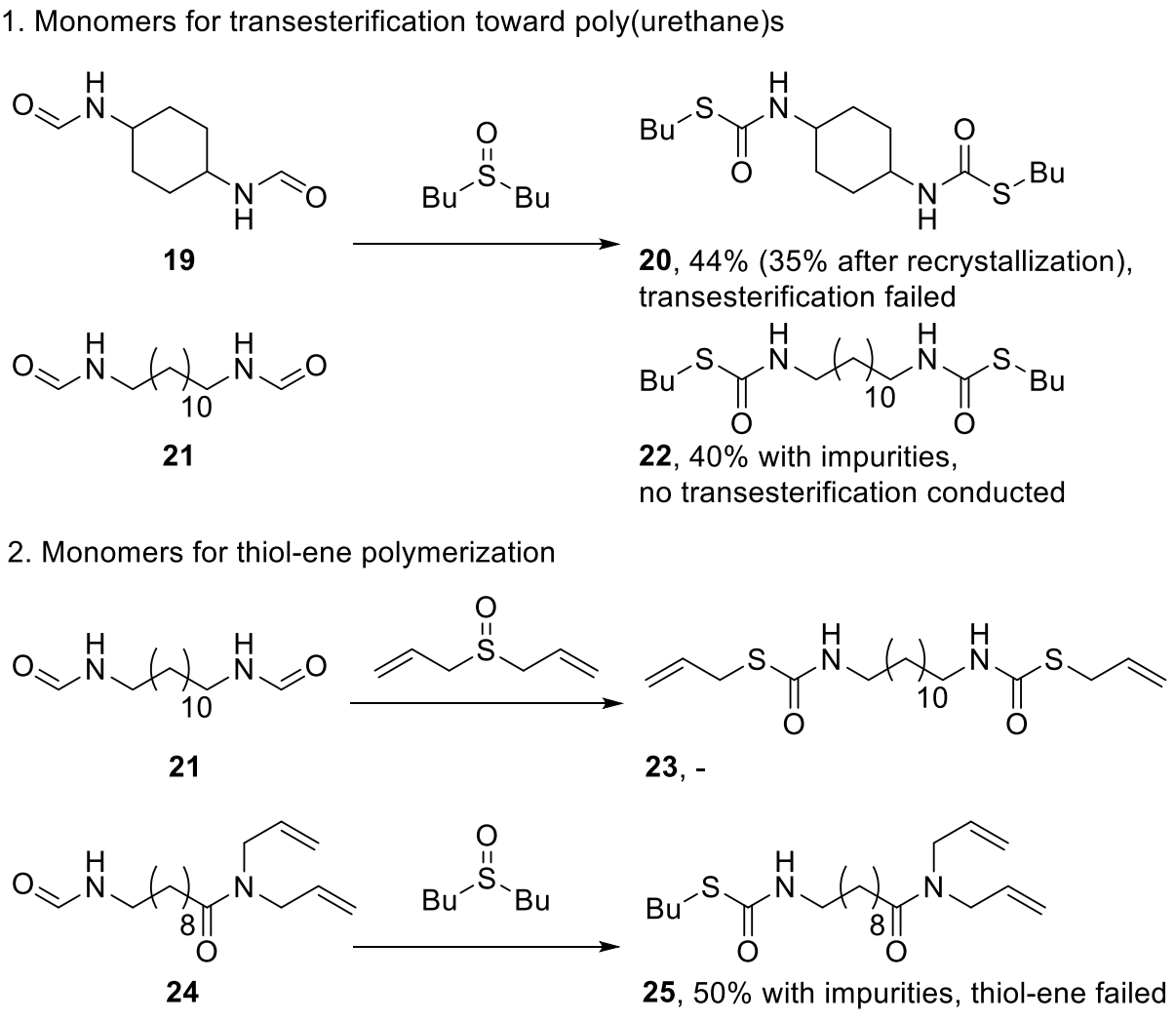

Scheme 59: Synthesis toward polymerizable thiocarbamates. 1. Monomers which allow for transesterification with diols. 2. Monomers designed to be polymerized *via* thiol-ene addition.

Neither the first nor the second approach was successful, as first yield was below average and often inseparable impurities remained within the isolated compounds and/or the suggested polymerization failed.

The final monomers were already presented within **Table 7** (p. 103) and are based on *N*-(5-norbornene-2-methyl) formamide, however several different pathways toward monomers were investigated. The associated intermediates are discussed within this chapter, yet as none of these syntheses was expedient, their analytics are **not** listed in **Chapter 6.3.2** for reasons of clarity.

In a first approach, the formamides **19** and **21** were reacted with butyl sulfoxide to their respective bis-thiocarbamates **20** and **22** (note that butyl sulfoxide was used instead of the cheaper DMSO, to omit the release of highly toxic methane thiol in the envisaged transesterification toward PUs). However, yields as well as purity were below-average for **22** (40% with remaining impurities). Also, the standardized work-up procedure (direct subjection to column chromatography) proved to be non-ideal due to the exceptionally poor solubility of the obtained compounds leading to smearing and contamination on the column. Hence, **20** was recrystallized in ethyl acetate after column chromatography, which yielded pure product in a yield of 35%. The ^{1}H NMR spectrum of the compound is depicted in **Figure 17**.

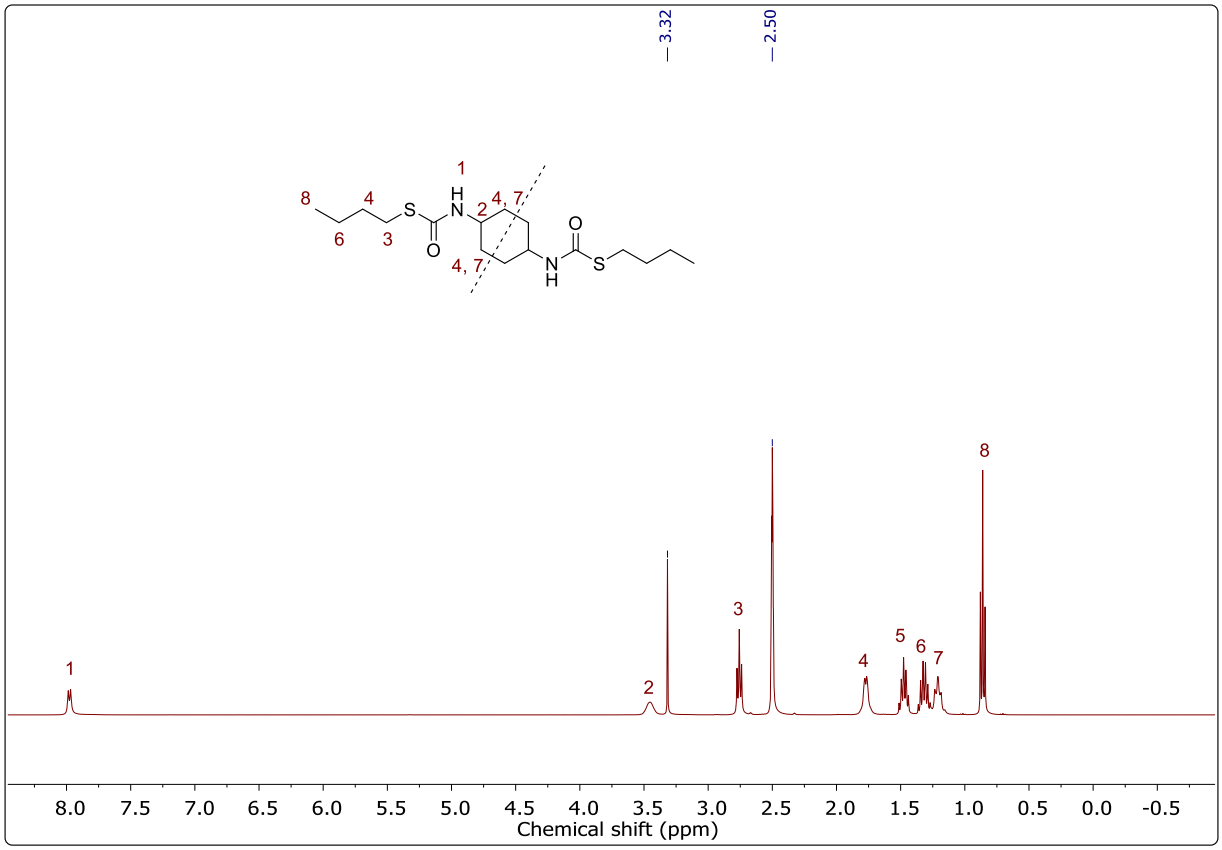

Figure 17: ^{1}H NMR spectrum of recrystallized **20** in deuterated dimethyl sulfoxide (DMSO-d_6). The peak at 3.32 ppm corresponds to water.

The subsequent transesterification, which was attempted in DMSO (0.25 M) and 10 mol% 1,8-diazabicyclo(5.4.0)undec-7ene (DBU) or 1,5,7-triazabicyclo(4.4.0)dec-5-en (TBD) at 75 °C under reduced pressure, only yielded low-molecular oligomers. These already precipitated in the hot DMSO hindering any further polymerization. Furthermore, a bulk polymerization was attempted, yet failed as compound **20** exhibited no melting point and just decomposed at elevated temperatures (at around 200 °C). Hence, the investigations toward these monomers were discontinued as the synthesis as well as the solubility/melting properties of the obtained compound **22** were unfavorable for subsequent polymerization.

Instead, an alternative pathway was investigated. Allyl sulfoxide was synthesized from allyl sulfide in a water/acetonitrile mixture utilizing Oxone® and obtained in moderate yield (49%) after column chromatography. Afterwards, the sulfoxide was employed together with *N*-formamide **21**, yet no product **23** was isolated. Further efforts to obtain monomers bearing the thiocarbamate in the backbone were unsuccessful. Alternatively, formamide **24** was synthesized and reacted with butyl sulfoxide to yield

monomer **25** bearing the thiocarbamate in the side chain. However, compound **25** could only be isolated in a moderate yield of 50% with some unknown impurity remaining. Nevertheless, a thiol-ene procedure from a previous publication of our working group was adapted, yet failed to deliver a polymeric compound.[358] Instead, only low-molecular oligomers were obtained according to an SEC measurement (**Figure 18**).

As both strategies led to a dead end, yet another pathway to monomers bearing thiocarbamate groups in the side chain was investigated (**Table 7**, entry 4). Here, molecules featuring a norbornene group and no other functional groups that might interfere with the thiocarbamate syntheses were employed. Hence, these monomers were obtained in moderate to good yields and it is planned to employ these in a ring-opening metathesis polymerization (**Scheme 60**). First experiments conducted by D. Barther already confirmed the reactivity of **ROMP-M2**, yet optimization of the ROMP as well as full analytical data is still pending.

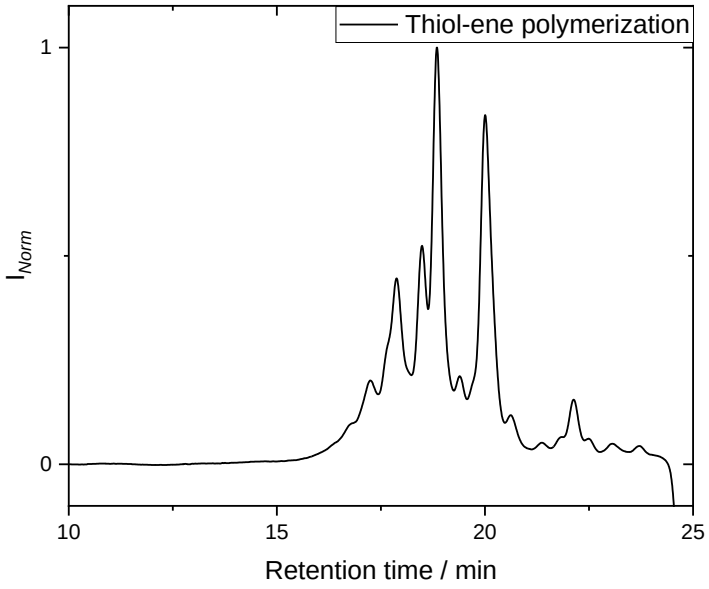

Figure 18: Crude SEC measurement in THF after employing compound **25** and 1,6-hexanedithiol in a thiol-ene polymerization. The normalized peak belongs to compound **25**, whereas the second highest peak at about 20 min belongs to the dithiol. Oligomeric species are visible at lower retention times (M_n = ~1000 g/mol).

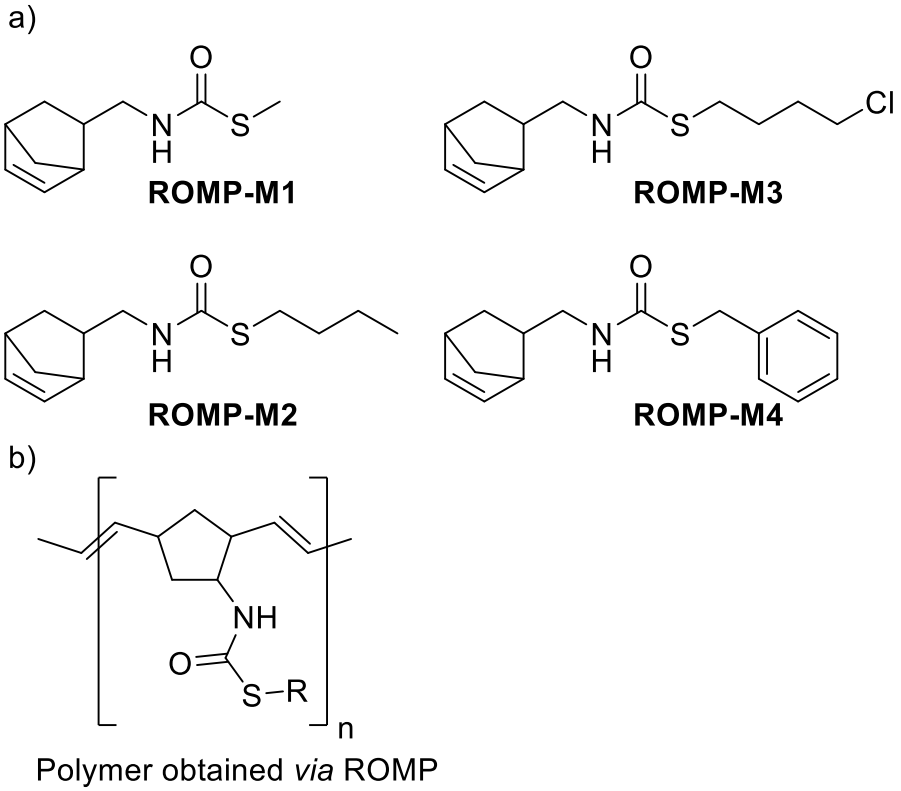

Scheme 60: a) Four ROMP monomers, each containing different thiocarbamates. Subsequent, polymerization leads to an unsaturated polymer bearing thiocarbamates as side chains. b) Simplified structure of a polymer obtained *via* ROMP utilizing one of the above-mentioned monomers.

Concluding, a novel reaction to synthesize diversely substituted thiocarbamates has been developed. The procedure is based on the previously described more sustainable isocyanide synthesis utilizing *p*-TsCl and features addition of an aliphatic sulfoxide after initial dehydration of the employed *N*-formamide. Hence, the procedure is considered one-pot as no work-up/isolation of the isocyanide is necessary for the thiocarbamate to be formed. This represents a distinct advantage over literature-known syntheses of thiocarbamates, which always employ pre-synthesized isocyanides, yet often misappropriate the fact, that the synthesis of the isocyanide is considered non-sustainable.

The newfound reaction was optimized regarding its conditions and then applied to synthesize a library of sixteen different thiocarbamates, which were obtained in moderate to good yields. The conducted reactions featured the commercially available sulfoxides DMSO, butyl sulfoxide, tetrahydrothiophene-1-oxide and dibenzyl sulfoxide. The employed *N*-formamides were already known from a previous publication (**Chapter 4.1**), with *N*-(5-norbornene-2-methyl) formamide being an exception, which was added last to the library.

Furthermore, several experiments featuring gas chromatographic analyses identified alkyl chlorides as byproducts, whereas the reduction of the sulfoxide to a sulfide and the respective oxidation of the isocyanide to an isocyanate was identified as side reaction. A mechanism was proposed and the excess *p*-TsCl from the formamide dehydration was found to be the driving force of the reaction, as it activates the sulfoxide in a Swern-like mechanism. Furthermore, as the employment of *p*-TsCl is not stoichiometric, recovery of the activating *p*-TsCl can be assumed yet is hard to prove. This analytical gap and the fact that after full conversion of the isocyanide component no *p*-TsCl remains within the reaction mixture, are the main reason why the term *catalysis* is omitted.

Finally, syntheses toward thiocarbamate monomers for subsequent polymerization were conducted yet failed to match the expectations. Poor yields, inseparable impurities as well as low solubility and reactivity did not allow the synthesis of polymers with thiocarbamate groups in the backbone. Hence, novel norbornene-based thiocarbamate monomers were synthesized and obtained in moderate to good yields and high purity. However, their employment in a ring-opening metathesis polymerization is still pending, yet a first test reaction confirmed the successful synthesis of the desired polymer.

4.3 The synthesis of uniform star-shaped macromolecules

It was already discussed in **Chapter 2.4** that the synthesis of uniform and sequence-defined macromolecules is a rather new area of research in polymer chemistry.[18,20,21,251,359]

The main targeted applications are the fundamental evaluation of differences between macromolecules exhibiting dispersity and ones that do not,[23] as well as understanding the sequence-property relationships and the application of sequence-defined macromolecules in data storage.[31,32,224,247]

Practically, research on this topic started when Merrifield first proposed his iterative procedure toward uniform oligopeptides, which relied on solid-phase synthesis as well as orthogonal protecting groups.[22] Also, both strategies are still employed as valuable tools in the preparation of uniform macromolecules. Recent publications on sequence-definition mostly feature novel manmade systems employing different kinds of chemistry for their synthesis,[23,25,26,235] whereas oligopeptides still have their foundation in natural chemistry.

However, whereas linear approaches toward uniform macromolecules have been evaluated quite intensely (mostly because of their applications in the field of molecular data storage),[26,31,32,232,248] multidirectional approaches have been neglected, with dendrimers being an exception.[264,275] To fill this gap in research, the synthesis of uniform star-shaped macromolecules has been targeted and will be evaluated in the next two sub-chapters.

4.3.1 The road to uniform star-shaped macromolecules – a core first approach

Abstract

The step-wise procedure toward sequence-defined macromolecules utilizing the P-3CR and subsequent hydrogenation is well established within our working group and was published in 2016.[26] Since then, the approach was employed to synthesize macromolecules in a linear as well as in a bidirectional fashion for several applications.[31,35,249]

Within this chapter, the protocol is adapted to fit the demands of a multidirectional synthesis of uniform star-shaped macromolecules in a core-first approach. The protocol had already been reliable in linear or bidirectional synthesis, while the novel multidirectional adaption revealed its limitations. The reaction procedure was accompanied by side reactions, which could not be resolved or suppressed. Several approaches were employed to address the mentioned challenges, yet none proved to be successful. Finally, due to the resulting inseparable impurities, the approach was abandoned and reworked into an arm-first approach, which is presented in **Chapter 4.3.2**.

State of the art

The synthesis of sequence-defined macromolecules employs mostly linear and bidirectional strategies, as well as the iterative exponential growth approach (IEG).[20,21,23,34] Hence, the obtained molecules are also linear and only a few other architectures are known.[24] However, in polymer science, research has been focused for a long time on sophisticated molecular architectures as unique structural insights and interesting applications derive from their structure.[36,306,313,315] Meanwhile, as polymers always come in a distribution in size, the question if their properties derive from their structure or rather their dispersity often remains unanswered. Sequence-definition aims to resolve this fundamental question with the main focus of revealing

the complex mechanisms of sophisticated structures, such as DNA or enzymes. Followingly, research would greatly benefit from the synthesis and evaluation of highly defined globular structures such as dendrimers or star-shaped structures. Whereas dendrimers are nearly always obtained in high definition and still represent a “hot topic” since their initial discovery in the late 20th century,[262,264] uniform star-shaped macromolecules have been neglected so far. Still, their unique structure and their immense versability offers a broad spectrum of applications like drug delivery,[316,328–330] catalysis,[332] biomedicine,[333,334] and other applications.[36]

The synthesis of linear uniform macromolecules, as well as the synthesis of star-shaped polymers *via* the P-3CR is already literature-known and has been established by our working group (**Scheme 61**).[26,37,312] Both procedures have already been thoroughly discussed within the theoretical background of this thesis (**Chapter 2.4** and **2.5**), yet the mechanisms are illustrated in the scheme above for clarity. As both are known for their reliable character, straightforward protocols, high yield and simple purification, the approaches were adapted and combined for the synthesis of uniform star-shaped macromolecules.

1. Iterative synthesis toward uniform macromolecules utilizing P-3CR and hydrogenation

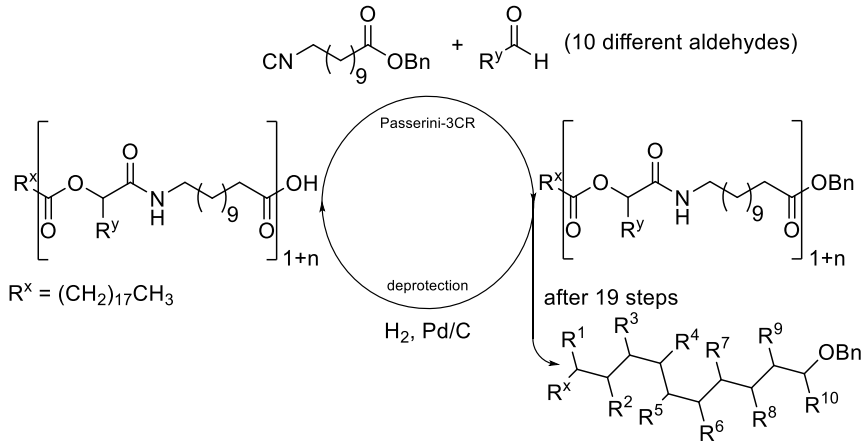

2. P-3CR polymerization toward star-shaped polymers and subsequent post-polymerization modification utilizing a PEG isocyanide and aldehyde

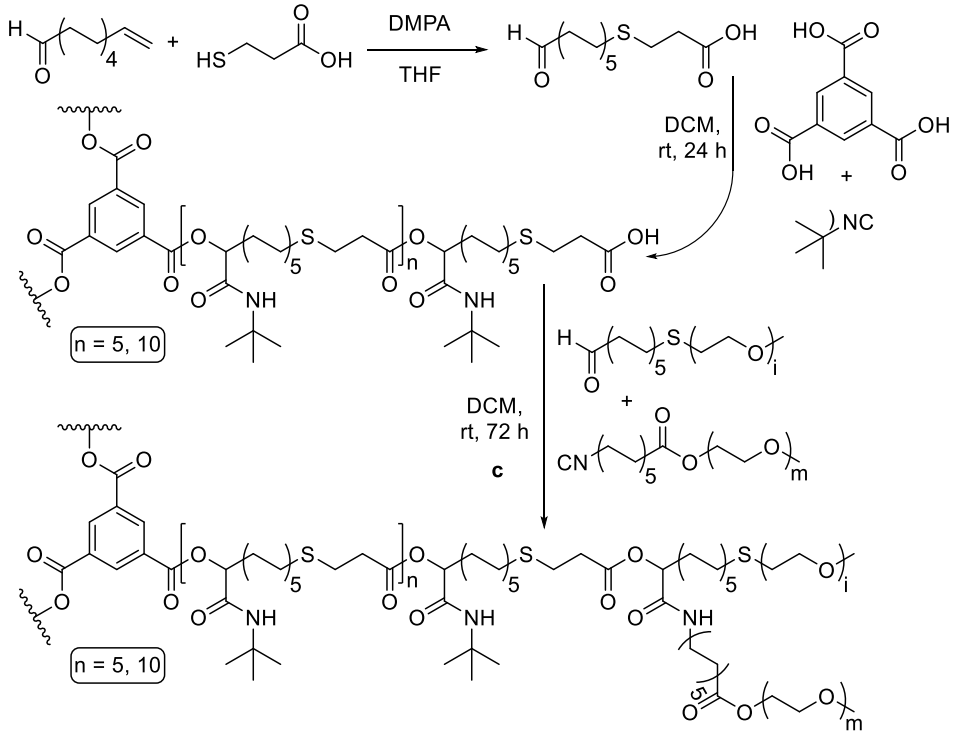

Scheme 61: 1. Synthesis of linear sequence-defined macromolecules *via* P-3CR and subsequent hydrogenation.[26] 2. Synthesis of star-shaped polymers and subsequent post-reaction modification with poly(ethylene glycol) *via* P-3CR.[26,37,312]

Results and discussion

Based on the preliminary work on disperse star-shaped macromolecules and linear uniform oligomers *via* the P-3CR, the strategy toward uniform stars was adjusted.[26,37,312] Four-arm star molecules were targeted with three, five and seven repeat units for each arm, respectively, to evaluated variances in their properties resulting from the different sizes. Therefore, the P-3CR is applied employing benzyl

11-isocyanoundecanoate **4**/**A1** (**Chapter 4.1**) as isocyanide component together with an aldehyde (mostly 2-ethylbutanal), which was commercially available in sufficient purity. Furthermore, it was targeted to employ the obtained uniform star-shaped macromolecules as potential hosts for dyes/drugs or as phase-transfer catalysts.

In the literature, the core-first approach is favored in the synthesis of star molecules as it is known to be more efficient[36] and hence early research was focused on adapting the protocols to its demands (**Scheme 62**). Therefore, the equivalents from previous publications about P-3CR-based sequence-definition were increased from 1.50 eq. of isocyanide and aldehyde to 2.00 eq. of isocyanide and 2.68 eq. of aldehyde per carboxylic acid, totaling in 8.00 eq. isocyanide and 10.7 eq. of aldehyde for tetra acids, respectively.[26]

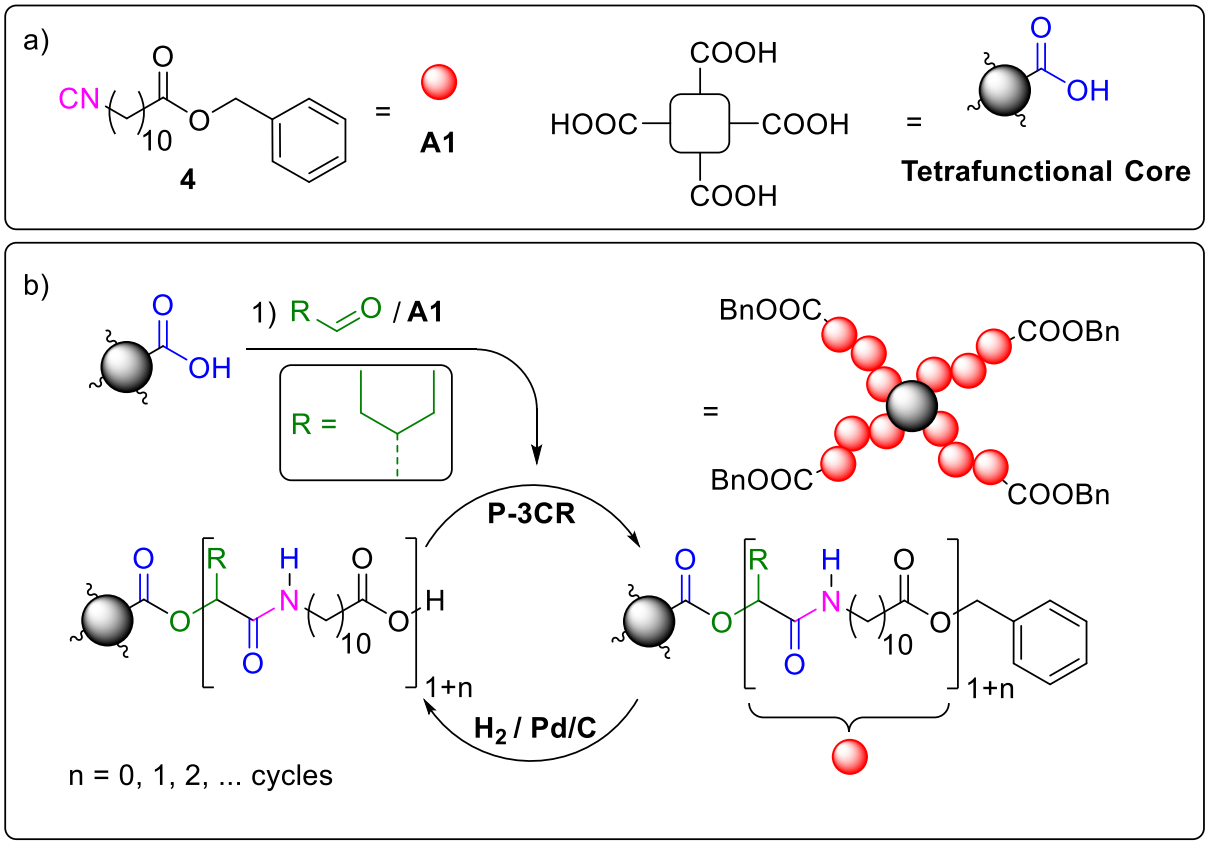

Scheme 62: a) Isocyanide **4** was used as building block throughout the synthesis and is hence labeled with **A1**. Several core units exhibiting four carboxylic acid moieties were employed within the synthesis. For reasons of clarity only one moiety is shown, whereas the other three are only implied. b) Iterative cycle toward star-shaped macromolecules *via* the core-first approach. A hypothetical end product is depicted schematically.

This change was introduced proactively to ensure full conversion of the tetrafunctional core unit. As the aldehyde component, solely 2-ethylbutanal was employed, if not stated otherwise.

In a first evaluation several, commercially available core moieties were employed by applying the adapted protocols (**Scheme 63**).

1. General conditions of the synthesis

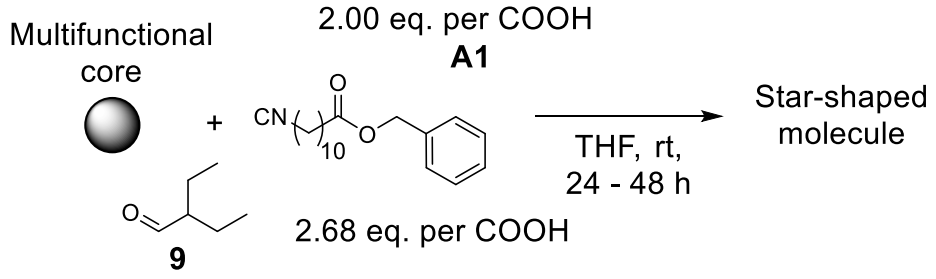

2. Employed multifunctional core moieties and obtained yields

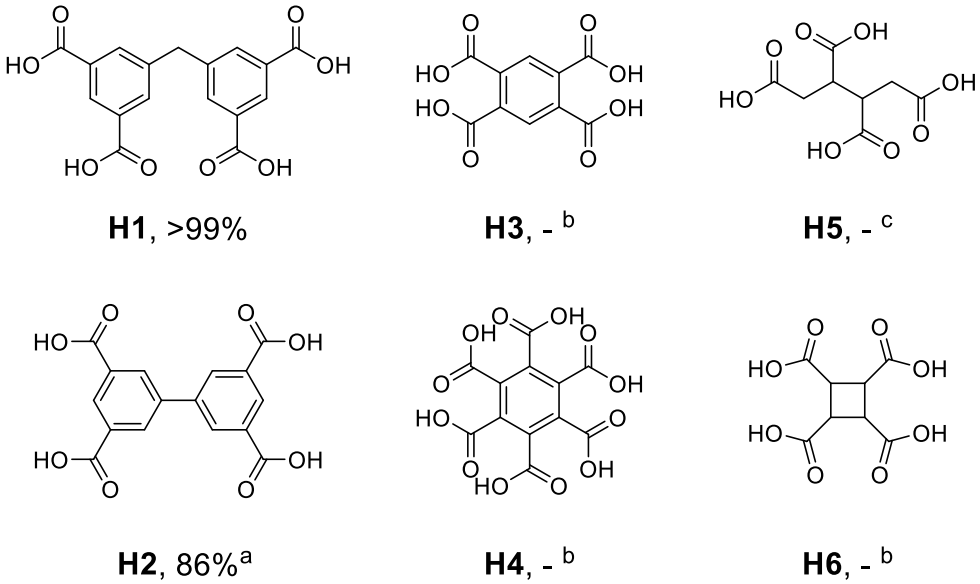

Scheme 63: 1. Conditions of the P-3CR toward star-shaped molecules. High conversion and yield justify large excess of reactants as this is only the first step of the iterative synthesis (**Scheme 62**). 2. The respective star-shaped molecule was only isolated for core **H1** and **H2**. [a] THF/water mixture (4:1 – volumetric) was employed as **H1** proofed to be insoluble in pure THF. [b] **26** was obtained as side product. [c] **26** was isolated and characterized. Its yield was determined as 38% regarding the stoichiometry of the core.

Previous publications have already established that the capacity of dye/drug encapsulation increases with the number of arms of the Passerini based star-shaped polymers (**Chapter 2.5.2**).[38] Hence, as encapsulation and drug-delivery also remained within the aims of the novel uniform star molecules, only tetra- and higher functional cores were employed. In total, six cores were tested in a first survey (**H1**-**6**). However, only **H1** and **H2** allowed for the isolation of the expected products (the analytical data for **H1** stars is described in a later paragraph). For the majority of

the employed core moieties, no product was obtained, but a side reaction was identified and the associated compound was isolated (**Scheme 64**).

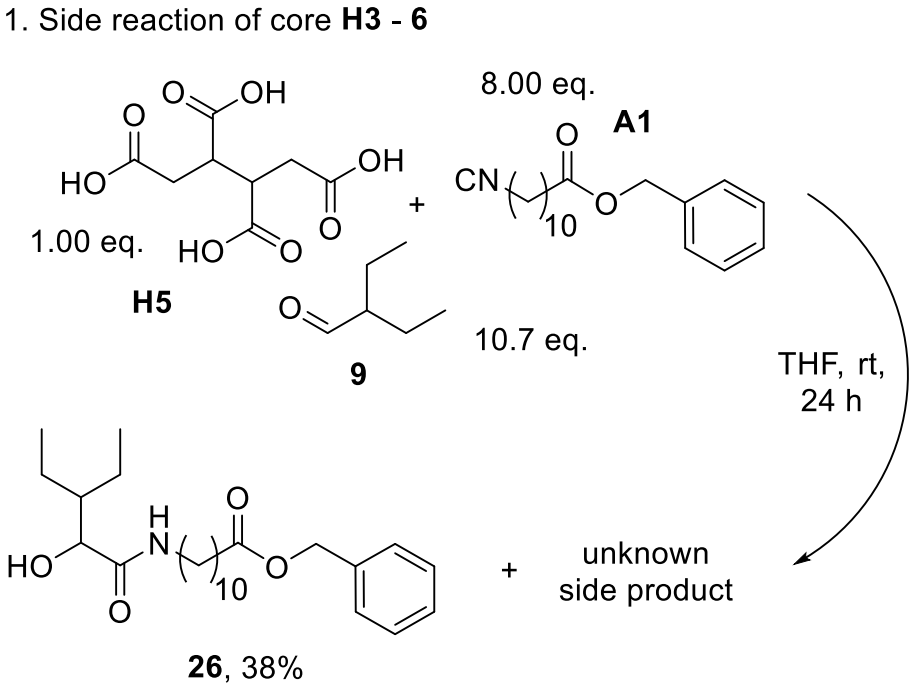

Scheme 64: Side reaction of core **H3** – **6** when employing the modified P-3CR conditions. The reaction proceeds like in the variation mentioned in **Chapter 2.3.4**, which utilizes strong acids (e.g. HCl) and yields the respective α-hydroxyamide.[174]

The main product resulting from **H5** was characterized and identified accordingly (**Figure 19**, **Chapter 6.3.3.2**) and proved to be the α-hydroxyamide **26**. However, the additional white insoluble precipitate, which accompanied the reaction, was neither isolated nor identified. The ^{1}H NMR spectrum of compound **26** is depicted in **Figure 19**. The characteristic signal of the hydroxy proton, labeled with the number 3, disappears when measured in deuterated chloroform as is often the case for acidic protons. In addition, high-resolution MS also confirmed the successful formation of the compound.

Furthermore, when reevaluating the structures of the core moieties **H3**-**6**, it was noticed that each one of them features adjacent carboxylic acid groups (herein considered as α-carboxy carboxylic acids). It is therefore hypothesized that the proximity of the carboxy functionalities is the reason for the altered outcome of the P-3CR. However, further experiments regarding the unidentified side product, which precipitated when employing core moiety **H3**, are needed to gain more insight in the mechanistical aspects of this reaction.

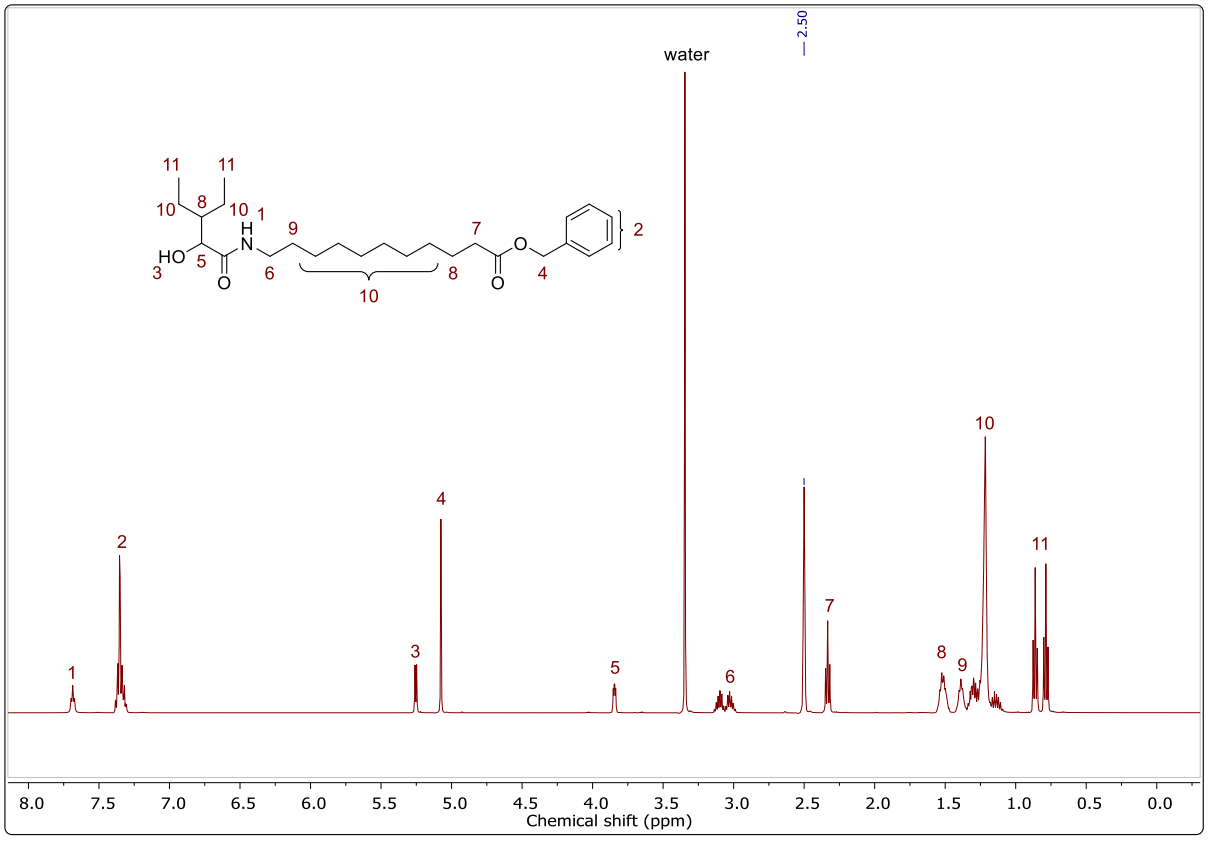

Figure 19: ^{1}H NMR spectrum of compound **26** in deuterated DMSO (DMSO-d_6). The characteristic signal 3 disappears if measured in deuterated chloroform indicating an acidic proton.

Employing core moiety **H1** and **H2**, however, allowed for the isolation of the targeted star-shaped molecules in high yields and purity. As an example, the ^{1}H NMR spectrum of the star molecule resulting from core **H1** (**CF-H1-1)** is shown in **Figure 20**. Subsequently, the iterative cycle presented in **Scheme 62** (p. 119) was continued for the molecules **CF-H1-1** and **CF-H2-1**. The hydrogenation was carried out with 10wt% palladium on charcoal in THF. Hydrogen was introduced into the solution *via* a balloon and a needle, as this proved to be efficient enough for full deprotection. The reactions were typically stirred overnight at room temperature. It is noted that the work-up of the P-3CR was performed by removing the solvent under reduced pressure and subsequent column chromatography utilizing different gradients of cyclohexane and ethyl acetate. The hydrogenation reaction mixture was simply dried over sodium sulfate and filtered through Celite® utilizing ethyl acetate with no further work-up than subsequent evaporation of the solvent. A more detailed description of the procedures is given in the experimental part (**Chapter 6.3.3.2**).

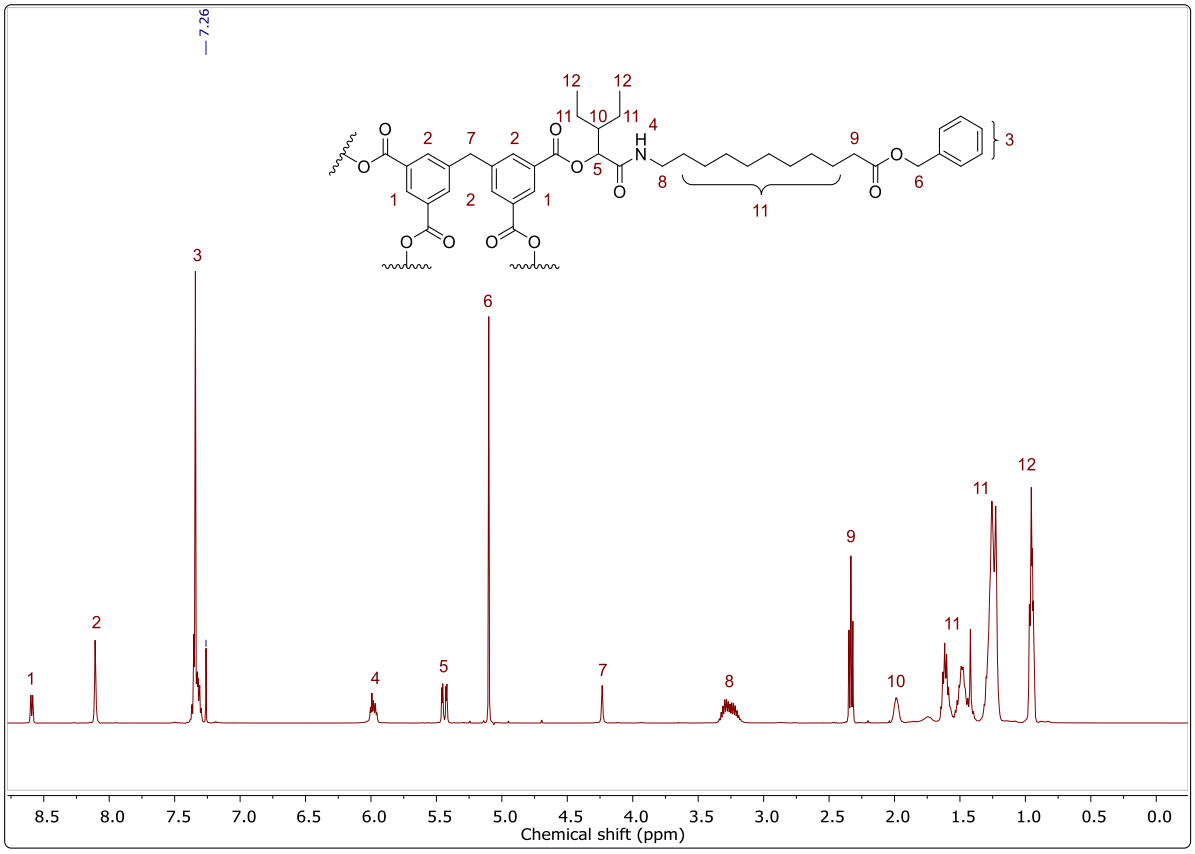

Figure 20: ^{1}H NMR spectrum of the star-shaped molecule **CF-H1-1** in deuterated chloroform ($CDCl_3$).

Yields of the respective P-3CR and hydrogenation reactions are displayed in **Table 9**. The resulting star molecules derived from **H1** and **H2** were each obtained in high yields, however during the second hydrogenation, the reactions were accompanied by an unknown side reaction, as will be described in the following paragraph. As this unknown side reaction also occurred for core **H2**, its further conversion was abandoned after conducting the second hydrogenation, whereas for **H1,** a third P-3CR was conducted to evaluate if the side product was separable *via* column chromatography. For reasons of clarity, only the SEC traces of the star-shaped macromolecules based on core **H1** are depicted and it is to presume that for both **H1** and **H2** the occurred side reaction is of the same character.

Table 9: Yields of the iterative stepwise synthesis toward star-shaped macromolecules utilizing the core moieties **H1** and **H2**.

Entry	*Reaction*	*Core **H1*** – yield (%)	*Core **H2*** – yield (%)
1	1st P-3CR	**CF-H1-1** – 99	**CF-H2-1** – 86
2	1st hydrogenation	**CF-H1-1$_b$** – 99	**CF-H2-1$_b$** – 98
3	2nd P-3CR	**CF-H1-2** – 94	**CF-H2-2** – 95
4	2nd	**CF-H1-2$_b$** – 94	**CF-H2-2$_b$** – no value
5	3rd P-3CR	**CF-H1-3** – 90	
	Overall yield (%)	78 after five steps	80.0 after three steps

The SEC traces of **CF-H1-1** – **3** including their impurities are depicted in **Figure 21**.

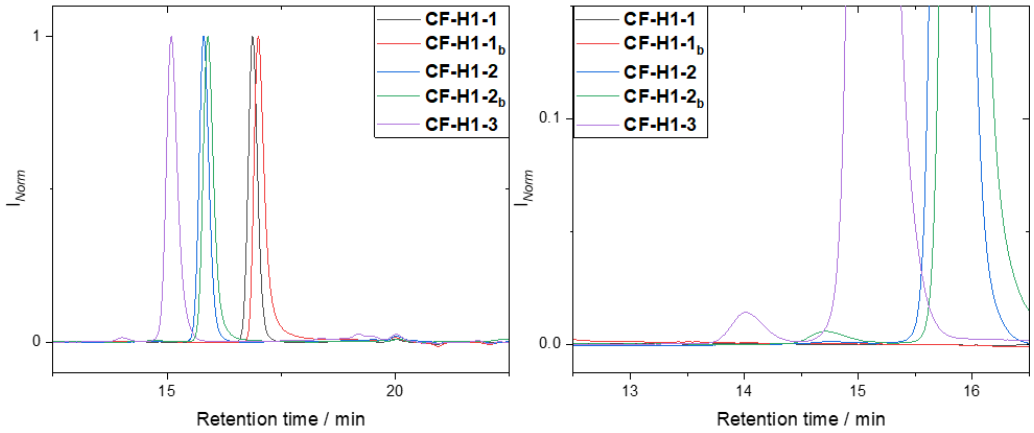

Figure 21: Left panel: SEC traces of **CF-H1-1** – **3** measured in THF. Right panel: for a better visibility, the important section containing the impurities is magnified. These first occurred in the second hydrogenation step and proofed inseparable *via* column chromatography after the third P-3CR and even increased during this reaction step.

The first three star-shaped macromolecules exhibit high purity, whereas **CF-H1-2$_b$** and **CF-H1-3** contained small amounts of contamination with higher hydrodynamic sizes (1-5% according to the SEC system) and hence the products cannot be considered uniform molecules as originally intended. Concludingly, these impurities must have formed *via* a coupling reaction, yet it remains unclear how this side reaction occurred.

A subsequent P-3CR was then performed to evaluate if this impurity was separable in the associated column chromatography, as purification of the tetra acid was omitted for polarity reasons. However, after the subsequent P-3CR and work-up, the amount

of impurity increased even further and proved to be inseparable from the product fraction by column chromatography. Additionally, the compound interacted surprisingly strongly with the silica employed for the purification, despite exhibiting an R_f value of 0.20 in cyclohexane/ethyl acetate 3:1, which was deemed sufficient for separation. Strong band broadening on the column was noticed, which contributed to the constantly decreasing product amounts over all the collected fractions. Moreover, control of the collected fractions by TLC analysis could not confirm an end to the chromatography, as spots were identified even after a huge elution volume (>5 L). Hence, to avoid loss in yield, the column was flushed with a more polar mixture of cyclohexane/ethyl acetate, which still was not sufficient to elute all product. This behavior was interpreted as the reason behind the higher amount of impurity in **CF-H1-3** in comparison to the employed reactant **CF-H1-2$_b$**. Also, any further hydrogenation steps conducted in small test batches exhibited increasing concentration of unknown side product. Consequently, this strategy was abandoned as the contaminations proved to be inseparable as well as persistent for each of the following hydrogenations (note that these reaction steps are neither included in **Table 9** nor in the experimental part for reasons of clarity). However, in **Figure 22** the ^{1}H NMR spectra of several star molecules based on core **H1** are shown. The panels label the respective impurities, which occurred during the syntheses and proved to be inseparable *via* column chromatography. Whereas the signals in panel **c** can at least be partially assigned to remaining ethyl acetate in the product, the signals in panel **a**, **b** and **d** belong to unknown impurities. As for the mechanistical aspects of the side reaction, it is herein hypothesized that a palladium-initiated coupling in the deprotection process occurred.

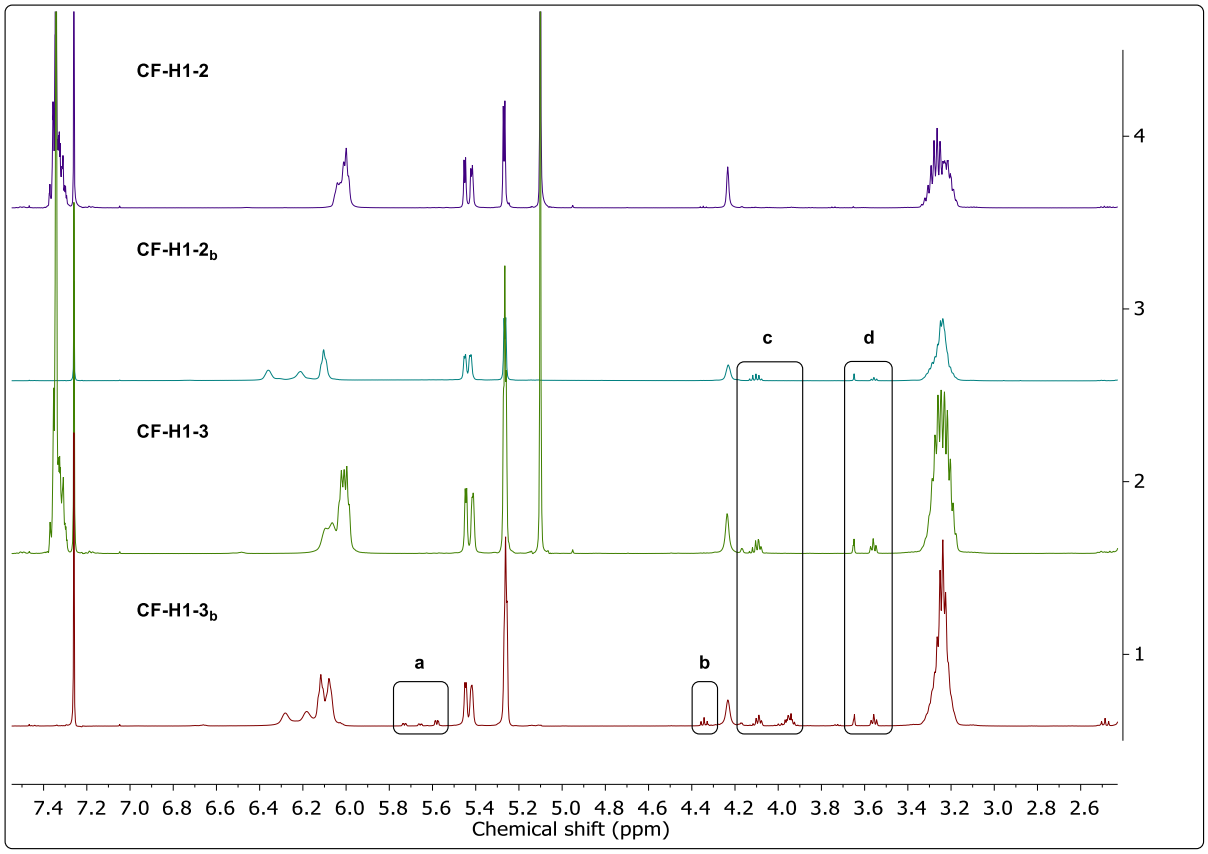

Figure 22: ^{1}H NMR spectra of the star molecules **CF-H1-2** – **3$_b$** in deuterated chloroform ($CDCl_3$). The panels labeled with **a** to **d** highlighted respective impurities, which occurred over the syntheses and proved inseparable in column chromatography.

In the first evaluation of core moieties, adjacent carboxylic acids proved to be problematic, hence a novel pathway was examined to exclude such interactions, as core **H1** and **H2** also possess carboxylic acid groups in proximity and were therefore suspected as a possible origin of the side reaction. Alternatively, the impurity is a result of the structural character of the star-shaped macromolecules, which is hard to prove directly, however would render all efforts obsolete. Therefore, an indirect proof was targeted to exclude the first assumption and hence indirectly confirm the second. The aliphatic sebacic acid **H7** was chosen as substrate, as it contains eight methylene groups separating the carboxylic acid functionalities. However, as sebacic acid is only a diacid, a second building block combining an aldehyde as well as a benzyl ester was synthesized. This allows for the synthesis of a star-shaped-molecule, which contains four benzyl esters after the first P-3CR of **H7** when employed in combination with **A1** (**Scheme 66**, p. 129). The aforementioned building block, named **F1**, was synthesized in a three-step procedure starting from ω-pentadecalactone (**Scheme 65**) and was obtained in an overall yield of 55.3%. The ^{1}H NMR spectra of all three compounds are depicted in **Figure 23**, whereas further analytical data can be found in **Chapter 6.3.3.1**.

First, ω-pentadecalactone **27** was dissolved in a water/ethanol mixture containing sodium hydroxide and heated at 50 °C for 18 h. Afterwards, the reaction solution was acidified until pH = 3 with 3 M hydrochloric acid upon which the product, 15-hydroxypentadanoic acid **28**, precipitated. The solid was filtered, thoroughly rinsed with ice cold water to remove any residual acid and dried at room temperature in a fume hood. **28** was obtained as a white solid (in 86% yield) and used without any further purification. To introduce the benzyl ester moiety, **28** was suspended in dichloromethane followed by addition of DBU, upon which the compound dissolved. Subsequently, benzyl bromide was added *via* a dropping funnel and the reaction mixture was stirred overnight at room temperature. TLC confirmed the complete conversion of **28**. After work-up, a beige crude product was obtained, which was recrystallized from 400 mL methanol, filtered off and rinsed with ice cold methanol. After allowing to dry, the pure product **29** was obtained in a yield of 96%.

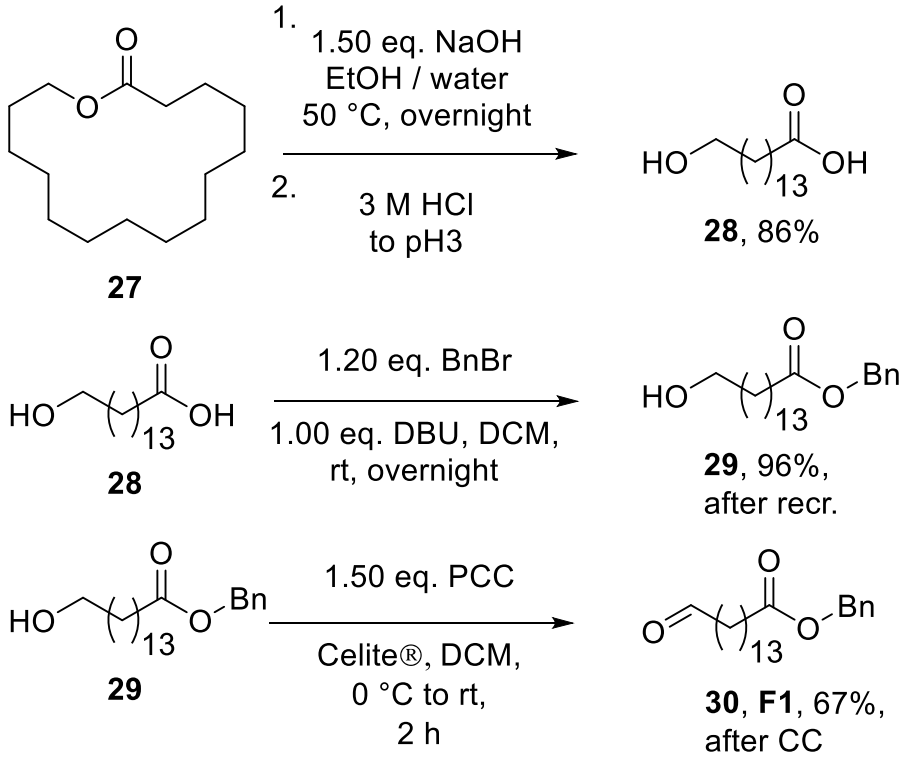

Scheme 65: Three-step synthesis toward building block **F1**, which incorporates an aldehyde function as well as a benzyl ester.

Finally, the hydroxy function of **29** was converted to an aldehyde by adding pyridinium chlorochromate (PCC) as oxidating agent. The reaction was carried out in DCM with Celite® as a binding agent for the insoluble chrome (III) compounds, which are generated as byproduct. After addition of PCC at 0 °C, the reaction was allowed to warm up to room temperature and stirred for 2 h, upon which the mixture color turned

from orange to brown-black. Diethyl ether was added to further decrease the solubility of chromium compounds. Afterwards, the solution was filtered through a large pad of silica and rinsed several times with diethyl ether. After evaporation of the solvent, the crude product was subjected to column chromatography, which yielded molecule **30** in high purity and a yield of 67%.

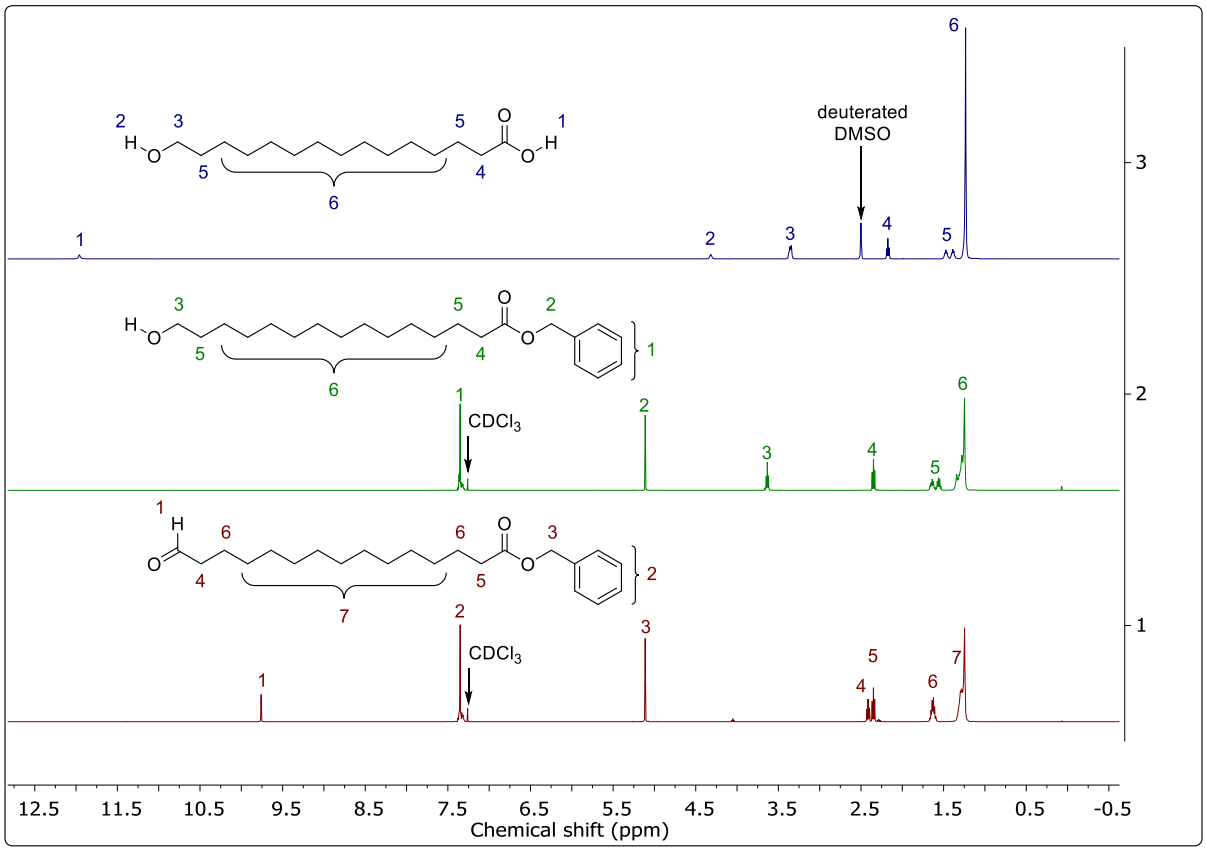

Figure 23: ^{1}H NMR spectra of the compounds **28**, **29** and **30**. The first sample was measured in deuterated DMSO (DMSO-d_6), whereas the other compounds were dissolved in deuterated chloroform ($CDCl_3$).

Afterwards, the novel building block **F1** was reacted with isocyanide **A1** and diacid **H7** toward the tetra benzylated structure **CF-H7-1** (**Scheme 66**). In the first P-3CR, 4.00 eq. of both **A1** and **F1** were employed to ensure full conversion. After isolation of pure **CF-H7-1** by column chromatography and subsequent hydrogenation of the benzyl esters, compound **CF-H7-1b** was obtained. Subsequently, the cycle presented in **Scheme 62** (p. 119) was continued, however utilizing isobutanal **31** instead of the 2-ethylbutanal **9**. 8.00 eq. of **A1** and 10.7 eq. of aldehyde **31** were consistently employed, as these conditions had already been favored in the previously conducted synthesis. The star-shaped macromolecules based on **H7** were isolated in high yields, yet the overall yield of 70% after five steps was about 8% lower than for **H1**. The respective molecules and their yields are displayed in **Table 10**.

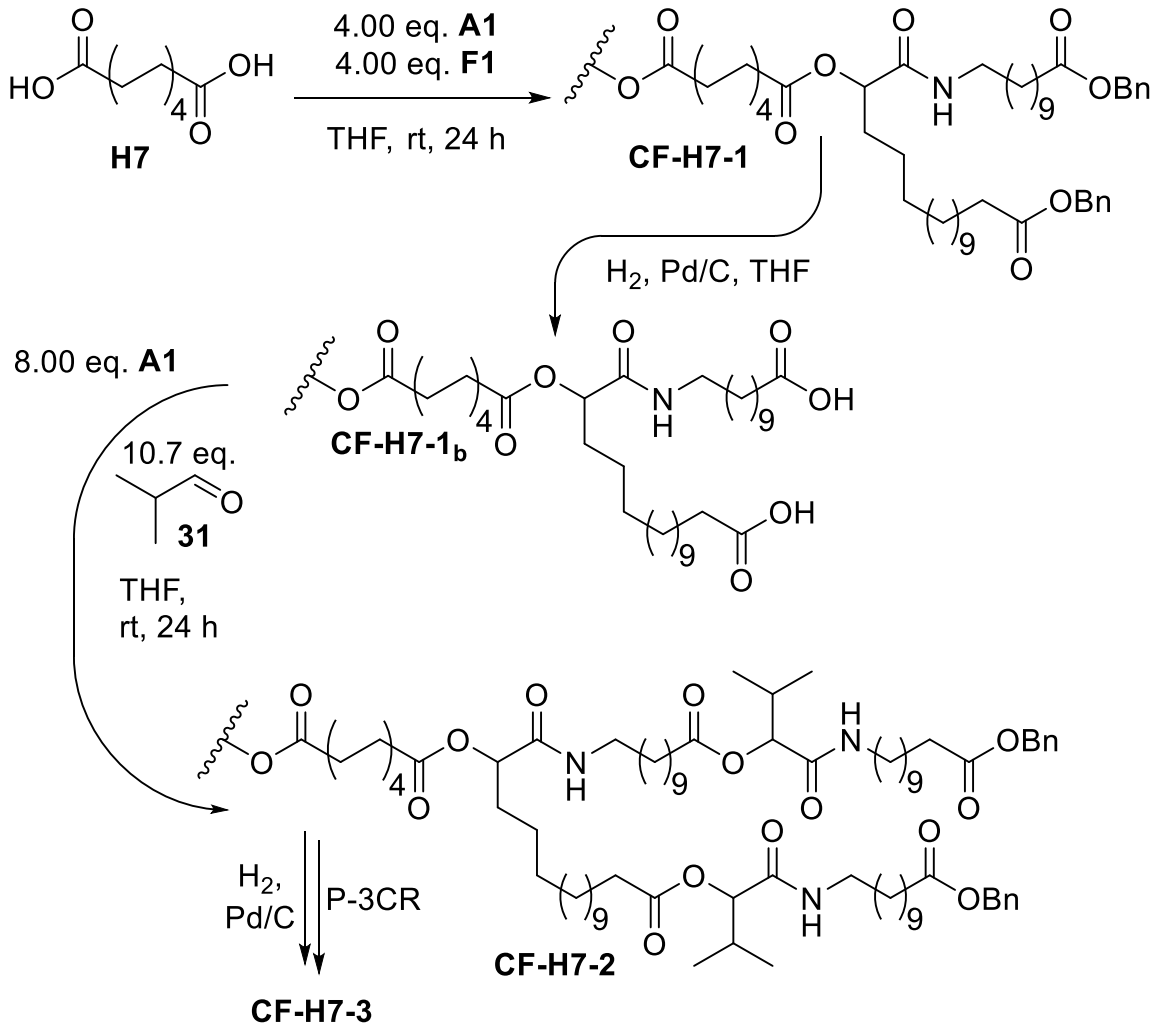

Scheme 66: Synthesis of **CF-H7-1** starting from sebacic acid **H7** utilizing the building blocks **A1** and **F1**. After subsequent hydrogenation, **CF-H7-1$_b$** was obtained, which was applied in the iterative cycle of P-3CR and hydrogenation employing building block **A1** and an aldehyde. For the subsequent molecules **CF-H7-2** and **CF-H7-3** isobutanal **31** was utilized.

Table 10: Yields of the iterative stepwise synthesis toward star-shaped macromolecules utilizing the core moiety **H7**, building block **A1** and **F1** as well as the aldehyde isobutanal **31** after entry 3.

Entry	*Reaction*	*Core **H7*** – yield (%)
1	1st P-3CR (utilizing **A1** and **F1**)	**CF-H7-1** – 92
2	1st hydrogenation	**CF-H7-1$_b$** – 95
3	2nd P-3CR (utilizing **A1** and **31**)	**CF-H7-2** – 91
4	2nd hydrogenation	**CF-H7-2$_b$** – 95
5	3rd P-3CR (utilizing **A1** and **31**)	**CF-H7-3** – 93
	Overall yield (%)	70 after five steps

The ^{1}H NMR spectrum of the final product **CF-H7-3** is displayed in **Figure 24** and suggests absence of impurities. However, SEC measurements carried out alongside the synthesis revealed that already **CF-H7-2$_b$** contained small amounts of impurities, comparably at the same stage as for star molecules based on core **H1**. The contaminations were, like for the previous star-shaped macromolecules, of higher hydrodynamic sizes as the respective signals appeared at lower retention times in the SEC graph. The SEC traces of the molecules **CF-H7-1** – **3** are displayed in **Figure 25**. It was concluded that the impurities were likely of the same character as for **H1**, and likewise could neither be characterized nor isolated. Attempts for purification *via* column chromatography were unsuccessful, similarly to the case of **CF-H1-3**. Further trials to purify the compound led to immense loss in obtained product (**Table 10**, entry 5 refers to the yield after the first column chromatography, whereas the value dropped below 70% after two additional attempts with less polar elution mixtures).

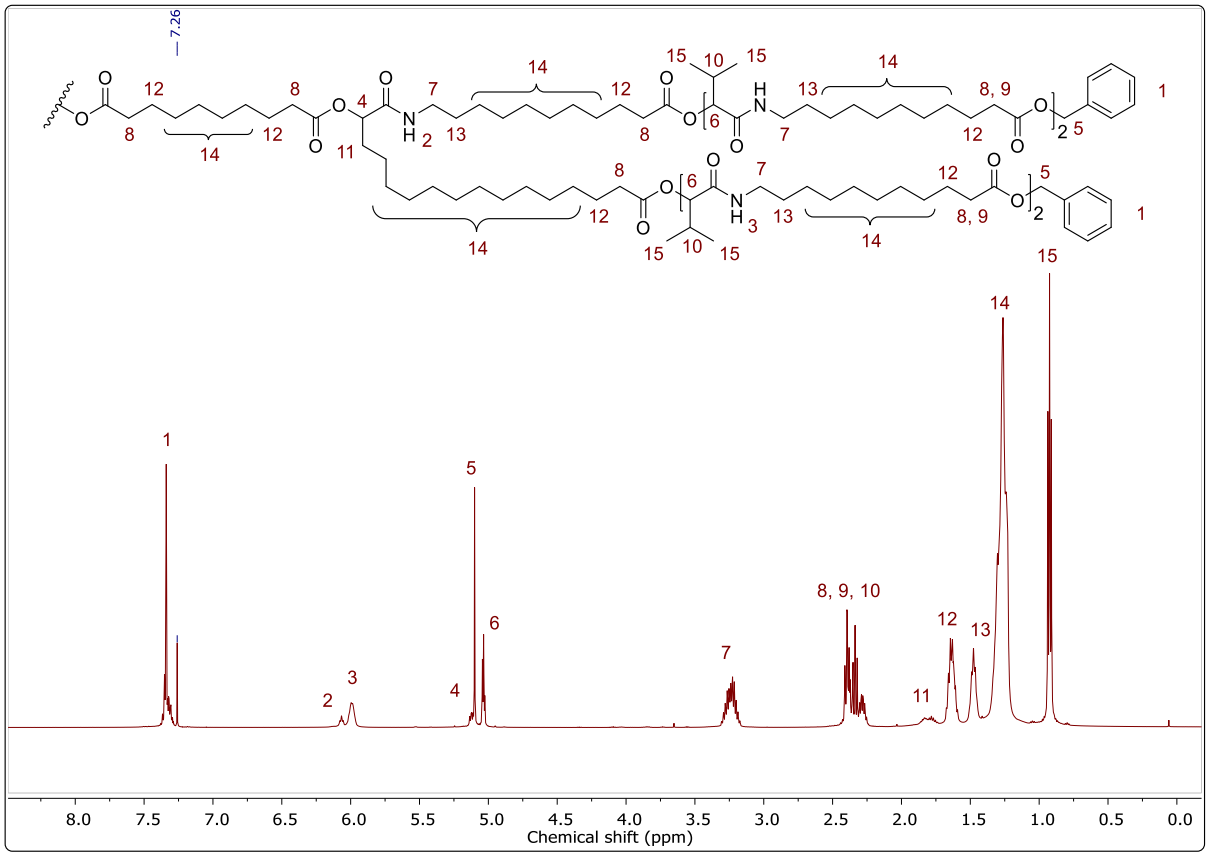

Figure 24: ^{1}H NMR spectrum of star-shaped molecule **CF-H7-1** in deuterated chloroform ($CDCl_3$).

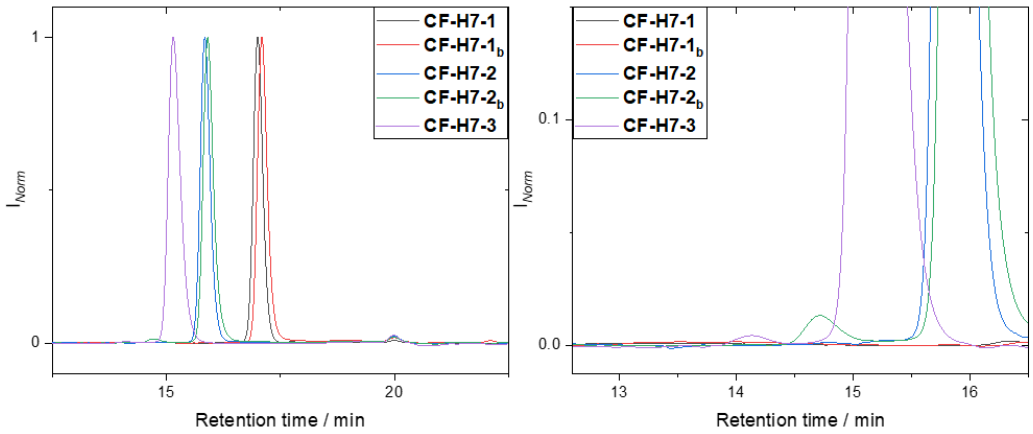

Figure 25: Left panel: SEC traces of **CF-H7-1** – **3** measured in THF. Right panel: for a better visibility, the important section containing the impurities is magnified. Contaminations first occurred during the second hydrogenation step and proved inseparable *via* column chromatography after the third P-3CR (**CF-H7-3**), however decreased in intensity compared to the reactant **CF-H7-2$_b$**.

Concludingly, the iterative procedure relying on the P-3CR and subsequent hydrogenation, which is already well-established within our working group, was transferred from a mono/bidirectional into a multifunctional approach toward uniform star-shaped macromolecules. A set of several core moieties containing four or more carboxylic acid groups were employed in the synthesis, yet only experiments featuring cores **H1** and **H2** proved to be successful. Employing core units **H3**-**6** yielded no uniform star-shaped macromolecules. Consequently, core moieties with adjacent carboxylic acids were not further employed in the synthesis, as the structural characteristic of such cores were deemed problematic.

Star-shaped macromolecules derived from **H1** and **H2** were synthesized in a five-step procedure in high yields. However, the second hydrogenation step was accompanied by an unknown side reaction. Hence the star-shaped macromolecules were no longer uniform. In order to evaluate whether the proximity of the acid groups was once again responsible, the novel building block **F1** was synthesized and employed together with **A1** and sebacic acid toward a star-shaped macromolecule with distant carboxylic acid moieties. Again, the second hydrogenation step proved problematic. As such, it was indirectly proven that the hydrogenation-based side reaction is connected to the structural character of the respective molecules. Hence, the core-first approach was abandoned. As alternative, an arm-first approach was investigated, which is described in the next chapter.

4.3.2 The road to uniform shar-shaped macromolecules – an arm-first approach

Parts of this chapter contain results that have already been published:

K. A. Waibel, D. Moatsou, M. A. R. Meier, *Macromol. Rapid Commun.* **2021**, *42*, 2000467, DOI: 10.1002/marc.202000467.

(The author planned the experiments, conducted the synthesis of the featured molecules and their evaluation, performed associated measurements and did most of the writing. D. Moatsou assisted with the planning and evaluation of the encapsulation experiments.)

Abstract

Within this chapter, the synthesis of uniform star-shaped macromolecules is described. Linear uniform oligomers obtained *via* a two-step iterative cycle, P-3CR and subsequent hydrogenation, are modified post-reaction with uniform octa(ethylene glycol) monomethyl ether. After coupling of the *arm* molecules *via* azide-alkyne cycloaddition uniform star-shaped block macromolecules with a mass of 9.13, 11.6 and 14.1 kDa, respectively, were obtained. Each molecule ranging from the linear oligomers up to the star-shaped macromolecules were characterized *via* NMR spectroscopy, electrospray ionization mass spectrometry (ESI-MS) and size exclusion chromatography (SEC) to prove their purity as well as their uniformity. Finally, the obtained star macromolecules were investigated in their ability to encapsulate dye molecules by conducting qualitative solid-liquid phase transfer experiments.

State of the art

In the previous chapter, it was shown that a multidirectional core-first approach toward *uniform* shar-shaped macromolecules *via* iterative P-3CR and subsequent hydrogenation is not possible due to unknown side reactions and byproducts that complicate the purification process. As the respective compounds did not match the criteria of uniformity an alternative approach has to be established.

In the publication from Meier *et al.* from 2016 (**Scheme 61**, **Chapter 4.3**, p. 118) is was already shown that the iterative cycle, P-3CR and deprotection, is capable of producing highly defined linear macromolecules.[26] Additionally, the procedure was successfully adapted into a bidirectional approach[35] and further used to synthesize large sets of oligomers with variation of the side chains or of the backbone, thus rendering them capable for data storage taking advantage of read-out *via* tandem MS.[31,249]

In **Chapter 2.5.2**, it was mentioned that star-shaped macromolecules can be synthesized using linear precursor molecules and coupling them with a core moiety. This is generally termed *arm-first approach*.[36] However, in the featured publications about sequence-defined macromolecules *via* P-3CR, only octadecanoic acid had been employed as a starting block.[26] This allows for subsequent buildup of long sequences but leaves only the carboxylic acid as a potential reactive functionality for attachment to a core moiety in the final step. Furthermore, since drug-delivery, phase transfer catalysis and encapsulation of dye molecules were considered as ultimate goals of this thesis, the introduction of a hydrophilic outer shell is necessary. In a publication featuring amphiphilic star-shaped polymers by Meier, this was achieved by a final functionalization utilizing poly(ethylene glycol),[37] which was also considered in this thesis. This approach requires two reactive functionalities on the uniform linear macromolecules: one for attachment to the core and one for the *PEGylation*. Consequently, the existent synthetic strategy by Meier *et al.* toward sequence-defined linear oligomers was adapted and improved in order to fit the requirements of the arm-first approach, which is described within this chapter.

Results and discussion

This chapter will be divided in three parts: synthesis and characterization of the necessary building blocks, synthesis and characterization of the linear oligomers and star-shaped macromolecules and finally their application in qualitative encapsulation experiments.

In **Chapter 4.3.1**, it was already mentioned that the targeted repeating numbers of building block **A1** in the star-shaped macromolecules are three, five and seven, respectively. To obtain a linear heptamer, it normally takes 14 reaction steps in total: seven P-3CRs and seven hydrogenations. This is independent from whether a core-first or an arm-first approach is employed. Since overall yield and expense in the laboratory mostly correlate with the total number of reactions, a more efficient way of synthesizing these linear oligomers was established. Therefore, the novel building block **A2** was designed, which still contains the functionalities of **A1**, but it also contains one repeating unit of the targeted oligomers. Hence, if employed in the synthesis, the size of the starting molecule does not increase by just one repeating unit, but rather by two, which effectively halves the numbers of total synthetic steps. This building block **A2** was synthesized in a five-step procedure starting from

11-aminoundecanoic acid **1**, or in a two-step procedure starting from building block **A1** as is depicted in **Scheme 67**.

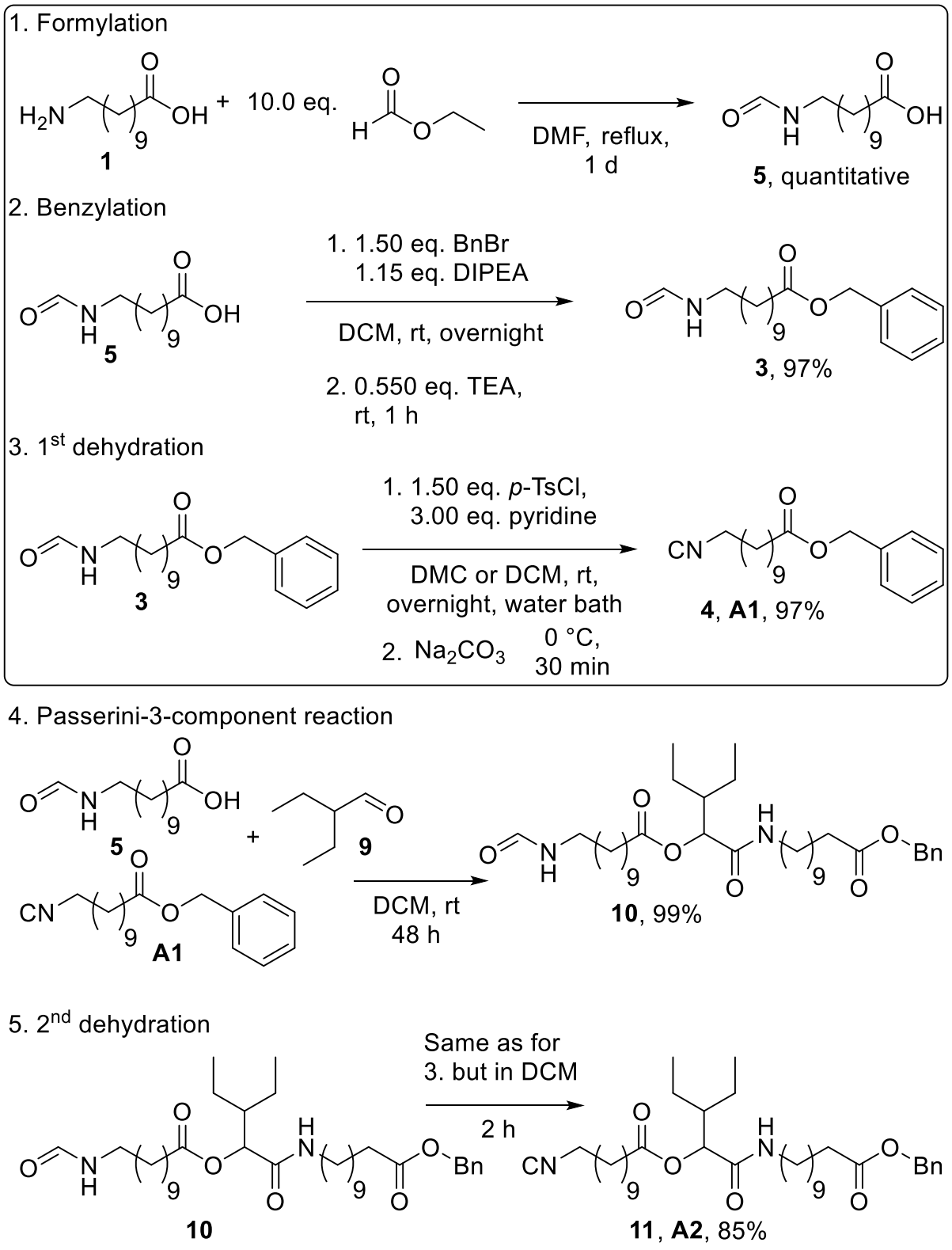

Scheme 67: Synthesis of building block **A2** starting from 11-aminoundecanoic acid **1**. The respective building block was obtained after a five-step synthesis in an overall yield of 79%. Note that the dehydration of **10** was carried out in DCM rather than in DMC because of the shorter reaction time. The framed part presents the synthesis of **A1** established in **Chapter 4.1**.

Note that this procedure was already briefly mentioned in the beginning of **Chapter 4.2**, as it led to the discovery of a novel path to thiocarbamates and is now evaluated in a more detailed way. As the first three steps have already been reviewed in detail in **Chapter 4.1**, they are not discussed again.

Building block **A1** was reacted together with 11-formamidoundecanoic acid and 2-ethylbutanal in DCM. After stirring for 48 h at room temperature and subsequent work-up *via* flash-column chromatography, the prolonged *N*-formamide **10** was obtained in a yield of 99%. Afterwards, **10** was dehydrated employing the conditions indicated in the third step of **Scheme 67**. This time, dichloromethane was used as solvent instead of the more benign dimethyl carbonate, as the reaction proceeds faster in DCM. Subsequent aqueous work-up and flash column chromatography yielded building block **A2** in a good yield of 85% and hence in an overall yield of 79% after five steps. The respective ^{1}H NMR spectra are shown in **Figure 26**. For a more detailed analytical analysis **Chapter 6.3.3.1** can be considered.

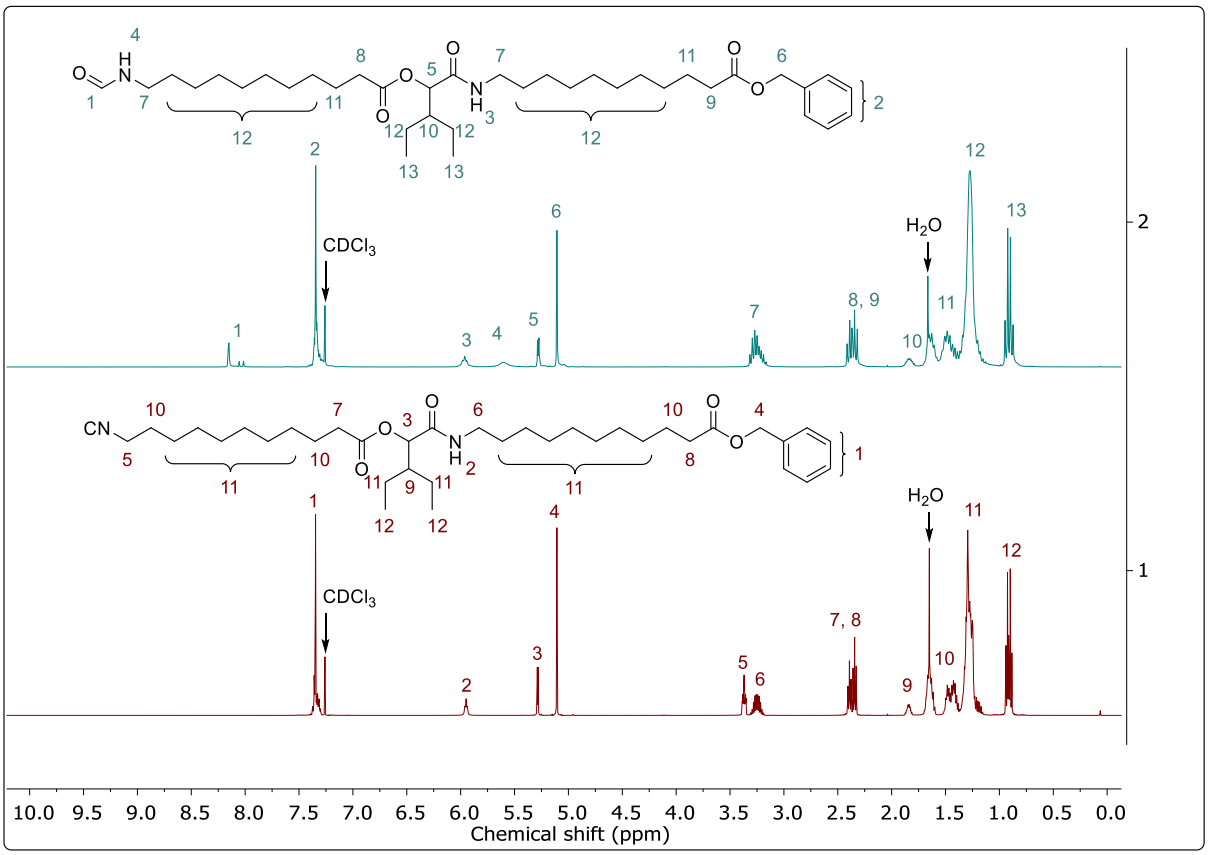

Figure 26: ^{1}H NMR spectra of **10** and building block **A2** in deuterated chloroform ($CDCl_3$).

It was briefly mentioned previously that the targeted applications of star-shaped macromolecules lie in phase-transfer and encapsulation. Hence, a hydrophilic shell

surrounding the hydrophilic core was introduced in a final step. In previous publications, poly(ethylene glycol) mono methyl ether was often employed, since it exhibits a decent water solubility.[37] In order to maintain uniformity of the star-shaped macromolecules, the poly(ethylene glycol) or oligo(ethylene glycol) (OEG) used needed to be monodisperse. However, the synthesis of uniform OEG is rather challenging and especially the purification process is time- and resource-consuming. In 2020, Meier published an extensive review about different literature-known strategies toward these compounds.[240] The following procedures are based on this publication and optimized to minimize the purification needed. In his comparative study, orthogonally protected OEGs were mostly employed in an iterative exponential growth strategy. Herein, a commercially available tetra(ethylene glycol) monomethyl ether (Me-4EG-OH) and a tetra(ethylene glycol) mono benzyl ether (Bn-4EG-OH) were purchased and subsequently employed in a three-step synthesis toward octa(ethylene glycol) mono methyl ether (Me-8EG-OH) (**Scheme 68**).

In the first step, **32** was activated by tosylation employing *p*-TsCl dissolved in THF, which was slowly added to a solution of **32** in aqueous sodium hydroxide. After stirring the reaction mixture overnight, subsequent extraction, drying over sodium sulfate and removal of the solvent, **33** was obtained in high yield and purity.[363] Subsequently, Bn-4EG-OH was dissolved in dry THF and deprotonated by addition of potassium *tert*-butoxide (KO^{t}Bu) in dry THF at 0 °C. Then, **33** in dry THF was slowly added *via* a dropping funnel and the reaction was allowed to warm up to room temperature. After stirring for 20 h, crude SEC measurements showed no further conversion of the reactants. The solution was cooled to 0 °C and neutralized by addition of 1 M hydrochloric acid. After aqueous work-up, the crude product was subjected to column chromatography twice, as the chromatographic separation of different OEG species was problematic. This was due to uncontrollable side reactions, such as elimination, false deprotection and further coupling, accompanying the Williamson ether synthesis, which is generally seen as non-ideal for aliphatic substrates. Further difficulties arose due to the character of the OEGs: these are quite polar compounds and so are their side and degradation products. However, until now, no alternative procedure toward larger quantities of uniform OEG other than the Williamson ether synthesis with orthogonal protecting groups has been reported in the literature.

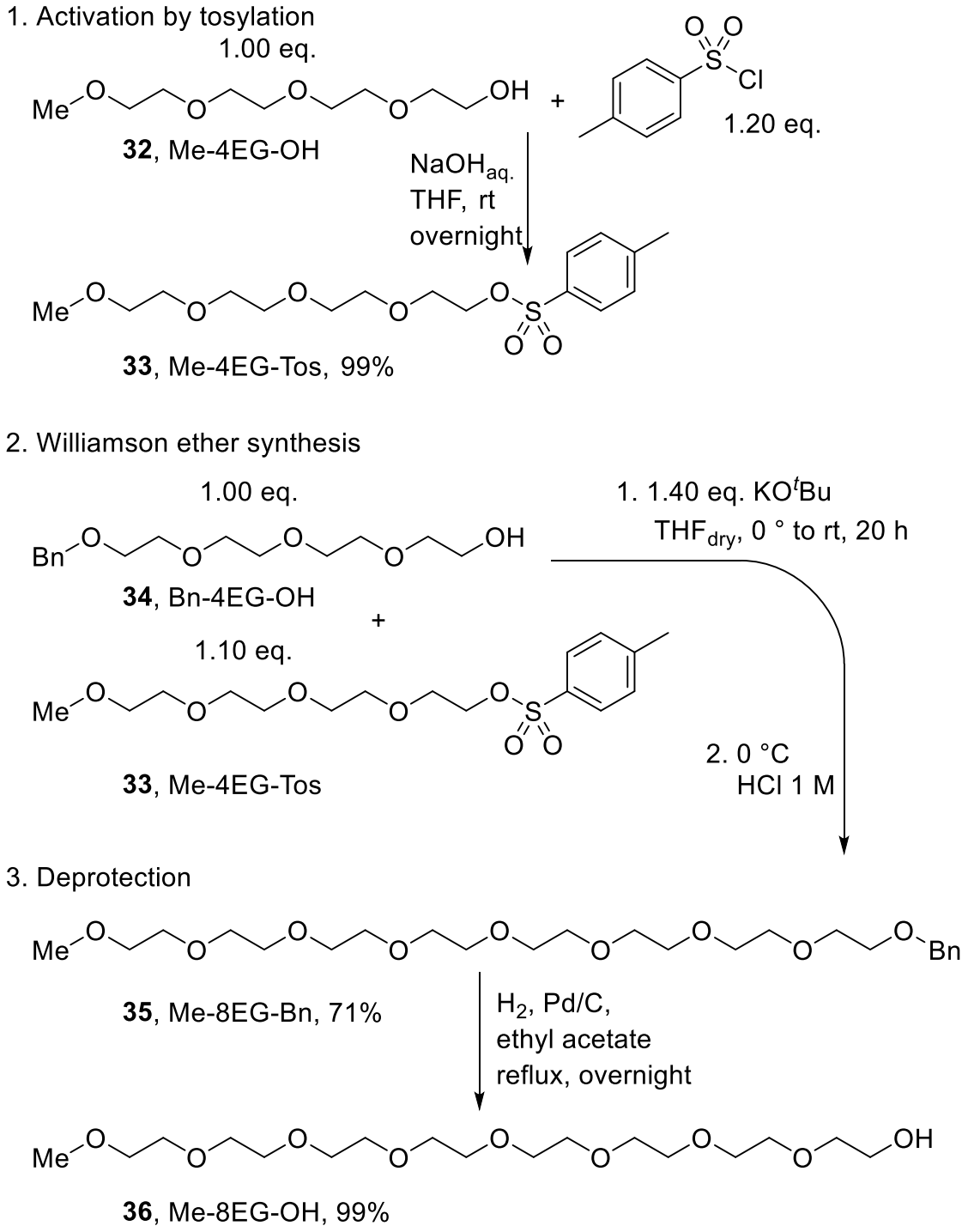

Scheme 68: Three-step synthesis toward octa(ethylene glycol) mono methyl ether (Me-8EG-OH) **35**. Starting reagent is commercially available Me-4EG-OH, which is activated *via* tosylation to yield **33**. Subsequent coupling of Bn-4EG-OH with **33** in THF yielded the respective Me-8EG-Bn **35** in a yield of 71% after two column chromatographies. A final deprotection of the benzyl ether yielded **36**.

Since two of the side-products exhibit slightly less polar character, the following strategy was employed for purification of compound **35**: The crude product was subjected to a first chromatographic separation utilizing a rather non-polar elution mixture (cyclohexane/ethyl acetate 1:1). This caused intentional band broadening, a

phenomenon that was already mentioned in the previous chapter, that leads to a rather slow elution of the desired compound. When the product started to be visible by TLC, the gradient was adjusted to ethyl acetate and then ethyl acetate/methanol 25:2. Subsequently, twenty 1 L fractions were collected and, after evaporation of the solvent, subjected to SEC analysis. Afterwards, the pure fractions were combined and the same was performed for the fractions containing only low amounts of impurity. Next, they were subjected to a second chromatography with the same protocol as the first one. Again, twenty 1 L fractions were collected and analyzed, which yielded similar SEC traces to the first. Therefore, all pure fractions were combined and added to the pure fraction of the first column chromatography. The rest was discarded and hence a final yield of 71% was obtained. Theoretically, the yield could have been increased by further column chromatographies, yet this was omitted due to a low cost-benefit ratio. As an example, selected SEC traces of the first column chromatography are depicted in **Figure 27**.

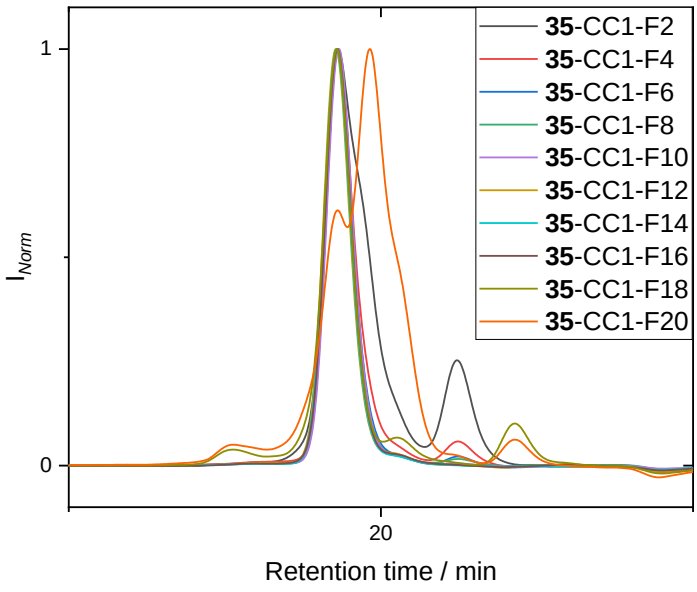

Figure 27: SEC traces of ten selected fractions of the first column chromatography of **35** measured in THF. The graphs are normalized to the respective product peak. Side products appear in fraction F2-F8 as well as F18-F20. Fractions F4-F8 and F17-20 were combined yet subjected to another column chromatography to increase the yield of **35**. Fractions F9-F16 were considered pure. The remaining small shoulder at 20 min is a system peak.

In total, about 60 L of solvent as well as 2 L of silica were necessary to obtain 28.7 g of pure product (60.4 mmol). Afterwards, **35** was deprotected by employing Pd/C and hydrogen. Compound **36** was obtained in high purity and nearly quantitative yield, after

refluxing the mixture overnight, filtering through Celite® and removal of the solvent. The ^{1}H NMR spectra of the pure compounds are depicted in **Figure 28**. Note that their respective SEC traces are shown together with the building blocks **B1** and **B2**, which were synthesized utilizing compound **36** in the next paragraph. The overall yield was 69.6% after three steps.

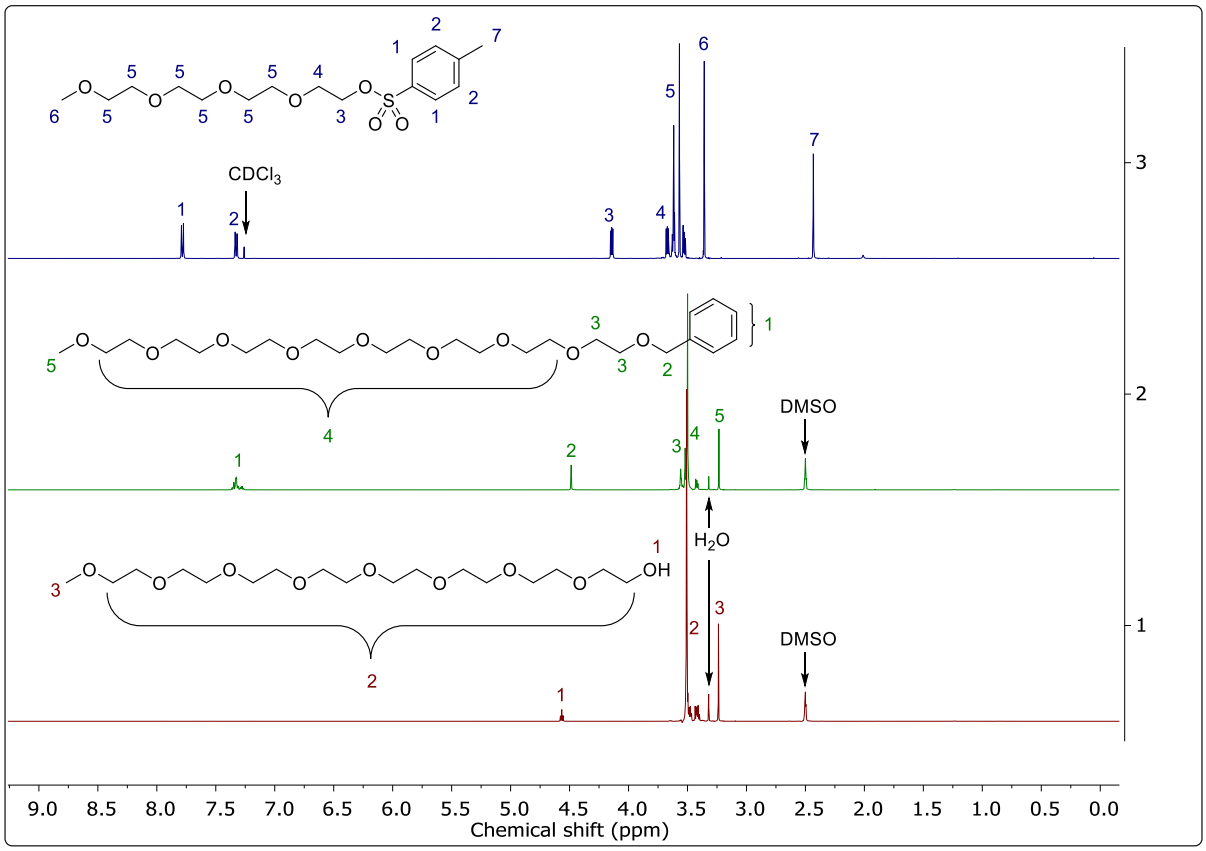

Figure 28: ^{1}H NMR spectra of the OEGs **33**, **35**, **36**. The first is conducted in deuterated chloroform ($CDCl_3$), whereas the latter two are measured in deuterated DMSO (DMSO-d_6).

In order to attach the previously obtained Me-8EG-OH units to the linear oligomers (arms of the star), whose synthesis is described in a later paragraph, a reactive functionality has to be introduced. As the P-3CR reaction was already well-established in this work, an aldehyde and isocyanide-functional OEG was synthesized in a one- or two-step procedure from their respective starting materials. For the isocyanide building block **B1**, 6-aminoundecanoic acid **37** was employed as substrate for subsequent formylation, Steglich esterification and dehydration. For the aldehyde component **B2**, 4-formylbenzoic acid **40** was chosen as it is commercially available in high purity and allows for a selective Steglich esterification with the Me-OEG-OH. Both procedures are depicted in **Scheme 69** and are described in detail in the following paragraph.

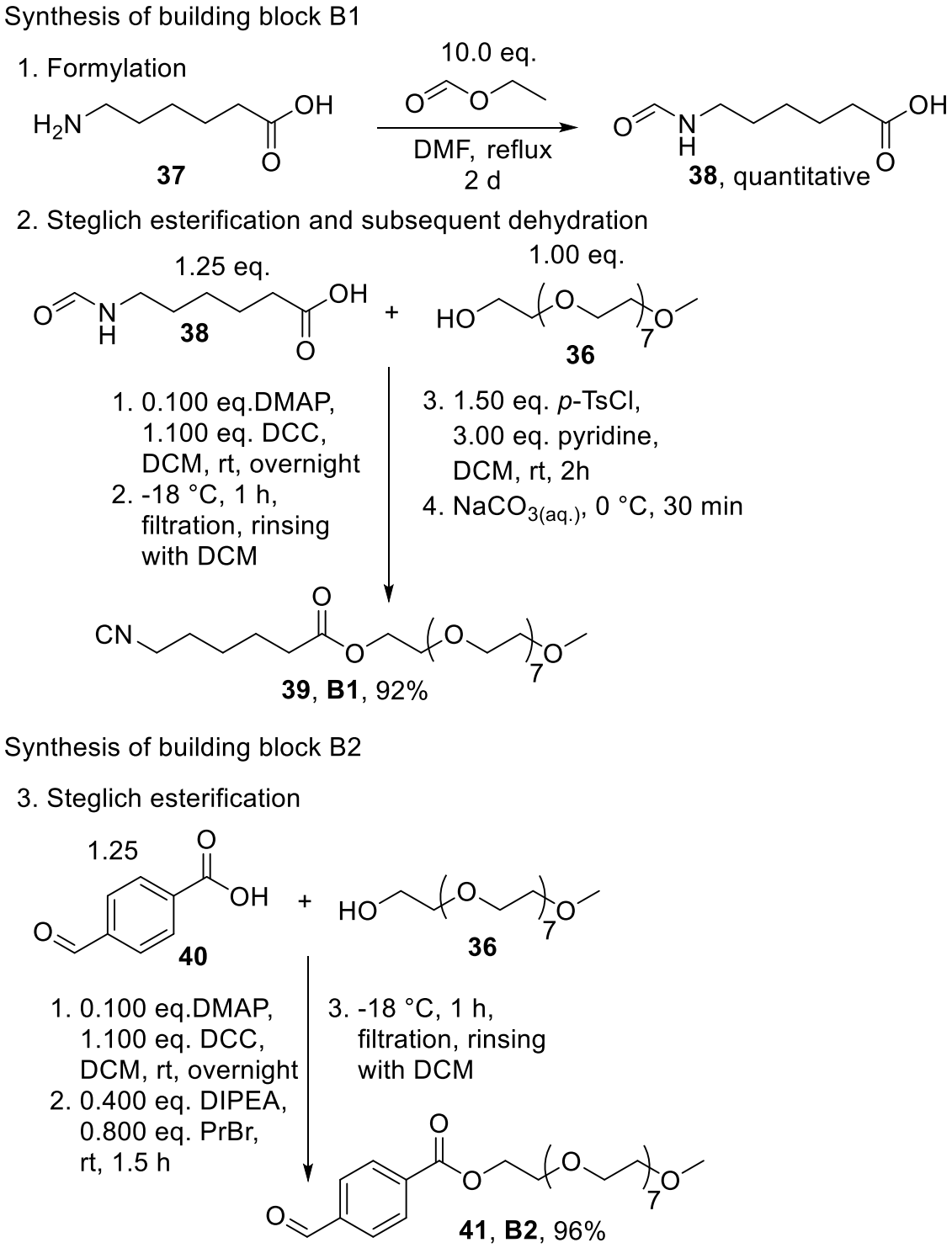

Scheme 69: Synthesis of the building blocks **B1** and **B2**. 1. Formylation of **37** yields **38** quantitatively. The conditions are the same as for 11-aminoundecanoic acid **1** (**Chapter 4.1**). 2. Combination of Steglich esterification and dehydration toward **B1**. 3. Steglich esterification of 4-formylbenzoic acid yields building block **B2** in one step.

In the first step, 6-aminohexanoic acid was formylated applying the conditions depicted in **Scheme 45** (**Chapter 4.1**). After removal of the solvent, the obtained formamide **38** was used without further purification. Subsequently, **38** was employed with Me-8EG-OH in a Steglich esterification utilizing 0.100 eq. *N,N*-dimethylpyridine

(DMAP) as catalyst and *N,N*-dicyclohexylcarbodiimide as activating reagent. To omit column chromatography of the highly polar PEGylated formamide, a novel one-pot procedure was established. After full conversion of **36**, the reaction mixture was cooled to -18 °C to allow precipitation of the insoluble dicyclohexylurea (DCU) byproduct. Afterwards, the reaction solution was filtrated, and the filter cake was rinsed with cold dichloromethane to extract remaining product. Drying and weighing of the obtained DCU confirmed removal of over 95% of the byproduct. Subsequently, 3.00 eq. pyridine were added and the solution was treated with 1.50 eq. *p*-TsCl. After quenching and subsequent aqueous work-up, the crude product was subjected to column chromatography yielding building block **B1** in high yield and purity (**Figure 29** and **Figure 30**). The overall yield was 64% starting from Me-4EG-OH **32** in five steps.

The Steglich reaction was also employed in the synthesis of **B2**. There, 4-formylbenzoic acid was reacted with **36**. Following complete conversion of the octa(ethylene glycol), 0.400 eq. DIPEA and 0.800 eq. propyl bromide (PrBr) were added to quench any remaining 4-formylbenzoic acid, which was used in excess (1.25 eq.). Afterwards, the reaction solution was also cooled to -18 °C for an hour, filtrated and rinsed with cold dichloromethane. The crude mixture was subjected to column chromatography and yielded the building block **B2** in a yield of 99% with high purity (**Figure 29** and **Figure 30**). The overall yield was 68.8% after four steps. The respective *Đ* was calculated using the software of the SEC system and found to be 1.00 for all OEGs as well as building blocks **B1** and **B2**, confirming their uniformity.

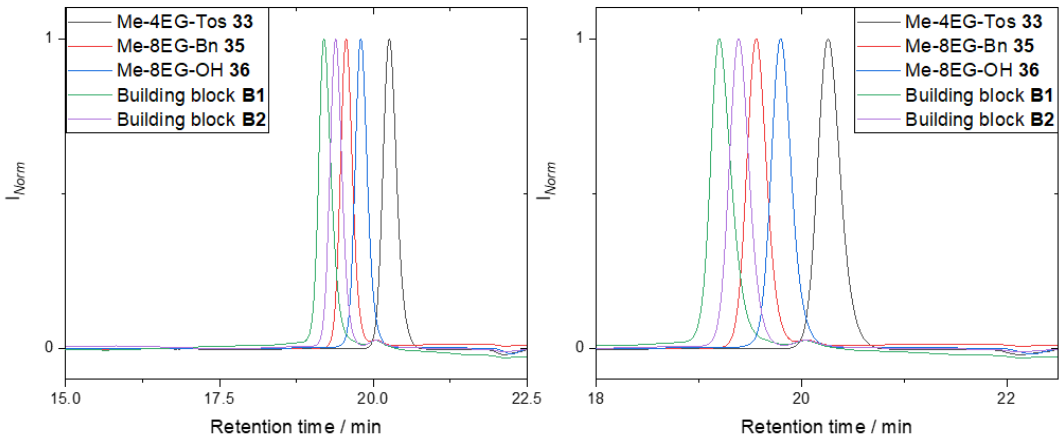

Figure 29: Left panel: SEC traces of the OEGs **33**, **35**, **36** and the building blocks **B1** and **B2**, all measured in THF. Right panel: magnified SEC traces, respectively. Note that the small peak at 20.0 is a system peak of the SEC device and not an impurity. Reprinted with permission from [224].

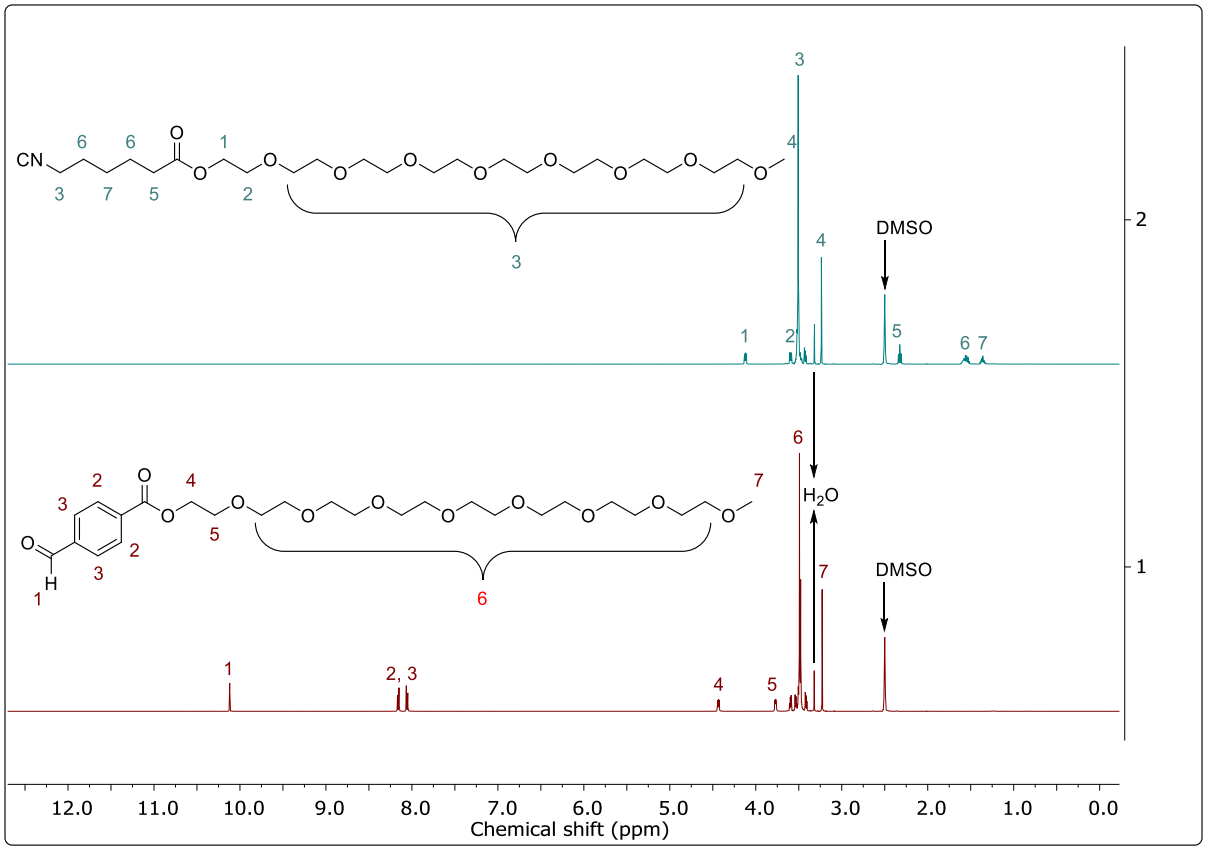

Figure 30: The ^{1}H NMR spectra of the building blocks **B1** and **B2** in deuterated DMSO (DMSO-d_6).

In order to connect the arm to the core, the azide-alkyne 'click' reaction was chosen as it is well-established and reliable reaction in organic chemistry (**Chapter 2.3.6**). Also, it is known for its versatile character as it can be carried out in a wide range of different solvents. Further, its high reaction rate and conversion were seen as invaluable for the final coupling step. In fact, the employed linear molecules were deemed to be sterically demanding and of a high molecular weight, while the attachment to the core is a tetra-functionalization, and hence full conversion was seen as absolute necessity, especially concerning the targeted uniformity of the final molecules.

The core was chosen to bear alkyne moieties since the iterative procedure of P-3CR and hydrogenation employed for the linear oligomer synthesis would compromise alkyne functionalities, which would be hydrogenated to the respective alkane. As substrate, 1,2,3,4-butan tetracarboxylic acid was chosen. The four alkyne functionalities were introduced by employing propargyl bromide as reagent together with DIPEA in dichloromethane as depicted in **Scheme 70**.

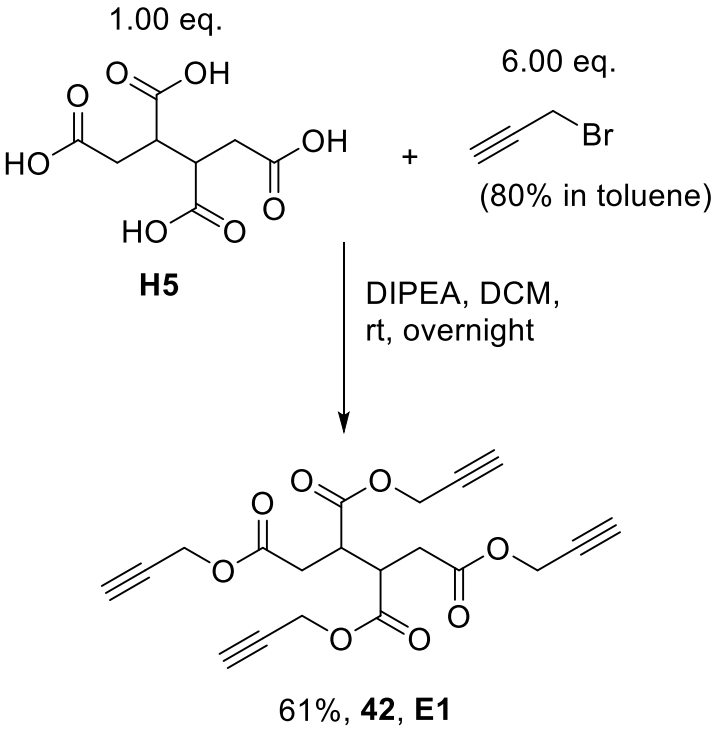

Scheme 70: Synthesis of a tetra alkyne starting from core **H5** by employing propargyl bromide in excess together with DIPEA in dichloromethane. The final product **42** is referred to as core **E1** and was obtained in 61% yield.

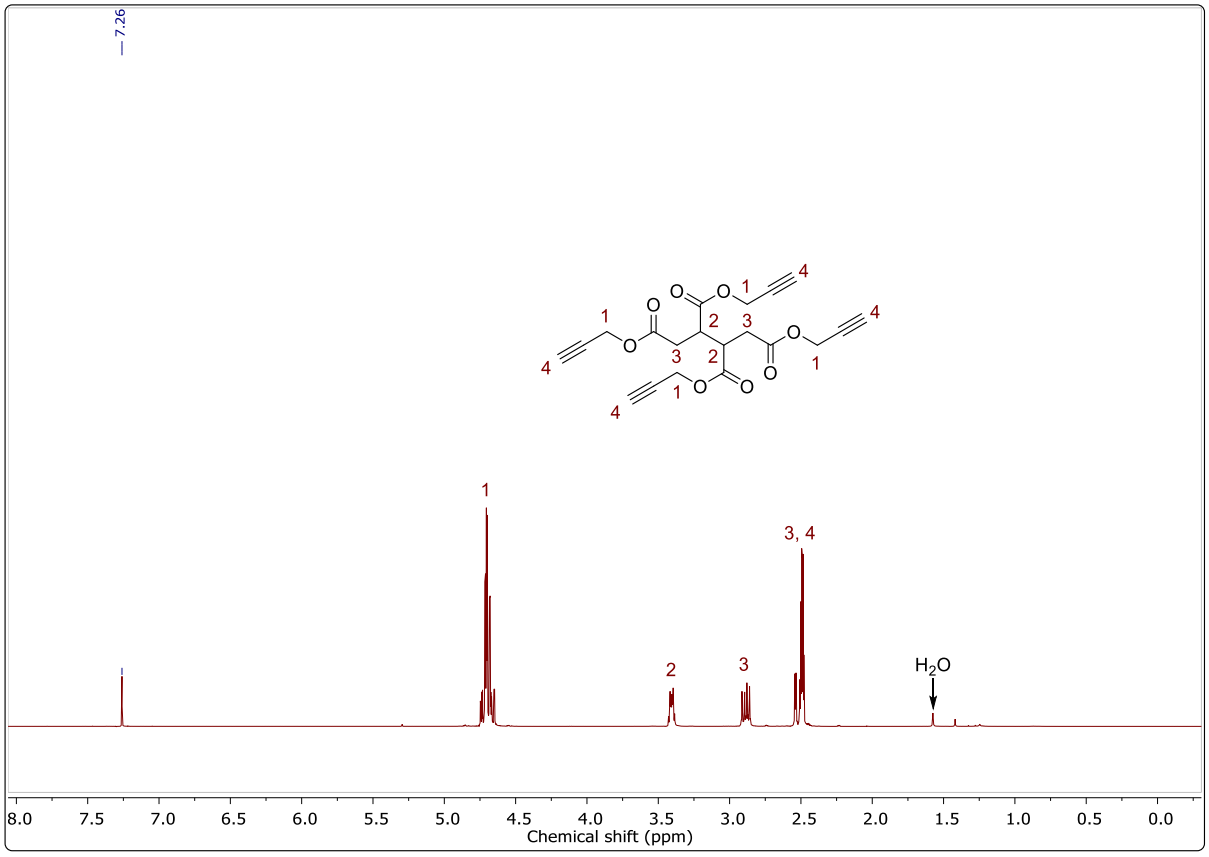

Figure 31: ^{1}H NMR spectrum of **E1** in deuterated chloroform ($CDCl_3$). Reprinted with permission from [224].

The reaction mixture was stirred for one day and then subjected to aqueous work-up. After subsequent column chromatography, the product was obtained in good yield and high purity. The ^{1}H NMR spectrum of **E1** is depicted in **Figure 31** (previous page), while a more detailed characterization is included in **Chapter 6.3.3.3**. Note that the core protons assigned with number 2 were of special importance as they were later employed to evaluate the proportion of core to arm after the final functionalization.

Finally, the linear oligomers were synthesized. As azide moieties do not tolerate hydrogenation, as they are converted to their respective primary amines, it was instead introduced in the final step *via* nucleophilic substitution employing sodium azide. Note that sodium azide is explosion endangered as well as highly toxic and thus has to be handled with outmost care. Bromide was chosen as leaving group to ensure sufficient reactivity in this reaction. Therefore, 11-bromoundecanoic acid **43** was employed as starting material, as it is commercially available in high purity (99% from Sigma Aldrich). Furthermore, three, five and seven repeating units were kept as goal and hence a novel iterative cycle employing a combination of building block **A1** and **A2** was designed. This allowed for reduction of the necessary reaction steps toward the targeted oligomers. Originally, the iterative cycle of P-3CR and subsequent hydrogenation has to be employed 7 times to reach a hypothetical heptamer, which totals in 14 reaction steps, two for each oligomer size increase. However, the novel approach only needs a total of 7 reaction steps to achieve the same, as it essentially halves the necessary reaction steps (note that the targeted oligomer numbers are uneven and hence do not allow for exact halving as therefore **A2** has to be employed in all reaction steps which was not done in order to obtain a tri-, penta- and heptamer). The novel approach allowed for less synthetic effort for all oligomer sizes, however, was only applicable if the employed aldehyde in the P-3CR is not meant to be varied. The iterative cycle is depicted in **Scheme 71**. In a first step, **43** was reacted with **A1** and 2-ethylbutanal **9** and hydrogenated to obtain the deprotected monomer **C1$_b$** in two steps (note that the protected oligomers are labeled **C1-4** and their respective deprotected counterparts **C1$_b$-4$_b$**). **C1$_b$** was then subjected to the iterative cycle employing **9** and **A2**. Therefore, **C2$_b$-4$_b$** were obtained after a total of 4, 6 and 8 steps. The respective yields and overall yields of selected compounds are given in **Table 11**.

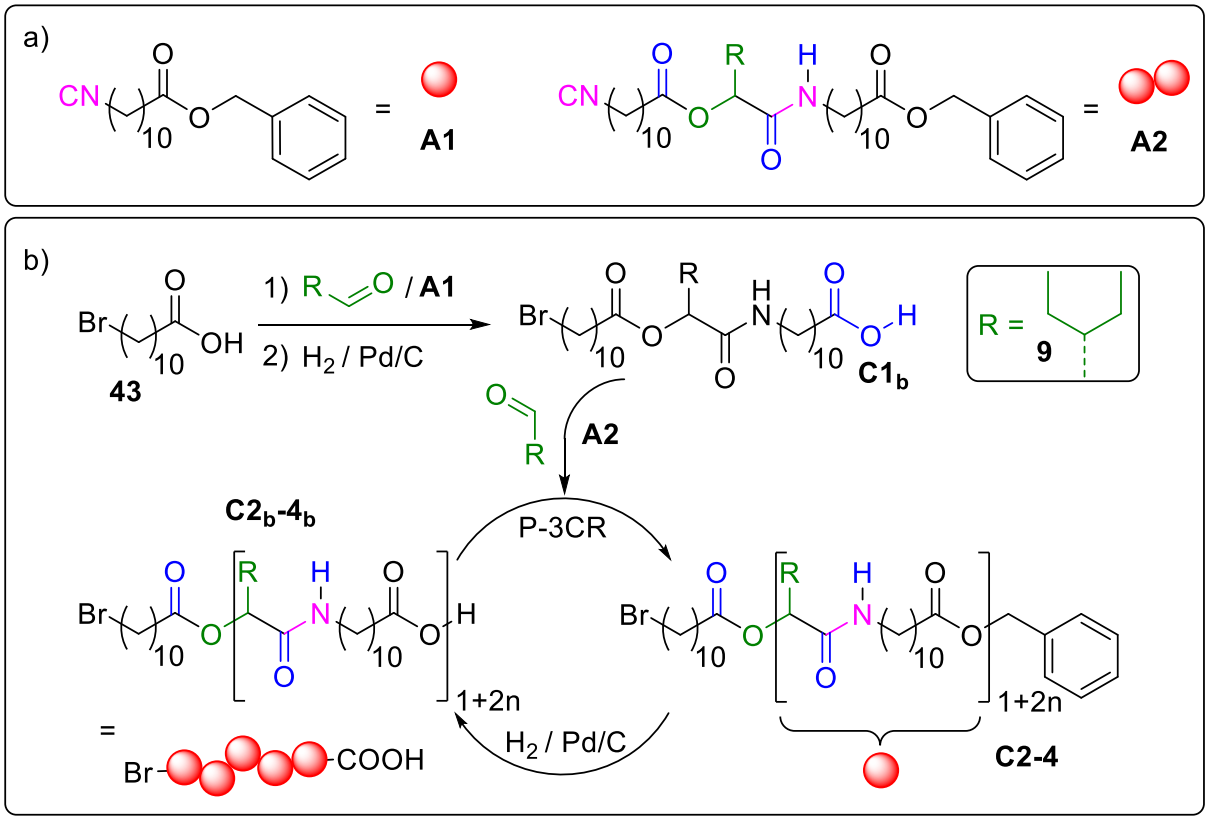

Scheme 71: a) The building blocks **A1** and **A2** were employed to reduce the necessary reaction steps toward the targeted oligomers. b) Iterative cycle of P-3CR and subsequent hydrogenation. Note that **A1** and a hydrogenation step were only employed to synthesize the monomer **C1$_b$**. Thereafter, **A2** was employed to reach the respective deprotected trimer, pentamer and heptamer (**C2$_b$**-**4$_b$**) in 2, 4 or 6 additional steps (or 4, 6 and 8 steps in total starting from **43**). Reprinted with permission from [224].

Table 11: Yields of the obtained oligomers. **C1**-**4** are the benzyl protected ones. The overall yields are given for the deprotected tri-, penta-, and heptamer (**C2$_b$**, **C3$_b$**, **C4$_b$**).

Entry	*Compound*	*Yield (%)*	*Overall yield (%)*
1	**C1** monomer	97	-
2	**C1$_b$**	98	-
3	**C2** trimer	92	-
4	**C2$_b$**	99	87 (4 steps)
5	**C3** pentamer	93	-
6	**C3$_b$**	98	79 (6 steps)
7	**C4** heptamer	92	-
8	**C4$_b$**	97	70 (8 steps)

The P-3CRs were carried out in dichloromethane utilizing 1.25-1.50 eq. of building block **A1**/**A2** and 1.50 eq. 2-ethylbutanal **9**. The concentration of the starting material in dichloromethane ranged between 1.00 and 1.50 mol L^{-1}. The reactions were stirred overnight at room temperature under argon atmosphere to prevent oxidation of the employed aldehyde. Work-up consisted of evaporation of the solvent and excess of aldehyde and subsequent column chromatography utilizing cyclohexane/ethyl acetate mixtures in different gradients. For the pentamer and heptamer, an additional 2.50 % v/v triethylamine was added, as the compound was found to exhibit band broadening similar to the compounds associated with the core-first approach. The hydrogenation was carried out in ethyl acetate and was purified by filtration trough Celite® and subsequent removal of the solvent. Furthermore, it was noticed that during the P-3CR, a side reaction occurred, which led to a species with lower retention time. These byproducts were identified by ESI-MS or SEC-ESI-MS measurements as results of chain-doubling: the deprotected acid reacted intramolecularly in a nucleophilic substitution featuring the bromide of the starting block as leaving group and was subsequently converted by a P-3CR (**Scheme 72**).

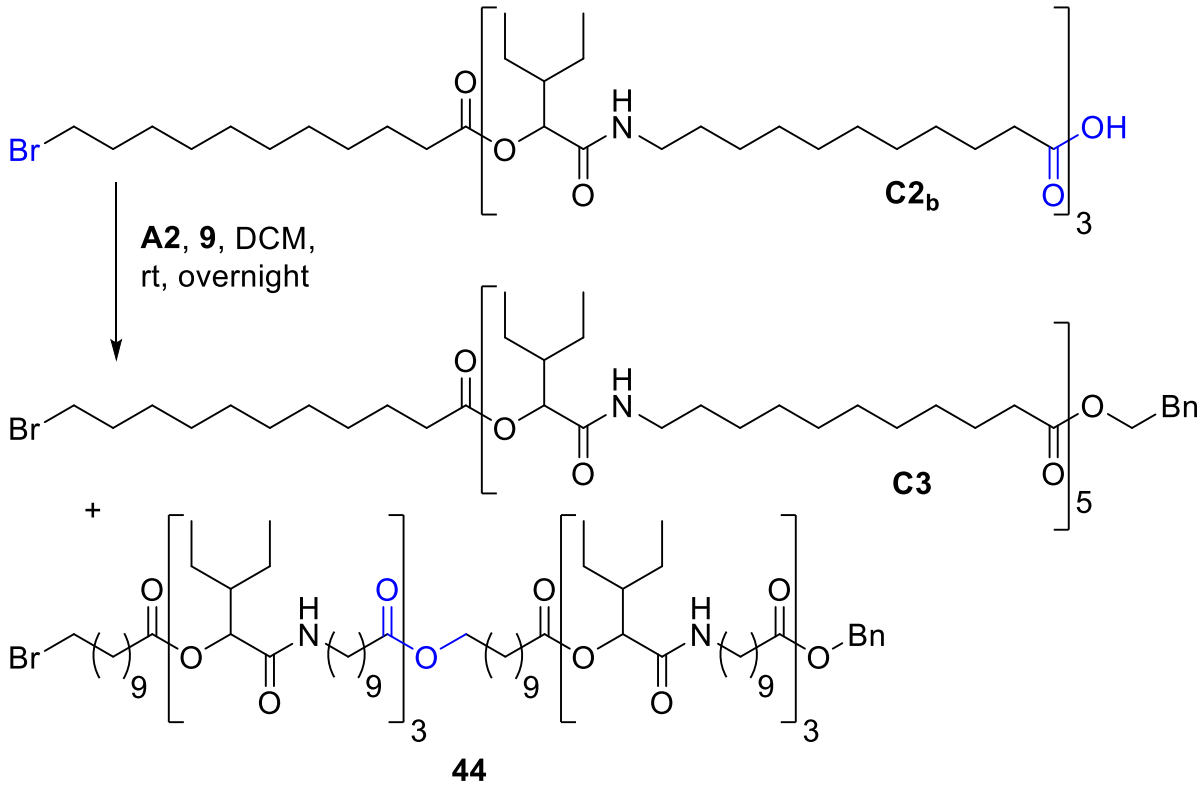

Scheme 72: Reaction of the deprotected trimer **C2$_b$** to the protected pentamer **C3**. The chain-doubled compound **44** was identified as byproduct and results from intermolecular nucleophilic substitution and subsequent P-3CR. The reactive functionalities are marked in blue.

In the given example, **C2$_b$** reacted with another molecule **C2$_b$** before it was converted *via* P-3CR as planned, giving a *hexameric* compound with a C_{11} spacer in between. These compounds were never isolated, as they exhibited quite similar polarity to the target compound, but clearly identified by HRMS. The calculated and found mass patterns of compound **44** are depicted in **Figure 32**, which confirm the chain-doubling side-reaction. More chain-doubling events were also confirmed in MS measurements, yet are left out for reasons of clarity. The byproduct was *ca.* 1-1.5% according to SEC and led to some mixed fractions in column chromatography, which explains the drop of yield to the lower nineties (92-93%) in **Table 11** for the trimer, pentamer and heptamer which was not observed for the monomer.

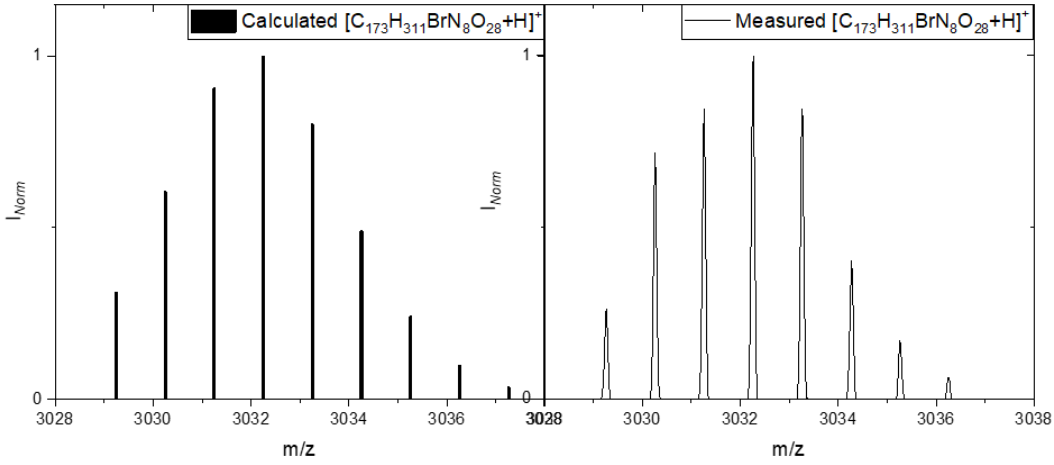

Figure 32: Left: Predicted mass spectrum of the chain-doubling product **44**. Right: Mass spectrum of **44**, which was obtained by ESI-MS of a mixed fraction. The predicted spectrum was calculated using the software MMass.

Nonetheless, the oligomers were obtained in high yields (>90%) and high overall yields, as depicted in **Table 11**. The respective SEC traces of the compounds are shown in **Figure 33** and confirm their high purity (>99%). Note that the trace of **C4$_b$** shows a small peak at lower retention times that was ascribed to the chain-doubled compound. The impurity occurred due to degradation over time as the sample had to be remeasured due to a change of pressure in the SEC system. All featured compounds exhibited a dispersity of 1.00 according to the SEC software.

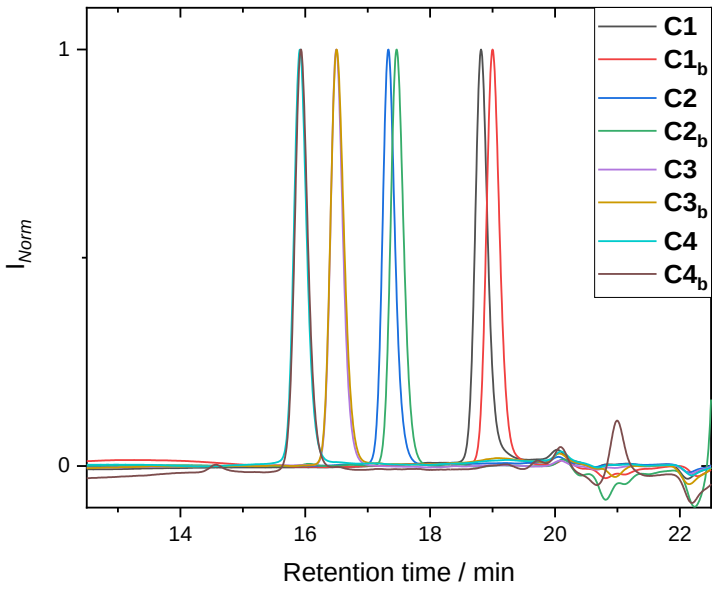

Figure 33: SEC traces of the oligomers **C1**-**C4$_b$** measured in THF. The trace of **C4$_b$** shows a peak at lower retention times, which belongs to the chain-doubled compound. The peak at 20 min is a system peak. Everything above 20 mins corresponds to solvent signals. The dispersity of all featured compounds was found to be 1.00 by the software of the SEC system.

Furthermore, NMR and IR spectroscopy, as well as mass spectrometry, were carried out to characterize the compounds and are depicted in **Chapter 6.3.3.3**. As an example, the ^{1}H NMR spectrum of the pentamers **C3** and **C3$_b$** are shown in **Figure 34** certifying the high purity of the synthesized compounds. After purification and characterization of the oligomer compounds, their post-reaction modification with uniform OEGs was carried out (**Scheme 73**). Originally, it was planned to employ the same reaction parameters as for the oligomer syntheses only exchanging the reactants: dichloromethane (1 M regarding the starting material), 1.50 eq. of isocyanide **B1** and aldehyde **B2** and overnight stirring at room temperature. However, the reaction mixture proved to be too viscous and hence the concentration was decreased to 0.330 mol L^{-1} for the PEGylation of the deprotected trimer **C2$_b$**. Still, after 24 h of stirring incomplete conversion was observed in the crude SEC and hence refluxing for another 24 h was employed.

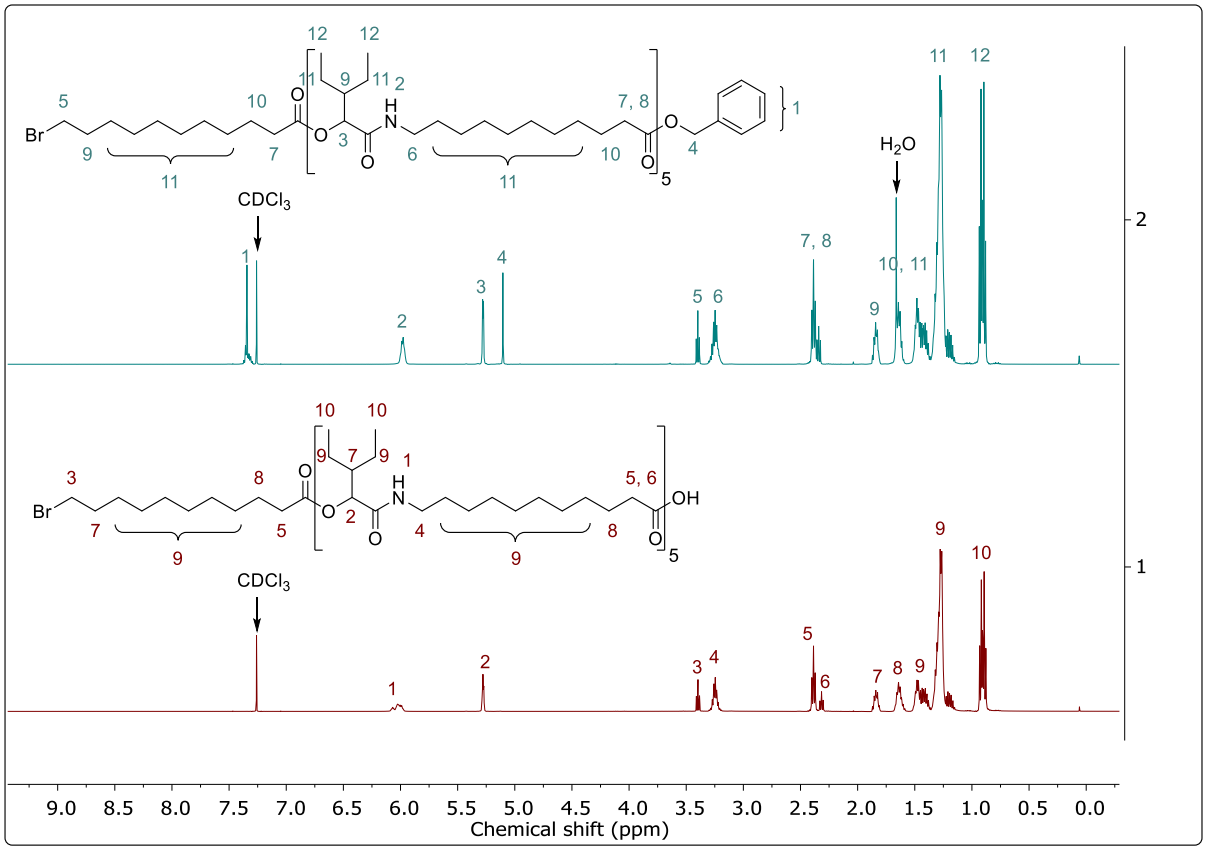

Figure 34: ^{1}H NMR spectra of the pentamers **C3** and **C3$_b$**. Both are measured in deuterated chloroform ($CDCl_3$) and show no visible impurities despite some silicon grease at 0.07 ppm.

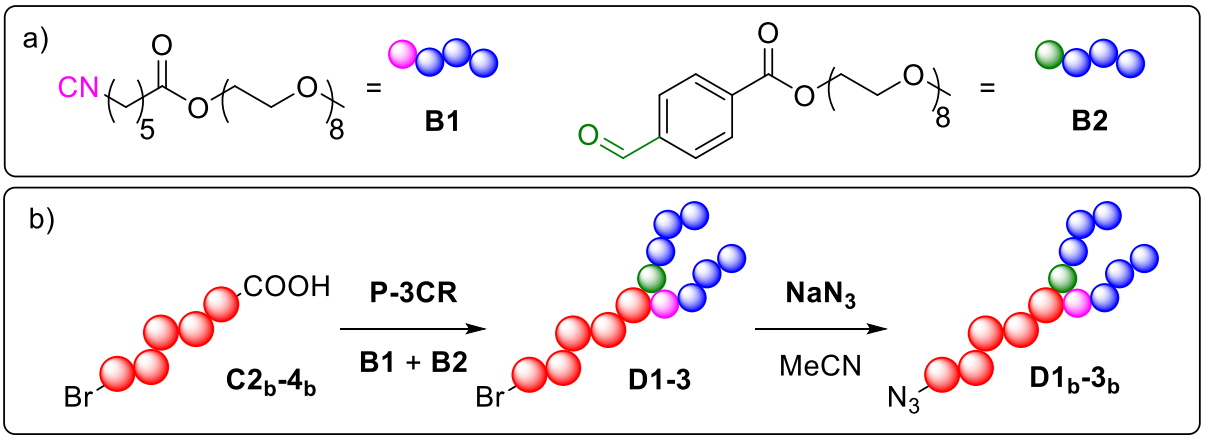

Scheme 73: a) PEGylated building blocks **B1** and **B2**. b) Post modification of the oligomers with **B1** and **B2** toward the oligomers **D1-3** and subsequent azidation yielding **D1$_b$-3$_b$**. Reprinted with permission from [224].

Consequently, the heating led to an increase of conversion, but also supported the chain-doubling reaction. For the PEGylation of the pentamer **C3$_b$**, chloroform was employed instead of dichloromethane to be able to achieve a higher temperature at reflux. Also, the mixture was only subjected to heating for 12 h, yet still chain-doubling

occurred. For both reactions, the SEC integration yielded about 1-1.5% percent of the PEGylated chain-doubled byproduct. Therefore, in the reaction of the heptamer, the equivalents of **B1** and **B2** were increased to 1.65 each and no heating was employed, which resulted in a lower conversion, but also in less byproduct. As for the OEGs presented in the beginning of this chapter, separation *via* column chromatography proved to be strenuous. The chain-doubled products and the target compounds exhibited only slight differences of polarity, which were not visible by TLC. However, by SEC measurements of the chromatographed fractions, it was established that the chain-doubled PEGylated byproducts are slightly less polar than the target compounds. Subsequently, the byproduct was carefully separated by employing a gradient column chromatography and adjusting the solvent accordingly (detailed information is presented in **Chapter 6.3.3.3**). As for the ethylene glycols, several fractions containing 1 L solvent each were collected and analyzed *via* SEC. For the trimer and pentamers, two column chromatographies were necessary to rid the PEGylated oligomers of their byproducts, while for the heptamer only one was sufficient. Each consumed about 30 L of solvent as well as 1 L of silica, which underlines the exhaustive efforts made to purify the compounds. Some product was lost due to mixed fractions in the column chromatography. The yields of **D1**-**3** were 81, 67 and 69%, respectively. As an example, the SEC traces of the fractions of the heptamer **D3** are displayed in **Figure 35**.

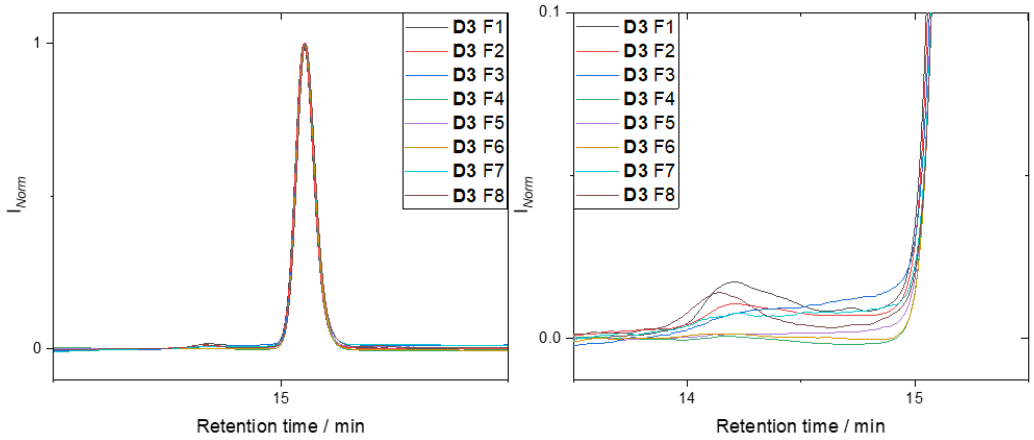

Figure 35: Left panel: SEC traces of the fractions of **D3** after column chromatography measured in THF. Right panel: The impurity at lower retention times is clearly visible in the magnified frame.

After purification, the three PEGylated oligomers **D1**-**3** were treated with 3.00 eq. of sodium azide at reflux in acetonitrile (MeCN) for a duration of 12-18 h to exchange the

bromide with an azide functionality. The work-up of these reactions featured filtration of the precipitated NaBr and the excess of NaN_3, washing with ethyl acetate and removal of the solvent. Subsequently, flash column chromatography provided the azides in quantitative yields and high purities. As an example, the ^{1}H NMR spectra of the PEGylated trimer **D1** and the azidated trimer **D1b** are depicted in **Figure 36**. A more detailed characterization is described in **Chapter 6.3.3.3**. The proton signal of the methylene group adjacent to the bromide (**Figure 36**, blue, number 11) vanished after **D1** was converted to its respective azide **D1b** and shifted into the signal of the CH_2 groups adjacent to the amide (**Figure 36**, red, number 12).

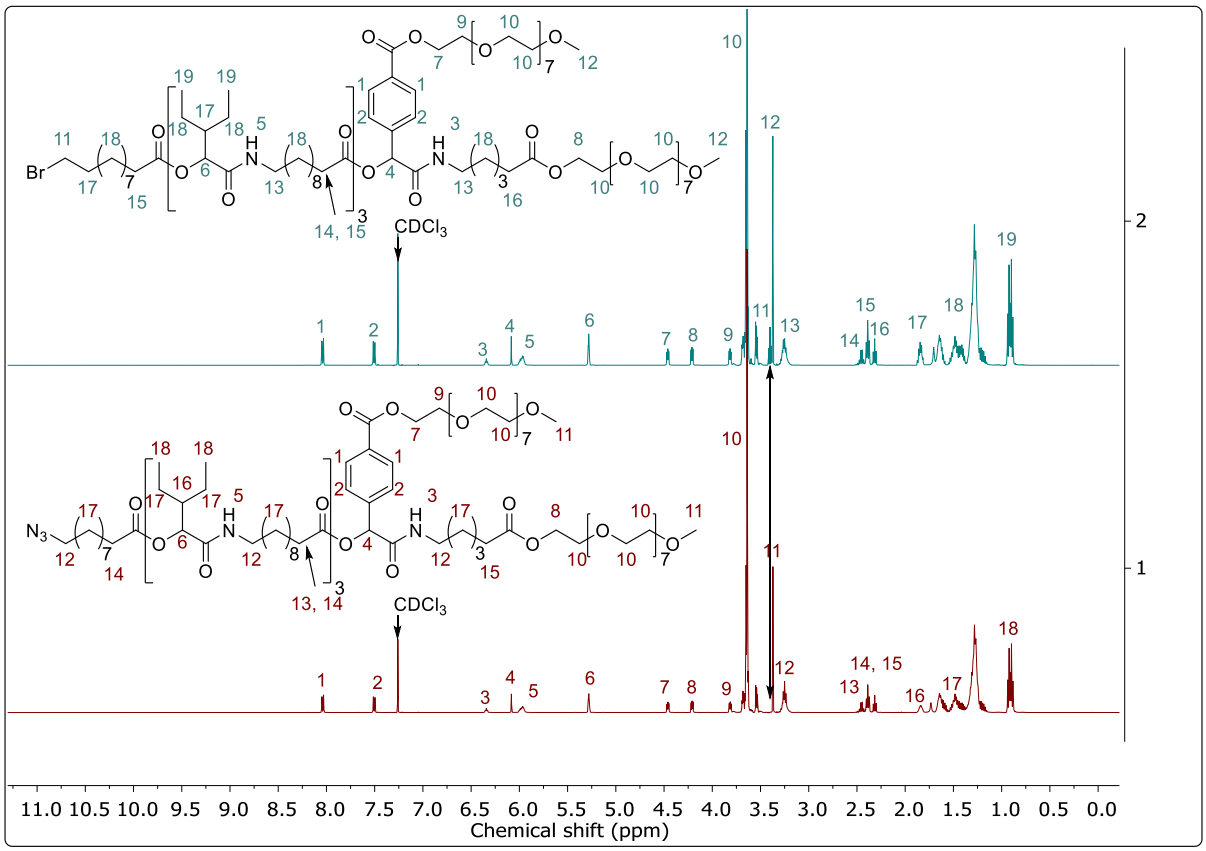

Figure 36: ^{1}H NMR spectra of **D1** and **D1b** in deuterated chloroform ($CDCl_3$). The proton signal of the methylene group adjacent to the bromide (blue, number 11) vanishes when the compound is converted to its respective azide.

Finally, the finished arm-molecules **D1b**-**3b** were coupled to core **E1** *via* CuAAC by exploiting the newly introduced azide moiety. These couplings were all conducted in chloroform at 65 °C for 24-40 h in a pressure vial. As copper catalyst Cu(I) iodide was used together with diisopropylethylamine (DIPEA) as ligand. All three reactions were flushed with argon for 5 min before the pressure vial was sealed to prevent Glaser coupling of the tetra-alkyne core **E1**. As an alternative, a procedure using the *in situ* reduction of copper(II)sulfate with L-ascorbic acid in THF/water was attempted

but yielded inferior results after a week of stirring at room temperature. In this case, elevated temperature was omitted due to the possibility of hydrolysis of the ester bonds by the water, which was used as co-solvent. In order to balance the increasing viscosity of the oligomer solutions, the concentration of the reactions was decreased with increasing arm-length (*i.e.*, 0.0350, 0.0258, and 0.0229 mol L^{-1} for the three star-shaped molecules **SM1-3**, respectively). In **Scheme 74**, the general reaction conditions of the CuAAC are depicted.

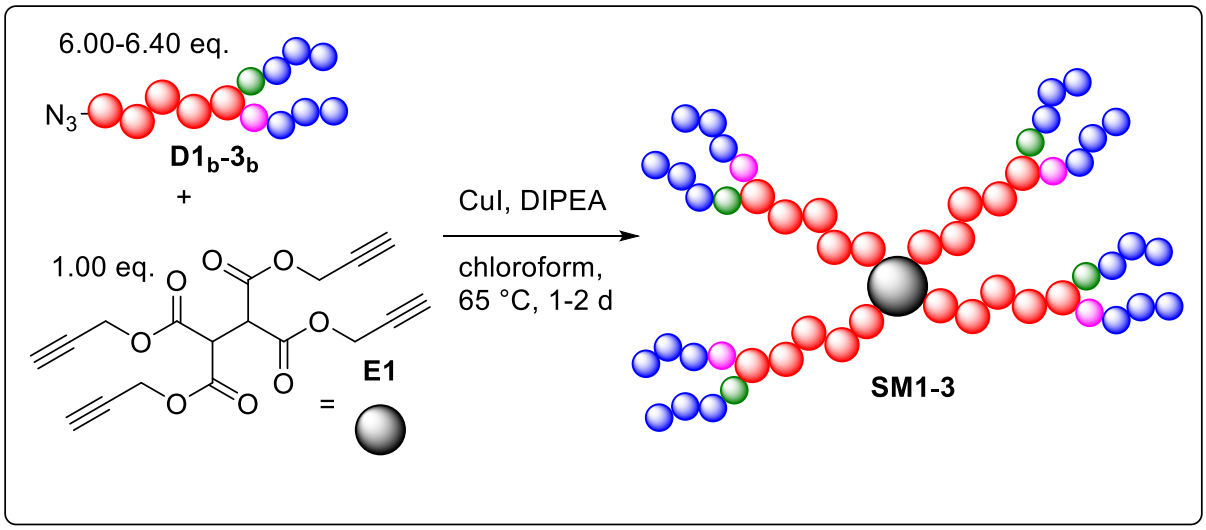

Scheme 74: Synthesis of the star-shaped macromolecules **SM1-3** *via* CuAAC utilizing core E1 and the previously synthesized azidated arms **D1$_b$-3$_b$**. The reaction was monitored by SEC measurements until full conversion was achieved (1-2 d). Reprinted with permission from [224].

The reactions were monitored *via* SEC measurements and subjected to column chromatography after full conversion to remove the excess of arm-molecules. **D1$_b$-3$_b$** were used in 1.50-1.60 eq. for each alkyne moiety, hence 6.00-6.40 eq. in total. Column chromatography yielded the trimer/pentamer/heptamer stars **SM1-3** in very good yields (90–91%) and high purities above 99% (determined by SEC, **Figure 37**). Finally, characterization of the star-shaped macromolecules *via* ^{1}H, ^{13}C NMR and IR spectroscopy, as well as mass spectrometry proved their successful synthesis (**Chapter 6.3.3.3**). As an example, the ^{1}H NMR spectrum of the trimer star **SM1** is depicted together with its predicted and measured mass spectrum in **Figure 38**. The ratio of the proton signals 8 and 14 confirm successful tetra functionalization. Altogether, the final star-shaped macromolecules **SM1-3** were obtained in an overall yield of 63, 48, and 44%, in a 7-/9-/11-step synthesis, respectively. Concluding, the implemented arm-first approach utilizing a P-3CR, hydrogenation, azidation and

CuAAC was capable to prepare uniform star-shaped block co-macromolecules in sufficient yield and high purity.

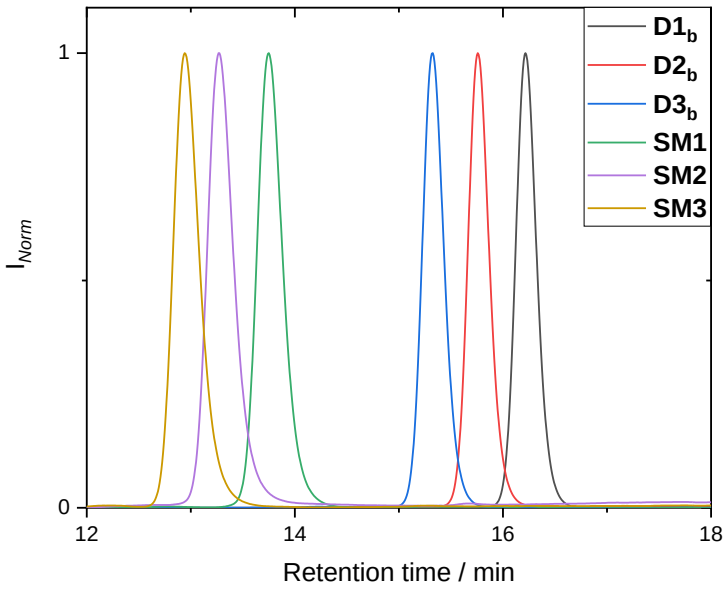

Figure 37: SEC traces of the azides **$D1_b$-3_b** and star-shaped macromolecules **SM1-3** measured in THF. Dispersity of the oligomers are 1.00, whereas the dispersity of the star-shaped molecules is 1.01 due to rounding, respectively.

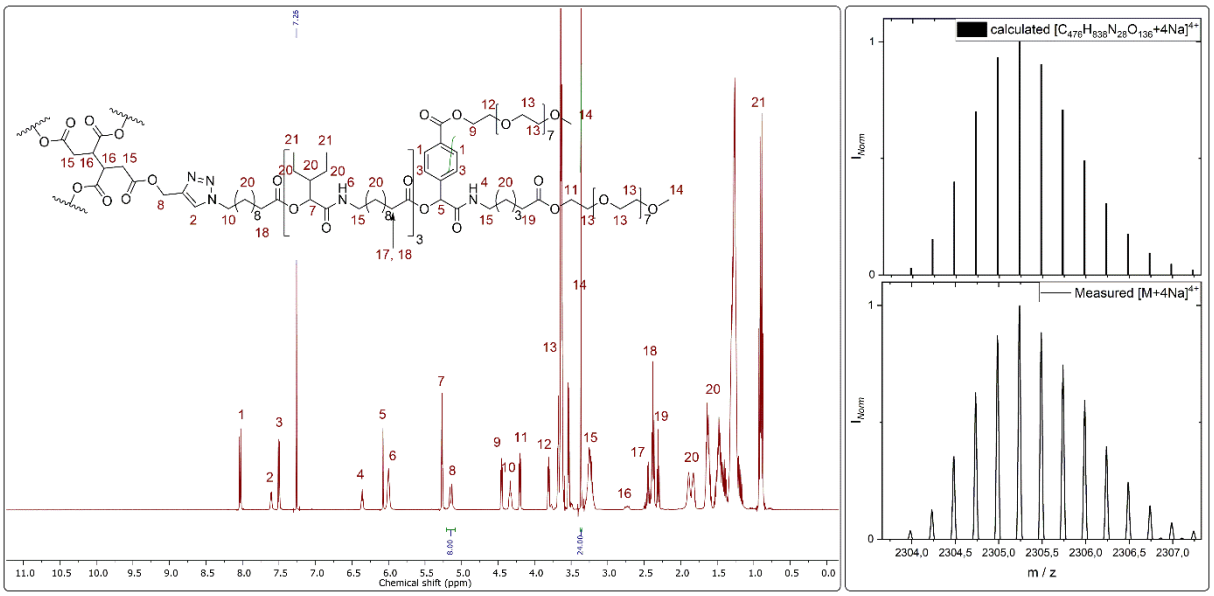

Figure 38: Left: Structure and ^{1}H NMR spectrum of the star-shaped macromolecule **SM1** in deuterated chloroform ($CDCl_3$). The ratio of the proton signals 8 and 14 confirm successful tetra functionalization. Right: Predicted and measured mass spectrum of **SM1**. The predicted spectrum was calculated using the software MMass. Reprinted with permission from [224].

The obtained star-shaped macromolecules were subsequently employed in phase-transfer experiments to establish their potential applications. Therefore, a previous publication by Meier was consulted, in which disperse star-shaped block copolymers were synthesized and applied in quantitative phase-transfer experiments utilizing the water-soluble organic dye Orange II (**Chapter 2.5.2**).[37] There, DCM solutions containing star polymers in different concentrations (0.1-10 mg mL^{-1}) were prepared, as well as a stock solution of Orange II in water (0.0225mg mL^{-1}). Mixing of these solutions allowed quantification of the phase-transfer *via* UV/Vis, spectroscopy after phase-separation. However, employing these conditions for the uniform star-shaped macromolecules **SM1**-**3** did not yield suitable data. Mixing of the prepared solutions resulted in bench-stable emulsions, which did not separate even after several days of standing. To counter these problems, sodium chloride was added as phase-separating agent, which was only partially successful. The addition of sodium chloride was non-beneficial for the UV/Vis measurements as it interfered with the absorption and the stars were found to encapsulate sodium chloride besides the targeted dye compound. Instead, an alternative dye was utilized: Nile red. However, as Nile red is partially soluble in water as well as organic solvents, another approach toward quantification was chosen. Originally, it was planned to dissolve all three star-shaped macromolecules in water to obtain solutions of different concentrations just as for the first experiment, but **SM2** and **SM3** were not soluble in pure water. Therefore, it was decided to employ a methanol/water mixture in which the dye, as well as the star-shaped macromolecules, were dissolved. The solutions were stirred for two days to allow for equilibrating. Afterwards, SEC measurements were conducted to verify that the star-shaped macromolecules were not degraded by the methanol/water mixture. However, SEC measurements of the mixtures showed that the star-shaped macromolecules had been broken down into smaller species and lacked uniformity. **Figure 39** depicts the pure uniform SEC trace of **SM3** next to measurements taken after 2 and 14 d of stirring in methanol/water, which show evident signs of degradation. After two days, a visible tailing appears as well as smaller species eluting at 15.5 and 17.8 mins. After two weeks, no traces of the original compound remain as it has degraded to different unknown species. Additionally, the SEC trace of the heptamer-arm $\mathbf{D3_b}$ is given as it matches the retention time of the species at 15 mins, which is found in both degradation residues. As their retention time is quite similar it potentially originates from the cleavage of the arm moiety of the core. Note that this cleavage

does not yield **D3b** but rather its hydroxymethyl triazole derivative, which therefore is depicted within the **Figure 39**. As no further analytics were conducted, this remains non-verified.

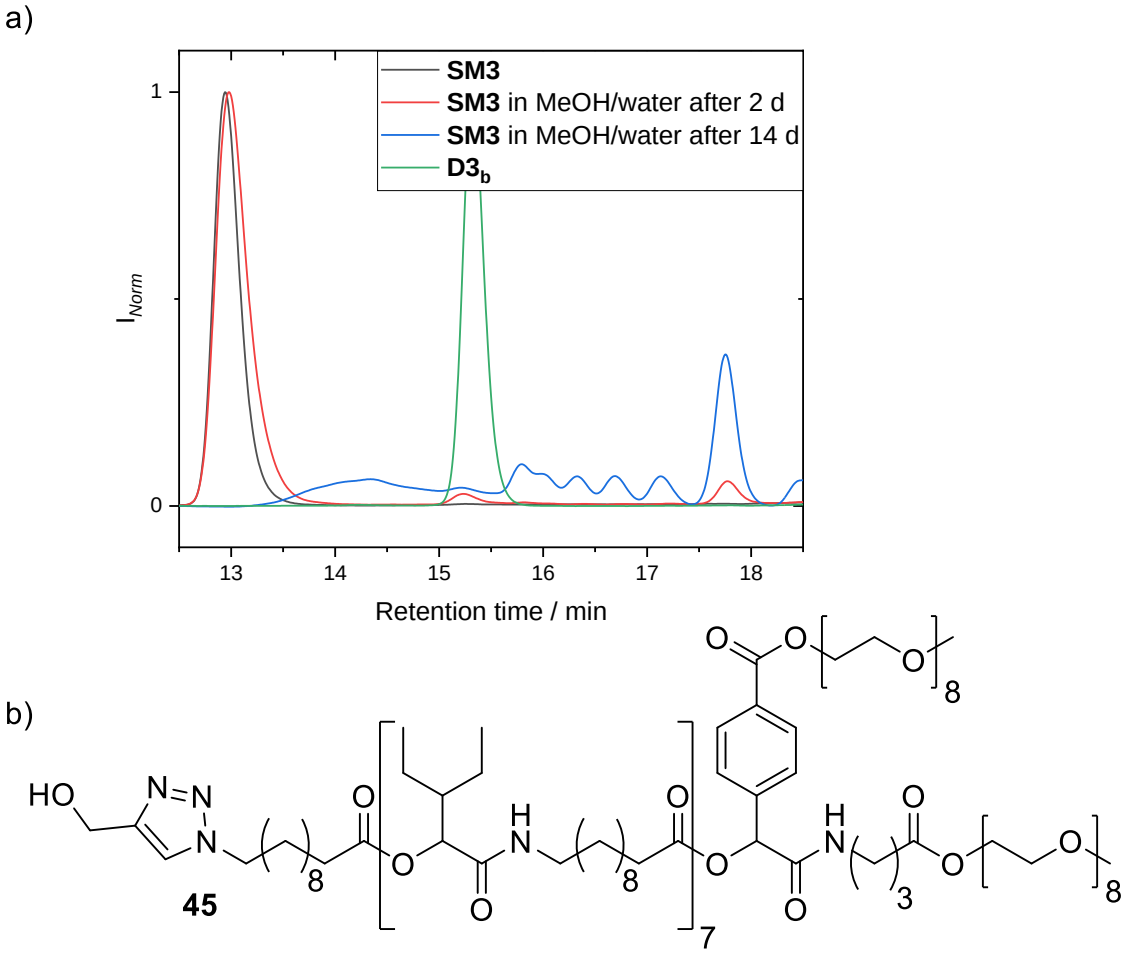

Figure 39: a) SEC traces of **SM3** as well as its degradation products after 2 and 14 d measured in THF. Additionally given is the trace of the PEGylated heptamer azide **D3b** as the degradation product visible at 15.5 mins is approximately the same size. b) Structure of the theoretical degradation product, which is associated with said peak. It is obtained by cleavage ester bond of the core unit **E1**.

Due to these degradation problems, an alternative way of evaluating their potential in encapsulation had to be sought. As employing water for long periods of time was not possible and liquid-liquid phase-transfer was found to be ineffective due to separation problems, qualitative solid-liquid phase-transfer experiments were established to evaluate their encapsulation of guest molecules, either as unimolecular micelles or as self-assembled co-macromolecules.

One experiment was conducted utilizing **SM1** for a dye transfer into aqueous phase as it was the only star-shaped macromolecule that was found to be water-soluble. Here,

Nile red was employed as its water solubility is low (0.1 mg mL^{-1}). For the other experiment, **SM3**, Orange II and DCM were employed. The goal was encapsulation of the insoluble Orange II to allow its transfer into the dichloromethane phase. For both experiments, a blank sample of pure solvent as well as five samples, which featured macromolecule concentrations of 0.1-5/10 mg/mL were prepared and vigorously shaken with an excess of dye for 6 h. Afterwards, the remaining solids were filtered off and the visibly colored solutions were measured by UV/Vis spectroscopy. In **Figure 40**, the set-up of the experiments and the absorption graphs are depicted. Within the graphs, the absorption maxima α at 556 nm for Nile red and at 484 nm is plotted against polymer concentration. It increases with higher concentration of star-shaped macromolecules, albeit nonlinearly. This indicated the formation of self-assembled structures in solution.

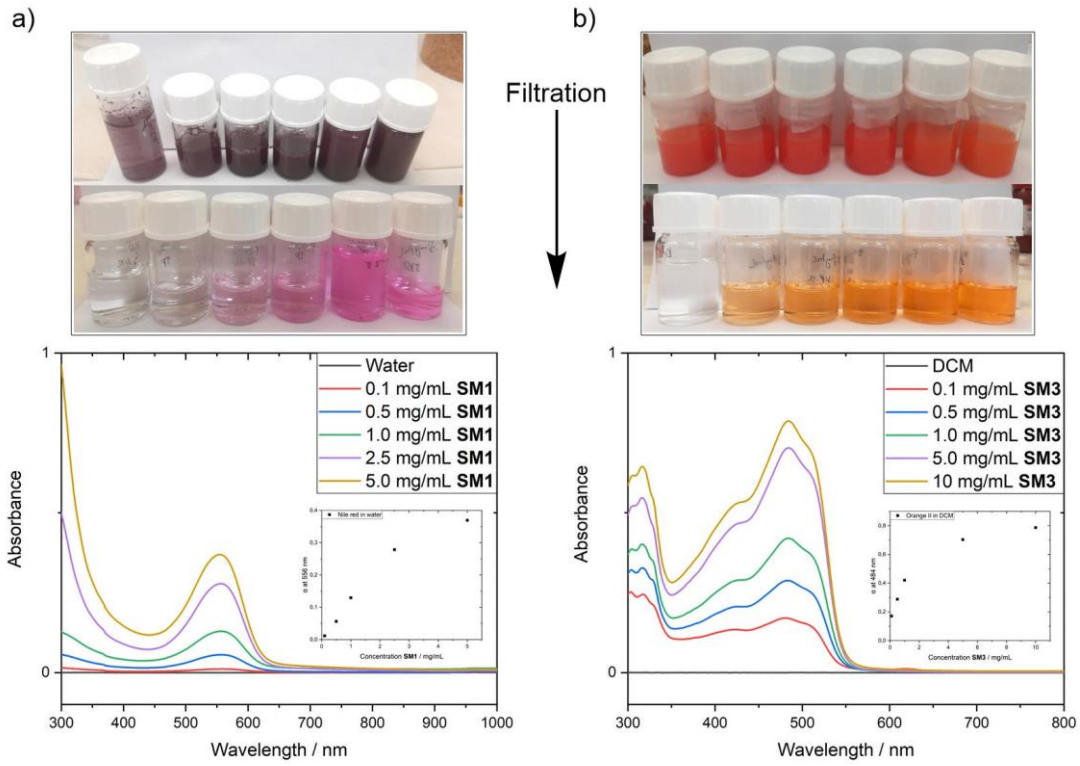

Figure 40: a) Solid-liquid phase transfer of Nile Red into an aqueous phase employing the star macromolecule **SM1**. b) Solid-liquid phase transfer of Orange II into dichloromethane employing the star macromolecule **SM3**. Both experiments were verified by UV/vis measurements. Reprinted with permission from [224].

To investigate this possibility, dynamic light scattering (DLS) measurements of **SM1** in mixtures of methanol and water were carried out. The choice of solvent was determined by the fact that methanol was a good solvent for **SM1** and indicated unimolecular structures (**Figure 41**).

For low water contents (0-20%), hydrodynamic radii (R_h) of 4.3-4.7 nm were measured for **SM1**, which indicates the presence of unimers in these solvent mixtures. However, with increasing water content, also higher R_h were found with a distinct increase above 80% water content.

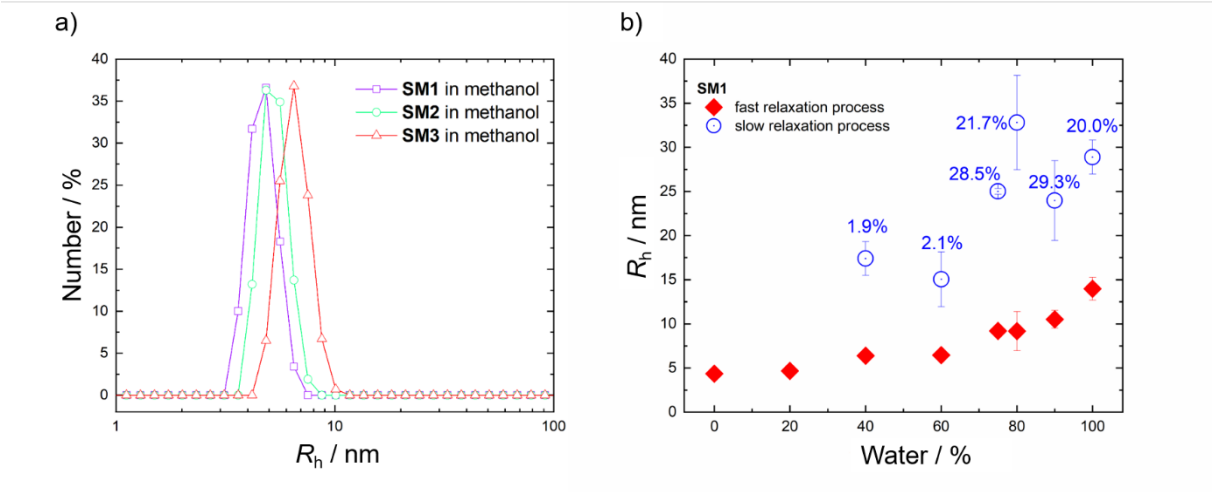

Figure 41: a) Hydrodynamic radii of the star-shaped co-macromolecules dissolved in methanol, measured by dynamic light scattering (DLS) at 25 °C: $R_{h,\mathbf{SM1}}$ = 4.2 nm, $R_{h,\mathbf{SM2}}$ = 4.7 nm, $R_{h,\mathbf{SM3}}$ = 5.8 nm. b) Hydrodynamic radii obtained from DLS measurements of **SM1** in mixtures of methanol and water: red diamonds are from the fast diffusing scatterers, blue circles from the slow ones; percentages indicate the relative concentration of the large scatterers in the mixture. Reprinted with permission from [224].

In the high water content area, multiple molecules of **SM1** self-assemble, which explains the larger sizes observed (9.1-14.0 nm). Furthermore, at a water content of 40% or higher, a prominent slower relaxation process, which corresponds to larger scatterers was observed (R_h ≈ 17.4-32.8 nm). These also increased with higher water percentages as they constituted <3% relative concentration until the water content reached 60% and ≈ 20% in pure water. This was attributed to the aggregation of the star shaped **SM1** molecules into larger structures.

DLS measurements in dichloromethane were not possible due to the low scattering intensity obtained. This is probably a result of refractive index matching of solvent and macromolecules, which could not be circumvented.

In conclusion, the iterative procedure relying on the P-3CR and subsequent hydrogenation was maintained in a monodirectional way, yet expanded by employing a bromide-bearing start block to allow for two post-synthesis modifications: the introduction of oligo(ethylene glycol)s and an azide moiety as they were both necessary for the targeted arm-first approach toward star-shaped macromolecules.

To allow for faster synthesis of the required linear oligomers, a novel building block **A2**, which already featured one iteration unit, was synthesized by employing a two-step synthesis from **A1**. It was obtained in high yield and purity and reduced the necessary steps toward a heptamer by 6 lowering the overall laboratorial effort of the synthesis. Furthermore, two novel uniform building blocks **B1** and **B2**, which both featured octa(ethylene glycol) methyl ether units, were synthesized and characterized. These were accessible starting from the commercially available tetra(ethylene glycol) mono benzyl ether and mono methyl ether and were obtained in moderate yields, but high purity after SEC measurement–assisted standard column chromatography.

The respective arm molecules **C2**-**C4** (tri-/penta-/heptamer) were synthesized and obtained in high overall yields and high purity, which was verified by employing several analytical methods, most importantly NMR spectroscopy, size-exclusion chromatography, and mass spectrometry. SEC measurements of the respective compounds confirmed their targeted uniformity. Afterwards, the oligomers were modified post-reaction by employing **B1** and **B2** and subsequently azidated to yield a set of three PEGylated and azidated oligomers: trimer **C1$_b$**, pentamer **C2$_b$**, and heptamer **C3$_b$**.

In a final CuAAC, the three oligomers were coupled to a tetra-alkyne bearing core **E1**. Column chromatography provided a set of highly pure star-shaped macromolecules **SM1**-**3**, which were obtained in high overall yields (63, 48, 44%) after 7/9/11 steps in total. After careful analysis by SEC, ESI-MS and NMR spectroscopy, potential applications were targeted and evaluated.

The star-shaped macromolecules were employed to evaluate their ability to carry water-insoluble compounds into an aqueous phase and water-soluble compounds into an organic phase. These experiments were supported by UV/Vis spectroscopy and indicate their potential application in phase-transfer catalysis or drug delivery. Further self-assembly of the star-shaped macromolecule **SM1** in water was noticed and evaluated in subsequent DLS experiments employing different mixtures of methanol/water. These experiments showed prominent slow relaxation processes of aggregated **SM1** besides **SM1** unimers above a water content of 40%.

5 Conclusions and outlook

In summary, this thesis is divided into three sub-chapters, all based on isocyanide chemistry: first, the sustainability and practicability of isocyanide synthesis and its improvement were evaluated. Second, the optimization and application of a novel one-pot synthesis utilizing isocyanides and sulfoxides was presented. Third, the application of the P-3CR in order to synthesize uniform star-shaped macromolecules in a core-first and an arm-first approach as well as their subsequent application in qualitative encapsulation experiments was discussed.

In the first chapter, procedures utilizing $POCl_3$, PPh_3/I_2 and *p*-TsCl to dehydrate *N*-formamides into isocyanides were evaluated in terms of sustainability. It was established that *p*-TsCl provided the highest yields of up to 97% for non-sterically demanding aliphatic isocyanides with E-factors down to 6.55, the latter often being much lower than in the literature, where mostly $POCl_3$ is used. In addition to the more benign dehydrating agent, the non-toxic dimethyl carbonate was introduced as a sustainable solvent alternative to the commonly applied highly hazardous dichloromethane. Procedures in dichloromethane and dimethyl carbonate were established and applied to the synthesis of ten different aliphatic isocyanides, which were obtained in high yields and excellent purity. Furthermore, it was shown that even flash column chromatography, which is generally applied for purification, can be omitted for some isocyanides, which were still obtained in sufficient purity for subsequent polymerization. However, sterically more demanding or aromatic compounds proved to be the limitation for this new procedure, as these were only obtained in low yields with high E-factor. Nonetheless, the novel procedure is straightforward and offers significant improvements in terms of sustainability. This especially provides an advantage for isocyanide-based chemistries, such as IMCRs, in which the isocyanide components constitute the only limiting factor in terms of sustainability. For future developments, the poor atom-economy of the isocyanide synthesis can be targeted. An enzyme-based dehydration of *N*-formamides would allow for a further decrease of the ecological fingerprint of the isocyanide synthesis. For their respective isomers (nitriles) this is already literature known and has been exploited toward their synthesis in laboratory scale. There are also living organisms that biosynthesize isocyanide-bearing compounds, a potential hint to an enzymatic mechanism, albeit only few are known.

In the second chapter, a novel reaction to synthesize diversely substituted thiocarbamates was investigated. The procedure is based on the isocyanide synthesis utilizing *p*-TsCl and features the addition of an aliphatic sulfoxide after initial dehydration of the employed *N*-formamide. The procedure features a one-pot protocol, as the isocyanide component does not need to be isolated in between, which represents a clear advantage over other isocyanide-based thiocarbamate syntheses. The reaction was optimized and subsequently applied to synthesize a library of sixteen different thiocarbamates, utilizing four commercially available sulfoxides. Furthermore, reduction of the sulfoxide to the respective sulfide was noticed as a side-reaction, whereas alkyl chlorides were identified as related products of the thiocarbamate reaction. Thereafter, a mechanism was proposed that attributes *p*-TsCl to be the driving force of the reaction, as it activates the sulfoxide in a Swern-like mechanism. Finally, syntheses of thiocarbamate bearing step-growth monomers for subsequent polymerization were conducted, yet failed to match the expectations. However, novel norbornene-based thiocarbamate monomers were synthesized and obtained in moderate to good yields and excellent purity. The author plans to employ them in a ring-opening metathesis polymerization and a first test reaction has already shown promising results. Thiocarbamate-based macromolecules still represent a niche in polymer science, however their unique character and reactivity not only enables possible post-polymerization modifications, but also allows for a supramolecular assembly based on the strong hydrogen bonding of the thiocarbamate functionality. Regarding the actual reaction, the employment of different solvent parameters, with focus on sustainable alternatives like DMC and Me-THF, can be considered as the next step. Further understanding of the mechanism would allow to improve the reaction conditions with a focus on side-reaction suppression. Also, temperature parameters and concentration of the reactants are to be considered for further optimization.

In the final chapter, an iterative protocol featuring the P-3CR and subsequent hydrogenation was employed to synthesize uniform star-shaped molecules. At first, a multi-directional core-first approach was evaluated, which proved to be unsuccessful. Several star-shaped macromolecules were synthesized in good to excellent yields, but the hydrogenation step was accompanied by an unknown side reaction that prevented the targeted uniformity. The respective byproduct could neither be isolated nor characterized, as it proved to be inseparable from the main product. Hence, the core-first approach was replaced by an arm-first approach.

Utilizing the arm-first approach, three uniform oligomers (tri-, penta-, and heptamer) were prepared and modified post-reaction with a uniform octa(ethylene glycol). In a final coupling, the block co-oligomers were attached to a core moiety *via* CuAAC yielding three star-shaped macromolecules of different, yet molecularly perfectly defined sizes. These were obtained in high overall yields (> 44%) after 7/9/11 steps in total and were analyzed *via* NMR spectroscopy, ESI-MS and SEC. Finally, the amphiphilic star-shaped macromolecules were employed to evaluate their ability to carry water-insoluble compounds into an aqueous phase and water-soluble compounds into an organic phase. These experiments were supported by UV/Vis spectroscopy and indicated their potential application in phase-transfer catalysis or drug delivery. However, further investigations of the actual loading potential of the obtained star-shaped macromolecules as well as their self-assembly properties remain to be conducted. Also, the respective arm length can be increased in further experiments, albeit the ratio between the hydrophobic parts of the arms and the hydrophilic oligo(ethylene glycol)s can be varied to establish a structure-property relationship regarding the possible drug/dye loading potential and their respective water solubility.

Overall, it was thus demonstrated that the molecule class of isocyanides still carries unrevealed synthetic potential, even more than a hundred years after their initial discovery by the chemist Lieke. Since then, isocyanides have seen a remarkable increase in use, shaping a whole area of chemistry: isocyanide-based multi-component reactions. The substance class is used in medicinal and combinatorial chemistry as well as in the synthesis of defined and disperse macromolecules, with applications like data storage or drug delivery. However, recent and future research focuses on the reevaluation of their synthesis with regard to efficiency and sustainability, and still novel applications for these remarkable compounds are in reach.

6 Experimental section

6.1 Materials

1,12-Diamino dodecane (98%), 3,3',5,5'-tetracarboxyldiphenylmethane (≥95%), 4-aminobutyric acid (≥99%),11-aminoundecanoic acid (97%), 11-bromoundecanoic acid (99%), 2-ethylbutyraldehyde (>92%), β-alanine (99%), benzyl bromide (98%), cerium(IV)-sulfate (99%), copper(I)iodide, cyclohexyl amine (99%), ethyl formate (reagent grade, 97%), heptanal (95%), *N,N*'-dicyclohexylcarbodiimide (DCC) (≥99%), oleylamine (>98%), palladium on activated charcoal (10wt%), phosphomolybdic acid hydrate (99%), *p*-toluenesulfonyl chloride (*p*-TsCl) (reagent grade, ≥98%), sebacic acid (99%), silica gel (technical grade, pore size 60 Å. 230-400 mesh particle size, TLC silica gel F_{254} and 40-63 µm particle size), sodium azide (ReagentPlus®, ≥99.5%), sodium carbonate (98%), tetradecane (≥99%) and ω-pentadecalactone (≥99%) were purchased from **Sigma-Aldrich**. Acetonitrile (HPLC-grade, ≥99.8%), chloroform (HPLC-grade, ≥99.8%), dichloromethane (HPLC-grade, ≥99.8%), DMSO (≥99.9%), pyridine (≥99.5%) and triethylamine (≥99.5%) were supplied by **Fisher chemical**. Anhydrous seasand, sodium hydroxide and sodium sulfate were purchased from **Bernd Kraft**. 1,8-Diazabicyclo(5.4.0)undec-7-ene (DBU) (>98%), 6-hydroxyhexyl amine (>97%), amino octadecane (>85%), norbornene-2-methylamine (>98%, mixture of isomers), tetra(ethylene glycol) monobenzyl ether (>95%), tetra(ethylene glycol) monomethyl ether (>98%) and tetrahydrothiophene-1-oxide (95%) were purchased from **TCI**. DMF (HPLC-grade) and methanol (HPLC-grade) were purchased from **VWR**. 4-Dimethylaminopyridine (DMAP) (99%), diisopropylethylamine (DIPEA) (99%) was purchased from **abcr GmbH**. 1,5-diamino pentane (98%), formic acid (99%), potassium *tert*-butoxide (98%), propargyl bromide (80% solution in toluene), pyridinium chlorochromate (PCC) (98%), thionyl chloride (>99.5%) and trimethyl orthoformate (99%) stabilized with MgO) were purchased from **ACROS Organics**. 1-bromopropane (99%) and 6-Aminohexanoic acid (>98.5%) were purchased from **FLUKA**. [1,1'-biphenyl]-3,3',5,5'-tetracarboxylate (95%) and formyl benzoic acid (99.75%) were purchased from **BLDPharm**. 1,2,3,4-butane tetracarboxylic acid (≥98%), 4-aminobenzoic acid (99%), adamantyl amine (98%), amino decane (97%), Celite® 545 and dibutyl sulfoxide (97%), were purchased from **Alfa Aesar**. Benzyl amine (>99%), benzyl sulfoxide (>99%) were purchased from **Merck kGaA**. Potassium carbonate (≥99.5%) was purchased from **Evonik**. Benzyl alcohol (≥99%) was purchased from **Honeywell**. Hydrogen (99.999%) was purchased from **Air Liquide**.

$CDCl_3$ (≥99.8%), DMSO-d_6 (≥99.8%) and MeOH-d_4 (≥99.8%) were purchased from **Euriso-top**. Solvents like cyclohexane and ethyl acetate were used in HPLC grade. Acetone and diethyl ether were used in technical grade.

6.2 Analytical instruments and methods

6.2.1 Nuclear magnetic resonance (NMR) spectroscopy

^{1}H NMR spectra were recorded using a Bruker Avance DRX 500 with 8 scans at ambient temperature. Data is reported in ppm relative to DMSO-d_6 at 2.50 ppm or $CDCl_3$ at 7.26 ppm. ^{13}C NMR spectra were recorded using a Bruker Avance DRX 500 with 1024 scans at ambient temperature. Data is reported in ppm relative to DMSO-d_6 at 39.51 ppm or $CDCl_3$ at 77.16 ppm.

For the different splittings of the NMR-data, following shortcuts were used: s = singlet, d = doublet, t = triplet, q = quartet, p = quintet, sex = sextet, m = multiplet, bs = broad signal.

6.2.2 Gas chromatography (GC)

Gas chromatography (GC) was performed on a Bruker 430 GC instrument equipped with capillary column FactorFour™ VF-5 ms (30.0 m × 0.25 mm × 0.25 µm), using flame ionization detection (FID). The oven temperature program was: initial temperature 95 °C, hold for 1 min, ramp at 15°C min^{-1} to 220 °C, hold for 4 min, ramp at 15°C min^{-1} to 300 °C, hold for 2 min, ramp at 15°C min^{-1} to 325 °C, hold for 3 min. Measurements were performed in split-split mode using nitrogen as the carrier gas (flow rate 30 mL min^{-1}).

6.2.3 Gas chromatography-mass spectrometry (GC-MS)

GC-MS (electron impact (EI)) measurements were performed on the following system: Varian 431 GC instrument with a capillary column FactorFour VF – 5 ms (30 m × 0.25 mm × 0.25 mm) and a Varian 210 ion trap mass detector. Scans were performed from 40 to 650 m/z at a rate of 1.0 scans s^{-1}. The oven temperature was adjusted as followed: initial temperature 95 °C, hold for 1 min, ramp at 15 °C min^{-1} to 220 °C, hold for 4 min, ramp at 15 °C min^{-1} to 300 °C, hold for 2 min. The injector transfer line temperature was set to 250 °C. Measurements were performed in the split-split mode (split ratio 50:1) using helium as carrier gas (flow rate 1.0 mL min^{-1}).

6.2.4 Size exclusion chromatography (SEC)

The obtained oligomers were characterized *via* size exclusion chromatography on a Shimadzu Size Exclusion Chromatography (SEC) system equipped with a Shimadzu

isocratic pump model LC-20AD, a Shimadzu refractive index detector (model RID-20A, a Shimadzu autosampler model SIL-20A and a Varian column oven model 510 (50°C). For separation, a three-column setup was sued with one SDV 3 µm, 8 × 50 mm precolumn and two SDV 3 µm, 1000 Å, 3 × 300 mm columns supplied by PSS, Germany. Tetrahydrofuran (THF) stabilized with 250 ppm butylated hydroxytoluene (BHT, ≥99.9%) supplied by Sigma-Aldrich was used at a flow rate of 1.0 mL min^{-1}. For calibration, linear poly(methyl methacrylate) standards (PSS) ranging from 875 Da to 1677 kDA were used. The peak around 20.15 min. is a system peak and does not belong to any impurities. Dispersity *Đ* was determined by integration of the peak in LabSolution software. The program calculates M_w/M_n, which are obtained *via* the calibration.

6.2.5 Size exclusion chromatography coupled to Electrospray ionization-Mass spectrometry (SEC-ESI-MS)

SEC-ESI-MS spectra were recorded on a Q Exactive (Orbitrap) mass spectrometer (Thermo Fisher Scientific, San Jose, CA, USA) equipped with a HESI II probe. The instrument was calibrated in the m/z range 74–1822 using premixed calibration solutions (Thermo Scientific). A constant spray voltage of 4.6 kV, a dimensionless gas flow rate of 8, and a dimensionless auxiliary gas flow rate of 2 were applied. The capillary temperature and the S-lens RF level were set to 320 °C and 62.0, respectively. The Q Exactive was coupled to an UltiMate 3000 UHPLC System (Dionex, Sunnyvale, CA, USA) consisting of a pump (LPG 3400SD), an autosampler (WPS 3000TSL), and a thermostated column department (TCC 3000SD). Separation was performed on two mixed bed size exclusion chromatography columns (Polymer Laboratories, Mesopore 250 × 4.6 mm, particle diameter 3 µm) with precolumn (Mesopore 50 × 4.6 mm) operating at 30 °C. THF at a flow rate of 0.30 mL min^{-1} was used as eluent. The mass spectrometer was coupled to the column in parallel to a RI detector (RefractoMax520, ERC, Japan). 0.27 mL min^{-1} of the eluent were directed through the RI-detector and 30 µL min^{-1} infused into the electrospray source after postcolumn addition of a 100 µM solution of sodium iodide in methanol at 20 µL min^{-1} by a micro-flow HPLC syringe pump (Teledyne ISCO, Model 100DM). A 20 µL aliquot of a polymer solution with a concentration of 2 mg mL^{-1} was injected onto the HPLC system.

6.2.6 Infrared spectroscopy (IR spectroscopy)

Infrared spectra of all samples were recorded on a Bruker alpha-p instrument in a frequency range of 3997.41 to 373.828 cm^{-1} using ATR technology.

6.2.7 Mass spectrometry (EI-MS)/High resolution mass spectrometry (HRMS)

High resolution electron ionization mass spectra were recorded on a Finnigan MAT 95 instrument.

6.2.8 Fast atom bombardment-mass spectrometry (FAB-MS)/High resolution mass spectrometry (HRMS)

High resolution-fast atom bombardment mass spectra recorded on a Finnigan MAT 95 instrument.

6.2.9 Electrospray ionization-mass spectrometry (ESI-MS)

Electrospray Ionization-Mass Spectrometry (ESI-MS) experiments were recorded on a Q-Exactive (Orbitrap) mass spectrometer (Thermo Fisher Scientific, San Jose, CA, USA) equipped with a HESI II probe. The spectra were interpreted by molecular peaks $[M]^+$, peaks of protonated molecules $[M+H]^+$ and also higher charged species for the higher molecular weight oligomers and polymers, for instance $[M+2H]^{2+}$ up to $[M+6Na]^{6+}$. All peaks are indicated with their mass-to-charge ratio (*m/z*).

6.2.10 Atmospheric solids analysis probe (ASAP) with atmospheric pressure chemical ionization-mass spectrometry (APCI-MS) and electrospray ionization-mass spectrometry (ESI-MS)

A CMS expression Advion atmospheric solids analysis probe (ASAP) system with atmospheric pressure chemical ionization-mass spectrometry (APCI-MS) and electrospray ionization-mass spectrometry (ESI-MS) was used. The range of the detector is 10 – 1200 g/mol. The device is equipped with an Edwards scroll pump type *15i* with serial nXDS and a Peak scientific nitrogen generator. Only the APCI-MS was used for ASAP investigations.

6.2.11 UV/Vis spectroscopy

Transmission was recorded on a LAMBDA 950 UV/Vis spectrophotometer, which was equipped with an integrating sphere.

6.2.12 Dynamic light scattering (DLS)

DLS measurements were carried out using a Zetasizer Nano ZS (Malvern Instruments Ltd.) equipped with a 4 mW He-Ne laser operating at 632.8 nm, while the scattered

intensity was measured at an angle of 173 °. The temperature of the solutions was 25 °C, while the refractive indices, dielectric constants and viscosity parameters were based on literature values.[360,361] The electric field autocorrelation functions $g_1(t)$ were fitted with eq. 4 to deconvolute the different relaxation processes and extract the relaxation times (τ) as well as the amplitudes (*A*) of each process.

$$g_1(t) = B + \sum_i A_i e^{-\Gamma_i t} \qquad \text{(eq. 4)}$$

where $\Gamma_i = \tau_i^{-1}$ and *B* is the baseline of the correlation function.

The R_h values were calculated by applying the Stokes-Einstein equation (eq. 6)

$$R_h = \frac{k_B T}{6\pi\eta D_s} \qquad \text{(eq. 6)}$$

where k_B is the Boltzmann constant, *T* is the temperature (in K), *η* is the solvent viscosity and $D_s = \Gamma q^{-2}$ is the diffusion coefficient (*q* is the scattering vector). In order to obtain the relative concentrations of the different relaxation processes, the approximation that is $A \sim N \cdot R_h^6$ was applied.[362,363] In the absence of Mie scattering parameters, this estimation is expected to be precise as qR < 1.

6.2.13 Thin layer chromatography (TLC)

Thin layer chromatography (TLC) experiments were performed on silica-gel-coated aluminum foil (silica gel 60 F254, Sigma-Aldrich). Compounds were visualized by irradiation with a UV lamp, by staining with Seebach solution (mixture of phosphomolybdic acid hydrate cerium(IV)-sulfate, sulfuric acid and water) or a solution of vanillin in sulfuric acid followed by heating with a heat gun.

6.2.14 Molecular mass (M) and exact mass [M]

Molecular mass (M) of the molecules in the SI were calculated *via* the application ChemDraw Professional.

Exact masses [M] of the molecules in the SI or its protonated/deprotonated species and metal adducts *i.e.* $[M + H]^+$, $[M - H]^-$, $[M + xNa]^{x+}$ were calculated by the application mMass.

6.3 Syntheses and analytical data

6.3.1 Isocyanides – Chapter 4.1

Note: Chapter 6.3.1 refers to the publication “A more sustainable and highly practicable synthesis of aliphatic isocyanides”. The following data is taken from the corresponding SI, yet slightly adjusted to fit the optics of this thesis. Figures are reprinted with permission [103].

Also, the calculation for the exact masses in this thesis was carried out with mMass. Therefore, the calculated values of the molecule/ion weight featured in this chapter differ slightly to the ones in the SI of the publication.

General isocyanide screening with internal standard (3.00 mmol scale)*

*The GC screening was carried out by N. Möhl in her bachelor thesis, which was supervised by the author. The respective data is taken from her thesis as well as the aforementioned publication for completeness.[103,336]

In order to determine the concentration of 1-isocyanooctadecane in the GC screening experiments, a gas chromatography calibration curve with tetradecane as internal standard (IS) was compiled by measuring six samples.

Table S 1: Six sample of different concentrations of 1-isocyanooctadecane and the same concentration of IS were measured and the ratio of the area of the 1-isocyano octadecane and the area of IS were calculated.[336]

Sample	*A(2)*	*A(IS)*	*c(2) (mg/mL)*	*c(IS) (mg/mL)*	*c(2)/c(IS)*	*A(2)/A(IS)*
1	2.76 E3	289	1.00	0.100	10.0	9.57
2	2.36 E3	289	0.800	0.100	8.00	8.16
3	1.81 E3	289	0.600	0.100	6.00	6.27
4	1.69 E3	289	0.500	0.100	5.00	5.85
5	1.11 E3	289	0.400	0.100	4.00	3.83
6	492	289	0.200	0.100	2.00	1.70

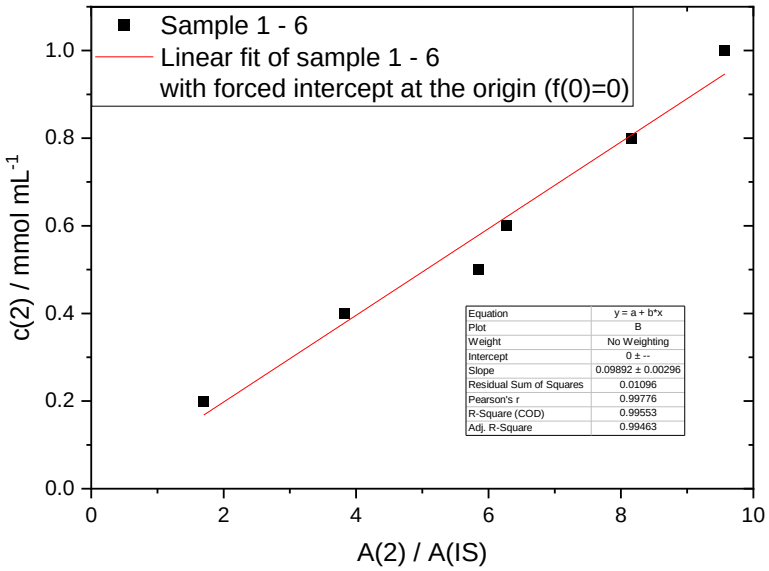

Figure S 1: Calibration curve calculated using a linear fit (red line). The obtained slope was 0.0989 and the R^2-value was 0.996. Adapted from [336].

In a typical GC screening experiment, 3.00 mmol of *N*-formamidooctadecane was dissolved in a solvent (various amount) and then, reacted with a dehydrating agent (various amounts) in presence of a base (various amounts) and a given amount of tetradecane (mostly 10 mol%). Samples were taken after different reactions times and the resulting areas of the signals of tetradecane and the product were determined to calculate the yield of each specific reaction condition applying the following formulas:

$$R_{x/is} = \frac{A_x/A_{is}}{c_x/c_{is}} \qquad \text{(eq.7)}$$

$R_{x/is}$ is the slope of the calibration curve, whereas A_x, A_{is}, c_x and c_{is} correspond to the measured area and concentration of standard (is) and analyte (x).

$$c_x = \frac{c_x}{c_{is}} c_{is} \qquad \text{(eq.8)}$$

As the amount of internal standard and therefore its concentration is known, the unknown concentration of analyte (x) and the corresponding yield can be calculated, respectively.

6.3.1.1 General synthesis of aliphatic *N*-formamides

The corresponding aliphatic amine (30.0 mmol, 1.00 eq.) and ethyl formate (24.2 mL, 22.2 g, 300 mmol, 10.0 eq.) were stirred under reflux overnight. Afterwards, remaining

ethyl formate and ethanol were removed under reduced pressure and the crude product was used without further purification or analysis.

Exceptions are: Adamantyl *N*-formamide, methyl-4-formamidobenzoate, *N*-(6-hydroxyhexyl)formamide and 11-formamidoundecanoic acid (The latter is described in **Chapter 6.3.3.1**).

Adamantyl *N*-formamide*

Adamantyl amine, chloroform and ethyl formate were refluxed for 48 hours. Afterwards, remaining ethyl formate, chloroform and ethanol were removed under reduced pressure and the crude product was used without further purification or analysis.

*This compound was synthesized by R. Seim under the author's supervision.

Methyl-4-formamidobenzoate*

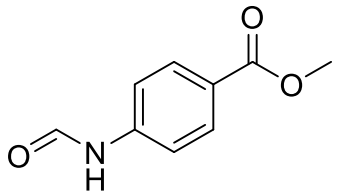

$C_9H_9NO_3$

M = 179.18 g/mol

In a flask equipped with a Dimroth-cooler, methyl 4-aminobenzoate (9.82 g, 65.0 mmol, 1.00 eq.) was dissolved in formic acid (9.80 mL, 12.0 g, 260 mmol, 4.00 eq.) and was heated to 60 °C for 24 h. Afterwards, formic acid and water were removed under reduced pressure and the product (11.0 g, 61.4 mmol) was obtained as white powder in a yield of 95% without further purification.

*This compound was synthesized by N. Seul, who conducted her "Vertieferarbeit" under the co-supervision of R. Nickisch.

TLC: R_f (cyclohexane/ethyl acetate 2:1) = 0.13

^{1}H NMR (500 MHz, DMSO-d_6): δ (ppm) = 10.56 – 10.47 (m, 1H, C**H**, ^{1}), 8.97 (d, *J* = 10.7 Hz, 1H, N**H**, ^{2}), 8.35 (d, *J* = 1.7 Hz, 1H, N**H**, ^{2}), 7.93 – 7.88 (m, 2H, C**H**$_{\text{aromatic}}$, ^{3}), 7.71 (d, J = 8.8 Hz, 2H, C**H**$_{\text{aromatic}}$, ^{4}), 7.31 (d, *J* = 8.6 Hz, 2H, C**H**$_{\text{aromatic}}$, ^{4}), 3.81 (s, 3H, C**H**$_3$, ^{5}).

^{13}C NMR (126 MHz, DMSO-d_6): δ (ppm) = 165.8, 163.2, 162.6, 160.2, 142.5, 130.8, 130.4, 124.4, 118.7, 116.5, 51.9.

HRMS (EI) *m/z*: [M] calculated (calcd) for $C_9H_9NO_3$, 179.0582; found, 179.0584.

IR (ATR): ṽ (cm^{-1}) = 3182, 3053, 2962, 2884, 1716, 1611, 1522, 1438, 1419, 1273, 1189, 1039, 1016, 963, 885, 847, 817, 763, 687, 636, 523, 506, 479, 457.

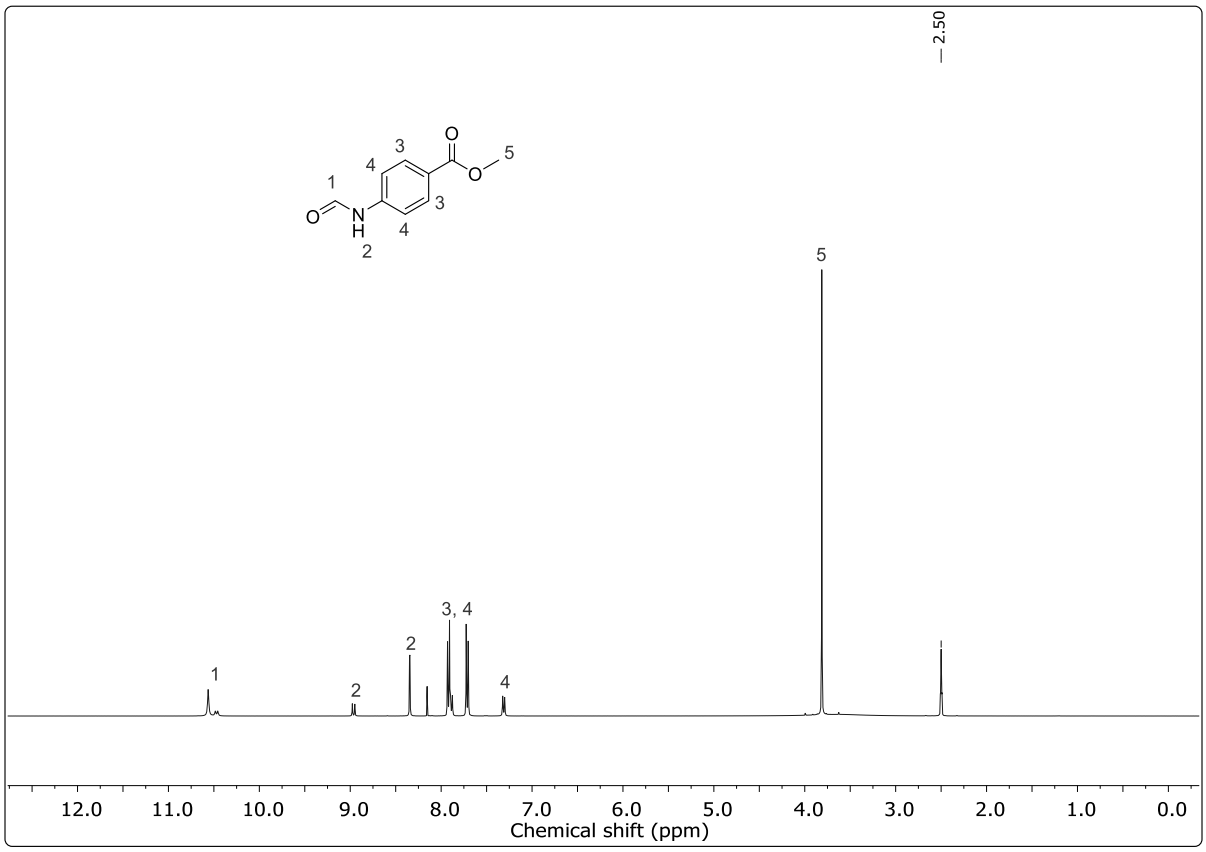

_N_-(6-hydroxyhexyl)formamide*

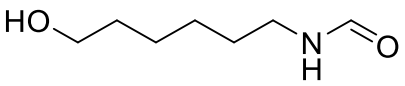

$C_7H_{15}NO_2$

M = 145.20 g/mol

6-Amino hexane-1-ol (5.00 g, 42.7 mmol, 1.00 eq.) and ethyl formate (34.4 mL, 34.6 g, 427 mmol, 10.0 eq.) were heated under reflux for 20 hours. Afterwards, remaining ethyl formate and ethanol were removed under reduced pressure, and the crude mixture was stored for two weeks at room temperature. The product crystalized from the solution and was obtained as white solid (1.70 g, 11.7 mmol) in a yield of 27% after filtration and washing with cyclohexane and ethyl acetate.

*This compound was synthesized R. Nickisch.

TLC: R_f (cyclohexane/ethyl acetate 1:1) = 0.16

^{1}H NMR (500 MHz, DMSO-d$_6$): δ (ppm) = 7.98 – 7.91 (m, 2H, N**H**, C**H**, ^{1}), 4.34 (t, *J* = 5.1 Hz, 2H, O**H**, ^{2}), 3.40 – 3.35 (m, 2H, C**H$_2$**, ^{3}), 3.07 (q, *J* = 6.5 Hz, 2H, C**H$_2$**, ^{4}), 1.43 – 1.37 (m, 4H, C**H$_2$**, ^{5}), 1.31 – 1.25 (m, 4H, C**H$_2$**, ^{6}).

^{13}C NMR (126 MHz, DMSO-d$_6$): δ (ppm) = 164.5, 160.9, 60.7, 40.8, 37.1, 32.5, 31.0, 29.1, 26.3, 25.8, 25.2.

HRMS (EI) *m/z*: [M - H]$^-$ calcd for $C_7H_{15}NO_2$, 144.1030; found, 144.1025.

IR (ATR): ṽ (cm^{-1}) = 3374, 3308, 3035, 2934, 2855, 1640, 1524, 1464, 1363, 1283, 1241, 1215, 1107, 1062, 1048, 1025, 1006, 975, 782, 739, 705, 638.

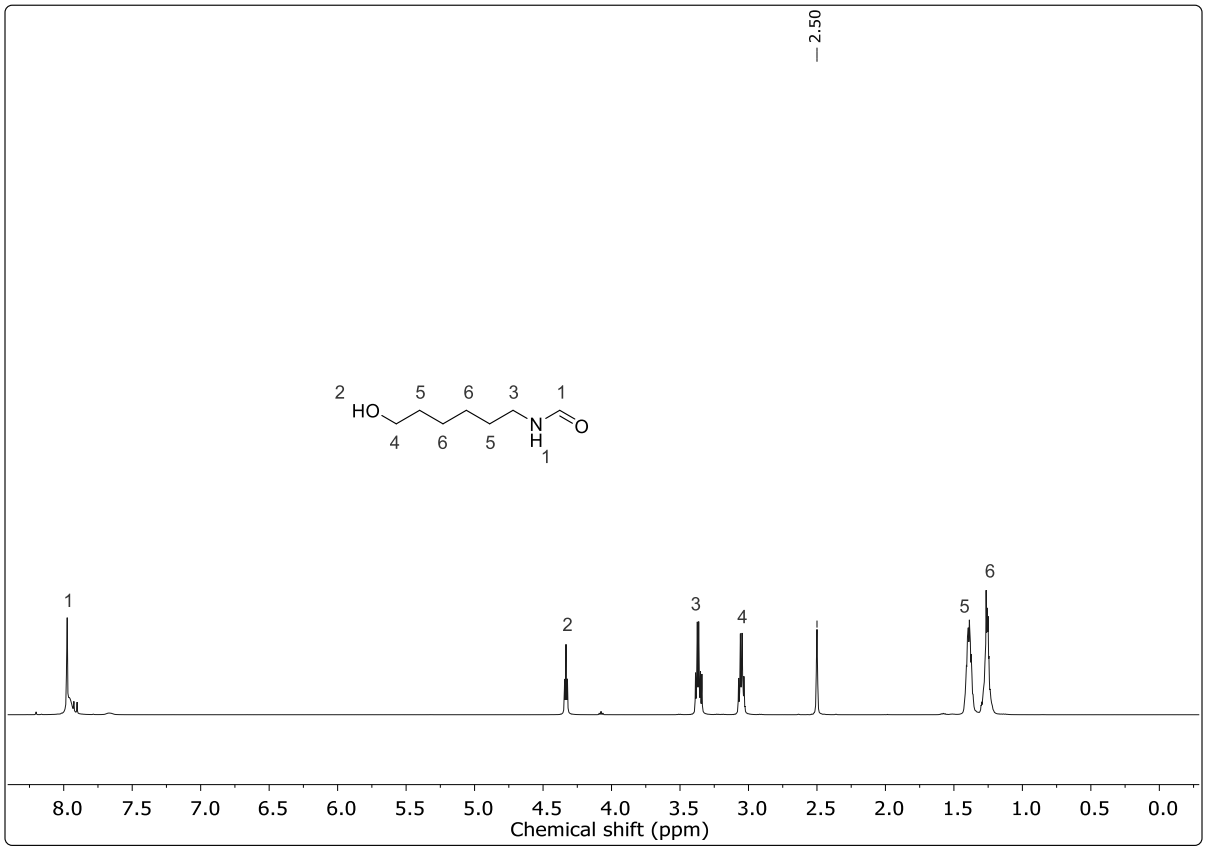

6.3.1.2 General isocyanide synthesis in DCM (5.00 mmol scale)

The formamide (5.00 mmol, 1.00 eq.) was dissolved in DCM (5 mL) and pyridine (15.0 mmol, 3.00 eq.) was added. Subsequently, *p*-TsCl (7.50 mmol, 1.50 eq.) was added under cooling with a water bath. The cooling was removed, and the reaction mixture was stirred until full conversion (monitored *via* TLC, average reaction time of 2 hours) was observed. Afterwards, aqueous Na_2CO_3-solution (5 mL, 20 wt%) was

added and the biphasic mixture was stirred for another 30 minutes. Water (10 mL) and DCM (10 mL) were added, and the organic phase was separated. The aqueous phase was extracted with DCM (3 × 5 mL), the organic extracts were combined and washed with water (3 × 5 mL) and saturated sodium chloride solution (2 × 5 mL). The organic extract was dried over sodium sulfate, filtered and the solvent was removed under reduced pressure. Further purification was not necessary in many cases. Nevertheless, purification by flash column chromatography (mixture of cyclohexane and ethyl acetate) can be applied to obtain the product in higher purity.

6.3.1.3 General isocyanide synthesis in DMC (5.00 mmol scale)

The formamide (5.00 mmol, 1.00 eq.) was dissolved in DMC (5 mL) and pyridine (15.0 mmol, 3.00 eq.) was added. Subsequently, *p*-TsCl (7.50 mmol, 1.50 eq.) was added under cooling with a water bath. The cooling was removed, and the reaction mixture was stirred until full conversion (monitored *via* TLC, average reaction time of 24 hours) was observed. Afterwards, aqueous Na_2CO_3-solution (5 mL, 20 wt%) was added and the biphasic mixture was stirred for another 30 minutes. Water (10 mL) and DMC (10 mL) were added, and the organic phase was separated. The aqueous phase was extracted with DMC (3 × 5 mL), the organic extracts were combined and washed with water (3 × 5 mL) and saturated sodium chloride solution (2 × 5 mL). The organic extract was dried over sodium sulfate, filtered and the solvent was removed under reduced pressure. Further purification was not necessary in many cases. Nevertheless, purification by flash column chromatography (mixture of cyclohexane and ethyl acetate) can be applied to obtain the product in higher purity).

Note: For the commercially available isocyanides no full analytic analysis was carried out.

6.3.1.4 Synthesized isocyanides

1-isocyanooctadecane*

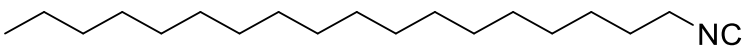

$C_{19}H_{37}N$

M = 279.52 g/mol

*This compound was synthesized by R. Seim under the author's supervision.

Was obtained as rose solid in a yield of 96% (DCM) or 89% (DMC).

TLC: R_f (cyclohexane/ethyl acetate 15:1) = 0.47

^{1}H NMR (500 MHz, $CDCl_3$): δ (ppm) = 3.31 (tt, J = 6.8, 1.8 Hz, 2H, C**H$_2$**, ^{1}), 1.61 (m, 2H, C**H$_2$**, ^{2}), 1.36 (m, 2H, C**H$_2$**, ^{3}), 1.23 – 1.19 (m, 28H, C**H$_2$**, ^{4}), 0.81 (t, J = 7.0 Hz, 3H, C**H$_3$**, ^{5}).

^{13}C NMR (126 MHz, $CDCl_3$): δ (ppm) = 155.72, 155.67, 155.62, 41.75, 41.70, 41.65 32.07, 29.84, 29.82, 29.80, 29.79, 29.74, 29.65, 29.51, 29.26, 28.85, 26.47, 22.84, 14.26.

HRMS (EI) *m/z*: [M] calcd for $C_{19}H_{37}N$, 279.2926; found, 279.2926.

IR (ATR): ṽ (cm^{-1}) = 2913, 2849, 2152, 1471, 718.

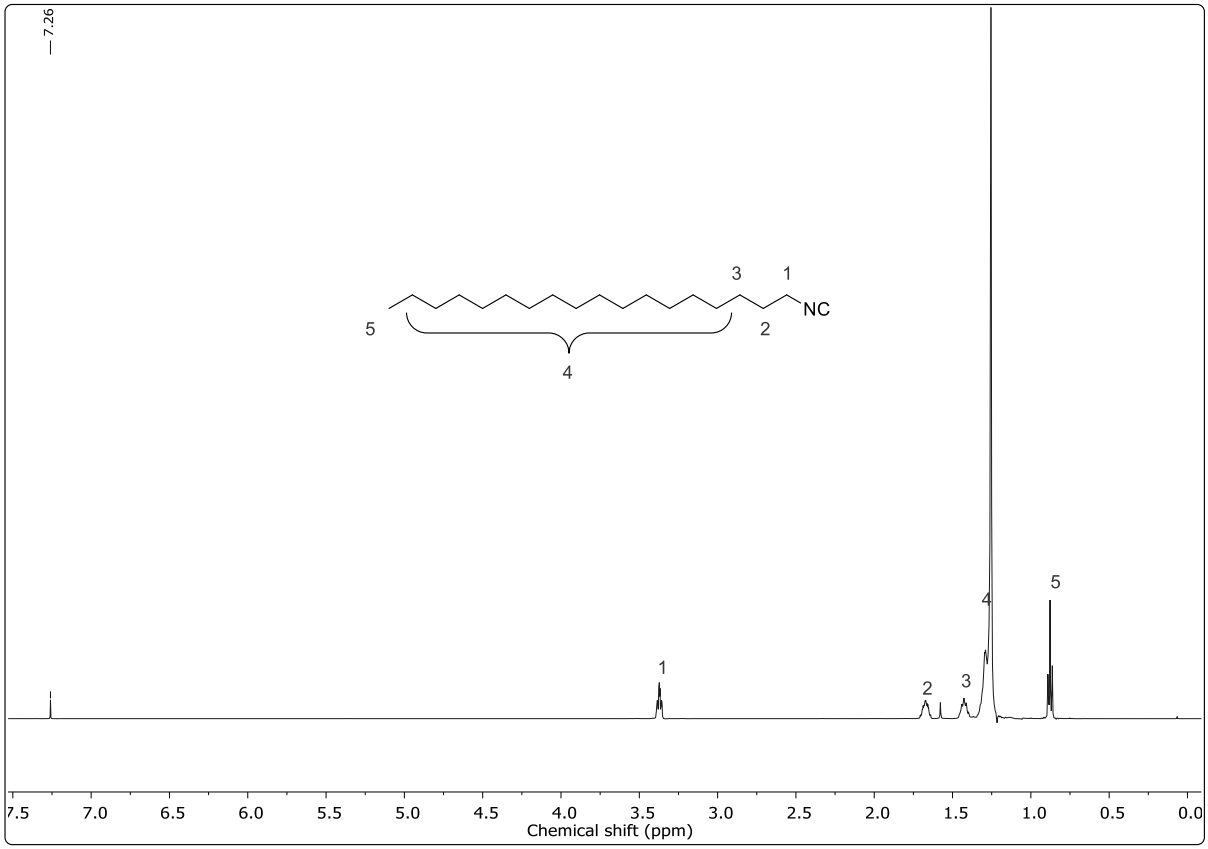

1-isocyanododecane*

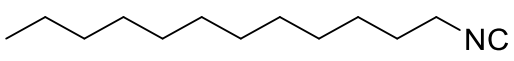

$C_{13}H_{25}N$

M = 195.35 g/mol

*This compound was synthesized by R. Seim under the author's supervision.

Was obtained as yellow liquid in a yield of 90% (DCM) and 94% (DMC).

TLC: R_f (cyclohexane/ethyl acetate 15:1) = 0.58

^{1}H NMR (500 MHz, $CDCl_3$): δ (ppm) = 3.37 (tt, J = 6.8, 1.9 Hz, 2H, C**H$_2$**, ^{1}), 1.70 – 1.62 (m, 2H, C**H$_2$**, ^{2}), 1.42 (p, J = 7.3 Hz, 2H, C**H$_2$**, ^{3}), 1.30 – 1.26 (m, 16H, C**H$_2$**, ^{4}), 0.87 (t, J = 7.0 Hz, 3H, C**H$_3$**, ^{5}).

^{13}C NMR (126 MHz, $CDCl_3$): δ (ppm) = 155.67, 41.72, 41.67, 41.61, 32.01, 29.71, 29.61, 29.48, 29.44, 29.22, 28.81, 26.43, 22.79, 14.21.

HRMS (EI) *m/z*: $[M - H]^-$ calcd for $C_{13}H_{25}N$, 194.1914; found, 194.1909.

IR (ATR): ṽ (cm^{-1}) = 2923, 2853, 2145, 1458.

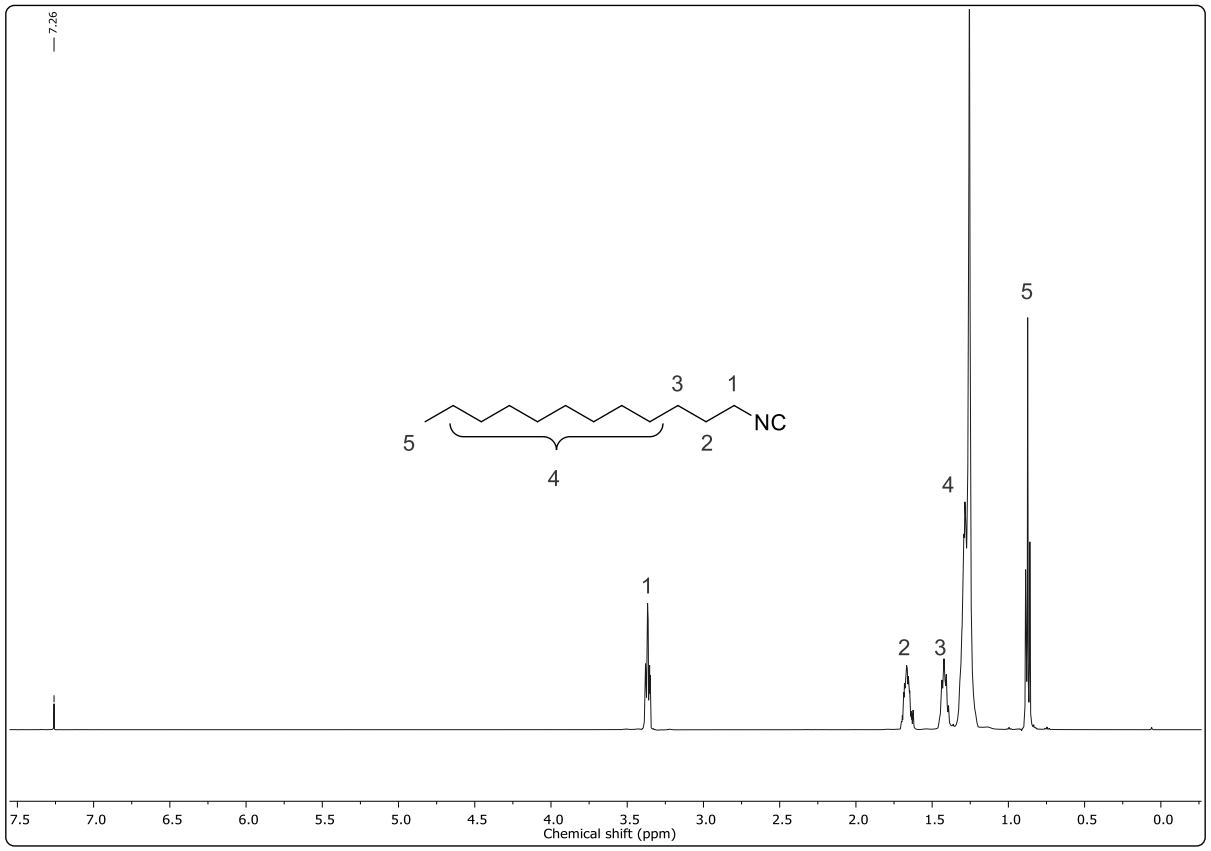

(*Z*)-1-isocyanooctadec-9-ene (Oleylisocyanide)*

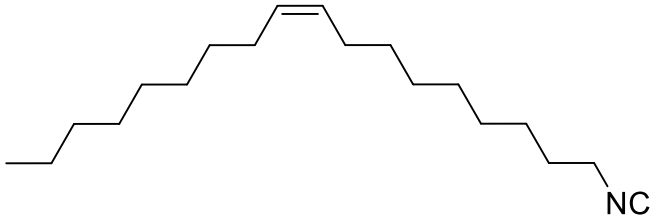

$C_{19}H_{35}N$

M = 277.50 g/mol

*This compound was synthesized by R. Seim under the author's supervision.

Was obtained as yellowish oil in a yield of 97% (DCM) and 98% (DMC).

TLC: R_f (cyclohexane/ethyl acetate 9:1) = 0.70

^{1}H NMR-spectrum is in accordance with the literature.[364]

^{1}H NMR (500 MHz, $CDCl_3$): δ (ppm) = 5.40 – 5.31 (m, 2H, C**H**, ^{1,2}), 3.37 (tt, *J* = 6.7, 1.9 Hz, 2H, C**H$_2$**, ^{3}), 2.06 – 1.94 (m, 4H, CHC**H$_2$**, ^{4}), 1.71 – 1.64 (m, 2H, C**H$_2$**, ^{5}), 1.47 – 1.40 (m, 2H, C**H$_2$**, ^{6}), 1.38 – 1.21 (m, 20H, C**H$_2$**, ^{7}), 0.88 (t, *J* = 6.9 Hz, C**H$_3$**, ^{8}).

^{13}C NMR (126 MHz, $CDCl_3$): δ (ppm) = 155.76, 155.71, 155.67, 130.17, 129.83, 41.74, 41.69, 41.64, 32.04, 29.90, 29.81, 29.73, 29.66, 29.50, 29.46, 29.40, 29.27, 29.24, 28.84, 28.82, 27.35, 27.28, 26.45, 25.76, 22.82, 22.80, 22.71, 22.69, 22.48, 14.25, 14.21.

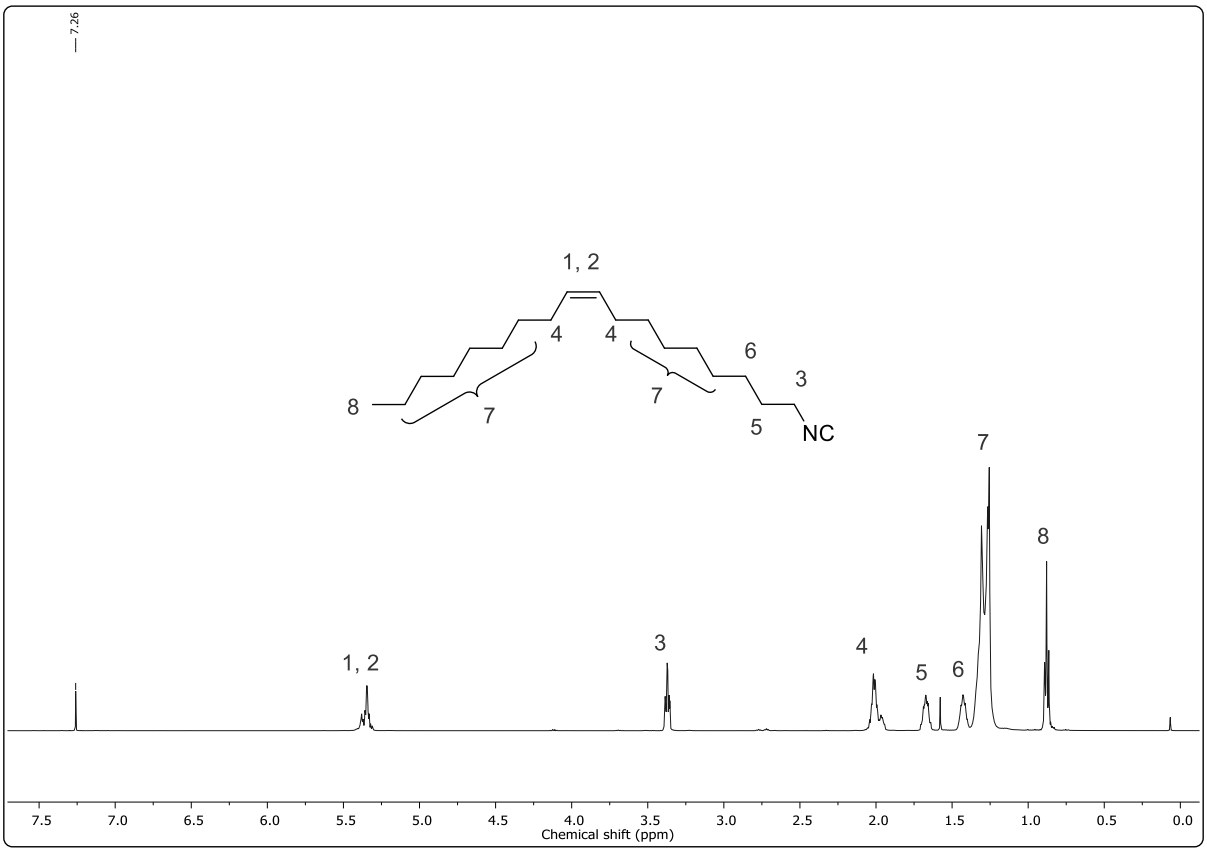

Benzyl 11-isocyanoundecanoate

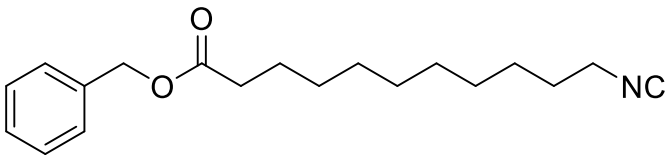

$C_{19}H_{27}NO_2$

M = 301.43 g/mol

Was obtained as yellowish liquid in a yield of 97% (DCM) and 87% (DMC).

TLC: R_f (cyclohexane/ethyl acetate 5:1) = 0.45

^{1}H NMR (500 MHz, $CDCl_3$): δ (ppm) = 7.37 – 7.30 (m, 5H, C**H**$_{\textbf{aromatic}}$, ^{1}), 5.11 (s, 2H, C**H**$_2$, ^{2}), 3.35 (tt, *J* = 6.8, 1.9 Hz, 2H, C**H**$_2$, ^{3}), 2.35 (t, *J* = 7.5 Hz, 2H, C**H**$_2$, ^{4}), 1.69 – 1.61 (m, 4H, C**H**$_2$, ^{5}), 1.41 (p, *J* = 7.3 Hz, 2H, C**H**$_2$, ^{6}), 1.33 – 1.28 (m, 10H, C**H**$_2$, ^{7}).

^{13}C NMR (126 MHz, $CDCl_3$): δ (ppm) = 173.57, 155.68, 155.63, 136.13, 128.51, 128.13, 66.01, 41.57, 41.52, 41.47, 34.27, 29.25, 29.14, 29.07, 29.04, 28.64, 26.27, 24.90.

HRMS (FAB) *m/z*: $[M + H]^+$ calcd for $C_{19}H_{27}NO_2$, 302.2115; found, 302.2113.

IR (ATR): ṽ (cm^{-1}) = 3032, 2924, 2853, 2146, 1733, 1497, 1454, 1380, 1350, 1212, 1161, 1101, 1001, 736, 697, 579, 501.

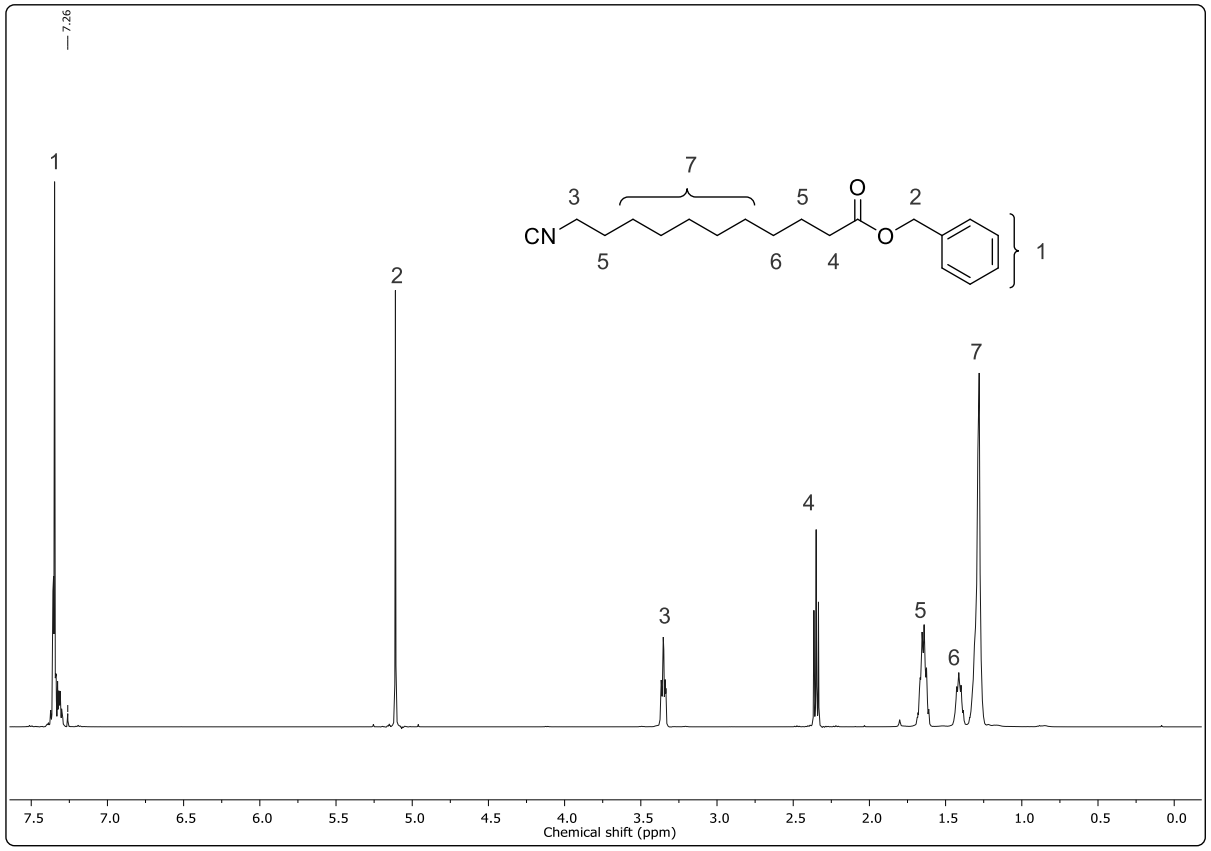

6-isocyanohexyl 4-methylbenzenesulfonate*

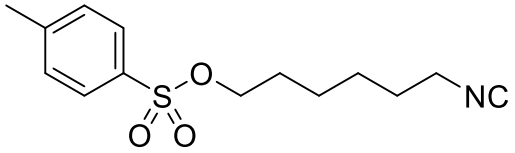

$C_{14}H_{19}NO_3S$

M = 281.37 g/mol

*This compound was synthesized by R. Seim under the author's supervision.

Was obtained as brown oil a yield of 53% (DCM) and 68% (DMC).

TLC: R_f (cyclohexane/ethyl acetate 2:1) = 0.69

^{1}H NMR (500 MHz, $CDCl_3$): δ (ppm) = 7.79 (d, *J* = 8.4 Hz, 2H, C**H**$_{\textbf{aromatic}}$, ^{1}), 7.35 (d, *J* = 8.0 Hz, 2H, C**H**$_{\textbf{aromatic}}$, ^{2}), 4.03 (t, *J* = 6.3 Hz, 2H, C**H**$_2$, ^{3}), 3.35 (tt, *J* = 6.6, 1.9 Hz, 2H, C**H**$_2$, ^{4}), 2.45 (s, 3H, C**H**$_3$, ^{5}), 1.69 – 1.61 (m, 4H, C**H**$_2$, ^{6}), 1.44 – 1.33 (m, 4H, C**H**$_2$, ^{7}).

^{13}C NMR (126 MHz, $CDCl_3$): δ (ppm) = ^{13}C NMR (126 MHz, $CDCl_3$) δ 156.08, 144.93, 133.22, 130.00, 128.01, 70.35, 41.56, 41.51, 41.46, 28.96, 28.76, 25.85, 24.76, 21.79.

HRMS (EI) *m/z*: [M] calcd for $C_{14}H_{19}NO_3S$, 281.1086; found, 281.1086.

IR (ATR): ṽ (cm^{-1}) = 2938, 2863, 2148, 1598, 1454, 1353, 1307, 1188, 1173, 1097, 1019, 957, 918, 814, 749, 725, 688, 662, 575, 553.

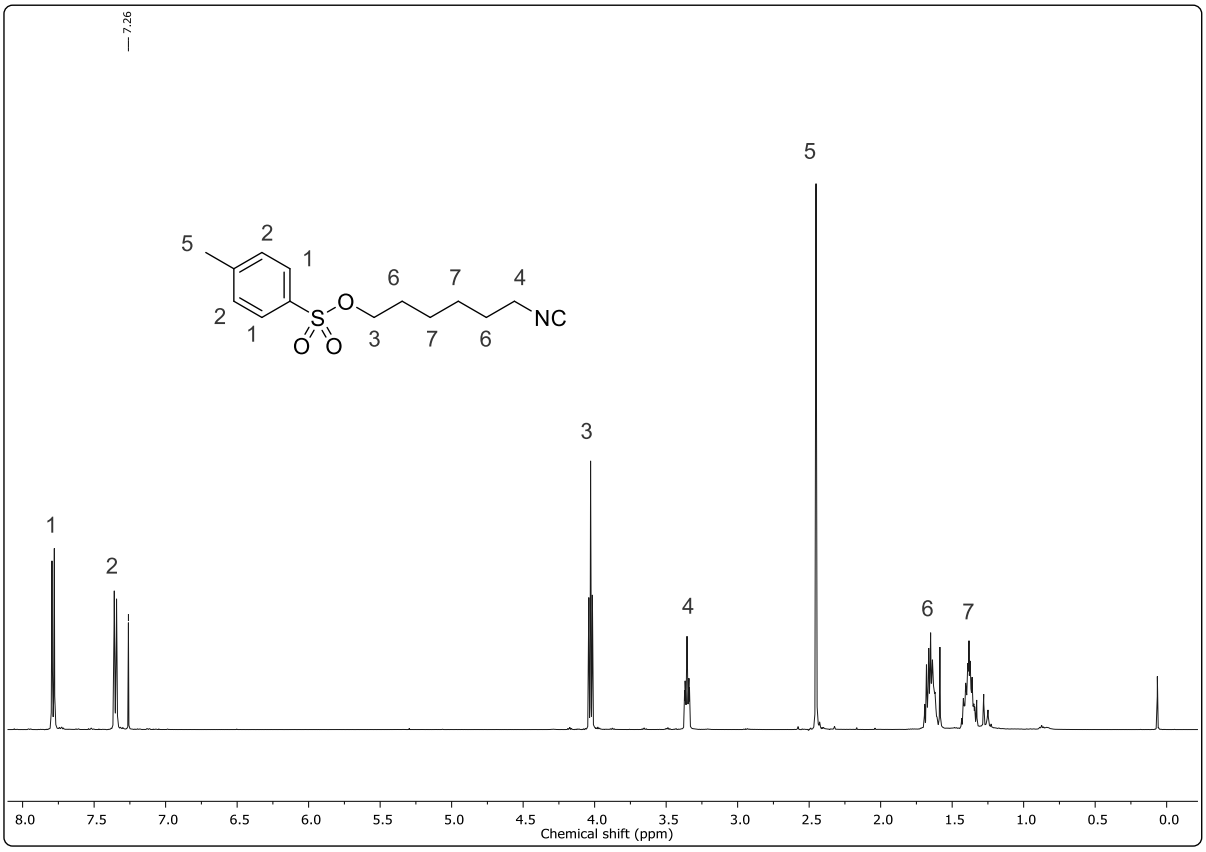

1,5-diisocyanopentane (Cadaverindiisocyanide)*

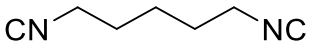

$C_7H_{10}N_2$

M = 122.17 g/mol

*This compound was synthesized by R. Seim under the author's supervision.

Was obtained as brownish liquid in a yield of 48% (DCM) and 82% (DMC).

TLC: R_f (cyclohexane/ethyl acetate 2:1) = 0.48

^{1}H NMR (500 MHz, $CDCl_3$): δ (ppm) = 3.37 (tt, *J* = 6.5, 2.0 Hz, 4H, C**H₂**, ^{1}), 1.71 – 1.64 (m, 4H, C**H₂**, ^{2}), 1.58 – 1.52 (m, 2H, C**H₂**, ^{3}).

^{13}C NMR (126 MHz, $CDCl_3$): δ (ppm) = 156.30, 41.35, 41.30, 41.24, 28.21, 23.28.

HRMS (EI) *m/z*: $[M - H]^-$ calcd for $C_7H_{10}N_2$, 121.0771; found, 121.0766.

IR (ATR): $\tilde{\nu}$ (cm^{-1}) = 2923, 2853, 2145, 1465, 1352, 722.

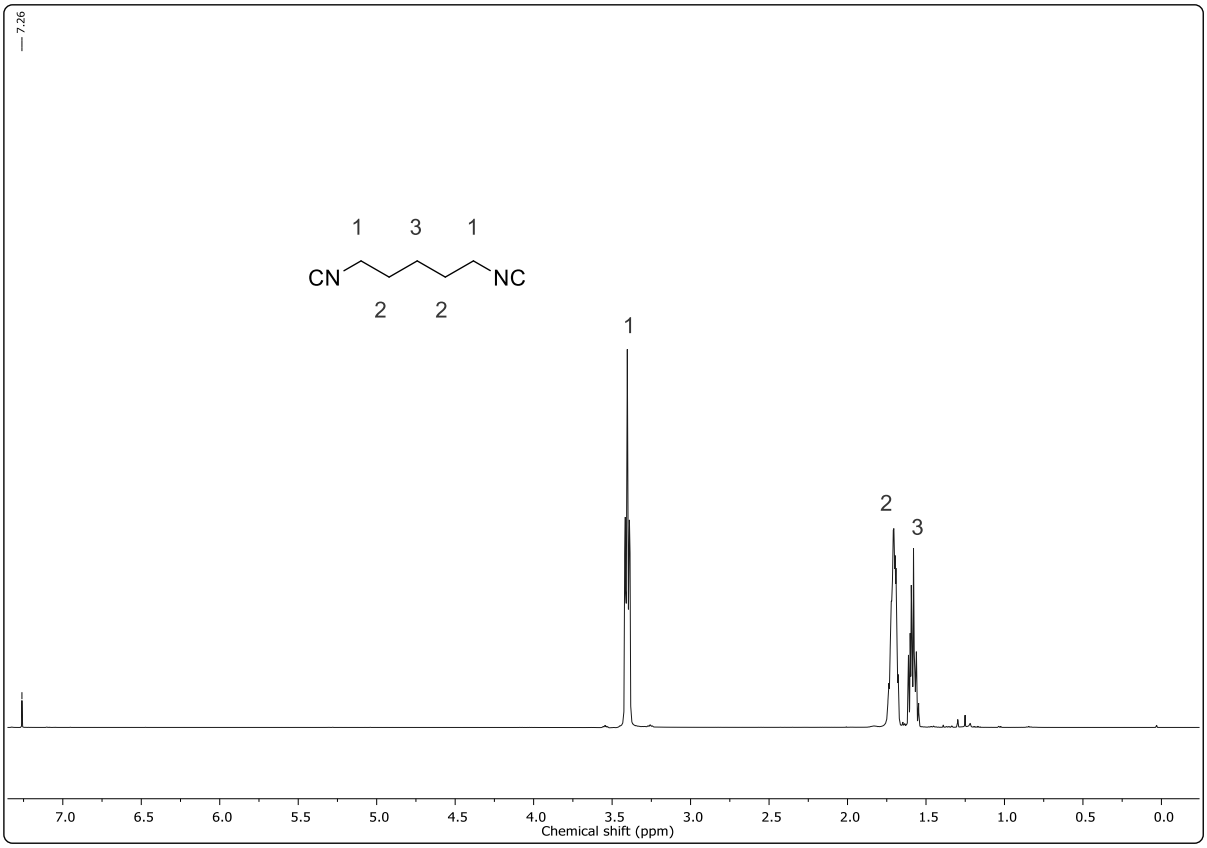

1,10-diisocyanodecane*

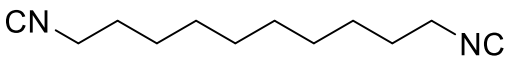

$C_{12}H_{20}N_2$

M = 192.31 g/mol

*This compound was synthesized by R. Seim under the author's supervision.

Was otained as yellow liquid in a yield of 93% (DCM) and 89% (DMC).

TLC: R_f (cyclohexane/ethyl acetate 4:1) = 0.44

^{1}H NMR (500 MHz, $CDCl_3$): δ (ppm) = 3.37 (tt, *J* = 6.8, 1.8 Hz, 4H, C**H$_2$**, ^{1}), 1.69 – 1.62 (m, 4H, C**H$_2$**, ^{2}), 1.42 (m, *J* = 7.1 Hz, 4H, C**H$_2$**, ^{3}), 1.31 – 1.29 (m, 8H, C**H$_2$**, ^{4}).

^{13}C NMR (126 MHz, $CDCl_3$): δ (ppm) = 155.80, 41.65, 41.60, 41.54, 29.23, 29.09, 28.65, 26.30.

HRMS (EI) *m/z*: $[M - H]^-$ calcd for $C_{12}H_{20}N_2$, 191.1554; found, 191.1547.

IR (ATR): $\tilde{\nu}$ (cm^{-1}) = 2927, 2857, 2145, 1454, 1351.

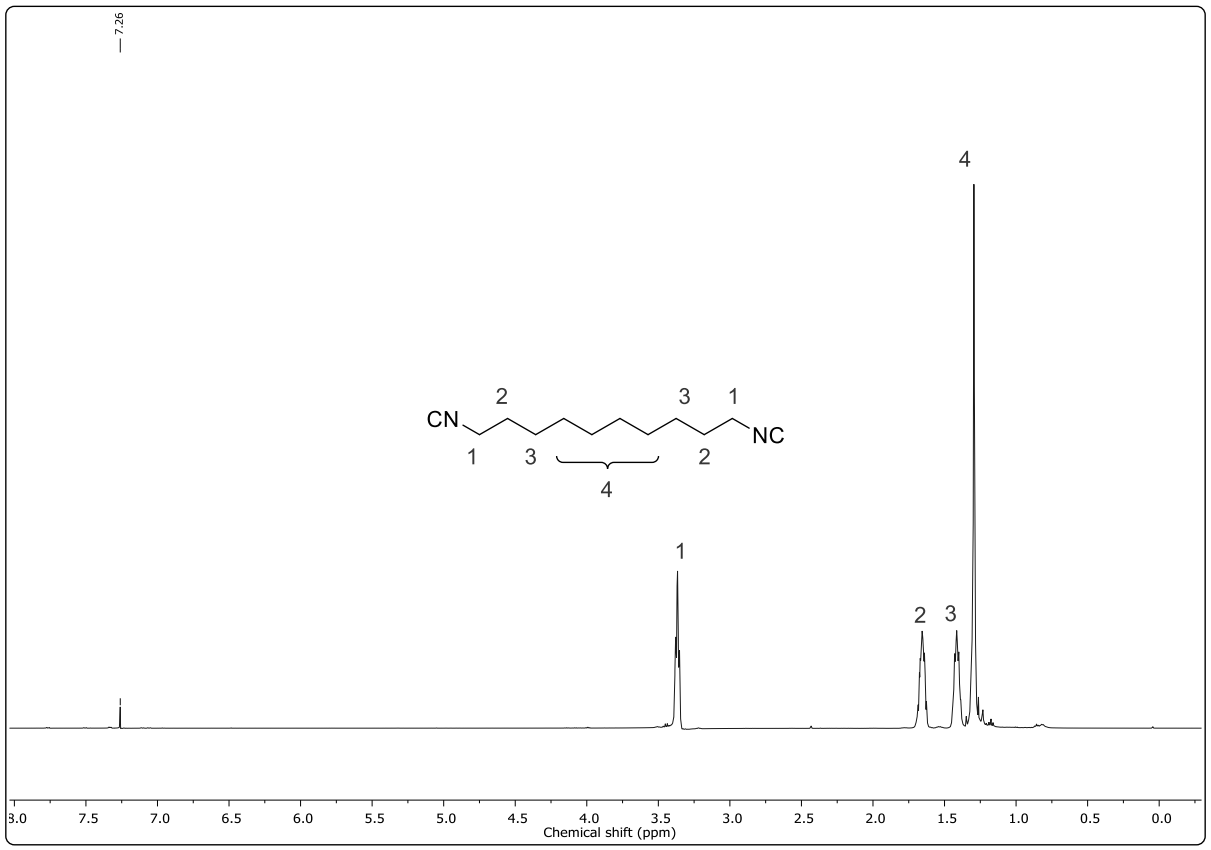

1,12-diisocyanododecane*

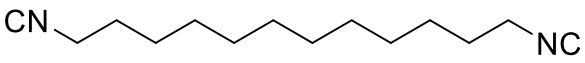

$C_{14}H_{24}N_2$

M = 220.36 g/mol

*This compound was synthesized by R. Seim under the author's supervision.

Was obtained as yellow liquid in a yield of 87% (DCM) and 97% (DMC).

TLC: R_f (cyclohexane/ethyl acetate 9:1) = 0.44

^{1}H NMR (500 MHz, $CDCl_3$): δ (ppm) = 3.36 (tt, *J* = 6.8, 1.9 Hz, 4H, C**H$_2$**, ^{1}), 1.68 – 1.62 (m, 4H, C**H$_2$**, ^{2}), 1.41 (p, *J* = 7.1 Hz, 4H, C**H$_2$**, ^{3}), 1.31– 1.23 (m, 12H, C**H$_2$**, ^{4}).

^{13}C NMR (126 MHz, $CDCl_3$): δ (ppm) = 155.63, 41.64, 41.59, 41.53, 29.40, 29.32, 29.09, 28.68, 26.30.

HRMS (EI) *m/z*: $[M - H]^-$ calcd for $C_{14}H_{24}N_2$, 219.1867; found, 219.1863.

IR (ATR): $\tilde{\nu}$ (cm^{-1}) = 2925, 2855, 2145, 1456.

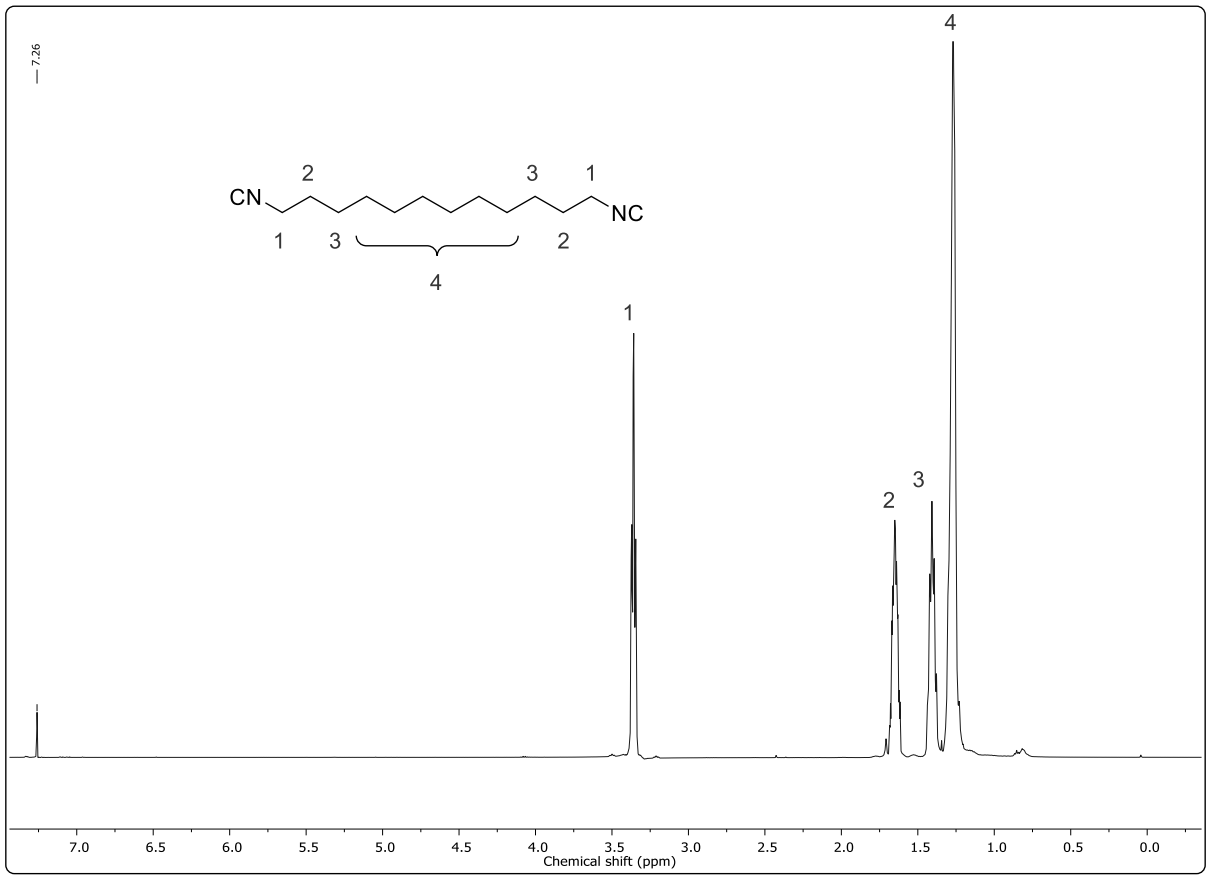

Cyclohexylisocyanide*

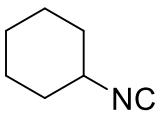

$C_7H_{11}N$

109.17 g/mol

*This compound was synthesized by R. Seim under the author's supervision.

Was obtained as yellowish liquid in a yield of 67% (DCM) and 68% (DMC).

TLC: R_f (cyclohexane/ethyl acetate 9:1) = 0.57

^{1}H NMR-spectrum was in accordance with the literature.[365]

^{1}H NMR (500 MHz, $CDCl_3$): δ (ppm) = 3.57 – 3.50 (m, 1H, C**H**, ^{1}), 1.86 – 1.77 (m, 2H, C**H**, ^{2}), 1.77– 1.57 (m, 4H, C**H**, ^{3}), 1.46– 1.27 (m, 4H, C**H₂**, ^{4}).

^{13}C NMR (126 MHz, $CDCl_3$): δ (ppm) = ^{13}C NMR (126 MHz, $CDCl_3$) δ 171.16, 60.42, 51.76, 51.72, 51.68, 32.70, 25.02, 22.81.

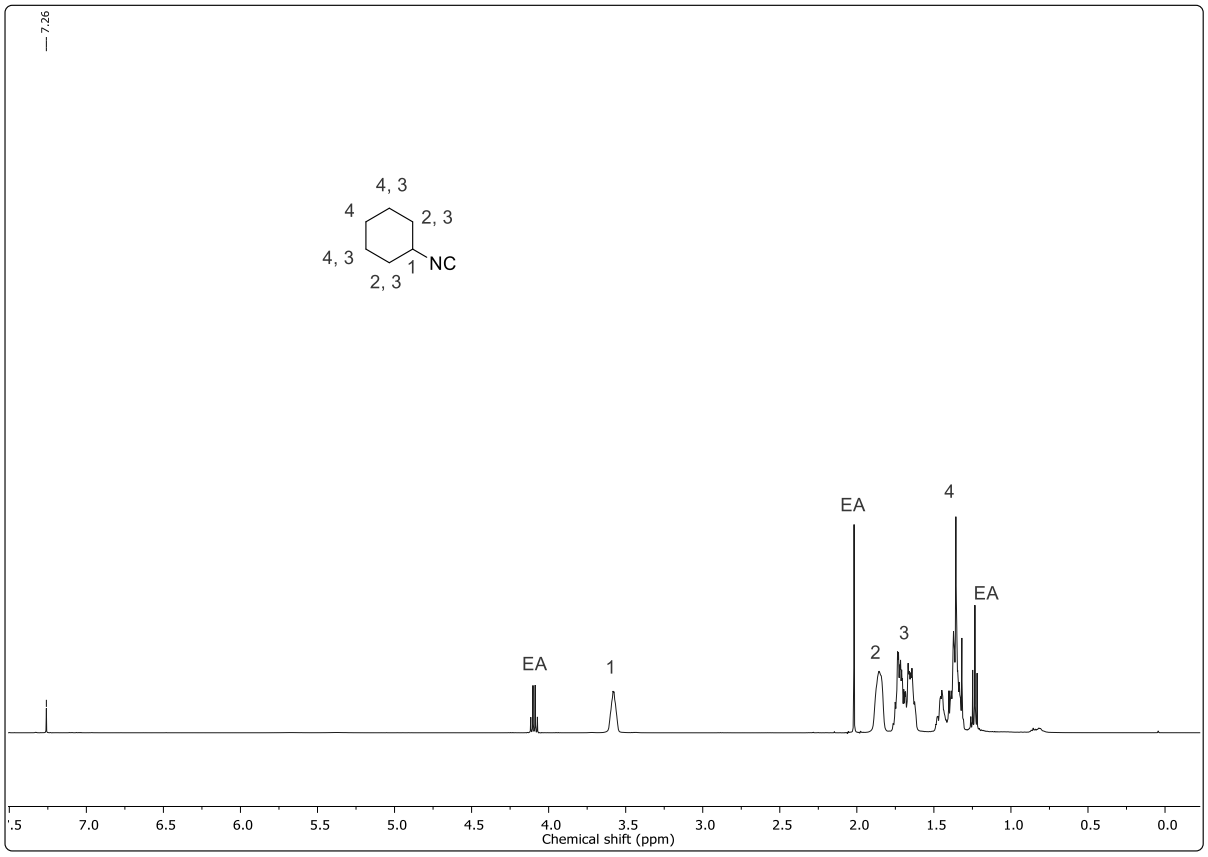

Benzylisocyanide*

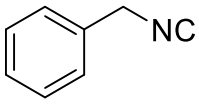

C_7H_7N

117.15 g/mol

*This compound was synthesized by R. Seim under the author's supervision.

Was obtained as yellowish liquid in a yield of 44% (DCM) and 62% (DMC).

TLC: R_f (cyclohexane/ethyl acetate 9:1) = 0.63

^{1}H NMR-spectrum is in accordance with the literature.[75]

^{1}H NMR (500 MHz, $CDCl_3$): δ (ppm) = 7.43 – 7.26 (m, 5H, C**H**$_{\textbf{aromatic}}$, ^{1}), 4.64 (m, 2H, C**H**$_{\textbf{2}}$, ^{2}).

^{13}C NMR (126 MHz, $CDCl_3$): δ (ppm) = 157.69, 132.38, 129.01, 128.45, 126.64, 45.62, 45.56, 45.51.

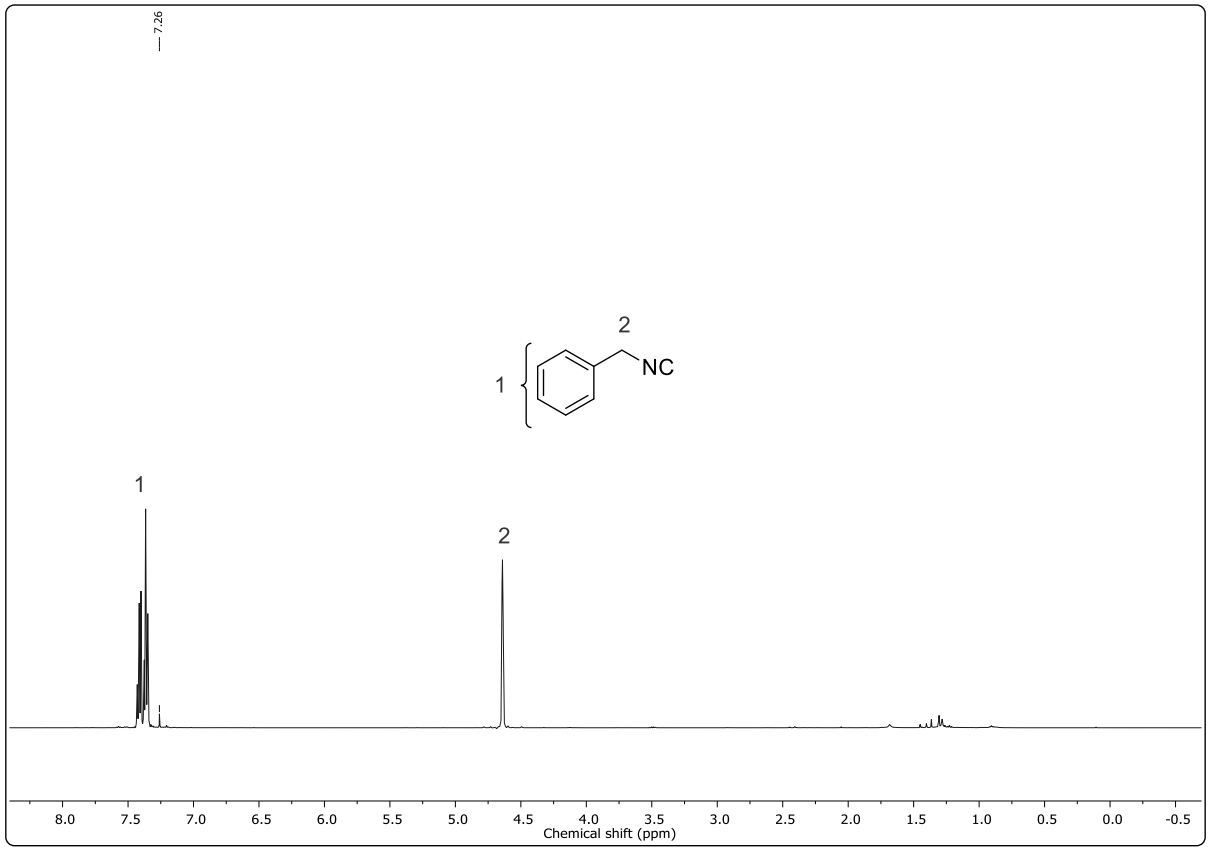

Adamantylisocyanide*

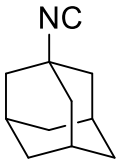

$C_{11}H_{15}N$

M = 161.25 g/mol

*This compound was synthesized by R. Seim under the author's supervision.

Was obtained as white solid in a yield of 79% (DCM) and 78% (DMC).

TLC: R_f (cyclohexane/ethyl acetate 4:1) = 0.83

^{1}H NMR spectrum is in accordance with the literature.[364]

^{1}H NMR (500 MHz, $CDCl_3$): δ (ppm) = 2.11 – 2.07 (m, 3H, C**H**, ^{1}), 2.04 – 2.01 (m, 6H, C**H₂**, ^{2}), 1.71 – 1.62 (m, 6H, C**H₂**, ^{3}).

^{13}C NMR (126 MHz, $CDCl_3$): δ (ppm) = 151.69, 151.65, 151.61, 54.37, 54.33, 54.28, 43.65, 35.59, 28.81.

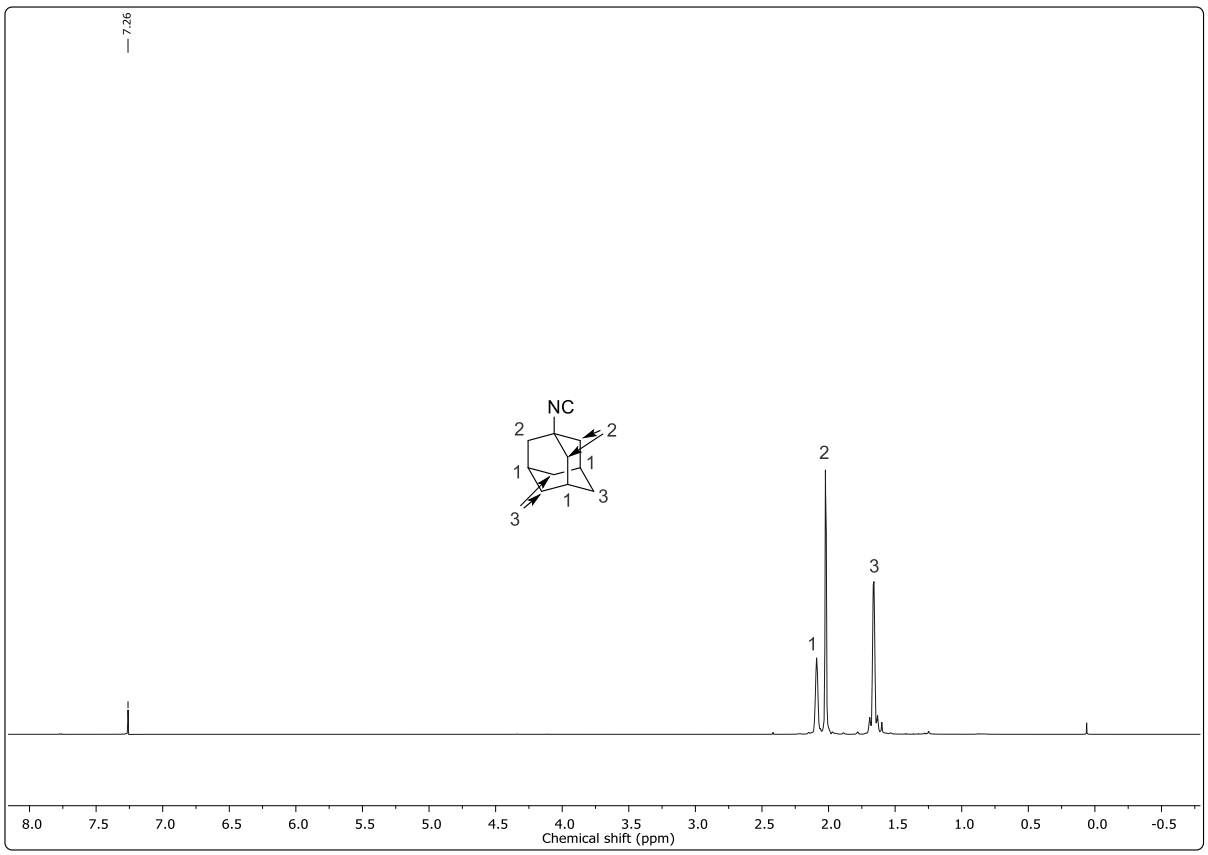

Methyl 4-isocyanobenzoate*

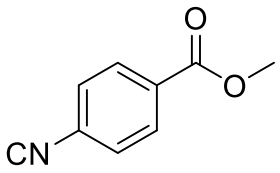

$C_{11}H_{15}N$

M = 161.25 g/mol

Methyl-4-formamidobenzoate (1.00 g, 5.58 mmol, 1.00 eq.) was dissolved in DCM (5.58 mL) and pyridine (1.53 mL, 1.50 g, 19.0 mmol, 3.40 eq.) was added. Subsequently, *p*-TsCl (1.81 g, 9.49 mmol, 1.70 eq.) was added under cooling with a water bath. The cooling was removed, and the reaction mixture was stirred for 165 min. Afterwards, aqueous, saturated Na_2CO_3-solution (24 mL) was added, and the biphasic mixture was stirred for another 30 minutes. Water (10 mL) and DCM (10 mL) were added, and the organic phase was separated. The aqueous phase was extracted with DCM (3 × 5 mL). The organic layers were dried over sodium sulfate, filtered and the

solvent was removed under reduced pressure. The product was obtained as black solid (120 mg, 740 µmol) after purification by column chromatography (cyclohexane/ethyl acetate 3:1) in a yield of 13%.

*This compound was synthesized by N. Seul, who conducted her “Vertieferarbeit” under the co-supervision of R. Nickisch.

TLC: R_f (cyclohexane/ethyl acetate 3:1) = 0.30

^{1}H NMR (400 MHz, DMSO-d_6): δ (ppm) = 8.02 (d, J = 8.5 Hz, 2H, C**H**$_{\text{aromatic}}$, ^{1}), 7.69 (d, J = 8.5 Hz, 2H, C**H**$_{\text{aromatic}}$, ^{2}), 3.86 (s, 3H, C**H**$_3$, ^{3}).

^{13}C NMR (101 MHz, DMSO-d_6): δ (ppm) = 166.6, 164.9, 130.6, 130.5, 129.2, 126.9.

HRMS (EI) *m/z*: [M] calcd for $C_9H_7NO_2$, 161.0477; found, 161.0475.

IR (ATR): ṽ (cm^{-1}) = 3088, 2953, 2128, 1716, 1605, 1504, 1428, 1272, 1169, 1103, 1018, 955, 865, 833, 760, 686, 637, 572, 513, 448.

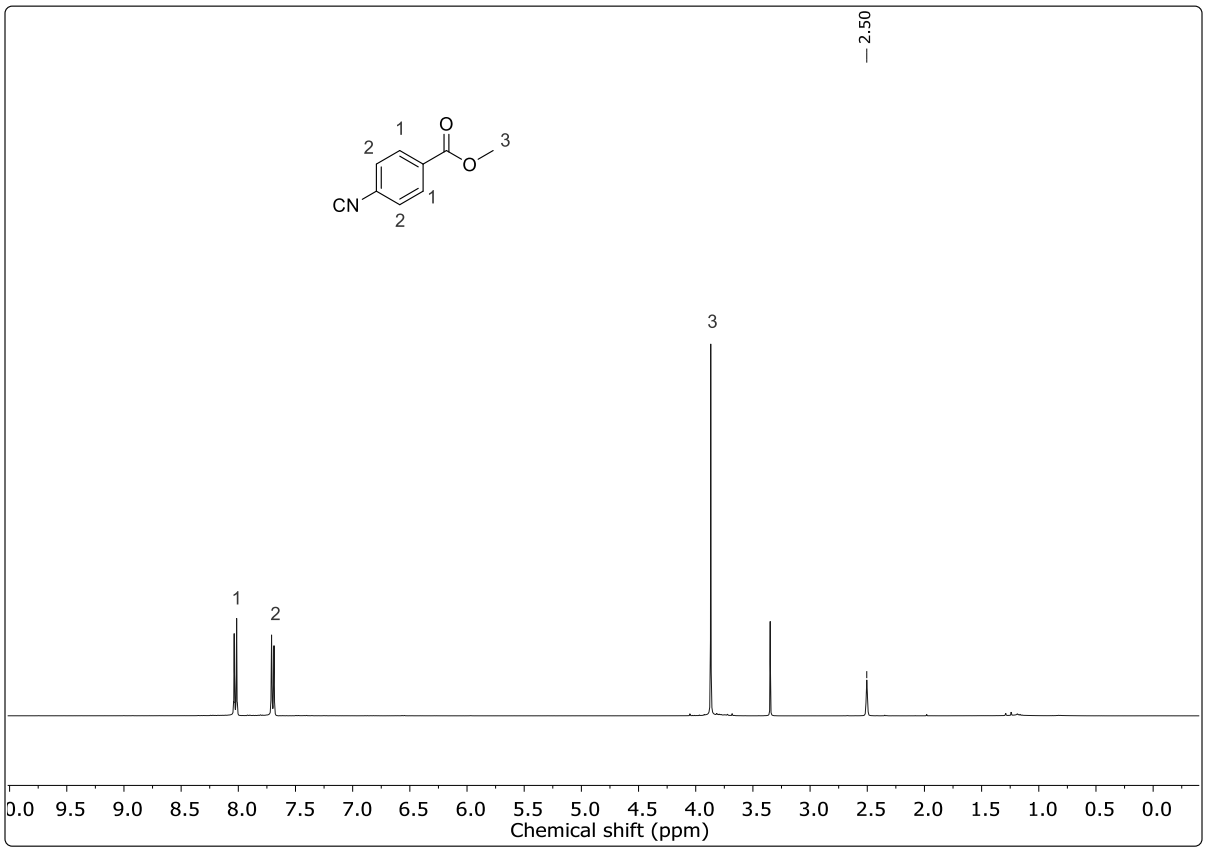

Polymer – Purified IC and Polymer – Crude IC*

Polymer 1 – synthesized with purified isocyanide

Decanedioic acid (405 mg, 2.00 mmol, 1.00 eq.), heptanal (1.69 mL, 1.37 g, 12.0 mmol, 6.00 eq.) and 1,12-diisocyanododecane (441 mg, 2.00 mmol, 1.00 eq.) were stirred under argon atmosphere at room temperature for 24 hours. The obtained solid was dissolved in DCM (3 mL) and was then precipitated into diethylether (75 mL). Polymer (886 mg, M_n = 10517 Da) was obtained after filtration and removal of remaining solvent under reduced pressure as a brownish highly viscous oil in a yield of 67% (in correspondence to the theoretical, maximal mass of the polymer).

Polymer 2 – synthesized with crude isocyanide

Decanedioic acid (405 mg, 2.00 mmol, 1.00 eq.), heptanal (1.69 mL, 1.37 g, 12.0 mmol, 6.00 eq.) and 1,12-diisocyanododecane (441 mg, 2.00 mmol, 1.00 eq.) were stirred under argon atmosphere at room temperature for 24 h. The obtained solid was dissolved in DCM (3 mL) and was then precipitated with diethylether (75 mL). Polymer (833 mg, M_n = 8350 Da) was obtained after filtration and removal of remaining solvent under reduced pressure as a brownish highly viscous oil in a yield of 63% (in correspondence to the theoretical, maximal mass of the polymer).

*These compounds were synthesized by R. Seim under the author's supervision.

^{1}H NMR (500 MHz, $CDCl_3$): δ (ppm) = 6.06 (s, 2H, N**H**, ^{1}), 5.17 – 5.13 (m, 2H, C**H**, ^{2}), 3.27 – 3.21 (m, 4H, C**H$_2$**, ^{3}), 2.38 (t, J = 7.5 Hz, 4H, C**H$_2$**, ^{4}), 1.88 – 1.75(m, 4H, C**H$_2$**, ^{5}), 1.68 – 1.59 (m, 4H, C**H$_2$**, ^{6}), 1.52-1.44 (m, 4H, **CH$_2$**, ^{7}), 1.35-1.24 (m, 40H, **CH$_2$**, ^{8}), 0.86 (t, J = 7.0 Hz, C**H$_3$**, ^{9}).

^{13}C NMR (126 MHz, $CDCl_3$): δ (ppm) = 172.6, 170.0, 74.1, 39.4, 34.4, 32.1, 31.8, 29.7, 29.2, 29.0, 27.0, 25.0, 24.8, 22.7, 14.2.

IR (ATR): $\tilde{\nu}$ (cm^{-1}) = 3291, 2923, 2854, 1741, 1653, 1538, 1464, 1376, 1237, 1162, 1096, 723.

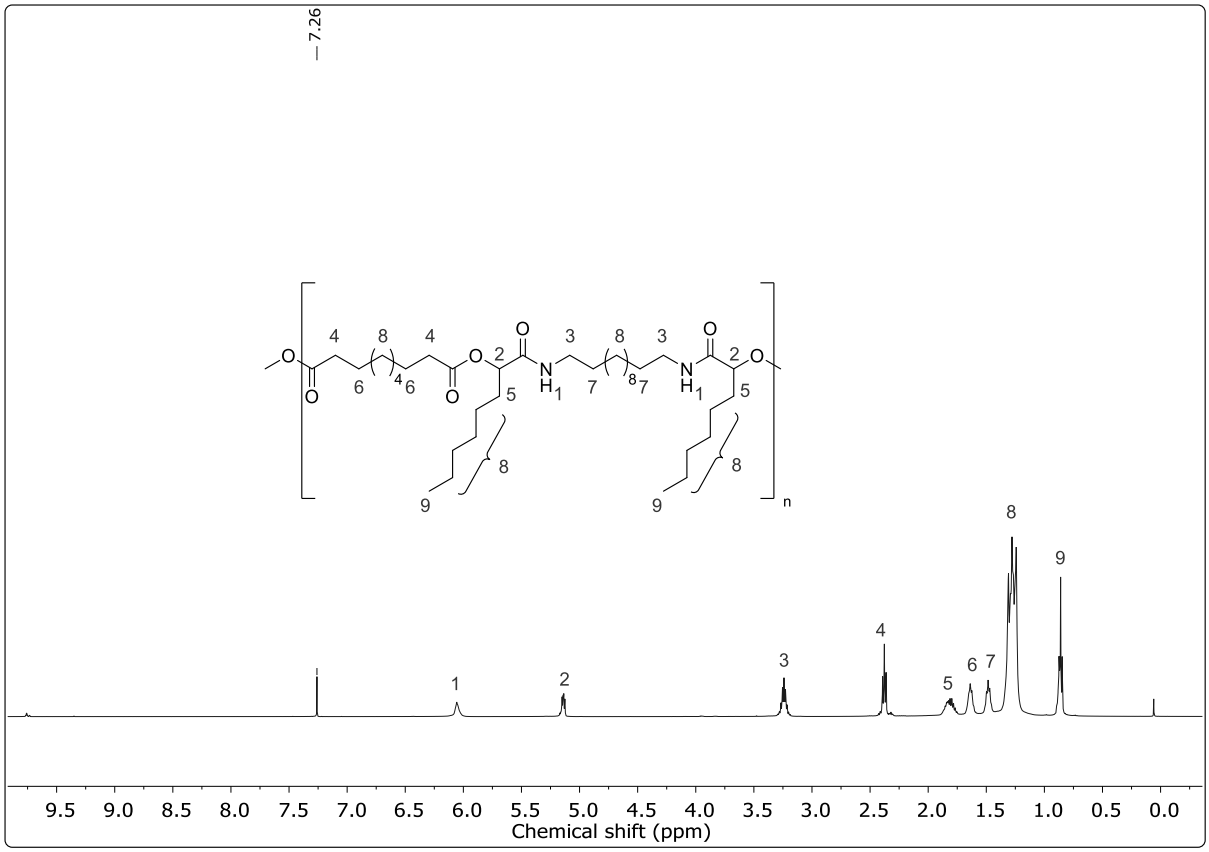

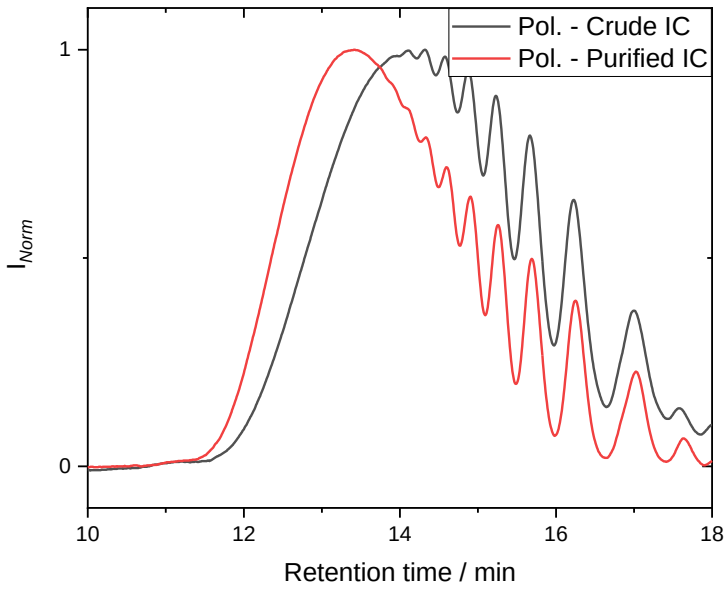

Figure S 2: Molecular weight distribution of the two obtained polymers measured in THF. Red line: obtained polymer using the purified isocyanide. Black line: obtained polymer using the *crude* isocyanide. Reprinted with permission from [103].

6.3.2 Thiocarbamates – Chapter 4.2

6.3.2.1 General synthesis of thiocarbamates/bis-thiocarbamates

N-formamide (1.00 eq.) was suspended in DCM (1.00 mol/L), then pyridine (3.00 eq.) and *p*-TsCl (1.50 eq) were added. The reaction mixture was stirred for 2 h at room temperature. Then, sulfoxide (1.50 eq.) was added and the reaction was allowed to stir for another two hours. Afterwards the crude reaction solution is directly subjected to column chromatography.

Di-*N*-formamide (1.00 eq.) was suspended in DCM (1.00 mol/L), then pyridine (6.00 eq.) and *p*-TsCl (3.00 eq) were added. The reaction mixture was stirred for 2 h at room temperature. Then, sulfoxide (3.00 eq.) in DCM (3.00 mol/L) was added *via* a dropping funnel over 5 minutes and the reaction was allowed to stir overnight. Afterwards the crude reaction solution is directly subjected to column chromatography.

6.3.2.2 Synthesized thiocarbamates

_S_-methyl dodecyl thiocarbamate

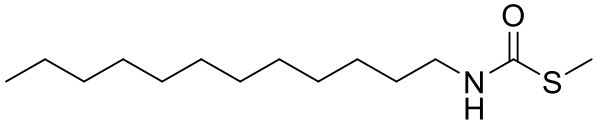

$C_{14}H_{29}NOS$

M = 259.45 g/mol

Was obtained as beige solid in a yield of 77%.

TLC: R_f (cyclohexane/ethyl acetate 9:1) = 0.41

^{1}H NMR (500 MHz, $CDCl_3$): δ (ppm) = 5.32 (bs, 1H, N**H**, ^{1}), 3.35 – 3.20 (m, 2H, C**H$_2$**, ^{2}), 2.34 (s, 3H, SC**H$_3$**, ^{3}), 1.55 – 1.47 (m, 2H, C**H$_2$**, ^{4}), 1.34 – 1.22 (m, 18H, C**H$_2$**, ^{5}), 0.88 (t, *J* = 6.96 Hz, 3H, C**H$_3$**, ^{6}).

^{13}C NMR (126 MHz, $CDCl_3$): δ (ppm) = 167.63, 41.67, 32.05, 29.87, 29.77, 29.76, 29.70, 29.64, 29.48, 29.37, 26.90, 22.83, 14.26, 12.48.

HRMS (EI) *m/z*: [M] calcd for $C_{14}H_{29}NOS$, 259.1970; found, 259.1966.

IR (ATR): ṽ (cm^{-1}) = 3331, 2953, 2918, 2849, 1644, 1508, 1466, 1377, 1315, 1289, 1264, 1233, 1209, 1197, 965, 891, 850, 722, 569, 503, 469, 429.

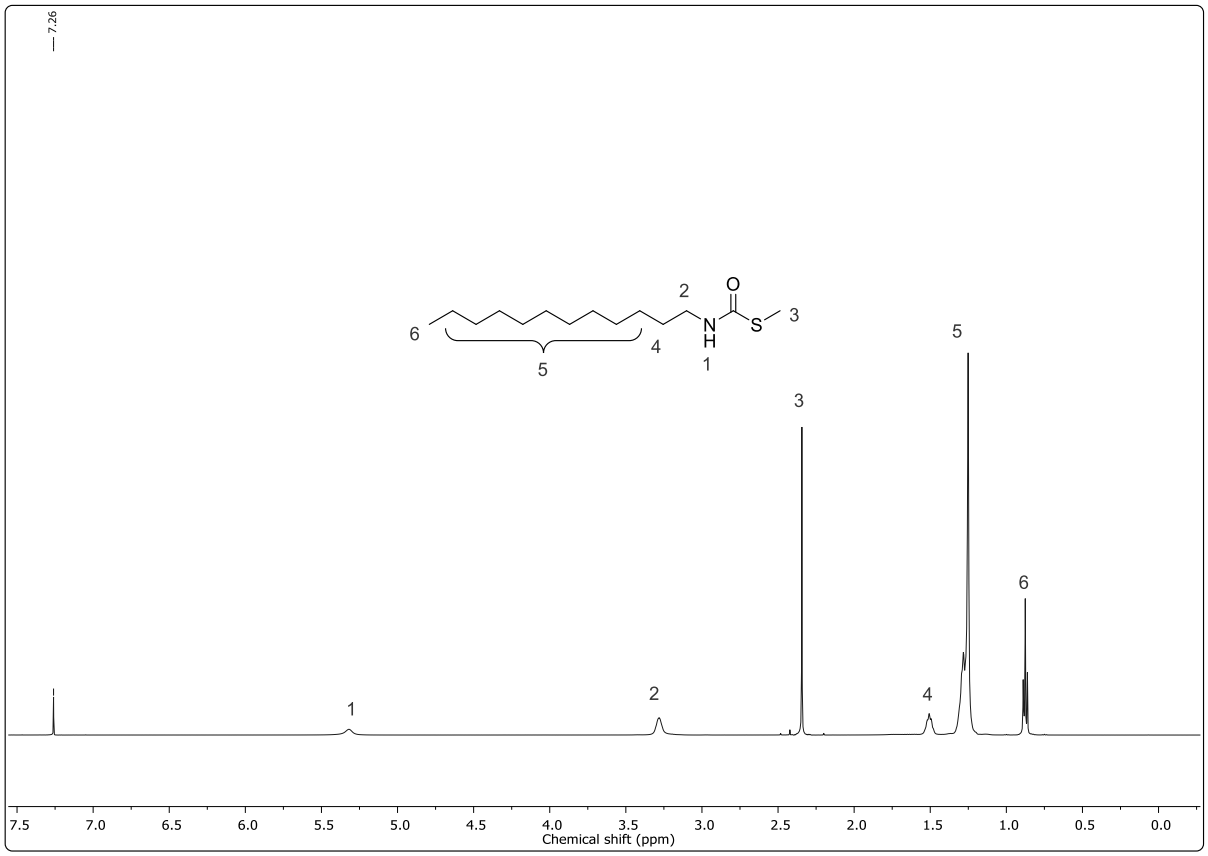

_S_-butyl dodecyl thiocarbamate

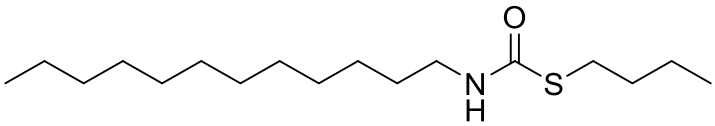

$C_{17}H_{35}NOS$

M = 301.53 g/mol

Was obtained as beige solid in a yield of 85%.

TLC: R_f (cyclohexane/ethyl acetate 9:1) = 0.69

^{1}H NMR (500 MHz, $CDCl_3$): δ (ppm) = 5.27 (bs, 1H, N**H**, ^{1}), 3.32 – 3.22 (m, 2H, C**H₂**, ^{2}), 2.90 (t, *J* = 7.34 Hz, 2H, SC**H₂**, ^{3}), 1.59 (p, *J* = 7.44 Hz, 2H, C**H₂**, ^{4}), 1.54 – 1.47 (m, 2H, C**H₂**, ^{5}), 1.47 – 1.36 (m, 2H, C**H₂**, ^{6}), 1.33 – 1.21 (m, 18H, C**H₂**, ^{7}), 0.91 (t, *J* = 7.36 Hz, 3H, C**H₃**, ^{8}), 0.88 (t, *J* = 6.97 Hz, 3H, C**H₃**, ^{9}).

^{13}C NMR (126 MHz, $CDCl_3$): δ (ppm) = 167.37, 41.55, 32.72, 32.05, 29.88, 29.83, 29.78, 29.76, 29.71, 29.65, 29.48, 29.37, 26.92, 22.83, 22.04, 14.26, 13.76.

HRMS (EI) *m/z*: [M] calcd for $C_{17}H_{35}NOS$, 301.2439; found, 301.2431.

IR (ATR): ṽ (cm^{-1}) = 3333, 2955, 2918, 2849, 1635, 1505, 1469, 1453, 1431, 1375, 1293, 1264, 1235, 1206, 1195, 916, 891, 851, 787, 760, 733, 721, 572, 509, 472, 431, 415.

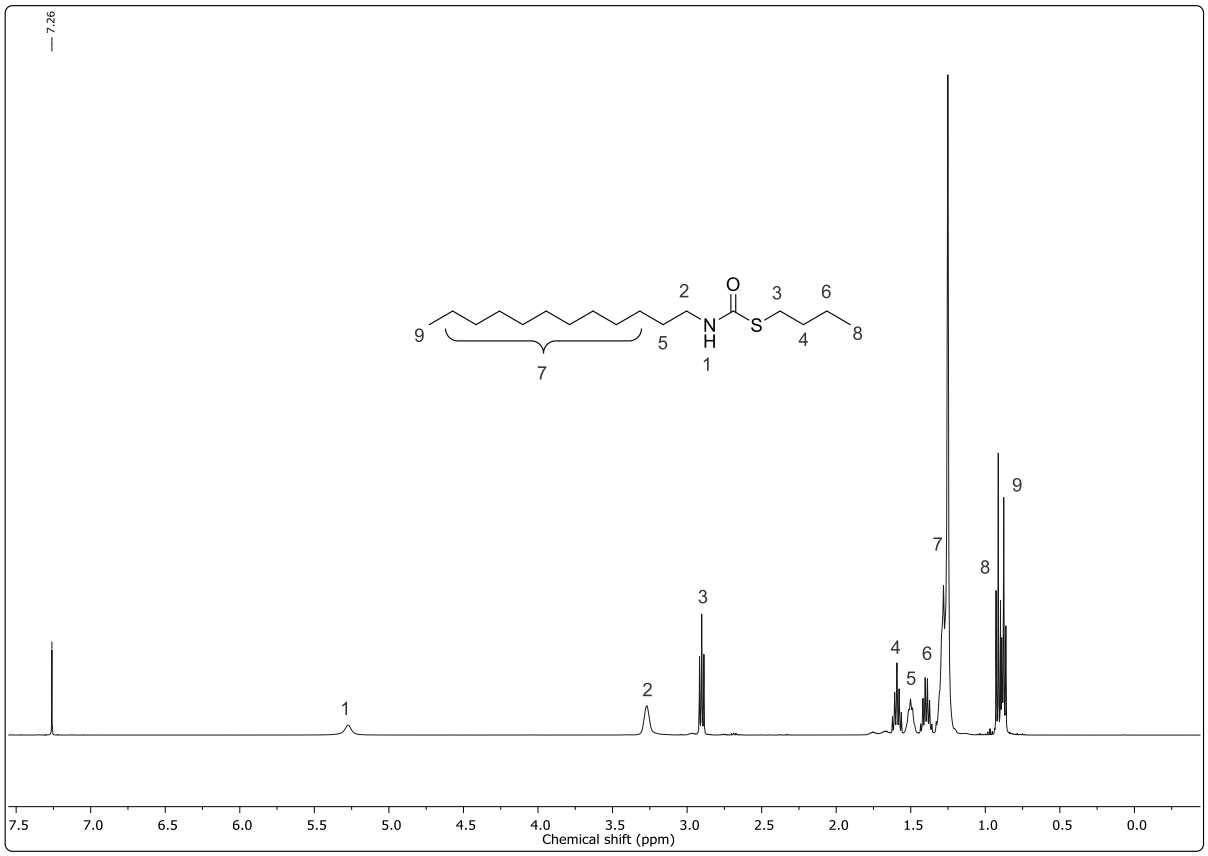

***S*-4-chlorobutyl dodecyl thiocarbamate**

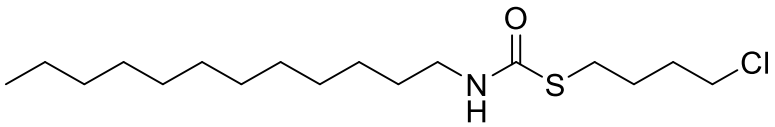

$C_{17}H_{34}ClNOS$

M = 335.98 g/mol

Was obtained as white solid in a yield of 80%.

TLC: R_f (cyclohexane/ethyl acetate 9:1) = 0.58

^{1}H NMR (500 MHz, $CDCl_3$): δ (ppm) = 5.28 (bs, 1H, N**H**, ^{1}), 3.55 (t, *J* = 6.50 Hz, 2H, ClC**H**$_2$, ^{2}), 3.31 – 3.24 (m, 2H, C**H**$_2$, ^{3}), 2.93 (t, *J* = 7.06, 2H, SC**H**$_2$, ^{4}), 1.90 – 1.84 (m, 2H, ClCH$_2$C**H**$_2$, ^{5}), 1.80 – 1.74 (m, 2H, SCH$_2$C**H**$_2$, ^{6}), 1.54 – 1.47 (m, 2H, C**H**$_2$, ^{7}), 1.34 – 1.21 (m, 18H, C**H**$_2$, ^{8}), 0.88 (t, *J* = 6.96 Hz, 3H, C**H**$_3$, ^{9}).

^{13}C NMR (126 MHz, $CDCl_3$): δ (ppm) = 166.91, 44.58, 41.63, 32.05, 31.54, 29.85, 29.77, 29.76, 29.70, 29.65, 29.48, 29.36, 29.27, 27.99, 26.91, 22.83, 14.26.

HRMS (EI) *m/z*: [M] calcd for $C_{17}H_{34}ClNOS$, 335.2050; found, 335.2044.

IR (ATR): ṽ (cm^{-1}) = 3325, 2957, 2918, 2848, 1638, 1508, 1467, 1455, 1425, 1379, 1322, 1292, 1264, 1234, 1213, 1196, 1019, 888, 850, 735, 723, 581, 510, 471, 405.

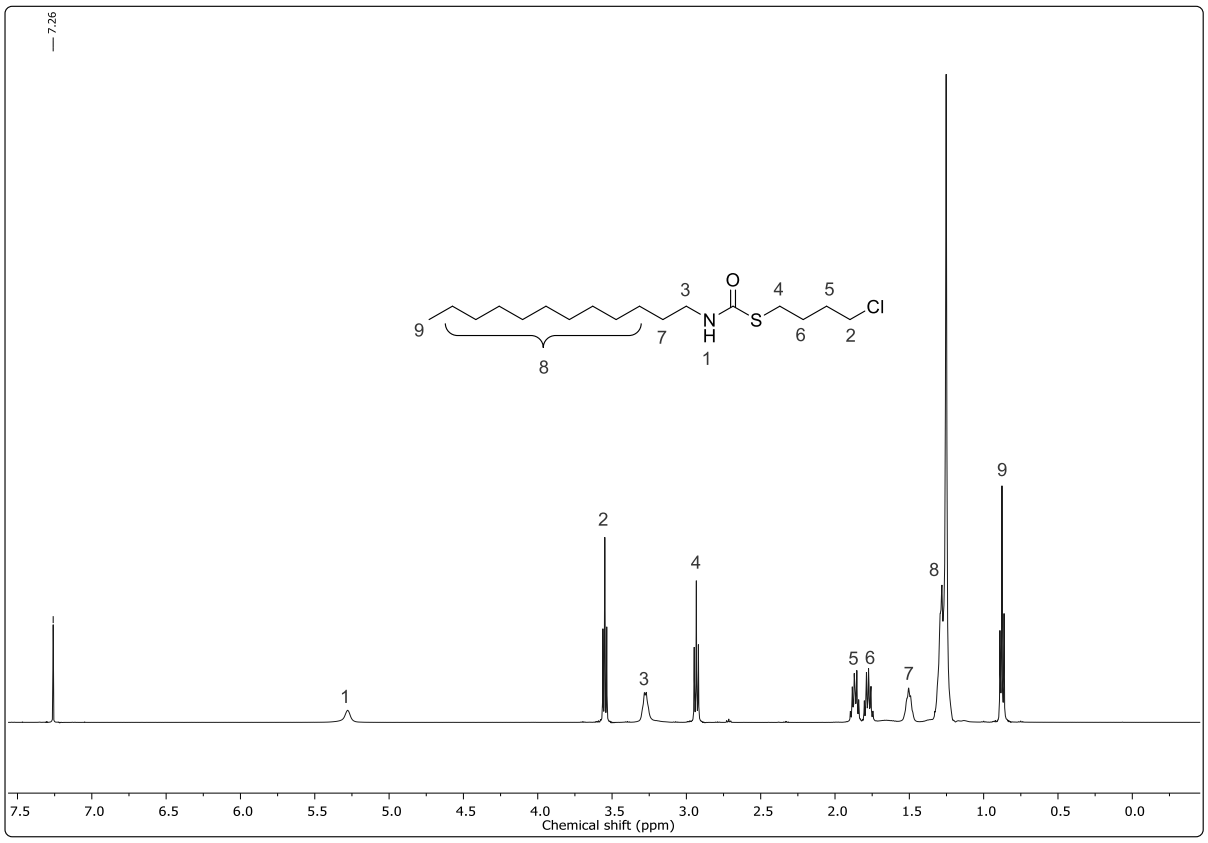

_S_-benzyl dodecyl thiocarbamate

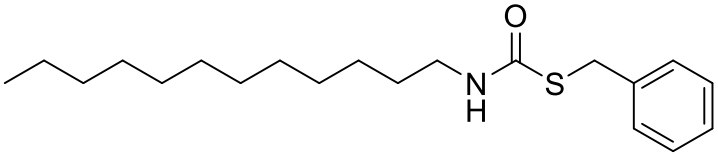

$C_{20}H_{33}NOS$

M = 335.55 g/mol

Was obtained as beige solid in a yield of 53%.

TLC: R_f (cyclohexane/ethyl acetate 9:1) = 0.49

^{1}H NMR (500 MHz, $CDCl_3$): δ (ppm) = 7.35 – 7.21 (m, 5H, C**H**$_{\text{Aromatic}}$, ^{1}), 5.27 (bs, 1H, N**H**, ^{2}), 4.16 (s, 1H, SC**H$_2$**, ^{3}), 3.36 – 3.29 (m, 2H, C**H$_2$**, ^{4}), 1.55 – 1.45 (m, 2H, C**H$_2$**, ^{5}), 1.34 – 1.22 (m, 18H, C**H$_2$**, ^{6}), 0.88 (t, *J* = 6.73 Hz, 3H, C**H$_3$**, ^{7}).

^{13}C NMR (126 MHz, $CDCl_3$): δ (ppm) = 166.64, 128.95, 128.70, 127.29, 41.73, 34.34, 32.06, 29.84, 29.78, 29.76, 29.70, 29.65, 29.49, 29.36, 26.90, 22.83, 14.27.

HRMS (FAB) *m/z*: $[M + H]^+$ calcd for $C_{20}H_{33}NOS$, 336.2356; found, 336.2357.

IR (ATR): ṽ (cm^{-1}) = 3276, 3027, 2956, 2919, 2871, 2845, 1659, 1632, 1523, 1494, 1476, 1454, 1409, 1379, 1289, 1263, 1232, 1214, 1199, 1073, 1028, 919, 889, 845, 764, 721, 699, 611, 561, 522, 505, 486, 462, 431.

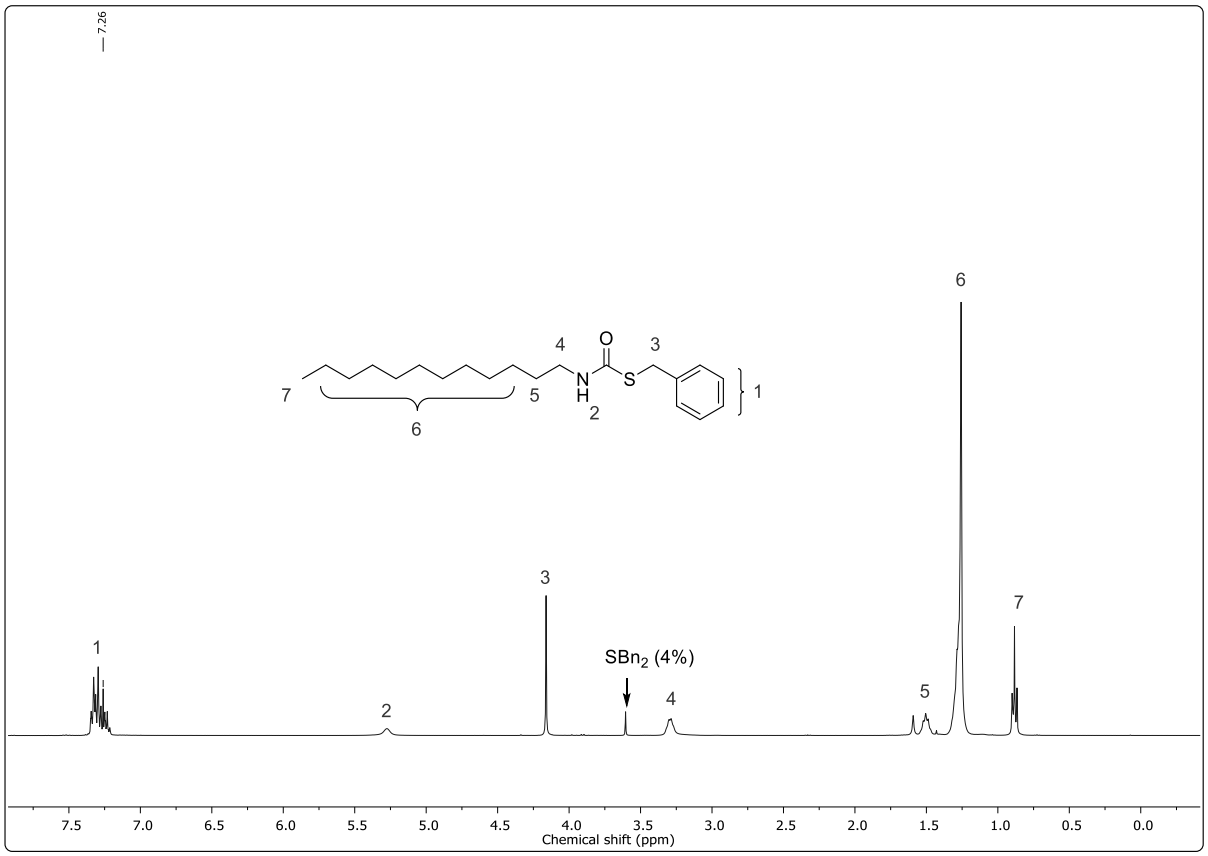

_S_-methyl cyclohexyl thiocarbamate

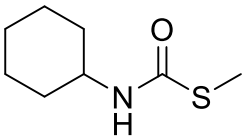

$C_8H_{15}NOS$

M = 173.27 g/mol

Was obtained as white solid in a yield of 69%.

TLC: R_f (cyclohexane/ethyl acetate 9:1) = 0.44

^{1}H NMR (500 MHz, $CDCl_3$): δ (ppm) = 5.24 (bs, 1H, N**H**, ^{1}), 3.84 – 3.68 (m, 1H, C**H**, ^{2}), 2.33 (s, 3H, SC**H**$_3$, ^{3}), 2.02 – 1.89 (m, 2H, C**H**, ^{4}), 1.76 – 1.66 (m, 2H, C**H**, ^{5}), 1.63 – 1.56 (m, 1H, C**H**, ^{6}), 1.39 – 1.30 (m, 2H, C**H**, ^{7}), 1.20 – 1.11 (m, 3H, C**H**, $^{8, 9}$).

^{13}C NMR (126 MHz, $CDCl_3$): δ (ppm) = 166.57, 50.66, 33.32, 25.54, 24.89, 12.44.

HRMS (EI) *m/z*: [M] calcd for $C_8H_{15}NOS$, 173.0874; found, 173.0868.

IR (ATR): ṽ (cm^{-1}) = 3319, 2929, 2853, 1647, 1511, 1454, 1349, 1302, 1266, 1246, 1208, 1188, 1082, 967, 925, 908, 889, 840, 786, 697, 594, 571, 486, 448.

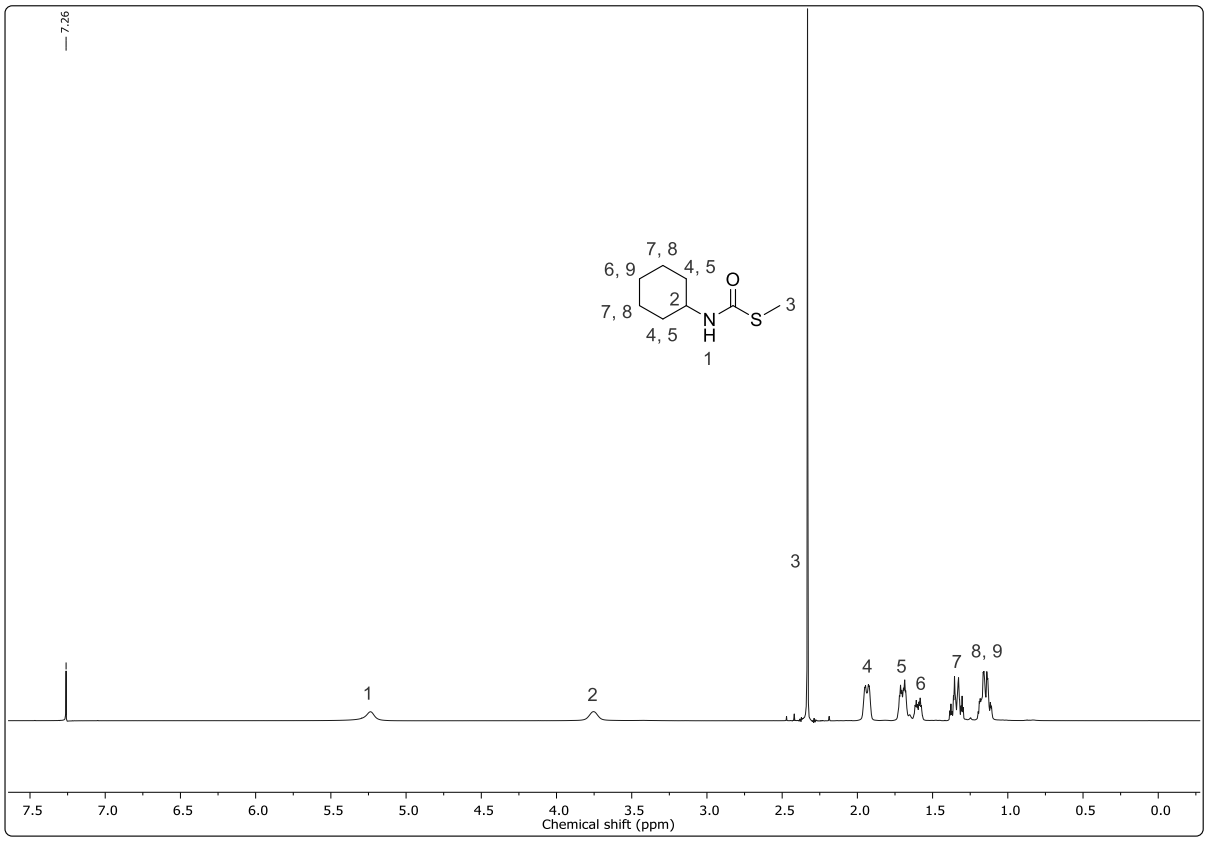

_S_-butyl cyclohexyl thiocarbamate

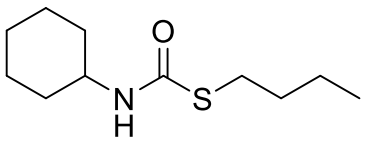

$C_{11}H_{21}NOS$

M = 215.36 g/mol

Was obtained as white solid in a yield of 70%.

TLC: R_f (cyclohexane/ethyl acetate 9:1) = 0.48

^{1}H NMR (500 MHz, $CDCl_3$): δ (ppm) = 5.20 (bs, 1H, N**H**, ^{1}), 3.79 – 3.67 (m, 1H, C**H**, ^{2}), 2.90 (t, *J* = 7.34 Hz, 2H, SC**H**$_2$, ^{3}), 1.99 – 1.90 (m, 2H, C**H**, ^{4}), 1.74 – 1.66 (m, 2H, C**H**, ^{5}), 1.62 – 1.56 (m, 3H, C**H$_2$**, C**H**, ^{6}), 1.43 – 1.29 (m, 4H, C**H$_2$**, C**H**, ^{7}), 1.19 – 1.10 (m, 2H, C**H**, $^{8, 9}$), 0.91 (t, *J* = 7.36 Hz, 3H, C**H$_3$**, ^{10}).

^{13}C NMR (126 MHz, $CDCl_3$): δ (ppm) = 166.36, 50.99, 50.58, 33.32, 32.72, 31.16, 29.76, 25.55, 24.91, 22.04, 13.74.

HRMS (EI) *m/z*: [M] calcd for $C_{11}H_{21}NOS$, 215.1344; found, 215.1340.

IR (ATR): ṽ (cm^{-1}) = 3248, 3028, 2930, 2855, 1660, 1636, 1528, 1464, 1446, 1404, 1371, 1349, 1303, 1264, 1248, 1209, 1150, 1086, 968, 927, 909, 889, 836, 785, 743, 714, 668, 630, 572, 470, 449.

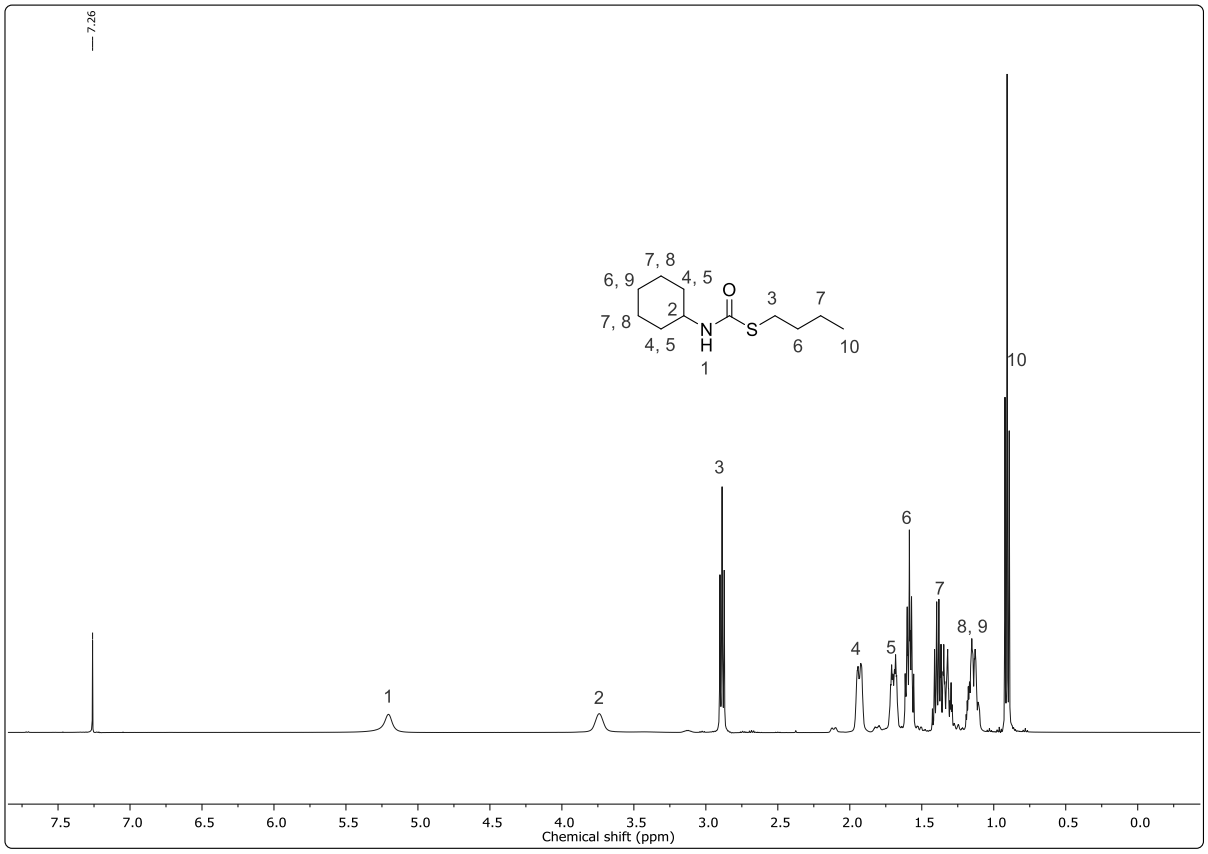

***S*-4-chlorobutyl cyclohexyl thiocarbamate**

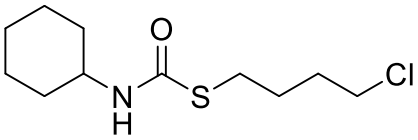

$C_{11}H_{20}ClNOS$

M = 249.80 g/mol

Was obtained as white solid in a yield of 70%.

TLC: R_f (cyclohexane/ethyl acetate 9:1) = 0.46

^{1}H NMR (500 MHz, $CDCl_3$): δ (ppm) = 5.20 (bs, 1H, N**H**, ^{1}), 3.79 – 3.69 (m, 1H, C**H**, ^{2}), 3.55 (t, *J* = 6.51 Hz, 2H, C**H**$_2$Cl, ^{3}), 2.92 (t, *J* = 7.06 Hz, 2H, SC**H**$_2$, ^{4}), 1.98 – 1.90 (m, 2H, C**H**, ^{5}), 1.89 – 1.84 (m, 2H, C**H**$_2$CH$_2$Cl, ^{6}), 1.80 – 1.74 (m, 2H, SCH$_2$C**H**$_2$, ^{7}), 1.74 – 1.66 (m, 2H, C**H**, ^{8}), 1.63 – 1.56 (m, 1H, C**H**, ^{9}), 1.39 – 1.29 (m, 2H, C**H**, ^{10}), 1.19 – 1.10 (m, 2H, C**H**, ^{11}).

^{13}C NMR (126 MHz, $CDCl_3$): δ (ppm) = 165.91, 50.70, 44.59, 33.29, 31.55, 29.21, 27.99, 25.53, 24.90.

HRMS (EI) *m/z*: [M] calcd for $C_{11}H_{20}ClNOS$, 249.0954; found, 249.0950.

IR (ATR): ṽ (cm^{-1}) = 3323, 2932, 2856, 1642, 1509, 1455, 1347, 1320, 1248, 1212, 1202, 1189, 1084, 1016, 967, 925, 884, 842, 786, 765, 738, 723, 646, 574, 505, 475, 449.

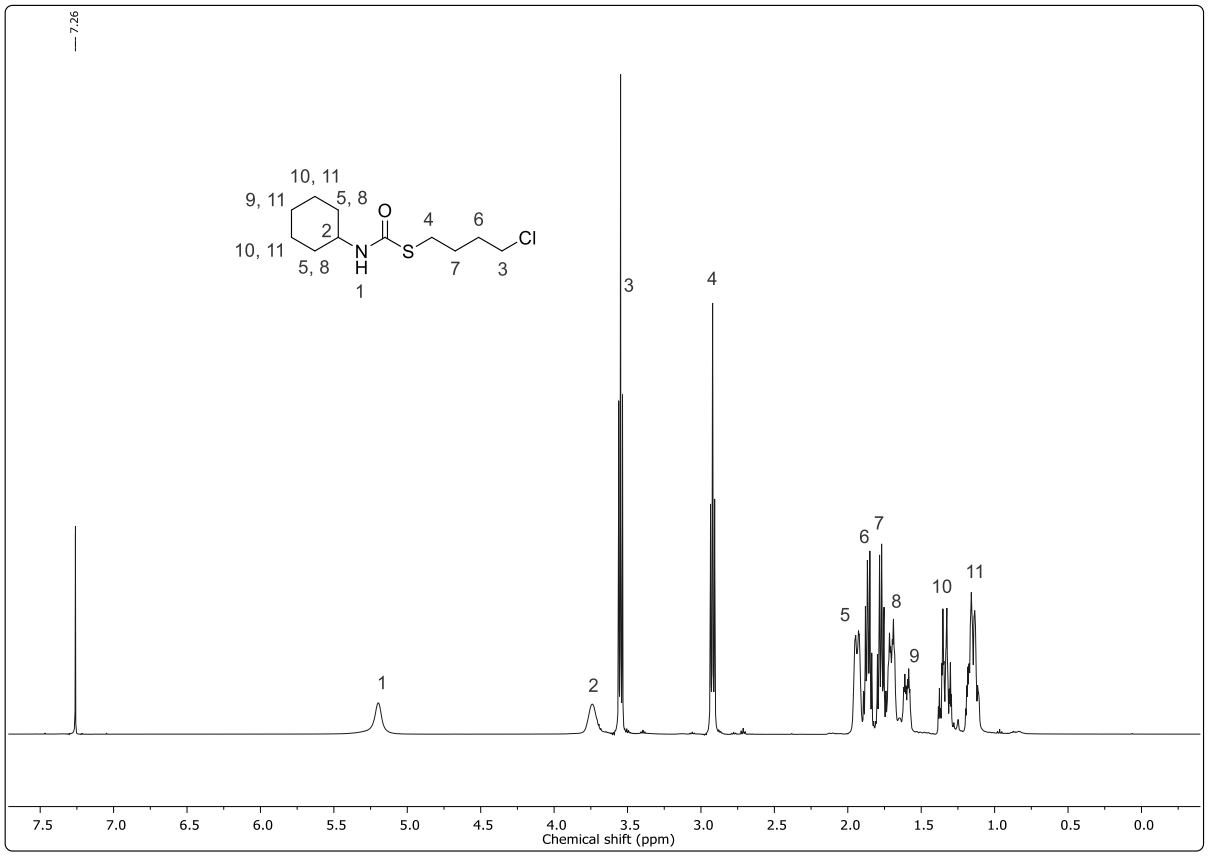

_S_-benzyl cyclohexyl thiocarbamate

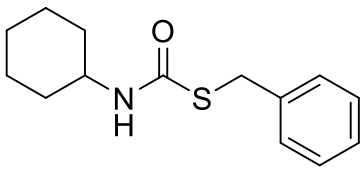

$C_{14}H_{19}NOS$

M = 249.37 g/mol

Was obtained as beige solid in a yield of 25%.

TLC: R_f (cyclohexane/ethyl acetate 9:1) = 0.36

^{1}H NMR (500 MHz, $CDCl_3$): δ (ppm) = 7.35 – 7. 21 (m, 5H, C**H**$_{\text{aromatic}}$, ^{1}), 5.20 (bs, 1H, N**H**, ^{2}), 4.15 (s, 2H, C**H**$_2$, ^{3}), 3.85 – 3.69 (m, 1H, C**H**, ^{4}), 2.00 – 1.89 (m, 2H, C**H**, ^{5}), 1.76 – 1.66 (m, 2H, C**H**, ^{6}), 1.64 – 1.55 (m, 1H, C**H**, ^{7}), 1.41 – 1.25 (m, 3H, C**H**, ^{8}), 1.21 – 1.08 (m, 2H, C**H**, ^{9}).

^{13}C NMR (126 MHz, $CDCl_3$): δ (ppm) = 165.63, 128.96, 128.70, 127.27, 50.82, 34.31, 33.29, 25.53, 24.90.

HRMS (EI) *m/z*: [M] calcd for $C_{14}H_{19}NOS$, 249.1187; found, 249.1181.

IR (ATR): ṽ (cm^{-1}) = 3294, 3029, 2925, 2845, 1635, 1520, 1494, 1447, 1347, 1312, 1269, 1247, 1206, 1191, 1068, 1028, 964, 911, 889, 836, 783, 713, 697, 630, 564, 505, 485, 461, 445.

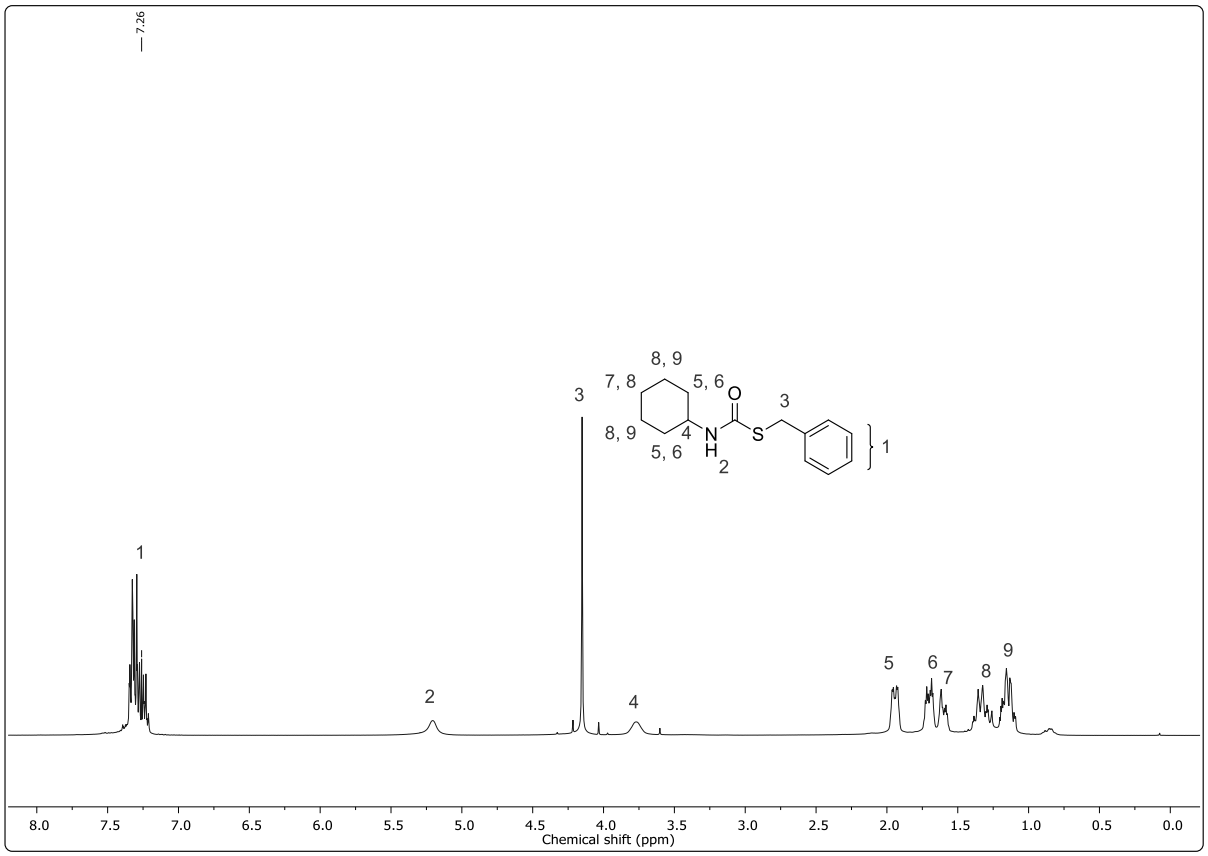

_S_-methyl benzyl thiocarbamate

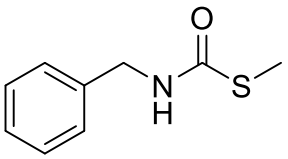

$C_9H_{11}NOS$

M = 181.25 g/mol

Was obtained as white solid in a yield of 72%.

TLC: R_f (cyclohexane/ethyl acetate 5:1) = 0.42

^{1}H NMR (500 MHz, $CDCl_3$): δ (ppm) = 7.36 – 7.33 (m, 2H, C**H**$_{\textbf{Aromatic}}$, ^{1}), 7.30 – 7.27 (m, 3H, C**H**$_{\textbf{Aromatic}}$, ^{2}), 5.68 (bs, 1H, N**H**, ^{3}), 4.47 (d, J = 5.27 Hz, 2H, C**H**$_2$, ^{4}), 2.38 (s, 3H, SC**H**$_3$, ^{5}).

^{13}C NMR (126 MHz, $CDCl_3$): δ (ppm) = 167.97, 137.85, 128.88, 128.88, 127.85, 127.82, 45.50, 12.54.

HRMS (EI) *m/z*: [M] calcd for $C_9H_{11}NOS$, 181.0561; found, 181.0556.

IR (ATR): ṽ (cm^{-1}) = 3313, 3029, 2927, 2852, 1640, 1498, 1462, 1450, 1359, 1310, 1203, 1151, 1076, 1054, 1025, 970, 877, 809, 785, 742, 694, 606, 578, 504, 479, 406.

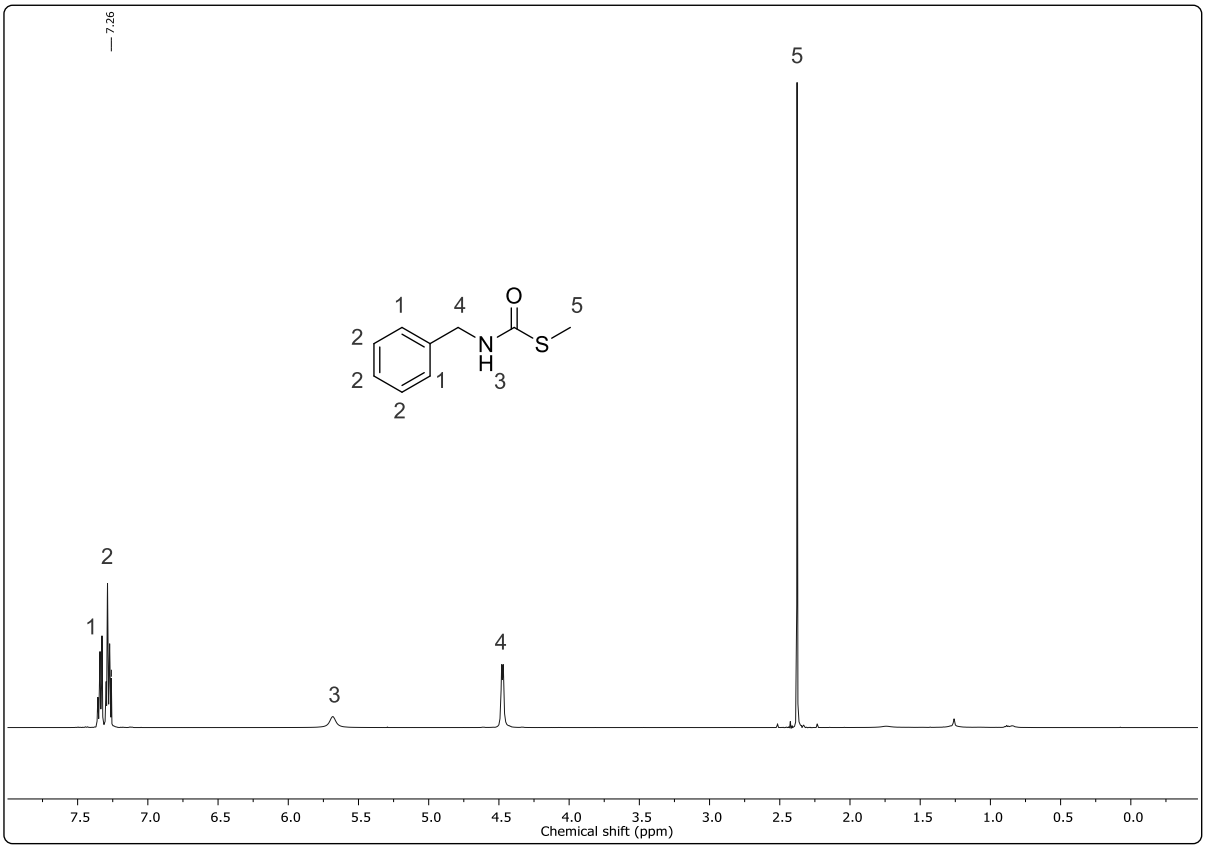

_S_-butyl benzyl thiocarbamate

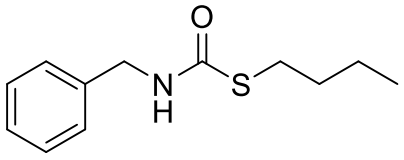

$C_{12}H_{17}NOS$

M = 223.33 g/mol

Was obtained as white solid in a yield of 59%.

TLC: R_f (cyclohexane/ethyl acetate 9:1) = 0.42

^{1}H NMR (500 MHz, $CDCl_3$): δ (ppm) = 7.36 – 7.33 (m, 2H, C**H**$_{\textbf{Aromatic}}$, ^{1}), 7.30 – 7.27 (m, 3H, C**H**$_{\textbf{Aromatic}}$, ^{2}), 5.61 (bs, 1H, N**H**, ^{3}), 4.47 (d, *J* = 5.24 Hz, 2H, C**H**$_{\textbf{2}}$, ^{4}), 2.94 (m,

2H, SC**H**$_2$, [5]), 1.62 (p, *J* = 7.42 Hz, 2H, C**H**$_2$, [6]), 1.42 (p, *J* = 7.37 Hz, 2H, C**H**$_2$, [7]), 2.38 (t, *J* = 7.36 Hz, 3H, C**H**$_3$, [8]).

^{13}C NMR (126 MHz, $CDCl_3$): δ (ppm) = 167.72, 137.91, 128.89, 127.87, 127.81, 45.41, 32.64, 31.98, 31.96, 29.91, 22.03, 13.75.

HRMS (EI) *m/z*: [M] calcd for $C_{12}H_{17}NOS$, 223.1031; found, 223.1025.

IR (ATR): ṽ (cm^{-1}) = 3305, 3031, 2957, 2929, 2872, 1649, 1496, 1454, 1379, 1358, 1211, 1186, 1080, 1029, 993, 902, 787, 725, 696, 600, 500.

_S_-4-chlorobutyl benzyl thiocarbamate

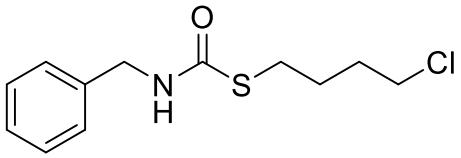

$C_{12}H_{16}ClNOS$

M = 257.78 g/mol

Was obtained as white solid in a yield of 81%.

TLC: R_f (cyclohexane/ethyl acetate 9:1) = 0.26

^{1}H NMR (500 MHz, $CDCl_3$): δ (ppm) = 7.36 – 7.33 (m, 2H, C**H**$_{\textbf{Aromatic}}$, ^{1}), 7.30 – 7.27 (m, 3H, C**H**$_{\textbf{Aromatic}}$, ^{2}), 5.62 (bs, 1H, N**H**, ^{3}), 4.47 (d, *J* = 5.45 Hz, 2H, C**H**$_{\textbf{2}}$, ^{4}), 3.56 (t, *J* = 6.46 Hz, 2H, C**H**$_{\textbf{2}}$Cl, ^{5}), 2.97 (t, 7.03 Hz, 2H, SC**H**$_{\textbf{2}}$, ^{6}), 1.62 (m, 2H, C**H**$_{\textbf{2}}$$CH_2$Cl, ^{7}), 1.42 (m, 2H, C**H**$_{\textbf{2}}$, ^{8}).

^{13}C NMR (126 MHz, $CDCl_3$): δ (ppm) = 167.27, 137.78, 128.92, 127.88, 45.49, 44.56, 31.53, 29.36, 27.93.

HRMS (EI) *m/z*: [M] calcd for $C_{12}H_{16}ClNOS$, 257.0641; found, 257.0636.

IR (ATR): ṽ (cm^{-1}) = 3337, 3032, 2959, 2939, 2927, 2858, 1646, 1508, 1453, 1431, 1411, 1361, 1313, 1286, 1249, 1217, 1183, 1081, 1032, 994, 877, 849, 802, 772, 739, 698, 675, 634, 608, 576, 492, 472, 423.

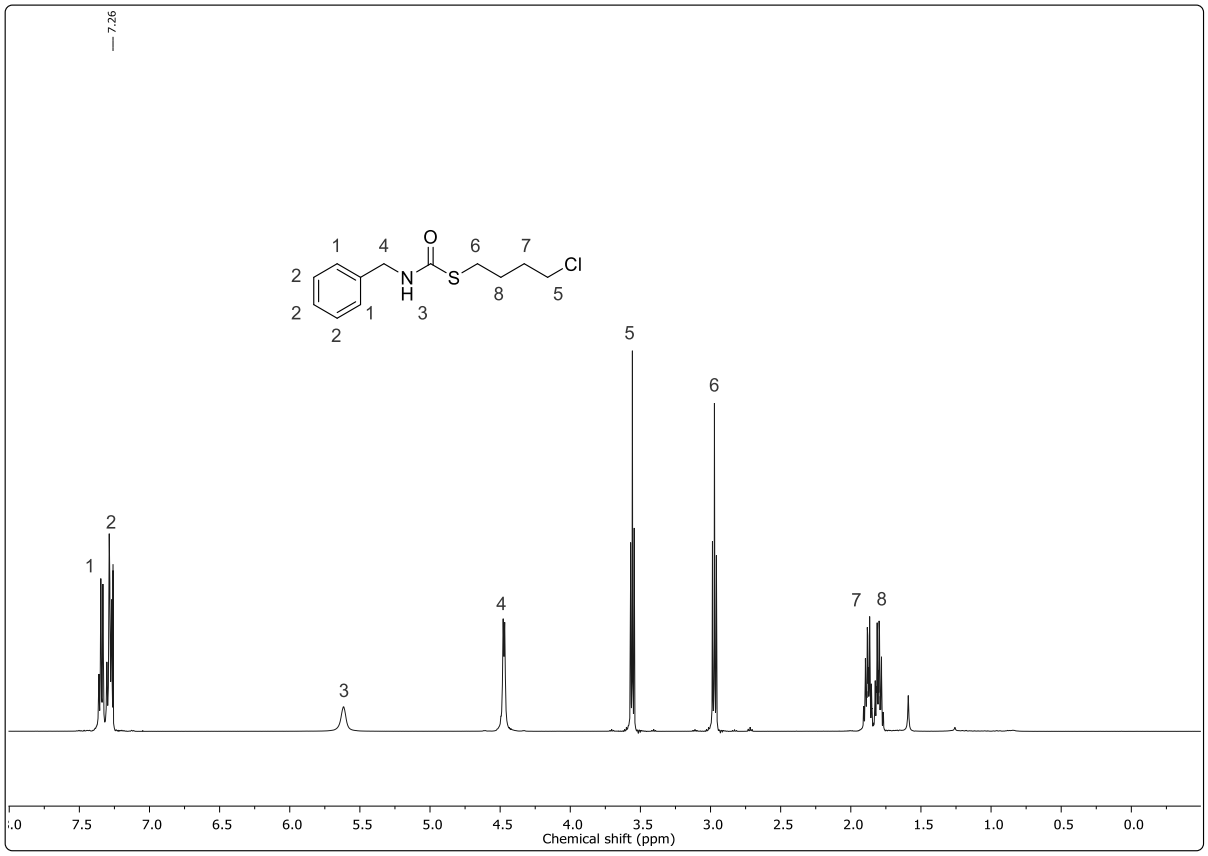

_S_-benzyl benzyl thiocarbamate

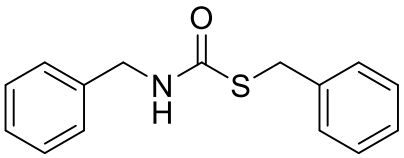

$C_{15}H_{15}NOS$

M = 257.35 g/mol

Was obtained as beige solid in a yield of 46%.

TLC: R_f (cyclohexane/ethyl acetate 9:1) = 0.32

^{1}H NMR (500 MHz, $CDCl_3$): δ (ppm) = 7.36 – 7.23 (m, 10H, C**H**$_{\text{Aromatic}}$, ^{1}), 5.61 (bs, 1H, N**H**, ^{2}), 4.49 (d, J = 4.86 Hz, 2H, C**H**$_2$, ^{3}), 4.20 (d, J = 4.86, 2H, C**H**$_2$, ^{4}).

^{13}C NMR (126 MHz, $CDCl_3$): δ (ppm) = 166.99, 138.37, 137.68, 128.98, 128.91, 128.73, 127.87, 127.36, 45.57, 34.42.

HRMS (EI) *m/z*: [M] calcd for $C_{15}H_{15}NOS$, 257.0874; found, 257.0869.

IR (ATR): ṽ (cm^{-1}) = 3245, 3029, 2925, 1810, 1662, 1633, 1536, 1493, 1452, 1407, 1354, 1236, 1206, 1080, 1026, 963, 917, 843, 786, 751, 695, 640, 588, 562, 509, 483, 470, 408.

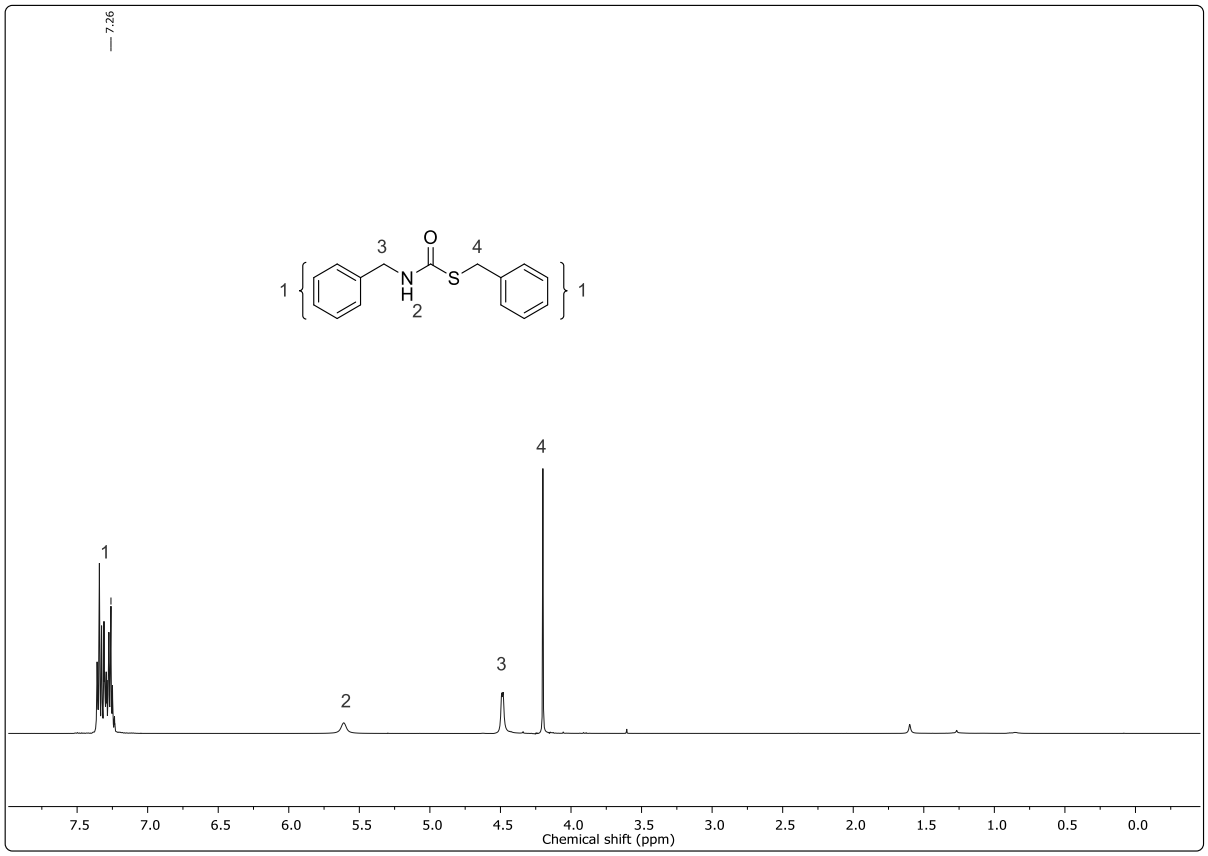

_S_-methyl (bicyclo[2.2.1]hept-5-en-2-ylmethyl)carbamothioate

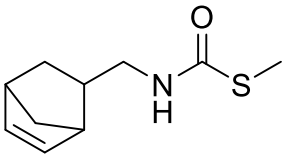

$C_{10}H_{15}NOS$

M = 197.30 g/mol

Was obtained as white solid in a yield of 60%. Note that the starting material norbornene-2-methylamine purchased from TCI is a mixture of isomers, which were not separable in column chromatography. Hence, in ^{1}H and ^{113}C NMR spectrum only the peaks associated with predominant isomer are assigned.

TLC: R_f (cyclohexane/ethyl acetate 7:1) = 0.40

^{1}H NMR (500 MHz, $CDCl_3$): δ (ppm) = 6.16 (dd, J = 5.53, 2.97 Hz, 1H, C=C**H**, ^{1}), 5.94 (dd, J = 5.71, 2.56 Hz, 1H, C=C**H**, ^{2}), 5.42 (bs, 1H, N**H**, ^{3}), 3.13 – 2.91 (m, 2H, C**H₂**, ^{4}), 2.82 – 2.80 (m, 2H, C**H**, ^{5}), 3.33 (s, 3H, C**H₃**, ^{6}), 2.29 – 2.22 (m, 1H, C**H**, ^{7}), 1.84 (ddd, J = 12.68, 9.20, 3.81 Hz, 1H, ½ C**H₂**, ^{8}), 1.45 – 1.43 (m, 1H, ½ C**H₂**, ^{9}), 1.24 – 1.23 (m, 1H, ½ C**H₂**, ^{9}), 0.54 (ddd, J = 11.59, 4.24, 2.66 Hz, 2H, C**H₂**, ^{10}).

^{13}C NMR (126 MHz, $CDCl_3$): δ (ppm) = 167.49, 137.96, 132.02, 49.62, 44.26, 42.49, 41.13, 39.12, 30.11, 12.48.

HRMS (EI) *m/z*: [M] calcd for $C_{10}H_{15}NOS$, 197.0874; found, 197.0871.

IR (ATR): ṽ (cm^{-1}) = 3296, 3056, 2965, 2931, 2866, 1645, 1518, 1437, 1368, 1338, 1259, 1205, 1124, 1091, 1020, 961, 929, 901, 865, 826, 809, 785, 769, 718, 659, 613, 467, 440.

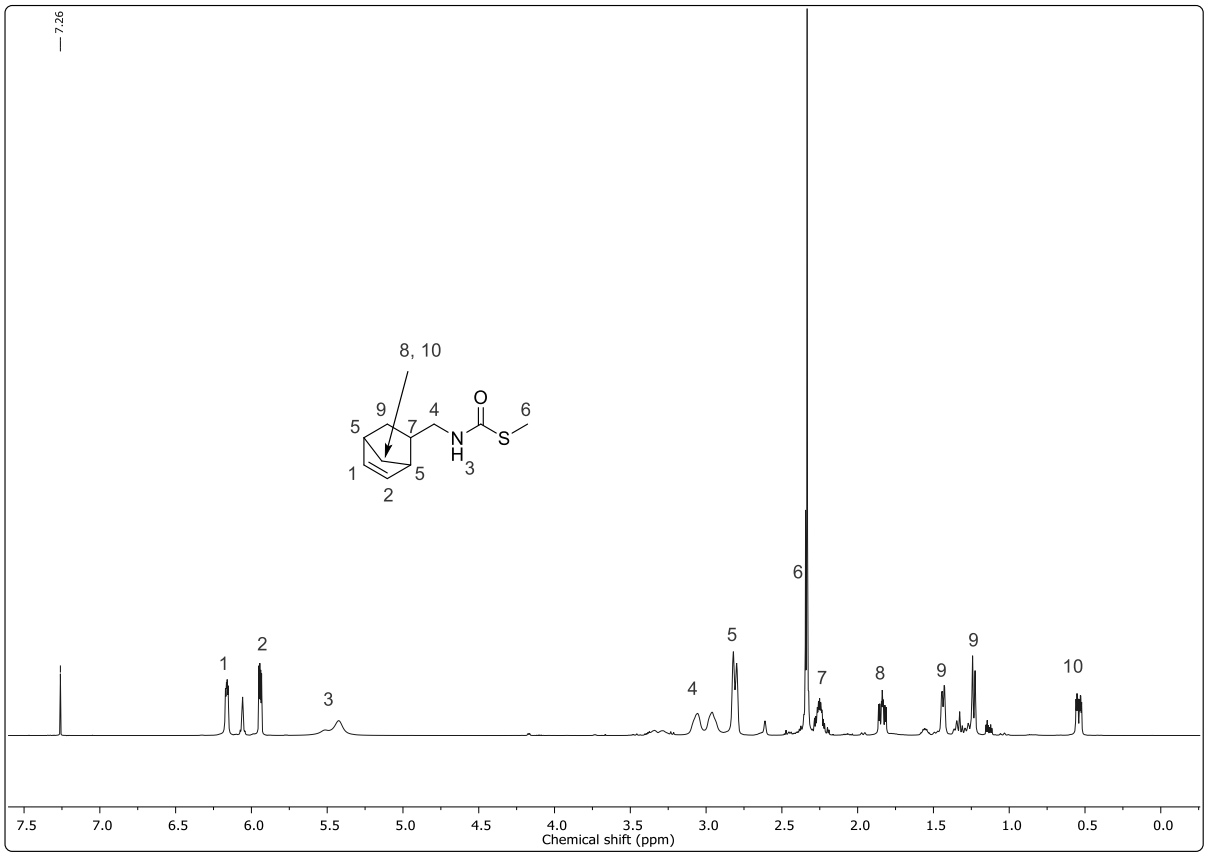

_S_-butyl (bicyclo[2.2.1]hept-5-en-2-ylmethyl)carbamothioate

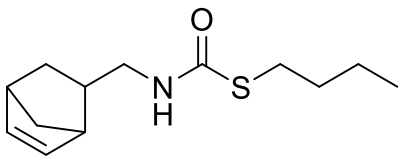

$C_{13}H_{21}NOS$

M = 239.38 g/mol

Was obtained as white solid in a yield of 73%. Note that the starting material norbornene-2-methylamine purchased from TCI is a mixture of isomers, which were not separable in column chromatography. Hence, in ^{1}H and ^{13}C NMR spectrum only the peaks associated with predominant isomer are assigned.

TLC: R_f (cyclohexane/ethyl acetate 7:1) = 0.47

^{1}H NMR (500 MHz, $CDCl_3$): δ (ppm) = 6.17 (dd, *J* = 5.55, 2.97 Hz, 1H, C=C**H**, [1]), 5.95 (dd, *J* = 5.72, 2.84 Hz, 1H, C=C**H**, [2]), 5.28 (bs, 1H, N**H**, [3]), 3.11 – 2.93 (m, 2H, C**H₂**, [4]), 2.92 – 2.89 (m, 2H, C**H₂**, [5]), 2.85 – 2.79 (m, 2H, C**H**, [6]), 2.25 (ddq, *J* = 12.59, 8.84, 4.02 Hz, 1H, C**H**, [7]), 1.84 (ddd, *J* = 12.59, 9.18, 3.77 Hz, 1H, ½ C**H₂**, [8]), 1.59 (p, *J* = 7.52 Hz, 3H, ½ C**H₂**, C**H₂**, [9]), 1.47 – 1.23 (m, 3H, C**H₂**, C**H**, [10, 11]), 0.92 (t, *J* = 7.36 Hz, 3H, C**H₃**, [12]), 0.55 (ddd, *J* = 11.59, 4.26, 2.65 Hz, 1H, ½ C**H₂**, [13]).

^{13}C NMR (126 MHz, $CDCl_3$): δ (ppm) = 167.26, 137.99, 132.07, 49.66, 44.31, 42.52, 41.88, 39.17, 32.72, 30.14, 29.85, 22.04, 13.76.

HRMS (EI) *m/z*: [M] calcd for $C_{13}H_{21}NOS$, 239.1344; found, 239.1338.

IR (ATR): ṽ (cm^{-1}) = 3300, 3057, 2959, 2932, 2866, 1645, 1518, 1464, 1367, 1338, 1259, 1205, 1124, 1098, 1019, 929, 901, 867, 827, 809, 785, 718, 659, 615, 469, 442.

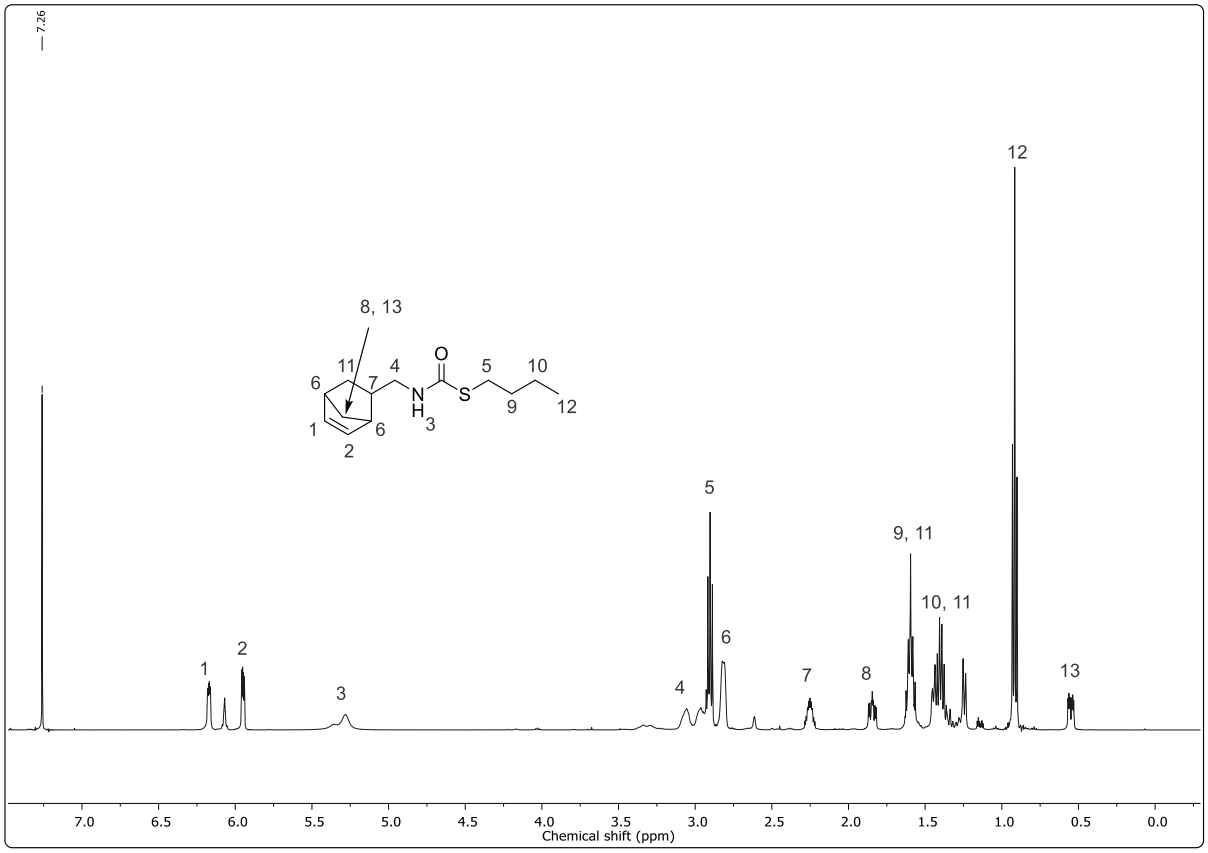

_S_-4-chlorobutyl (bicyclo[2.2.1]hept-5-en-2-ylmethyl)carbamothioate

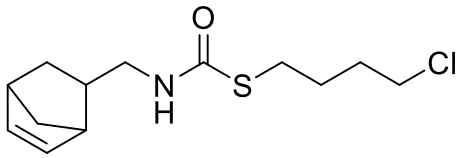

$C_{13}H_{20}ClNOS$

M = 273.82 g/mol

Was obtained as white solid in a yield of 79%. Note that the starting material norbornene-2-methylamine purchased from TCI is a mixture of isomers, which were not separable in column chromatography. Hence, in ^{1}H and ^{13}C NMR spectrum only the peaks associated with predominant isomer are assigned.

TLC: R_f (cyclohexane/ethyl acetate 7:1) = 0.30

^{1}H NMR (500 MHz, $CDCl_3$): δ (ppm) = 6.17 (dd, J = 5.46, 2.93 Hz, 1H, C=C**H**, [1]), 5.95 (dd, J = 5.76, 2.83 Hz, 1H, C=C**H**, [2]), 5.30 (bs, 1H, N**H**, [3]), 3.55 (t, J = 6.51 Hz, 2H, C**H₂**Cl, [4]), 3.12 – 2.92 (m, 2H, C**H₂**, [5]), 2.93 (t, J = 7.06 Hz, 2H, SC**H₂**, [6]), 2.86 – 2.79 (m, 2H, C**H**, [7]), 2.25 (ddq, J = 12.51, 8.89, 4.15 Hz, 1H, C**H**, [8]), 1.91 – 1.83 (m, 3H, C**H₂**, C**H**, [9]), 1.80 – 1.74 (m, 2H, C**H₂**, [10]), 1.46 – 1.44 (m, 1H, ½ C**H₂**, [11]), 1.25 – 1.24 (m, 1H, ½ C**H₂**, [11]), 0.55 (ddd, J = 11.61, 4.26, 2.65 Hz, 1H, ½ C**H₂**, [12]).

^{13}C NMR (126 MHz, $CDCl_3$): δ (ppm) = 166.78, 138.03, 137.07, 132.03, 49.66, 44.58, 44.30, 42.52, 39.16, 31.54, 30.13, 29.29, 27.99.

HRMS (EI) *m/z*: [M] calcd for $C_{13}H_{20}ClNOS$, 273.0954; found, 273.0950.

IR (ATR): ṽ (cm^{-1}) = 3305, 3056, 2961, 2866, 1646, 1512, 1446, 1367, 1338, 1317, 1284, 1258, 1203, 1124, 1091, 970, 929, 801, 827, 809, 769, 719, 650, 469.

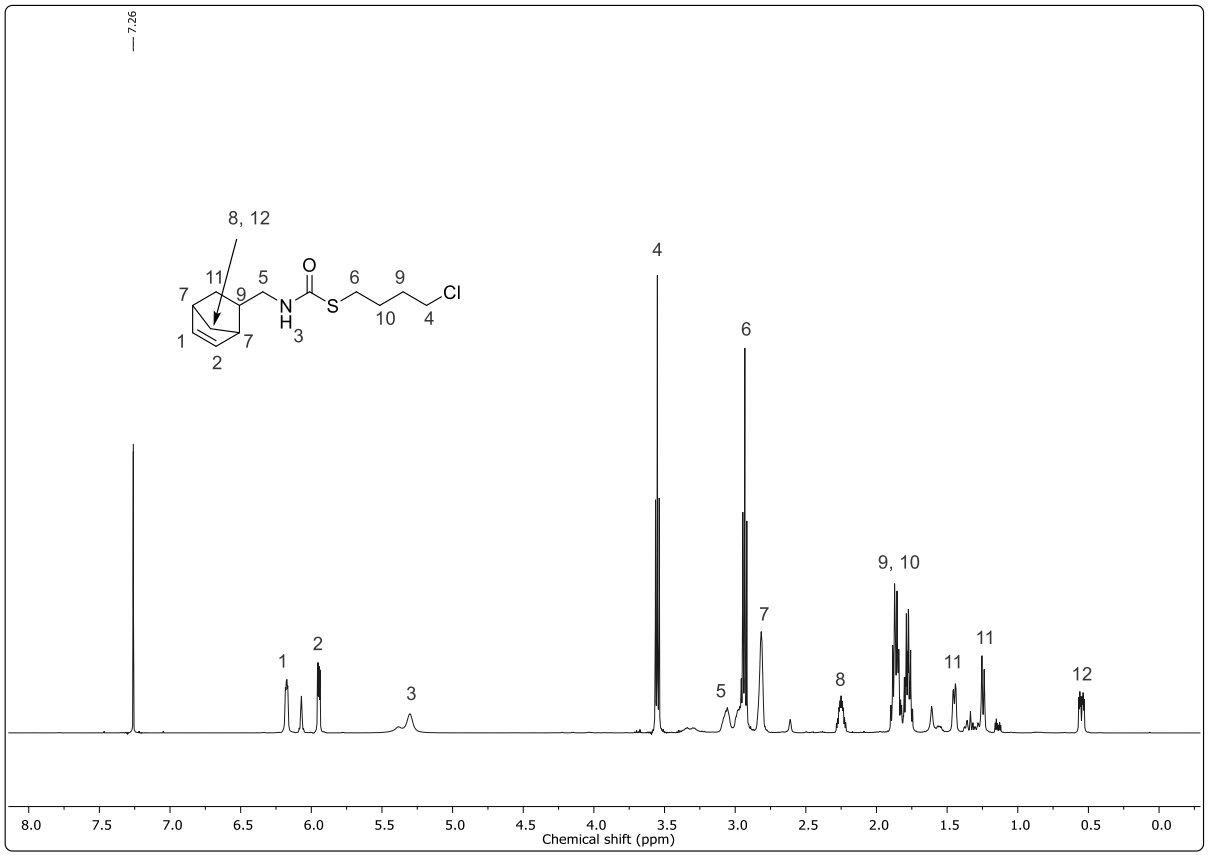

_S_-benzyl (bicyclo[2.2.1]hept-5-en-2-ylmethyl)carbamothioate

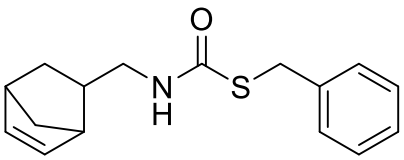

$C_{16}H_{19}NOS$

M = 273.39 g/mol

Was obtained as white solid in a yield of 50%. Note that the starting material norbornene-2-methylamine purchased from TCI is a mixture of isomers, which were not separable in column chromatography. Hence, in ^{1}H and ^{13}C NMR spectrum only the peaks associated with predominant isomer are assigned.

TLC: R_f (cyclohexane/ethyl acetate 7:1) = 0.44

^{1}H NMR (500 MHz, $CDCl_3$): δ (ppm) = 7.35 – 7.22 (m, 5H, C**H**$_{\text{aromatic}}$, ^{1}) 6.17 (dd, J = 5.65, 3.21 Hz, 1H, C=C**H**, ^{2}), 5.94 (dd, J = 5.53, 2.84 Hz, 1H, C=C**H**, ^{3}), 5.30 (bs, 1H, N**H**, ^{4}), 4.16 (s, 2H, C**H**$_2$, ^{5}), 3.13 – 2.95 (m, 2H, C**H**$_2$, ^{6}), 2.81 (m, 2H, C**H**, ^{7}), 2.25 (ddt, J = 11.96, 8.75, 4.39 Hz, 1H, C**H**, ^{8}), 1.84 (ddd, J = 11.51, 9.02, 3.75 Hz, 1H, ½

C**H**$_2$, [9]), 1.47 – 1.42 (m, 1H, ½ C**H**$_2$, [10]), 1.25 – 1.23 (m, 1H, ½ C**H**$_2$, [10]), 0.54 (ddd, *J* = 11.58, 4.34, 2.63 Hz, 2H, C**H**$_2$, [11]).

^{13}C NMR (126 MHz, $CDCl_3$): δ (ppm) = 166.50, 138.62, 138.01, 137.05, 136.31, 132.04, 128.95, 128.71, 127.30, 49.65, 44.29, 42.51, 41.87, 39.12, 34.37, 30.94, 30.13.

HRMS (EI) *m/z*: [M] calcd for $C_{16}H_{19}NOS$, 273.1187; found, 273.1182.

IR (ATR): ṽ (cm^{-1}) = 3287, 3055, 2963, 2932, 2865, 1742, 1634, 1513, 1453, 1335, 1248, 1205, 1193, 1087, 1069, 1027, 959, 917, 903, 865, 827, 767, 708, 693, 659, 600, 569, 525, 501, 480, 462, 434.

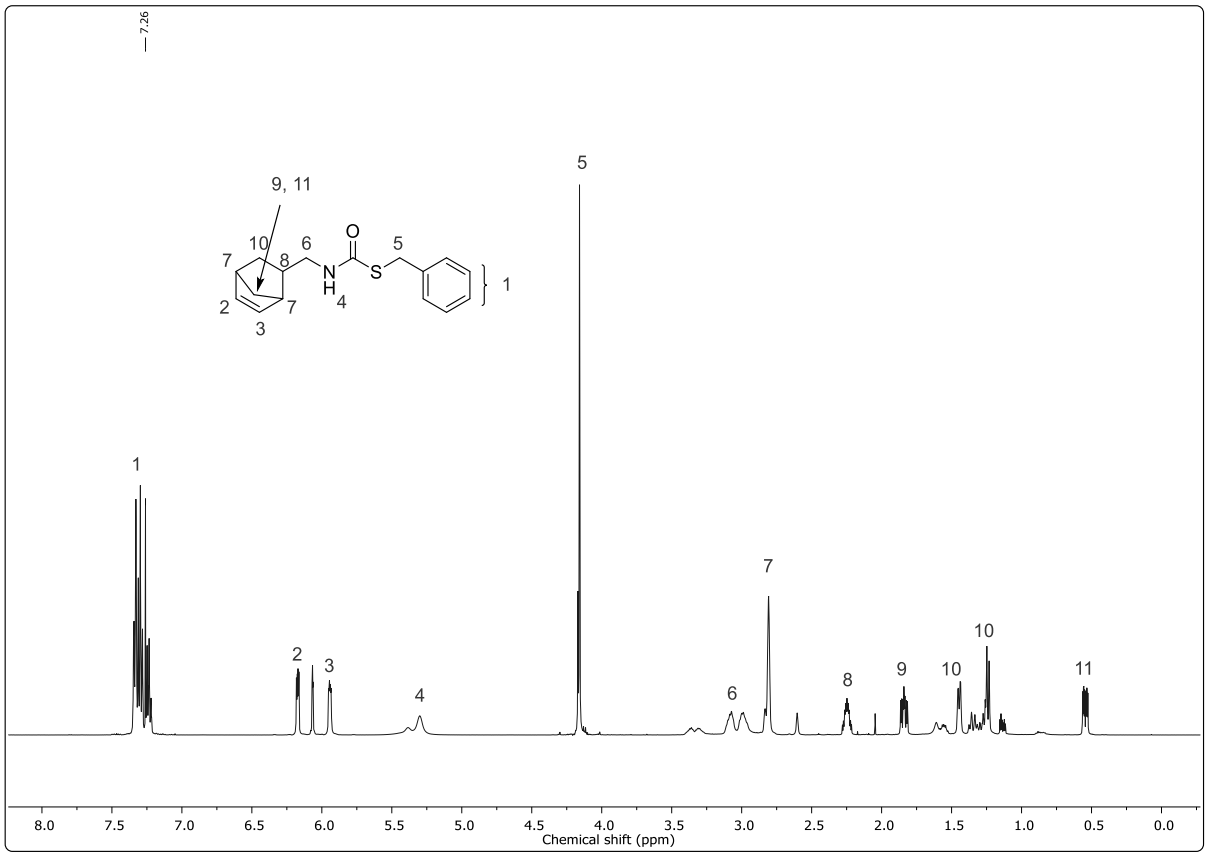

_S,S_'-dibutyl cyclohexane-,_trans_-1,4-diyldithiocarbamate

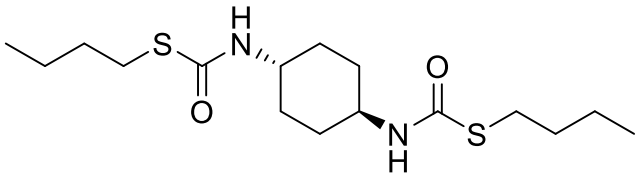

$C_{16}H_{30}N_2O_2S_2$

M = 346.55 g/mol

Was obtained as white solid in a yield of 44%.

TLC: R_f (cyclohexane/ethyl acetate 3:1) = 0.45

^{1}H NMR (500 MHz, $CDCl_3$): δ (ppm) = 7.98 (d, J = 7.37, 2H, N**H**, ^{1}), 3.51 – 3.41 (m, 2H, C**H**, ^{2}), 2.76 (t, J = 7.20 Hz, 4H, SC**H**$_2$, ^{3}), 1.77 (d, J = 6.03 Hz, 4H, C**H**, ^{4}), 1.47 (p, J = 7.37 Hz, 4H, C**H**$_2$, ^{5}), 1.32 (p, J = 7.30 Hz, 4H, C**H**$_2$, ^{6}), 1.32 (p, J = 11.0 Hz, 4H, C**H**, ^{7}), 0.86 (p, J = 7.35 Hz, 6H, C**H**, ^{8}).

^{13}C NMR (126 MHz, $CDCl_3$): δ (ppm) = 164.74, 49.28, 32.35, 30.92, 28.26, 21.29, 13.49.

HRMS (FAB) m/z: $[M + H]^+$ calcd for $C_{16}H_{30}N_2O_2S_2$, 347.1821; found, 347.1821.

IR (ATR): ṽ (cm^{-1}) = 3315, 2931, 2865, 1639, 1509, 1456, 1434, 1378, 1296, 1253, 1200, 1094, 979, 950, 914, 890, 827, 760, 732, 698, 594, 501, 445, 411.

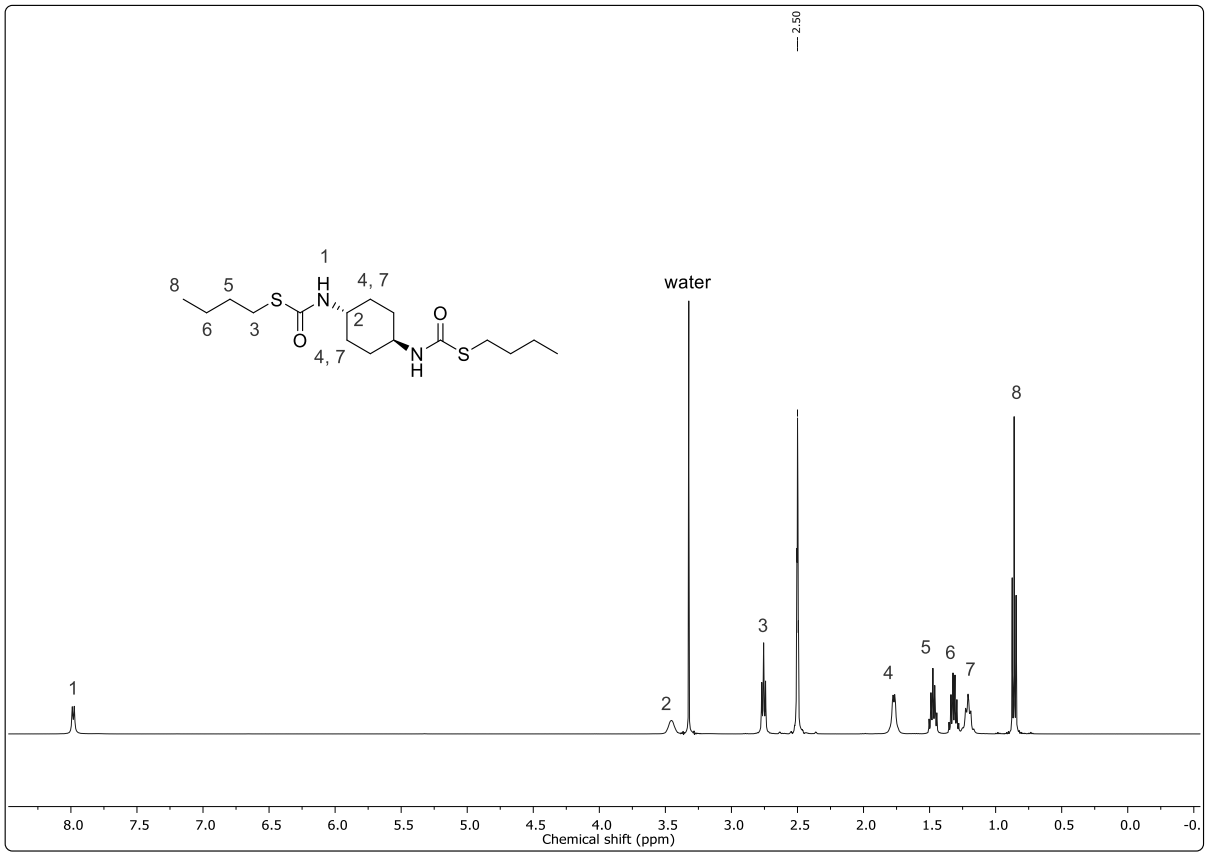
2.50
water
1
2
3
4
5
6
7
8
8.0
7.5
7.0
6.5
6.0
5.5
5.0
4.5
4.0
3.5
3.0
2.5
2.0
1.5
1.0
0.5
0.0
Chemical shift (ppm)

6.3.3 Building blocks and uniform macromolecules – Chapter 4.3

Note: Chapter 6.3.3 refers to the publication “Synthesis and encapsulation of uniform star-shaped block-macromolecules”. Parts of the following data is taken from the corresponding SI, yet slightly adjusted to fit the optics of this thesis. Figures are reprinted with permission from [224].

6.3.3.1 Building blocks

11-formamidoundecanoic acid

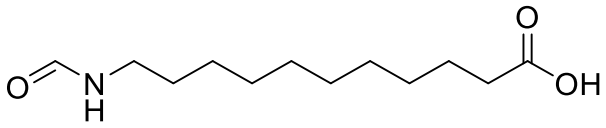

$C_{12}H_{23}NO_3$

M = 229.32 g/mol

11-aminoundecanoic acid **1** (25.1 g, 125 mmol, 1.00 eq.) was placed in a round-bottom flask. Ethyl formate (92.6 g, 1.25 mol, 101 mL, 10.0 eq.) and 50 mL of DMF were added and the suspension was heated at 75 °C and stirred until it became clear (~20 to 26 h). After the reaction was finished, the solvent was removed under reduced pressure and the product was used without further purification. The product **5** was obtained as white solid (28.7 g, 125 mmol, quant. yield). The analytical data is according to the literature.[103]

^{1}H NMR (500 MHz, DMSO-d_6): δ (ppm) = 11.93 (bs, 1H, COO**H**, ^{1}), 7.98 – 7.91 (m, 1H, NHCO**H**, ^{2}), 7.96 (bs, 1H, CHON**H**, ^{3}), 3.08 – 3.04 (m, 2H, CONHC**H$_2$**, ^{4}), 2.19 (t, *J* = 7.37 Hz, 2H, C**H$_2$**COOH, ^{5}), 1.51 – 1.46 (m, 2H, C**H$_2$**, ^{6}), 1.42 – 1.36 (m, 2H, C**H$_2$**, ^{7}), 1.25 (m, 12H, C**H$_2$**, ^{8}).

^{13}C NMR (126 MHz, DMSO-d_6): δ (ppm) = 174.55, 164.49, 160.89, 37.08, 33.70, 30.92, 29.02, 28.96, 28.88, 28.87, 27.83, 28.76, 28.70, 28.64, 28.58, 26.37, 25.89, 24.53.

HRMS (FAB) *m/z*: $[M + H]^+$ calcd for $C_{12}H_{23}NO_3$, 230.1751; found, 230.1755.

IR (ATR): $\tilde{\nu}$ (cm^{-1}) = 3359, 2939, 2919, 2849, 2578, 1721, 1647, 1626, 1526, 1471, 1438, 1410. 1363, 1319, 1294, 1273, 1243, 1207, 1178, 1109, 1055, 934, 897, 806, 765, 740, 713, 663, 548, 529, 448.

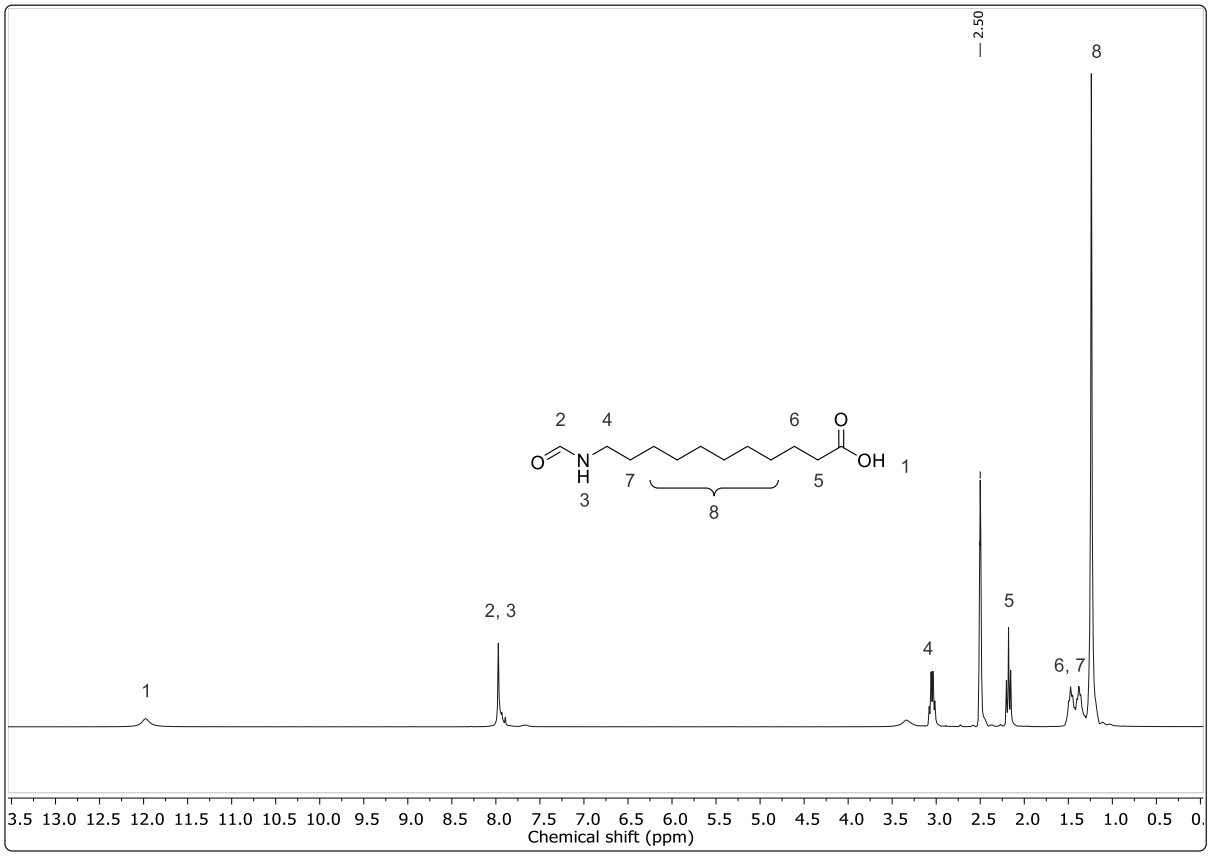

Benzyl 11-formamidoundecanoate

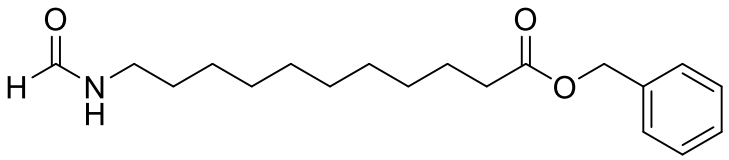

$C_{19}H_{29}NO_3$

M = 319.45 g/mol

11-Formamidoundecanoic acid **5** (22.9 g, 100 mmol, 1.00 eq.) was suspended in 50 mL of DCM, then DIPEA (14.9 g, 115 mmol, 19.6 mL, 1.15 eq.) was added. Under stirring, benzyl bromide (25.7 g, 150 mmol, 17.8 mL, 1.50 eq.) in 25 mL of DCM was slowly added *via* a dropping funnel. The reaction was stirred overnight and monitored by TLC. After the reaction was finished, triethylamine (5.57 g, 55.0 mmol, 7.62 mL, 0.55 eq.) was added and the reaction was stirred for another 1 h. Afterwards, the reaction mixture was poured into a separation funnel and 150 mL of water were added. The phases were separated, and the aqueous phase was extracted with DCM (3 × 75 mL). Then, the organic phases were combined and washed water (3 × 150 mL). The second aqueous phase (450 mL) was checked *via* TLC for remaining product. If the test was positive, it was extracted another time with 50 mL of DCM. The combined

organic layers were then dried over sodium sulfate and the solvent was removed under reduced pressure to yield the crude product **3** as slightly yellow solid (32.6 g, 102%). It was used without further purification (purity calculated *via* ^{1}H-NMR: 95%; yield: 31.0 g, 97.0 mmol, 97%). The analytical data is according to the literature.[26,103]

TLC: R_f (cyclohexane/ethyl acetate 1:2) = 0.25

^{1}H NMR (500 MHz, $CDCl_3$): δ (ppm) = 8.15, 8.04, 8.02 (m (cis + trans), 1H, C**H**ONH, ^{1}), 7.37 – 7.26 (m, 5H, C$\mathbf{H}_{\mathbf{aromatic}}$, ^{2}), 5.65 (bs, 1H, CON**H**, ^{3}), 5.11 (s. 2H, C$\mathbf{H_2}$, ^{4}), 3.28 (q (cis), J = 6.74 Hz, 2H, HCONHC$\mathbf{H_2}$, ^{5}), 3.19 (q (trans), J = 6.79 Hz, 2H, HCONHC$\mathbf{H_2}$, ^{5}), 2.34 (t, J = 7.54 Hz, 2H, C$\mathbf{H_2}$COOBn, ^{6}), 1.63 (p, J = 7.52 Hz, 2H, C$\mathbf{H_2}$, ^{7}), 1.51 (p, J = 7.36 Hz, 2H, C$\mathbf{H_2}$, ^{8}), 1.28 – 1.25 (m. 12H, C$\mathbf{H_2}$, ^{9}).

^{13}C NMR (126 MHz, $CDCl_3$): δ (ppm) = 173.83, 173.80, 164.66, 161.27, 145.13, 136.22, 128.65, 128.51, 128.28, 128.26, 66.19, 41.86, 38.30, 34.43, 31.35, 29.62, 29.49, 29.48, 29.40, 29.28, 29.20, 29.18, 27.02, 26.91, 26.47, 25.15, 25.03.

HRMS (FAB) *m/z*: $[M + H]^+$ calcd for $C_{19}H_{29}NO_3$, 320.2220; found, 320.2222.

IR (ATR): ṽ (cm^{-1}) = 3266, 3070, 2915, 2877, 2848, 1732, 1653, 1557, 1497, 1471, 1451, 1417, 1380, 1352, 1330, 1300, 1268, 1247, 1234, 1213, 1200, 1161, 1109, 1083, 1055, 1029, 997, 938, 924, 904, 867, 826, 807, 754, 719, 696, 609, 520, 488, 452.

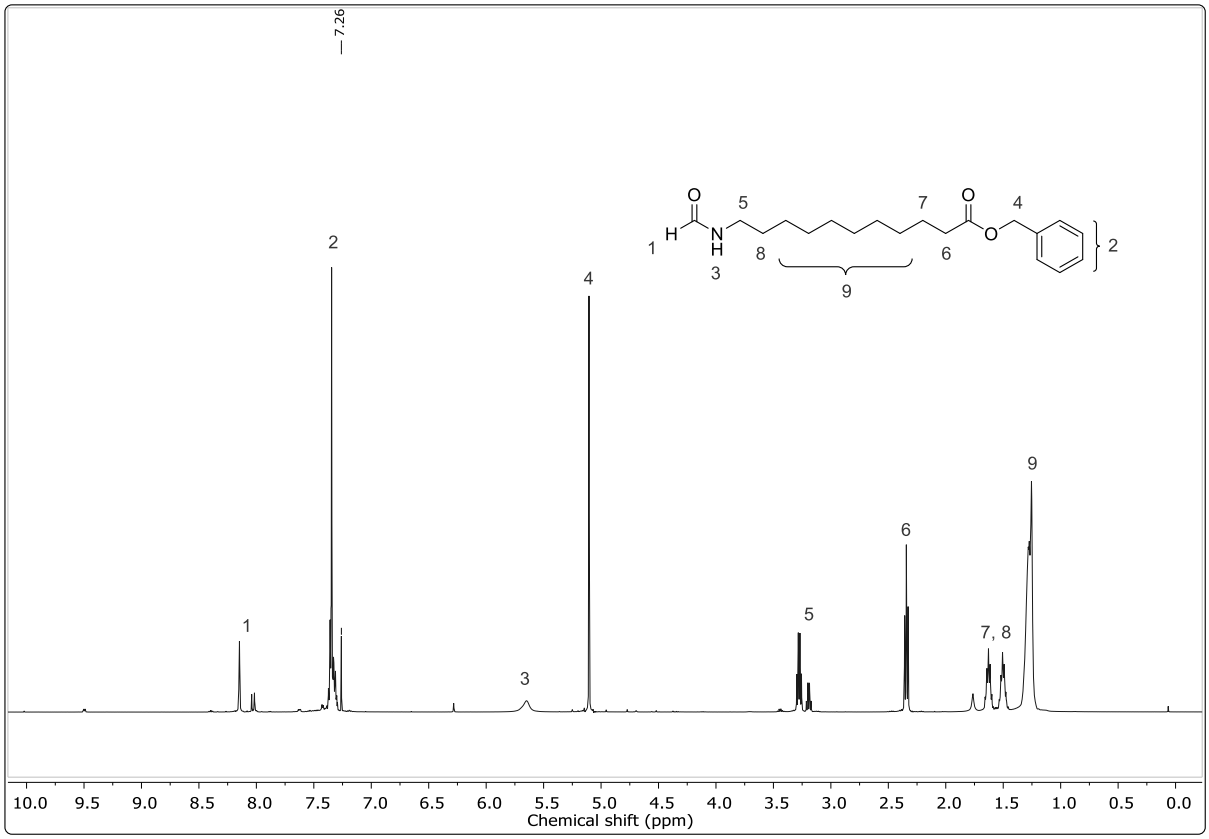

Benzyl 11-isocyanoundecanoate – Building Block A1

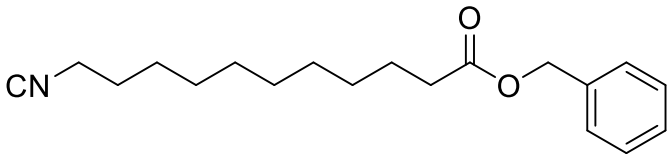

$C_{19}H_{27}NO_2$

M = 301.43 g/mol

Benzyl 11-formamidoundecanoate **3** (31.0 g, 96.9 mmol, 1.00 eq.) was suspended in 97.0 mL (1.00 mol/L) of DCM. Then pyridine (23.0 g, 291 mmol, 23.4 mL, 3.00 eq.) was added. The solution was cooled with a water bath and subsequently *p*-TsCl (27.7 g, 145 mmol, 1.50 eq) was added *via* a dropping funnel. Then, the reaction mixture was stirred for 1 h, while maintaining room temperature. After the reaction was finished (TLC control), cooling was applied and 97.0 mL of aqueous sodium carbonate solution (20%) was added slowly. The mixture was stirred for another 30 minutes, when another 50 mL of water and 50 mL DCM were added. Afterwards, the phases were separated, and the aqueous phase was extracted with DCM (3 × 100 mL). The organic phase was dried over sodium sulfate and filtrated. Then, the solvent was evaporated under reduced pressure to yield the crude isocyanide, which was purified *via* column chromatography (cyclohexane/ethyl acetate 7:1). The product **4**/**A1** was obtained as a colorless oil (28.2 g, 94.0 mmol, 97%). The analytical data is according to the literature.[26,103]

TLC: R_f (cyclohexane/ethyl acetate 5:1) = 0.45

^{1}H NMR (500 MHz, $CDCl_3$): δ (ppm) = 7.37 – 7.30 (m, 5H, C**H**$_{\text{aromatic}}$, ^{1}), 5.11 (s, 2H, C**H**$_2$, ^{2}), 3.35 (tt, *J* = 6.8, 1.9 Hz, 2H, C**H**$_2$, ^{3}), 2.35 (t, *J* = 7.5 Hz, 2H, C**H**$_2$, ^{4}), 1.69 – 1.61 (m, 4H, C**H**$_2$, ^{5}), 1.41 (q, *J* = 7.3 Hz, 2H, C**H**$_2$, ^{6}), 1.33 – 1.28 (m, 10H, C**H**$_2$, ^{7}).

^{13}C NMR (126 MHz, $CDCl_3$): δ (ppm) = 173.57, 155.68, 155.63, 136.13, 128.51, 128.13, 66.01, 41.57, 41.52, 41.47, 34.27, 29.25, 29.14, 29.07, 29.04, 28.64, 26.27, 24.90.

HRMS (FAB) *m/z*: $[M + H]^+$ calcd for $C_{19}H_{27}NO_2$, 302.2115; found, 302.2113.

IR (ATR): ṽ (cm^{-1}) = 3032, 2924, 2853, 2146, 1733, 1497, 1454, 1380, 1350, 1212, 1161, 1101, 1001, 736, 697, 579, 501.

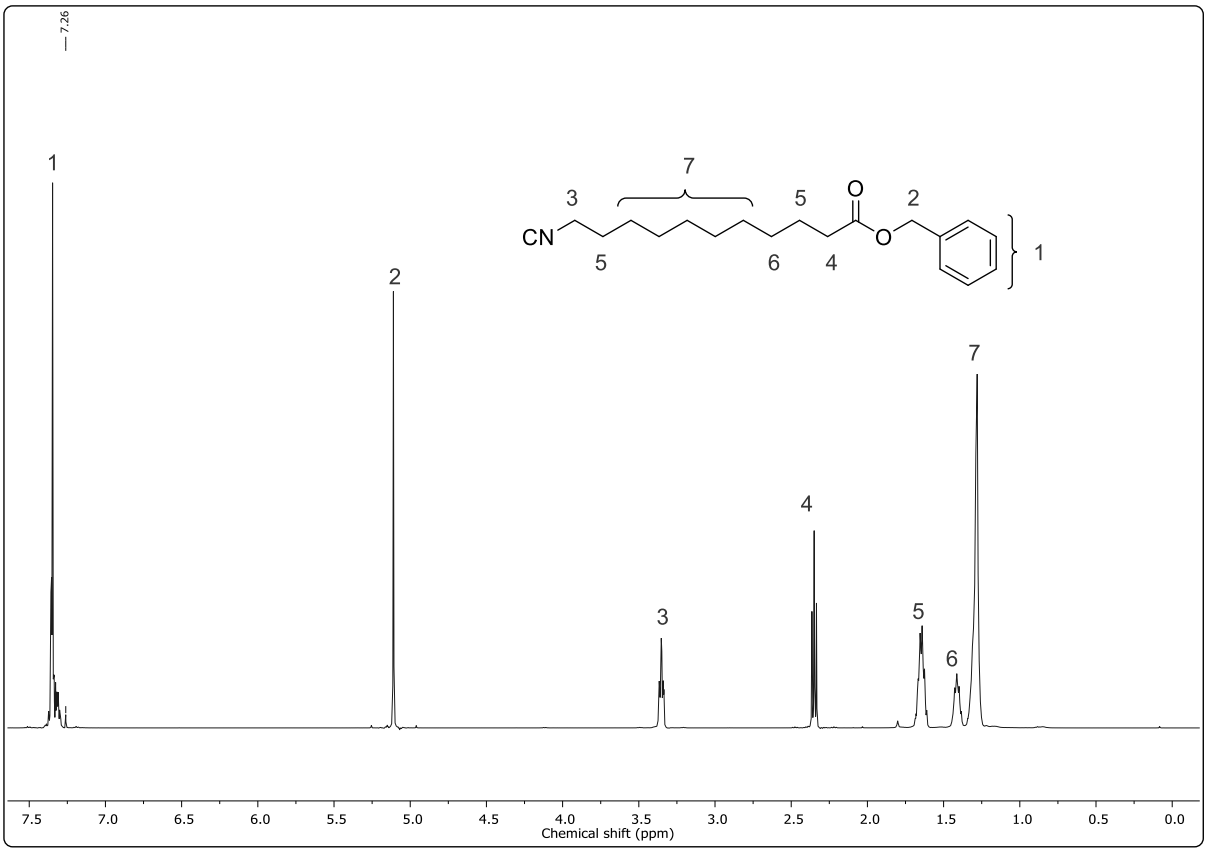

Benzyl 11-(3-ethyl-2-((11-formamidoundecanoyl)oxy)pentanamido)undecanoate

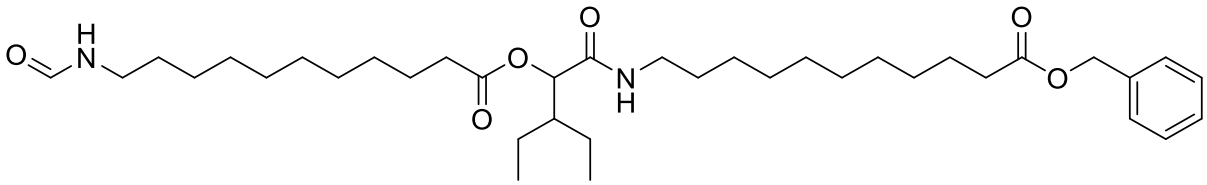

$C_{37}H_{62}N_2O_6$

M = 630.91 g/mol

11-Formamidoundecanoic acid **5** (17.2 g, 75.0 mmol, 1.00 eq.) was placed in a round bottom flask and dissolved in 50 mL DCM (1.50 mol L^{-1}). Subsequently, 2-ethylbutyraldehyde **9** (12.4 g, 124 mmol, 1.65 eq.) and benzyl 11-isocyanidodecanoate **A1** (31.7 g, 105 mmol, 1.40 eq.) were added. The reaction was monitored *via* TLC and the solvent was evaporated under reduced pressure when completed (typically 2 to 3 days). The crude product was purified *via* column chromatography (cyclohexane/ethyl acetate 7:1 → 1:2 + 5.00% methanol). The product **10** was obtained as a dark colored oil (47.0 g, 74.5 mmol, 99%).

TLC: R_f (cyclohexane/ethyl acetate 5:1) = 0.00

^{1}H NMR (500 MHz, $CDCl_3$): δ (ppm) = 8.15, 8.05, 8.02 (m (cis + trans), 1H, C**H**ONH, ^{1}), 7.38 – 7.30 (m, 5H, C**H$_{aromatic}$**, ^{2}), 6.00 – 5.95 (m, 1H, CON**H**, ^{3}), 5.61 (bs, 1H, CHON**H**, ^{4}), 5.28 – 5.27 (d, *J* = 3.84 Hz, 1H, C**H**, ^{5}), 5.11 (s. 2H, C**H$_2$**, ^{6}), 3.30 – 3.18 (m, 4H, CONC**H$_2$**, CHONC**H$_2$**, ^{7}), 2.39 (t, 2H, *J* = 7.63 Hz, C**H$_2$**COOR, ^{8}), 2.34 (t, 2H, *J* = 7.55 Hz, C**H$_2$**COOBn, ^{9}), 1.87 – 1.81 (m, 1H, C**H**, ^{10}), 1.70 – 1.60 (m, 4H, C**H$_2$**, ^{11}), 1.54 – 1.16 (m, 35H, C**H$_2$**, ^{12}), 0.94 – 0.88 (m. 6H, C**H$_3$**, ^{12}).

^{13}C NMR (126 MHz, $CDCl_3$): δ (ppm) = 173.85, 173.82, 172.64, 172.62, 169.87, 169.84, 164.64, 161.27, 136.23, 128.67, 128.53, 128.30, 128.28, 75.16, 75.14, 66.21, 43.62, 43.59, 41.83, 41.14, 39.34, 38.30, 34.47, 34.45, 29.66, 29.65, 29.58, 29.51, 29.48, 29.46, 29.42, 29.39, 29.35, 29.29, 29.27, 29.24, 29.21, 29.18, 26.99, 26.92, 25.12, 25.09, 25.07, 22.35, 22.03, 11.75, 11.73, 11.70, 11.67.

HRMS (ESI) *m/z*: $[M + H]^+$ calcd for $C_{37}H_{62}N_2O_6$, 631.4681; found, 631.46741.

IR (ATR): ṽ (cm^{-1}) = 3292, 2925, 2854, 1737, 1660, 1533, 1457, 1382, 1232, 1160, 1109, 1049, 1010, 735, 697, 501, 456.

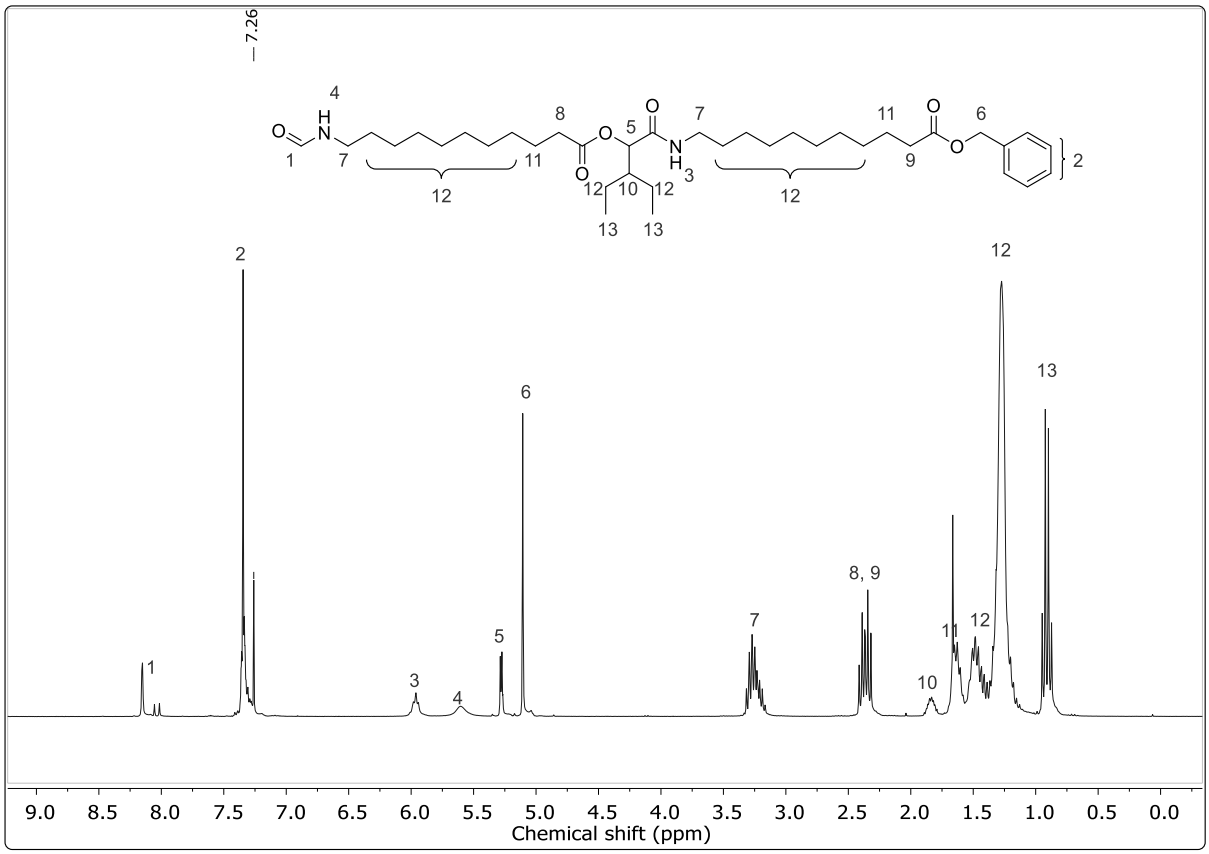

Benzyl 11-(3-ethyl-2-((11-isocyanoundecanoyl)oxy)pentanamido)undecanoate – Building Block A2

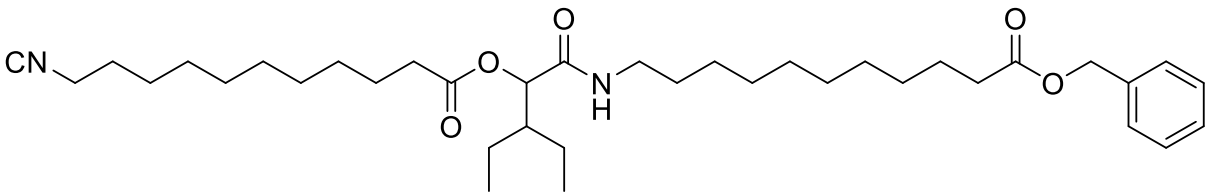

$C_{37}H_{60}N_2O_5$

612.90 g/mol

The formamide derivative **10** (47.0 g, 74.5 mmol, 1.00 eq.) was dissolved in 37.3 mL (1.50 mol L^{-1}) of DCM, then 18.1 mL pyridine (17.7 g, 224 mmol, 18.1 mmol, 3.00 eq.) were added. The solution was cooled with a water bath and subsequently 21.3 g *p*-TsCl (112 mmol, 1.50 eq) was added *via* a dropping funnel. Then, the reaction mixture was stirred for 1 h, while maintaining room temperature. After the reaction was finished (TLC control), cooling was applied and 75 mL of aqueous sodium carbonate solution (20%) was added slowly. The mixture was stirred for another 30 minutes, when another 50 mL of water and 50 mL DCM were added. Afterwards, sodium chloride was added to the aqueous phase and then extracted with DCM (3 × 50 mL). Afterwards, the combined organic phases were washed with brine (3 × 100 mL). The aqueous phase was tested by TLC, if further product was remaining inside, it was extracted with another 50 mL of DCM. The organic phase was dried over sodium sulfate and filtrated. Then the solvent was evaporated under reduced pressure to yield the crude isocyanide, which was purified *via* column chromatography (cyclohexane/ethyl acetate 4:1). The product **11**/**A2** was obtained as a colorless oil (38.8 g, 63.3 mmol, 85%).

TLC: R_f (cyclohexane/ethyl acetate 3:1) = 0.42

^{1}H NMR (500 MHz, $CDCl_3$): δ (ppm) = 7.38 – 7.30 (m, 5H, C**H**$_{\textbf{aromatic}}$, [1]), 5.94 (t, 1H, *J* = 5.61 Hz, CON**H**, [2]), 5.28 (d, 1H, *J* = 3.84 Hz, C**H**, [3]), 5.11 (s. 2H, C**H$_2$**, [4]), 3.37 (tt, 2H, *J* = 6.69, 1.88 Hz, CNC**H$_2$**, [5]), 3.25 (dp, 2H, *J* = 19.1, 6.08 Hz, CONHC**H$_2$**, [6]), 2.39 (t, 2H, *J* = 7.63 Hz, C**H$_2$**COOR, [7]), 2.34 (t, 2H, *J* = 7.55 Hz, C**H$_2$**COOBn, [8]), 1.87 – 1.81 (m, 1H, C**H**, [9]), 1.70 – 1.60 (m, 6H, C**H$_2$,** [10]), 1.50 – 1.16 (m, 30H, C**H$_2$**, [11]), 0.94 – 0.88 (m. 6H, C**H$_3$**, [12]).

^{13}C NMR (126 MHz, $CDCl_3$): δ (ppm) = 173.80, 172.57, 169.83, 155.75, 155.70, 155.66, 136.24, 128.66, 128.28, 75.12, 66.19, 43.62, 41.73, 41.68, 39.32, 34.46,

34.44, 29.67, 29.57, 29.47, 29.41, 29.33, 29.30, 29.23, 29.22, 29.19, 28.78, 26.98, 26.41, 25.12, 25.06, 22.35, 22.03, 11.75, 11.70.

HRMS (ESI) *m/z*: $[M + H]^+$ calcd for $C_{37}H_{60}N_2O_5$, 613.4575; found, 613.4575.

IR (ATR): $\tilde{\nu}$ (cm^{-1}) = 3340, 2926, 2855, 2147, 1737, 1660, 1530, 1456, 1379, 1160 1109, 1004, 735, 697.

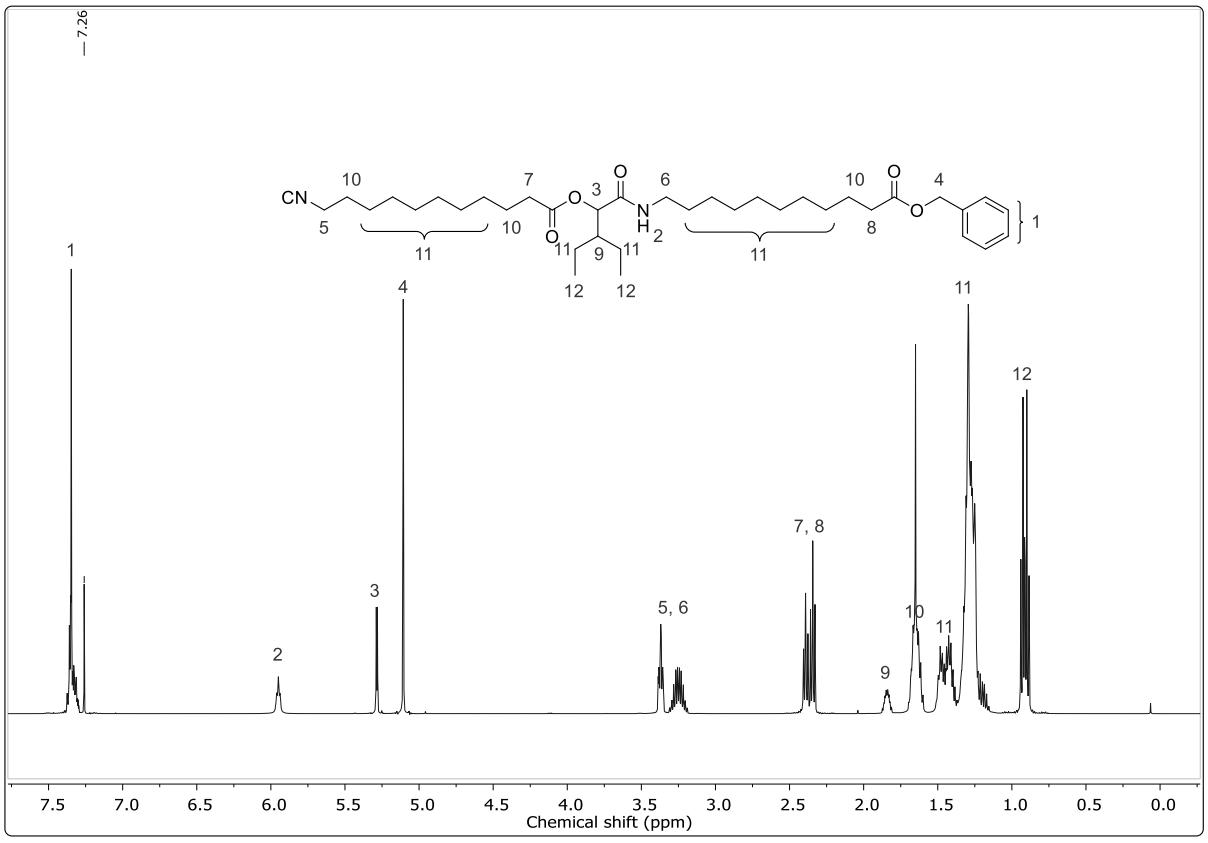

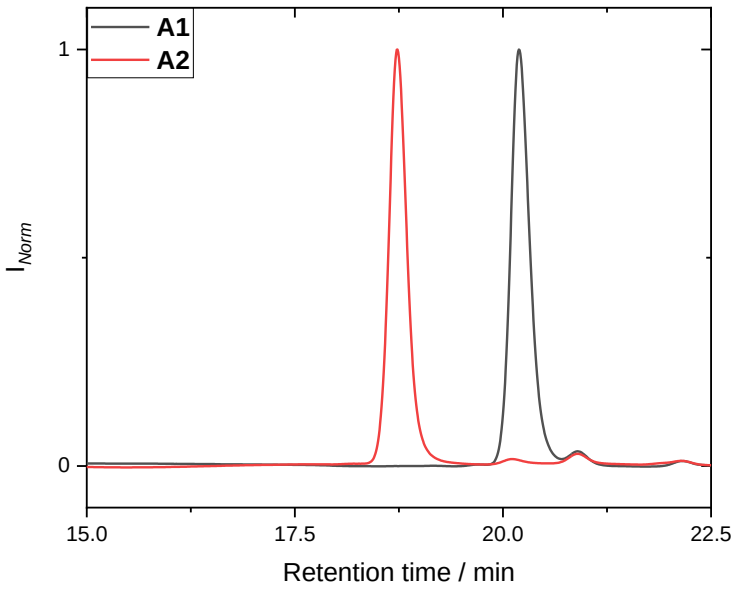

Figure S 3: SEC traces of the building blocks **A1** and **A2** measured in THF.

6-Formamidohexanoic acid

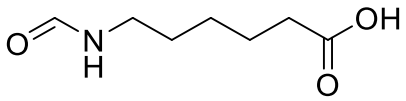

$C_7H_{13}NO_3$

M = 159.19 g/mol

6-Aminohexanoic acid **37** (6.56 g, 50.0 mmol, 1.00 eq.) was placed in a round-bottom flask. Ethyl formate (37.0 g, 500 mmol, 40.4 mL, 10.0 eq.) and 20 mL of DMF were added and the suspension was heated at 75 °C and stirred until it became clear (24 h). After the reaction was finished, the solvent was removed under reduced pressure and the product was used without further purification. The product **38** was obtained as white solid (7.96 g, 50.0 mmol, quant. yield).

^{1}H NMR (500 MHz, DMSO-d_6): δ (ppm) = 11.99 (bs, 1H, COO**H**, ^{1}), 7.98 – 7.90 (m. 1H, NHCO**H**, ^{2}), 7.96 (bs, 1H, CHON**H**, ^{3}), 3.07 – 3.03 (m, 2H, CONHC**H$_2$**, ^{4}), 2.19 (t, *J* = 7.38 Hz, 2H, C**H$_2$**COOH, ^{5}), 1.48 (p, *J* = 7.43 Hz, 2H, C**H$_2$**, ^{6}), 1.39 (p, *J* = 7.25 Hz, 2H, C**H$_2$**, ^{7}), 1.26 (m, 2H, C**H$_2$**, ^{8}).

^{13}C NMR (126 MHz, DMSO-d_6): δ (ppm) = 174.43, 160.86, 36.92, 33.60, 28.76, 25.92, 24.17.

HRMS (FAB) *m/z*: [M] calcd for $C_7H_{13}NO_3$, 159.0895; found, 159.0889.

IR (ATR): $\tilde{\nu}$ (cm^{-1}) = 3324, 2940, 2870, 2477, 1913, 1690, 1627, 1528, 1480, 1437, 1414, 1361, 1299, 1260, 1226, 1199, 1102, 988, 900, 841, 789, 741, 687, 669, 534.

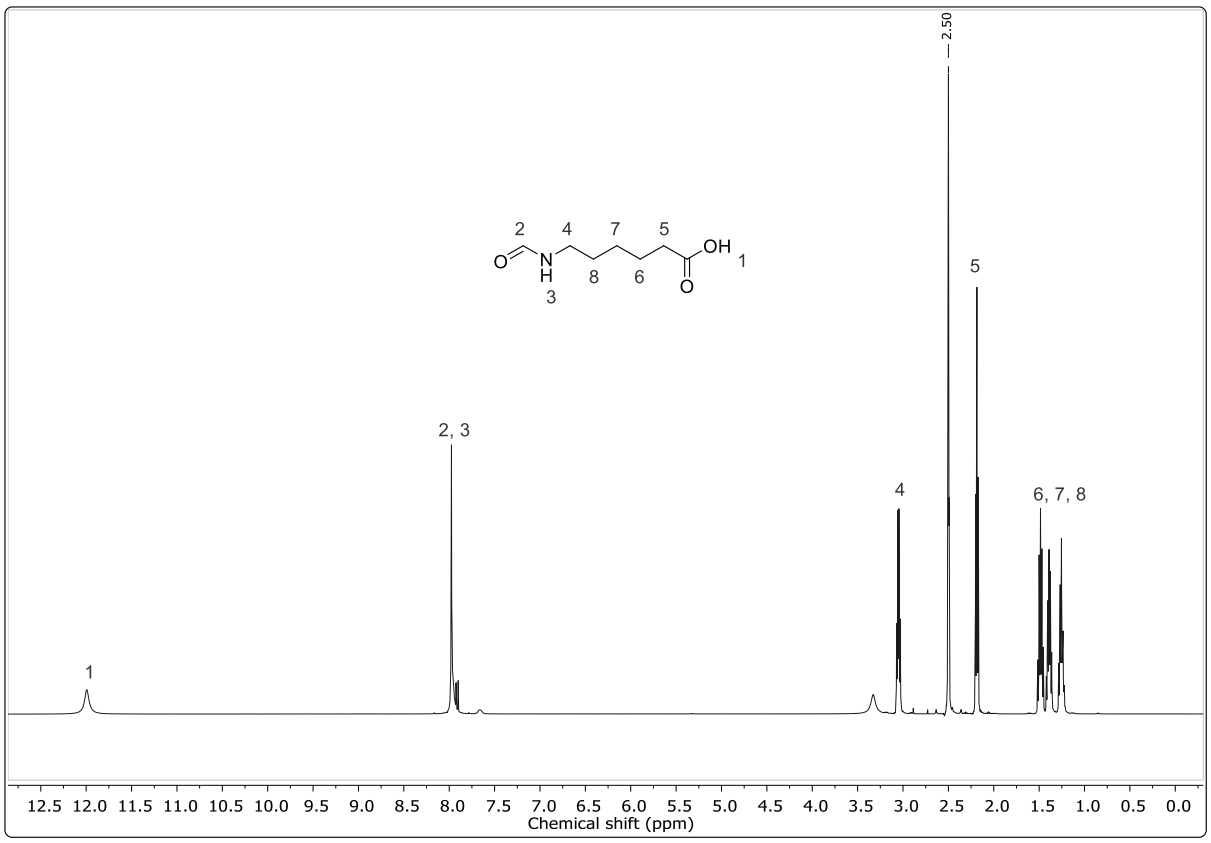

15-Hydroxypentadecanoic acid

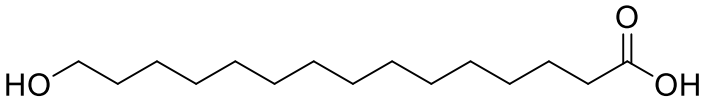

$C_{15}H_{30}O_3$

M = 258.4 g/mol

24.0 g ω-Pentadecalactone **27** (100 mmol, 1.00 eq.) were dissolved 200 mL ethanol. Then 6.00 g sodium hydroxide (150 mmol, 1.50 eq.) in 150 mL water were added to the solution. The reaction was stirred overnight at 50 °C and controlled *via* TLC. Afterwards the ethanol was evaporated under reduced pressure. The remaining solution was acidified up to a pH value of 2 with 3M hydrochloric acid. Afterwards the precipitate was collected, washed with water and dried on air. The crude product **28** was stored in the freezer and used as obtained (22.2 g, 86.0 mmol, 86%).

TLC: R_f (dichloromethane/ethyl acetate 95:5) = 0.28

^{1}H NMR (500 MHz, DMSO-d_6): δ (ppm) = 11.96 (bs, 1H, COO**H**, ^{1}), 4.32 (bs, 1H, O**H**, ^{2}), 3.39 – 3.33 (m, 2H, C**H$_2$**OH, ^{3}), 2.17 (t, *J* = 7.37 Hz, 2H, C**H$_2$**CO, ^{4}), 1.51 – 1.44 (m, 2H, HOOCCH$_2$C**H$_2$**, ^{5}), 1.42 – 1.36 (m, 2H, HOCH$_2$C**H$_2$**, ^{6}), 1.28 – 1.20 (m, 20H, C**H$_2$**, ^{7}).

^{13}C NMR (126 MHz, DMSO-d_6): δ (ppm) = 174.50, 60.74, 33.68, 32.58, 29.16, 29.09, 29.05, 29.01, 28.97, 28.80, 28.59, 25.55, 24.52.

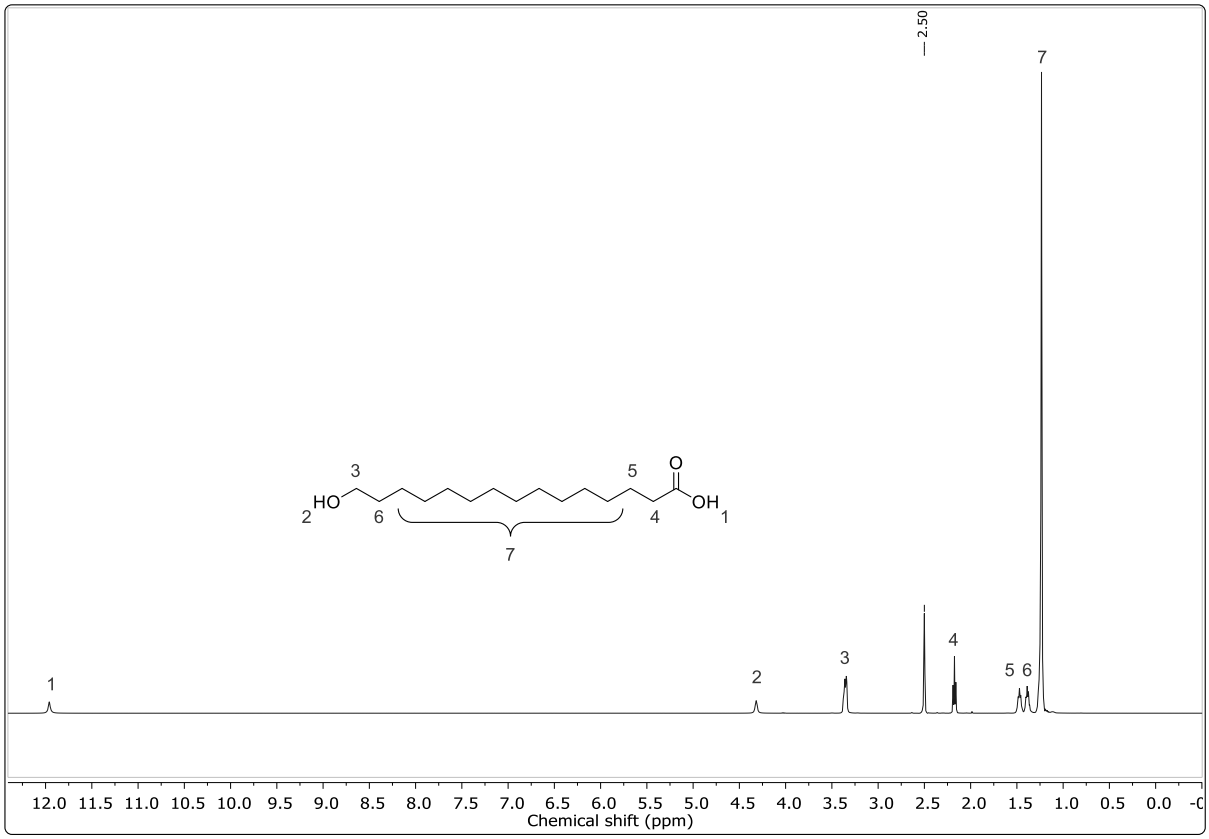

Benzyl 15-hydroxypentadecanoate

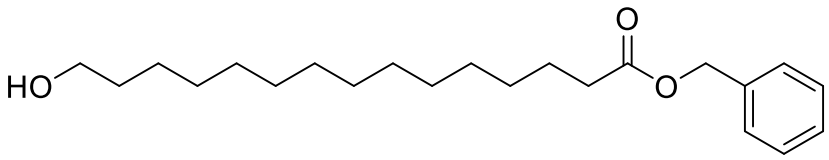

$C_{22}H_{36}O_3$

M = 348.53 g/mol

21.9 g 15-Hydroxypentadecanoic acid **28** (85.0 mmol, 1.00 eq.) were suspended in 75 mL DCM and 12.9 g DBU (12.7 mL, 85.0 mmol, 1.00 eq) were added. Afterwards 12.1 g benzyl bromide (17.4 mmol, 12.1 mL, 1.20 eq.) dissolved in DCM (25 mL) were added while maintaining the temperature. After addition of the benzyl bromide, the solution stirred until the reaction was completed. Afterwards, 200 mL water were

added, the phases were separated, and the aqueous phase was extracted 3 times with 75 mL DCM. The organic phases were dried over sodium sulfate and the solvent was removed under reduced pressure. The product was purified *via* recrystallization in methanol (ca. 400 mL). After filtration the filter cake was washed three times with 50 mL ice cold methanol. The pure product **29** was obtained as white solid (28.4 g, 81.5 mmol, 96%).

TLC: R_f (cyclohexane/ethyl acetate 5:1) = 0.41

^{1}H NMR (500 MHz, $CDCl_3$): δ (ppm) = 7.38 – 7.30 (m, 5H, C**H**$_{\textbf{aromatic}}$, ^{1}), 5.11 (s, 2H, C**H**$_2$, ^{2}), 3.63 (t, *J* = 6.65 Hz, 2H, C**H**$_2$OH, ^{3}), 2.35 (t, *J* = 7.56 Hz, 2H, C**H**$_2$COOBn, ^{4}), 1.64 (p, *J* = 7.34 Hz, 2H, C**H**$_2$CH$_2$COOBn, ^{5}), 1.64 (p, *J* = 7.67 Hz, 2H, C**H**$_2$CH$_2$OH, ^{6}), 1.34 – 1.25 (m, 20H, C**H**$_2$, ^{7}).

^{13}C NMR (126 MHz, $CDCl_3$): δ (ppm) = 173.87, 136.24, 128.66, 128.29, 66.20, 63.21, 34.47, 32.94, 29.74, 29.71, 29.69, 29.56, 29.37, 29.26, 25.87, 25.09.

HRMS (ESI) *m/z*: $[M + H]^+$ calcd for $C_{22}H_{36}O_3$, 349.2737; found, 349.2735.

IR (ATR): ṽ (cm^{-1}) = 3350, 2916, 2848, 1734, 1496, 1472, 1462, 1414, 1390, 1355, 1340, 1319, 1284, 1263, 1239, 1217, 1189, 1164, 1115, 1073, 1041, 1010, 962, 924, 886, 843, 807, 776, 746, 730, 697, 589, 537, 501, 459, 420.

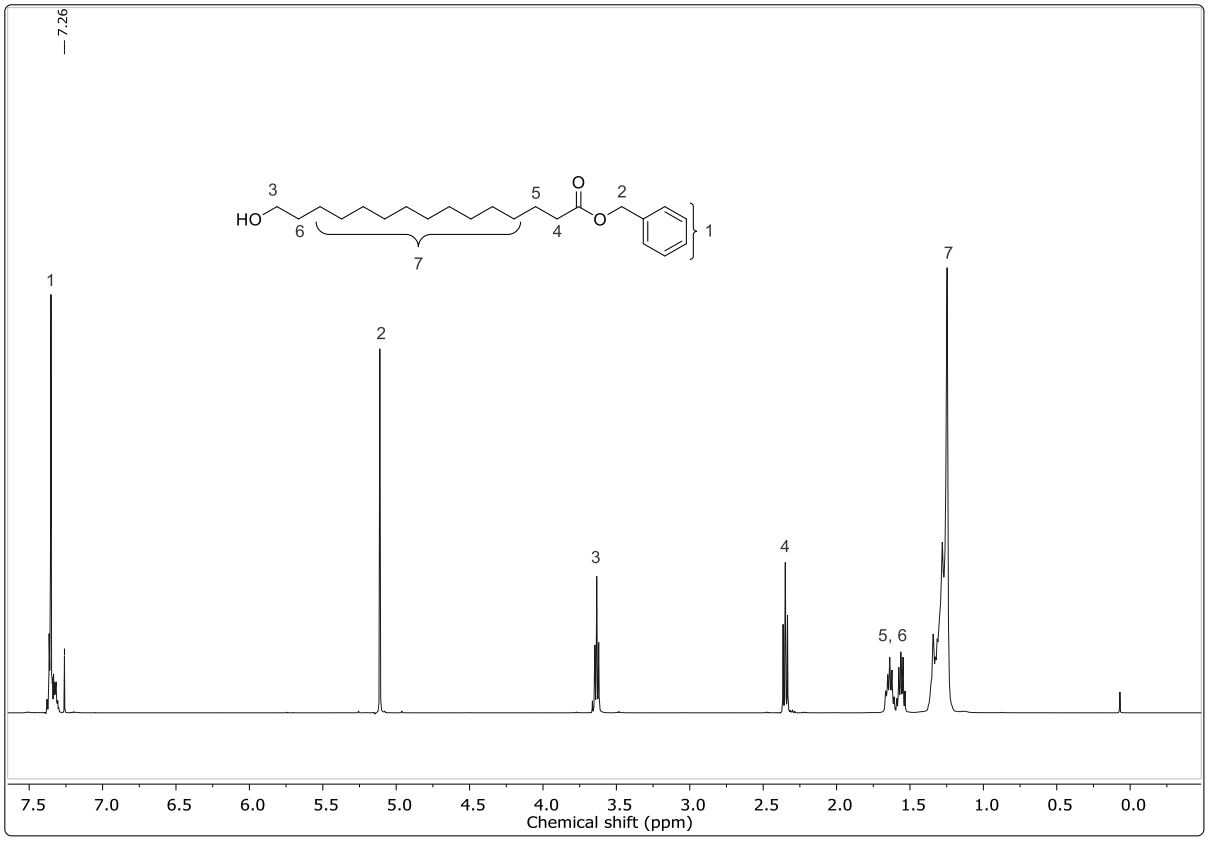

Benzyl 15-oxopentadecanoate – Building block F1

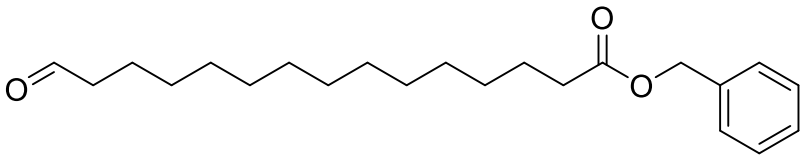

$C_{22}H_{34}O_3$

M = 346.51 g/mol

16.2 g PCC (75.0 mmol, 1.50 eq.) and 16.2 g Celite® (100 weight%) were suspended in 84.5 mL DCM. Cooling was applied (0 °C), then a solution of benzyl 15-hydroxypentadecanoate **29** (17.4 g, 50.0 mmol, 1.00 eq.) in 75 mL DCM was added. The reaction was stirred for 2.5 h, then diluted with 100 mL EtO_2 and filtrated through a short pad of SiO_2. The filter cake was thoroughly rinsed with Et_2O (4 × 100 mL). Afterwards the solvent was evaporated under reduced pressure and the crude product was purified *via* column chromatography (cyclohexane/ethyl acetate 7:1). The pure product **30**/**F1** was obtained as white solid (12.2 g, 33.5 mmol, 67%).

TLC: R_f (cyclohexane/ethyl acetate 5:1) = 0.61

^{1}H NMR (500 MHz, $CDCl_3$): δ (ppm) = 9.76 (t, *J* = 1.88 Hz, 1H, C**H**O, [1]), 7.38 – 7.30 (m, 5H, C**H**$_{\text{aromatic}}$, [2]), 5.11 (s, 2H, C**H$_2$**, [3]), 2.41 (td, *J* = 7.38, 1.88 Hz, 2H, C**H$_2$**CHO, [4]), 2.35 (t, *J* = 7.55 Hz, 2H, C**H$_2$**CO, [5]), 1.67 – 1.59 (m, 4H, C**H$_2$**, [6]), 1.30 – 1.25 (m, 18H, C**H$_2$**, [7]).

^{13}C NMR (126 MHz, $CDCl_3$): δ (ppm) = 203.09, 173.83, 136.27, 128.66, 128.52, 128.28, 66.18, 44.05, 34.55, 34.47, 29.76, 29.74, 29.71, 29.68, 29.61, 29.59, 29.56, 29.55, 29.48, 29.42, 29.39, 29.37, 29.30, 29.26, 25.09, 22.22.

HRMS (ESI) *m/z*: $[M + H]^+$ calcd for $C_{22}H_{34}O_3$, 347.2581; found, 347.2584.

IR (ATR): ṽ (cm^{-1}) = 2914, 2849, 2740, 1726, 1711, 1499, 1472, 1411, 1389, 1362, 1338, 1296, 1268, 1247, 1224, 1195, 1168, 1102, 1078, 1047, 988, 892, 744, 717, 695, 662, 578, 494, 457, 425.

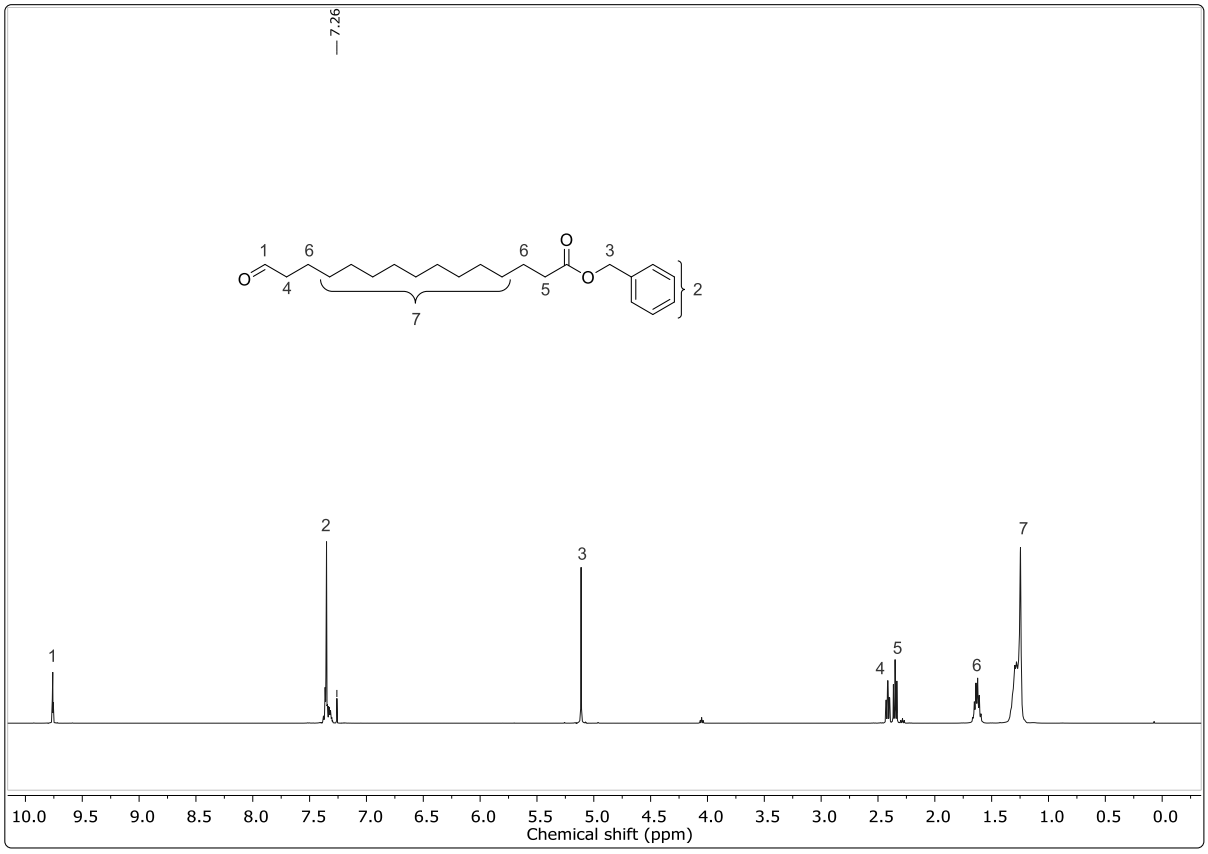

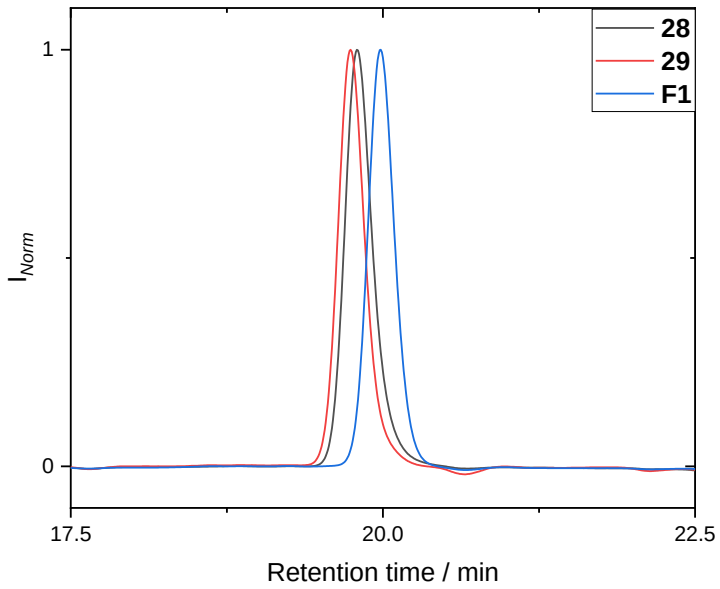

Figure S 4: SEC traces of building block **F1** and its precursors **28** and **29** measured in THF.

Mono methyl tetra(ethylene glycol) tosylat – Me-4EG-Tos

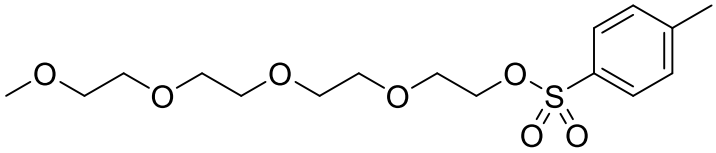

$C_{16}H_{26}O_7S$

M = 362.44 g/mol

Tetra(ethylene glycol) monomethyl ether **32** (25.0 g, 27.1 mL, 120 mmol, 1.00 eq.) was dissolved in aqueous NaOH (10.1 g, 252 mmol, 50.4 mL, 2.10 eq./5 mol L^{-1}) and cooled to 0 °C. Then, *p*-TsCl (27.5 g, 144 mL, 1.20 eq.) in THF (62.5 mL) is slowly added into the mixture and stirred for 1 d. Afterwards, the reaction mixture was extracted with dichloromethane (3 × 150 mL). The organic phase is washed with brine (2 × 100 mL), dried over sodium sulfate and the solvent was evaporated. The crude product **33** was obtained as a yellowish oil (43.1 g, 119 mmol, 99%) and used without further purification. The analytical data is according to the literature.[363]

^{1}H NMR (500 MHz, $CDCl_3$): δ (ppm) = 7.78 (d, *J* = 8.33 Hz, 2H, C**H**$_{\mathbf{aromatic}}$, ^{1}), 7.33 (d, *J* = 7.98 Hz, 2H, C**H**$_{\mathbf{aromatic}}$, ^{2}), 4.15 – 4.13 (m, 2H, SOOOC**H**$_\mathbf{2}$, ^{3}), 3.68 – 3.66 (m, 2H, SOOOCH_2C**H**$_\mathbf{2}$, ^{4}), 3.63 – 3.52 (m, 12H, OC**H**$_\mathbf{2}$, ^{5}), 3.36 (s, 3H, OC**H**$_\mathbf{3}$, ^{6}), 2.43 (s, 2H, PhC**H**$_\mathbf{3}$, ^{7}).

^{13}C NMR (126 MHz, $CDCl_3$): δ (ppm) = 144.89, 133.09, 129.92, 128.08, 72.02, 70.83, 70.69, 70.68, 70.62, 69.35, 68.77, 59.13, 21.75.

HRMS (ESI) *m/z*: $[M + H]^+$ calcd for $C_{16}H_{26}O_7S$, 363.1472; found, 363.1468.

IR (ATR): ṽ (cm^{-1}) = 2872, 1598, 1452, 1353, 1292, 1248, 1189, 1175, 1095, 1016, 917, 816, 774, 706, 662, 582, 553.

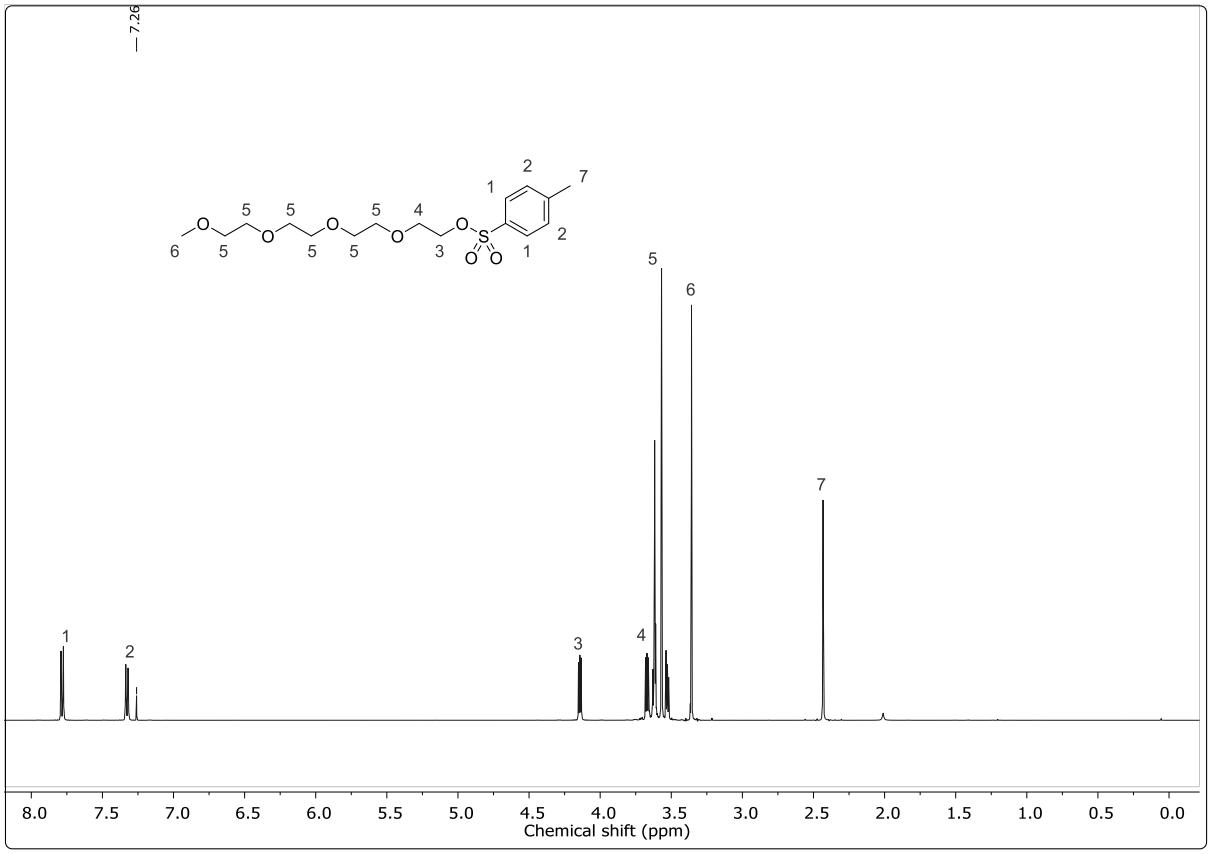

Mono methyl mono benzyl octa(ethylene glycol) – Me-8EG-Bn

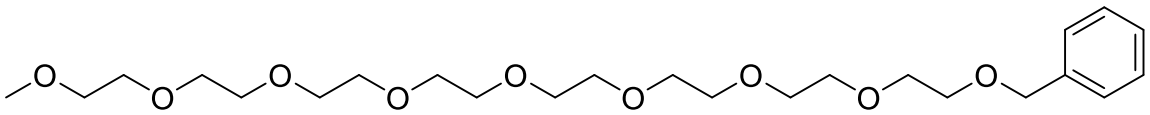

$C_{24}H_{42}O_9$

M = 474.59 g/mol

Monobenzyl tetra(ethylene glycol) **34** (24.2 g, 85.0 mmol, 1.00 eq.), dissolved in dry THF (130 mL), was added over 30 minutes to a solution of KO*t*Bu (13.4 g, 119 mmol, 1.40 eq.) in dry THF (120 mL) at 0 °C. Then, monomethyl tetra(ethylene glycol) tosylate **33** (33.9 g, 93.5 mmol, 1.10 eq.) in dry THF (85 mL) was added over three hours at the same temperature. The reaction mixture was gradually warmed up to room temperature and left stirring for 20 hours. The mixture was cooled again to 0 °C with an ice bath and the solution was neutralized with cold 1 M aqueous HCl. The solvent was evaporated and water (50 ml) was added to the residue. The product was extracted with DCM (5 × 100 mL). The combined organic layers were washed with brine (2 × 100 mL), dried over anhydrous sodium sulfate and filtered. After evaporation of the solvent, the crude product was purified *via* column chromatography

(cyclohexane/ethyl acetate 1:1 → ethyl acetate → ethyl acetate/methanol 25:2). The product **35** was obtained as yellow oil (28.7 g, 60.4 mmol, 71%).

^{1}H NMR (500 MHz, DMSO-*d*$_6$): δ (ppm) = 7.36 – 7.26 (m, 5H, C**H**$_{\mathbf{aromatic}}$, ^{1}), 4.49 (s, 2H, C**H**$_{\mathbf{2}}$, ^{2}), 3.59 – 3.54 (m, 4H, OCH$_2$OC**H**$_{\mathbf{2}}$OBn, OC**H**$_{\mathbf{2}}$OCH$_2$OBn, ^{3}), 3.53 – 3.41 (m, 28H, OC**H**$_{\mathbf{2}}$, ^{4}), 3.23 (s, 3H, OC**H**$_{\mathbf{3}}$, ^{5}).

^{13}C NMR (126 MHz, DMSO-*d*$_6$): δ (ppm) = 138.48, 128.20, 127.47, 127.35, 72.01, 71.27, 69.84, 66.79, 69.78, 69.58, 69.13, 58.04.

HRMS (ESI) *m/z*: $[M + H]^+$ calcd for $C_{24}H_{42}O_9$, 475.2902; found, 475.2890.

IR (ATR): ṽ (cm^{-1}) = 2864, 1454, 1350, 1297, 1248, 1200, 1095, 1028, 946, 850, 739, 699, 517.

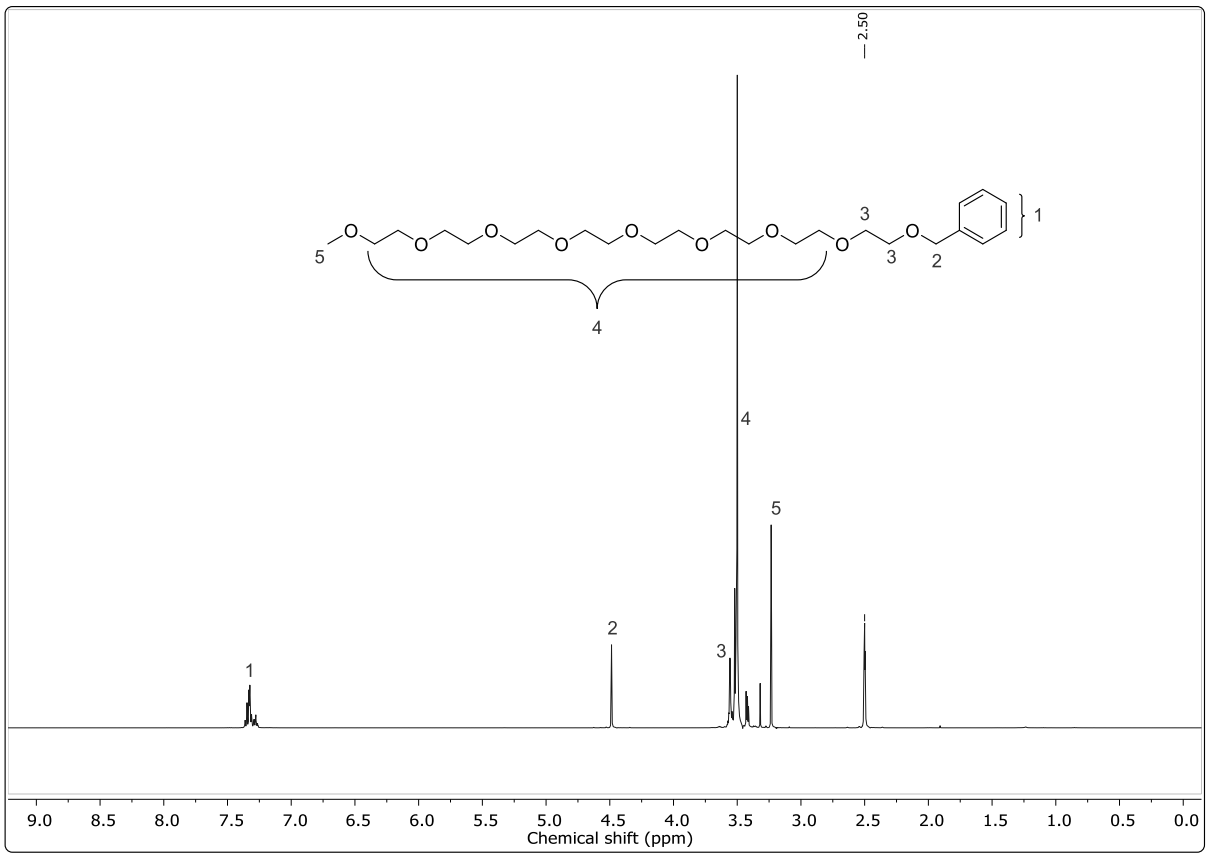

Mono methyl octa(ethylene glycol) – Me-8EG-OH

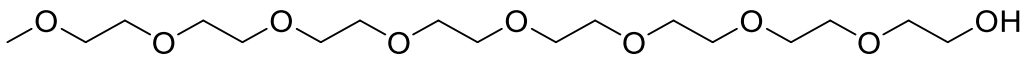

$C_{17}H_{36}O_9$

M = 384.47 g/mol

Benzyl protected octaethylene glycol **35** (26.6 g, 56.0 mmol, 1.00 eq.) and 10 wt% Pd on activated charcoal (2.66 g) were placed in a round bottom flask and dissolved in ethyl acetate, after vigorous stirring for a few minutes the solution was purged with hydrogen. Subsequently, the reaction was heated to reflux and stirred until the reactant was consumed completely. Then, the solution was allowed to cool down and filtered through Celite®. The solvent was evaporated, and the product was used as obtained. The product **36** was obtained as slightly yellowish oil (23.3 g, 55.4 mmol, 99%).

^{1}H NMR (500 MHz, DMSO-d_6): δ (ppm) = 4.57 (t, *J* = 5.50 Hz, 1H, O**H**, ^{1}), 3.52 – 3.40 (m, 32H, OC**H$_2$**, ^{2}), 3.23 (s, 3H, OC**H$_3$**, ^{3}).

^{13}C NMR (126 MHz, DMSO-d_6): δ (ppm) = 72.35, 71.28, 70.41, 69.82, 69.79, 69.58, 60.21, 58.05.

HRMS (ESI) *m/z*: $[M + H]^+$ calcd for $C_{17}H_{36}O_9$, 385.2432; found, 385.2420.

IR (ATR): ṽ (cm^{-1}) = 3471, 2866, 1454, 1349, 1296, 1249, 1199, 1096, 944, 849, 524.

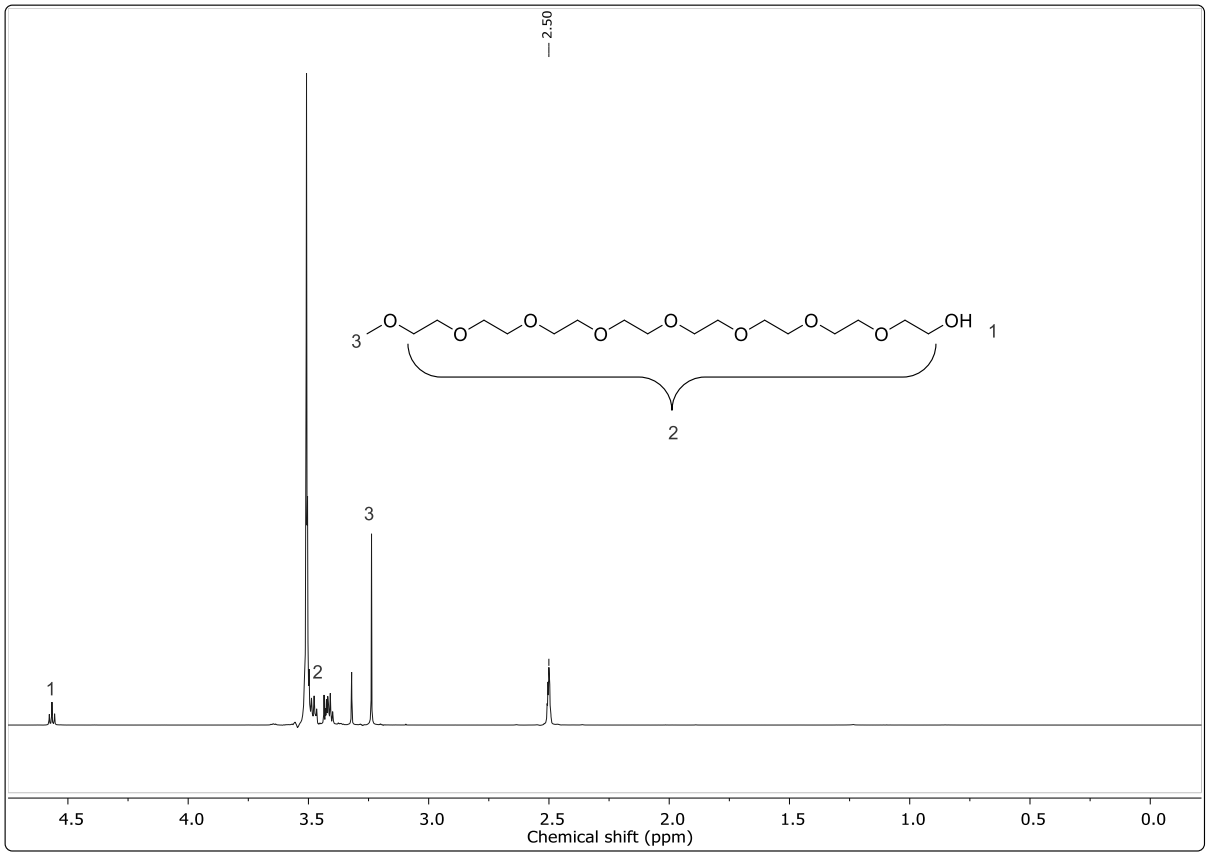

6-Isocyano (octa(ethylene glycol) mono methyl ether) hexanoate – Building Block B1

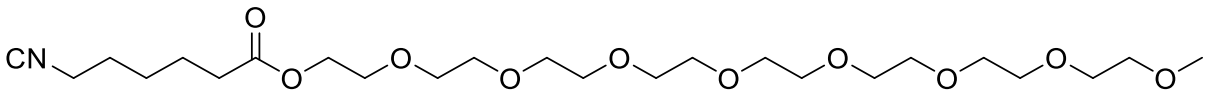

$C_{24}H_{45}NO_{10}$

M = 507.62 g/mol

HO-8EG-Me **36** (9.61 g, 25.0 mmol, 1.00 eq.), 6-formamidohexanoic acid **38** (4.97 g, 31.3 mmol, 1.25 eq.) and DMAP (305 mg, 2.50 mmol, 0.100 eq) were suspended in 30 mL of DCM (1 mol L^{-1}), then DCC (5.67 g, 27.5 mmol, 1.10 eq.) was added. The reaction was stirred overnight and monitored by SEC. After the reaction was finished, it was cooled to -18 °C and filtrated. The filter cake was washed with cold DCM (3 × 30 mL), then the organic phase was reduced to 30 mL. Afterwards, pyridine (5.93 g, 6.04 mL, 75.0 mmol, 3.00 eq.) and *p*-TsCl (7.15 g, 37.5 mmol, 1.50 eq.) were added and the reaction was stirred for another 2 h. Then, the reaction mixture was quenched with 40 mL of 20% sodium carbonate solution and stirred for 30 min. Another 50 mL of water and DCM were added, and the phases were separated. Subsequently, the aqueous phase was extracted with DCM (5 × 30 mL), combined,

dried over sodium sulfate and the solvent was evaporated under reduced pressure. The crude product was purified *via* column chromatography (cyclohexane/ethyl acetate 1:1 → ethyl acetate → ethyl acetate/methanol 20:1). The product **39**/**B1** was obtained as yellow oil (11.6 g, 22.9 mmol, 92%).

TLC: R_f (ethyl acetate/methanol 20:1) = 0.29

^{1}H NMR (500 MHz, DMSO-d_6): δ (ppm) = 4.12 (m, 2H, COOC**H$_2$**, ^{1}), 3.59 (m, 2H, COOCH$_2$C**H$_2$**, ^{2}), 3.54 – 3.42 (m, 30H, OC**H$_2$**, CNC**H$_2$**, ^{3}), 3.24 (s, 3H, OC**H$_3$**, ^{4}), 2.33 (t, *J* = 7.34 Hz, 2H, C**H$_2$**COOR, ^{5}), 1.55 (m, 4H, C**H$_2$**, ^{6}), 1.37 (m, 2H, C**H$_2$**, ^{7}).

^{13}C NMR (126 MHz, DMSO-d_6): δ (ppm) = 172.74, 155.46, 155.42, 155.37, 71.27, 69.78, 69.74, 69.58, 68.29, 63.10, 58.05, 41.05, 41.00, 40.96, 40.11, 40.02, 39.95, 39.85, 39.78, 39.69, 39.61, 39.52, 39.44, 39.35, 39.19, 39.02, 33.18, 28.09, 25.21, 23.56.

HRMS (ESI) *m/z*: $[M + H]^+$ calcd for $C_{24}H_{45}NO_{10}$, 508.3116; found, 508.3109.

IR (ATR): ṽ (cm^{-1}) = 2867, 2147, 1732, 1455 1350, 1248, 1097, 947, 850, 544.

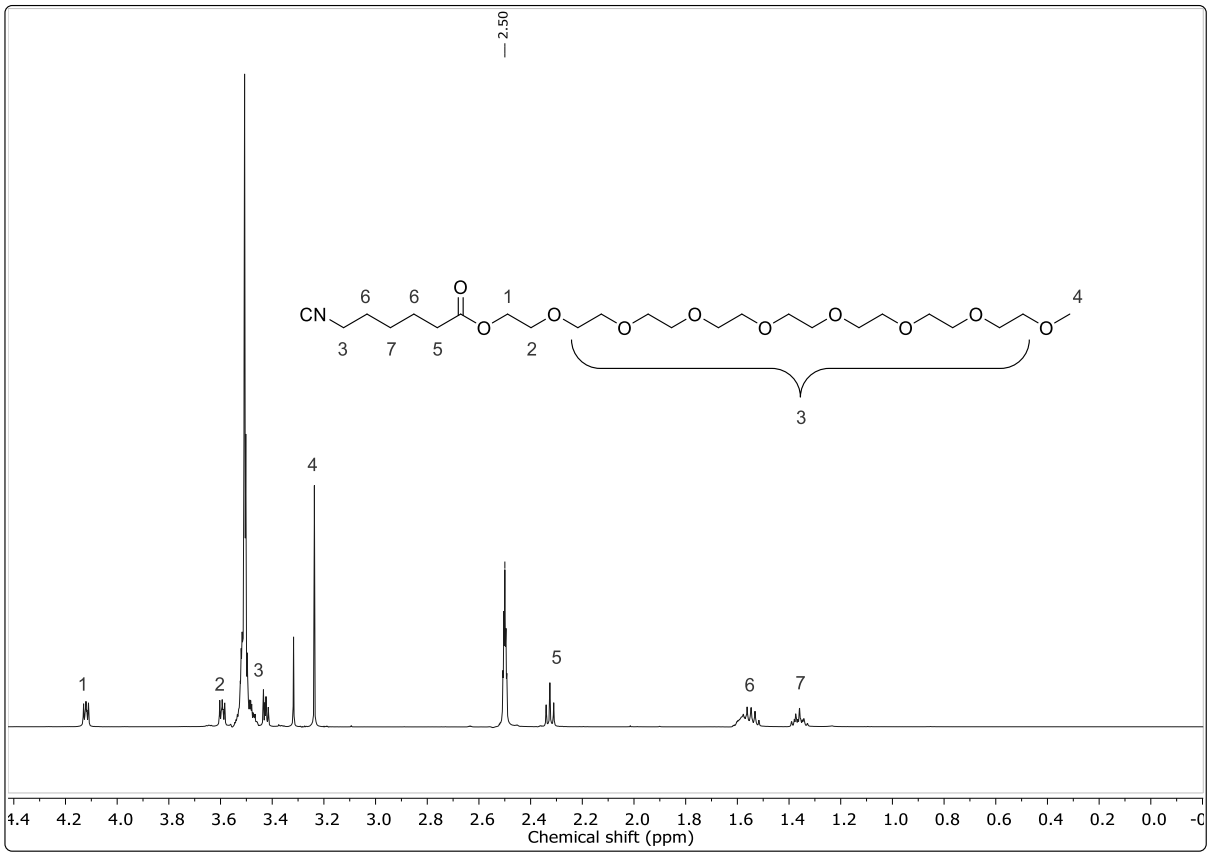

4-Formyl (octa(ethylene glycol) mono methyl ether) benzoate – Building Block B2

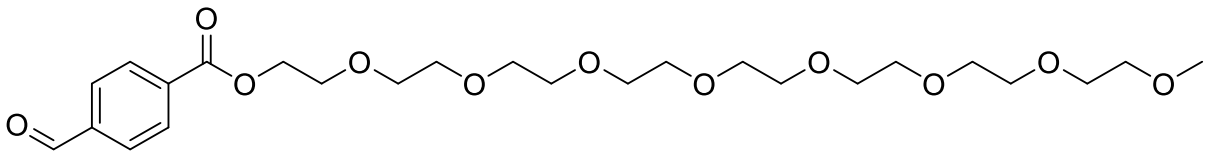

$C_{25}H_{40}O_{11}$

M = 516.58 g/mol

HO-8EG-Me **36** (9.61 g, 25.0 mmol, 1.00 eq.), formyl benzoic acid **40** (4.69 g, 31.3 mmol, 1.25 eq.) and DMAP (305 mg, 2.50 mmol, 0.100 eq) were suspended in 30 mL of DCM (1 mol/L), then DCC (5.67 g, 27.5 mmol, 1.10 eq.) was added. The reaction was stirred overnight monitored by SEC. After the reaction was finished, it was cooled to -18 °C and filtrated. The filter cake was washed with cold DCM (3 × 50 mL). The organic phase was reduced to 25 mL, then DIPEA (1.29 g, 10.0 mmol, 1.74 mL, 0.400 eq.) and propyl bromide (2.46 g, 20 mmol, 1.82 mL, 0.800 eq) were added and the reaction was stirred for another 1.5 h. Then, the organic phase was washed with brine (75 mL). The phases were separated, and the aqueous phase was extracted with DCM (5 × 30 mL). The product was purified *via* column chromatography (cyclohexane/ethyl acetate 1:1 → ethyl acetate → ethyl acetate/methanol 20:1). The product **41**/**B2** was obtained as slightly yellow oil (12.4 g, 24.0 mmol, 96%).

TLC: R_f (ethyl acetate/methanol 20:1) = 0.26

^{1}H NMR (500 MHz, DMSO-d_6): δ (ppm) = 10.12 (s, 1H, C**H**O, ^{1}), 8.16 (d, *J* = 8.20 Hz, 2H, C**H**$_{\textbf{aromatic}}$, ^{2}), 8.06 (d, *J* = 8.50 Hz, 2H, C**H**$_{\textbf{aromatic}}$, ^{3}), 4.43 (m, 2H, COOC**H**$_{\textbf{2}}$, ^{4}), 3.77 (m, 2H, COOCH$_2$C**H**$_{\textbf{2}}$, ^{5}), 3.61 – 3.41 (m, 28H, OC**H**$_{\textbf{2}}$, ^{6}), 3.23 (s, 3H, OC**H**$_{\textbf{3}}$, ^{7}).

^{13}C NMR (126 MHz, DMSO-d_6): δ (ppm) = 192.97, 164.99, 139.16, 134.35, 129.85, 129.67, 71.26, 69.86, 69.80, 69.76, 69.57, 68.21, 64.58, 58.04.

HRMS (ESI) *m/z*: $[M + H]^+$ calcd for $C_{25}H_{40}O_{11}$, 517.2643; found, 517.2638.

IR (ATR): $\tilde{\nu}$ (cm^{-1}) = 2867, 1721, 1703, 1577, 1453, 1350, 1272, 1201, 1092, 946, 853, 760, 689, 513.

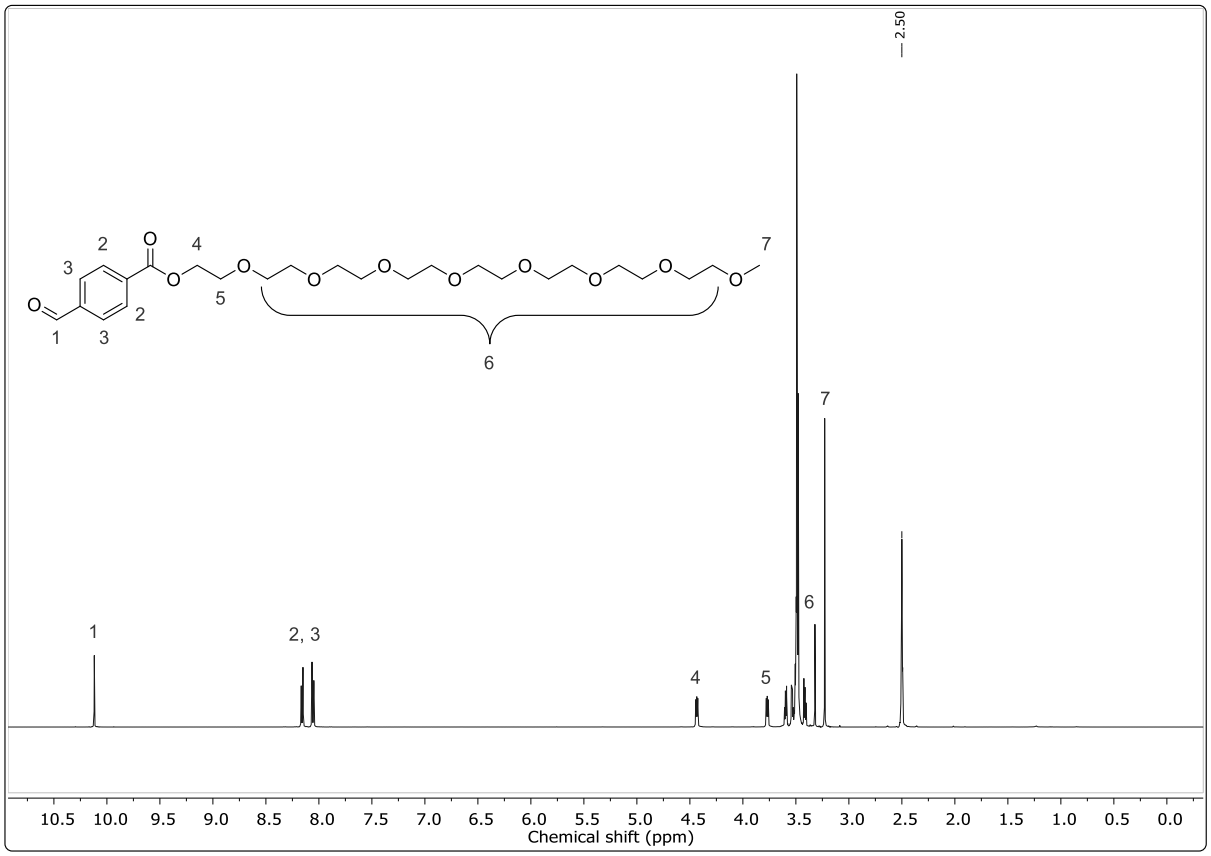

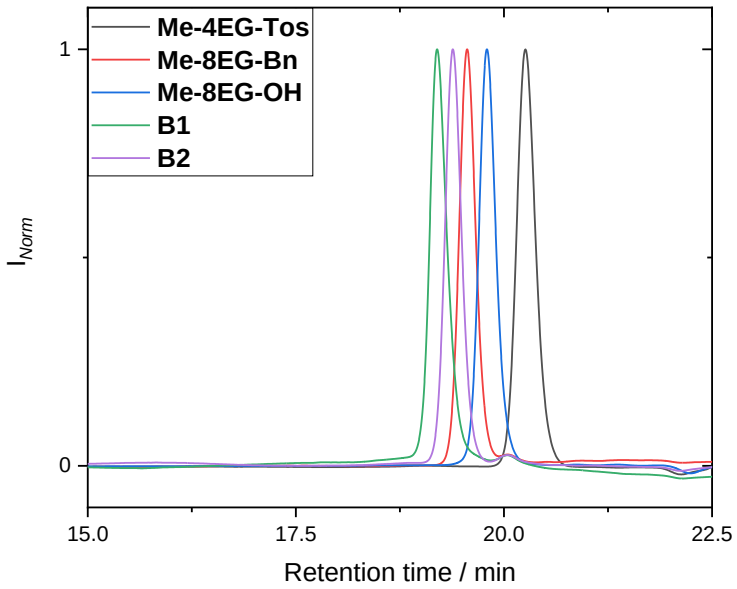

Figure S 5: SEC traces of the uniform oligo(ethylene glycol)s and the building blocks **B1** and **B2** measured in THF.

6.3.3.2 Star-shaped macromolecules *via* the core-first approach

Star-shaped macromolecule CF-H1-1

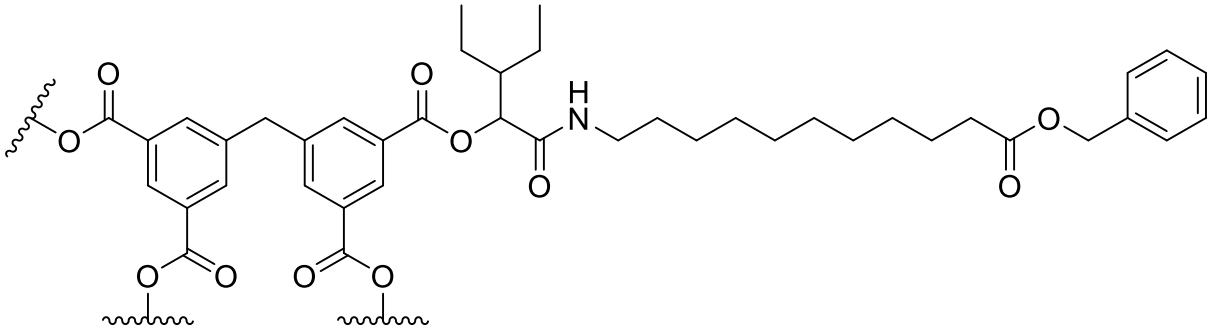

$C_{117}H_{168}N_4O_{20}$

M = 1950.64 g/mol

5,5'-Methylendiisophtalic acid **H1** (500 mg, 1.45 mmol, 1.00 eq.) were placed in a round bottom flask and dissolved in 4.50 mL THF, after vigorous stirring for a few minutes the solution was purged with Argon. Subsequently, benzyl 11-isocyanidodecanoate (building block **A1**) (3.50 g, 11.6 mol, 8.00 eq.) and 2-ethylbutanal **9** (1.55 g, 15.5 mmol, 1.93 mL, 10.7 eq.) were added. After the reaction was completed (18 h) the solvent was evaporated under reduced pressure. Then the crude product was purified *via* column chromatography (cyclohexane/ethyl acetate 4:1 → 5:2) and dried *in vacuo*. The product **CF-H1-**1 was obtained as a viscous colorless oil (2.69 g, 1.38 mmol, 99%).

TLC: R_f (cyclohexane/ethyl acetate 2:1) = 0.44

^{1}H NMR (500 MHz, $CDCl_3$): δ (ppm) = 8.60 (s, 2H, C**H**$_{\textbf{aromatic}}$, ^{1}), 8.58 (s, 1H, C**H**$_{\textbf{aromatic}}$, ^{1}), 8.11 (s, 4H, C**H**$_{\textbf{aromatic}}$, ^{2}), 7.37 – 7.29 (m. 20H, C**H**$_{\textbf{aromatic}}$, ^{3}), 6.00 – 5.96 (m, 4H, CON**H**, ^{4}), 5.46 (d, *J* = 3.61 Hz, 2H,C**H**, ^{5}), 5.42 (d, *J* = 3.83 Hz, 2H, C**H**, ^{5}), 5.10 (s, 8H, C**H$_2$**, ^{6}), 4.23 (s. 2H, C**H$_2$**, ^{7}), 3.35 – 3.18 (m, 8H, CONHC**H$_2$**, ^{8}), 2.33 (t, *J* = 7.55 Hz, 8H, C**H$_2$**COOBn, ^{9}), 2.02 – 1.95 (m, 4H, C**H**, ^{10}), 1.65 – 1.23 (m, 80H, C**H$_2$**, ^{11}), 0.97 – 0.94 (m, 24H, C**H$_3$**, ^{12}).

^{13}C NMR (126 MHz, $CDCl_3$): δ (ppm) = 173.81, 169.24, 169.22, 164.62, 164.53, 141.32, 141.25, 141.23, 136.21, 135.32, 130.81, 130.81, 130.78, 130.76, 129.11, 128.99, 128.65, 128.51, 128.37, 128.28, 128.27, 76.57, 76.49, 76.46, 66.19, 43.76, 43.78, 43.74, 43.67, 40.96, 39.58, 39.55, 34.42, 29.73, 29.71, 29.56, 29.46, 29.33, 29.30, 29.22, 27.03, 26.96, 25.05, 22.59, 22.49, 22.25, 22.19, 11.81, 11.78, 11.75, 11.72.

HRMS (ESI) *m/z*: $[M + H]^+$ calcd for $C_{117}H_{168}N_4O_{20}$, 1950.2325; found, 1950.2343.

IR (ATR): $\tilde{\nu}$ (cm^{-1}) = 3308, 2926, 2854, 1727, 1653, 1538, 1456, 1223, 1187, 1002, 750, 697, 577.

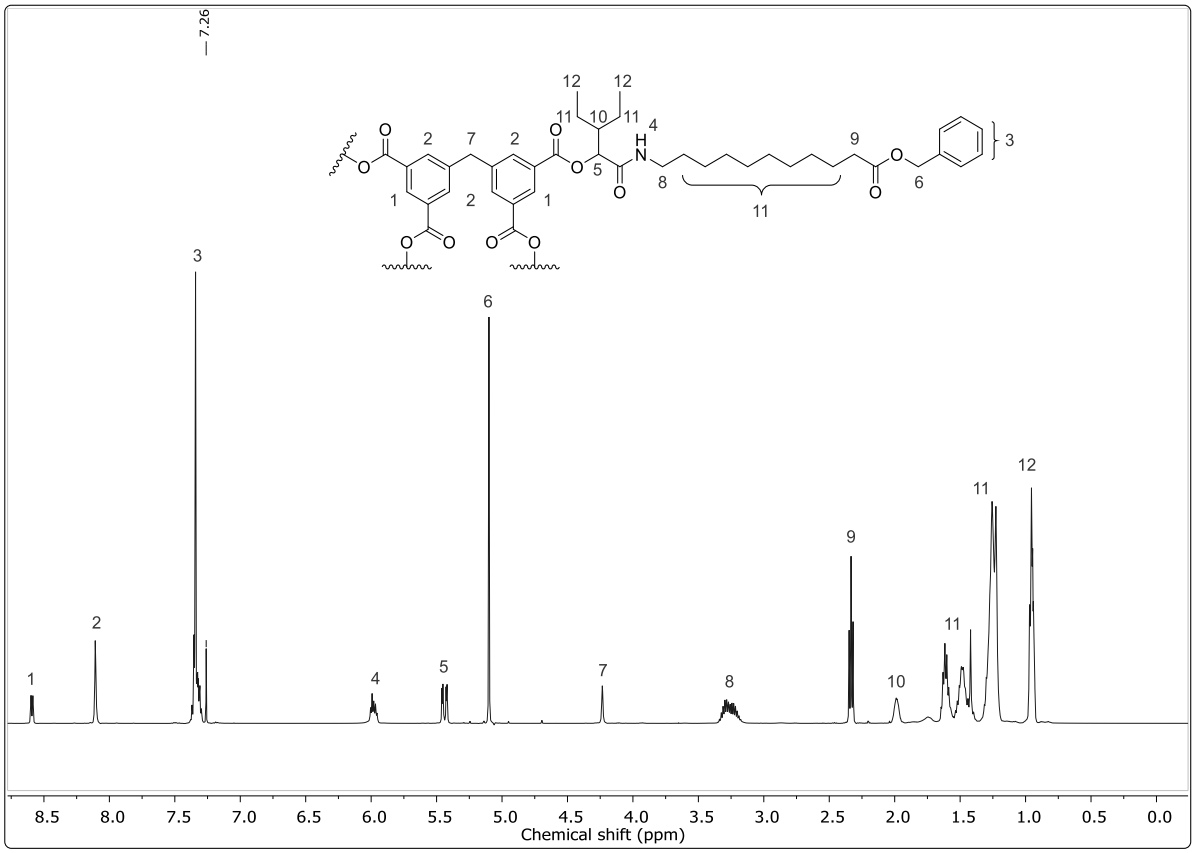

Deprotected star-shaped macromolecule CF-H1-1$_b$

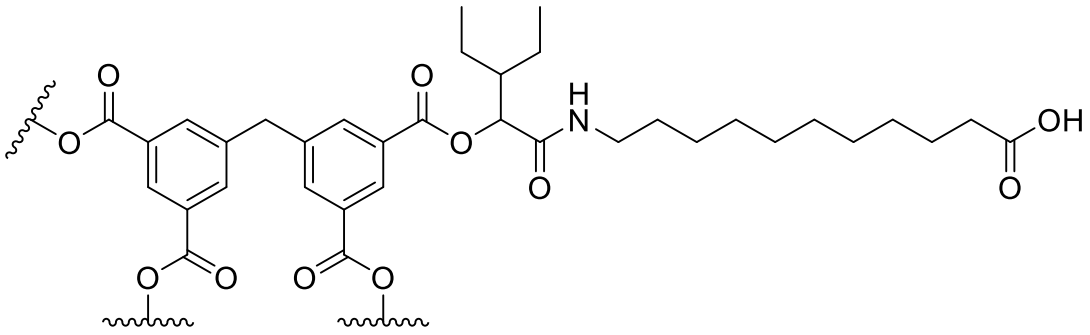

$C_{89}H_{144}N_4O_{20}$

M = 1590.14 g/mol

Benzyl protected star molecule **CF-H1-1** (2.57 g, 1.32 mmol, 1.00 eq.) and 10wt% Pd on Carbon (257 mg) were placed in a round bottom flask and dissolved in ethyl acetate, after vigorous stirring for a few minutes the solution was purged with Hydrogen. The reaction was controlled *via* TLC until no benzyl protected starting material was left. The

solution was dried over Sodium sulfate and filtered through Celite®. Subsequently, the solvent was evaporated under reduced pressure and the residue was dried *in vacuo*. The product **CF-H1-1$_b$** was obtained as a yellowish foam (2.08 g, 1.31 mmol, 99%).

TLC: R_f (cyclohexane/ethyl acetate 2:1) = 0.00

^{1}H NMR (500 MHz, $CDCl_3$): δ (ppm) = 10.45 (bs, 4H, COO**H**, [1]), 8.61 – 8.55 (s, 2H, C**H**$_{aromatic}$, [2]), 8.13 – 8.07 (s, 4H, C**H**$_{aromatic}$, [3]), 6.78 – 6.58 (bs, 2H, CON**H**, [4]), 6.18 (t, *J* = 5.35 Hz, 1H, CON**H**, [4]), 6.07 (t, *J* = 5.35 Hz, 1H, CON**H**, [4]), 5.46 (d, *J* = 3.62 Hz, 1H, C**H**, [5]), 5.44 (d, *J* = 3.71 Hz, 1H, C**H**, [5]), 5.39 (bs, 2H, C**H**, [5]), 4.25 (s. 2H, C**H$_2$**, [6]), 3.35 – 3.09 (m, 8H, CONHC**H$_2$**, [7]), 2.33 – 2.26 (m, 8H, C**H$_2$**COOH, [8]), 2.05 – 1.92 (m, 4H, C**H**, [9]), 1.61 – 1.24 (m, 80H, C**H$_2$**, [10]), 0.97 – 0.94 (m, 24H, C**H$_3$**, [11]).

^{13}C NMR (125 MHz, $CDCl_3$): δ (ppm) = 179.28, 179.13, 178.85, 169.61, 169.51, 164.66, 164.60, 135.37, 130.81, 130.73, 129.23, 100.12,76.55, 43.71, 39.60, 34.25, 34.10, 29.86, 29.56, 29.43, 29.32, 29.29, 29.25, 29.13, 29.09, 29.07, 28.86, 26.98, 26.81, 24.87, 24.74, 22.55, 22.50, 22.23, 22.19, 11.82, 11.79, 11.77, 11.72.

HRMS (ESI) *m/z*: $[M + H]^+$ calcd for $C_{89}H_{144}N_4O_{20}$, 1590.0447; found, 1590.0415.

IR (ATR): ṽ (cm^{-1}) = 3305, 2925, 2855, 1726, 1646, 1541, 1459, 1294, 1222, 1188, 1128, 1107, 1004, 944, 751, 721, 654.

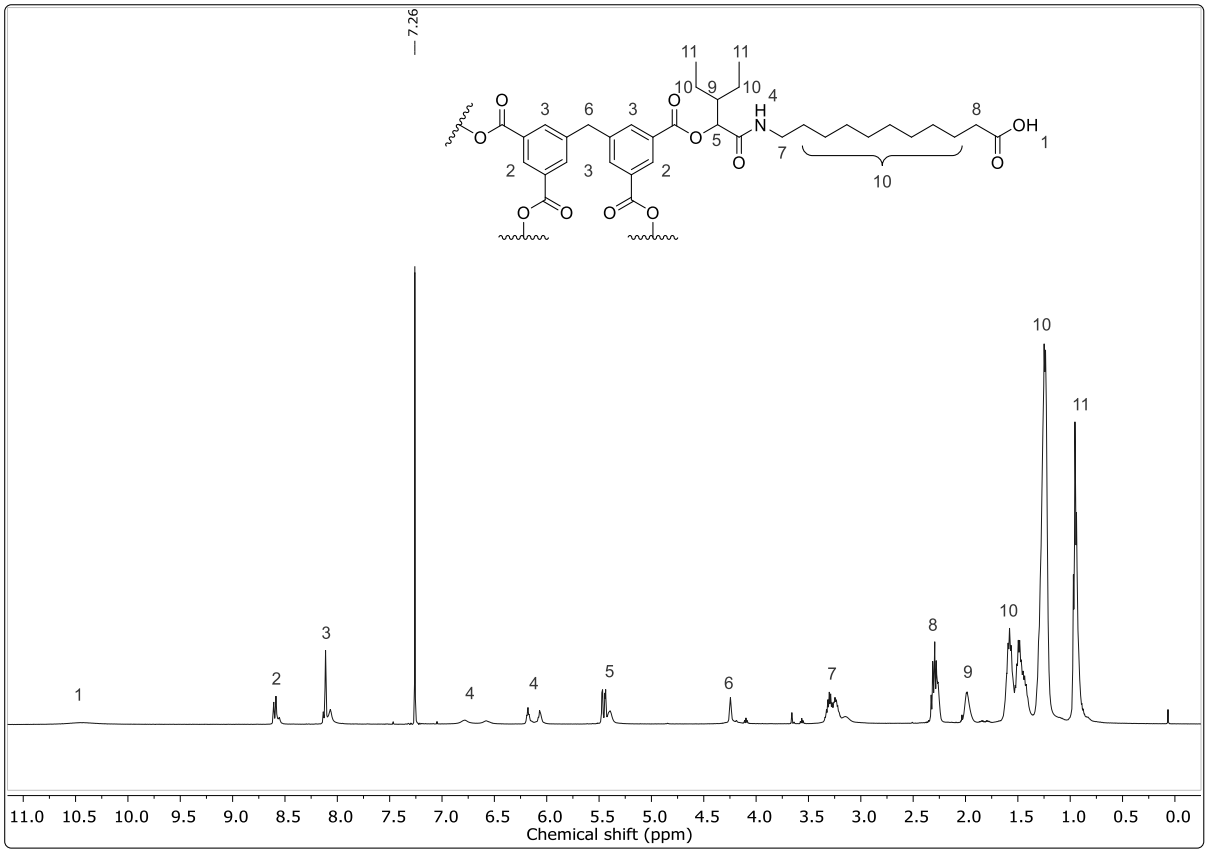

Star-shaped macromolecule CF-H1-2

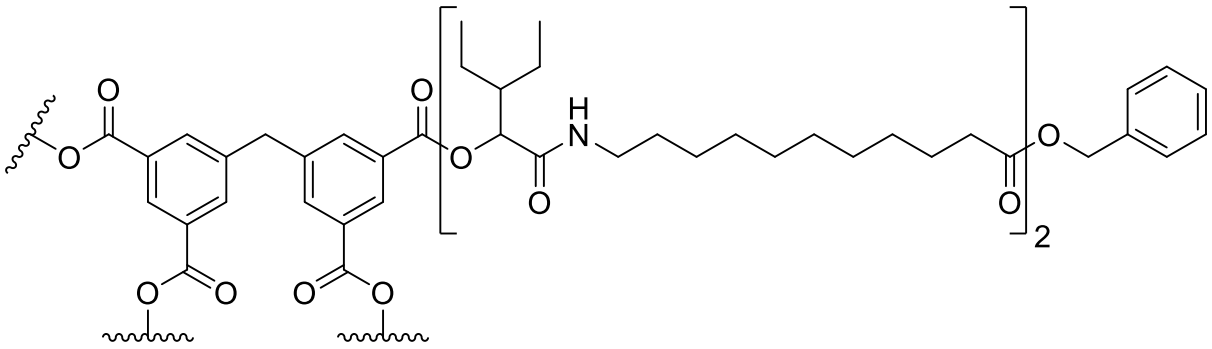

$C_{189}H_{300}N_8O_{32}$

M = 3196.50 g/mol

Tetra acid **CF-H1-1$_b$** (1.91 g, 1.20 mmol, 1.00 eq.) was placed in a round bottom flask and dissolved in 5.00 mL THF, after vigorous stirring for a few minutes the solution was purged with Argon. Subsequently, building block **A1** (2.89 g, 9.60 mol, 8.00 eq.) and 2-ethylbutyr aldehyde **9** (1.28 g, 12.8 mmol, 10.7 eq.) were added. The reaction was controlled *via* TLC and the solvent was evaporated under reduced pressure when the tetra acid was consumed. The crude product was purified *via* column chromatography (cyclohexane/ethyl acetate 3:1 → 2:1) and dried *in vacuo*. The product **CF-H1-2** was obtained as a viscous colorless oil (3.59 g, 1.12 mmol, 94%).

TLC: R_f (cyclohexane/ethyl acetate 3:2) = 0.25

^{1}H NMR (500 MHz, $CDCl_3$): δ (ppm) = 8.59 (s, 1H, C**H**$_{aromatic}$, ^{1}), 8.58 (s, 1H, C**H**$_{aromatic}$, ^{1}), 8.10 (s, 4H, C**H**$_{aromatic}$, ^{2}), 7.37 – 7.30 (m. 20H, C**H**$_{aromatic}$, ^{3}), 6.04 – 5.99 (m, 8H, CON**H**, ^{4}), 5.45 (d, *J* = 3.63 Hz, 2H,C**H**, ^{5}), 5.42 (d, *J* = 3.74 Hz, 2H, C**H**, ^{5}), 5.27 (d, *J* = 3.78 Hz, 4H, C**H** (second repeating unit), ^{6}), 5.10 (s, 8H, C**H$_2$**, ^{7}), 4.23 (s. 2H, C**H$_2$**, ^{8}), 3.32 – 3.19 (m, 16H, CONHC**H$_2$**, ^{9}), 2.38 (t, *J* = 7.54 Hz, 8H, C**H$_2$**COOR, ^{10}), 2.34 (t, *J* = 7.55 Hz, 8H, C**H$_2$**COOBn, ^{11}), 2.02 – 1.95 (m, 4H, C**H**, ^{12}), 1.87 – 1.80 (m, 4H, C**H** (second repeating unit), ^{13}), 1.67 – 1.15 (m, 160H, C**H$_2$**, ^{14}), 0.97 – 0.88 (m, 48H, C**H$_3$**, ^{15}).

^{13}C NMR (126 MHz, $CDCl_3$): δ (ppm) =173.82, 172.61, 169.84, 169.27, 169.25, 164.64, 164.56, 141.32, 141.25, 136.22, 135.32, 130.82, 130.77, 129.13, 129.02, 128.6, 128.29, 128.28, 76.58, 76.49, 75.09, 66.20, 43.63, 39.58, 39.55, 39.34, 34.45, 29.27, 29.73, 29.68, 29.59, 29.48, 29.36, 29.34, 29.30, 29.24, 26.99, 25.12, 25.07, 22.03, 22.02, 11.82, 11.79, 11.75, 11.73, 11.70.

HRMS (ESI) *m/z*: $[M + Na]^+$ calcd for $C_{189}H_{300}N_8O_{32}$, 3217.1986; found, 3217.2065.

IR (ATR): ṽ (cm^{-1}) = 3309, 2926, 2854, 1731, 1651, 1535, 1457, 1379, 1352, 1224, 1163, 1108, 1004, 750, 697, 576, 501.

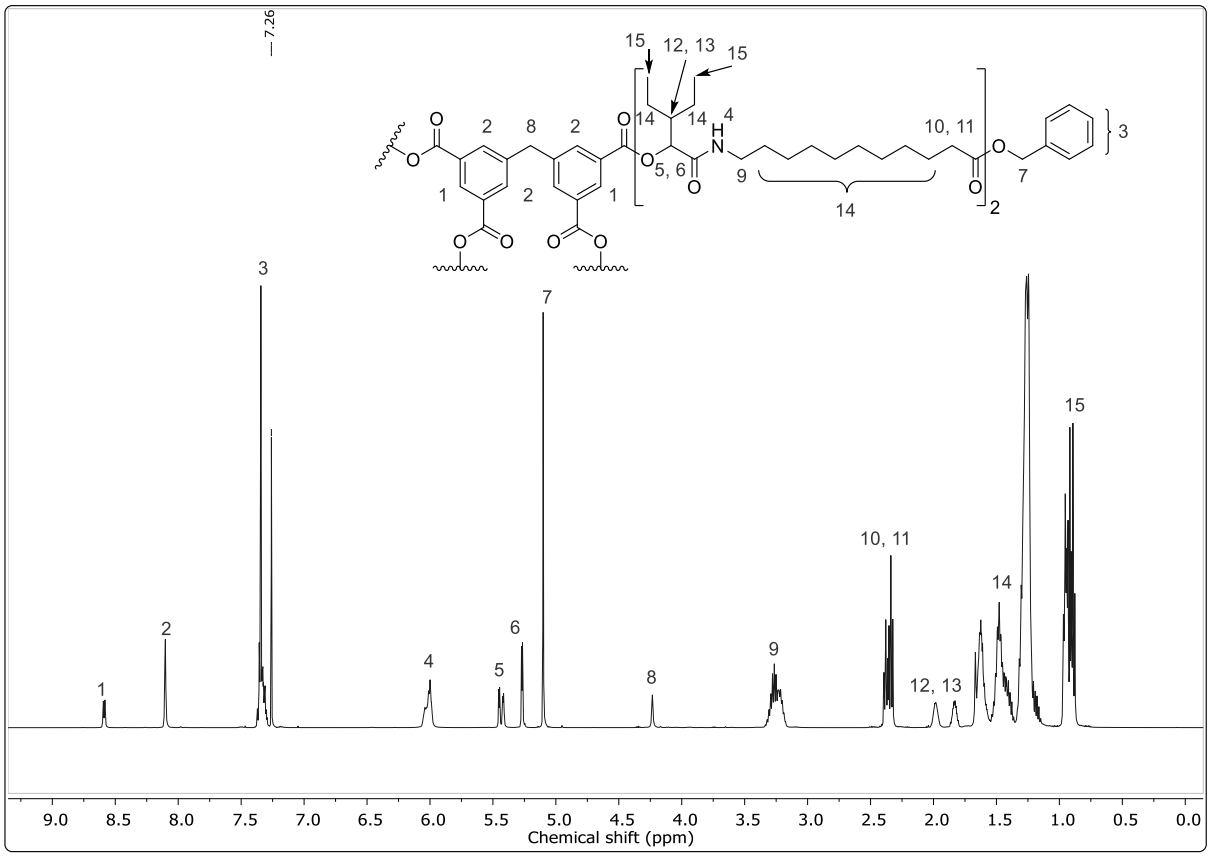

Deprotected star-shaped macromolecule CF-H1-2$_b$

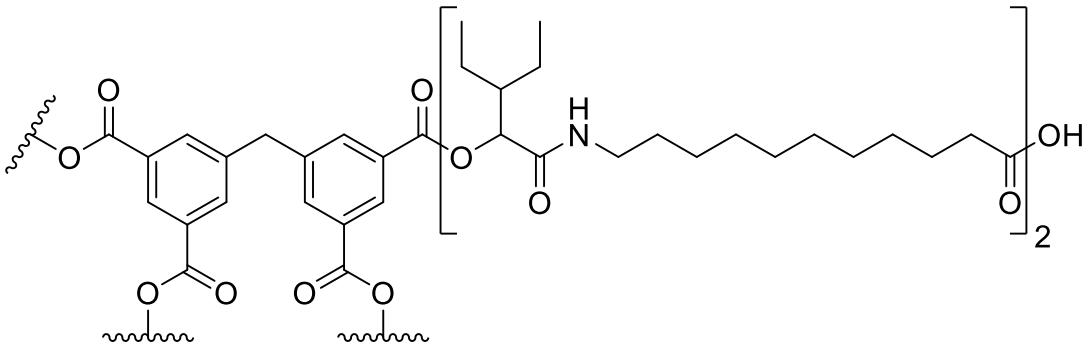

$C_{161}H_{276}N_8O_{32}$

M = 2836.00 g/mol

Benzyl protected star molecule **CF-H1-2** (3.06 g, 957 µmol, 1.00 eq.) and 10wt% Pd on Carbon (306.0 mg) were placed in a round bottom flask and dissolved in ethyl acetate, after vigorous stirring for a few minutes the solution was purged with Hydrogen. The reaction was controlled *via* TLC until no benzyl protected starting material was left. The solution was dried over sodium sulfate and filtered through Celite®. Subsequently, the solvent was evaporated under reduced pressure and the residue was dried *in vacuo*. The product **CF-H1-2$_b$** was obtained as a yellowish foam (2.54 g, 896 µmol, 94%).

TLC: R_f (cyclohexane/ethyl acetate 3:2 = 0.00

^{1}H NMR (500 MHz, $CDCl_3$): δ (ppm) = 8.60(s, 2H, C**H**$_{aromatic}$, [1]), 8.57 (s, 1H, C**H**$_{aromatic}$, [1]), 8.09 (s, 4H, C**H**$_{aromatic}$, [2]), 6.40 – 6.33 (m, 2H, CON**H**, [3]), 6.25 – 6.16 (m, 2H, CON**H**, [3]), 6.13 – 6.07 (m, 4H, CON**H** (second repeating unit), [4]), 5.45 (d, *J* = 3.18 Hz, 2H,C**H**, [5]), 5.42 (d, *J* = 2.81 Hz, 2H, C**H**, [5]), 5.26 (d, *J* = 3.69 Hz, 4H, C**H** (second repeating unit), [6]), 4.23 (s. 2H, C**H$_2$**, [7]), 3.25 (m, 16H, CONHC**H$_2$**, [8]), 2.38 (t, *J* = 7.46 Hz, 8H, C**H$_2$**COOR, [9]), 2.31 – 2.26 (m, 8H, C**H$_2$**COOH, [10]), 2.02 – 1.94 (m, 4H, C**H**, [11]), 1.86 – 1.79 (m, 4H, C**H** (second repeating unit), [12]), 1.67 – 1.14 (m, 160H, C**H$_2$**, [13]), 0.98 – 0.86 (m, 48H, C**H$_3$**, [14]).

^{13}C NMR (126 MHz, $CDCl_3$): δ (ppm) = 178.29, 178.28, 178.28, 178.24, 178.19, 178.15, 172.67, 170.06, 169.67, 169.55, 164.68, 164.62, 135.31, 130.78, 130.69, 129.28, 129.10, 76.47, 75.09, 43.70, 43.56, 39.66, 39.61, 39.34, 34.43, 34.13, 29.66, 29.63, 29.58, 29.54, 29.48, 29.37, 29.35, 29.30, 29.26, 29.10, 26.98, 26.92, 25.13, 24.86, 22.55, 22.48, 22.30, 22.20, 22.15, 21.99, 11.77, 11.75, 11.71, 11.69, 11.68.

HRMS (ESI) *m/z*: $[M + H]^+$ calcd for $C_{161}H_{276}N_8O_{32}$, 2835.0288; found, 2835.0313.

IR (ATR): $\tilde{\nu}$ (cm^{-1}) = 3300, 2926, 2854, 1729, 1650, 1538, 1460, 1379, 1294, 1224, 1187, 1128, 1108, 1045, 1006, 922, 752, 721, 651.

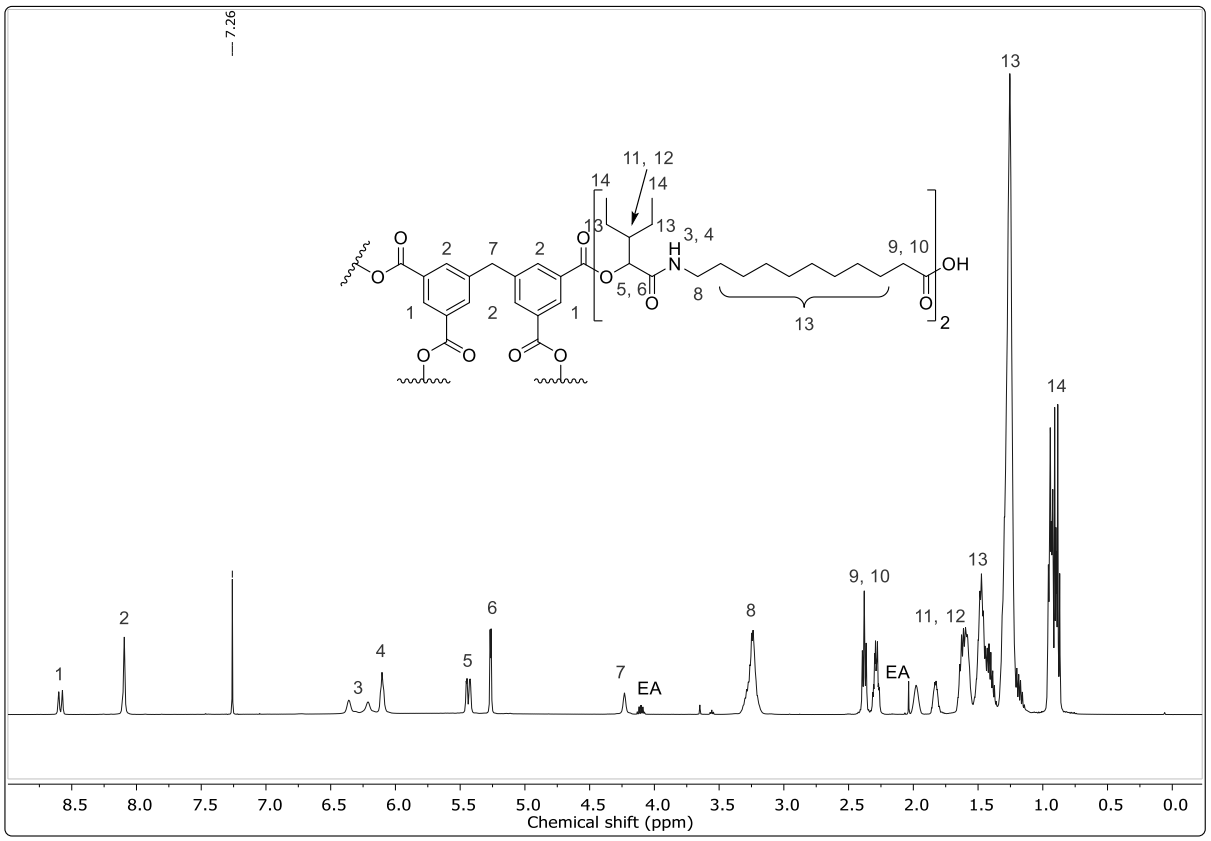

Star-shaped macromolecule CF-H1-3

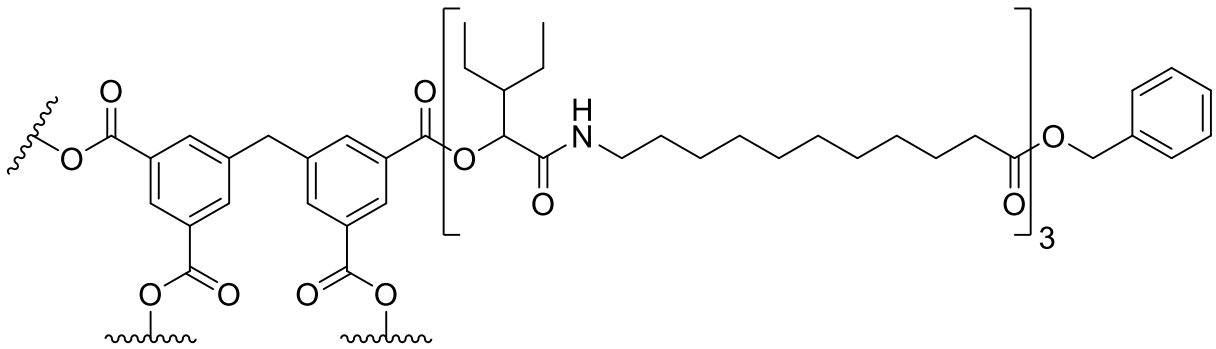

$C_{261}H_{432}N_{12}O_{44}$

M = 4442.37 g/mol

Tetra acid **CF-H1-2b** (2.46 g, 867 µmol, 1.00 eq.) was placed in a round bottom flask and dissolved in 5.00 mL THF, after vigorous stirring for a few minutes the solution was purged with Argon. Subsequently, building block **A1** (2.62 g, 8.69 mol, 10.0 eq.) and 2-ethylbutanal **9** (1.04 g, 10.4 mmol, 12.0 eq.) were added. The reaction was

controlled *via* TLC and the solvent was evaporated under reduced pressure when the tetra acid was consumed. The crude product was purified *via* column chromatography (cyclohexane/ethyl acetate 3:1 → 1:1) and dried *in vacuo*. The product **CF-H1-3** was obtained as a viscous colorless oil (3.46 g, 779 µmol, 90%).

TLC: R_f (cyclohexane/ethyl acetate 1:1) = 0.75

^{1}H NMR (500 MHz, $CDCl_3$): δ (ppm) = 8.59(s, 1H, C**H**$_{\text{aromatic}}$, [1]), 8.58 (s, 1H, C**H**$_{\text{aromatic}}$, [1]), 8.10 (s, 4H, C**H**$_{\text{aromatic}}$, [2]), 7.37 – 7.30 (s. 20H, C**H**$_{\text{aromatic}}$, [3]), 6.13 – 5.98 (m, 12H, CON**H**, [4]), 5.45 (d, *J* = 3.35 Hz, 2H,C**H**, [5]), 5.41 (m, 2H, C**H**, [5]), 5.27 (d, *J* = 3.00 Hz, 4H, C**H**, [5]), 5.26 (d, *J* = 3.17 Hz, 4H, C**H** (second and third repeating unit), [6]), 5.10 (s, 8H, C**H$_2$**, [6]), 4.24 (s. 2H, C**H$_2$**, [8]), 3.34 – 3.18 (m, 24H, CONHC**H$_2$**, [9]), 2.38 (t, *J* = 7.24 Hz, 12H, C**H$_2$**COOR, [10]) 2.35 (t, *J* = 7.56 Hz, 8H, C**H$_2$**COOBn, [11]), 2.01 – 1.95 (m, 4H, C**H**, [12]), 1.87 – 1.80 (m, 8H, C**H** (second and third repeating unit), [13]), 1.65 – 1.15 (m, 240H, C**H$_2$**, [14]), 0.96 – 0.88 (m, 72H, C**H$_3$**, [15]).

^{13}C NMR (126 MHz, $CDCl_3$): δ (ppm) = 173.82, 172.63, 172.61, 169.87, 169.85, 169.30, 169.27, 164.66, 164.57, 136.22, 135.22, 130.81, 130.76, 129.04, 128.66, 128.29, 128.27, 75.56, 76.48, 75.08, 66.19, 63.50, 43.75, 43.68, 43.62, 40.97, 39.59, 39.56, 39.33, 34.46, 34.44, 29.75, 29.73, 29.69, 29.67, 29.59, 29.58, 29.49, 29.47, 29.35, 29.34, 29.32, 29.25, 29.23, 26.98, 26.22, 25.13, 25.12, 25.06, 22.50, 22.49, 22.33, 22.25, 22.20, 22.02, 11.82, 11.78, 11.75, 11.72, 11.70.

HRMS (ESI) *m/z*: $[M + 2H]^{2+}$ calcd for $C_{261}H_{432}N_{12}O_{44}$, 2220.6040, found: 2220.6094.

IR (ATR): ṽ (cm^{-1}) = 3314, 2925, 2854, 1733, 1651, 1534, 1458, 1379, 1225, 1160, 1109, 1046, 1005, 750, 697.

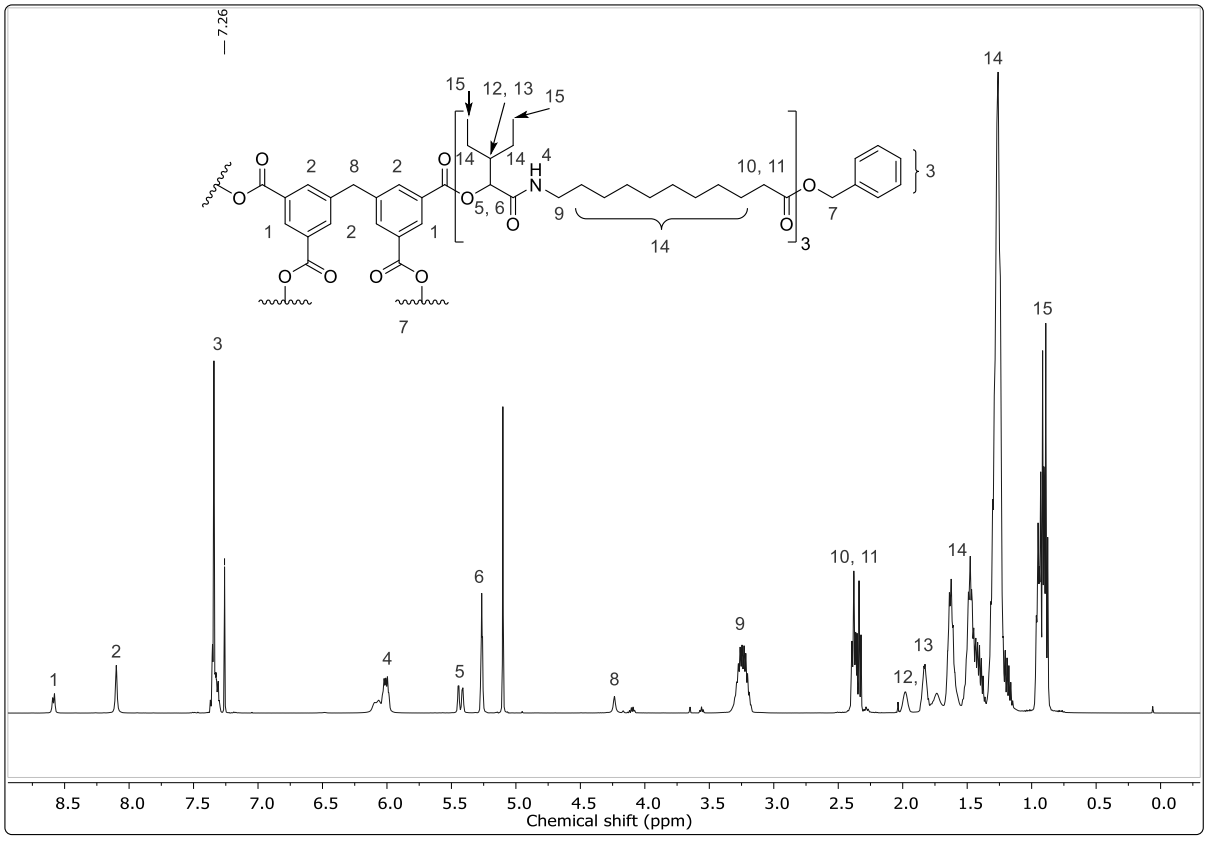

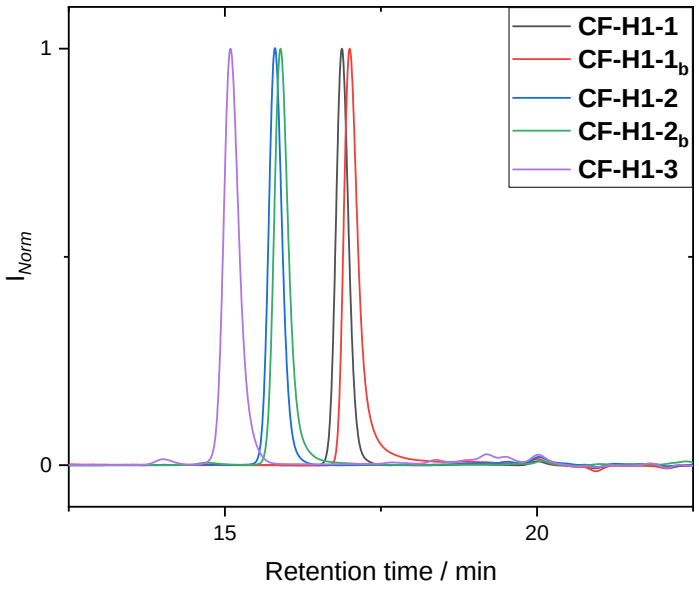

Figure S 6: SEC traces of the star-shaped macromolecules based on core **H1** measured in THF.

Benzyl 11-(3-ethyl-2-hydroxypentanamido)undecanoate

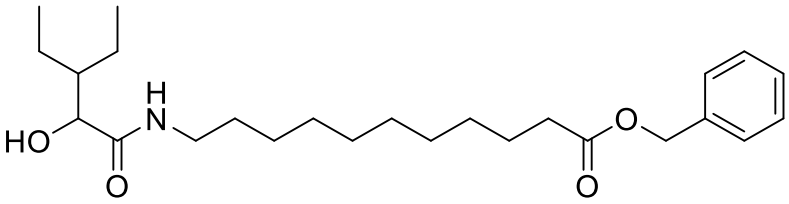

$C_{25}H_{41}NO_4$

M = 419.61 g/mol

Butane-1,2,3,4-tetracarboxylic acid **H5** (351.2 mg, 1.50 mmol, 1.00 eq.) was placed in a round bottom flask and dissolved in 2.50 mL THF, after vigorous stirring for a few minutes the solution was purged with Argon. Subsequently, benzyl 11-isocyanidoundecanoate (building block **A1**) (3.62 g, 12.0 mmol, 8.00 eq.) and 2-ethylbutanal **9** (1.60 g, 16.0 mmol, 10.7 eq.) were added. (The reaction was accompanied by precipitation of a white solid, which did not elute from the subsequent column chromatography). The crude product was purified *via* column chromatography (cyclohexane/ethyl acetate 2:1 → 3:2). The side product **26** was obtained as a white sticky solid (1.05 g, 0.570 mmol, 38%).

TLC: R_f (cyclohexane/ethyl acetate 2:1) = 0.38

^{1}H NMR (500 MHz, DMSO-d_6): δ (ppm) = 7.69 (t, 1H, CON**H**, ^{1}), 7.38 – 7.31 (m. 5H, C**H**$_{\text{aromatic}}$, ^{2}), 5.25 (d, J = 5.69 Hz, 1H, O**H**, ^{3}), 5.08 (s, 2H, C**H$_2$**, ^{4}), 3.84 (dd, J = 5.48, 3.26 Hz, 1H, C**H**, ^{5}), 3.14 – 2.99 (m, 2H, CONHC**H$_2$**, ^{6}), 2.33 (t, J = 7.35 Hz, 2H, C**H$_2$**COOBn, ^{7}), 1.56 – 1.47 (m, 3H, C**H$_2$**, C**H**, ^{8}), 1.43 – 1.34 (m, 2H, C**H$_2$**, ^{9}) 1.34 – 1.09 (m, 16H, C**H$_2$**, ^{10}), 0.86 (t, J = 7.39 Hz, 3H, C**H$_3$**, ^{11}), 0.79 (t, J = 7.48 Hz, 3H, C**H$_3$**, ^{11}).

^{13}C NMR (126 MHz, DMSO-d_6): δ (ppm) = 173.66, 172.79, 136.31, 128.42, 127.99, 127.94, 71.76, 65.29, 44.36, 38.09, 33.48, 29.21, 28.96, 28.84, 28.74, 28.68, 28.43, 26.38, 24.49, 22.15, 21.06, 11.89, 11.78.

HRMS (ESI) *m/z*: $[M + H]^+$ calcd for $C_{25}H_{41}NO_4$, 420.3108; found, 420.3095.

IR (ATR): ṽ (cm^{-1}) = 3305, 2925, 2854, 1736, 1621, 1538, 1498, 1456, 1378, 1354, 1294, 1212, 1160, 1133, 1050, 1026, 734, 696, 606, 502.

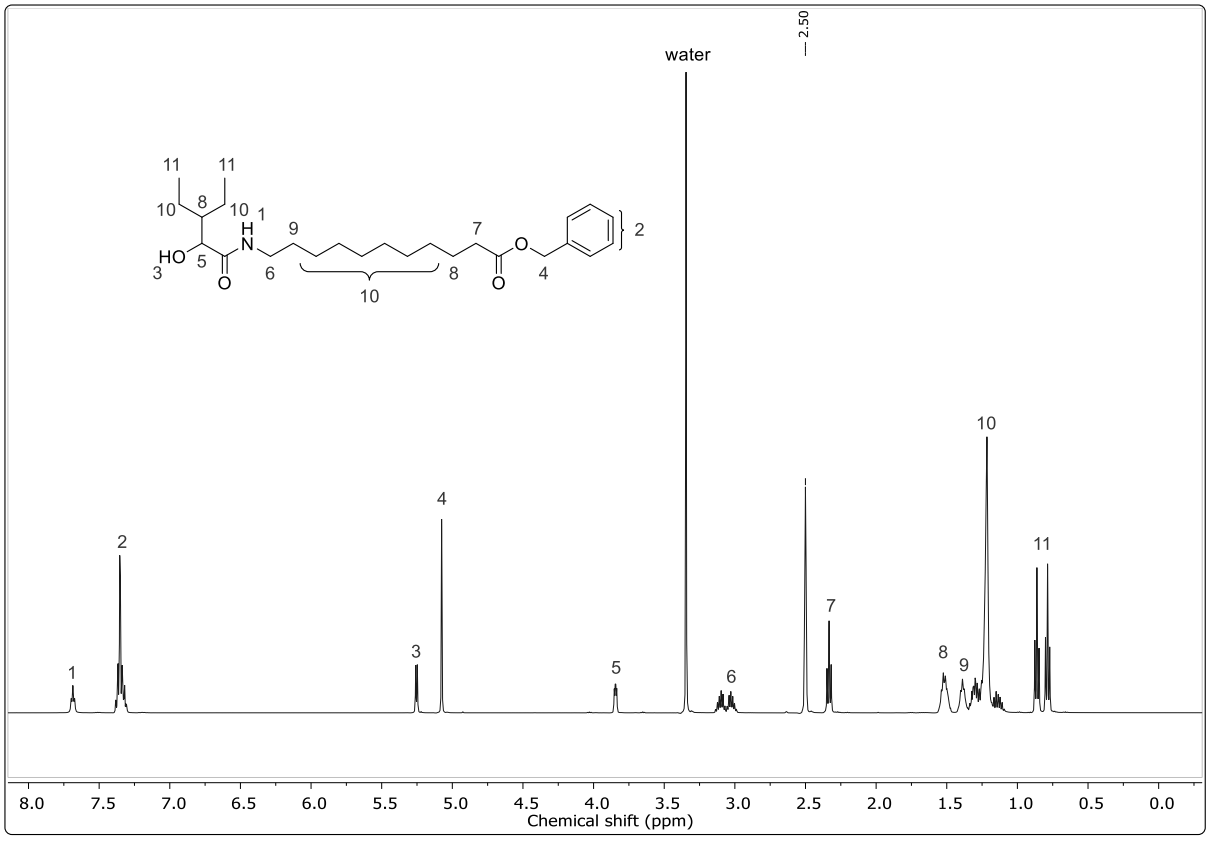

Star-shaped macromolecule CF-H2-1

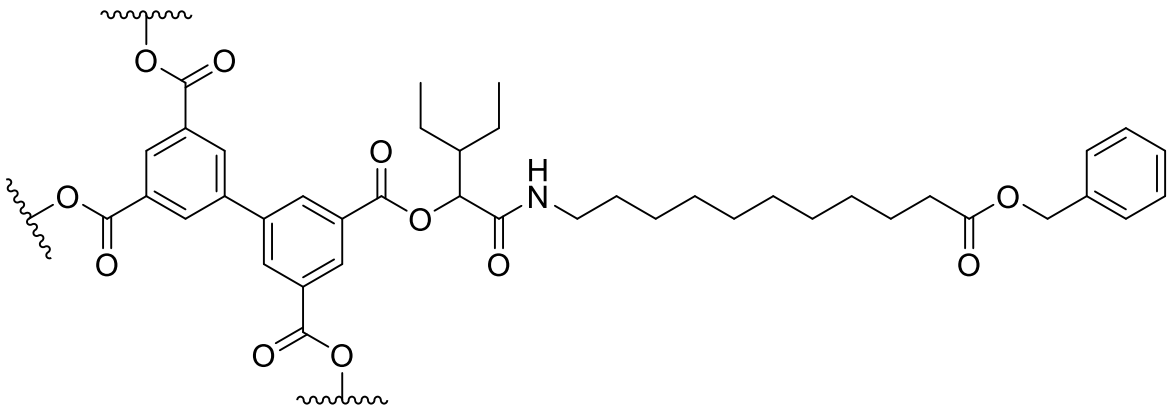

$C_{116}H_{166}N_4O_{20}$

M = 1936.61 g/mol

[1,1'-Biphenyl]-3,3',5,5'-tetracarboxylic acid **H2** (495 mg, 1.50 mmol, 1.00 eq.) were placed in a round bottom flask and dissolved in 10 mL THF and 2.5 mL water, after vigorous stirring for a few minutes the solution was purged with Argon. Subsequently, benzyl 11-isocyanidodecanoate (building block **A1**) (3.62 g, 12.0 mol, 8.00 eq.) and 2-ethylbutanal **9** (1.60 g, 16.0 mmol, 1.99 mL, 10.7 eq.) were added. The reaction was controlled *via* TLC and then 20 mL DCM and 10 mL water were added when the tetra acid was consumed. The phases were separated and the aqueous one was extracted

three times with 20 mL DCM. Afterwards, the organic phase was dried over sodium sulfate and the solvent was removed under reduced pressure. The crude product was purified *via* column chromatography (cyclohexane/ethyl acetate 4:1 → 2:1). The product **CF-H2-1** was obtained as a viscous orange oil (2.36 g, 1.22 mmol, 86%).

TLC: R_f (cyclohexane/ethyl acetate 2:1) = 0.43

^{1}H NMR (500 MHz, $CDCl_3$): δ (ppm) = 8.77 – 8.75 (m, 2H, C**H**$_{\textbf{aromatic}}$, ^{1}), 8.55 (s, 4H, C**H**$_{\textbf{aromatic}}$, ^{2}), 7.37 – 7.29 (s. 20H, C**H**$_{\textbf{aromatic}}$, ^{3}), 6.06 – 5.98 (m, 4H, CON**H**, ^{4}), 5.49 (d, *J* = 3.85 Hz, 2H, C**H**, ^{5}), 5.47 (d, *J* = 4.06 Hz, 2H, C**H**, ^{5}), 5.09 (s, 8H, C**H$_2$**, ^{6}), 3.34 – 3.22 (m, 8H, CONHC**H$_2$**, ^{7}), 2.32 (t, *J* = 7.55 Hz, 8H, C**H$_2$**COOBn, ^{8}), 2.06 – 1.99 (m, 4H, C**H**, ^{10}), 1.68 – 1.19 (m, 80H, C**H$_2$**, ^{10}), 1.00 – 0.97 (m, 24H, C**H$_3$**, ^{11}).

^{13}C NMR (126 MHz, $CDCl_3$): δ (ppm) = 173.80, 169.16, 169.14, 164.46, 164.41, 140.45, 140.42, 140.38, 136.19, 133.32, 133.29, 131.36, 131.30, 130.33, 130.25, 128.64, 128.50, 128.35, 128.27, 128.25, 76.81, 76.76, 66.17, 43.67, 43.60, 39.61, 39.59, 34.41, 29.70, 29.69, 29.54, 29.43, 29.31, 29.28, 29.20, 26.96, 25.03, 22.47, 22.23, 22.18, 11.77, 11.75, 11.70.

HRMS (ESI) *m/z*: $[M + H]^+$ calcd for $C_{116}H_{166}N_4O_{20}$, 1936.2168; found, 1936.2162.

IR (ATR): ṽ (cm^{-1}) = 3294, 2926, 2854, 1729, 1655, 1537, 1456, 1381, 1297, 1224, 1137, 1107, 1085, 1002, 904, 749, 696, 660, 579, 497.

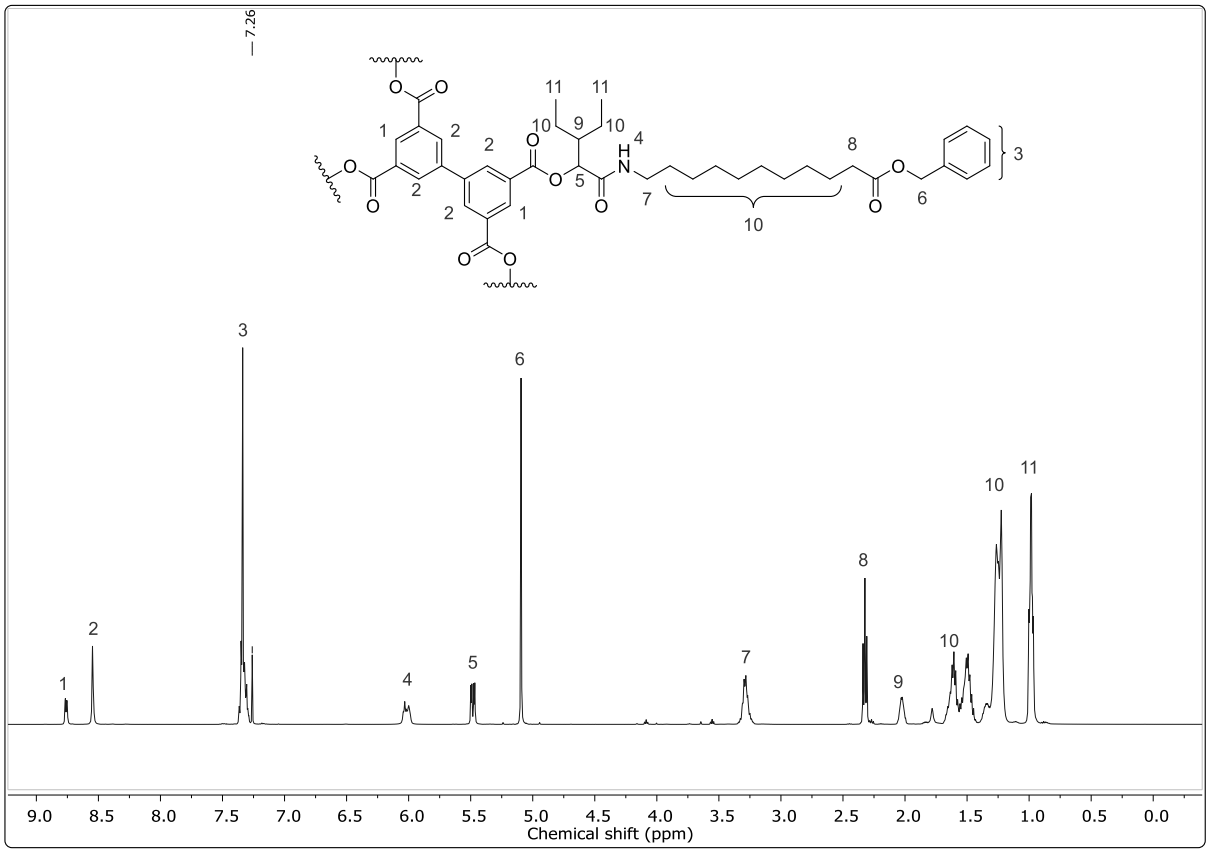

Deprotected star-shaped macromolecule CF-H2-1$_b$

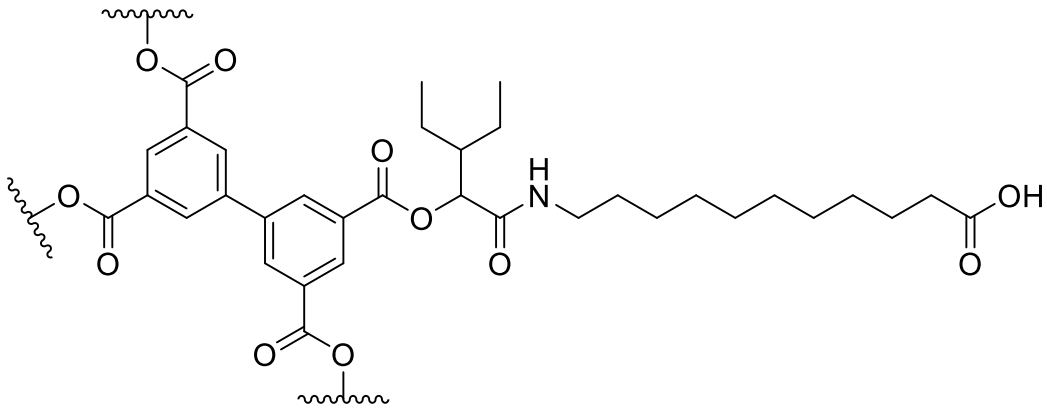

$C_{88}H_{142}N_4O_{20}$

M = 1576.11 g/mol

Benzyl protected star molecule **CF-H2-1** (2.32 g, 1.20 mmol, 1.00 eq.) and 10wt% Pd on Carbon (232 mg) were placed in a round bottom flask and dissolved in ethyl acetate, after vigorous stirring for a few minutes the solution was purged with Hydrogen. The reaction was controlled *via* TLC until no benzyl protected starting material was left. The solution dried over sodium sulfate and filtered through Celite®. Subsequently, the

solvent was evaporated under reduced pressure and the residue was dried *in vacuo*. The product **CF-H2-1$_b$** was obtained as a yellowish foam (1.85 g, 1.18 mmol, 98%).

TLC: R_f (cyclohexane/ethyl acetate 2:1) = 0.00

^{1}H NMR (500 MHz, DMSO-d_6): δ (ppm) = 11.95 (bs, 4H, COO**H**, ^{1}), 8.66 – 8.65 (s, 2H, C**H**$_{aromatic}$, ^{2}), 8.53 (s, 4H, C**H**$_{aromatic}$, ^{3}), 8.18 – 8.11 (bs, 4H, CON**H**, ^{4}), 5.20 (d, J = 3.71 Hz, 4H, C**H**, ^{5}), 3.14 – 3.03 (m, 8H, CONHC**H$_2$**, ^{6}), 2.15 (t, J = 7.36 Hz, 8H, C**H$_2$**COOH, ^{7}), 1.91 – 1.84 (m, 4H, C**H**, ^{8}), 1.61 – 1.14 (m, 80H, C**H$_2$**, ^{9}), 0.97 – 0.94 (t, J = 7.18 Hz, 24H, C**H$_3$**, ^{10}).

^{13}C NMR (126 MHz, DMSO-d_6): δ (ppm) = 174.50, 174.45, 168.27, 164.20, 164.17, 139.32, 132.12, 131.26, 131.21, 129.95, 75.87, 75.82, 62.94, 44.94, 42.77, 42.74, 38.38, 33.64, 28.98, 28.96, 28.85, 28.75, 28.70, 28.66, 28.56, 28.42, 26.29, 25.67, 24.48, 22.16, 21.56, 21.53, 11.53, 11.40, 11.38, 11.31.

HRMS (ESI) *m/z*: $[M + H]^+$ calcd for $C_{88}H_{142}N_4O_{20}$, 1576.0290; found, 1576.0280.

IR (ATR): ṽ (cm^{-1}) = 3310, 2926, 2855, 1729, 1650, 1541, 1461, 1380, 1296, 1222, 1134, 1108, 1085, 1037, 1002, 904, 751, 723, 659.

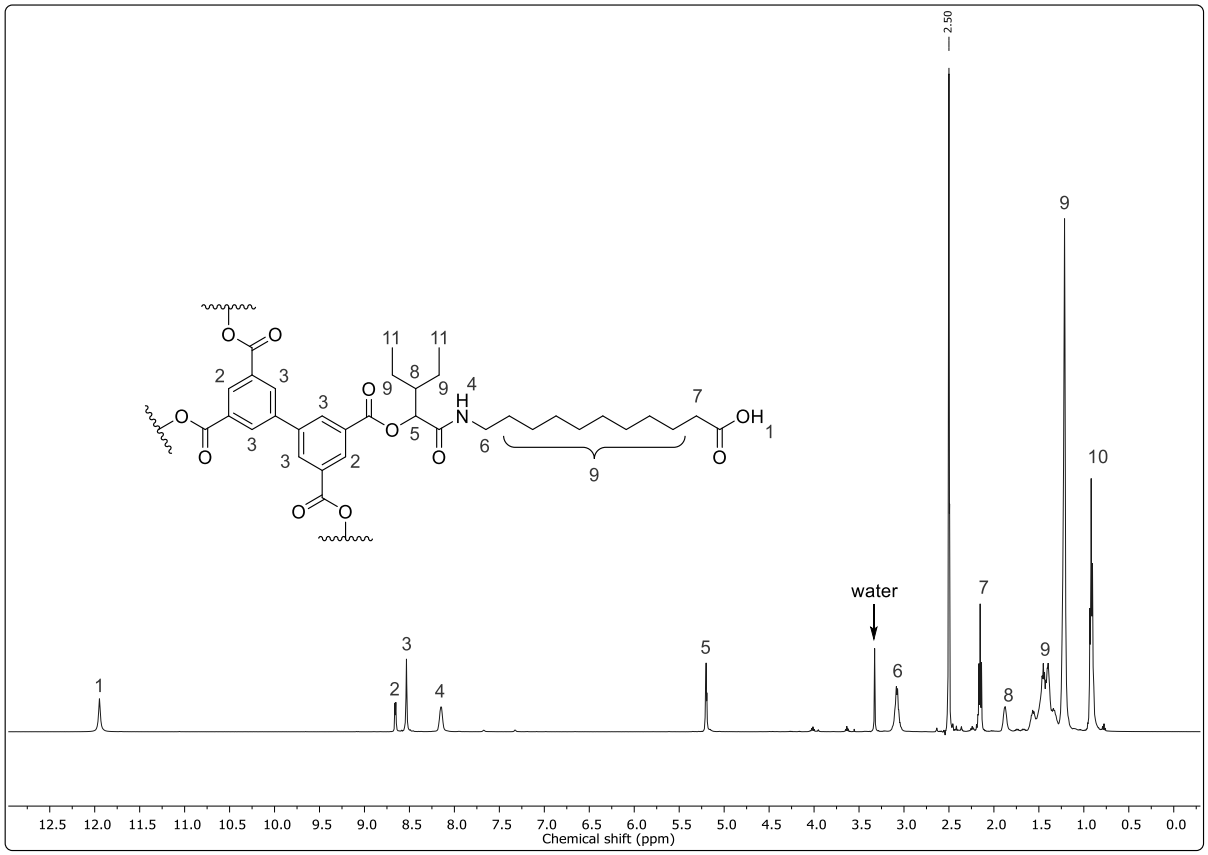

Star-shaped macromolecule CF-H2-2

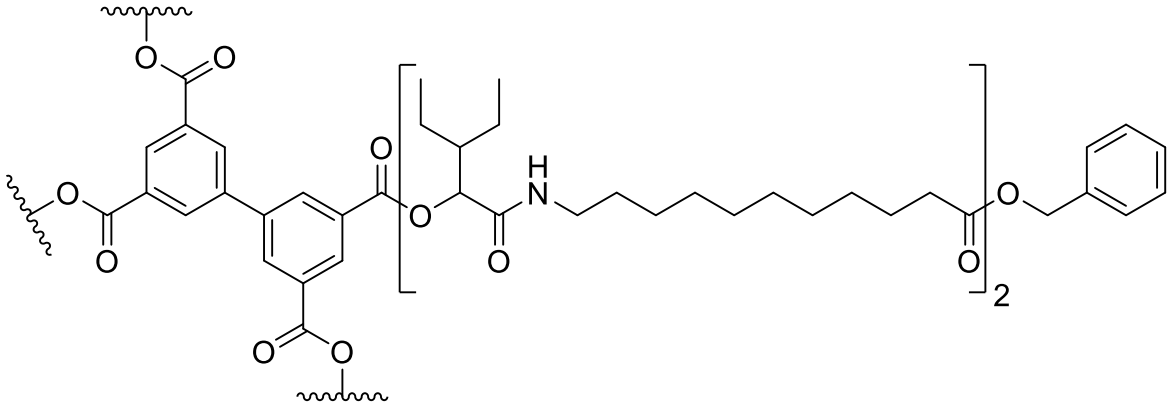

$C_{188}H_{298}N_8O_{32}$

M = 3182.48 g/mol

Tetra acid **CF-H2-1$_b$** (1.81 g, 1.15 mmol, 1.00 eq.) were placed in a round bottom flask and dissolved in 2.50 mL THF, after vigorous stirring for a few minutes the solution was purged with Argon. Subsequently, building block **A1** (2.77 g, 9.20 mol, 8.00 eq.) and 2-ethylbutanal **9** (1.23 g, 12.3 mmol, 1.53 mL, 10.7 eq.) were added. The reaction was controlled *via* TLC and the solvent was evaporated under reduced pressure when the tetra acid was consumed. The crude product was purified *via* column chromatography (cyclohexane/ethyl acetate 3:1 → 2:1). The product **CF-H2-2** was obtained as a viscous orange oil (3.47 g, 1.09 mmol, 95%).

TLC: R_f (cyclohexane/ethyl acetate 3:2) = 0.24

^{1}H NMR (500 MHz, $CDCl_3$): δ (ppm) = 8.76 – 8.75 (m, 2H, C**H**$_{aromatic}$, ^{1}), 8.54 (s, 4H, C**H**$_{aromatic}$, ^{2}), 7.37 – 7.30 (s. 20H, C**H**$_{aromatic}$, ^{3}), 6.12 – 6.04 (m, 4H, CON**H**, ^{4}), 6.12 – 6.00 (m, 4H, CON**H** (second repeating unit), ^{5}), 5.48 (d, *J* = 3.81 Hz, 2H, C**H**, ^{6}), 5.46 (d, *J* = 4.10 Hz, 2H, C**H**, ^{6}), 5.26 (d, *J* = 3.72 Hz, 4H, C**H** (second repeating unit), ^{7}), 5.10 (s, 8H, C**H$_2$**, ^{8}), 3.31 – 3.18 (m, 16H, CONHC**H$_2$**, ^{9}), 2.37 (t, *J* = 7.56 Hz, 8H, C**H$_2$**COOR, ^{10}), 2.34 (t, *J* = 7.56 Hz, 8H, C**H$_2$**COOBn, ^{11}), 2.06 – 1.99 (m, 4H, C**H**, ^{12}), 1.86 – 1.80 (m, 4H, C**H** (second repeating unit, ^{13}), 1.68 – 1.19 (m, 160H, C**H$_2$**, ^{14}), 1.00 – 0.96 (m, 24H, C**H$_3$**, ^{15}), 0.93 – 0.88 (m, 24H, C**H$_3$** (second repeating unit), ^{16}).

^{13}C NMR (126 MHz, $CDCl_3$): δ (ppm) = 173.82, 172.61, 169.85, 169.23, 169.19, 164.51, 164.46, 136.23, 133.30, 131.39, 131.32, 128.66, 128.29, 128.27, 75.10, 66.20, 43.69, 43.64, 39.61, 39.35, 34.45, 29.74, 29.72, 29.68, 29.58, 29.48, 29.34, 29.30,

29.24, 26.99, 25.12, 25.07, 22.59, 22.50, 22.34, 22.24, 22.20, 22.03, 11.78, 11.77, 11.75, 11.72, 11.70.

HRMS (ESI) *m/z*: $[M + H]^+$ calcd for $C_{188}H_{298}N_8O_{32}$, 3181.2010; found, 3181.2051.

IR (ATR): $\tilde{\nu}$ (cm^{-1}) = 3313, 2926, 2854, 1732, 1651, 1535, 1457, 1380, 1225, 1160, 1108, 1004, 905, 750, 697, 659.

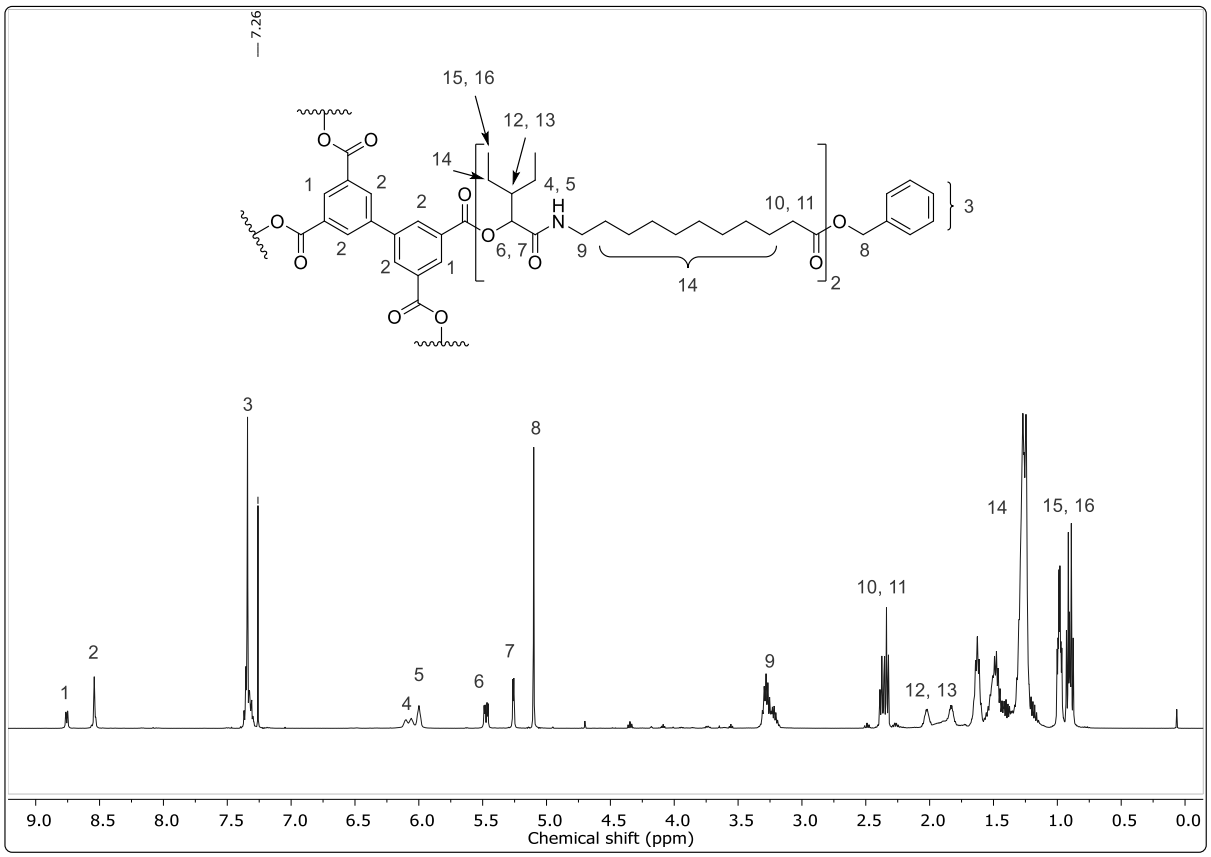

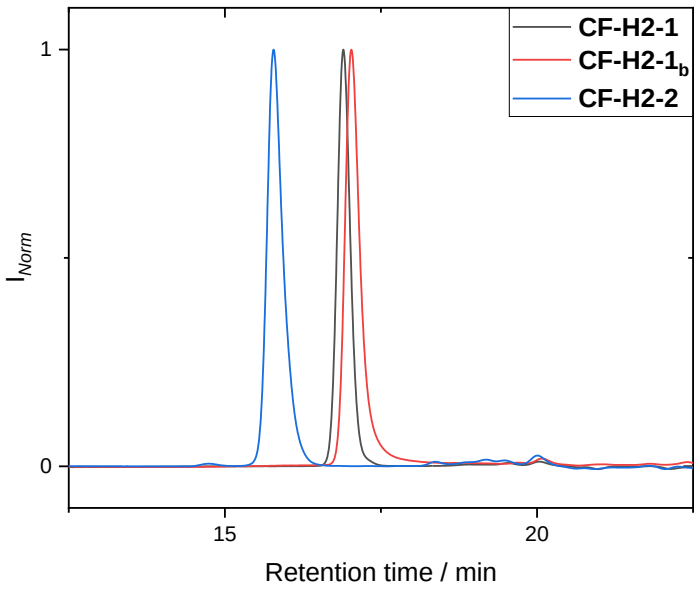

Figure S 7: SEC traces of the star-shaped macromolecules based on core **H2** measured in THF.

Star-shaped macromolecule CF-H7-1

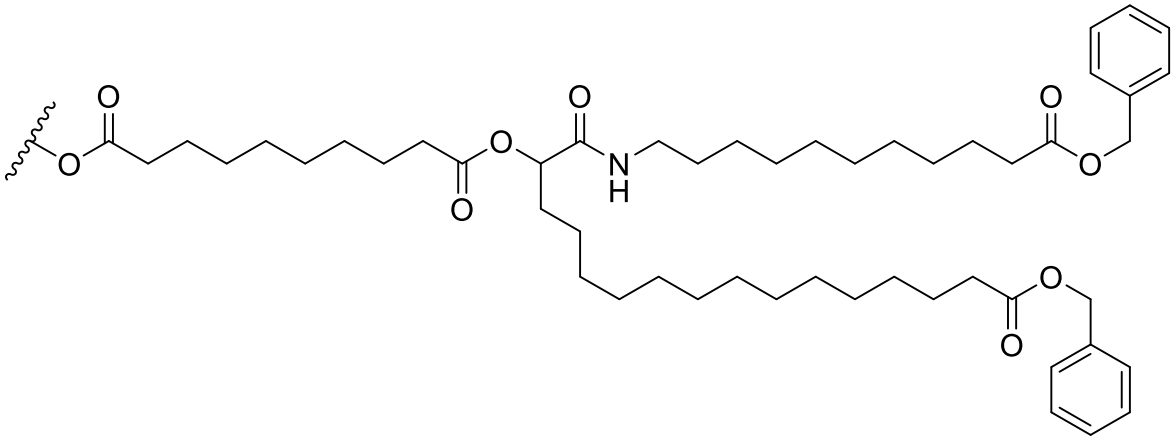

$C_{92}H_{140}N_2O_{14}$

M = 1498.13 g/mol

Sebacic acid **H7** (405 mg, 2.00 mmol, 1.00 eq.) was placed in a vial and dissolved in 5.00 mL THF. The solution was purged with Argon after vigorous stirring for a few minutes. Subsequently, benzyl 15-oxopentadecanoate (building block **F1**) (2.77 g, 8.00 mmol, 4.00 eq.) and benzyl 11-isocyanidodecanoate (building block **A1**) (2.41 g, 8.00 mol, 4.00 eq.) were added. The reaction was controlled *via* TLC until completed, then the solvent was evaporated under reduced pressure. The crude product was

purified *via* column chromatography (cyclohexane/ethyl acetate 5:1 → 2:1). The product **CF-H7-1** was obtained as colorless wax (2.73 g, 1.82 mmol, 92%).

TLC (cyclohexane/ethyl acetate 3:1) R_f = 0.39

^{1}H NMR (500 MHz, $CDCl_3$): δ (ppm) = 7.34 (s. 20H, C**H**$_{\text{aromatic}}$, [1]), 6.01 (t, *J* = 5.77 Hz, 2H, CON**H**, [2]), 5.16 – 5.13 (m, 2H, C**H**, [3]), 5.11 (s, 8H, C**H**$_2$, [4]), 3.30 – 3.19 (m, 4H, CONHC**H**$_2$, [5]), 2.38 (t, *J* = 7.50 Hz, 4H, C**H**$_2$COOR, [6]), 2.35 (t, *J* = 7.50 Hz, 8H, C**H**$_2$COOBn, [7]), 1.89 – 1.75 (m, 4H, C**H**$_2$, [8]), 1.68 – 1.60 (m, 12H, C**H**$_2$, [9]), 1.51 – 1.46 (m, 4H, C**H**$_2$, [10]),1.37 – 1.20 (m, 72H, C**H**$_2$, [11]).

^{13}C NMR (126 MHz, $CDCl_3$): δ (ppm) = 173.83, 173.79, 172.53, 169.92, 136.24, 136.23, 128.66, 128.52, 128.38, 128.28, 74.09, 66.19, 66.18, 39.32, 34.46, 34.44, 34.38, 29.76, 29.74, 29.72, 29.69, 29.59, 29.48, 29.41, 29.39, 29.35, 29.27, 29.24, 29.22, 29.18, 26.96, 25.09, 25.06, 25.00, 24.92.

HRMS (ESI) *m/z*: $[M + H]^+$ calcd for $C_{92}H_{140}N_2O_{14}$, 1498.0377; found, 1498.0356.

IR (ATR): ṽ (cm^{-1}) = 3332, 2920, 2851, 1734, 1662, 1532, 1498, 1468, 1452, 1387, 1362, 1291, 1261, 1237, 1205, 1161, 992, 963, 736, 696, 579, 507, 457.

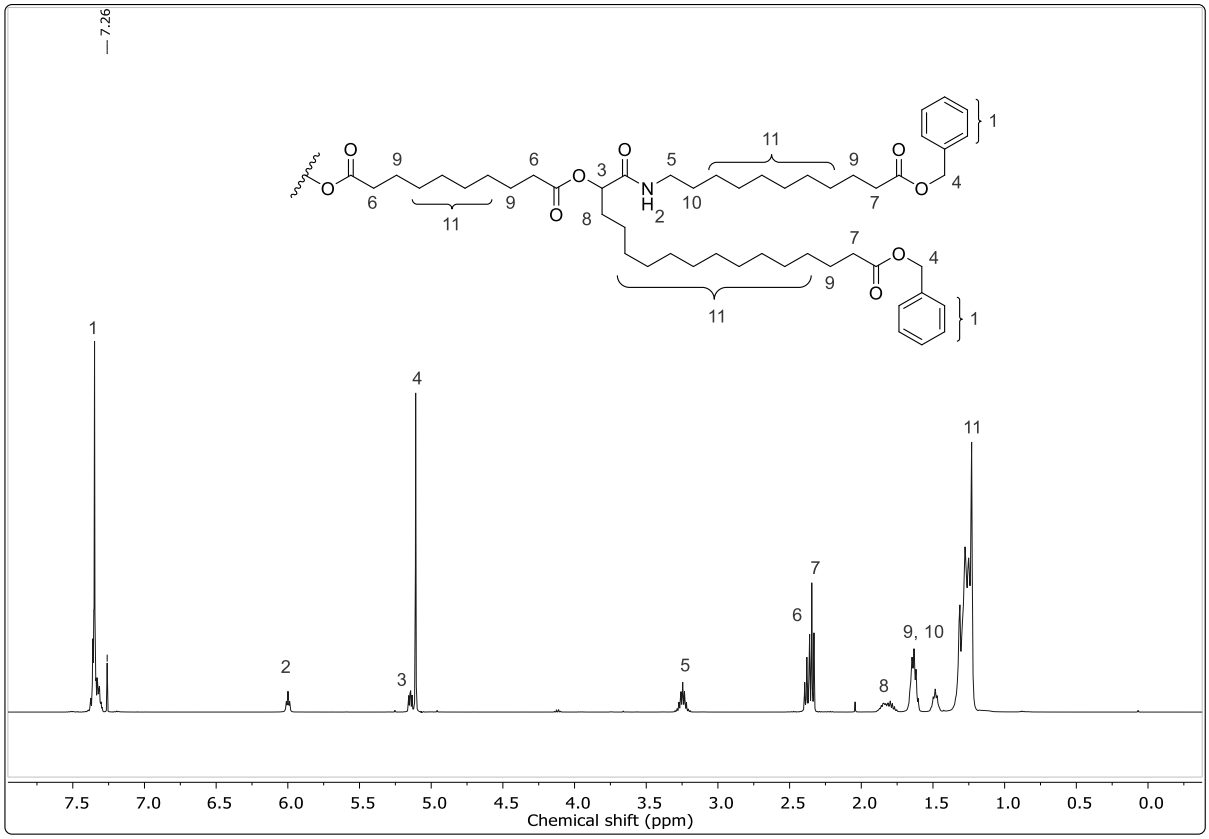

Deprotected star-shaped macromolecule CF-H7-1$_b$

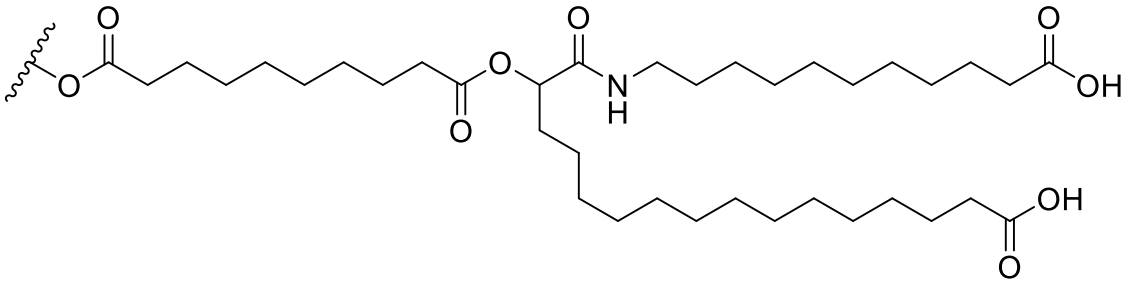

$C_{64}H_{116}N_2O_{14}$

M = 1137.63 g/mol

Benzyl protected star molecule **CF-H7-1** (2.67 g, 1.78 mmol, 1.00 eq.) and 10wt% Pd on Carbon (267 mg) were placed in a round bottom flask and dissolved in THF, after vigorous stirring for a few minutes the solution was purged with Hydrogen. The reaction was controlled *via* TLC until no benzyl protected Polymer was left. The solution was dried over sodium sulfate and filtered through Celite®. Subsequently, the solvent was evaporated under reduced pressure and the residue was dried *in vacuo*. The product **CF-H7-1$_b$** was obtained as a colorless solid (1.93 g, 1.69 mmol, 95%).

TLC (cyclohexane/ethyl acetate 3:1) R_f = 0.00

^{1}H NMR (500 MHz, $CDCl_3$): δ (ppm) = 11.95 (bs, 4H, COO**H**, ^{1}), 6.07 (t, *J* = 5.73 Hz, 2H, CON**H**, ^{2}), 4.80 (d, *J* = 6.28 Hz, 2H, C**H**, ^{3}), 3.09 – 2.97 (m, 4H, CONHC**H$_2$**, ^{4}), 2.33 (t, *J* = 7.30 Hz, 4H, C**H$_2$**COOR, ^{5}), 2.17 (t, *J* = 7.36 Hz, 8H, C**H$_2$**COOH, ^{6}), 1.68 – 1.61 (m, 4H, C**H$_2$**, ^{7}), 1.53 – 1.44 (m, 12H, C**H$_2$**, ^{8}), 1.39 – 1.34 (m, 4H, C**H$_2$**, ^{9}), 1.29 – 1.18 (m, 72H, C**H$_2$**, ^{10}).

^{13}C NMR (126 MHz, $CDCl_3$): δ (ppm) = 174.46, 172.32, 169.08, 97.17, 73.07, 39.26, 39.09, 38.21, 33.67, 33.44, 31.42, 29.08, 29.05, 29.02, 29.00, 28.97, 28.90, 28.81, 28.75, 28.60, 28.57, 28.37, 26.26, 24.52, 24.45. 24.40.

HRMS (ESI) *m/z*: $[M + H]^+$ calcd for $C_{64}H_{116}N_2O_{14}$, 1137.8499; found, 1137.8472.

IR (ATR): ṽ (cm^{-1}) = 3284, 2915, 2849, 1733, 1698, 1657, 1547, 1467, 1435, 1412, 1364, 1292, 1247, 1216, 1170, 1108, 922, 721, 681, 536.

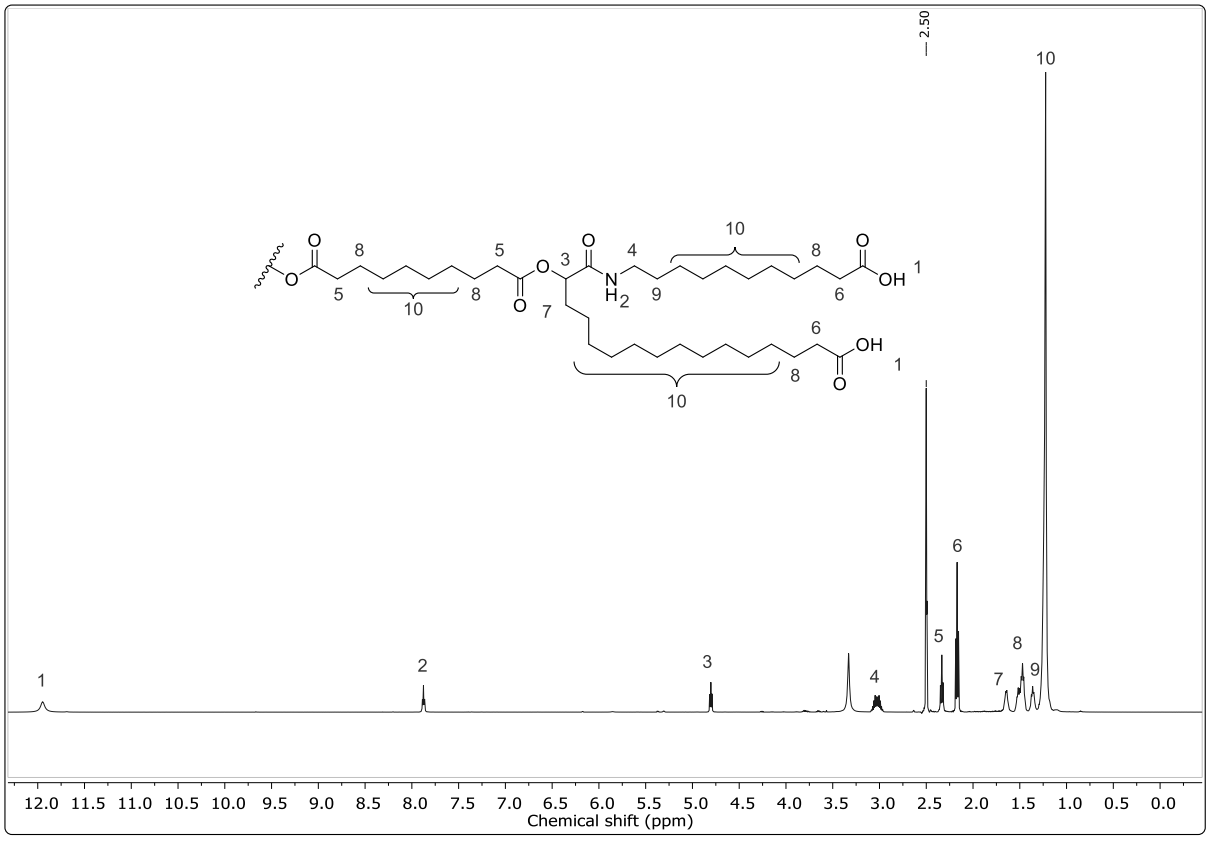

Star-shaped macromolecule CF-H7-2

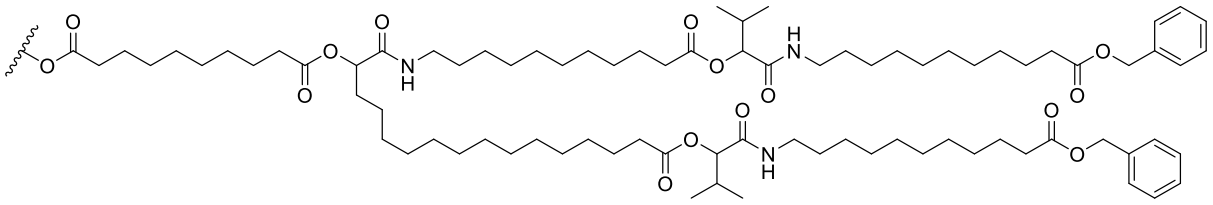

$C_{156}H_{256}N_6O_{26}$

M = 2631.78 g/mol

Tetra acid **CF-H7-1b** (1.82 g, 1.60 mmol, 1.00 eq.) were placed in a round bottom flask and dissolved in 6.00 mL THF, after vigorous stirring for a few minutes the solution was purged with Argon. Subsequently, building block **A1** (3.86 g, 12.80 mol, 8.00 eq.) and isobutanal **31** (1.23 g, 17.1 mmol, 10.7 eq.) were added. The reaction was controlled *via* TLC and the solvent was evaporated under reduced pressure when the tetra acid was consumed. The crude product was purified *via* column chromatography (cyclohexane/ethyl acetate 3:2). The product **CF-H7-2** was obtained as a viscous colorless oil (3.84 g, 1.46 mmol, 91%).

TLC: R_f (cyclohexane/ethyl acetate 3:2) = 0.27

^{1}H NMR (500 MHz, $CDCl_3$): δ (ppm) = 7.37 – 7.29 (s. 20H, C**H**$_{\text{aromatic}}$, ^{1}), 6.03 (t, *J* = 5.79 Hz, 2H, CON**H**, ^{2}), 5.99 – 5.95 (m, 4H, CON**H**, ^{3}), 5.14 – 5.12 (m, 2H, C**H**, ^{4}), 5.11 (s, 8H, C**H$_2$**, ^{5}), 5.05 (d, *J* = 4.42 Hz, 2H, C**H**, ^{6}), 5.04 (d, *J* = 4.46 Hz, 2H, C**H**, ^{6}), 3.31 – 3.18 (m, 12H, CONHC**H$_2$**, ^{7}), 2.41 – 2.36 (m, 12H, C**H$_2$**COOR, ^{8}), 2.34 (t, *J* = 7.56 Hz, 8H, C**H$_2$**COOBn, ^{9}), 2.33 – 2.25 (m, 4H, C**H**, ^{10}), 1.88 – 1.74 (m, 4H, C**H$_2$**, ^{11}), 1.68 – 1.60 (m, 20H, C**H$_2$**, ^{12}), 1.52 – 1.44 (m, 12H, C**H$_2$**, ^{13}),1.35 – 1.21 (m, 120H, C**H$_2$**, ^{14}), 0.94 (d, *J* = 6.65 Hz, 12H, C**H$_3$**, ^{15}), 0.92 (d, *J* = 6.10 Hz, 12H, C**H$_3$**, ^{15}).

^{13}C NMR (126 MHz, $CDCl_3$): δ (ppm) = 173.80, 172.68, 172.56, 171.28, 169.95, 169.38, 169.37, 136.24, 128.66, 128.29, 128.28, 78.05, 78.01, 74.09, 66.19, 39.29, 34.45, 34.41, 30.65, 29.75, 29.72, 29.60, 29.57, 29.50, 29.47, 29.42, 29.32, 29.33, 29.30, 29.26, 29.23, 29.19, 26.98, 25.17, 25.13, 25.07, 18.93, 17.10, 17.08, 14.34.

HRMS (ESI) *m/z*: $[M + H]^+$ calcd for $C_{156}H_{256}N_6O_{26}$, 2630.8967; found, 2630.9043.

IR (ATR): ṽ (cm^{-1}) = 3308.58, 2923.60, 2852.95, 1737.07, 1654.61, 1535.20, 1456.75, 1370.40, 1233.08, 1160.82, 1107.97, 1003.23, 733.62, 696.93, 502.29.

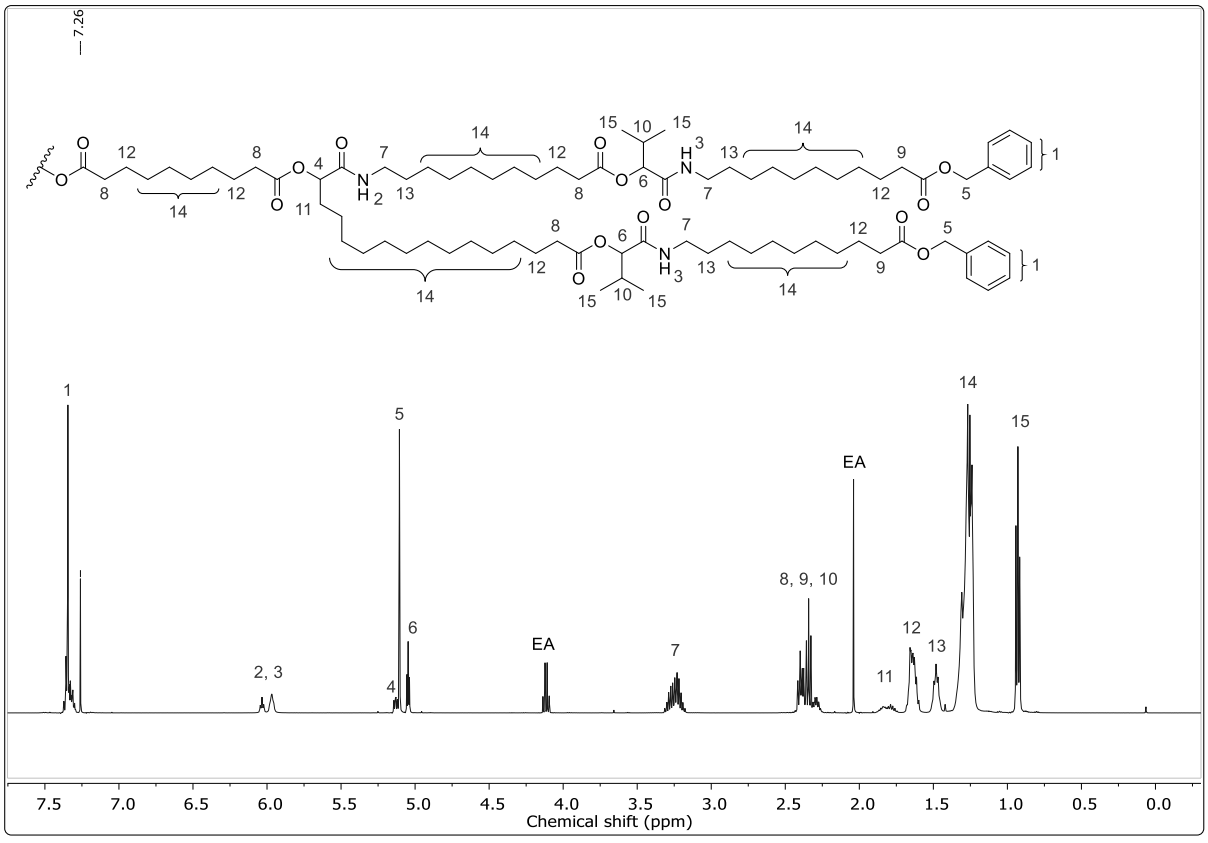

Deprotected star-shaped macromolecule CF-H7-2$_b$

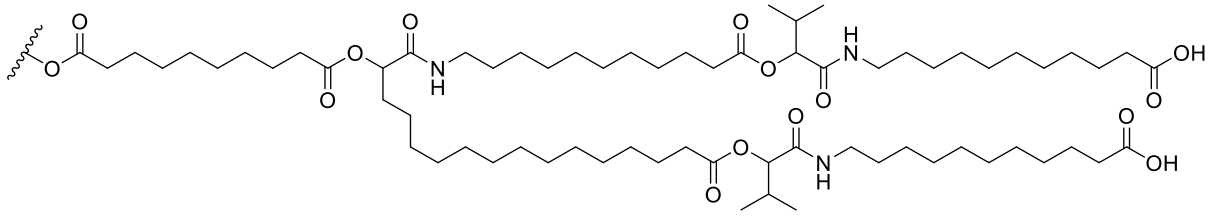

$C_{128}H_{232}N_6O_{26}$

2271.28 g/mol

Benzyl protected star molecule **CF-H7-2** (3.42 g, 1.30 mmol, 1.00 eq.) and 10wt% Pd on Carbon (342 mg) were placed in a round bottom flask and dissolved in ethyl acetate, after vigorous stirring for a few minutes the solution was purged with hydrogen. The reaction was controlled *via* TLC until no benzyl protected polymer was left. The solution was dried over sodium sulfate and filtered through Celite®. Subsequently, the solvent was evaporated under reduced pressure and the residue was dried *in vacuo*. The product **CF-H7-2$_b$** was obtained as a colorless solid (2.82 g, 1.24 mmol, 95%).

TLC: R_f (cyclohexane/ethyl acetate 3:2) = 0.00

^{1}H NMR (500 MHz, $CDCl_3$): δ (ppm) = 6.17 (t, *J* = 5.60 Hz, 2H, CON**H**, ^{1}), 6.09 – 6.03 (m, 4H, CON**H**, ^{2}), 5.15 – 5.13 (m, 2H, C**H**, ^{3}), 5.06 (d, *J* = 4.70 Hz, 2H, C**H**, ^{4}), 5.05 (d, *J* = 4.80 Hz, 2H, C**H**, ^{4}), 3.31 – 3.19 (m, 12H, CONHC**H$_2$**, ^{5}), 2.42 – 2.36 (m, 12H, C**H$_2$**COOR, ^{6}), 2.33 (t, *J* = 7.42 Hz, 8H, C**H$_2$**COOH, ^{7}), 2.33 – 2.25 (m, 4H, C**H**, ^{8}), 1.88 – 1.75 (m, 4H, C**H$_2$**, ^{9}), 1.69 – 1.57 (m, 20H, C**H$_2$**, ^{10}), 1.53 – 1.44 (m, 12H, C**H$_2$**, ^{11}), 1.29 – 1.18 (m, 120H, C**H$_2$**, ^{12}), 0.93 (t, *J* = 6.67 Hz, 24H, C**H$_2$**, ^{13}).

^{13}C NMR (126 MHz, $CDCl_3$): δ (ppm) = 178.63, 172.74, 172.68, 170.27, 169.58, 78.05, 78.02, 74.06, 39.41, 39.30, 34.43, 34.40, 34.36, 34.15, 32.03, 30.62, 29.73, 29.68, 29.63, 29.61, 29.59, 29.56, 29.49, 29.47, 29.40, 29.37, 29.32, 29.26, 29.20, 29.16, 29.13, 29.11, 26.95, 26.93, 26.91, 25.17, 25.14, 24.99, 24.92, 24.86, 18.92, 17.10, 17.08.

HRMS (ESI) *m/z*: $[M + H]^+$ calcd for $C_{128}H_{232}N_6O_{26}$, 2270.7089; found, 2270.7129.

IR (ATR): ṽ (cm^{-1}) = 3311, 2923, 2853, 1738, 1651, 1540, 1464, 1370, 1164, 1109, 1007, 921, 722, 647.

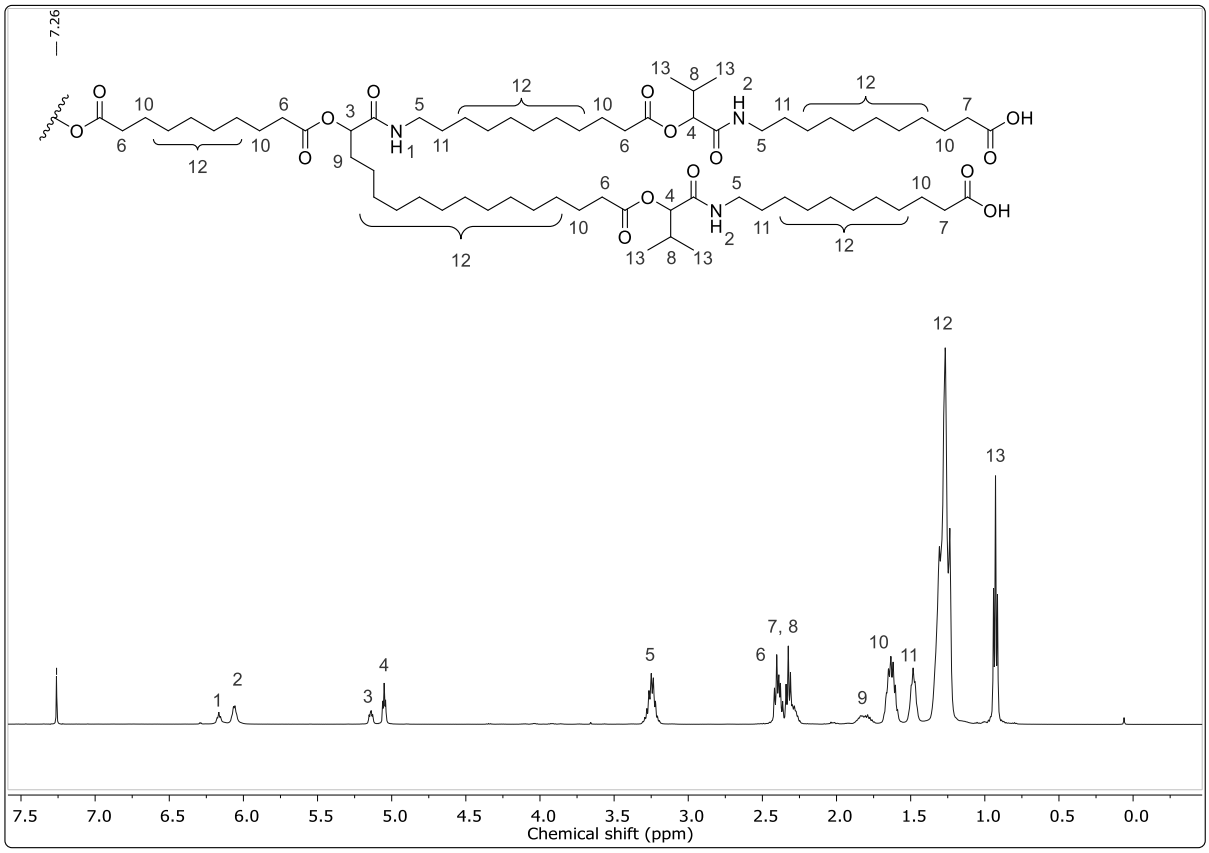

Star-shaped macromolecule CF-H7-3

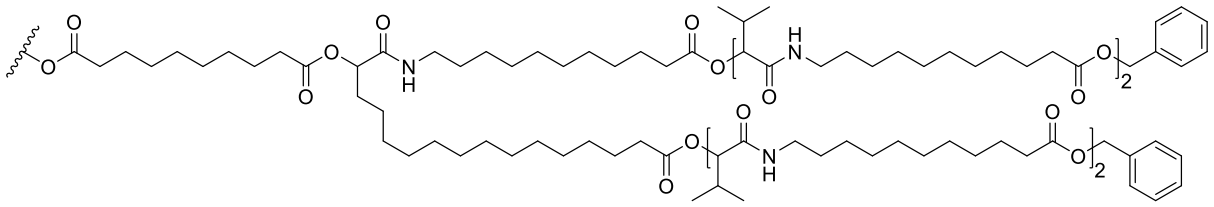

$C_{220}H_{372}N_{10}O_{38}$

3765.43 g/mol

Tetra acid **CF-H7-2b** (2.58 g, 1.14 mmol, 1.00 eq.) was placed in a round bottom flask and dissolved in 5.00 mL THF, after vigorous stirring for a few minutes the solution was purged with Argon. Subsequently, building block **A1** (2.74 g, 9.08 mol, 8.00 eq.) and isobutanal **31** (982 mg, 1.24 mL, 13.6 mmol, 12.0 eq.) were added. The reaction was controlled *via* GPC and the solvent was evaporated under reduced pressure when the tetra acid was consumed. The crude product was purified *via* column chromatography (cyclohexane/ethyl acetate 1:1). The product **CF-H7-3** was obtained as a viscous colorless oil (3.99 g, 1.06 mmol, 93%).

TLC: R_f (cyclohexane/ethyl acetate 3:2) = 0.53

^{1}H NMR (500 MHz, $CDCl_3$): δ (ppm) = 7.37 – 7.29 (s. 20H, C**H**$_{\text{aromatic}}$, ^{1}), 6.07 (t, *J* = 5.60 Hz, 2H, CON**H**, ^{2}), 6.03 – 5.95 (m, 8H, CON**H**, ^{3}), 5.13 – 5.11 (m, 2H, C**H**, ^{4}), 5.10 (s, 8H, C**H$_2$**, ^{5}), 5.04 – 5.03 (m, 8H, C**H**, ^{6}), 3.31 – 3.17 (m, 20H, CONHC**H$_2$**, ^{7}), 2.41 – 2.36 (m, 20H, C**H$_2$**COOR, ^{8}), 2.34 (t, *J* = 7.55 Hz, 8H, C**H$_2$**COOBn, ^{9}), 2.32 – 2.24 (m, 8H, C**H**, ^{10}), 1.88 – 1.74 (m, 4H, C**H$_2$**, ^{11}), 1.67 – 1.59 (m, 28H, C**H$_2$**, ^{12}), 1.52 – 1.42 (m, 20H, C**H$_2$**, ^{13}),1.35 – 1.21 (m, 168H, C**H$_2$**, ^{14}), 0.93 (d, *J* = 6.25 Hz, 48H, C**H$_3$**, ^{15}).

^{13}C NMR (126 MHz, $CDCl_3$): δ (ppm) = 173.79, 172.70, 172.67, 172.57, 169.97, 169.44, 169.40, 169.37, 136.22, 128.65, 128.27, 128.26, 78.02, 78.00, 74.07, 66.18, 39.33, 39.27, 34.43, 34.42, 34.40, 34.35, 32.07, 30.64, 29.75, 29.70, 29.59, 29.57, 29.55, 29.49, 29.46, 29.41, 29.35, 29.32, 29.29, 29.28, 29.24, 29.22, 29.18, 26.96, 25.15, 25.12, 25.05, 24.99, 24.95, 18.91, 17.10, 17.08.

HRMS (ESI) *m/z*: $[M + H]^+$ calcd for $C_{220}H_{372}N_{10}O_{38}$, 3763.7557; found, 3763.7585.

IR (ATR): ṽ (cm^{-1}) = 3303, 2924, 2853, 1738, 1653, 1535, 1463, 1370, 1233, 1161, 1109, 1005, 723, 697, 409.

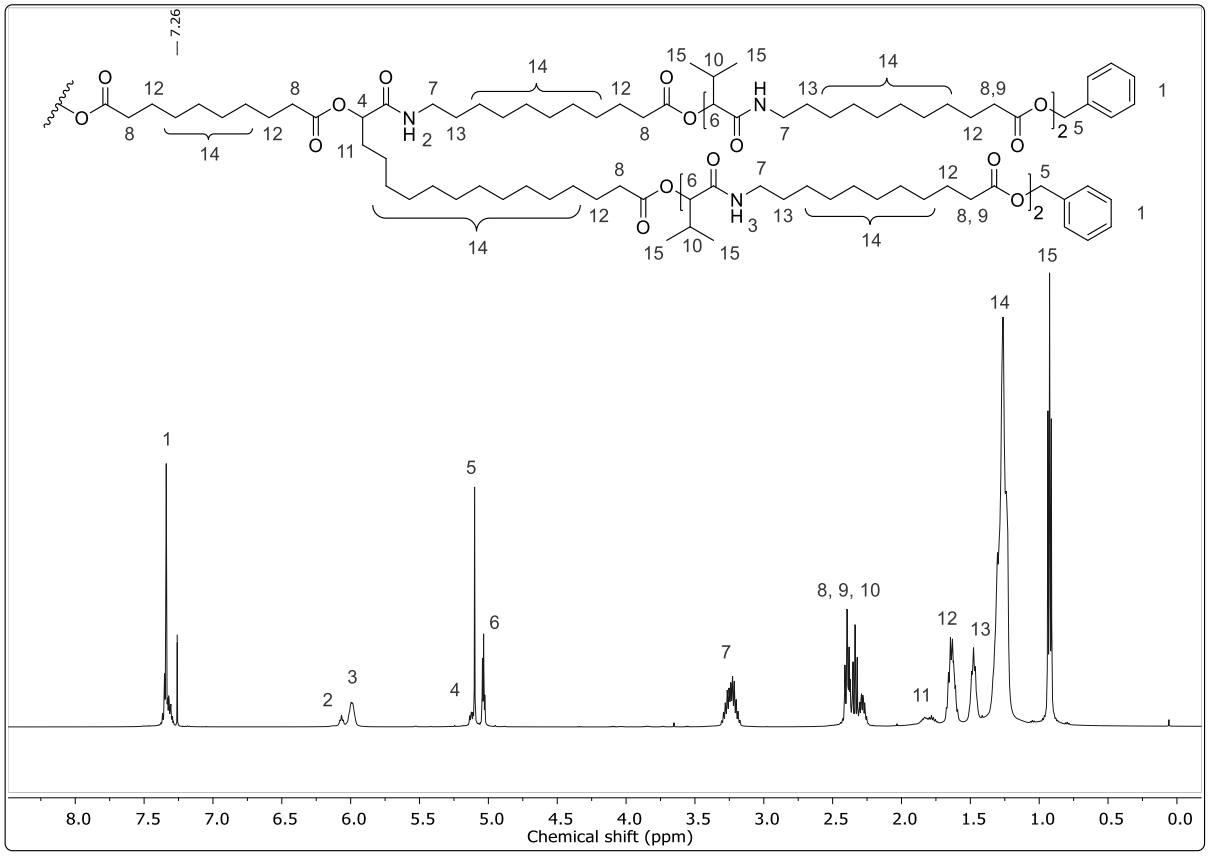

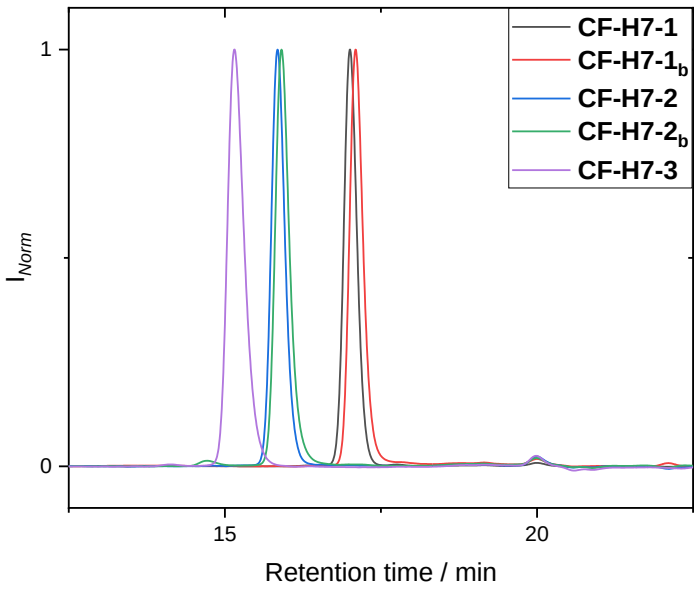

Figure S 8: SEC traces of the star-shaped macromolecules based on core **H7** measured in THF.

6.3.3.3 Linear oligomers and star-shaped macromolecules *via* the arm-first approach

Monomer C1

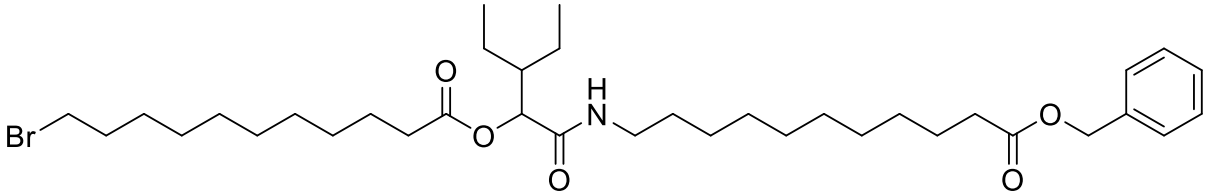

$C_{36}H_{60}BrNO_5$

M = 666.78 g/mol

11-Bromoundecanoic acid **43** (10.7 g, 40.4 mmol, 1.00 eq.) was placed in a round bottom flask and dissolved in 27.0 mL DCM (1.50 mol L^{-1}), after vigorous stirring for a few minutes the solution was purged with argon. Subsequently, 2-ethylbutanal **9** (6.07 g, 60.6 mmol, 7.59 mL, 1.50 eq.) and benzyl 11-isocyanidoundecanoate (building block **A1**) (15.1 g, 50.5 mmol, 1.50 eq.) were added. The reaction was stirred overnight, then the solvent was evaporated under reduced pressure. Subsequently, the crude product was purified *via* column chromatography (cyclohexane/ethyl acetate 7:1 → 5:1). The product **C1** was obtained as slightly yellow oil (26.0 g, 39.0 mmol, 97%).

TLC: R_f (cyclohexane/ethyl acetate 5:1) = 0.41

^{1}H NMR (500 MHz, $CDCl_3$): δ (ppm) = 7.38 – 7.30 (m, 5H, C**H**$_{\text{aromatic}}$, [1]), 5.94 (t, 1H, *J* = 5.36 Hz, CON**H**, [2]), 5.29 (d, 1H, *J* = 3.82 Hz, C**H**, [3]), 5.11 (s. 2H, C**H**$_2$, [4]), 3.40 (t, 2H, *J* = 6.85 Hz, BrC**H**$_2$, [5]), 3.31 – 3.19 (m, 2H, CONHC**H**$_2$, [6]), 2.39 (t, 2H, *J* = 7.65 Hz, C**H**$_2$COOR, [7]), 2.35 (t, 2H, *J* = 7.55 Hz, C**H**$_2$COOBn, [8]), 1.87 – 1.82 (m, 3H, C**H**, C**H**$_2$, [9]), 1.68 – 1.60 (m, 4H, C**H**$_2$, [10]), 1.50 – 1.37 (m, 6H, C**H**$_2$, [11]), 1.34 – 1.16 (m, 24H, C**H**$_2$, [12]), 0.94 – 0.89 (m. 6H, C**H**$_3$, [13]).

^{13}C NMR (126 MHz, $CDCl_3$): δ (ppm) = 173.81, 172.58, 169.85, 136.25, 128.67, 128.29, 75.13, 66.20, 43.63, 39.33, 34.49, 34.45, 34.16, 32.93, 29.68, 29.58, 29.49, 29.46, 29.34, 29.25, 28.86, 28.27, 26.99, 25.15, 25.07, 22.36, 22.05, 11.76, 11.71.

HRMS (ESI) *m/z*: $[M + H]^+$ calcd for $C_{36}H_{60}BrNO_5$, 666.3728; found, 666.3728.

IR (ATR): ṽ (cm^{-1}) = 3332, 2925, 2854, 1737, 1656, 1530, 1457, 1380, 1241, 1159, 1115, 1004, 735, 697, 644, 563, 503.

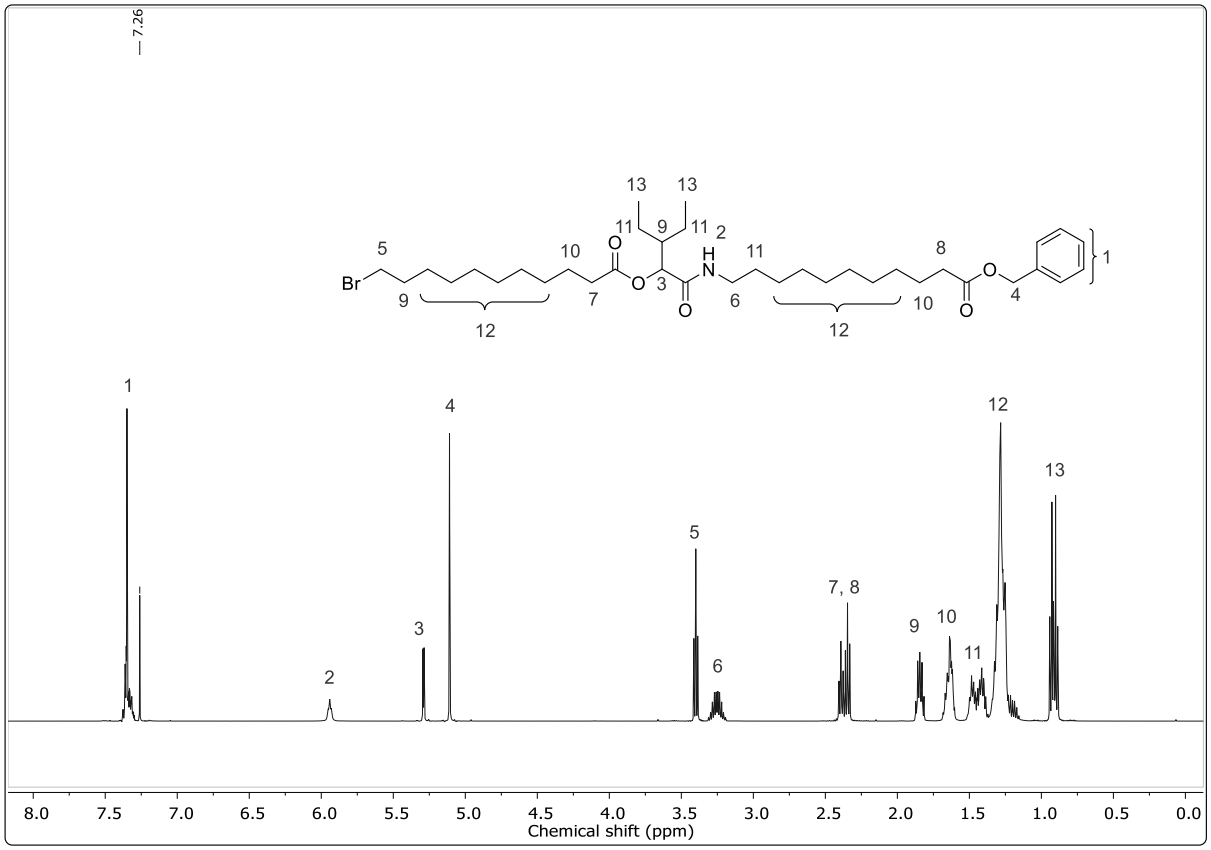

Deprotected Monomer C1$_b$

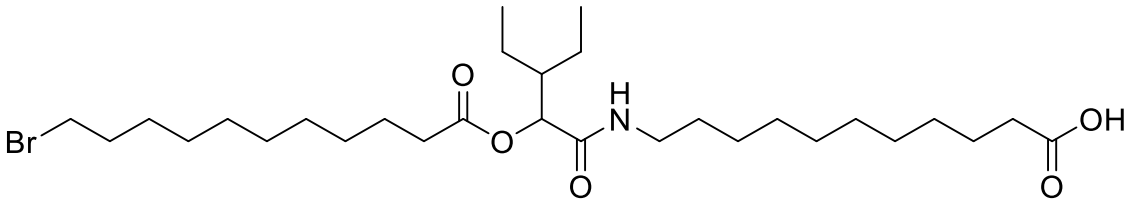

$C_{29}H_{54}BrNO_5$

M = 576.66 g/mol

Benzyl protected monomer **C1** (26.0 g, 39.0 mmol, 1.00 eq.) and 10wt% Pd on activated charcoal (2.60 g) were placed in a round bottom flask and dissolved in ethyl acetate, after vigorous stirring for a few minutes the solution was purged with hydrogen. The reaction was monitored *via* TLC until no benzyl protected oligomer was left. The solution was dried over sodium sulfate and filtered through Celite®. Subsequently, the solvent was evaporated under reduced pressure and the residue was dried *in vacuo*. The product **C1$_b$** was obtained as slightly yellow oil (22.1 g, 38.3 mmol, 98%).

TLC: R_f (cyclohexane/ethyl acetate 5:1) = 0.41

^{1}H NMR (500 MHz, $CDCl_3$): δ (ppm) = 6.00 (t, 1H, *J* = 5.66 Hz, CON**H**, ^{1}), 5.28 (d, 1H, *J* = 3.86 Hz, C**H**, ^{2}), 3.40 (t, 2H, *J* = 6.85 Hz, BrC**H$_2$**, ^{3}), 3.31 – 3.19 (m, 2H, CONHC**H$_2$**, ^{4}), 2.39 (t, 2H, *J* = 7.62 Hz, C**H$_2$**COOR, ^{5}), 2.32 (t, 2H, *J* = 7.50 Hz, C**H$_2$**COOH, ^{6}), 1.87 – 1.81 (m, 3H, C**H**, C**H$_2$**, ^{7}), 1.68 – 1.58 (m, 4H, C**H$_2$**, ^{8}), 1.50 – 1.38 (m, 6H, C**H$_2$**, ^{9}), 1.32 – 1.15 (m, 24H, C**H$_2$**, ^{10}), 0.93 – 0.88 (m. 6H, C**H$_3$**, ^{11}).

^{13}C NMR (126 MHz, $CDCl_3$): δ (ppm) = 179.35, 172.64, 169.98, 75.12, 43.59, 39.36, 34.47, 34.24, 34.15, 32.92, 29.62, 29.51, 29.48, 29.45, 29.40, 29.33, 29.27, 29.24, 29.14, 28.85, 28.76, 28.26, 26.95, 25.15, 24.85, 22.34, 22.02, 11.73, 11.68.

HRMS (ESI) *m/z*: $[M + H]^+$ calcd. for $C_{29}H_{54}BrNO_5$, 576.3258; found, 576.3259.

IR (ATR): ṽ (cm^{-1}) = 2925, 2854, 1740, 1710, 1651, 1537, 1461, 1379, 1240, 1159, 1121, 1046, 1010, 930, 722, 645, 563.

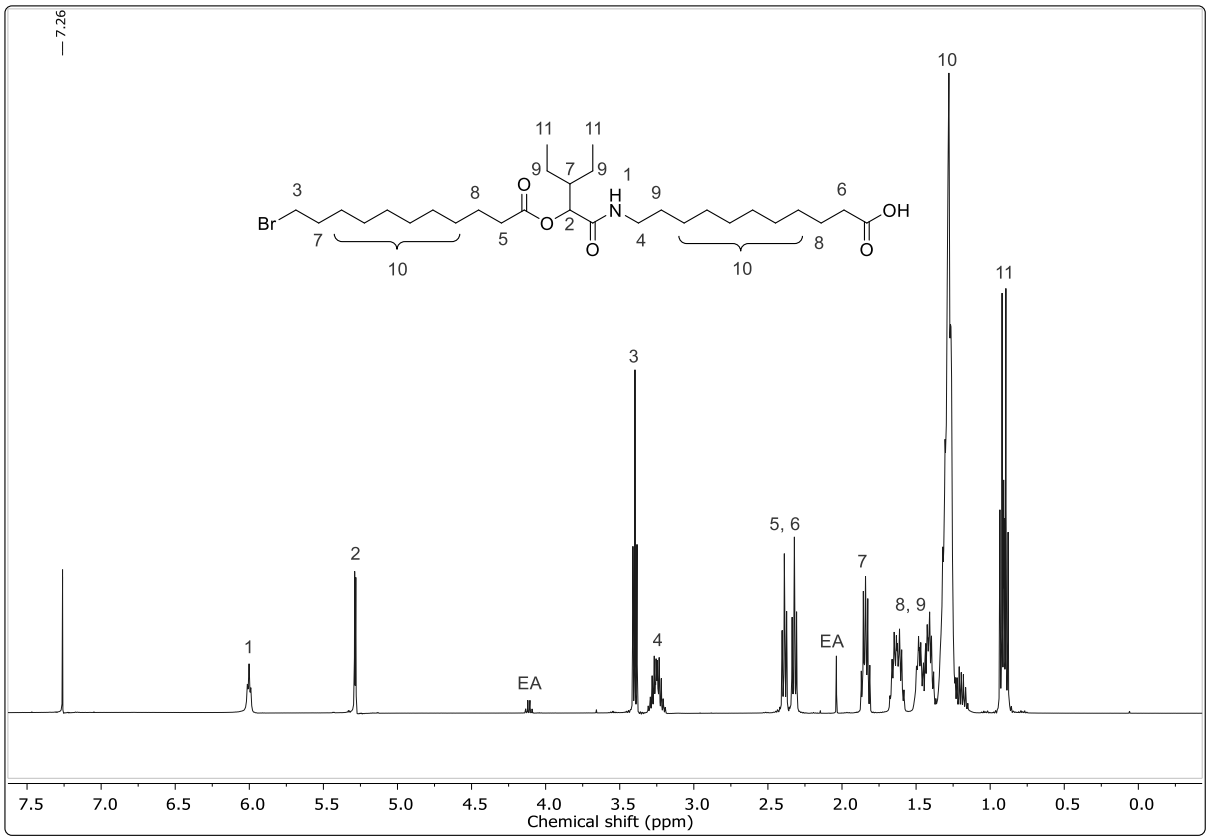

Trimer C2

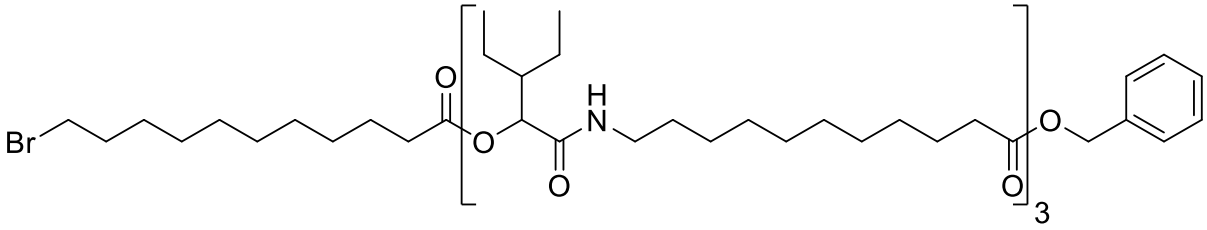

$C_{72}H_{126}BrN_3O_{11}$

M = 1289.71 g/mol

Deprotected monomer **C1d** (21.8 g, 37.8 mmol, 1.00 eq.) was placed in a round bottom flask and dissolved in 25.2 mL DCM (1.5 mol/L), after vigorous stirring for a few minutes the solution was purged with Argon. Subsequently, 2-ethylbutanal **9** (5.68 g, 56.7 mmol, 7.06 mL, 1.50 eq.) and Benzyl 11-(3-ethyl-2-((11-isocyanoundecanoyl)oxy)pentanamido)undecanoate (building block **A2**) (29.0 g, 50.3 mmol, 1.25 eq.) were added. The reaction was stirred overnight, then the solvent was evaporated under reduced pressure. Subsequently, the crude product was purified *via* gradient column chromatography (cyclohexane/ethyl acetate 7:1 → 4:1). The product **C2** was obtained as slightly yellow oil (44.9 g, 37.8 mmol, 92%).

TLC: R_f (cyclohexane/ethyl acetate 5:1) = 0.41

^{1}H NMR (500 MHz, $CDCl_3$): δ (ppm) = 7.37 – 7.29 (m, 5H, C**H**$_{\text{aromatic}}$, ^{1}), 5.99 – 5.98 (m, 3H, CON**H**, ^{2}), 5.29 – 5.27 (m, 3H, C**H**, ^{3}), 5.10 (s. 2H, C**H$_2$**, ^{4}), 3.39 (t, 2H, *J* = 6.84 Hz, BrC**H$_2$**, ^{5}), 3.29 – 3.18 (m, 6H, CONHC**H$_2$**, ^{6}), 2.38 (t, 6H, *J* = 7.75 Hz, C**H$_2$**COOR, ^{7}), 2.33 (t, 2H, *J* = 7.55 Hz, C**H$_2$**COOBn, ^{8}), 1.86 – 1.81 (m, 5H, C**H**, C**H$_2$**, ^{9}), 1.67 – 1.59 (m, 8H, C**H$_2$**, ^{10}), 1.51 – 1.15 (m, 66H, C**H$_2$**, ^{11}), 0.92 (t. 9H, *J* = 7.44 Hz, C**H$_3$**, ^{12}), 0.89 (t. 9H, *J* = 7.44 Hz, C**H$_3$**, ^{12}).

^{13}C NMR (126 MHz, $CDCl_3$): δ (ppm) = 173.77, 172.57, 169.83, 169.82, 136.21, 128.63, 128.26, 128.24, 75.08, 66.16, 53.55, 43.60, 39.30, 39.29, 34.44, 34.42, 34.13, 32.89, 29.66, 29.65, 29.56, 29.55, 29.47, 29.45, 29.42, 29.32, 29.31, 29.29, 29.22, 29.21, 28.82, 28.23, 26.95, 25.11, 25.04, 22.32, 22.01, 11.72, 11.68, 11.59.

HRMS (ESI) *m/z*: $[M + H]^+$ calcd for $C_{72}H_{126}BrN_3O_{11}$, 1288.8649; found, 1288.8669.

IR (ATR): $\tilde{\nu}$ (cm^{-1}) = 3317, 2925, 2854, 1739, 1652, 1532, 1459, 1378, 1240, 1158, 1111, 1047, 1007, 733, 697, 646.

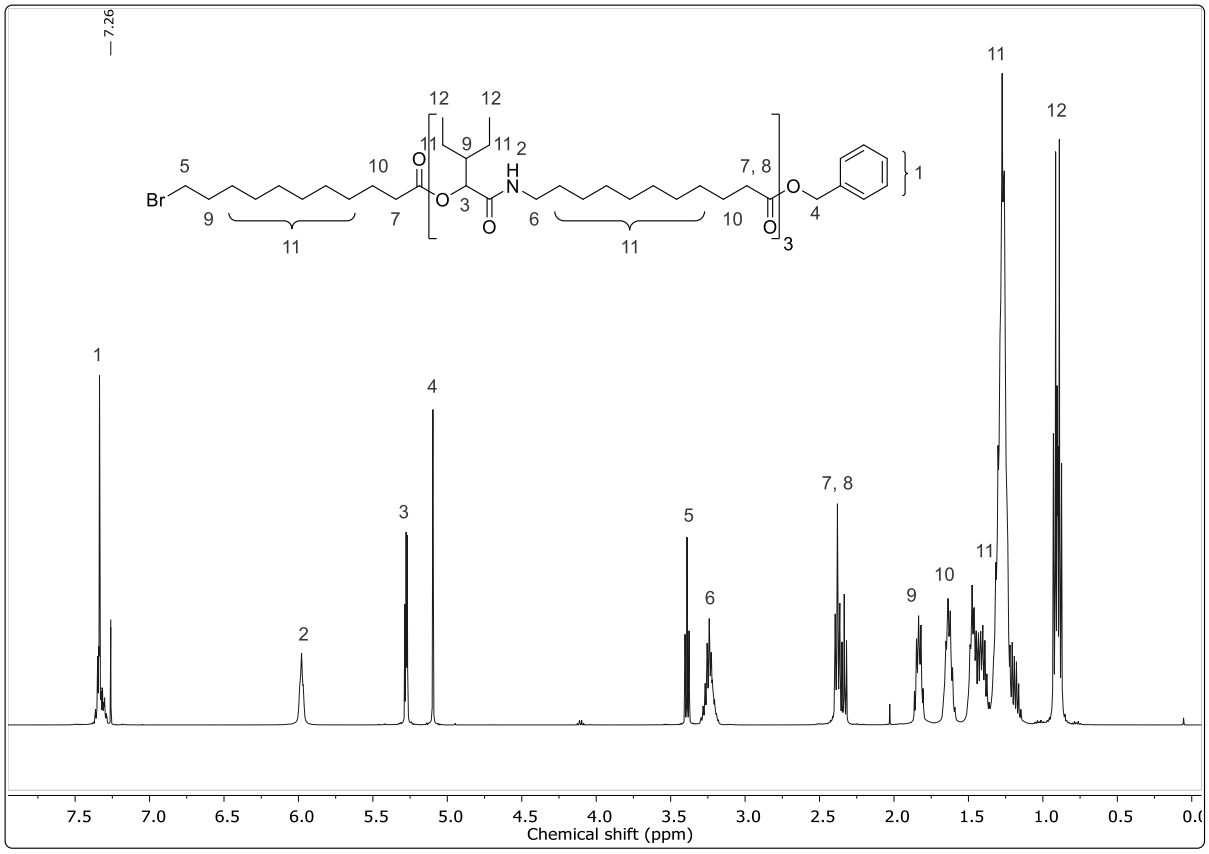

Deprotected trimer C2$_b$

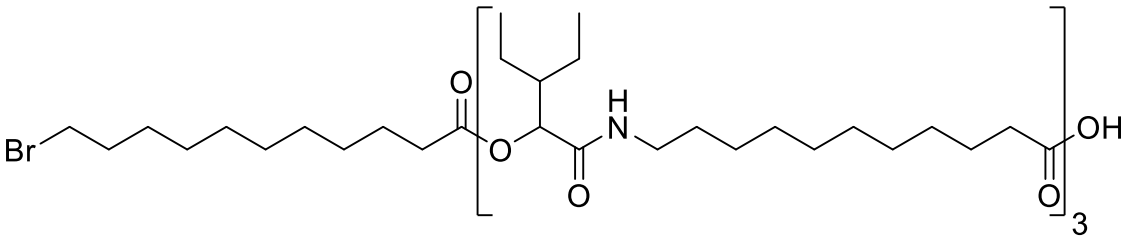

$C_{65}H_{120}BrN_3O_{11}$

M = 1199.59 g/mol

Benzyl protected trimer **C2** (26.1 g, 20.2 mmol, 1.00 eq.) and 10wt% Pd on activated charcoal (2.61 g) were placed in a round bottom flask and dissolved in ethyl acetate, after vigorous stirring for a few minutes the solution was purged with hydrogen. The reaction was monitored *via* TLC until no benzyl protected oligomer was left. The solution was dried over sodium sulfate and filtered through Celite®. Subsequently, the solvent was evaporated under reduced pressure and the residue was dried *in vacuo*. The product **C2$_b$** was obtained as slightly yellow oil (23.9 g, 19.9 mmol, 99%).

TLC: R_f (cyclohexane/ethyl acetate 3:2) = 0.21

^{1}H NMR (500 MHz, $CDCl_3$): δ (ppm) = 6.05 – 5.99 (m, 3H, CON**H**, ^{1}), 5.29 – 5.28 (m, 3H, C**H**, ^{2}), 3.40 (t, 2H, *J* = 6.84 Hz, BrC**H$_2$**, ^{3}), 3.31 – 3.20 (m, 6H, CONHC**H$_2$**, ^{4}), 2.39 (t, 6H, *J* = 7.46 Hz, C**H$_2$**COOR, ^{5}), 2.33 (t, 2H, *J* = 7.45 Hz, C**H$_2$**COOH, ^{6}), 1.87 – 1.82 (m, 5H, C**H**, C**H$_2$**, ^{7}), 1.66 – 1.59 (m, 8H, C**H$_2$**, ^{8}), 1.50 – 1.15 (m, 66H, C**H$_2$**, ^{9}), 0.94 – 0.88 (m. 18H, C**H$_3$**, ^{10}).

^{13}C NMR (126 MHz, $CDCl_3$): δ (ppm) = 177.13, 172.71, 172.64, 172.63, 170.05, 169.98, 169.95, 75.15, 75.13, 75.12, 43.61, 43.58, 39.40, 39.36, 39.31, 34.48, 34.17, 3400, 33.97, 32.93, 29.68, 29.67, 29.61, 29.59, 29.49, 29.46, 29.38, 29.34, 29.32, 29.28, 29.25, 29.21, 28.86, 28.27, 26.98, 25.18, 25.14, 24.90, 22.35, 22.32, 22.03, 22.01, 11.74,11.73, 11.70, 11.67.

HRMS (ESI) *m/z*: $[M + H]^+$ calcd for $C_{65}H_{120}BrN_3O_{11}$, 1198.8179; found, 1198.8176.

IR (ATR): ṽ (cm^{-1}) = 3324, 2925, 2854, 1740, 1651, 1536, 1461, 1373, 1239, 1158, 1111, 1046, 1009, 924, 722, 646.

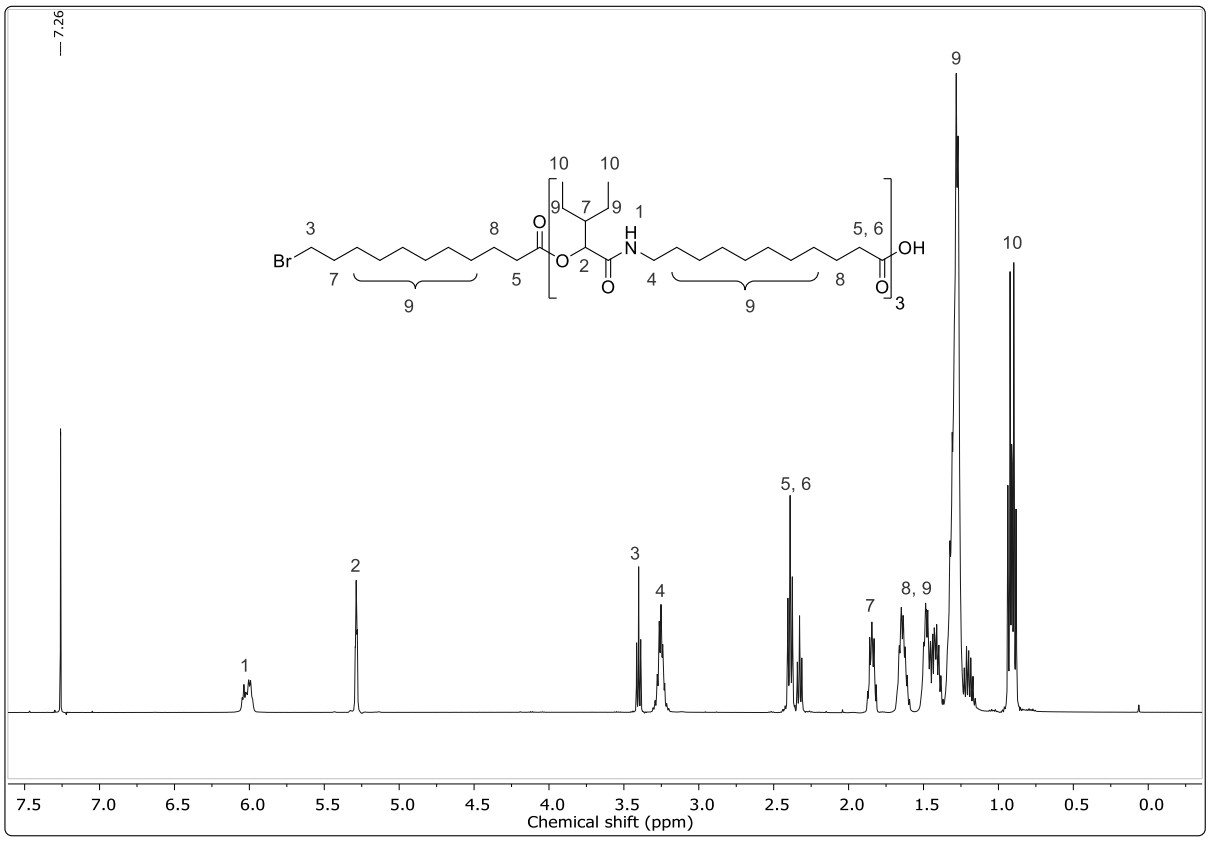

PEGylated Trimer D1

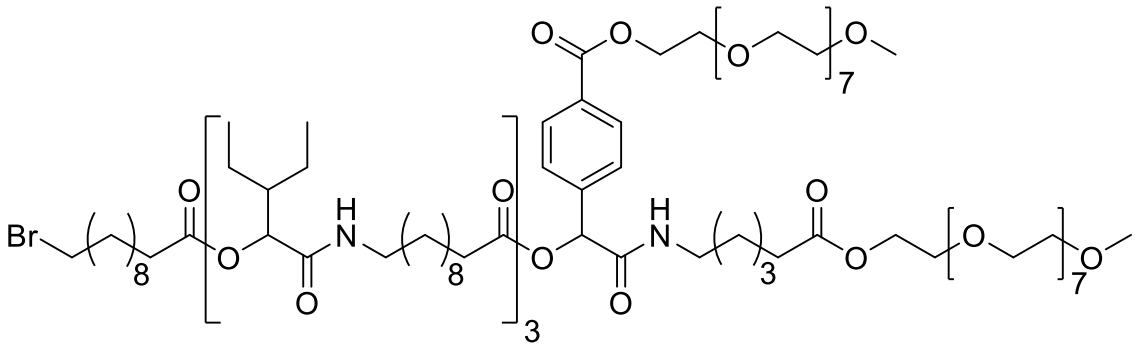

$C_{114}H_{205}BrN_4O_{32}$

M = 2223.79 g/mol

Deprotected trimer **C2b** (5.94 g, 4.95 mmol, 1.00 eq.) was placed in a round bottom flask and dissolved in 15.0 mL DCM (0.330 mol L^{-1}), after vigorous stirring for a few minutes the solution was purged with argon. Subsequently, 4-formyl (octa(ethylene glycol) mono methyl ether) benzoate (building block **B2**) (3.84 g, 7.43 mmol, 1.50 eq.) and 6-isocyano (octa(ethylene glycol) mono methyl ether) hexanoate (building block **B1**) (3.77 g, 7.43 mmol 1.50 eq.) were added. The reaction was stirred under argon for 48 h and then refluxed for another 24 h. Then, the solvent was evaporated, and the crude product was purified *via* column chromatography (ethyl acetate → ethyl acetate/methanol 40:1 → ethyl acetate/methanol 20:1 → ethyl acetate/acetone 1:1). The product **D1** was obtained as slightly yellow oil (8.91 g, 4.01 mmol, 81%).

TLC: R_f (ethyl acetate/methanol 5:1) = 0.21

^{1}H NMR (500 MHz, $CDCl_3$): δ (ppm) = 8.04 (d, 2H, *J* = 8.35 Hz, C**H**$_{\textbf{aromatic}}$, [1]), 7.50 (d, 2H, *J* = 8.32 Hz, C**H**$_{\textbf{aromatic}}$, [2]), 6.34 (t, 1H, *J* = 5.65 Hz, CON**H**, [3]), 6.08 (s, 1H, C**H**, [4]), 6.00 – 5.95 (m, 3H, CON**H**, [5]), 5.29 – 5.27 (m, 3H, C**H**, [6]), 4.47 – 4.45 (m, 2H, PhCOOC**H$_2$**CH_2OR, [7]), 4.22 – 4.20 (m, 2H, COOC**H$_2$**CH_2OR, [8]), 3.82 – 3.81 (m, 2H, PhCOOCH_2**CH_2**OR, [9]), 3.70 – 3.53 (m, 58H, OC**H$_2$**, [10]), 3.40 (t, 2H, *J* = 6.85 Hz, BrC**H$_2$**, [11]), 3.37 (s, 6H, OC**H$_3$**, [12]), 3.30 – 3.20 (m, 8H, CONHC**H$_2$**, [13]), 2.48 – 2.43 (m, 2H, C**H$_2$**COOR (third repeating unit), [14]), 2.39 (t, 6H, *J* = 7.79 Hz, C**H$_2$**COOR (startblock + first and second repeating unit), [15]), 2.32 (t, 2H, *J* = 7.39 Hz, C**H$_2$**COOCH_2CH_2O, [16]), 1.87 – 1.82 (p, 5H, *J* = 6.88 Hz, C**H**, C**H$_2$**, [17]), 1.70 – 1.16 (m, 82H, C**H$_2$**, [18]), 0.94 – 0.88 (m. 18H, C**H$_3$**, [19]).

^{13}C NMR (126 MHz, $CDCl_3$): δ (ppm) = 173.61, 172.61, 171.94, 169.87, 167.79, 166.14, 140.88, 130.59, 130.17, 127.26, 75.12, 74.93, 72.08, 70.82, 70.78, 70.77, 70.75, 70.71, 70.66, 69.32, 69.28, 64.39, 63.59, 59.18, 43.64, 39.37, 39.33, 34.49, 34.28, 34.17, 34.01, 32.93, 29.71, 29.60, 29.58, 29.51, 29.49, 29.46, 29.36, 29.34, 29.33, 29.31, 29.26, 29.25, 29.18, 28.86, 28.27, 26.99, 26.34, 25.15, 24.90, 24.43, 22.36, 22.05, 11.76, 11.72.

HRMS (ESI) *m/z*: $[M + H]^+$ calcd for $C_{114}H_{205}BrN_4O_{32}$, 2222.3793; found, 2222.3801.

IR (ATR): ṽ (cm^{-1}) = 3317, 2926, 2856, 1738, 1657, 1532, 1459, 1351, 1274, 1245, 1101, 1042, 947, 851, 723, 559.

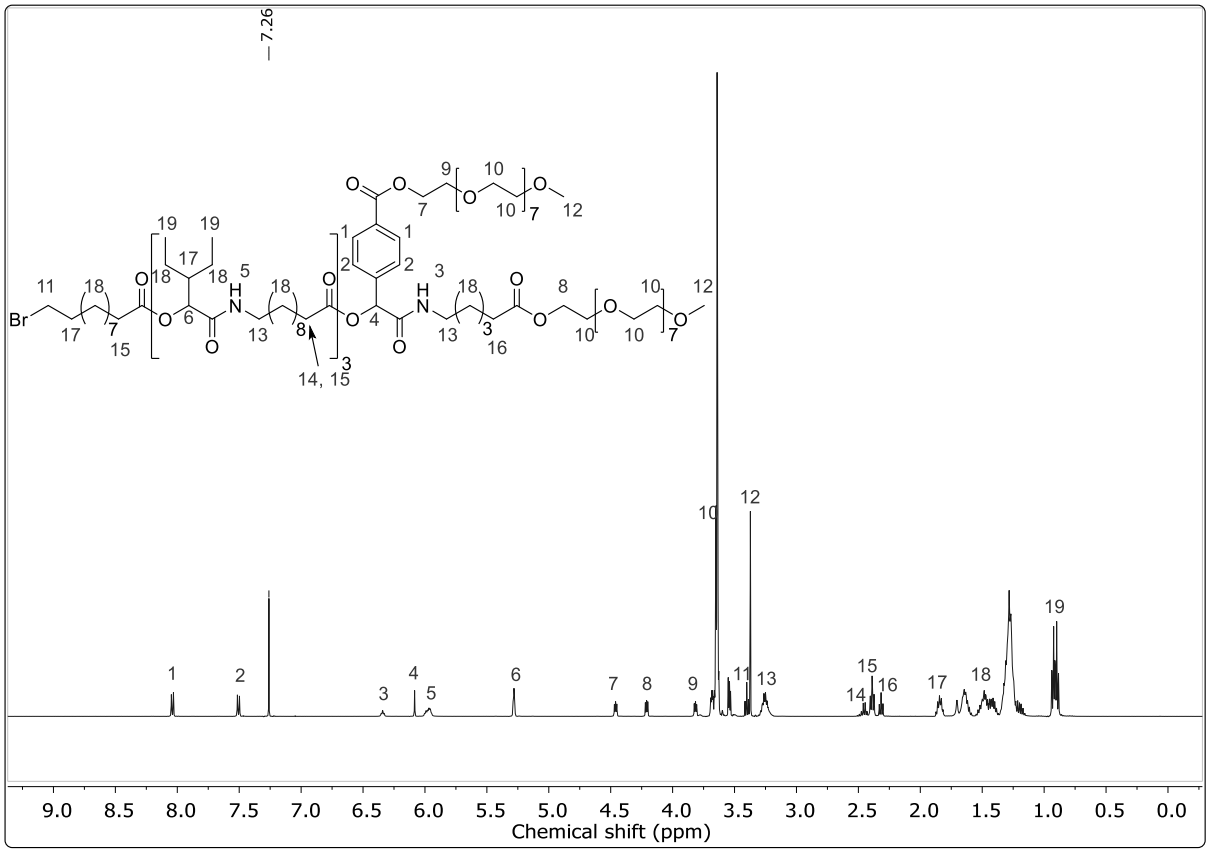

Azidated Trimer D1$_b$

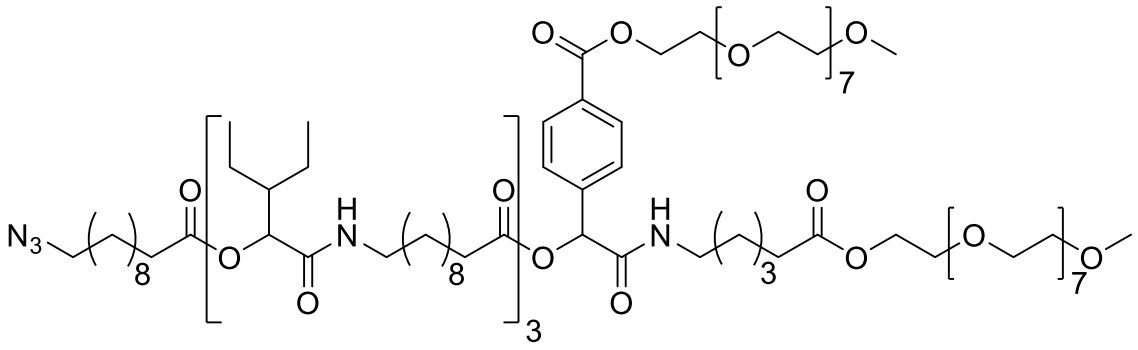

$C_{114}H_{205}N_7O_{32}$

M = 2185.91 g/mol

PEGylated trimer **D1** (4.15 g, 1.86 mmol, 1.00 eq.) was dissolved in MeCN (5 mL). Subsequently, sodium azide (363 mg, 5.58 mmol, 3.00 eq.) was added and the reaction was stirred overnight at 75 °C. Afterwards, the reaction was filtrated and subjected to flash column chromatography (acetone). The product **D1$_b$** was obtained as slightly yellow oil (4.07 g, 1.86 mmol, quant. yield).

TLC: R_f (ethyl acetate/methanol 5:1) = 0.21

^{1}H NMR (500 MHz, $CDCl_3$): δ (ppm) = 8.04 (d, 2H, *J* = 8.37 Hz, C**H**$_{aromatic}$, ^{1}), 7.50 (d, 2H, *J* = 8.32 Hz, C**H**$_{aromatic}$, ^{2}), 6.34 (t, 1H, *J* = 5.69 Hz, CON**H**, ^{3}), 6.08 (s, 1H, C**H**, ^{4}), 6.00 – 5.95 (m, 3H, CON**H**, ^{5}), 5.29 – 5.27 (m, 3H, C**H**, ^{6}), 4.47 – 4.45 (m, 2H, PhCOOC**H$_2$**CH$_2$OR, ^{7}), 4.22 – 4.20 (m, 2H, COOC**H$_2$**CH$_2$OR, ^{8}), 3.82 – 3.80 (m, 2H, PhCOOCH$_2$**CH$_2$**OR, ^{9}), 3.69 – 3.53 (m, 58H, OC**H$_2$**, ^{10}), 3.37 (s, 6H, OC**H$_3$**, ^{11}), 3.30 – 3.19 (m, 10H, CONHC**H$_2$**, C**H$_2$**N$_3$, ^{12}), 2.47 – 2.43 (m, 2H, C**H$_2$**COOR (third repeating unit), ^{13}), 2.39 (t, 6H, *J* = 7.74 Hz, C**H$_2$**COOR (startblock + first and second repeating unit), ^{14}), 2.32 (t, 2H, *J* = 7.39 Hz, C**H$_2$**COOCH$_2$CH$_2$O, ^{15}), 1.88 – 1.80 (m, 3H, C**H**, ^{16}), 1.73 – 1.16 (m, 82H, C**H$_2$**, ^{17}), 0.94 – 0.88 (m. 18H, C**H$_3$**, ^{18}).

^{13}C NMR (126 MHz, $CDCl_3$): δ (ppm) = 173.61, 172.61, 171.93, 169.86, 167.78, 166.14, 140.88, 130.59, 130.17, 127.25, 75.11, 74.92, 72.07, 70.81, 70.78, 70.77, 70.75, 70.71, 70.66, 69.32, 69.28, 64.38, 63.59, 59.18, 51.60, 43.64, 39.36, 39.33, 34.48, 34.28, 34.00, 29.70, 29.60, 29.58, 29.53, 29.50, 29.46, 29.36, 29.35, 29.32, 29.31, 29.26, 29.25, 29.17, 28.96, 26.98, 26.83, 26.34, 25.15, 24.90, 24.43, 22.36, 22.04, 11.76, 11.71.

HRMS (ESI) *m/z*: $[M + H]^+$ calcd for $C_{114}H_{205}N_7O_{32}$, 2185.4702; found, 2185.4712.

IR (ATR): $\tilde{\nu}$ (cm^{-1}) = 3325, 2925, 2856, 2095, 1738, 2095, 1738, 1658, 1532, 1460, 1351, 1274, 1245, 1102, 1043, 946, 851, 722, 550.

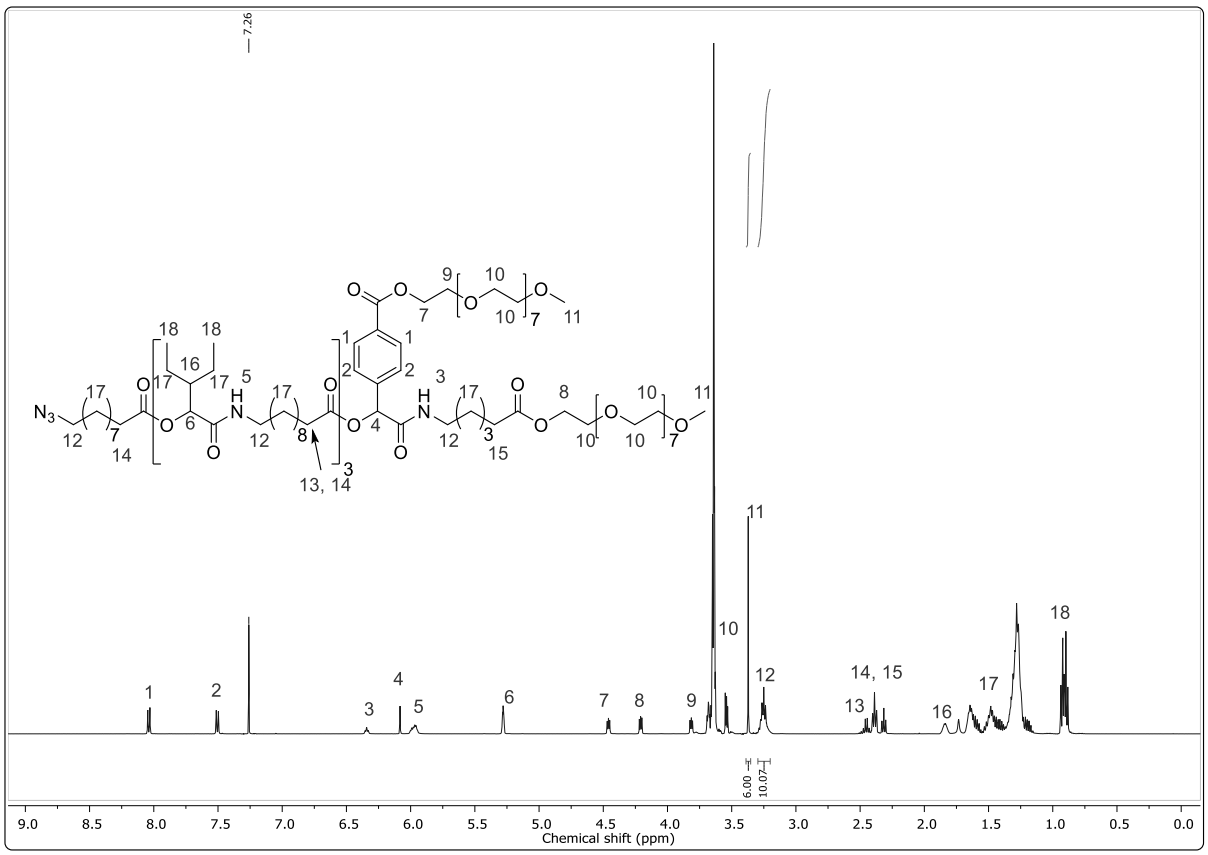

Pentamer C3

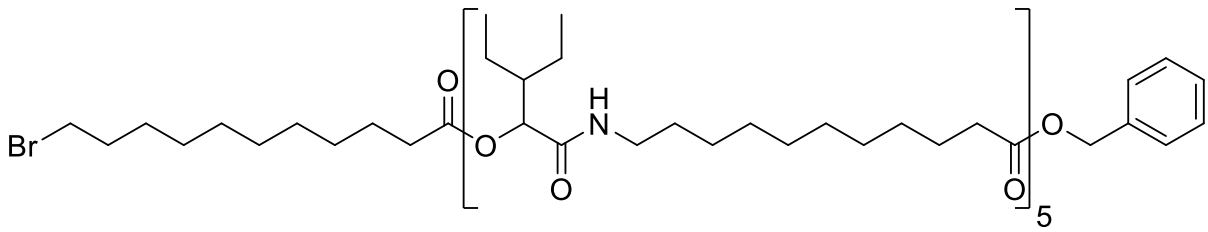

$C_{108}H_{192}BrN_5O_{17}$

M = 1912.65 g/mol

Deprotected trimer **C2b** (23.2 g, 19.3 mmol, 1.00 eq.) was placed in a round bottom flask and dissolved in 19.3 mL DCM (1.00 mol L^{-1}), after vigorous stirring for a few minutes the solution was purged with argon. Subsequently, 2-ethylbutanal **9** (3.61 g, 29.0 mmol, 3.61 mL, 1.50 eq.) and building block **A2** (17.7 g, 29.0 mmol, 1.50 eq.) were added. The reaction was stirred overnight, then the solvent was evaporated under reduced pressure. Subsequently, the crude product was purified *via* gradient column chromatography (cyclohexane/ethyl acetate 10:1 → 5:1 + 2.50%

triethylamine). The product **C3** was obtained as slightly yellow oil (34.3 g, 17.9 mmol, 93%)

TLC: R_f (cyclohexane/ethyl acetate 2:1) = 0.43

^{1}H NMR (500 MHz, $CDCl_3$): δ (ppm) = 7.37 – 7.29 (m, 5H, C**H**$_{\mathbf{aromatic}}$, ^{1}), 5.99 – 5.98 (m, 5H, CON**H**, ^{2}), 5.28 (d, 5H, *J* = 3.32 Hz, C**H**, ^{3}), 5.10 (s. 2H, C**H$_2$**, ^{4}), 3.40 (t, 2H, *J* = 6.84 Hz, BrC**H$_2$**, ^{5}), 3.30 – 3.19 (m, 10H, CONHC**H$_2$**, ^{6}), 2.39 (t, 10H, *J* = 7.57 Hz, C**H$_2$**COOR, ^{7}), 2.33 (t, 2H, *J* = 7.55 Hz, C**H$_2$**COOBn, ^{8}), 1.87 – 1.82 (m, 7H, C**H**, C**H$_2$**, ^{9}), 1.68 – 1.60 (m, 12H, C**H$_2$**, ^{10}), 1.50 – 1.15 (m, 102H, C**H$_2$**, ^{11}), 0.94 – 0.88 (m. 30H, C**H$_3$**, ^{12}).

^{13}C NMR (126 MHz, $CDCl_3$): δ (ppm) = 173.81, 172.61, 169.87, 169.85, 136.24, 128.66, 128.28, 75.11, 66.19, 43.63, 39.32, 34.47, 34.45, 34.16, 32.92, 27.70, 29.68, 29.59, 29.58, 29.50, 29.48, 29.45, 29.36, 29.34, 29.32. 29.26, 29.24, 26.98, 25.14, 25.08, 22.35, 22.03, 11.75, 11.70.

HRMS (ESI) *m/z*: $[M + H]^+$ calcd for $C_{108}H_{192}BrN_5O_{17}$, 1911.3569; found, 1911.3593.

IR (ATR): ṽ (cm^{-1}) = 3313, 2925, 2854, 1740, 1651, 1532, 1461, 1378, 1239, 1156.98, 1111, 1047, 1008, 723, 697, 648.

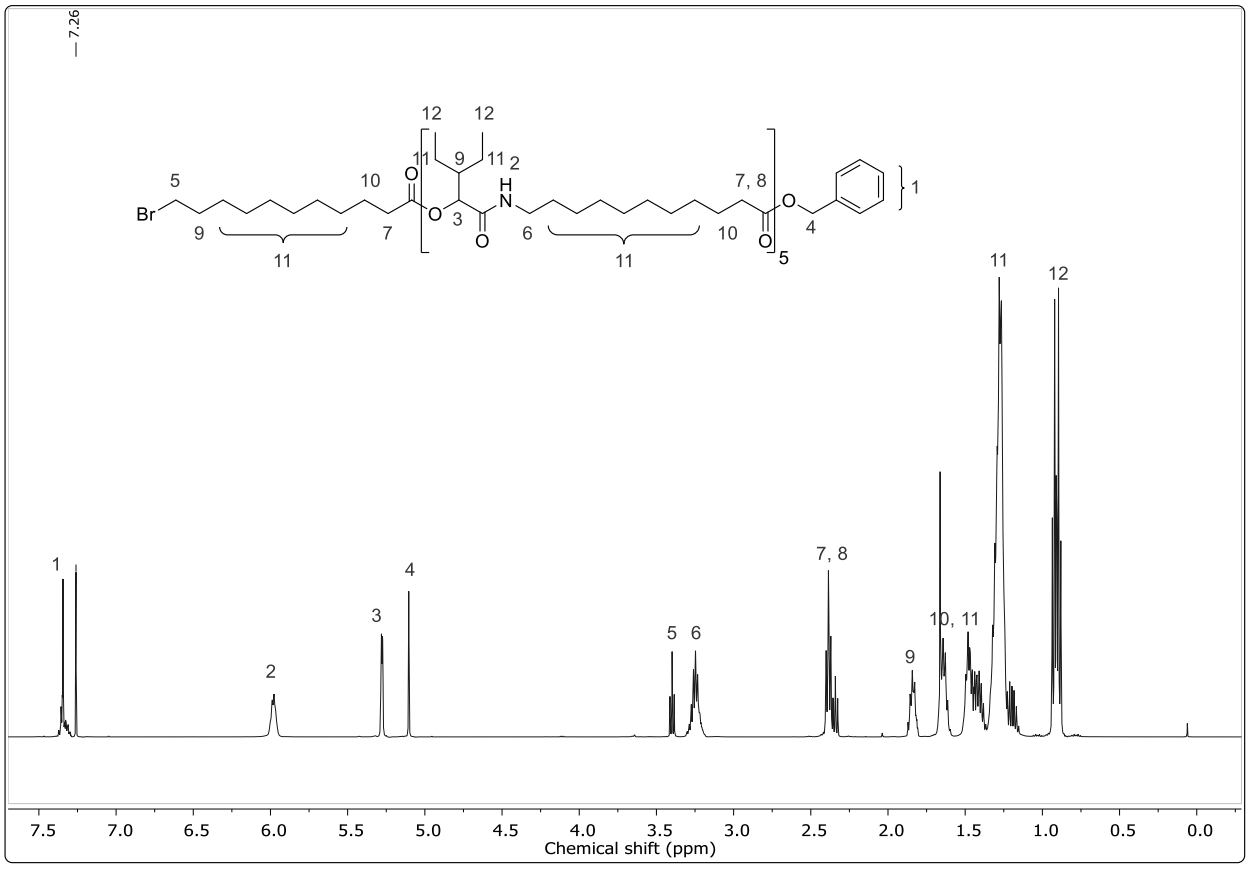

Deprotected Pentamer C3$_b$

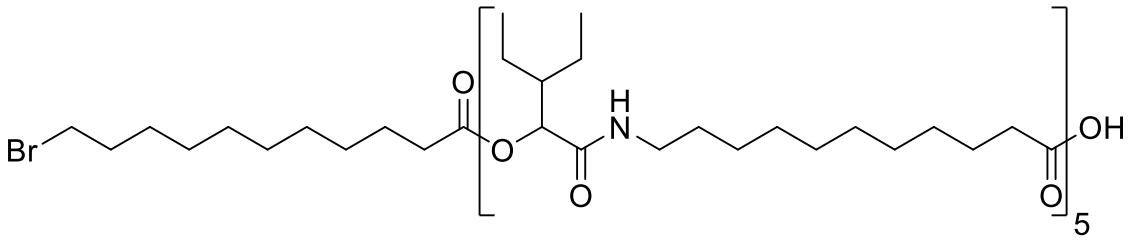

$C_{101}H_{186}BrN_5O_{17}$

M = 1822.52 g/mol

Benzyl protected pentamer **C3** (16.7 g, 8.75 mmol, 1.00 eq.) and 10 wt% Pd on activated charcoal (1.67 g) were placed in a round bottom flask and dissolved in ethyl acetate, after vigorous stirring for a few minutes the solution was purged with hydrogen. The reaction was monitored *via* TLC until no benzyl protected oligomer was left. The solution was dried over sodium sulfate and filtered through Celite®. Subsequently, the solvent was evaporated under reduced pressure and the residue was dried *in vacuo*. The product **C3$_b$** was obtained as slightly yellow oil (15.6 g, 8.57 mmol, 98%).

TLC: R_f (cyclohexane/ethyl acetate 2:1) = 0.00

^{1}H NMR (500 MHz, $CDCl_3$): δ (ppm) = 6.08 – 5.98 (m, 5H, CON**H**, ^{1}), 5.29 – 5.27 (m, 5H, C**H**, ^{2}), 3.40 (t, 2H, *J* = 6.84 Hz, BrC**H$_2$**, ^{3}), 3.30 – 3.19 (m, 10H, CONHC**H$_2$**, ^{4}), 2.39 (t, 10H, *J* = 7.53 Hz, C**H$_2$**COOR, ^{5}), 2.32 (t, 2H, *J* = 7.46 Hz, C**H$_2$**COOBn, ^{6}), 1.87 – 1.81 (m, 7H, C**H**, C**H$_2$**, ^{7}), 1.66 – 1.59 (m, 12H, C**H$_2$**, ^{8}), 1.49 – 1.15 (m, 102H, C**H$_2$**, ^{9}), 0.93 – 0.88 (m. 30H, C**H$_3$**, ^{10}).

^{13}C NMR (126 MHz, $CDCl_3$): δ (ppm) = 176.86, 172.72, 172.66, 172.63, 170.04, 169.98, 169.95, 169.93, 75.14, 75.12, 75.11, 43.61, 43.57, 39.39, 39.34, 39.30, 34.47, 34.16, 34.03, 32.92, 29.68, 29.65, 29.61, 29.59, 29.54, 29.50, 29.48, 29.45, 29.43, 29.37, 29.35, 29.33, 29.32, 29.27, 29.25, 29.24, 29.21, 29.10, 28.85, 28.26, 26.97, 25.17, 25.14, 22.34, 22.31, 22.02, 21.99, 11.73, 11.71, 11.69, 11.66.

HRMS (ESI) *m/z*: $[M + H]^+$ calcd for $C_{101}H_{186}BrN_5O_{17}$, 1821.3100; found, 1821.3126.

IR (ATR): ṽ (cm^{-1}) = 3319, 2925, 2854, 1741, 1651, 1534, 1461, 1378, 1233, 1158, 1110, 1047, 1009, 927, 754, 722, 665.

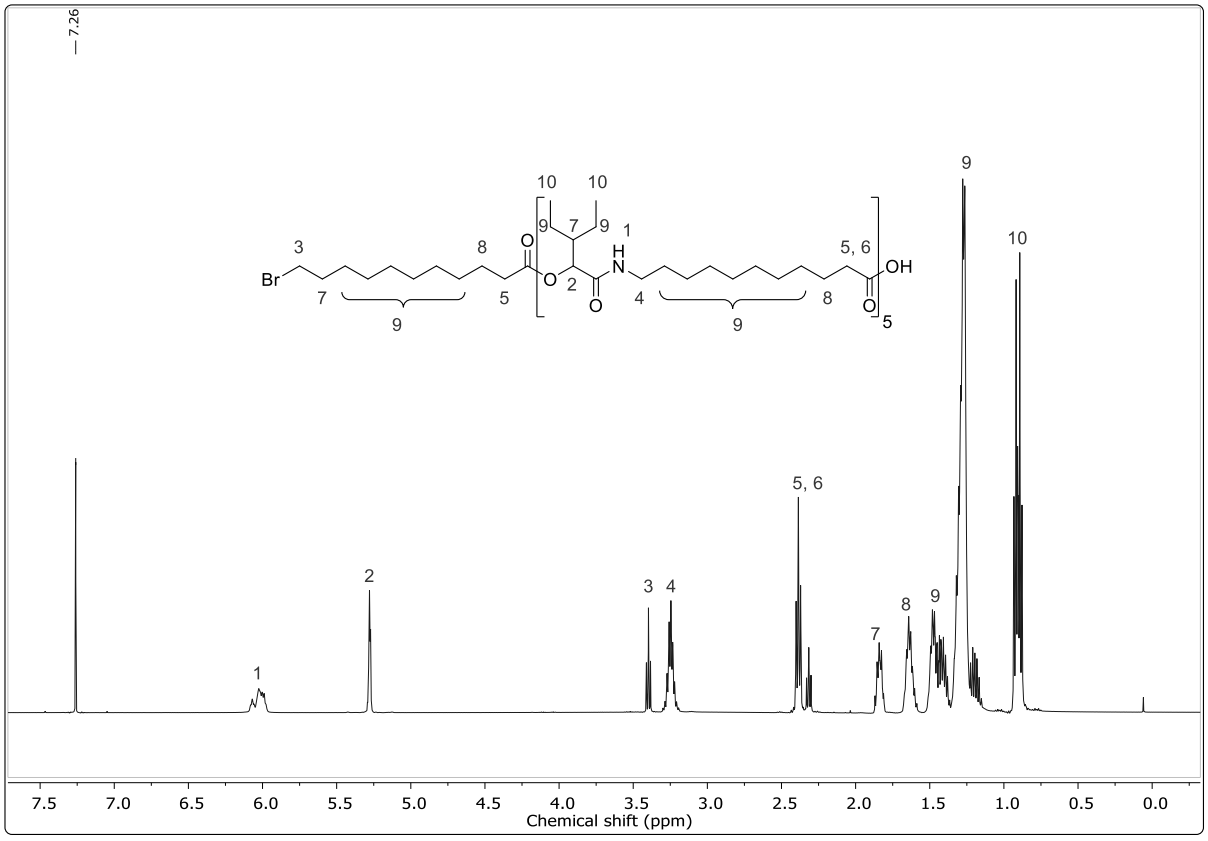

PEGylated Pentamer D2

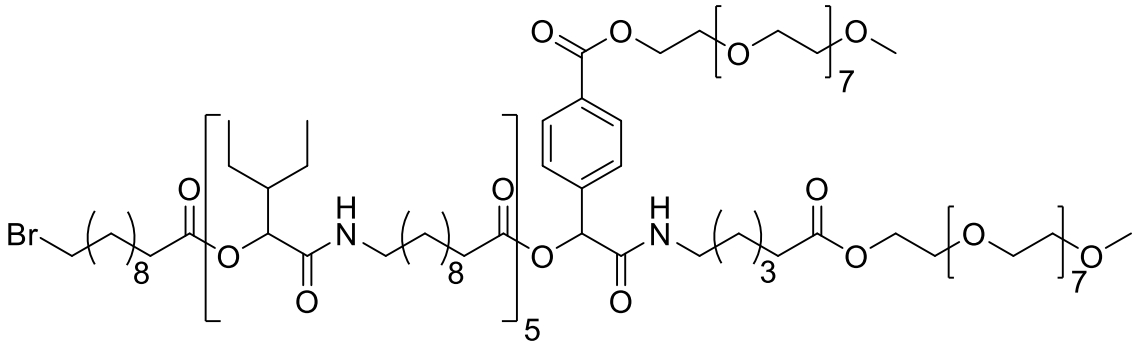

$C_{150}H_{271}BrN_6O_{38}$

M = 2846.73 g/mol

Deprotected pentamer **C3$_b$** (8.02 g, 4.40 mmol, 1.00 eq.) was placed in a round bottom flask and dissolved in 15.0 mL chloroform (0.293 mol L^{-1}), after vigorous stirring for a few minutes the solution was purged with argon. Subsequently, building block **B2** (3.41 g, 6.60 mmol 1.50 eq.) and building block **B1** (3.35 g, 6.60 mmol, 1.50 eq.) were added. The reaction was stirred under argon for 48 h and then refluxed for another 8 h. Then, the solvent was evaporated, and the crude product was purified *via* column chromatography (ethyl acetate → ethyl acetate/methanol 40:1 → ethyl

acetate/methanol 20:1 → ethyl acetate/acetone 1:1). The product **D2** was obtained as slightly yellow oil (8.43 g, 2.86 mmol, 67%).

TLC: R_f (ethyl acetate/methanol 5:1) = 0.21

^{1}H NMR (500 MHz, $CDCl_3$): δ (ppm) = 8.03 (d, 2H, *J* = 8.33 Hz, C**H**$_{\textbf{aromatic}}$, ^{1}), 7.50 (d, 2H, *J* = 8.32 Hz, C**H**$_{\textbf{aromatic}}$, ^{2}), 6.37 (t, 1H, *J* = 5.41 Hz, CON**H**, ^{3}), 6.08 (s, 1H, C**H**, ^{4}), 6.03 – 5.94 (m, 3H, CON**H**, ^{5}), 5.29 – 5.26 (m, 5H, C**H**, ^{6}), 4.47 – 4.45 (m, 2H, PhCOOC**H$_2$**CH_2OR, ^{7}), 4.22 – 4.20 (m, 2H, COOC**H$_2$**CH_2OR, ^{8}), 3.82 – 3.80 (m, 2H, PhCOOCH_2**CH_2**OR, ^{9}), 3.71 – 3.52 (m, 58H, OC**H$_2$**, ^{10}), 3.40 (t, 2H, *J* = 6.84 Hz, BrC**H$_2$**, ^{11}), 3.37 (s, 6H, OC**H$_3$**, ^{12}), 3.30 – 3.18 (m, 12H, CONHC**H$_2$**, ^{13}), 2.49 – 2.42 (m, 2H, C**H$_2$**COOR (fifth repeating unit), ^{14}), 2.38 (t, 10H, *J* = 7.47 Hz, C**H$_2$**COOR (startblock + first to fourth repeating unit), ^{15}), 2.32 (t, 2H, *J* = 7.39 Hz, C**H$_2$**COOC$H_2$$CH_2$O, ^{16}), 1.86 – 1.80 (m, 7H, C**H**, C**H$_2$**, ^{17}), 1.68 – 1.15 (m, 120H, C**H$_2$**, ^{18}), 0.94 – 0.88 (m. 30H, C**H$_3$**, ^{19}).

^{13}C NMR (126 MHz, $CDCl_3$): δ (ppm) = 173.61, 172.63, 172.60, 171.95, 169.87, 167.80, 166.13, 140.87, 130.58, 130.16, 127.25, 75.10, 74.92, 72.06, 70.80, 70.76, 70.75, 70.73, 70.69, 70.65, 70.64, 69.31, 69.27, 64.37, 63.58, 59.16, 43.62, 39.35, 39.32, 34.47, 34.27, 34.16, 34.00, 32.91, 29.69, 29.59, 29.57, 29.49, 29.48, 29.45, 29.35, 29.33, 29.31, 29.25, 29.24, 29.16, 28.84, 28.26, 26.97, 26.32, 25.14, 24.89, 24.42, 22.34, 22.03, 11.75, 11.70.

HRMS (ESI) *m/z*: $[M + H]^+$ calcd for $C_{150}H_{271}BrN_6O_{38}$, 2844.8714; found, 2844.8752.

IR (ATR): ṽ (cm^{-1}) = 3326, 2926, 2855, 1738, 1655, 1532, 1461, 1373, 1243, 1103, 1045, 944, 850, 722.

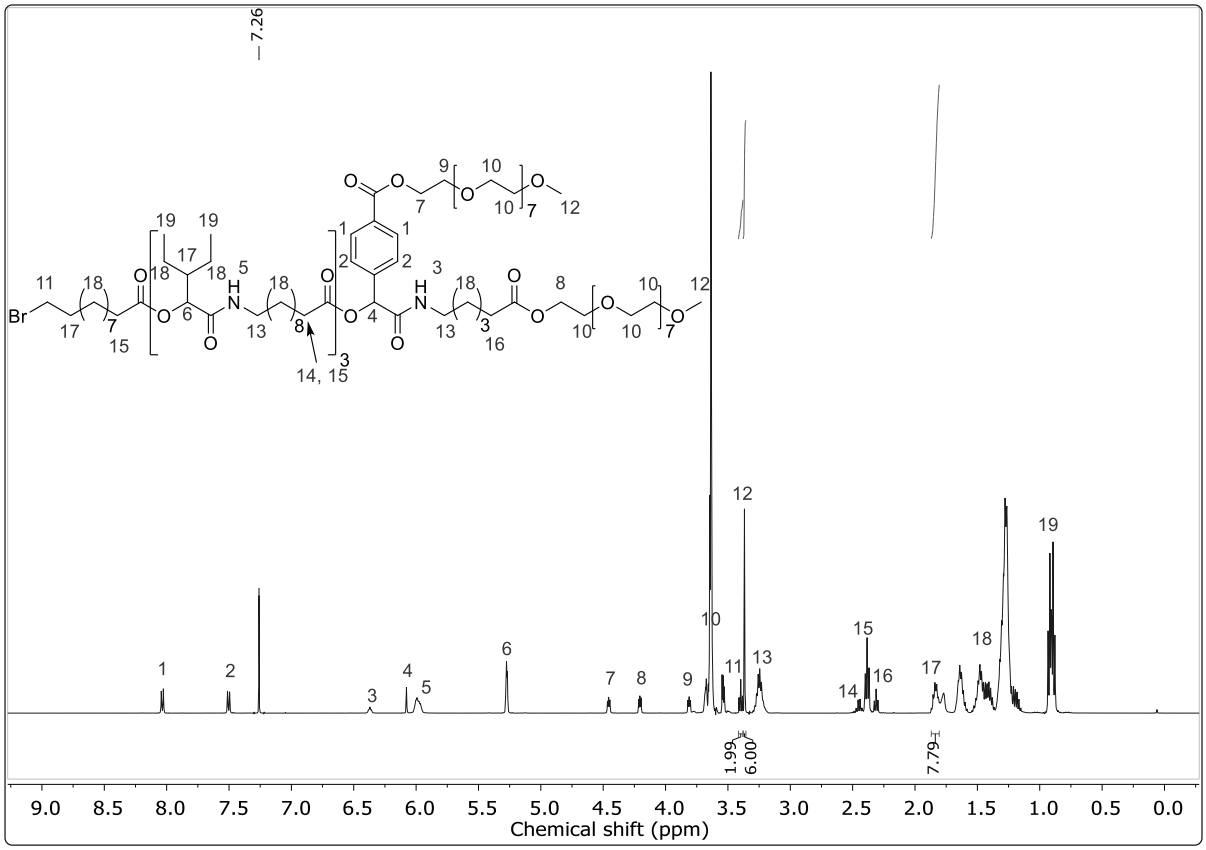

Azidated Pentamer D2$_b$

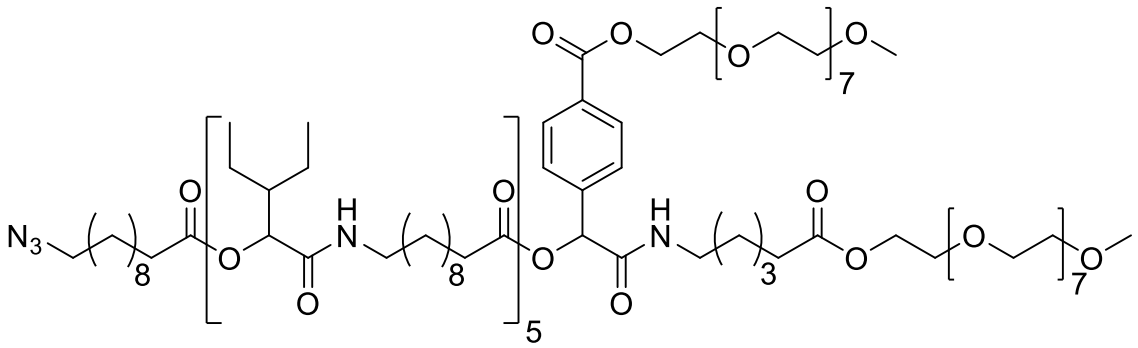

$C_{150}H_{271}N_9O_{38}$

M = 2808.84 g/mol

PEGylated pentamer **D2** (2.45 g, 1.10 mmol, 1.00 eq.) was dissolved in MeCN (5 mL). Subsequently, sodium azide (215 mg, 3.30 mmol, 3.00 eq.) was added and the reaction was stirred overnight at 75 °C. Afterwards, the reaction was filtrated and subjected to flash column chromatography (acetone). The product **D2$_b$** was obtained as slightly yellow oil (2.40 g, 1.10 mmol, quant.).

TLC: R_f (ethyl acetate/methanol 5:1) = 0.21

^{1}H NMR (500 MHz, $CDCl_3$): δ (ppm) = 8.03 (d, 2H, *J* = 8.29 Hz, C**H**$_{\textbf{aromatic}}$, ^{1}), 7.50 (d, 2H, *J* = 8.30 Hz, C**H**$_{\textbf{aromatic}}$, ^{2}), 6.38 (t, 1H, *J* = 5.42 Hz, CON**H**, ^{3}), 6.08 (s, 1H, C**H**, ^{4}), 6.03 – 5.95 (m, 5H, CON**H**, ^{5}), 5.29 – 5.26 (m, 5H, C**H**, ^{6}), 4.47 – 4.45 (m, 2H, PhCOOC**H$_2$**CH_2OR, ^{7}), 4.21 – 4.20 (m, 2H, COOC**H$_2$**CH_2OR, ^{8}), 3.82 – 3.80 (m, 2H, PhCOOCH_2**CH_2**OR, ^{9}), 3.70 – 3.52 (m, 58H, OC**H$_2$**, ^{10}), 3.37 (s, 6H, OC**H$_3$**, ^{11}), 3.30 – 3.18 (m, 14H, CONHC**H$_2$**, C**H$_2$**N_3, ^{12}), 2.47 – 2.43 (m, 2H, C**H$_2$**COOR (fifth repeating unit), ^{13}), 2.38 (t, 10H, *J* = 7.47 Hz, C**H$_2$**COOR (startblock + first to fourth repeating unit), ^{14}), 2.31 (t, 2H, *J* = 7.37 Hz, C**H$_2$**COOCH_2CH_2O, ^{15}), 1.88 – 1.77 (m, 5H, C**H**, ^{16}), 1.69 – 1.15 (m, 122H, C**H$_2$**, ^{17}), 0.94 – 0.88 (m. 30H, C**H$_3$**, ^{18}).

^{13}C NMR (126 MHz, $CDCl_3$): δ (ppm) = 173.61, 172.63, 172.61, 171.95, 169.87, 167.80, 166.13, 140.87, 130.57, 130.15, 127.25, 75.10, 74.91, 72.05, 70.80, 70.76, 70.74, 70.72, 70.68, 70.63, 69.30, 69.26, 64.37, 63.57, 59.16, 51.58, 43.62, 39.35, 39.32, 34.46, 34.26, 33.99, 29.68, 29.58, 29.56, 29.52, 29.49, 29.45, 29.35, 29.31, 29.25, 29.23, 29.16, 28.95, 26.97, 26.82, 26.32, 25.13, 24.88, 24.41, 22.34, 22.02, 11.74, 11.69.

HRMS (ESI) *m/z*: $[M + Na]^+$ calcd for $C_{150}H_{271}N_9O_{38}$, 2829.9442; found, 2829.9509.

IR (ATR): ṽ (cm^{-1}) =3319, 2926, 2855, 2096, 1739, 1654, 1532, 1461, 1352, 1274, 1103, 947, 850, 723.

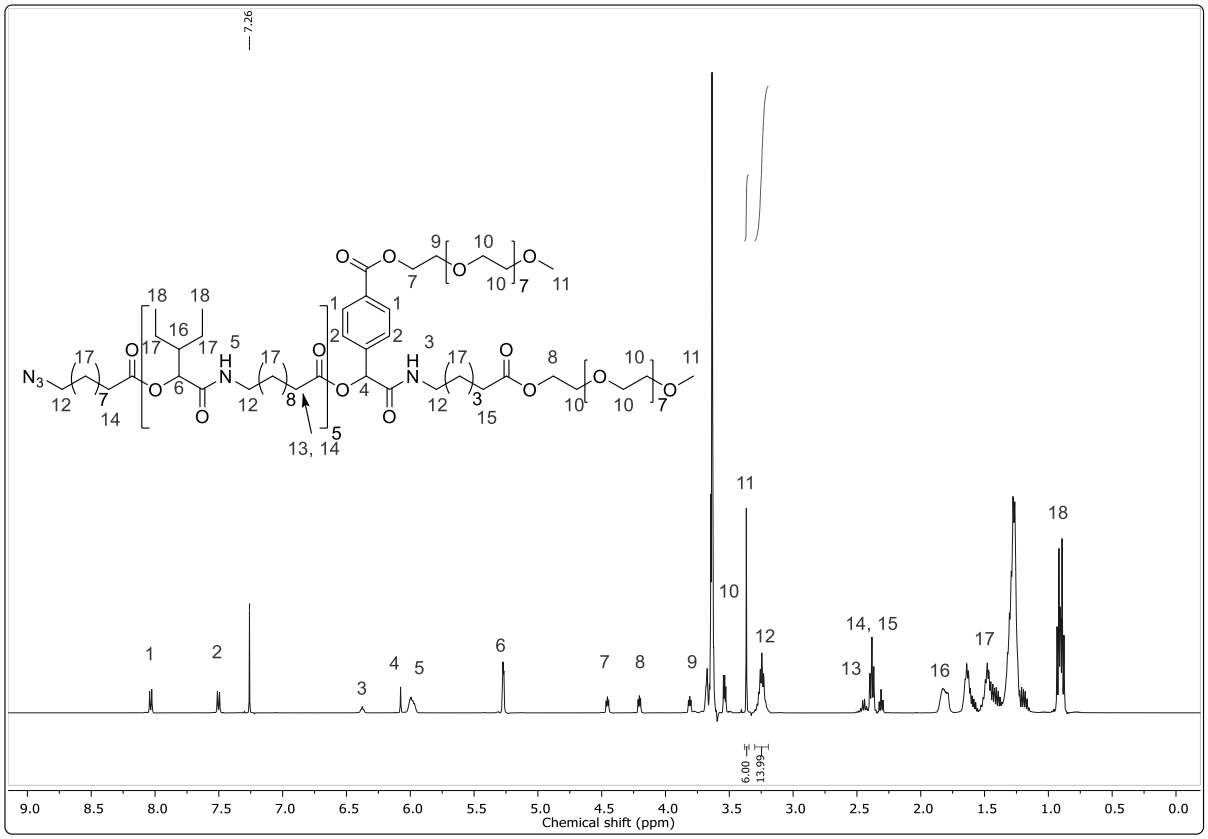

Heptamer C4

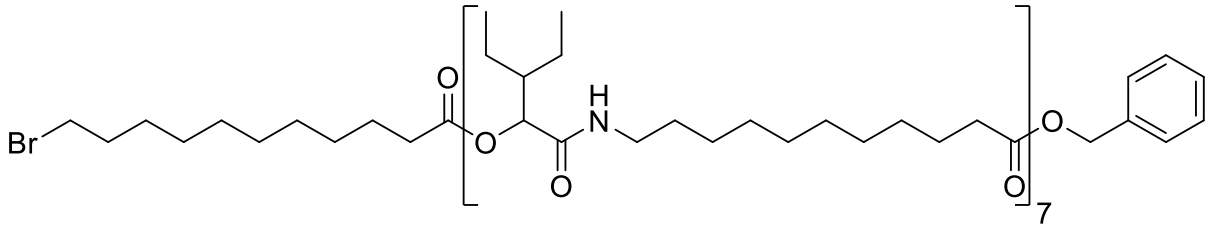

$C_{144}H_{258}BrN_7O_{23}$

M = 2535.58 g/mol

Deprotected heptamer **C3d** (15.9 g, 8.70 mmol, 1.00 eq.) was placed in a round bottom flask and dissolved in 9.0 mL DCM (1.00 mol L^{-1}), after vigorous stirring for a few minutes the solution was purged with argon. Subsequently, 2-ethylbutanal **9** (1.31 g, 13.1 mmol, 1.63 mL, 1.50 eq.) and building block **A2** (8.00 g, 13.1 mmol, 1.50 eq.) were added. The reaction was stirred overnight, then the solvent was evaporated under reduced pressure. Subsequently, the crude product was purified *via* gradient column chromatography (cyclohexane/ethyl acetate 9:1 → 4:1 + 2.50% triethylamine). The product **C4** was obtained as slightly yellow oil (20.3 g, 8.01 mmol, 92%)

TLC: R_f (cyclohexane/ethyl acetate 3:2) = 0.59

^{1}H NMR (500 MHz, $CDCl_3$): δ (ppm) = 7.36 – 7.28 (m, 5H, C**H**$_{\text{aromatic}}$, ^{1}), 6.04 – 5.96 (m, 7H, CON**H**, ^{2}), 5.27 (d, 7H, *J* = 3.71 Hz, C**H**, ^{3}), 5.09 (s. 2H, C**H$_2$**, ^{4}), 3.39 (t, 2H, *J* = 6.84 Hz, BrC**H$_2$**, ^{5}), 3.29 – 3.18 (m, 14H, CONHC**H$_2$**, ^{6}), 2.38 (t, 14H, *J* = 7.51 Hz, C**H$_2$**COOR, ^{7}), 2.33 (t, 2H, *J* = 7.55 Hz, C**H$_2$**COOBn, ^{8}), 1.86 – 1.80 (m, 9H, C**H**, C**H$_2$**, ^{9}), 1.66 – 1.59 (m, 16H, C**H$_2$**, ^{10}), 1.49 – 1.15 (m, 138H, C**H$_2$**, ^{11}), 0.91 (t. 21H, *J* = 7.44 Hz, C**H$_3$**, ^{12}), 0.88 (t. 21H, *J* = 7.44 Hz, C**H$_3$**, ^{12}).

^{13}C NMR (126 MHz, $CDCl_3$): δ (ppm) = 173.78, 172.60, 172.58, 169.85, 169.82, 136.21, 128.63, 128.26, 128.25, 75.08, 66.16, 53.55, 43.60, 39.29, 34.44, 34.42, 34.14, 32.89, 29.80, 29.67, 29.65, 29.57, 29.55, 29.47, 29.45, 29.43, 29.37, 29.33, 29.31, 29.29, 29.23, 29.21, 28.82, 28.23, 26.95, 25.12, 25.05, 22.32, 22.01, 11.72, 11.68.

HRMS (ESI) *m/z*: $[M + H]^+$ calcd for $C_{144}H_{258}BrN_7O_{23}$, 2533.8490; found, 2533.8508.

IR (ATR): ṽ (cm^{-1}) = 3309, 2925, 2854, 1740, 1651, 1532, 1460, 1378, 1242, 1157, 1110, 1047, 1008, 723, 697, 646.

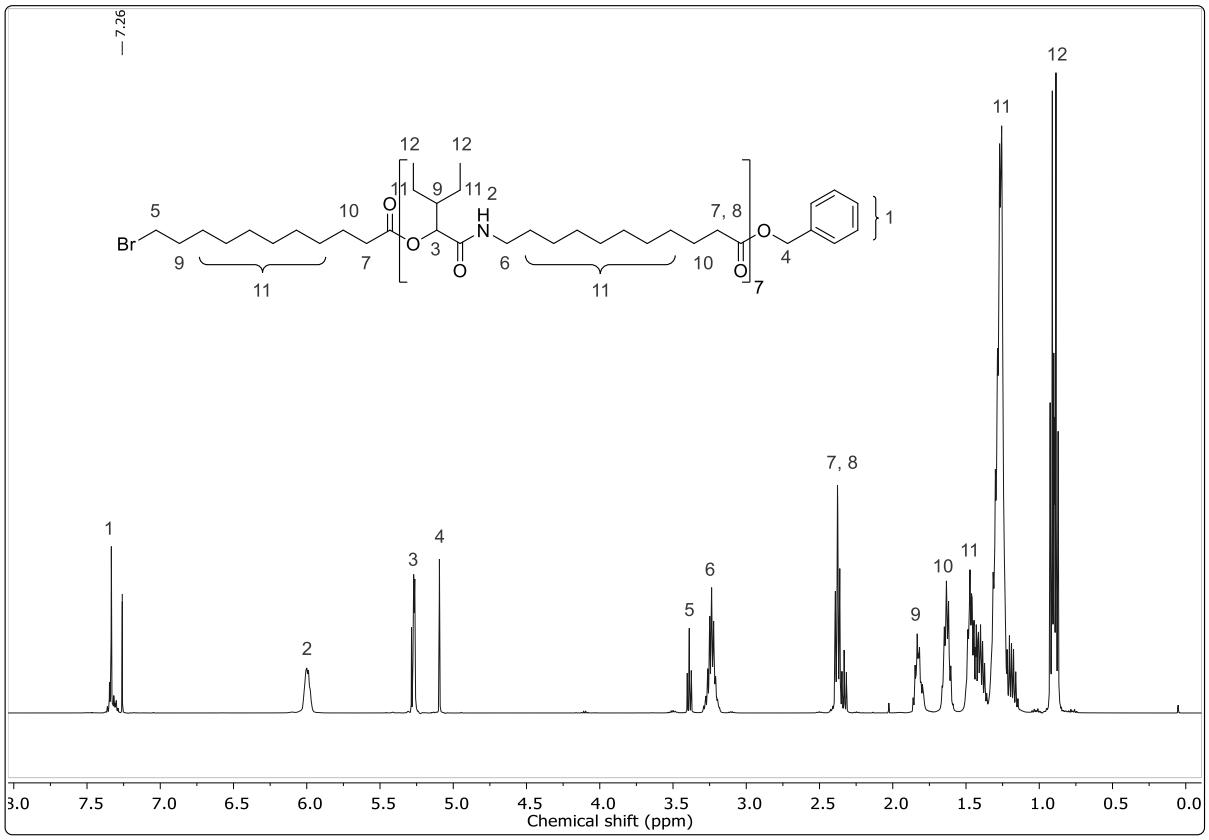

Deprotected Heptamer C4$_b$

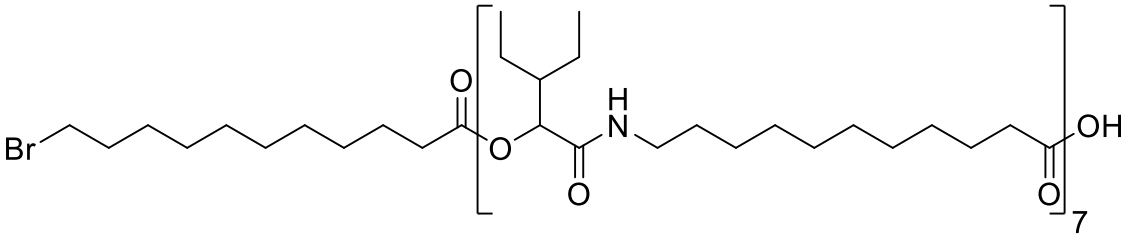

$C_{137}H_{252}BrN_7O_{23}$

M = 2445.45 g/mol

Benzyl protected oligomer **C4** (8.65 g, 3.41 mmol, 1.00 eq.) and 10 wt% Pd on activated charcoal (864 mg) were placed in a round bottom flask and dissolved in ethyl acetate, after vigorous stirring for a few minutes the solution was purged with hydrogen. The reaction was monitored *via* TLC until no benzyl protected oligomer was left. The solution was dried over sodium sulfate and filtered through Celite®. Subsequently, the solvent was evaporated under reduced pressure and the residue was dried *in vacuo*. The product **C4$_b$** was obtained as slightly yellow oil (8.11 g, 3.31 mmol, 97%).

TLC: R_f (cyclohexane/ethyl acetate 3:2) = 0.00

^{1}H NMR (500 MHz, $CDCl_3$): δ (ppm) = 6.11 – 5.95 (m, 7H, CON**H**, ^{1}), 5.28 – 5.27 (m, 7H, C**H**, ^{2}), 3.40 (t, 2H, *J* = 6.84 Hz, BrC**H$_2$**, ^{3}), 3.30 – 3.20 (m, 14H, CONHC**H$_2$**, ^{4}), 2.39 (t, 14H, *J* = 7.56 Hz, C**H$_2$**COOR, ^{5}), 2.32 (t, 2H, *J* = 7.43 Hz, C**H$_2$**COOBn, ^{6}), 1.87 – 1.81 (m, 9H, C**H**, C**H$_2$**, ^{7}), 1.69 – 1.58 (m, 16H, C**H$_2$**, ^{8}), 1.49 – 1.15 (m, 138H, C**H$_2$**, ^{9}), 0.94 – 0.88 (m. 42H, C**H$_3$**, ^{10}).

^{13}C NMR (126 MHz, $CDCl_3$): δ (ppm) = 176.01, 172.74, 172.66, 172.63, 170.07, 169.99, 169.95, 169.92, 75.16, 75.14, 75.11, 43.63, 43.57, 39.40, 39.35, 39.29, 34.48, 34.17, 33.87, 32.93, 29.69, 29.67, 29.60, 29.53, 29.51, 29.49, 29.46, 29.41, 29.38, 29.36, 29.34, 29.33, 29.31, 29.27, 29.25, 29.19, 29.08, 29.08, 28.86, 28.27, 26.98, 26.89, 25.18, 25.15, 24.93, 22.35, 22.31, 22.03, 22.00, 11.75, 11.70, 11.67.

HRMS (ESI) *m/z*: $[M + H]^+$ calcd for $C_{137}H_{252}BrN_7O_{23}$, 2443.8021; found, 2443.8023.

IR (ATR): ṽ (cm^{-1}) = 3332, 2925, 2854, 1737, 1656, 1530, 1457, 1380, 1241, 1159, 1115, 1004, 735, 697, 644, 563, 503.

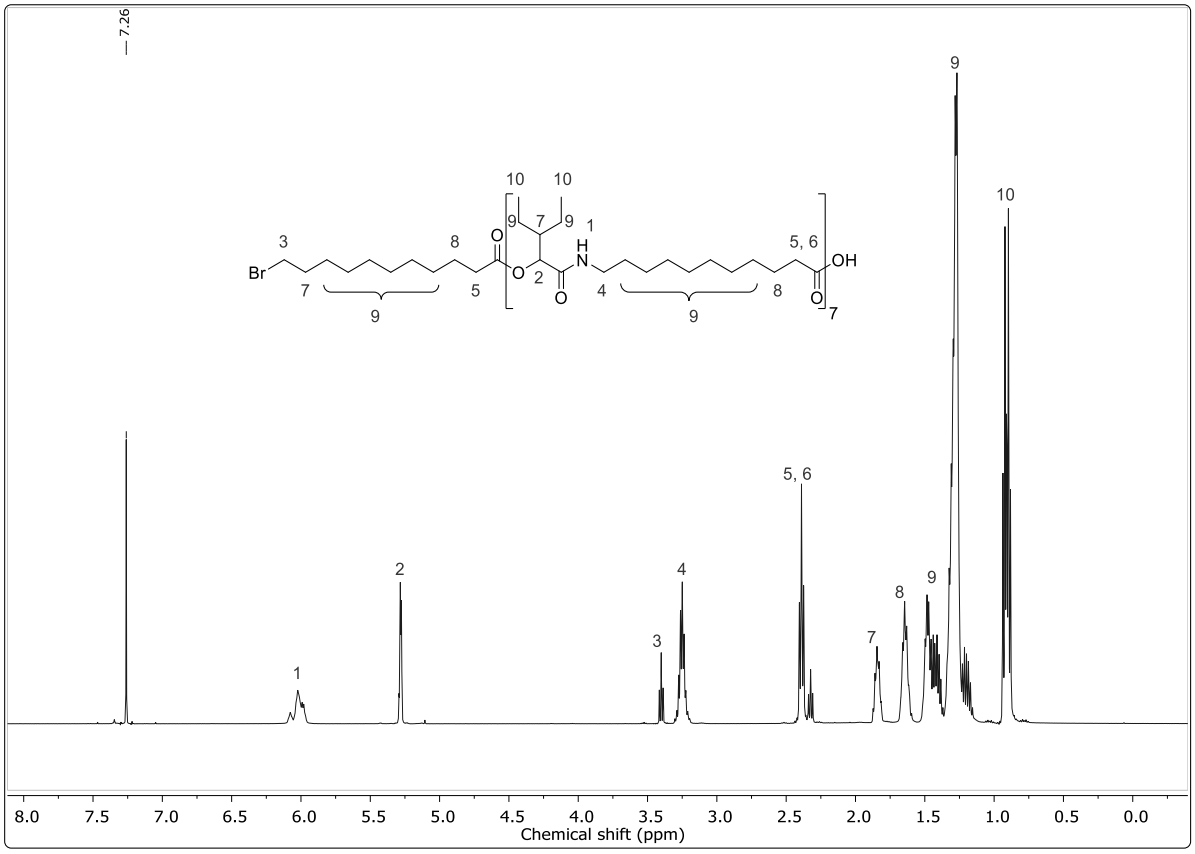

PEGylated Heptamer D3

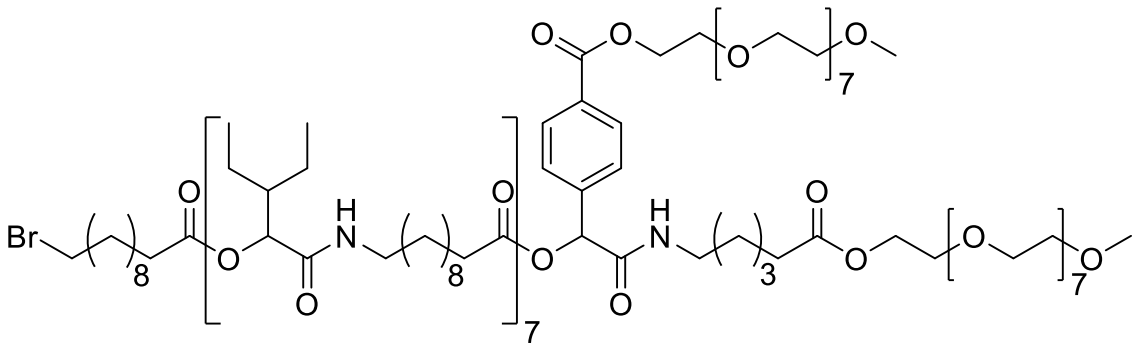

$C_{186}H_{337}BrN_8O_{44}$

M = 3469.69 g/mol

Deprotected heptamer **C4b** (8.19 g, 3.35 mmol, 1.00 eq.) was placed in a round bottom flask and dissolved in 15.0 mL chloroform (0.223 mol L^{-1}), after vigorous stirring for a few minutes the solution was purged with argon. Subsequently, building Block **B2** (2.86 g, 5.53 mmol, 1.65 eq.) and building block **B1** (2.81 g, 5.53 mmol, 1.65 eq.) were added. The reaction was monitored *via* TLC and the solvent was evaporated under reduced pressure when completed. The crude product was purified *via* column

chromatography (ethyl acetate → ethyl acetate/acetone 4:1 → ethyl acetate/acetone 2:1). The product **D3** was obtained as a viscous colorless oil (8.01 g, 2.31 mmol, 69%).

TLC: R_f (ethyl acetate/methanol 5:1) = 0.21

^{1}H NMR (500 MHz, $CDCl_3$): δ (ppm) = 8.04 (d, 2H, *J* = 8.36 Hz, C**H**$_{\textbf{aromatic}}$, ^{1}), 7.50 (d, 2H, *J* = 8.30 Hz, C**H**$_{\textbf{aromatic}}$, ^{2}), 6.38 (t, 1H, *J* = 5.67 Hz, CON**H**, ^{3}), 6.08 (s, 1H, C**H**, ^{4}), 6.04 – 5.95 (m, 7H, CON**H**, ^{5}), 5.28 – 5.27 (m, 7H, C**H**, ^{6}), 4.47 – 4.45 (m, 2H, PhCOOC**H$_2$**CH_2OR, ^{7}), 4.22 – 4.20 (m, 2H, COOC**H$_2$**CH_2OR, ^{8}), 3.82 – 3.80 (m, 2H, PhCOOCH_2**C H$_2$**OR, ^{9}), 3.70 – 3.53 (m, 58H, OC**H$_2$**, ^{10}), 3.40 (t, 2H, *J* = 6.84 Hz, BrC**H$_2$**, ^{11}), 3.37 (s, 6H, OC**H$_3$**, ^{12}), 3.30 – 3.19 (m, 16H, CONHC**H$_2$**, ^{13}), 2.49 – 2.40 (m, 2H, C**H$_2$**COOR (seventh repeating unit), ^{14}), 2.38 (t, 14H, *J* = 7.46 Hz, C**H$_2$**COOR (startblock + first to sixth repeating unit), ^{15}), 2.31 (t, 2H, *J* = 7.39 Hz, C**H$_2$**COOCH_2CH_2O, ^{16}), 1.87 – 1.80 (m, 9H, C**H**, C**H$_2$**, ^{17}), 1.68 – 1.15 (m, 120H, C**H$_2$**, ^{18}), 0.93 – 0.88 (m. 42H, C**H$_3$**, ^{19}).

^{13}C NMR (126 MHz, $CDCl_3$): δ (ppm) = 173.62, 172.63, 171.95, 169.88, 167.81, 166.14, 140.88, 130.57, 130.16, 127.25, 77.36, 75.10, 74.92, 72.05, 70.80, 70.76, 70.74, 70.72, 70.69, 70.63, 69.30, 69.27, 64.37, 63.58, 59.16, 43.62, 39.35, 39.32, 34.47, 34.27, 34.16, 34.00, 32.91, 29.69, 29.59, 29.57, 29.49, 29.48, 29.45, 29.35, 29.31, 29.25, 29.24, 29.16, 28.84, 28.26, 26.97, 26.32, 25.14, 24.89, 24.42, 22.34, 22.03, 11.74, 11.70.

HRMS (ESI) *m/z*: $[M + H]^{2+}$ calcd for $C_{186}H_{337}BrN_8O_{44}$, 1734.1854; found, 1734.1836.

IR (ATR): ṽ (cm^{-1}) = 3324, 2926, 2855, 1739, 1653, 1532, 1461, 1374, 1244, 1102, 753.

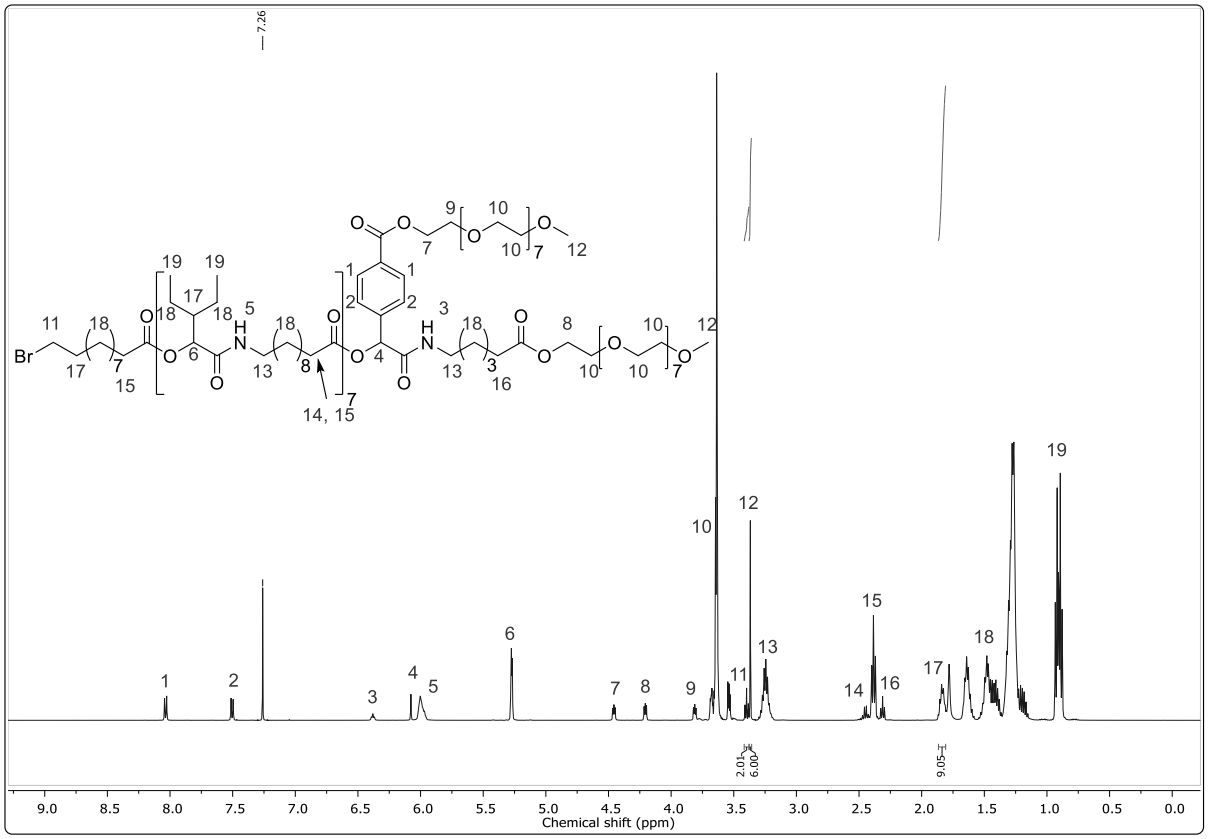

Azidated Heptamer D3$_b$

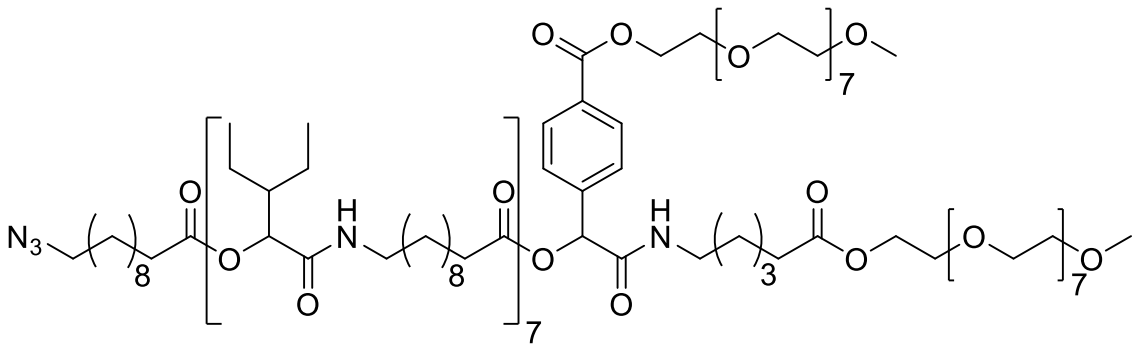

$C_{186}H_{337}N_{11}O_{44}$

M = 3431.775 g/mol

PEGylated heptamer **D3** (5.38 g, 1.55 mmol, 1.00 eq.) was dissolved in MeCN (10 mL). Subsequently, sodium azide (302 mg, 4.65 mmol, 3.00 eq.) was added and the reaction was stirred overnight at 85 °C. Afterwards, the reaction was filtrated and subjected to flash column chromatography (acetone). The product **D3$_b$** was obtained as slightly yellow oil (5.32 g, 1.55 mmol, quant.).

TLC: R_f (ethyl acetate/methanol 5:1) = 0.21

^{1}H NMR (500 MHz, $CDCl_3$): δ (ppm) = 8.03 (d, 2H, *J* = 8.36 Hz, C**H**$_{\textbf{aromatic}}$, ^{1}), 7.50 (d, 2H, *J* = 8.30 Hz, C**H**$_{\textbf{aromatic}}$, ^{2}), 6.37 (t, 1H, *J* = 5.66 Hz, CON**H**, ^{3}), 6.08 (s, 1H, C**H**, ^{4}), 6.03 – 5.96 (m, 7H, CON**H**, ^{5}), 5.29 – 5.26 (m, 7H, C**H**, ^{6}), 4.46 – 4.44 (m, 2H, PhCOOC**H$_2$**CH_2OR, ^{7}), 4.21 – 4.19 (m, 2H, COOC**H$_2$**CH_2OR, ^{8}), 3.82 – 3.80 (m, 2H, PhCOOCH_2**CH_2**OR, ^{9}), 3.70 – 3.52 (m, 58H, OC**H$_2$**, ^{10}), 3.37 (s, 6H, OC**H$_3$**, ^{11}), 3.30 – 3.18 (m, 18H, CONHC**H$_2$**, C**H$_2$**N_3, ^{12}), 2.49 – 2.41 (m, 2H, C**H$_2$**COOR (seventh repeating unit), ^{13}), 2.38 (t, 14H, *J* = 7.45 Hz, C**H$_2$**COOR (startblock + first to sixth repeating unit), ^{14}), 2.31 (t, 2H, *J* = 7.39 Hz, C**H$_2$**COOCH_2CH_2O, ^{15}), 1.88 – 1.77 (m, 7H, C**H**, ^{16}), 1.68 – 1.15 (m, 162H, C**H$_2$**, ^{17}), 0.94 – 0.88 (m. 42H, C**H$_3$**, ^{18}).

^{13}C NMR (126 MHz, $CDCl_3$): δ (ppm) = 173.60, 172.62, 171.94, 169.86, 167.79, 166.13, 140.87, 130.57, 130.15, 127.24, 75.10, 74.91, 72.05, 70.80, 70.76, 70.74, 70.73, 70.69, 70.64, 69.30, 69.26, 64.37, 63.57, 59.16, 51.58, 43.62, 39.35, 39.32, 34.46, 34.26, 33.99, 29.69, 29.59, 29.56, 29.52, 29.49, 29.45, 29.35, 29.31, 29.25, 29.24, 29.16, 28.95, 26.97, 26.82, 26.32, 25.13, 24.88, 24.41, 22.34, 22.02, 11.74, 11.69.

HRMS (ESI) *m/z*: $[M + H]^{2+}$ calcd for $C_{186}H_{337}N_{11}O_{44}$, 1715.7308; found, 1715.7318.

IR (ATR): ṽ (cm^{-1}) =3314, 2926, 2855, 2096, 1739, 1653, 1532, 1461, 1373, 1241, 1105, 1045, 940, 848, 722.

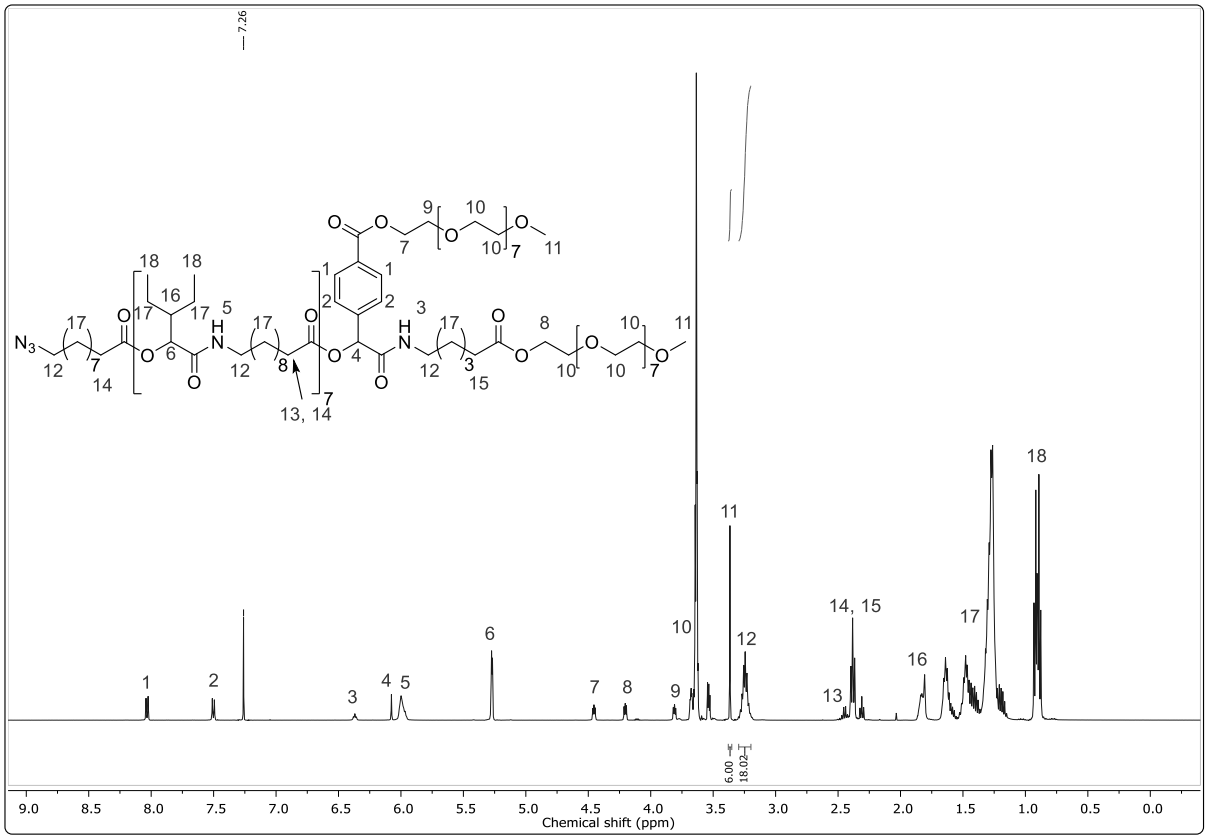

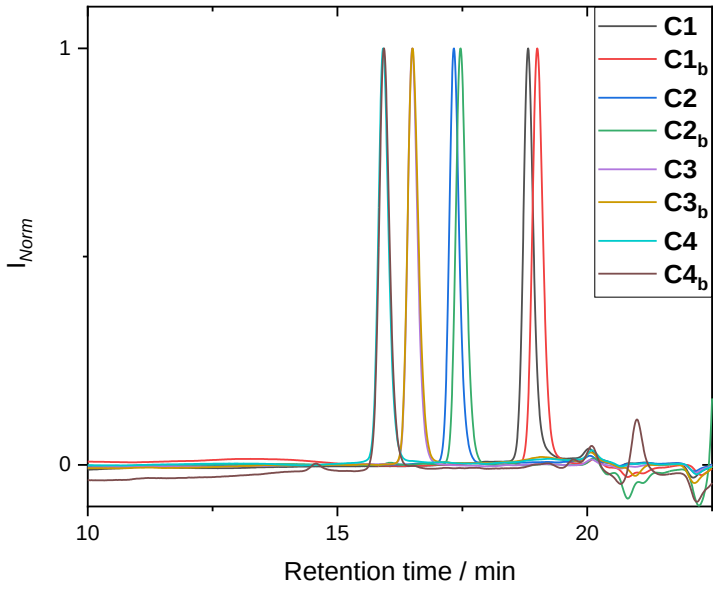

Figure S 9: SEC traces of the protected and deprotected linear oligomers **C1**-**C4$_b$** (monomer to deprotected heptamer) measured in THF.

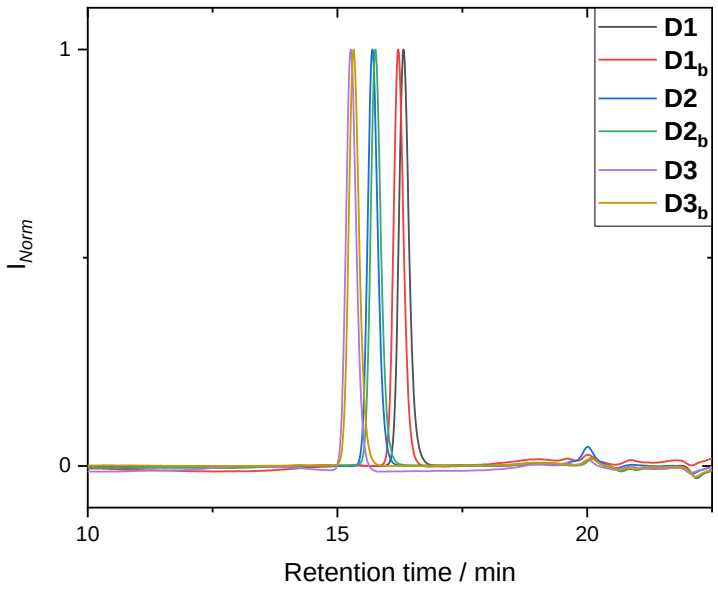

Figure S 10: SEC traces of the PEGylated and azidated oligomers **D1**-**D3$_b$** (trimer, pentamer and heptamer) measured in THF.

Tetra(prop-2-yn-1-yl) butane-1,2,3,4-tetracarboxylate – E1

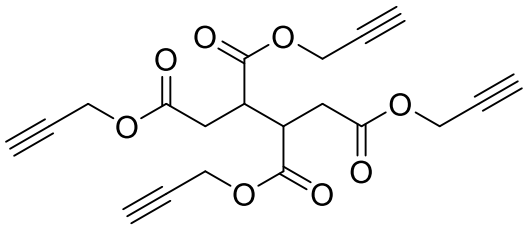

$C_{20}H_{18}O_8$
M = 386.36 g/mol

Butane-1,2,3,4-tetracarboxylic acid **H5** (2.34 g, 10.0 mmol, 1.00 eq.) was dissolved in 10 mL DCM and DIPEA (5.69 g, 44.0 mmol, 4.40 eq.). Afterwards, propargyl bromide (80wt% solution in toluene, 8.92 g, 60.0 mmol, 6.68 mL, 6.00 eq.) was slowly added *via* syringe. The reaction was monitored *via* TLC. Afterwards, the reaction mixture was poured into a separation funnel and 50 mL of water were added. The phases were separated, and the aqueous phase was extracted with DCM (3 × 15 mL). Then, the organic phases were combined and washed water (3 × 25 mL). The aqueous phase (75 mL) was checked *via* TLC for remaining product. If the test was positive, it was extracted another time with 15 mL of DCM. The combined organic layers were then dried over sodium sulfate and the solvent was removed under reduced pressure to yield crude product. The crude product was purified *via* column chromatography

(cyclohexane/ethyl acetate 4:1 → 2:1). The product **42**/**E1** was obtained as yellow viscous oil (6.11 g, 6.11 mmol, 61%).

TLC: R_f (cyclohexane/ethyl acetate 3:1) = 0.33

^{1}H NMR (500 MHz, $CDCl_3$): δ (ppm) = 4.75 – 4.65 (m, 8H, C≡CC**H$_2$**, ^{1}), 3.43 – 3.39 (m, 2H, C**H**COOR, ^{2}), 2.92 – 2.85 (m, 2H, C**H$_2$**COOR, ^{3}), 2.54 – 2.48 (m, C**H$_2$**COOR, **H**C≡C, ^{4}).

^{13}C NMR (126 MHz, $CDCl_3$): δ (ppm) = 171.00, 170.39, 77.31, 77.08, 75.61, 75.40, 53.02, 52.67, 42.10, 33.03.

HRMS (ESI) *m/z*: $[M + H]^+$ calcd for $C_{20}H_{18}O_8$, 387.1074; found, 387.1071.

IR (ATR): ṽ (cm^{-1}) = 3287, 2130, 1732, 1436, 1384, 1336, 1152, 991, 831, 640, 430.

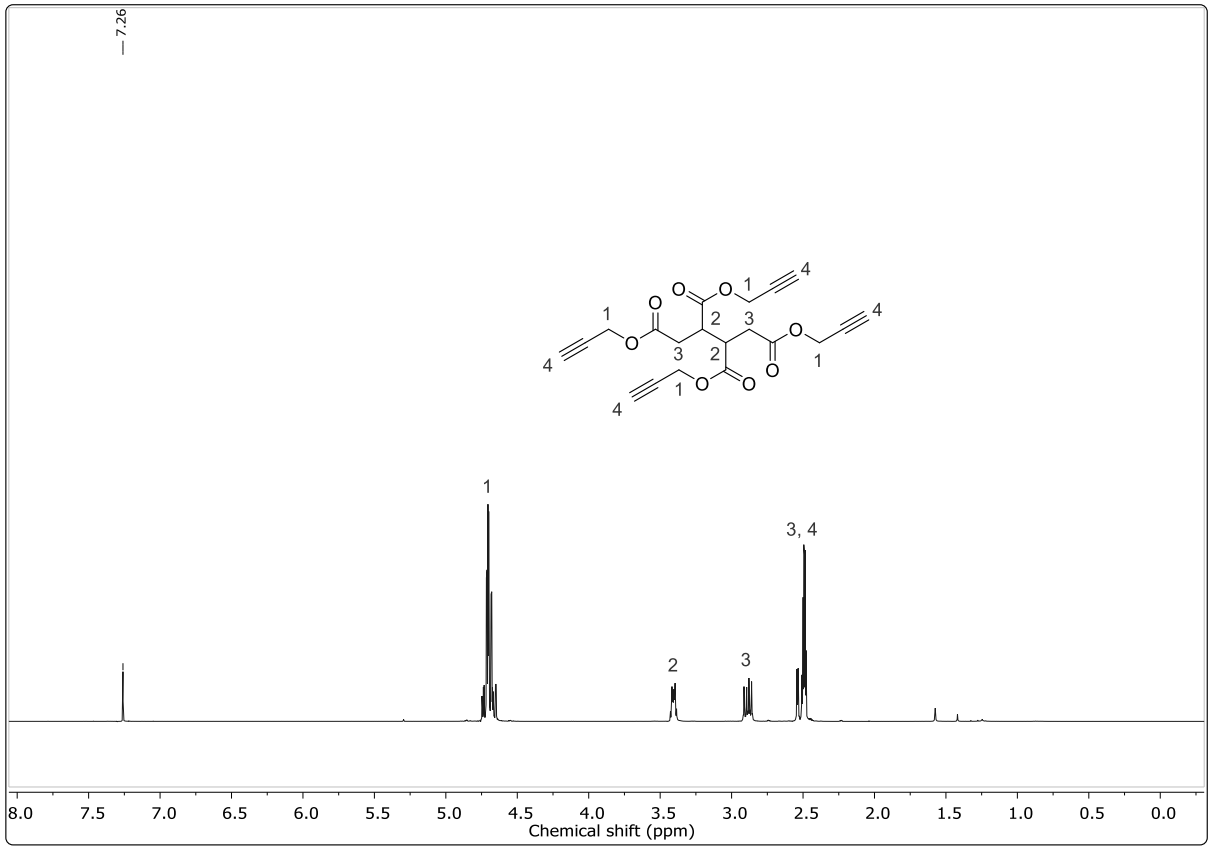

Trimer-star-shaped macromolecule SM1

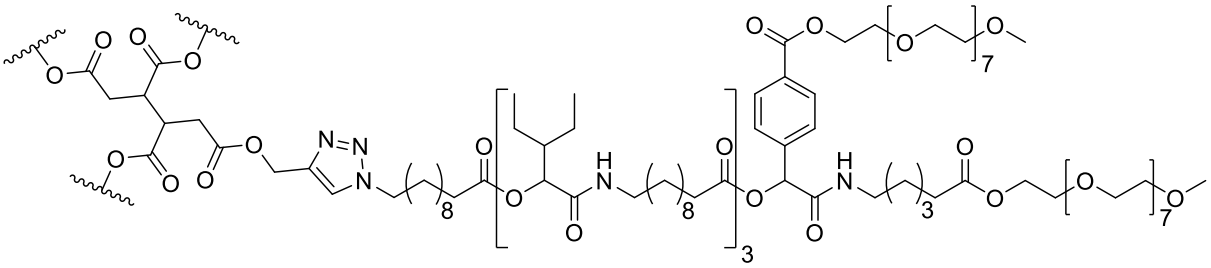

$C_{476}H_{838}N_{28}O_{136}$

9130.00 g/mol

Copper(I)iodide (53.3 mg, 0.280 mmol, 1.00 eq.) and DIPEA (289 mg, 2.24 mmol, 390 µL, 8.00 eq.) were added to a solution of **D1b** (3.92 g, 1.79 mmol, 6.40 eq.) in 6.50 mL chloroform. Then, core **E1** (108 mg, 0.280 mmol, 1.00 eq.) in 1.50 mL chloroform was added and the reaction mixture was saturated with argon. Subsequently, the reaction mixture was stirred in a pressure vial at 65 °C until the reaction was finished. Then, the solvent was evaporated, and the product was purified *via* column chromatography (ethyl acetate → ethyl acetate/acetone 2:1 → ethyl acetate/acetone 1:1 → acetone → ethyl acetate/methanol 1:1). The product **SM1** was obtained as a viscous yellow oil (2.43 g, 0.266 mmol, 90%).

^{1}H NMR (500 MHz, $CDCl_3$): δ (ppm) = 8.03 (d, 8H, *J* = 8.37 Hz, C**H**$_{\textbf{aromatic}}$, [1]), 7.61 (d, 4H, *J* = 6.80 Hz, C=C**H**-N, [2]), 7.50 (d, 8H, *J* = 8.31 Hz, C**H**$_{\textbf{aromatic}}$, [3]), 6.38 (t, 4H, *J* = 5.66 Hz, CON**H**, [4]), 6.08 (s, 4H, C**H**, [5]), 6.04 – 5.97 (m, 12H, CON**H**, [6]), 5.29 – 5.24 (m, 12H, C**H**, [7]), 5.18 – 5.11 (m, 8H, COOC**H$_2$**C(N)=C, [8]), 4.46 – 4.44 (m, 8H, PhCOOC**H$_2$**CH_2OR, [9]), 4.35 – 4.32 (m, 8H, NC**H$_2$**, [10]), 4.21 – 4.19 (m, 8H, COOC**H$_2$**CH_2OR, [11]), 3.82 – 3.80 (m, 8H, PhCOOCH_2**CH$_2$**OR, [12]), 3.69 – 3.53 (m, 232H, OC**H$_2$**, [13]), 3.36 (s, 24H, OC**H$_3$**, [14]), 3.30 – 3.18 (m, 36H, CONHC**H$_2$** + core, [15]), 2.76 – 2.71 (m, 2H, C**H**COOR (core), [16]), 2.47 – 2.42 (m, 8H, C**H$_2$**COOR (third repeating unit), [17]), 2.38 (t, 24H, *J* = 7.41 Hz, C**H$_2$**COOR (startblock + first and second repeating unit), [18]), 2.31 (t, 8H, *J* = 7.39 Hz, C**H$_2$**$COOCH_2CH_2O$, [19]), 1.94 – 1.15 (m, 340H, C**H**, C**H$_2$**, [20]), 0.93 – 0.87 (m. 72H, C**H$_3$**, [21]).

^{13}C NMR (126 MHz, $CDCl_3$): δ (ppm) = 173.58, 172.60, 171.92, 170.98, 169.84, 167.77, 166.10, 140.85, 130.54, 130.12, 127.22, 75.06, 74.89, 72.03, 70.77, 70.73, 70.71, 70.69, 70.66, 70.62, 70.61, 69.27, 69.24, 64.35, 63.55, 59.13, 50.53, 43.61, 42.10, 39.32, 39.30, 34.43, 34.42, 34.24, 33.97, 30.39, 29.79, 29.67, 29.65, 29.57,

29.54, 29.47, 29.45, 29.42, 29.33, 29.29, 29.27, 29.22, 29.21, 29.13, 29.09, 26.95, 26.60, 26.29, 25.11, 25.08, 24.86, 24.39, 22.31, 22.00, 11.72, 11.67.

HRMS (ESI) *m/z*: $[M + 4Na]^{4+}$ calcd for $C_{476}H_{838}N_{28}O_{136}$, 2303.9772; found, 2303.9832.

IR (ATR): $\tilde{\nu}$ (cm^{-1}) = 3317, 2925, 2856, 1737, 1658, 1533, 1460, 1351, 1274, 1101, 948, 849.

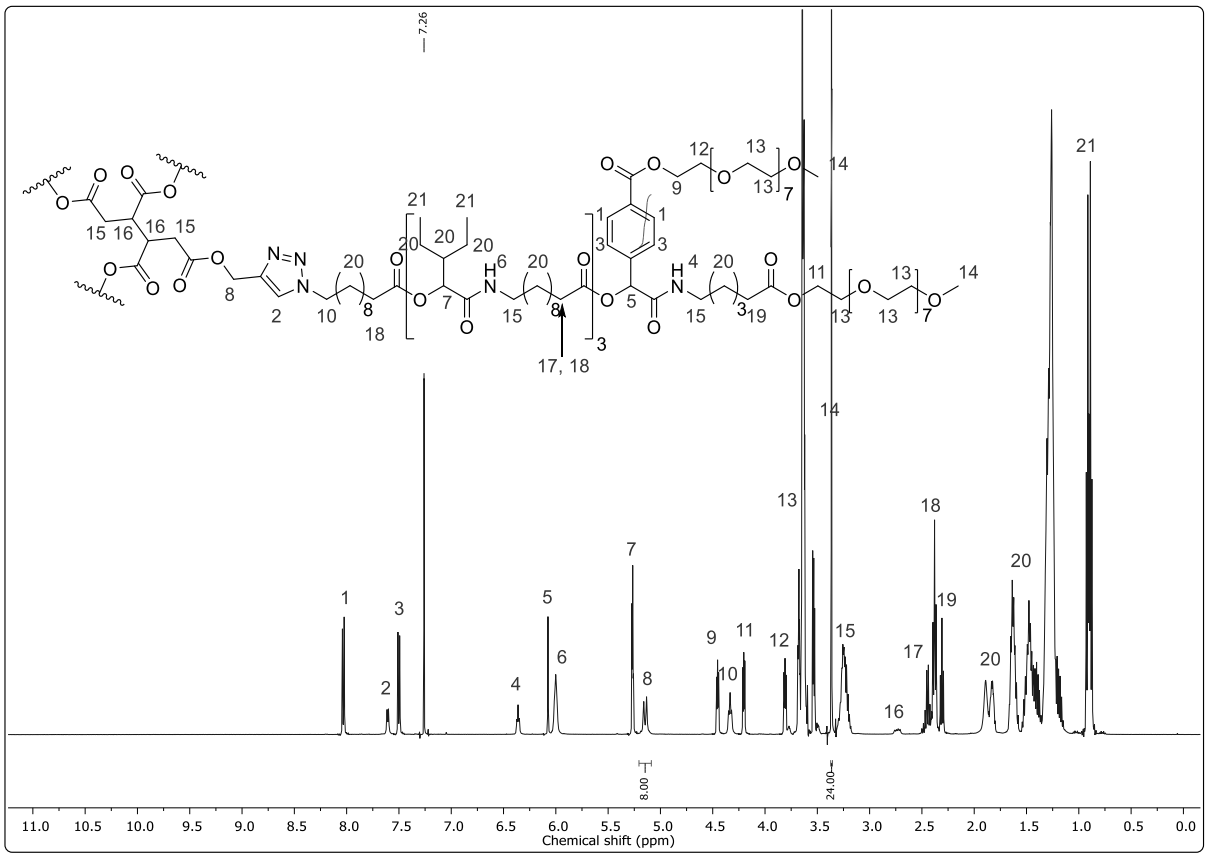

Pentamer-star-shaped macromolecule SM2

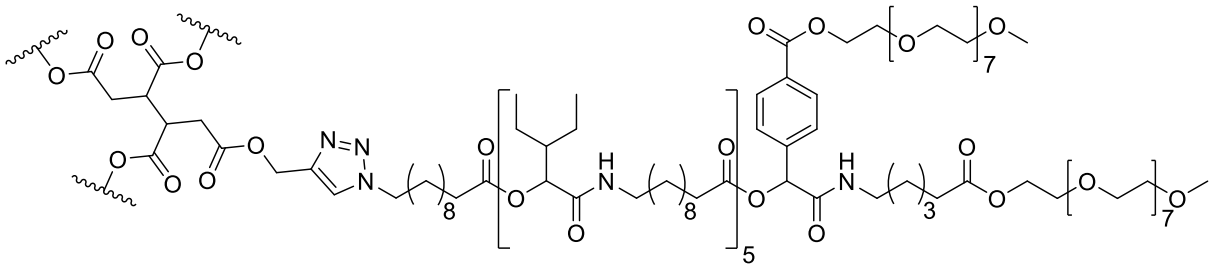

$C_{620}H_{1102}N_{36}O_{160}$

11621.73 g/mol

Copper(I)iodide (29.5 mg, 0.155 mmol, 1.00 eq.) and DIPEA (160 mg, 1.24 mmol, 8.00 eq.) were added to a solution of **D2b** (2.61 g, 0.930 mmol, 6.00 eq.) in 4.50 mL chloroform. Then, core **E1** (59.9 mg, 0.155 mmol, 1.00 eq.) in 1.50 mL chloroform was

added and the reaction mixture was saturated with argon. Subsequently, the reaction mixture stirred in a pressure vial at 65 °C until the reaction was finished. Then, the solvent was evaporated, and the product was purified *via* column chromatography (ethyl acetate → ethyl acetate/acetone 2:3 → acetone → ethyl acetate/methanol 1:1). The product **SM2** was obtained as a viscous yellow oil (1.64 g, 0.141 mmol, 91%).

^{1}H NMR (500 MHz, $CDCl_3$): δ (ppm) = 8.03 (d, 8H, *J* = 8.39 Hz, C**H**$_{\text{aromatic}}$, [1]), 7.60 (d, 4H, *J* = 6.50 Hz, C=C**H**-N, [2]), 7.50 (d, 8H, *J* = 8.30 Hz, C**H**$_{\text{aromatic}}$, [3]), 6.37 (t, 4H, *J* = 5.76 Hz, CON**H**, [4]), 6.07 (s, 4H, C**H**, [5]), 6.04 – 5.97 (m, 20H, CON**H**, [6]), 5.29 – 5.25 (m, 20H, C**H**, [7]), 5.14 (m, 8H, COOC**H$_2$**C(N)=C, [8]), 4.46 – 4.44 (m, 8H, PhCOOC**H$_2$**CH_2OR, [9]), 4.35 – 4.32 (m, 8H, NC**H$_2$**, [10]), 4.21 – 4.19 (m, 8H, COOC**H$_2$**CH_2OR, [11]), 3.82 – 3.80 (m, 8H, PhCOOCH_2**C**H_2OR, [12]), 3.69 – 3.53 (m, 232H, OC**H$_2$**, [13]), 3.37 (s, 24H, OC**H$_3$**, [14]), 3.29 – 3.18 (m, 52H, CONHC**H$_2$** + core, [15]), 2.76 – 2.71 (m, 2H, C**H**COOR (core), [16]), 2.46 – 2.42 (m, 8H, C**H$_2$**COOR (fifth repeating unit), [17]), 2.38 (t, 40H, *J* = 7.41 Hz, C**H$_2$**COOR (startblock + first to fourth repeating unit), [18]), 2.31 (t, 8H, *J* = 7.39 Hz, C**H$_2$**COOC$H_2$$CH_2$O, [19]), 1.92 – 1.15 (m, 508H, C**H**, C**H$_2$**, [20]), 0.93 – 0.87 (m. 120H, C**H$_3$**, [21]).

^{13}C NMR (126 MHz, $CDCl_3$): δ (ppm) = 173.59, 172.61, 171.93, 171.64, 170.98, 169.85, 167.78, 166.12, 142.37, 142.10, 140.87, 130.56, 130.14, 127.23, 123.97, 123.80, 75.08, 74.90, 72.05, 70.79, 70.75, 70.74, 70.72, 70.69, 70.65, 70.63, 69.29, 69.26, 64.36, 63.57, 59.15, 58.66, 58.32, 50.56, 43.62, 42.11, 39.34, 39.31, 34.45, 34.43, 34.25, 33.99, 33.14, 30.40, 29.69, 29.67, 29.58, 29.55, 29.48, 29.46, 29.44, 29.34, 29.30, 29.29, 29.24, 29.15, 29.10, 26.97, 26.61, 26.31, 25.12, 25.10, 24.88, 24.41, 22.33, 22.02, 11.74, 11.69.

HRMS (ESI) *m/z*: $[M + 5Na]^{5+}$ calcd for $C_{620}H_{1102}N_{36}O_{160}$, 2345.7733; found, 2345.7871.

IR (ATR): $\tilde{\nu}$ (cm^{-1}) = 3324, 2926, 2855, 1738, 1655, 1532, 1461, 1373, 1241, 1103, 1045, 947, 848, 723.

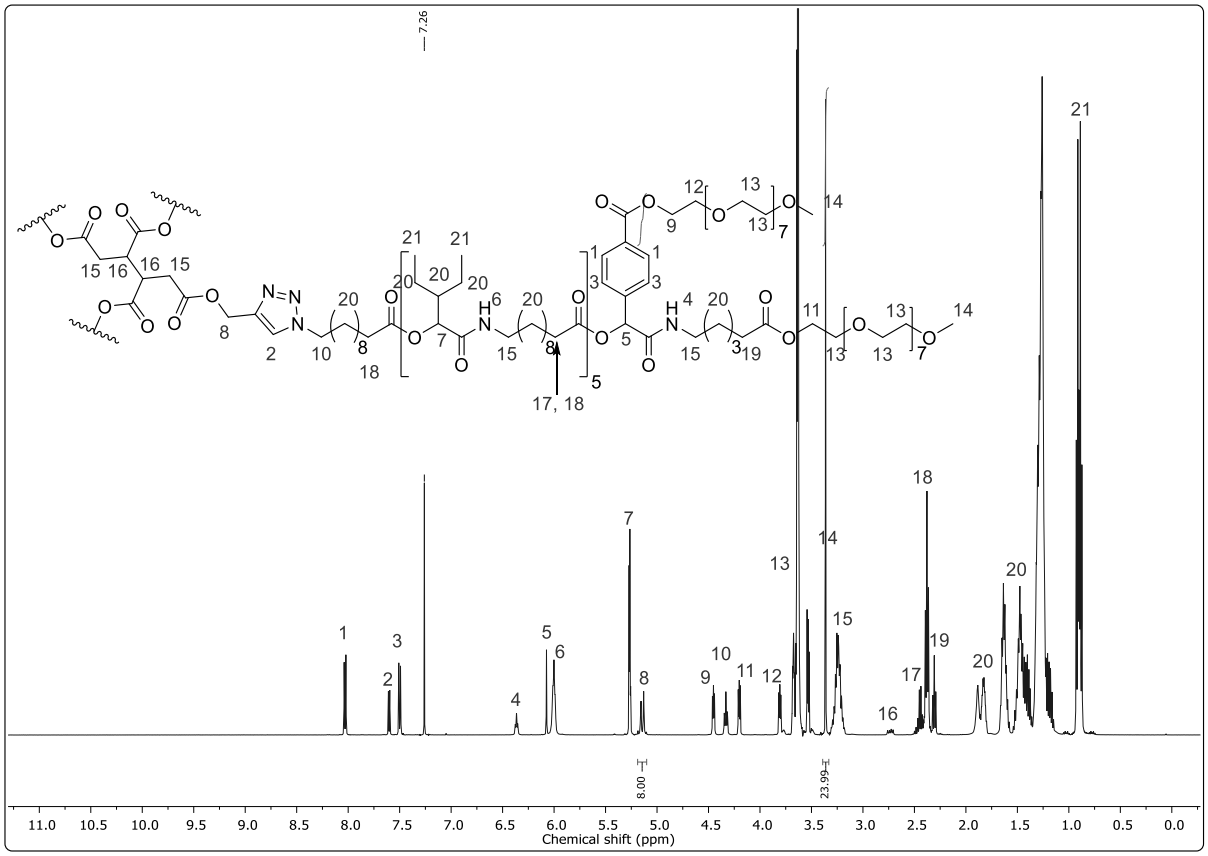

Heptamer-star-shaped macromolecule SM3

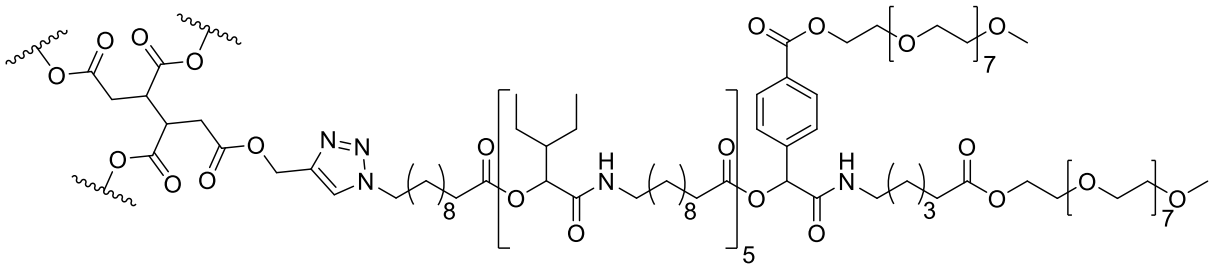

$C_{764}H_{1366}N_{44}O_{184}$

14113.46 g/mol

Copper(I)iodide (45.7 mg, 0.240 mmol, 1.00 eq.) and DIPEA (248 mg, 1.92 mmol, 8.00 eq.) were added to a solution of **D3b** (5.27 g, 1.54 mmol, 6.40 eq.) in 8.50 mL chloroform. Then, core **E1** (92.7 mg, 0.240 mmol, 1.00 eq.) in 2.00 mL chloroform was added and the reaction mixture was saturated with argon. The reaction mixture stirred in a pressure vial at 65 °C until the reaction was finished. Subsequently, the reaction mixture was refluxed until the reaction was finished. Then, the solvent was evaporated, and the product was purified *via* column chromatography (ethyl acetate → ethyl acetate/acetone 2:3 → acetone → ethyl acetate/methanol 1:1). The product **SM3** was obtained as a viscous yellow oil (2.30 g, 0.216 mmol, 90%).

^{1}H NMR (500 MHz, $CDCl_3$): δ (ppm) = 8.03 (d, 8H, *J* = 8.39 Hz, C**H**$_{\text{aromatic}}$, [1]), 7.60 (d, 4H, *J* = 6.21 Hz, C=C**H**-N, [2]), 7.50 (d, 8H, *J* = 8.30 Hz, C**H**$_{\text{aromatic}}$, [3]), 6.37 (t, 4H, *J* = 5.74 Hz, CON**H**, [4]), 6.07 (s, 4H, C**H**, [5]), 6.04 – 5.96 (m, 28H, CON**H**, [6]), 5.29 – 5.25 (m, 28H, C**H**, [7]), 5.18 – 5.10 (m, 8H, COOC**H$_2$**C(N)=C, [8]), 4.46 – 4.44 (m, 8H, PhCOOC**H$_2$**CH_2OR, [9]), 4.35 – 4.32 (m, 8H, NC**H$_2$**, [10]), 4.21 – 4.19 (m, 8H, COOC**H$_2$**CH_2OR, [11]), 3.81 – 3.80 (m, 8H, PhCOOCH_2**CH_2**OR, [12]), 3.71 – 3.52 (m, 232H, OC**H$_2$**, [13]), 3.36 (s, 24H, OC**H$_3$**, [14]), 3.31 – 3.18 (m, 68H, CONHC**H$_2$** + core, [15]), 2.76 – 2.71 (m, 2H, C**H**COOR (core), [16]), 2.48 – 2.41 (m, 8H, C**H$_2$**COOR (seventh repeating unit), [17]), 2.38 (t, 56H, *J* = 7.43 Hz, C**H$_2$**COOR (startblock + first to sixth repeating unit), [18]), 2.31 (t, 8H, *J* = 7.40 Hz, C**H$_2$**COOCH_2CH_2O, [19]), 1.92 – 1.15 (m, 676H, C**H**, C**H$_2$**, [20]), 0.93 – 0.87 (m. 168H, C**H$_3$**, [21]).

^{13}C NMR (126 MHz, $CDCl_3$): δ (ppm) = 173.59, 172.61, 171.93, 171.64, 170.98, 169.85, 167.78, 166.12, 142.37, 142.11, 140.87, 130.56, 130.14, 127.23, 123.96, 123.79, 75.08, 74.90, 72.05, 70.79, 70.75, 70.74, 70.72, 70.68, 70.64, 70.63, 69.29, 69.25, 64.36, 63.56, 59.15, 58.67, 58.32, 50.55, 43.62, 42.11, 39.34, 39.31, 34.45, 34.43, 34.25, 33.98, 33.14, 30.41, 29.68, 29.66, 29.58, 29.55, 29.48, 29.46, 29.44, 29.34, 29.30, 29.24, 29.15, 29.10, 26.96, 26.60, 26.31, 25.12, 25.10, 24.87, 24.41, 22.33, 22.01, 11.73, 11.69.

HRMS (ESI) *m/z*: $[M + Na]^{6+}$ calcd for $C_{764}H_{1366}N_{44}O_{184}$, 2373.6373; found, 2373.6487.

IR (ATR): ṽ (cm^{-1}) = 3325, 2926, 2855, 1739, 1653, 1532, 1461, 1376, 1245, 1104, 948, 848, 722.

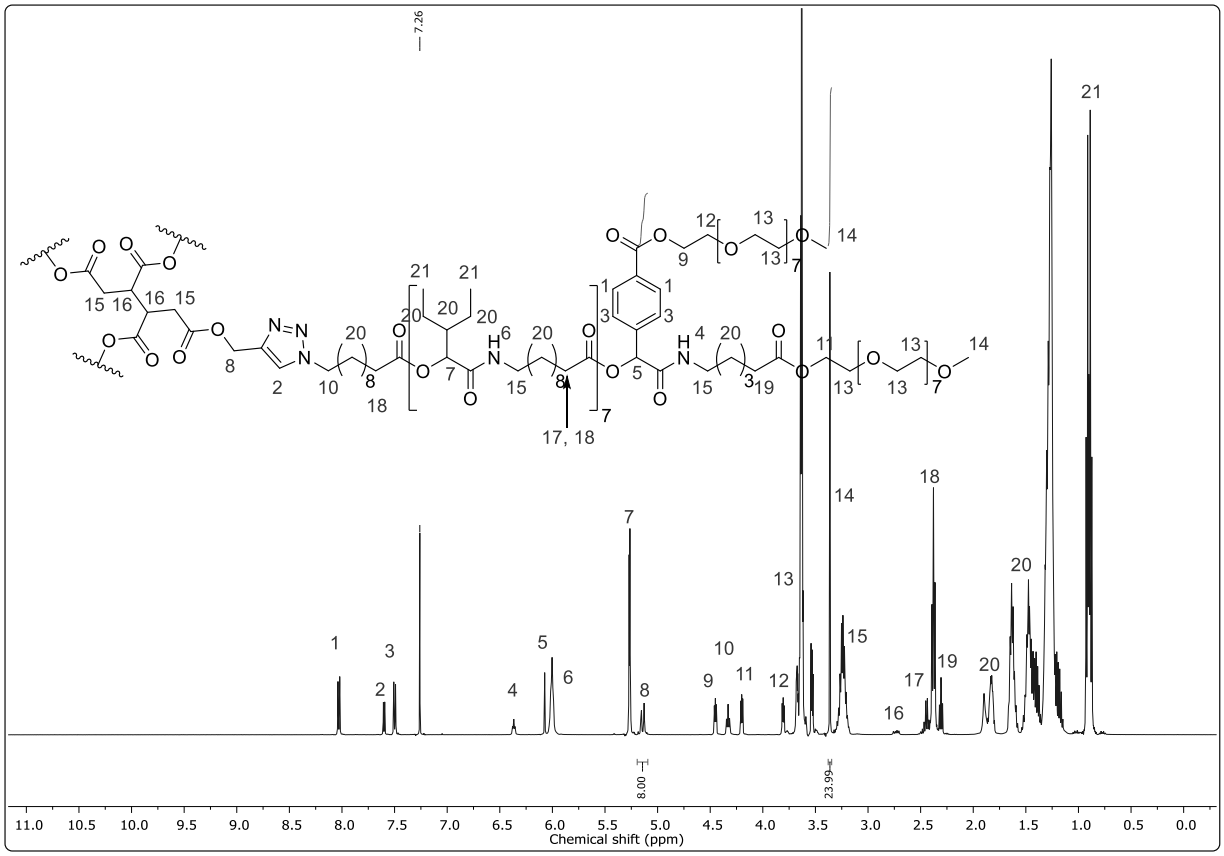

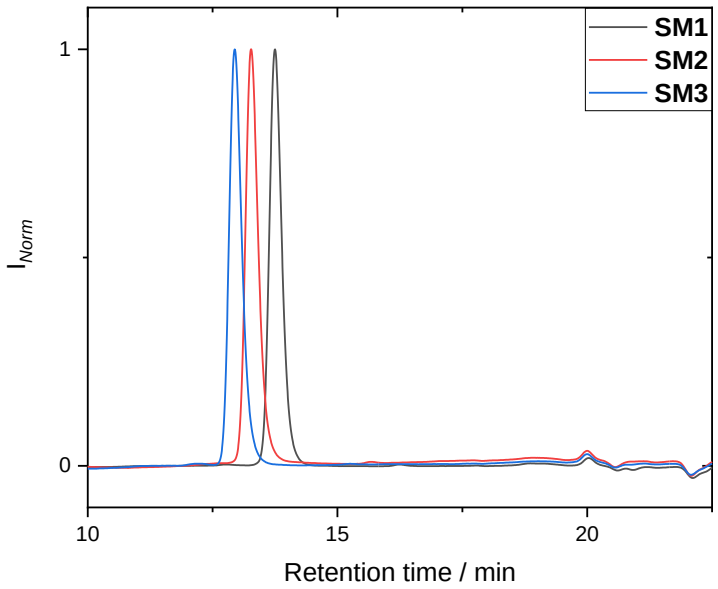

Figure S 11: SEC trace of the three star-shaped macromolecules **SM1**-**3** measured in THF.

7 Appendix

7.1 Index of abbreviations

18-C-6	18-crown-six ether
3-CR	three-component reaction
4EG	tetra(ethylene glycol)
8EG	octa(ethylene glycol)
AIDS	acquired immune deficiency syndrome
ADMET	acyclic diene metathesis
Ala	alanine
APCI-MS	atmospheric pressure chemical ionization-mass spectrometry
ASAP	atmospheric solids analysis probe
Asp	asparagine
ATRP	atom transfer radical polymerization
Bn	benzyl
BnBr	benzyl bromide
Boc	*tert*-butyloxycarbonyl
BTEAC	benzyl triethyl ammonium bromide
calcd	calculated
CuAAC	copper-catalyzed azide-alkyne cycloaddition
Cy	cysteine
DBU	1,8-diazabicyclo[5.4.0]undec-7-ene
DCC	*N,N'*-dicylcohexylcarbodiimide
DCM	dichloromethane
DCU	*N,N'*-dicyclohexylurea

DIA	diisopropylamine
DIPEA	diisopropylethylamine
DFT	density functional theory
DLS	dynamic light scattering
DMC	dimethyl carbonate
DMAP	dimethyl aminopyridine
DMF	dimethylformamide
DMSO	dimethylsulfoxide
DNA	deoxyribonucleic acid
EA	ethyl acetate
EI-MS	electron impact ionization-mass spectrometry
ESI-MS	electrospray ionization-mass spectrometry
ESI-MS(/MS)	electrospray ionization fragmentation mass spectrometry
EWGs	electron withdrawing groups
FAB-MS	fast atom bombardment-mass spectrometry
FLOW-IEG	flow synthesis and iterative exponential growth
FSPE	fluorous solid-phase extraction
GBL	γ-butyrolactone
GC	gas chromatography
GC-MS	gas chromatography mass spectrometry
GHS	global harmonized system
Glu	glutamic acid
HIV	immunodeficiency virus
HPLC	high pressure liquid chromatography
HRMS	high resolution mass spectrometry

HTS	high-throughput screening
IEG	iterative exponential growth
IMCR	isocyanide-based multi-component reaction
IUPAC	international union of pure and applied chemistry
IR	infrared
KO^{t}Bu	potassium *tert*-butoxide
Leu	leucine
Lys	lysine
MALDI	matrix assisted laser desorption ionization
MCR	multi-component reaction
MeCN	acetonitrile
Me-THF	2-methyl tetrahydrofuran
M_n	number average molar mass
MS	mass spectrometry
NaAsc	Sodium ascorbate
NMP	nitroxide-mediated radical polymerization
NMR	nuclear magnetic resonance
OEG	oligo(ethylene glycol)
OTos	tosylate
P-3CR	Passerini-3-component reaction
PCC	pyridinium chlorochromate
Pd/C	palladium on charcoal
PEG	poly(ethylene glycol)
PFG	pulsed field gradient
PG	protecting group

PLA	poly(lactic acid)
PMA	poly(methacrylate)
ppb	parts per billion
PPh_3	triphenylphosphane
ppm	parts per million
p-TsOH	para-toluenesulfonic acid
p-TsCl	*para*-toluenesulfonyl chloride
PrBr	propyl bromide
PU	poly(urethane)
Py	pyridine
RAFT	reversible addition-fragmentation chain transfer polymerization
RDRP	reversible deactivation radical polymerization
ROMP	ring opening metathesis polymerization
R_f	retention factor
RNA	ribonucleic acid
RU	repeating unit
SEC	size exclusion chromatography
SEC-ESI-MS	size exclusion chromatography coupled to electrospray ionization-mass spectrometry
Ser	serine
SPPS	solid phase peptide synthesis
TAD	1,2,4-triazoline-3,5-dione
TBDMS	*tert*-butyldimethylsilyl
TEA	triethylamine
TEMPO	2,2,5,5-tetramethylpiperidinyloxyl

TFA	trifluoro acetic acid
THP	2-tetrahydropyranyl
THF	tetrahydrofuran
Ser	serine
TAD	1,2,4-triazoline-3,5-dione
TEMPO	2,2,5,5-tetramethylpiperidinyloxyl
TFA	trifluoro acetic acid
THF	tetrahydrofuran
THP	tetrahydropyrane
TIPS	triisopropylsilyl
TLC	thin layer chromatography
ToF-MS	time of flight mass spectrometry
Trt	trityl
Tyr	tyrosine
U-4CR	Ugi-4-component reaction
UV/Vis	ultraviolet/visible light
Val	valine

7.2 Publications

[1] K. A. Waibel, D. Moatsou, M. A. R. Meier, *Macromol. Rapid Commun.* **2021**, *42*, 2000467, DOI: 10.1002/marc.202000467.

[2] K. A. Waibel, R. Nickisch, N. Möhl, R. Seim, M. A. R. Meier, *Green Chem.* **2020**, *22*, 933–941.

[3] R. V. Schneider, K. A. Waibel, A. P. Arndt, M. Lang, R. Seim, D. Busko, S. Bräse, U. Lemmer, M. A. R. Meier, *Sci. Rep.* **2018**, *8*, 6–13.

8 List of figures, schemes, and tables

8.1 List of figures

8.2 List of supporting figures

8.3 List of schemes

8.4 List of tables

8.5 List of supporting tables

9 Bibliography

All sources with weblink in the bibliography were last accessed on **February 27, 2021**.

[1] “Cellulose,” can be found under https://roempp.thieme.de/lexicon/RD-03-00833, **2021**.

[2] H.-H. Greve, in *Ullmann’s Encycl. Ind. Chem.*, Wiley-VCH, Weinheim, **2000**, pp. 583–594.

[3] “Lignin,” can be found under https://roempp.thieme.de/lexicon/RD-12-01138, **2021**.

[4] “Wolle,” can be found under https://roempp.thieme.de/lexicon/RD-23-01058, **2021**.

[5] “Baumwolle,” can be found under https://roempp.thieme.de/lexicon/RD-02-00425, **2021**.

[6] “Seide,” can be found under https://roempp.thieme.de/lexicon/RD-19-01696, **2021**.

[7] “Polysaccharide,” can be found under https://roempp.thieme.de/lexicon/RD-16-03559, **2021**.

[8] H. Staudinger, *Berichte der Dtsch. Chem. Gesellschaft* **1920**, *53*, 1073.

[9] H. Staudinger, *Berichte der Dtsch. Chem. Gesellschaft* **1924**, *57B*, 1203–1208.

[10] H. Staudinger, *Berichte der Dtsch. Chem. Gesellschaft* **1926**, *59*, 3019–3043.

[11] “Kunstoffe,” can be found under https://roempp.thieme.de/lexicon/RD-11-02403, **2021**.

[12] L. L. Böhm, *Angew. Chemie* **2003**, *115*, 5162–5183.

[13] R. Mülhaupt, *Macromol. Chem. Phys.* **2003**, *204*, 289–327.

[14] “DNA,” can be found under https://roempp.thieme.de/lexicon/RD-04-00730, **2021**.

[15] “Proteine,” can be found under https://roempp.thieme.de/lexicon/RD-16-04546, **2021**.

[16] M. Szwarc, *Chem. Eng. News* **1956**, *178*, 1168–1169.

[17] N. Badi, J.-F. Lutz, *Chem. Soc. Rev.* **2009**, *38*, 3383–3390.

[18] J.-F. Lutz, *Polym. Chem.* **2010**, *1*, 55–62.

[19] J.-F. Lutz, J.-M. Lehn, E. W. Meijer, K. Matyjaszewski, *Nat. Rev. Mater.* **2016**, *1*, 16024.

[20] S. C. Solleder, R. V. Schneider, K. S. Wetzel, A. C. Boukis, M. A. R. Meier, *Macromol. Rapid Commun.* **2017**, *38*, 1–45.

[21] J.-F. Lutz, *Macromol. Rapid Commun.* **2017**, *38*, 1–12.

[22] R. B. Merrifield, *J. Am. Chem. Soc.* **1963**, *85*, 2149–2154.

[23] K. Takizawa, C. Tang, C. J. Hawker, *J. Am. Chem. Soc.* **2008**, *130*, 1718–1726.

[24] F. A. Leibfarth, J. A. Johnson, T. F. Jamison, *Proc. Natl. Acad. Sci. U. S. A.* **2015**, *112*, 10617–10622.

[25] A. Al Ouahabi, L. Charles, J.-F. Lutz, *J. Am. Chem. Soc.* **2015**, *137*, 5629–5635.

[26] S. C. Solleder, D. Zengel, K. S. Wetzel, M. A. R. Meier, *Angew. Chem. Int. Ed.* **2016**, *55*, 1204.

[27] B. Zhao, Z. Gao, Y. Zheng, C. Gao, *J. Am. Chem. Soc.* **2019**, DOI 10.1021/jacs.9b00172.

[28] M. B. Koo, S. W. Lee, J. M. Lee, K. T. Kim, *J. Am. Chem. Soc.* **2020**, *142*, 14028–14032.

[29] A. Al Ouahabi, J. Amalian, L. Charles, J.-F. Lutz, *Nat. Commun.* **2017**, *8*, 967.

[30] A. C. Boukis, K. Reiter, M. Frölich, D. Hofheinz, M. A. R. Meier, *Nat. Commun.* **2018**, *9*, 1439.

[31] K. S. Wetzel, M. Frölich, S. C. Solleder, R. Nickisch, P. Treu, M. A. R. Meier, *Commun. Chem.* **2020**, *3*, 1–10.

[32] J. O. Holloway, F. Van Lijsebetten, N. Badi, H. A. Houck, F. E. Du Prez, *Adv. Sci.* **2020**, *7*, DOI 10.1002/advs.201903698.

[33] R. V. Schneider, K. A. Waibel, A. P. Arndt, M. Lang, R. Seim, D. Busko, S. Bräse, U. Lemmer, M. A. R. Meier, *Sci. Rep.* **2018**, *8*, 6–13.

[34] M. A. R. Meier, C. Barner-Kowollik, *Adv. Mater.* **2019**, *31*, 1–5.

[35] K. S. Wetzel, M. A. R. Meier, *Polym. Chem.* **2019**, *10*, 2716–2722.

[36] N. Hadjichristidis, M. Pitsikalis, H. Iatrou, P. Driva, G. Sakellariou, M. Chatzichristidi, *Polymers with Star-Related Structures: Synthesis, Properties, and Applications*, Elsevier B.V., **2012**.

[37] S. Oelmann, M. A. R. Meier, *RSC Adv.* **2017**, *7*, 45195–45199.

[38] S. Oelmann, A. Travanut, D. Barther, M. Romero, S. M. Howdle, C. Alexander, M. A. R. Meier, *Biomacromolecules* **2019**, *20*, 90–101.

[39] “macro-,” can be found under https://www.oxfordlearnersdictionaries.com/definition/english/macro_2, **2021**.

[40] “molecule,” can be found under https://www.oxfordlearnersdictionaries.com/definition/american_english/molecule, **2021**.

[41] “Makromolekül,” can be found under https://www.duden.de/rechtschreibung/Makromolekuel, **2021**.

[42] “Makromoleküle,” can be found under https://roempp.thieme.de/lexicon/RD-13-00294, **2021**.

[43] F. C. H. Crick, J. D. Watson, *Nature* **1953**, *171*, 737–738.

[44] M. Ouchi, D. R. Liu, M. Sawamoto, *Science (80-.).* **2013**, *341*, 1238149.

[45] H. Staudinger, J. Fritschi, *Helv. Chim. Acta* **1922**, *5*, 785–806.

[46] “Viren,” can be found under https://roempp.thieme.de/lexicon/RD-22-00869, **2021**.

[47] “Bakterien,” can be found under https://roempp.thieme.de/lexicon/RD-02-00123, **2021**.

[48] “Polynucleotide,” can be found under https://roempp.thieme.de/lexicon/RD-16-03449, **2021**.

[49] “Proteine,” can be found under https://roempp.thieme.de/lexicon/RD-16-04546, **2021**.

[50] “Naturkautschuk,” can be found under https://roempp.thieme.de/lexicon/RD-14-00569, **2021**.

[51] Zephyris, “Structure of DNA,” can be found under https://en.wikipedia.org/wiki/DNA#/media/File:DNA_Structure+Key+Labelled.pn_NoBB.png, **2021**.

[52] K. Munk, *Biochemie - Zellbiologie*, Georg Thieme Verlag, Stuttgart, **2008**.

[53] N. A. Campbell, J. B. Reece, L. A. Urry, M. L. Cain, S. A. Wasserman, P. V. Minorsky, R. B. Jackson, *Biologie*, Pearson Studium, **2015**.

[54] A. Gutteridge, J. M. Thornton, *Trends Biochem. Sci.* **2005**, *30*, 622–629.

[55] W. Kauzmann, *J. Cell. Physiol.* **1956**, *47*, 113–131.

[56] T. Shafee, “Protein structure,” can be found under https://upload.wikimedia.org/wikipedia/commons/5/5f/Protein_structure_%28full%29.png, **2021**.

[57] J. Lucas-Lenard, F. Lipmann, *Annu. Rev. Biochem* **1971**, *40*, 409–448.

[58] J.-F. Lutz, *Sequence-Controlled Polymers*, Wiley-VCH, Weinheim, **2018**.

[59] J.-F. Lutz, M. Ouchi, D. R. Liu, M. Sawamoto, *Science (80-.).* **2013**, *341*, 1238149.

[60] D. Moatsou, C. F. Hansell, R. K. O’Reilly, *Chem. Sci.* **2014**, *5*, 2246–2250.

[61] S. Martens, A. Landuyt, P. Espeel, B. Devreese, P. Dawyndt, F. E. Du Prez, *Nat. Commun.* **2018**, *9*, 4451.

[62] M. Anthea, J. Hopkins, C. W. McLaughlin, S. Johnson, M. Q. Warner, D. Lahart, J. D. Wright, *Human Biology and Health*, Englewood Cliffs, New Jersey, **1993**.

[63] “Sickle Cell Disease,” can be found under https://www.nhlbi.nih.gov/health-topics/sickle-cell-disease, **2021**.

[64] H. Eiberg, J. Troelsen, M. Nielsen, A. Mikkelsen, J. Mengel-From, K. W. Kjaer, L. Hansen, *Hum. Genet.* **2008**, *123*, 177–187.

[65] C. Keyser, C. Bouakaze, E. Crubézy, V. G. Nikolaev, D. Montagnon, T. Reis, B. Ludes, *Hum. Genet.* **2009**, *126*, 395–410.

[66] “What is cancer?,” can be found under https://www.cancer.gov/about-cancer/understanding/what-is-cancer, **2021**.

[67] P. A. Wender, S. T. Handy, D. L. Wright, *Chem. Ind.* **1997**, *19*, 765–769.

[68] A. Dömling, I. K. Ugi, *Angew. Chemie - Int. Ed.* **2000**, *39*, 3168–3210.

[69] K. Alfonsi, J. Colberg, P. J. Dunn, T. Fevig, S. Jennings, T. A. Johnson, H. P. Kleine, C. Knight, M. A. Nagy, D. A. Perry, M. Stefaniak, *Green Chem.* **2008**, 31.

[70] "GSK Solvent Selection Guide," **2010**.

[71] R. K. Henderson, C. Jimenez-Gonzalez, D. J. C. Constable, S. R. Alston, G. G. A. Inglis, G. Fisher, J. Sherwood, S. P. Binks, A. D. Curzons, *Green Chem.* **2011**, 854.

[72] D. Prat, J. Hayler, A. Wells, *Green Chem.* **2014**, *16*, 4546–4551.

[73] R. K. Henderson, A. P. Hill, A. M. Redman, H. F. Sneddon, *Green Chem.* **2015**, *17*, 945–949.

[74] M. Passerini, L. Simone, *Gazz. Chim. Ital.* **1921**, *51*, 126–129.

[75] A. Sehlinger, L. M. De Espinosa, M. A. R. Meier, *Macromol. Chem. Phys.* **2013**, *214*, 2821–2828.

[76] A. Sehlinger, O. Kreye, M. A. R. Meier, *Macromolecules* **2013**, *46*, 6031–6037.

[77] R. Huisgen, *J. Org. Chem.* **1976**, *41*, 403–419.

[78] M. Meldal, C. W. Tomøe, *Chem. Rev.* **2008**, *108*, 2952–3015.

[79] J. E. Hein, V. V. Fokin, *Chem. Soc. Rev.* **2010**, *39*, 1302–1315.

[80] L. Liang, D. Astruc, *Coord. Chem. Rev.* **2011**, *255*, 2933–2945.

[81] W. Lieke, *Ann. der Chemie und Pharm.* **1859**, *112*, 316–321.

[82] I. K. Ugi, *Angew. Chemie* **1962**, *I*, 8–21.

[83] I. K. Ugi, U. Fetzer, U. Eholzer, H. Knupfer, K. Offermann, *Angew. Chem. Int. Ed.* **1965**, *4*, 472–484.

[84] I. K. Ugi, B. Werner, A. Dömling, *Molecules* **2003**, *8*, 53–66.

[85] M. C. Pirrung, S. Ghorai, *J. Am. Chem. Soc.* **2006**, *128*, 11772–11773.

[86] A. W. Hoffmann, *Ber. Dtsch. Chem. Ges.* **1867**, *144*, 114.

[87] R. Meyr, I. K. Ugi, *Angew. Chemie* **1958**, *70*, 702–703.

[88] R. Appel, R. Kleinstück, K.-D. Ziehn, *Angew. Chemie Int. Ed. English* **1971**, *10*, 132.

[89] P. G. Gassman, T. L. Guggenheim, *J. Am. Chem. Soc.* **1982**, *104*, 5849–5850.

[90] X. Wang, Q. G. Wang, Q. L. Luo, *Synth.* **2015**, *47*, 49–54.

[91] K. Pérez-Labrada, I. Brouard, I. Méndez, D. G. Rivera, *J. Org. Chem.* **2012**, *77*, 4660–4670.

[92] A. Sehlinger, P. K. Dannecker, O. Kreye, M. A. R. Meier, *Macromolecules* **2014**, *47*, 2774–2783.

[93] M. K. W. Mackwitz, A. Hamacher, J. D. Osko, J. Held, A. Schöler, D. W. Christianson, M. U. Kassack, F. K. Hansen, *Org. Lett.* **2018**, *20*, 3255–3258.

[94] J. G. Polisar, L. Li, J. R. Norton, *Tetrahedron Lett.* **2011**, *52*, 2933–2934.

[95] K. Škoch, I. Císařová, P. Štěpnička, *Chem. - A Eur. J.* **2018**, *24*, 13788–13791.

[96] M. S. Edenborough, R. B. Herbert, *Nat. Prod. Rep.* **1988**, *55*, 299.

[97] P. J. Scheuer, *Acc. Chem. Res.* **1992**, *25*, 433.

[98] C. W. J. Chang, P. J. Scheuer, *Top. Curr. Chem.* **1993**, *167*, 33.

[99] R. E. Schuster, J. E. Scott, J. Casanova Jr., *J. Mol. Spectrosc.* **1979**, *76*, 55–70.

[100] S. M. Creedon, H. K. Crowley, D. G. McCarthy, *J. Chem. Soc. Perkin Trans. 1* **1998**, *16*, 1015–1018.

[101] G. Skorna, I. K. Ugi, *Angew. Chemie Int. Ed. English* **1977**, *16*, 259–260.

[102] I. K. Ugi, R. Meyr, U. Fetzer, C. Steinbrückner, *Angew. Chem.* **1959**, *71*, 386.

[103] K. A. Waibel, R. Nickisch, N. Möhl, R. Seim, M. A. R. Meier, *Green Chem.* **2020**, *22*, 933–941.

[104] P. Patil, M. Ahmadian-Moghaddam, A. Dömling, *Green Chem.* **2020**.

[105] G. Qiu, Q. Ding, J. Wu, *Chem. Soc. Rev.* **2013**, *42*, 5257–5269.

[106] T. Vlaar, E. Ruijter, B. U. W. Maes, R. V. A. Orru, *Angew. Chemie - Int. Ed.* **2013**, *52*, 7084–7097.

[107] V. P. Boyarskiy, N. A. Bokach, K. V. Luzyanin, V. Y. Kukushkin, *Chem. Rev.* **2015**, *115*, 2698–2779.

[108] J. W. Collet, T. R. Roose, E. Ruijter, B. U. W. Maes, R. V. A. Orru, *Angew. Chemie* **2020**, *132*, 548–566.

[109] O. H. Oldenziel, D. van Leusen, A. M. van Leusen, *J. Org. Chem.* **1977**, *42*, 3114–3118.

[110] A. Dömling, *Chem. Rev.* **2006**, *106*, 17–89.

[111] X. X. Deng, L. Li, Z. L. Li, A. Lv, F. S. Du, Z. C. Li, *ACS Macro Lett.* **2012**, *1*, 1300–1303.

[112] A. Lv, X.-X. Deng, L. Li, Z.-L. Li, Y.-Z. Wang, F.-S. Du, Z.-C. Li, *Polym. Chem.* **2013**, *4*, 3659.

[113] A. Sehlinger, R. Schneider, M. A. R. Meier, *Macromol. Rapid Commun.* **2014**, 1866–1871.

[114] X. X. Deng, Y. Cui, Y. Z. Wang, F. S. Du, Z. C. Li, *Aust. J. Chem.* **2014**, *67*, 555–561.

[115] B. Yang, Y. Zhao, Y. Wei, C. Fu, L. Tao, *Polym. Chem.* **2015**, *6*, 8233–8239.

[116] P. Mampuys, Y. Zhu, S. Sergeyev, E. Ruijter, R. V. A. Orru, S. Van Doorslaer, B. U. W. Maes, *Org. Lett.* **2016**, *18*, 2808–2811.

[117] S. Wu, X. Lei, E. Fan, Z. Sun, *Org. Lett.* **2018**, *20*, 522–525.

[118] W. Wei, P. Bao, H. Yue, S. Liu, L. Wang, Y. Li, D. Yang, *Org. Lett.* **2018**, *20*, 5291–5295.

[119] P. Bao, L. Wang, H. Yue, Y. Shao, J. Wen, D. Yang, X. Zhao, H. Wang, W. Wei, *J. Org. Chem.* **2019**, *84*, 2976–2983.

[120] A. Strecker, *Justus Liebigs Ann. Chem.* **1850**, *75*, 27–45.

[121] O. Kreye, T. Tóth, M. A. R. Meier, *J. Am Chem. Soc.* **2011**, *133*, 1790–1792.

[122] R. Kakuchi, *Angew. Chemie - Int. Ed.* **2014**, *53*, 46–48.

[123] B. M. Trost, *Science (80-.).* **1991**, *254*, 1471–1477.

[124] A. Váradi, T. C. Palmer, R. N. Dardashti, S. Majumdar, **2016**, DOI 10.3390/molecules21010019.

[125] L. Weber, *Curr. Med. Chem.* **2002**, *9*, DOI 10.2174/0929867023368719.

[126] K. Harada, *Nature* **1963**, *200*, 1201.

[127] F. A. Davis, R. E. Reddy, P. S. Portonovo, *Tetrahedron Lett.* **1994**, *35*, 9351–9354.

[128] M. S. Iyer, K. M. Gigstad, N. D. Namdev, M. Lipton, *J. Am. Chem. Soc.* **1996**, *118*, 4910–4911.

[129] H. Ishitani, S. Komiyama, Y. Hasegawa, S. Kobayashi, *J. Am. Chem. Soc.* **2000**, *122*, 762–766.

[130] J. Huang, E. J. Corey, *Org. Lett.* **2004**, *6*, 5027–5029.

[131] A. Hantzsch, *Chem. Ber.* **1881**, 1637–1638.

[132] J. J. Xia, G. W. Wang, *Synthesis (Stuttg).* **2005**, 2379–2383.

[133] “Nifepidine,” can be found under https://web.archive.org/web/20180808043257/https://www.drugs.com/monograph/nifedipine.html, **2021**.

[134] V. H. Meyer, F. Bossert, K. Wehinger, K. Stoepel, W. Vater, *Patent US 3 485 847*, **1969**, US 3 485 847.

[135] M. F. Gordeev, D. V. Patel, E. M. Gordon, *J. Org. Chem.* **1996**, *61*, 924–928.

[136] H. A. J. Struyker-Boudier, J. F. M. Smits, J. G. R. De Mey, *J. Cardiovasc. Pharmacol.* **1994**, *15*, 1–10.

[137] D. J. Triggle, *Cell. Mol. Neurobiol.* **2003**, *23*, 293–303.

[138] S. Sepehri, H. P. Sanchez, A. Fassihi, *J. Pharm. Pharm. Sci.* **2015**, *18*, 1–52.

[139] P. Biginelli, *Chem. Ber.* **1891**, 1317–1319.

[140] P. Biginelli, *Chem. Ber.* **1891**, 2962–2967.

[141] C. O. Kappe, *J. Org. Chem.* **1997**, *62*, 7201–7204.

[142] G. C. Rovnyak, K. S. Atwal, S. D. Kimball, B. C. O’Reilly, J. Schwartz, A. Hedberg, S. Moreland, J. Z. Gougoutas, M. F. Malley, *J. Med. Chem.* **1992**, *35*, 3254–3263.

[143] A. Cunningham, P. Wipf, *Tetrahedron Lett.* **1995**, *36*, 7819–7822.

[144] C. O. Kappe, *Bioorganic Med. Chem. Lett.* **2000**, *10*, 49–51.

[145] T. Panneer Selvam, C. Richa James, P. Vijaysarathy Dniandev, S. Karyn Valzita, *Res. Pharm.* **2012**, *2*, 1–9.

[146] Â. de Fátima, T. C. Braga, L. da S. Neto, B. S. Terra, B. G. F. Oliveira, D. L. da Silva, L. V. Modolo, *J. Adv. Res.* **2015**, *6*, 363–373.

[147] H. Nagarajaiah, A. Mukhopadhyay, J. N. Moorthy, *Tetrahedron Lett.* **2016**, *57*, 5135–5149.

[148] H. Xue, Y. Zhao, H. Wu, Z. Wang, B. Yang, Y. Wei, Z. Wang, L. Tao, *J. Am. Chem. Soc.* **2016**, *138*, 8690–8693.

[149] A. C. Boukis, B. Monney, M. A. R. Meier, *Beilstein J. Org. Chem.* **2017**, *13*, 54–62.

[150] A. C. Boukis, M. A. R. Meier, *Eur. Polym. J.* **2018**, *104*, 32–38.

[151] C. Mannich, W. Krösche, *Mitteilung aus dem phamazeutischen Inst. der Univ. Berlin* **1912**, 647–667.

[152] M. Arend, B. Westermann, N. Risch, *Angew. Chemie - Int. Ed.* **1998**, *37*, 1044–1070.

[153] B. List, *J. Am. Chem. Soc.* **2000**, *122*, 9336–9337.

[154] R. G. Arrayás, J. C. Carretero, *Chem. Soc. Rev.* **2009**, *38*, 1940–1948.

[155] M. Hartweg, C. R. Becer, *Green Chem.* **2016**, *18*, 3272–3277.

[156] B. Yang, Y. Zhao, C. Fu, C. Zhu, Y. Zhang, S. Wang, Y. Wei, L. Tao, *Polym. Chem.* **2014**, *5*, 2704–2708.

[157] S. C. Solleder, M. A. R. Meier, *Angew. Chemie - Int. Ed.* **2014**, *53*, 711–714.

[158] S. C. Solleder, K. S. Wetzel, M. A. R. Meier, *Polym. Chem.* **2015**, *6*, 3201–3204.

[159] Y. Wu, J. Zhang, F. Du, Z. Li, *ACS Macro Lett.* **2017**, 6–11.

[160] J. O. Holloway, K. S. Wetzel, S. Martens, F. E. Du Prez, M. A. R. Meier, *Polym. Chem.* **2019**, *10*, 3859–3867.

[161] N. Chéron, R. Ramozzi, L. El Kaïm, L. Grimaud, P. Fleurat-Lessard, *J. Org. Chem.* **2012**, *77*, 1361–1366.

[162] O. Mumm, *Ber. Dtsch. Chem. Ges.* **1910**, *43*, 886–893.

[163] R. O. Rocha, M. O. Rodrigues, B. A. D. Neto, *ACS Omega* **2020**, *5*, 972–979.

[164] A. C. Boukis, Moleküle Als Potentielle Datenspeichersysteme : Multikomponentenreaktionen Sind Der Schlüssel, KIT, **2018**.

[165] I. K. Ugi, C. Steinbrückner, *Aus dem Inst. für Org. Chemie der Univ. München* **1961**, 734–742.

[166] P. Stiernet, P. Lecomte, J. De Winter, A. Debuigne, *ACS Macro Lett.* **2019**, *8*, 427–434.

[167] L. El Kaïm, L. Grimaud, J. Oble, *Angew. Chemie - Int. Ed.* **2005**, *44*, 7961–7964.

[168] L. El Kaïm, M. Gizolme, L. Grimaud, J. Obie, *J. Org. Chem.* **2007**, *72*, 4169–4180.

[169] X. Zhang, S. Wang, J. Liu, Z. Xie, S. Luan, C. Xiao, Y. Tao, X. Wang, *ACS Macro Lett.* **2016**, *5*, 1049–1054.

[170] C. V. Robotham, C. Baker, B. Cuevas, K. Abboud, D. L. Wright, *Mol. Divers.* **2003**, *6*, 237–244.

[171] O. Kreye, O. Türünç, A. Sehlinger, J. Rackwitz, M. A. R. Meier, *Chem. - A Eur. J.* **2012**, *18*, 5767–5776.

[172] A. Sehlinger, K. Ochsenreither, N. Bartnick, M. A. R. Meier, *Eur. Polym. J.* **2015**, *65*, 313–324.

[173] R. H. Baker, D. Stanonis, *J. Am Chem. Soc.* **1951**, *73*, 699–702.

[174] I. Hagedorn, U. Eholzer, *Chem. Ber.* **1965**, *98*, 936–940.

[175] M. C. Pirrung, K. Das Sarma, *J. Am. Chem. Soc.* **2004**, *126*, 444–445.

[176] S. Maeda, S. Komagawa, M. Uchiyama, K. Morokuma, *Angew. Chemie - Int. Ed.* **2011**, *50*, 644–649.

[177] R. Ramozzi, K. Morokuma, *J. Org. Chem.* **2015**, *80*, 5652–5657.

[178] K. N. Onwukamike, S. Grelier, E. Grau, H. Cramail, M. A. R. Meier, *RSC Adv.* **2018**, *8*, 31490–31495.

[179] L. El Kaim, M. Gizolme, L. Grimaud, *Org. Lett.* **2006**, *8*, 5021–5023.

[180] J. M. Saya, R. Berabez, P. Broersen, I. Schuringa, A. Kruithof, R. V. A. Orru, E. Ruijter, *Org. Lett.* **2018**, *20*, 3988–3991.

[181] A. L. Chandgude, A. Dömling, *Green Chem.* **2016**, *18*, 3718–3721.

[182] T. Nixey, C. Hulme, *Tetrahedron Lett.* **2002**, *43*, 6833–6835.

[183] T. Ngouansavanh, J. Zhu, *Angew. Chemie - Int. Ed.* **2006**, *45*, 3495–3497.

[184] L. J. Zhang, X. X. Deng, F. S. Du, Z. C. Li, *Macromolecules* **2013**, *46*, 9554–9562.

[185] S. Sebti, A. Foucaud, *Communications* **1983**.

[186] H. Bock, I. K. Ugi, *J. Prakt. Chem.* **1997**, *339*, 385–389.

[187] U. Kusebauch, B. Beck, K. Messer, E. Herdtweck, A. Dömling, *Org. Lett.* **2003**, *5*, 4021–4024.

[188] P. R. Andreana, C. C. Liu, S. L. Schreiber, *Org. Lett.* **2004**, *6*, 4231–4233.

[189] T. Yue, M. X. Wang, D. X. Wang, J. Zhu, *Angew. Chemie - Int. Ed.* **2008**, *47*, 9454–9457.

[190] P. Slobbe, E. Ruijter, R. V. A. Orru, *Medchemcomm* **2012**, *3*, 1189–1218.

[191] T. Sperka, J. Pitlik, P. Bagossi, J. Tözsér, *Bioorganic Med. Chem. Lett.* **2005**, *15*, 3086–3090.

[192] N. A. M. Yehia, W. Antuch, B. Beck, S. Hess, V. Schauer-Vukašinović, M. Almstetter, P. Furer, E. Herdtweck, A. Dömling, *Bioorganic Med. Chem. Lett.* **2004**, *14*, 3121–3125.

[193] A. Dömling, B. Beck, W. Baumbach, G. Larbig, *Bioorganic Med. Chem. Lett.* **2007**, *17*, 379–384.

[194] A. Dömling, W. Wang, K. Wang, *Chem. Rev.* **2012**, *112*, 3083–3135.

[195] A. Sehlinger, R. Schneider, M. A. R. Meier, *Eur. Polym. J.* **2014**, *50*, 150–157.

[196] L. Li, A. Lv, X. X. Deng, F. S. Du, Z. C. Li, *Chem. Commun.* **2013**, *49*, 8549–8551.

[197] B. T. Tuten, L. De Keer, S. Wiedbrauk, P. H. M. Van Steenberge, D. R. D'hooge, C. Barner-Kowollik, *Angew. Chemie* **2019**, *131*, 5728–5732.

[198] S. Luleburgaz, G. Hizal, H. Durmaz, U. Tunca, *Polymer (Guildf).* **2017**, *127*, 45–51.

[199] S. Bräse, C. Gil, K. Knepper, V. Zimmermann, *Angew. Chemie - Int. Ed.* **2005**, *44*, 5188–5240.

[200] E. A. Betterton, *Crit. Rev. Environ. Sci. Technol.* **2003**, *33*, 423–458.

[201] C. Lang, K. Pahnke, C. Kiefer, A. S. Goldmann, P. W. Roesky, C. Barner-Kowollik, *Polym. Chem.* **2013**, *4*, 5456–5462.

[202] L. Benati, G. Bencivenni, R. Leardini, M. Minozzi, D. Nanni, R. Scialpi, P. Spagnolo, G. Zanardi, *J. Org. Chem.* **2006**, *71*, 5822–5825.

[203] L. Díaz, J. Bujons, J. Casas, A. Llebaria, A. Delgado, *J. Med. Chem.* **2010**, *53*, 5248–5255.

[204] A. J. Marshall, J. M. Lin, A. Grey, I. R. Reid, J. Cornish, W. A. Denny, *Bioorganic Med. Chem.* **2013**, *21*, 4112–4119.

[205] R. Huisgen, *Proc. Chem. Soc.* **1961**, 357–396.

[206] V. V. Rostovtsev, L. G. Green, V. V. Fokin, K. B. Sharpless, *Angew. Chemie - Int. Ed.* **2002**, *41*, 2596–2599.

[207] C. W. Tornøe, C. Christensen, M. Meldal, *J. Org. Chem.* **2002**, *67*, 3057–3064.

[208] H. Stöckmann, A. A. Neves, S. Stairs, K. M. Brindle, F. J. Leeper, *Org. Biomol. Chem.* **2011**, *9*, 7303–7305.

[209] N. K. Devaraj, R. Weissleder, S. A. Hilderbrand, *Bioconjug. Chem.* **2008**, *19*, 2297–2299.

[210] M. L. Blackman, M. Royzen, J. M. Fox, *J. Am. Chem. Soc.* **2008**, *130*, 13518–13519.

[211] C. E. Hoyle, C. N. Bowman, *Angew. Chemie - Int. Ed.* **2010**, *49*, 1540–1573.

[212] A. B. Lowe, *Polym. Chem.* **2010**, *1*, 17–36.

[213] A. B. Lowe, *Polymer (Guildf).* **2014**, *55*, 5517–5549.

[214] V. O. Rodionov, V. V. Fokin, M. G. Finn, *Angew. Chemie - Int. Ed.* **2005**, *44*, 2210–2215.

[215] C. Iacobucci, S. Reale, J. F. Gal, F. De Angelis, *Angew. Chemie - Int. Ed.* **2015**, *54*, 3065–3068.

[216] Y. Özkllç, N. S. Tüzün, *Organometallics* **2016**, *35*, 2589–2599.

[217] M. S. Ziegler, K. V. Lakshmi, T. D. Tilley, *J. Am. Chem. Soc.* **2017**, *139*, 5378–5386.

[218] V. Aragão-Leoneti, V. L. Campo, A. S. Gomes, R. A. Field, I. Carvalho, *Tetrahedron* **2010**, *66*, 9475–9492.

[219] X. Wang, B. Huang, X. Liu, P. Zhan, *Drug Discov. Today* **2016**, *21*, 118–132.

[220] V. Castro, H. Rodríguez, F. Albericio, *ACS Comb. Sci.* **2016**, *18*, 1–14.

[221] C. Ornelas, J. Ruiz Aranzaes, E. Cloutet, S. Alves, D. Astruc, *Angew. Chemie - Int. Ed.* **2007**, *46*, 872–877.

[222] G. Franc, A. Kakkar, *Chem. Commun.* **2008**, 5267–5276.

[223] M. Meldal, *Macromol. Rapid Commun.* **2008**, *29*, 1016–1051.

[224] K. A. Waibel, D. Moatsou, M. A. R. Meier, *Macromol. Rapid Commun.* **2021**, *42*, 2000467.

[225] “Ein Molekül für 007,” can be found under https://www.spiegel.de/wissenschaft/mensch/verschluesselung-dank-chemie-ein-molekuel-fuer-007-a-1203713.html, **2018**.

[226] M. Kato, M. Kamigaito, M. Sawamoto, T. Higashimura, *Macromolecules* **1995**, *28*, 1721–1723.

[227] A. C. Wicker, F. A. Leibfarth, T. F. Jamison, *Polym. Chem.* **2017**, *8*, 5786–5794.

[228] H. Mutlu, J.-F. Lutz, *Angew. Chem. Int. Ed.* **2014**, *53*, 13010–13019.

[229] R. K. Roy, A. Meszynska, C. Laure, L. Charles, C. Verchin, J.-F. Lutz, *Nat. Commun.* **2015**, *6*, 7237.

[230] J.-F. Lutz, *Macromolecules* **2015**, *48*, 4759–4767.

[231] G. Cavallo, S. Poyer, J. A. Amalian, F. Dufour, A. Burel, C. Carapito, L. Charles, J.-F. Lutz, *Angew. Chemie - Int. Ed.* **2018**, *57*, 6266–6269.

[232] J. A. Amalian, G. Cavallo, A. Al Ouahabi, J.-F. Lutz, L. Charles, *Anal. Chem.* **2019**, *91*, 7266–7272.

[233] K. Launay, J.-A. Amalian, E. Laurent, L. Oswald, A. Al Ouahabi, A. Burel, F. Dufour, C. Carapito, J.-L. Clément, J.-F. Lutz, L. Charles, D. Gigmes, *Angew. Chemie - Int. Ed.* **2020**, *59*, 2–12.

[234] S. C. Solleder, S. Martens, P. Espeel, F. E. Du Prez, M. A. R. Meier, *Chem. - A Eur. J.* **2017**, *23*, 13906–13909.

[235] S. Martens, J. O. Holloway, F. E. Du Prez, *Macromol. Rapid Commun.* **2017**, *38*, 1–15.

[236] C. J. Burns, L. D. Field, K. Hashimoto, B. J. Petteys, D. D. Ridley, K. R. A. Samankumara Sandanayake, *Synth. Commun.* **1999**, *29*, 2337–2347.

[237] F. A. Loiseau, K. K. Hii, A. M. Hill, *J. Org. Chem.* **2004**, *69*, 639–647.

[238] S. A. Ahmed, M. Tanaka, *J. Org. Chem.* **2006**, *71*, 9884–9886.

[239] A. C. French, A. L. Thompson, B. G. Davis, *Angew. Chemie - Int. Ed.* **2009**, *48*, 1248–1252.

[240] P. Bohn, M. A. R. Meier, *Polym. J.* **2020**, *52*, 165–178.

[241] X. Guo, K. S. Wetzel, S. C. Solleder, S. Spann, M. A. R. Meier, M. Wilhelm, B. Luy, G. Guthausen, *Macromol. Chem. Phys.* **2019**, *220*, DOI 10.1002/macp.201900155.

[242] A. Al Ouahabi, M. Kotera, L. Charles, J.-F. Lutz, *ACS Macro Lett.* **2015**, *4*, 1077–1080.

[243] R. L. Kanasty, A. J. Vegas, L. M. Ceo, M. Maier, K. Charisse, J. K. Nair, R. Langer, D. G. Anderson, *Angew. Chemie - Int. Ed.* **2016**, *55*, 9529–9533.

[244] E. A. Hoff, G. X. De Hoe, C. M. Mulvaney, M. A. Hillmyer, C. A. Alabi, *J. Am. Chem. Soc.* **2020**, *142*, 6729–6736.

[245] J. J. Haven, T. Junkers, *Polym. Chem.* **2019**, *10*, 679–682.

[246] J. M. Lee, M. B. Koo, S. W. Lee, H. Lee, J. Kwon, Y. H. Shim, S. Y. Kim, K. T. Kim, *Nat. Commun.* **2020**, *11*, 56.

[247] E. Laurent, J. A. Amalian, M. Parmentier, L. Oswald, A. Al Ouahabi, F. Dufour, K. Launay, J. L. Clément, D. Gigmes, M. A. Delsuc, L. Charles, J.-F. Lutz, *Macromolecules* **2020**, *53*, 4022–4029.

[248] T. Mondal, V. Greff, B. É. Petit, L. Charles, J. F. Lutz, *ACS Macro Lett.* **2019**, *8*, 1002–1005.

[249] M. Frölich, D. Hofheinz, M. A. R. Meier, *Commun. Chem.* **2020**, *3*, 1–10.

[250] J.-F. Lutz, *ACS Macro Lett.* **2020**, 185–189.

[251] J.-F. Lutz, *Isr. J. Chem.* **2020**, *60*, 151–159.

[252] “Forscher hoffen auf Durchbruch für die Medikamentenforschung,” can be found under https://www.spiegel.de/wissenschaft/medizin/kuenstliche-intelligenz-sagt-faltung-von-proteinen-praezise-voraus-a-c52705ef-d3b0-440b-b325-acb6da0bd50b, **2020**.

[253] S. Yang, Y. Yan, J. Huang, A. V. Petukhov, L. M. J. Kroon-Batenburg, M. Drechsler, C. Zhou, M. Tu, S. Granick, L. Jiang, *Nat. Commun.* **2017**, *8*, 1–7.

[254] H. Hu, M. Gopinadhan, C. O. Osuji, *Soft Matter* **2014**, *10*, 3867–3889.

[255] T. P. Lodge, *Macromol. Chem. Phys.* **2003**, *204*, 265–273.

[256] G. M. Dykes, *J. Chem. Technol. Biotechnol.* **2001**, *76*, 903–918.

[257] E. Buhlleier, W. Wehner, F. Vögtle, *Communications* **1978**, 155–158.

[258] R. G. Denkewalter, J. F. Kolc, W. J. Lukasavage, *Macromolecular Highly Branched Homogeneous Compound Based on Lysine Units*, **1979**, US4289872A.

[259] R. G. Denkewalter, J. F. Kolc, W. J. Lukasavage, *Macromolecular Highly Branched Homogeneous Compound*, **1981**, US4410688A.

[260] D. A. Tomalia, J. R. Dewald, *Dense Star Polymers Having Core, Core Branches, Terminal Groups*, **1983**, US4507466A.

[261] G. R. Newkome, Z. Q. Yao, G. R. Baker, V. K. Gupta, *J. Org. Chem.* **1985**, *50*, 2003–2004.

[262] D. A. Tomalia, H. Baker, J. Dewald, M. Hall, G. Kallos, S. Martin, J. Roeck, J. Ryder, P. Smith, *Polym. J.* **1985**, *17*, 117–132.

[263] C. J. Hawker, J. M. J. Fréchet, *J. Am. Chem. Soc.* **1990**, *112*, 7638–7647.

[264] E. Abbasi, S. F. Aval, A. Akbarzadeh, M. Milani, H. T. Nasrabadi, S. W. Joo, Y. Hanifehpour, K. Nejati-Koshki, R. Pashaei-Asl, *Nanoscale Res. Lett.* **2014**, *9*, 1–10.

[265] C. Gorman, *Adv. Mater.* **1998**, *10*, 295–309.

[266] E. Alonso, J. Ruiz, **1999**, 1747–1751.

[267] F. J. Stoddart, T. Welton, *Polyhedron* **1999**, *18*, 3575–3591.

[268] I. Cuadrado, M. Moran, C. M. Casado, B. Alonso, J. Losada, *Coord. Chem. Rev.* **1999**, *193–195*, 395–445.

[269] G. Smith, R. Chen, S. Mapolie, *J. Organomet. Chem.* **2003**, *673*, 111–115.

[270] G. S. Smith, S. F. Mapolie, *J. Mol. Catal. A Chem.* **2004**, *213*, 187–192.

[271] K. L. Killops, L. M. Campos, C. J. Hawker, *J. Am. Chem. Soc.* **2008**, *130*, 5062–5064.

[272] G. Franc, A. K. Kakkar, *Chem. - A Eur. J.* **2009**, *15*, 5630–5639.

[273] J. A. Jee, L. A. Spagnuolo, J. G. Rudick, *Org. Lett.* **2012**, *14*, 3292–3295.

[274] J. G. Rudick, *J. Polym. Sci. Part A Polym. Chem.* **2013**, *51*, 3985–3991.

[275] O. Kreye, D. Kugele, L. Faust, M. A. R. Meier, *Macromol. Rapid Commun.* **2014**, *35*, 317–322.

[276] X. X. Deng, F. S. Du, Z. C. Li, *ACS Macro Lett.* **2014**, *3*, 667–670.

[277] A. Sehlinger, M. A. R. Meier, in *Multi-Component Seq. React. Polym. Synth. Adv. Polym. Sci.* (Ed.: P. Theato), Springer, **2015**.

[278] A. Llevot, A. C. Boukis, S. Oelmann, K. S. Wetzel, M. A. R. Meier, in *Polym. Synth. Based Triple-Bond Build. Blocks. Top. Curr. Chem. Collect.* (Eds.: B. Tang, R. Hu), Springer, **2017**.

[279] U. Tunca, *Macromol. Chem. Phys.* **2018**, *219*, 1–9.

[280] P. Antoni, Y. Hed, A. Nordberg, D. Nyström, H. Von Holst, A. Hult, M. Malkoch, *Angew. Chemie - Int. Ed.* **2009**, *48*, 2126–2130.

[281] J. R. McElhanon, D. V. McGrath, *J. Org. Chem.* **2000**, *65*, 3525–3529.

[282] C. O. Liang, J. M. J. Fréchet, *Macromolecules* **2005**, *38*, 6276–6284.

[283] M. Fischer, V. Fritz, *Angew. Chem. Int. Ed.* **1999**, *38*, 884–905.

[284] S. Hecht, J. M. J. Fréchet, *Angew. Chemie - Int. Ed.* **2001**, *40*, 74–91.

[285] J. M. J. Fréchet, *Science (80-.).* **1994**, *263*, 1710–1715.

[286] M. Liu, K. Kono, J. M. J. Fréchet, *J. Control. Release* **2000**, *65*, 121–131.

[287] D. A. Tomalia, A. M. Naylor, W. A. Goddard, *Angew. Chemie - Int. Ed.* **1990**, *29*, 138–175.

[288] S. Stevelmans, J. C. M. Van Hest, J. F. G. A. Jansen, D. A. F. J. Van Boxtel, E. M. M. De Brabander-van Den Berg, E. W. Meijer, *J. Am. Chem. Soc.* **1996**, *118*, 7398–7399.

[289] D. Bhadra, S. Bhadra, S. Jain, N. K. Jain, *Int. J. Pharm.* **2003**, *257*, 111–124.

[290] A. Asthana, A. S. Chauhan, P. V. Diwan, N. K. Jain, *AAPS PharmSciTech* **2005**, *6*, 536–542.

[291] T. P. Thomas, I. J. Majoros, A. Kotlyar, J. F. Kukowska-Latallo, A. Bielinska, A. Myc, J. R. Baker, *J. Med. Chem.* **2005**, *48*, 3729–3735.

[292] U. Gupta, H. B. Agashe, A. Asthana, N. K. Jain, *Biomacromolecules* **2006**, *7*, 649–658.

[293] A. J. Khopade, F. Caruso, P. Tripathi, S. Nagaich, N. K. Jain, *Int. J. Pharm.* **2002**, *232*, 157–162.

[294] R. N. Prajapati, R. K. Tekade, U. Gupta, V. Gajbhiye, N. K. Jain, *Mol. Pharm.* **2009**, *6*, 940–950.

[295] A. S. Chauhan, S. Sridevi, K. B. Chalasani, A. K. Jain, S. K. Jain, N. K. Jain, P. V. Diwan, *J. Control. Release* **2003**, *90*, 335–343.

[296] J. F. Kukowska-Latallo, K. A. Candido, Z. Cao, S. S. Nigavekar, I. J. Majoros, T. P. Thomas, L. P. Balogh, M. K. Khan, J. R. Baker, *Cancer Res.* **2005**, *65*, 5317–5324.

[297] A. Quintana, E. Raczka, L. Piehler, I. Lee, A. Myc, I. Majoros, A. K. Patri, T. Thomas, J. Mulé, J. R. Baker, *Pharm. Res.* **2002**, *19*, 1310–1316.

[298] M. S. Shchepinov, I. A. Udalova, A. J. Bridgman, E. M. Southern, *Nucleic Acids Res.* **1997**, *25*, 4447–4454.

[299] M. Liu, J. M. J. Fréchet, *Pharm. Sci. Technol. Today* **1999**, *2*, 393–401.

[300] P. Singh, U. Gupta, A. Asthana, N. K. Jain, *Bioconjug. Chem.* **2008**, *19*, 2239–2252.

[301] W. Wijagkanalan, S. Kawakami, M. Hashida, *Pharm. Res.* **2011**, *28*, 1500–1519.

[302] J. Lim, E. E. Simanek, *Adv. Drug Deliv. Rev.* **2012**, *64*, 826–835.

[303] A. M. Caminade, C. O. Turrin, *J. Mater. Chem. B* **2014**, *2*, 4055–4066.

[304] H. Wang, Q. Huang, H. Chang, J. Xiao, Y. Cheng, *Biomater. Sci.* **2016**, *4*, 375–390.

[305] A. S. Chauhan, *Molecules* **2018**, *23*, DOI 10.3390/molecules23040938.

[306] J. R. Schaefgen, P. J. Flory, *J. Am. Chem. Soc.* **1948**, *70*, 2709–2718.

[307] M. Morton, T. E. Helminiak, S. D. Gadkary, F. Bueche, *J. Polym. Sci.* **1962**, *57*, 471–482.

[308] A. Chremos, E. Glynos, P. F. Green, *J. Chem. Phys.* **2015**, *142*, DOI 10.1063/1.4906085.

[309] A. Chremos, C. Jeong, J. F. Douglas, *Soft Matter* **2017**, *13*, 5778–5784.

[310] J. M. Ren, T. G. McKenzie, Q. Fu, E. H. H. Wong, J. Xu, Z. An, S. Shanmugam, T. P. Davis, C. Boyer, G. G. Qiao, *Chem. Rev.* **2016**, *116*, 6743–6836.

[311] J. R. Schaefgen, P. J. Flory, *J. Am. Chem. Soc.* **1948**, *70*, 2823–2824.

[312] S. Oelmann, S. C. Solleder, M. A. R. Meier, *Polym. Chem.* **2016**, *7*, 1857–1860.

[313] N. Hadjichristidis, M. Pitsikalis, S. Pispas, H. Iatrou, *Chem. Rev.* **2001**, *101*, 3747–3792.

[314] N. Hadjichristidis, S. Pispas, M. Pitsikalis, *End-Functionalized Polymers with Zwitterionic End-Groups*, **1999**.

[315] N. Hadjichristidis, *J. Polym. Sci. Part A Polym. Chem.* **1999**, *37*, 857–871.

[316] K. Khanna, S. Varshney, A. Kakkar, *Polym. Chem.* **2010**, *1*, 1171–1185.

[317] Y. K. Choi, Y. H. Bae, S. W. Kim, *Macromolecules* **1998**, *31*, 8766–8774.

[318] S. Kanaoka, M. Sawamoto, T. Higashimura, *Macromolecules* **1991**, *24*, 2309–2313.

[319] K. Y. Baek, M. Kamigaito, M. Sawamoto, *Macromolecules* **2001**, *34*, 215–221.

[320] R. Aksakal, M. Resmini, C. R. Becer, *Polym. Chem.* **2016**, *7*, 171–175.

[321] C. Zhang, Y. Zhou, Q. Liu, S. Li, S. Perrier, Y. Zhao, *Macromolecules* **2011**, *44*, 2034–2049.

[322] P. Pahl, C. Schwarzenböck, F. A. D. Herz, B. S. Soller, C. Jandl, B. Rieger, *Macromolecules* **2017**, *50*, 6569–6576.

[323] Z. Sun, K. Morishita, K. Nomura, *Catalysts* **2018**, *8*, DOI 10.3390/catal8120670.

[324] R. Hoogenboom, B. C. Moore, U. S. Schubert, *Chem. Commun.* **2006**, 4010–4012.

[325] V. P. Beyer, B. Cattoz, C. R. Becer, *Macromol. Rapid Commun.* **2020**, *2000519*, 2000519.

[326] A. J. Inglis, P. Pierrat, T. Muller, S. Bräse, C. Barner-Kowollik, *Soft Matter* **2009**, *6*, 82–84.

[327] E. Doganci, M. A. Tasdelen, F. Yilmaz, *Macromol. Chem. Phys.* **2015**, *216*, 1823–1830.

[328] J. Deng, N. Li, K. Mai, C. Yang, L. Yan, L. M. Zhang, *J. Mater. Chem.* **2011**, *21*, 5273–5281.

[329] L. Li, Y. Wang, F. Ji, Y. Wen, J. Li, B. Yang, F. Yao, *J. Biomater. Sci. Polym. Ed.* **2014**, *25*, 1641–1657.

[330] D. P. Yang, M. N. N. L. Oo, G. R. Deen, Z. Li, X. J. Loh, *Macromol. Rapid Commun.* **2017**, *38*, 1–25.

[331] K. Knoll, N. Nierner, *Macromol. Symp.* **1998**, *132*, 231–243.

[332] Z. Sun, P. Unruean, H. Aoki, B. Kitiyanan, K. Nomura, *Organometallics* **2020**, *39*, 2998–3009.

[333] X. Liu, X. Jin, P. X. Ma, *Nat. Mater.* **2011**, *10*, 398–406.

[334] Y. Zhang, Y. Wang, C. Zhang, J. Wang, D. Pan, J. Liu, F. Feng, *ACS Appl. Mater. Interfaces* **2016**, *8*, 3719–3724.

[335] C. V. Rieker, Sustainability Evaluation of Isocyanide Synthesis, KIT, **2019**.

[336] N. D. C. L. Möhl, Improving the Sustainability of Isocyanide Synthesis, KIT, **2019**.

[337] U. S. Department of Health and Human Services, *Toxicol. Profile Methylene Chloride* **2000**, 1–313.

[338] R. A. Sheldon, *Chem. Ind.* **1992**, 903–906.

[339] H.-J. Buysch, in *Ullmann's Encycl. Ind. Chem.*, Wiley-VCH, Weinheim, **2005**.

[340] H. E. Hoydonckx, V. M. van Rhijn, D. E. de Vos, P. A. Jacobs, in *Ullmann's Encycl. Ind. Chem.*, Wiley-VCH, Weinheim, **2012**.

[341] S. Sharma, R. A. Maurya, K. I. Min, G. Y. Jeong, D. P. Kim, *Angew. Chemie - Int. Ed.* **2013**, *52*, 7564–7568.

[342] X. Wang, Q. Wang, *Synthesis (Stuttg).* **2015**, *47*, 49.

[343] Merck, *Sicherheitsdatenblatt - POCl3* **2021**, 1–11.

[344] Merck, *Sicherheitsdatenblatt - p-TsCl* **2021**, 1–10.

[345] C. Fahlberg, I. Remsen, *Berichte der Dtsch. Chem. Gesellschaft* **1879**, *12*, 469–473.

[346] D. J. Ager, D. P. Pantaleone, S. A. Henderson, A. R. Katritzky, I. Prakash, D. E. Walters, *Angew. Chemie Int. Ed.* **1998**, *37*, 1802–1817.

[347] W. Bull, *US 2686811*, **1954**, US 2686811.

[348] F. Haese, J. Wulff-Döring, U. Köhler, P. Gaa, F.-F. Pape, J.-P. Melder, M. Julius, *Patent WO2006/136571 A1*, **2006**, Patent WO2006/136571 A1.

[349] J. Eberhardt, H. Meissner, B. W. Hoffer, J.-P. Melder, E. Schwab, *Patent US2010/267948 A1*, **2010**, Patent US2010/267948 A1.

[350] S. Shimizu, N. Watanabe, T. Kataoka, T. Shoji, N. Abe, S. Morishita, H. Ichimura, in *Ullmann's Encycl. Ind. Chem.*, Wiley-VCH, Weinheim, **2005**.

[351] W. Reppe, W. J. Schweckendiek, *Justus Liebigs Ann. Chem.* **1948**, *560*, 104–116.

[352] K. Eller, E. Henkes, R. Rossbacher, H. Höke, in *Ullmann's Encycl. Ind. Chem.*, Wiley-VCH, Weinheim, **2005**.

[353] A. V. Gulevich, L. S. Koroleva, O. V. Morozova, V. N. Bakhvalova, V. N. Silnikov, V. G. Nenajdenko, *Beilstein J. Org. Chem.* **2011**, *7*, 1135–1140.

[354] H. Mutlu, M. A. R. Meier, *Eur. J. Lipid Sci. Technol.* **2010**, *112*, 10–30.

[355] T. Malliaridou, GC-Optimierung Einer Neuartigen Synthese von Thiolocarbamaten, KIT, **2020**.

[356] H. V. Le, B. Ganem, *Org. Lett.* **2011**, *13*, 2584–2585.

[357] L. Zhu, X. Xu, F. Zheng, *Turkish J. Chem.* **2018**, *42*, 75–85.

[358] L. Filippi, M. A. R. Meier, *Macromol. Rapid Commun.* **2021**, *42*, 2000440.

[359] S. Martens, J. O. Holloway, F. E. Du Prez, in *Seq. Polym.* (Ed.: J.-F. Lutz), Wiley-VCH, Weinheim, **2018**, p. 379.

[360] S. Z. Mikhail, W. R. Kimel, *J. Chem. Eng. Data* **1961**, *6*, 533–537.

[361] A. Arce, A. Blanco, A. Soto, I. Vidal, *J. Chem. Eng. Data* **1993**, *38*, 336–340.

[362] C. E. Barnett, *J. Phys. Chem.* **1942**, *46*, 69–75.

[363] J. Stetefeld, S. A. McKenna, T. R. Patel, *Biophys. Rev.* **2016**, *8*, 409–427.

[364] R. Mocci, S. Murgia, L. De Luca, E. Colacino, F. Delogu, A. Porcheddu, *Org. Chem. Front.* **2018**, *5*, 531–538.

[365] A. Guirado, A. Zapata, J. L. Gómez, L. Trabalón, J. Gálvez, *Tetrahedron* **1999**, *55*, 9631–9640.